CHILDREN'S EDUCATION SOCIETY (Regd.)
THE OXFORD COLLEGE OF ENGINEERING
(Recognised by the Govt. of Karnataka, Affiliated to Visvesvaraya Technological University, Belagavi &
amp; Approved by A.I.C.T.E. New Delhi, Accredited by NAAC &
NBA New Delhi and Recognised by UGC Under Section 2(f))
Bommanahalli, Hosur Road, Bangalore – 560 068.
Ph: 080 -61754601/602, Fax: 080 – 25730551
E-mail: engprincipal@theoxford.edu Web: www.theoxford.edu

List of teachers along with the department affiliation, title of the funded project, the amount and the funding agency during the last academic year

Index

PRINCIPAL
The Oxford College of Engineering
Bommanahalli, Hosur Road
Bengaluru-560 068

CHILDREN'S EDUCATION SOCIETY (Regd.)
THE OXFORD COLLEGE OF ENGINEERING
(Recognised by the Govt. of Karnataka, Affiliated to Visvesvaraya Technological University, Belagavi &
amp; Approved by A.I.C.T.E. New Delhi, Accredited by NAAC &
NBA New Delhi and Recognised by UGC Under Section 2(f))
Bommanahalli, Hosur Road, Bangalore – 560 068.
Ph: 080 -61754601/602, Fax: 080 – 25730551
E-mail: engprincipal@theoxford.edu Web: www.theoxford.edu

LIST OF GRANTS RECEIVED FOR THE ACADEMIC YEAR 2021-22 ALONG WITH THE NATURE OF AWARD, THE AWARDING AGENCY AND THE AMOUNT

Sl.No	Year	Project	Faculties involved	Funding Agencies	Amounts in Rs.
1.	2021-22	16	18	3	1300000
Total		**16**	**18**	**3**	**1300000**

PRINCIPAL
The Oxford College of Engineering
Bommanahalli, Hosur Road
Bangalore-560 068

CHILDREN'S EDUCATION SOCIETY (Regd.)
THE OXFORD COLLEGE OF ENGINEERING
(Recognised by the Govt. of Karnataka, Affiliated to Visvesvaraya Technological University, Belagavi &
amp; Approved by A.I.C.T.E. New Delhi, Accredited by NAAC &
NBA New Delhi and Recognised by UGC Under Section 2(f))
Bommanahalli, Hosur Road, Bangalore – 560 068.
Ph: 080 -61754601/602, Fax: 080 – 25730551
E-mail: engprincipal@theoxford.edu Web: www.theoxford.edu

2021-22

SL No	Name of the Project/ Endowments, Chairs	Name of the Principal Investigator or/Co-investigator	Department of Principal Investigator	Year of Award	Amount Sanctioned	Duration of the project	Name of the Funding Agency	Type (Government/non-Government)
1.	Use Of Super Capacitors In Permanent Magnet Synchronous Motor Drive For E-Mobility	Mr. N JAYAKUMAR	EEE	2021-22	8000	6 MONTHS	KSCST	Government
2.	Iot Based Development Of Smart Dustbin With Monitoring And Tracking System	Mr. N JAYAKUMAR	EEE	2021-22	7000	6 MONTHS	KSCST	Government
3.	Voice And Gesture Controlled Wheel Chair	Prof. SUMITH A T L	EEE	2021-22	8000	6 MONTHS	KSCST	Government
4.	Automatic Self Driving Cars	Dr. V S BHARATH	EEE	2021-22	7000	6 MONTHS	KSCST	Government
5.	Studies On Hot Corosion And Erosion Behaviour Of Thermally Sprayed Composite Coating For High Temperature Industrial Application	DR.MADHUSHUDANA REDDY /Mr. ANUP M UPADHYAYA	ME	2021-22	11,000,00	2 YEARS	VTU RGS	Government

6.	Design And Realization Of 3d Printed Pulse Monitoring Probes	Mr. ANUP M UPADHYAYA	ME	2021-22	7000	6 MONTHS	KSCST	Government
7.	Design And Development Of 3d Printed Bite Force Monitoring Device For Dental Application	Mr. ANUP M UPADHYAYA	ME	2021-22	7000	6 MONTHS	KSCST	Government
8.	Prosthetic Leg	Mr. JAYARAJN/ Dr. PREETA SHARAN	ECE	2021-22	6000	6 MONTHS	KSCST	Government
9.	Supervision Of Water Distribution Using Iot And Android	Dr. M. NIRMALA	CSE	2021-22	6000	6 MONTHS	KSCST	Government
10	Iot Based Night Patrolling Robot Using Multi Model Neural Network	Dr. P. BINDHU MADHAVI	CSE	2021-22	5000	6 MONTHS	KSCST	Government
11	Smart Blind Stick With Object Detection And Assistance	Mr. YADHUKRISHNA M R Dr. R KANAGAVALLI	ISE	2021-22	5000	6 MONTHS	KSCST	Government
12	Compact NN Based Smart Pen	Mrs. S VIDHYA	ISE	2021-22	5000	6 MONTHS	KSCST	Government
13	Smart Portable Bio-Mechanical Patient Monitoring Ventilator	Prof. ANNAIAH C SHETTER	MECHATRONICS	2021-22	7000	6 MONTHS	KSCST	Government
14	Design, Fabrication And Performance Evaluation Of Hybrid Motor	Dr. RAJU B R /Mr. PRADEEP C	AUTOMOBILE	2021-22	10,000	6 MONTHS	KSCST	Government

	Cycle							
15	Bioremediation Of Carcinogenic Polycyclic Aromatic Hydrocarbons(Pahs) Rich Effluent From Petrochemical Industries	Dr. B K MANJUNATHA/Prof. DIVAKARA R	BT	2021-22	12,000	6 MONTHS	KSCST	Government
16	Atma Nirbha Bharat For Highly Innovative Level Of Acquiring Students Harmony	Dr. M.S.SHASHIDARA	MCA	2021-22	100000	1 year	AICTE	Government

PRINCIPAL
The Oxford College of Engineering
Bommanahalli, Hosur Road
Bengaluru-560 068

CHILDREN'S EDUCATION SOCIETY (Regd.)
THE OXFORD COLLEGE OF ENGINEERING
(Recognised by the Govt. of Karnataka, Affiliated to Visvesvaraya Technological University, Belagavi &
amp; Approved by A.I.C.T.E. New Delhi, Accredited by NAAC &
NBA New Delhi and Recognised by UGC Under Section 2(f))
Bommanahalli, Hosur Road, Bangalore – 560 068.
Ph: 080 -61754601/602, Fax: 080 – 25730551
E-mail: engprincipal@theoxford.edu Web: www.theoxford.edu

Karnataka State Council for Science and Technology
(An autonomous organisation under the Dept. of Science & Technology, Govt. of Karnataka)
Indian Institute of Science Campus, Bengaluru – 560 012
Telephone: 080-23341652, 23348848, 23348849, 23348840
Email: office.kscst@iisc.ac.in, office@kscst.org.in • **Website:** www.kscst.iisc.ernet.in, www.kscst.org.in

Mr. H. Hemanth Kumar
Executive Secretary

11th May, 2022

Ref: 7.1.01/SPP/91

The Principal,
The Oxford College of Engineering,
Bommanahalli Hosur Road,
Bengaluru – 560 068

Dear Sir/Madam,

Sub : Sanction of Student Project - 45th Series: Year 2021-2022

Project Proposal Reference No. : **45S_BE_3095**
Ref : Project Proposal entitled **USE OF SUPER CAPACITORS IN PERMANENT MAGNET SYNCHRONOUS MOTOR DRIVE FOR E-MOBILITY**

We are pleased to inform that your student project proposal referred above, has been approved by the Council under "Student Project Programme - 45th Series". The project details are as below:

Student(s)	Ms. SAHANA G H	**Department**	ELECTRICAL AND ELECTRONICS ENGINEERING
	Mr. ROSHAN S TELIGI		
	Ms. SHASHI KUMAR M		
	Mr. ABHILASH D S	**Sanctioned Amount (in Rs.)**	8,000.00
Guide(s)	Mr. N JAYAKUMAR		

Comments / Suggestions of the Experts

Application is mentioned in broad manner, bring out the practical model.

Instructions:

a) The project should be performed based on the objectives of the proposal submitted.
b) Any changes in the project title,objectives or students team is liable for rejection of the project and your institution shall return the sanctioned funds to KSCST.
c) Please quote your project reference number printed above in all your future correspondences.
d) After completing the project, 2 to 3 page write-up (synopsis) needs to be uploaded on to the following Google Forms link https://forms.gle/YMn9K7XETu96i8KbA. The synopsis should include following:
   1) Project Reference Number
   2) Title of the project
   3) Name of the College & Department

CHILDREN'S EDUCATION SOCIETY (Regd.)
THE OXFORD COLLEGE OF ENGINEERING
(Recognised by the Govt. of Karnataka, Affiliated to Visvesvaraya Technological University, Belagavi &
amp; Approved by A.I.C.T.E. New Delhi, Accredited by NAAC &
NBA New Delhi and Recognised by UGC Under Section 2(f))
Bommanahalli, Hosur Road, Bangalore – 560 068.
Ph: 080 -61754601/602, Fax: 080 – 25730551
E-mail: engprincipal@theoxford.edu Web: www.theoxford.edu

4) Name of the students & Guide(s)
5) Keywords
6) Introduction / background (with specific reference to the project, work done earlier, etc) - about 20 lines
7) Objectives (about 10 lines)
8) Methodology (about 20 lines on materials, methods, details of work carried out, including drawings, diagrams etc)
9) Results and Conclusions (about 20 lines with specific reference to work carried out)
10) Scope for future work (about 20 lines).

e) In case of incompeted projects, the sanctioned amount shall be returned to KSCST.
f) The sanctioned amount will be transferred by NEFT to the bank account provided by the College/Institute.
g) The sponsored projects evaluation will be held in the Nodal Centre/Online Mode and the details of the same will be intimated shortly by email / Website announcement.
h) After completion of the project, soft copy of the project report duly signed by the Principal, the HoD, Guide(s) and studetn(s) shall be uploaded in the following Google Forms Link https://forms.gle/PciAaAVisn6bn8AM7. The report should be prepared in the format prescribed by the university.

Please visit our website for further announcements / information and for any clarifications please email to spp@kscst.org.in

Thanking you and with best regards,

Yours sincerely,

(H. Hemanth Kumar)

Copy to:

1) The HoD
ELECTRICAL AND ELECTRONICS ENGINEERING
THE OXFORD COLLEGE OF ENGINEERING, BENGALURU

2) Mr. N JAYAKUMAR
ELECTRICAL AND ELECTRONICS ENGINEERING
THE OXFORD COLLEGE OF ENGINEERING, BENGALURU

3) THE ACCOUNTS OFFICER
KSCST, BENGALURU

CHILDREN'S EDUCATION SOCIETY (Regd.)
THE OXFORD COLLEGE OF ENGINEERING
(Recognised by the Govt. of Karnataka, Affiliated to Visvesvaraya Technological University, Belagavi &
amp; Approved by A.I.C.T.E. New Delhi, Accredited by NAAC &
NBA New Delhi and Recognised by UGC Under Section 2(f))
Bommanahalli, Hosur Road, Bangalore – 560 068.
Ph: 080 -61754601/602, Fax: 080 – 25730551
E-mail: engprincipal@theoxford.edu Web: www.theoxford.edu

Karnataka State Council for Science and Technology
(An autonomous organisation under the Dept. of Science & Technology, Govt. of Karnataka)
Indian Institute of Science Campus, Bengaluru – 560 012
Telephone: 080-23341652, 23348848, 23348849, 23348840
Email: office.kscst@iisc.ac.in, office@kscst.org.in ♦ **Website:** www.kscst.iisc.ernet.in, www.kscst.org.in

Mr. H. Hemanth Kumar
Executive Secretary

11th May, 2022

Ref: 7.1.01/SPP/91

The Principal,
The Oxford College of Engineering,
Bommanahalli Hosur Road,
Bengaluru – 560 068

Dear Sir/Madam,

Sub : Sanction of Student Project - 45th Series: Year 2021-2022

Project Proposal Reference No. : **45S_BE_3197**
Ref : Project Proposal entitled **IoT BASED DEVELOPMENT OF SMART DUSTBIN WITH MONITORING AND TRACKING SYSTEM**

We are pleased to inform that your student project proposal referred above, has been approved by the Council under "Student Project Programme - 45th Series". The project details are as below:

Student(s)	Mr. HARSHITH JG	**Department**	ELECTRICAL AND ELECTRONICS ENGINEERING
	Ms. GAGANA S M		
	Ms. NISHA H N		
	Mr. SANDEEP K	**Sanctioned Amount (in Rs.)**	7,000.00
Guide(s)	Prof. JAYAKUMAR N		

Comments / Suggestions of the Experts

Project seems to be very simple, as it is useful for mass, considered for proving the model in next phase

Instructions:

a) The project should be performed based on the objectives of the proposal submitted.
b) Any changes in the project title,objectives or students team is liable for rejection of the project and your institution shall return the sanctioned funds to KSCST.
c) Please quote your project reference number printed above in all your future correspondences.
d) After completing the project, 2 to 3 page write-up (synopsis) needs to be uploaded on to the following Google Forms link https://forms.gle/YMn9K7XETu96i8KbA. The synopsis should include following:
   1) Project Reference Number
   2) Title of the project
   3) Name of the College & Department

45S_BE_3197

4) Name of the students & Guide(s)
5) Keywords
6) Introduction / background (with specific reference to the project, work done earlier, etc) - about 20 lines
7) Objectives (about 10 lines)
8) Methodology (about 20 lines on materials, methods, details of work carried out, including drawings, diagrams etc)
9) Results and Conclusions (about 20 lines with specific reference to work carried out)
10) Scope for future work (about 20 lines).

e) In case of incompeted projects, the sanctioned amount shall be returned to KSCST.
f) The sanctioned amount will be transferred by NEFT to the bank account provided by the College/Institute.
g) The sponsored projects evaluation will be held in the Nodal Centre/Online Mode and the details of the same will be intimated shortly by email / Website announcement.
h) After completion of the project, soft copy of the project report duly signed by the Principal, the HoD, Guide(s) and studetn(s) shall be uploaded in the following Google Forms Link https://forms.gle/PciAaAVisn6bn8AM7. The report should be prepared in the format prescribed by the university.

Please visit our website for further announcements / information and for any clarifications please email to spp@kscst.org.in

Thanking you and with best regards,

Yours sincerely,

(H. Hemanth Kumar)

Copy to:

1) The HoD
ELECTRICAL AND ELECTRONICS ENGINEERING
THE OXFORD COLLEGE OF ENGINEERING, BENGALURU

2) Prof. JAYAKUMAR N
ELECTRICAL AND ELECTRONICS ENGINEERING
THE OXFORD COLLEGE OF ENGINEERING, BENGALURU

3) THE ACCOUNTS OFFICER
KSCST, BENGALURU

CHILDREN'S EDUCATION SOCIETY (Regd.)
THE OXFORD COLLEGE OF ENGINEERING
(Recognised by the Govt. of Karnataka, Affiliated to Visvesvaraya Technological University, Belagavi &
amp; Approved by A.I.C.T.E. New Delhi, Accredited by NAAC &
NBA New Delhi and Recognised by UGC Under Section 2(f))
Bommanahalli, Hosur Road, Bangalore – 560 068.
Ph: 080 -61754601/602, Fax: 080 – 25730551
E-mail: engprincipal@theoxford.edu Web: www.theoxford.edu

Karnataka State Council for Science and Technology
(An autonomous organisation under the Dept. of Science & Technology, Govt. of Karnataka)
Indian Institute of Science Campus, Bengaluru – 560 012
Telephone: 080-23341652, 23348848, 23348849, 23348840
Email: office.kscst@iisc.ac.in, office@kscst.org.in ♦ **Website:** www.kscst.iisc.ernet.in, www.kscst.org.in

Mr. H. Hemanth Kumar
Executive Secretary

11th May, 2022

Ref: 7.1.01/SPP/91

The Principal,
The Oxford College of Engineering,
Bommanahalli Hosur Road,
Bengaluru – 560 068

Dear Sir/Madam,

Sub : Sanction of Student Project - 45th Series: Year 2021-2022

Project Proposal Reference No. : 45S_BE_3150
Ref : Project Proposal entitled **VOICE AND GESTURE CONTROLLED WHEEL CHAIR**

We are pleased to inform that your student project proposal referred above, has been approved by the Council under "Student Project Programme - 45th Series". The project details are as below:

Student(s)	Mr. SUHARSHA L	**Department**	ELECTRICAL AND ELECTRONICS ENGINEERING
	Ms. AISHWARYA A K		
	Ms. ASHWINI M R		
	Ms. SANJANA K G	**Sanctioned Amount (in Rs.)**	8,000.00
Guide(s)	Prof. SUMITHA T L		

Comments / Suggestions of the Experts

Google assistant & Arduino chip provides support, include valve addition & demonstrate.

Instructions:

a) The project should be performed based on the objectives of the proposal submitted.
b) Any changes in the project title,objectives or students team is liable for rejection of the project and your institution shall return the sanctioned funds to KSCST.
c) Please quote your project reference number printed above in all your future correspondences.
d) After completing the project, 2 to 3 page write-up (synopsis) needs to be uploaded on to the following Google Forms link https://forms.gle/YMn9K7XETu96i8KbA. The synopsis should include following:
   1) Project Reference Number
   2) Title of the project
   3) Name of the College & Department

CHILDREN'S EDUCATION SOCIETY (Regd.)
THE OXFORD COLLEGE OF ENGINEERING
(Recognised by the Govt. of Karnataka, Affiliated to Visvesvaraya Technological University, Belagavi &
amp; Approved by A.I.C.T.E. New Delhi, Accredited by NAAC &
NBA New Delhi and Recognised by UGC Under Section 2(f))
Bommanahalli, Hosur Road, Bangalore – 560 068.
Ph: 080 -61754601/602, Fax: 080 – 25730551
E-mail: engprincipal@theoxford.edu Web: www.theoxford.edu

4) Name of the students & Guide(s)
5) Keywords
6) Introduction / background (with specific reference to the project, work done earlier, etc) - about 20 lines
7) Objectives (about 10 lines)
8) Methodology (about 20 lines on materials, methods, details of work carried out, including drawings, diagrams etc)
9) Results and Conclusions (about 20 lines with specific reference to work carried out)
10) Scope for future work (about 20 lines).

e) In case of incompeted projects, the sanctioned amount shall be returned to KSCST.
f) The sanctioned amount will be transferred by NEFT to the bank account provided by the College/Institute.
g) The sponsored projects evaluation will be held in the Nodal Centre/Online Mode and the details of the same will be intimated shortly by email / Website announcement.
h) After completion of the project, soft copy of the project report duly signed by the Principal, the HoD, Guide(s) and studetn(s) shall be uploaded in the following Google Forms Link https://forms.gle/PciAaAVisn6bn8AM7. The report should be prepared in the format prescribed by the university.

Please visit our website for further announcements / information and for any clarifications please email to spp@kscst.org.in

Thanking you and with best regards,

Yours sincerely,

(H. Hemanth Kumar)

Copy to:

1) The HoD
ELECTRICAL AND ELECTRONICS ENGINEERING
THE OXFORD COLLEGE OF ENGINEERING, BENGALURU

2) Prof. SUMITHA T L
ELECTRICAL AND ELECTRONICS ENGINEERING
THE OXFORD COLLEGE OF ENGINEERING, BENGALURU

3) THE ACCOUNTS OFFICER
KSCST, BENGALURU

CHILDREN'S EDUCATION SOCIETY (Regd.)
THE OXFORD COLLEGE OF ENGINEERING
(Recognised by the Govt. of Karnataka, Affiliated to Visvesvaraya Technological University, Belagavi &
amp; Approved by A.I.C.T.E. New Delhi, Accredited by NAAC &
NBA New Delhi and Recognised by UGC Under Section 2(f))
Bommanahalli, Hosur Road, Bangalore – 560 068.
Ph: 080 -61754601/602, Fax: 080 – 25730551
E-mail: engprincipal@theoxford.edu Web: www.theoxford.edu

Karnataka State Council for Science and Technology
(An autonomous organisation under the Dept. of Science & Technology, Govt. of Karnataka)
Indian Institute of Science Campus, Bengaluru – 560 012
Telephone: 080-23341652, 23348848, 23348849, 23348840
Email: office.kscst@iisc.ac.in, office@kscst.org.in • **Website:** www.kscst.iisc.ernet.in, www.kscst.org.in

Mr. H. Hemanth Kumar
Executive Secretary

11th May, 2022

Ref: 7.1.01/SPP/91

The Principal,
The Oxford College of Engineering,
Bommanahalli Hosur Road,
Bengaluru – 560 068

Dear Sir/Madam,

Sub : Sanction of Student Project - 45th Series: Year 2021-2022

Project Proposal Reference No. : **45S_BE_3194**
Ref : Project Proposal entitled **AUTOMATIC SELF DRIVING CARS**

We are pleased to inform that your student project proposal referred above, has been approved by the Council under "Student Project Programme - 45th Series". The project details are as below:

Student(s)	Ms. NITHYA N	**Department**	ELECTRICAL AND ELECTRONICS ENGINEERING
	Ms. KUSUMA G NAIK		
	Mr. SHIVAPRASAD L KULKARNI		
	Mr. SURYA B	**Sanctioned Amount (in Rs.)**	7,000.00
Guide(s)	Dr. V S BHARATH		

Instructions:

a) The project should be performed based on the objectives of the proposal submitted.
b) Any changes in the project title,objectives or students team is liable for rejection of the project and your institution shall return the sanctioned funds to KSCST.
c) Please quote your project reference number printed above in all your future correspondences.
d) After completing the project, 2 to 3 page write-up (synopsis) needs to be uploaded on to the following Google Forms link https://forms.gle/YMn9K7XETu96i8KbA. The synopsis should include following:
   1) Project Reference Number
   2) Title of the project
   3) Name of the College & Department
   4) Name of the students & Guide(s)
   5) Keywords
   6) Introduction / background (with specific reference to the project, work done earlier, etc) - about 20 lines
   7) Objectives (about 10 lines)

CHILDREN'S EDUCATION SOCIETY (Regd.)
THE OXFORD COLLEGE OF ENGINEERING
(Recognised by the Govt. of Karnataka, Affiliated to Visvesvaraya Technological University, Belagavi &
amp; Approved by A.I.C.T.E. New Delhi, Accredited by NAAC &
NBA New Delhi and Recognised by UGC Under Section 2(f))
Bommanahalli, Hosur Road, Bangalore – 560 068.
Ph: 080 -61754601/602, Fax: 080 – 25730551
E-mail: engprincipal@theoxford.edu Web: www.theoxford.edu

8) Methodology (about 20 lines on materials, methods, details of work carried out, including drawings, diagrams etc)
9) Results and Conclusions (about 20 lines with specific reference to work carried out)
10) Scope for future work (about 20 lines).

e) In case of incompeted projects, the sanctioned amount shall be returned to KSCST.
f) The sanctioned amount will be transferred by NEFT to the bank account provided by the College/Institute.
g) The sponsored projects evaluation will be held in the Nodal Centre/Online Mode and the details of the same will be intimated shortly by email / Website announcement.
h) After completion of the project, soft copy of the project report duly signed by the Principal, the HoD, Guide(s) and studetn(s) shall be uploaded in the following Google Forms Link https://forms.gle/PciAaAVisn6bn8AM7. The report should be prepared in the format prescribed by the university.

Please visit our website for further announcements / information and for any clarifications please email to spp@kscst.org.in

Thanking you and with best regards,

Yours sincerely,

(H. Hemanth Kumar)

Copy to:

1) The HoD
ELECTRICAL AND ELECTRONICS ENGINEERING
THE OXFORD COLLEGE OF ENGINEERING, BENGALURU

2) Dr. V S BHARATH
ELECTRICAL AND ELECTRONICS ENGINEERING
THE OXFORD COLLEGE OF ENGINEERING, BENGALURU

3) THE ACCOUNTS OFFICER
KSCST, BENGALURU

CHILDREN'S EDUCATION SOCIETY (Regd.)
THE OXFORD COLLEGE OF ENGINEERING
(Recognised by the Govt. of Karnataka, Affiliated to Visvesvaraya Technological University, Belagavi &
amp; Approved by A.I.C.T.E. New Delhi, Accredited by NAAC &
NBA New Delhi and Recognised by UGC Under Section 2(f))
Bommanahalli, Hosur Road, Bangalore – 560 068.
Ph: 080 -61754601/602, Fax: 080 – 25730551
E-mail: engprincipal@theoxford.edu Web: www.theoxford.edu

ವಿಶ್ವೇಶ್ವರಯ್ಯ ತಾಂತ್ರಿಕ ವಿಶ್ವವಿದ್ಯಾಲಯ
("ವಿ ಟಿ ಯುಅಧಿನಿಯಮ ೧೯೯೪" ರ ಅಡಿಯಲ್ಲಿ ಕರ್ನಾಟಕ ಸರ್ಕಾರದಿಂದ ಸ್ಥಾಪಿತವಾದ ರಾಜ್ಯ ವಿಶ್ವವಿದ್ಯಾಲಯ)
'ಜ್ಞಾನ ಸಂಗಮ', ಬೆಳಗಾವಿ - ೫೯೦ ೦೧೮ ಕರ್ನಾಟಕ ರಾಜ್ಯ
Visvesvaraya Technological University
(State University of Government of Karnataka Established as per the VTU Act,1994)
"Jnana Sangama" , Belagavi-590 018, Karnataka State, India

Prof. A. S. Deshpande B.E., M.Tech., Ph.D.
REGISTRAR
Phone : (0831) 2498100
Fax : (0831) 2405467

Ref: VTU/BGM/Aca/A-12/ VTU RGS /DIS -ME/2021-22/ 5869 Date : 18 FEB 2022

To,

The Principal,
The Oxford College of Engineering, Bengaluru

Sub: Grants for Research Proposal for the year 2021-22
Ref:. 1. VTU/Aca./2021-22/ PS/2019-20/9707, dated 18-03-2020.
2. Hon'ble Vice-Chancellor's approval dt: 11-02-2022

At the outset please accept our congratulations and greetings.

We are pleased to inform you that, the grant of **Rs. 11.00 Lakhs (Rupees Eleven Lakh only**) is sanctioned to the research proposal entitled as "**Studies on Hot Corrosion and Erosion Behaviour of Thermaly Sprayed Composite Coating for High Temperature Industrial Application** ." submitted by **Dr.Madhu Sudana Reddy (PI) and Anup M Upadhyaya (CoI)** under VTU Research Grants Scheme -2021.

The expenditure of the sanctioned amount needs to be planned as under.

Expenditure Particulars		First Year (Rs. in Lakhs)	Second Year (Rs. in Lakhs)	Total (Rs. in Lakhs)
Non - Recurring	Fellowship for Research Scholar	0.00	0.00	0.00
	Equipments/Software/Instruments (Purchase of Desktops/Laptops are not permitted)	8.00	1.50	9.50
Recurring	Consumables (Glass wares/Chemicals)	0.50	0.35	0.85
	Others (Expenditure towards/ testing / consultancy / publications of research work in terms IPR Registrations **(not for paper publications in journals)** / TA – DA to present a paper in conferences or workshop or symposia in India .	0.40	0.25	0.65
Total (Rs. in Lakhs)		**8.90**	**2.10**	**11.00**
VTU Contribution (75% of the Sanctioned Amount) This amount will be released after receiving the acceptance letter and compliance of Point Number 10,11 & 12 mentioned in **"Terms and Conditions"**		6.675	1.575	8.25
Institute Contribution (25% of the Sanctioned Amount) Please Refer Point Number 10,11 & 12 in the **"Terms and Conditions"** and comply accordingly		2.225	0.525	2.75

CHILDREN'S EDUCATION SOCIETY (Regd.)
THE OXFORD COLLEGE OF ENGINEERING
(Recognised by the Govt. of Karnataka, Affiliated to Visvesvaraya Technological University, Belagavi &
amp; Approved by A.I.C.T.E. New Delhi, Accredited by NAAC &
NBA New Delhi and Recognised by UGC Under Section 2(f))
Bommanahalli, Hosur Road, Bangalore – 560 068.
Ph: 080 -61754601/602, Fax: 080 – 25730551
E-mail: engprincipal@theoxford.edu Web: www.theoxford.edu

Applicable Terms and Conditions:

1. The grant will be released in the name of the Principal of the Institute and Principal Investigator of the project.
2. The grant shall be utilized for the purpose for which it has been sanctioned.
3. The research activities of the sanctioned projects will be evaluated at the end of each year by committee constituted by VTU. Also, the LIC team of VTU may review the progress.
4. Change in heads of expenditure mentioned in the table on the previous page is not permitted.
5. The grantee institute has to abide by the guidelines of VTU Research Grant Scheme.
6. VTU reserves all the rights to change/modify rules/guidelines in this regard.
7. The Principal of the institute shall submit year wise Utilization Certificate (UC) and in the prescribed format and Audit Report (Duly signed by CA) to the undersigned. The subsequent grant will be released only after submission of UC for the grant released earlier along with details of expenditure and satisfactory work progress report.
8. The project will last for two years from the day that the Grantee Institute receives the amount of first Installment.
9. Any correspondence by the Investigators to the Registrar of VTU shall be routed through the Principal of the Grantee Institute.
10. VTU shall release the amount of first installment, after an exclusive Joint Bank Account for the sanctioned project is opened and remitted the Institute share of 25% of the First Year Installment as mentioned in the above table and same shall be intimated to VTU by submitting copy of account statement.
11. The exclusive Bank Account must be Join Account in the name of Principal of the Institute and Principal Investigator with the title of the project mentioned as purpose.
12. Grantee Institute shall submit account details in the *mandate form (enclosed)* along with duly signed *acceptance letter (Format Enclosed)*. These are required for issuing the sanction order and release of fund from our end.

Thanking you,

Yours faithfully,

Registrar

Encl:
1) Format of Mandate Form
2) Format of Acceptance letter

CHILDREN'S EDUCATION SOCIETY (Regd.)
THE OXFORD COLLEGE OF ENGINEERING
(Recognised by the Govt. of Karnataka, Affiliated to Visvesvaraya Technological University, Belagavi &
amp; Approved by A.I.C.T.E. New Delhi, Accredited by NAAC &
NBA New Delhi and Recognised by UGC Under Section 2(f))
Bommanahalli, Hosur Road, Bangalore – 560 068.
Ph: 080 -61754601/602, Fax: 080 – 25730551
E-mail: engprincipal@theoxford.edu Web: www.theoxford.edu

Karnataka State Council for Science and Technology
(An autonomous organisation under the Dept. of Science & Technology, Govt. of Karnataka)
Indian Institute of Science Campus, Bengaluru – 560 012
Telephone: 080-23341652, 23348848, 23348849, 23348840
Email: office.kscst@iisc.ac.in, office@kscst.org.in ♦ **Website:** www.kscst.iisc.ernet.in, www.kscst.org.in

Mr. H. Hemanth Kumar
Executive Secretary

11th May, 2022

Ref: 7.1.01/SPP/91

The Principal,
The Oxford College of Engineering,
Bommanahalli Hosur Road,
Bengaluru – 560 068

Dear Sir/Madam,

Sub : Sanction of Student Project - 45th Series: Year 2021-2022

Project Proposal Reference No. : **45S_BE_3115**
Ref : Project Proposal entitled **DESIGN AND REALIZATION OF 3D PRINTED PULSE MONITORING PROBES**

We are pleased to inform that your student project proposal referred above, has been approved by the Council under "Student Project Programme - 45th Series". The project details are as below:

Student(s)	Mr. HARSHITH D	**Department**	MECHANICAL ENGINEERING
	Mr. RANJITH KUMAR V		
	Mr. J JACKSON		
	Mr. BHARATH KUMAR S	**Sanctioned Amount (in Rs.)**	7,000.00
Guide(s)	Mr. ANUP M UPADHYAYA		

Instructions:

a) The project should be performed based on the objectives of the proposal submitted.
b) Any changes in the project title,objectives or students team is liable for rejection of the project and your institution shall return the sanctioned funds to KSCST.
c) Please quote your project reference number printed above in all your future correspondences.
d) After completing the project, 2 to 3 page write-up (synopsis) needs to be uploaded on to the following Google Forms link https://forms.gle/YMn9K7XETu96i8KbA. The synopsis should include following:
   1) Project Reference Number
   2) Title of the project
   3) Name of the College & Department
   4) Name of the students & Guide(s)
   5) Keywords
   6) Introduction / background (with specific reference to the project, work done earlier, etc) - about 20 lines
   7) Objectives (about 10 lines)

CHILDREN'S EDUCATION SOCIETY (Regd.)
THE OXFORD COLLEGE OF ENGINEERING
(Recognised by the Govt. of Karnataka, Affiliated to Visvesvaraya Technological University, Belagavi &
amp; Approved by A.I.C.T.E. New Delhi, Accredited by NAAC &
NBA New Delhi and Recognised by UGC Under Section 2(f))
Bommanahalli, Hosur Road, Bangalore – 560 068.
Ph: 080 -61754601/602, Fax: 080 – 25730551
E-mail: engprincipal@theoxford.edu Web: www.theoxford.edu

8) Methodology (about 20 lines on materials, methods, details of work carried out, including drawings, diagrams etc)
9) Results and Conclusions (about 20 lines with specific reference to work carried out)
10) Scope for future work (about 20 lines).

e) In case of incompeted projects, the sanctioned amount shall be returned to KSCST.
f) The sanctioned amount will be transferred by NEFT to the bank account provided by the College/Institute.
g) The sponsored projects evaluation will be held in the Nodal Centre/Online Mode and the details of the same will be intimated shortly by email / Website announcement.
h) After completion of the project, soft copy of the project report duly signed by the Principal, the HoD, Guide(s) and studetn(s) shall be uploaded in the following Google Forms Link https://forms.gle/PciAaAVisn6bn8AM7. The report should be prepared in the format prescribed by the university.

Please visit our website for further announcements / information and for any clarifications please email to spp@kscst.org.in

Thanking you and with best regards,

Yours sincerely,

(H. Hemanth Kumar)

Copy to:

1) The HoD
MECHANICAL ENGINEERING
THE OXFORD COLLEGE OF ENGINEERING, BENGALURU

2) Mr. ANUP M UPADHYAYA
MECHANICAL ENGINEERING
THE OXFORD COLLEGE OF ENGINEERING, BENGALURU

3) THE ACCOUNTS OFFICER
KSCST, BENGALURU

CHILDREN'S EDUCATION SOCIETY (Regd.)
THE OXFORD COLLEGE OF ENGINEERING
(Recognised by the Govt. of Karnataka, Affiliated to Visvesvaraya Technological University, Belagavi &
amp; Approved by A.I.C.T.E. New Delhi, Accredited by NAAC &
NBA New Delhi and Recognised by UGC Under Section 2(f))
Bommanahalli, Hosur Road, Bangalore – 560 068.
Ph: 080 -61754601/602, Fax: 080 – 25730551
E-mail: engprincipal@theoxford.edu Web: www.theoxford.edu

Karnataka State Council for Science and Technology
(An autonomous organisation under the Dept. of Science & Technology, Govt. of Karnataka)
Indian Institute of Science Campus, Bengaluru – 560 012
Telephone: 080-23341652, 23348848, 23348849, 23348840
Email: office.kscst@iisc.ac.in, office@kscst.org.in ♦ **Website:** www.kscst.iisc.ernet.in, www.kscst.org.in

Mr. H. Hemanth Kumar
Executive Secretary

11th May, 2022

Ref: 7.1.01/SPP/91

The Principal,
The Oxford College of Engineering,
Bommanahalli Hosur Road,
Bengaluru – 560 068

Dear Sir/Madam,

Sub : Sanction of Student Project - 45th Series: Year 2021-2022

Project Proposal Reference No. : **45S_BE_3103**
Ref : Project Proposal entitled **DESIGN AND DEVELOPMENT OF 3D PRINTED BITE FORCE MONITORING DEVICE FOR DENTAL APPLICATION**

We are pleased to inform that your student project proposal referred above, has been approved by the Council under "Student Project Programme - 45th Series". The project details are as below:

Student(s)	Mr. NAVEEN KUMAR JAISHWAL	**Department**	MECHANICAL ENGINEERING
	Mr. BHARGAV REDDY S		
	Mr. SHREYAS D		
	Mr. AMITHKUMAR H P	**Sanctioned Amount (in Rs.)**	7,000.00
Guide(s)	Mr. ANUP M UPADHAYAYA		

Instructions:

a) The project should be performed based on the objectives of the proposal submitted.
b) Any changes in the project title,objectives or students team is liable for rejection of the project and your institution shall return the sanctioned funds to KSCST.
c) Please quote your project reference number printed above in all your future correspondences.
d) After completing the project, 2 to 3 page write-up (synopsis) needs to be uploaded on to the following Google Forms link https://forms.gle/YMn9K7XETu96i8KbA. The synopsis should include following:
   1) Project Reference Number
   2) Title of the project
   3) Name of the College & Department
   4) Name of the students & Guide(s)
   5) Keywords
   6) Introduction / background (with specific reference to the project, work done earlier, etc) - about 20 lines
   7) Objectives (about 10 lines)

45S_BE_3103

8) Methodology (about 20 lines on materials, methods, details of work carried out, including drawings, diagrams etc)
9) Results and Conclusions (about 20 lines with specific reference to work carried out)
10) Scope for future work (about 20 lines).

e) In case of incompeted projects, the sanctioned amount shall be returned to KSCST.
f) The sanctioned amount will be transferred by NEFT to the bank account provided by the College/Institute.
g) The sponsored projects evaluation will be held in the Nodal Centre/Online Mode and the details of the same will be intimated shortly by email / Website announcement.
h) After completion of the project, soft copy of the project report duly signed by the Principal, the HoD, Guide(s) and studetn(s) shall be uploaded in the following Google Forms Link https://forms.gle/PciAaAVisn6bn8AM7. The report should be prepared in the format prescribed by the university.

Please visit our website for further announcements / information and for any clarifications please email to spp@kscst.org.in

Thanking you and with best regards,

Yours sincerely,

(H. Hemanth Kumar)

Copy to:

1) The HoD
MECHANICAL ENGINEERING
THE OXFORD COLLEGE OF ENGINEERING, BENGALURU

2) Mr. ANUP M UPADHAYAYA
MECHANICAL ENGINEERING
THE OXFORD COLLEGE OF ENGINEERING, BENGALURU

3) THE ACCOUNTS OFFICER
KSCST, BENGALURU

CHILDREN'S EDUCATION SOCIETY (Regd.)
THE OXFORD COLLEGE OF ENGINEERING
(Recognised by the Govt. of Karnataka, Affiliated to Visvesvaraya Technological University, Belagavi &
amp; Approved by A.I.C.T.E. New Delhi, Accredited by NAAC &
NBA New Delhi and Recognised by UGC Under Section 2(f))
Bommanahalli, Hosur Road, Bangalore – 560 068.
Ph: 080 -61754601/602, Fax: 080 – 25730551
E-mail: engprincipal@theoxford.edu Web: www.theoxford.edu

Karnataka State Council for Science and Technology
(An autonomous organisation under the Dept. of Science & Technology, Govt. of Karnataka)
Indian Institute of Science Campus, Bengaluru – 560 012
Telephone: 080-23341652, 23348848, 23348849, 23348840
Email: office.kscst@iisc.ac.in, office@kscst.org.in • **Website:** www.kscst.iisc.ernet.in, www.kscst.org.in

Mr. H. Hemanth Kumar
Executive Secretary

11th May, 2022

Ref: 7.1.01/SPP/91

The Principal,
The Oxford College of Engineering,
Bommanahalli Hosur Road,
Bengaluru – 560 068

Dear Sir/Madam,

Sub : Sanction of Student Project - 45th Series: Year 2021-2022

Project Proposal Reference No. : **45S_BE_3300**
Ref : Project Proposal entitled **PROSTHETIC LEG**

We are pleased to inform that your student project proposal referred above, has been approved by the Council under "Student Project Programme - 45th Series". The project details are as below:

Student(s)	Ms. KUSUMA M	**Department**	ELECTRONICS AND COMMUNICATION ENGINEERING
	Mr. NITHIN B K		
	Mr. ABHISHEK		
	Ms. BHAVANA D G	**Sanctioned Amount (in Rs.)**	6,000.00
Guide(s)	Mr. JAYARAJ N		
	Dr. PREETA SHARAN		

Instructions:

a) The project should be performed based on the objectives of the proposal submitted.

b) Any changes in the project title,objectives or students team is liable for rejection of the project and your institution shall return the sanctioned funds to KSCST.

c) Please quote your project reference number printed above in all your future correspondences.

d) After completing the project, 2 to 3 page write-up (synopsis) needs to be uploaded on to the following Google Forms link https://forms.gle/YMn9K7XETu96i8KbA. The synopsis should include following:

1) Project Reference Number

2) Title of the project

3) Name of the College & Department

4) Name of the students & Guide(s)

5) Keywords

6) Introduction / background (with specific reference to the project, work done earlier, etc) - about 20 lines

7) Objectives (about 10 lines)

CHILDREN'S EDUCATION SOCIETY (Regd.)
THE OXFORD COLLEGE OF ENGINEERING
(Recognised by the Govt. of Karnataka, Affiliated to Visvesvaraya Technological University, Belagavi &
amp; Approved by A.I.C.T.E. New Delhi, Accredited by NAAC &
NBA New Delhi and Recognised by UGC Under Section 2(f))
Bommanahalli, Hosur Road, Bangalore – 560 068.
Ph: 080 -61754601/602, Fax: 080 – 25730551
E-mail: engprincipal@theoxford.edu Web: www.theoxford.edu

8) Methodology (about 20 lines on materials, methods, details of work carried out, including drawings, diagrams etc)
9) Results and Conclusions (about 20 lines with specific reference to work carried out)
10) Scope for future work (about 20 lines).

e) In case of incompeted projects, the sanctioned amount shall be returned to KSCST.
f) The sanctioned amount will be transferred by NEFT to the bank account provided by the College/Institute.
g) The sponsored projects evaluation will be held in the Nodal Centre/Online Mode and the details of the same will be intimated shortly by email / Website announcement.
h) After completion of the project, soft copy of the project report duly signed by the Principal, the HoD, Guide(s) and studetn(s) shall be uploaded in the following Google Forms Link https://forms.gle/PciAaAVisn6bn8AM7. The report should be prepared in the format prescribed by the university.

Please visit our website for further announcements / information and for any clarifications please email to spp@kscst.org.in

Thanking you and with best regards,

Yours sincerely,

(H. Hemanth Kumar)

Copy to:

1) The HoD
ELECTRONICS AND COMMUNICATION ENGINEERING
THE OXFORD COLLEGE OF ENGINEERING, BENGALURU

2) Mr. JAYARAJ N Dr. PREETA SHARAN
ELECTRONICS AND COMMUNICATION ENGINEERING
THE OXFORD COLLEGE OF ENGINEERING, BENGALURU

3) THE ACCOUNTS OFFICER
KSCST, BENGALURU

CHILDREN'S EDUCATION SOCIETY (Regd.)
THE OXFORD COLLEGE OF ENGINEERING
(Recognised by the Govt. of Karnataka, Affiliated to Visvesvaraya Technological University, Belagavi &
amp; Approved by A.I.C.T.E. New Delhi, Accredited by NAAC &
NBA New Delhi and Recognised by UGC Under Section 2(f))
Bommanahalli, Hosur Road, Bangalore – 560 068.
Ph: 080 -61754601/602, Fax: 080 – 25730551
E-mail: engprincipal@theoxford.edu Web: www.theoxford.edu

Karnataka State Council for Science and Technology
(An autonomous organisation under the Dept. of Science & Technology, Govt. of Karnataka)
Indian Institute of Science Campus, Bengaluru – 560 012
Telephone: 080-23341652, 23348848, 23348849, 23348840
Email: office.kscst@iisc.ac.in, office@kscst.org.in • **Website:** www.kscst.iisc.ernet.in, www.kscst.org.in

Mr. H. Hemanth Kumar
Executive Secretary

11th May, 2022

Ref: 7.1.01/SPP/91

The Principal,
The Oxford College of Engineering,
Bommanahalli Hosur Road,
Bengaluru – 560 068.

Dear Sir/Madam,

Sub : Sanction of Student Project - 45th Series: Year 2021-2022

Project Proposal Reference No. : **45S_BE_3375**
Ref : Project Proposal entitled **SUPERVISION OF WATER DISTRIBUTION USING IOT AND ANDROID**

We are pleased to inform that your student project proposal referred above, has been approved by the Council under "Student Project Programme - 45th Series". The project details are as below:

Student(s)	Mr. ABHISHEK C	**Department**	COMPUTER SCIENCE AND ENGINEERING
	Ms. BANU PRIYA U		
	Mr. DARSHAN P		
	Mr. GOWDUCHERUVU PAVAN KUMAR REDDY	**Sanctioned Amount (in Rs.)**	6,000.00
Guide(s)	Dr. M. NIRMALA		

Instructions:

a) The project should be performed based on the objectives of the proposal submitted.
b) Any changes in the project title,objectives or students team is liable for rejection of the project and your institution shall return the sanctioned funds to KSCST.
c) Please quote your project reference number printed above in all your future correspondences.
d) After completing the project, 2 to 3 page write-up (synopsis) needs to be uploaded on to the following Google Forms link https://forms.gle/YMn9K7XETu96i8KbA. The synopsis should include following:
   1) Project Reference Number
   2) Title of the project
   3) Name of the College & Department
   4) Name of the students & Guide(s)
   5) Keywords
   6) Introduction / background (with specific reference to the project, work done earlier, etc) - about 20 lines
   7) Objectives (about 10 lines)

CHILDREN'S EDUCATION SOCIETY (Regd.)
THE OXFORD COLLEGE OF ENGINEERING
(Recognised by the Govt. of Karnataka, Affiliated to Visvesvaraya Technological University, Belagavi &
amp; Approved by A.I.C.T.E. New Delhi, Accredited by NAAC &
NBA New Delhi and Recognised by UGC Under Section 2(f))
Bommanahalli, Hosur Road, Bangalore – 560 068.
Ph: 080 -61754601/602, Fax: 080 – 25730551
E-mail: engprincipal@theoxford.edu Web: www.theoxford.edu

45S_BE_3375

8) Methodology (about 20 lines on materials, methods, details of work carried out, including drawings, diagrams etc)
9) Results and Conclusions (about 20 lines with specific reference to work carried out)
10) Scope for future work (about 20 lines).

e) In case of incompeted projects, the sanctioned amount shall be returned to KSCST.
f) The sanctioned amount will be transferred by NEFT to the bank account provided by the College/Institute.
g) The sponsored projects evaluation will be held in the Nodal Centre/Online Mode and the details of the same will be intimated shortly by email / Website announcement.
h) After completion of the project, soft copy of the project report duly signed by the Principal, the HoD, Guide(s) and studetn(s) shall be uploaded in the following Google Forms Link https://forms.gle/PciAaAVisn6bn8AM7. The report should be prepared in the format prescribed by the university.

Please visit our website for further announcements / information and for any clarifications please email to spp@kscst.org.in

Thanking you and with best regards,

Yours sincerely,

(H. Hemanth Kumar)

Copy to:

1) The HoD
COMPUTER SCIENCE AND ENGINEERING
THE OXFORD COLLEGE OF ENGINEERING, BENGALURU

2) Dr. M. NIRMALA
COMPUTER SCIENCE AND ENGINEERING
THE OXFORD COLLEGE OF ENGINEERING, BENGALURU

3) THE ACCOUNTS OFFICER
KSCST, BENGALURU

CHILDREN'S EDUCATION SOCIETY (Regd.)
THE OXFORD COLLEGE OF ENGINEERING
(Recognised by the Govt. of Karnataka, Affiliated to Visvesvaraya Technological University, Belagavi &
amp; Approved by A.I.C.T.E. New Delhi, Accredited by NAAC &
NBA New Delhi and Recognised by UGC Under Section 2(f))
Bommanahalli, Hosur Road, Bangalore – 560 068.
Ph: 080 -61754601/602, Fax: 080 – 25730551
E-mail: engprincipal@theoxford.edu Web: www.theoxford.edu

Karnataka State Council for Science and Technology
(An autonomous organisation under the Dept. of Science & Technology, Govt. of Karnataka)
Indian Institute of Science Campus, Bengaluru – 560 012
Telephone: 080-23341652, 23348848, 23348849, 23348840
Email: office.kscst@iisc.ac.in, office@kscst.org.in • **Website:** www.kscst.iisc.ernet.in, www.kscst.org.in

Mr. H. Hemanth Kumar
Executive Secretary

11th May, 2022

Ref: 7.1.01/SPP/91

The Principal,
The Oxford College of Engineering,
Bommanahalli Hosur Road,
Bengaluru – 560 068

Dear Sir/Madam,

Sub : Sanction of Student Project - 45th Series: Year 2021-2022

Project Proposal Reference No. : **45S_BE_3529**
Ref : Project Proposal entitled **IOT BASED NIGHT PATROLLING ROBOT USING MULTI MODEL NEURAL NETWORK**

We are pleased to inform that your student project proposal referred above, has been approved by the Council under "Student Project Programme - 45th Series". The project details are as below:

Student(s)	Mr. KAUSHIK M	**Department**	COMPUTER SCIENCE AND ENGINEERING
	Mr. MUSTAFA A MULLA		
	Mr. VIKASH CHANDRA		
	Mrs. SARIGA V R	**Sanctioned Amount (in Rs.)**	5,000.00
Guide(s)	Dr. P. BINDHU MADHAVI		

Instructions:

a) The project should be performed based on the objectives of the proposal submitted.
b) Any changes in the project title,objectives or students team is liable for rejection of the project and your institution shall return the sanctioned funds to KSCST.
c) Please quote your project reference number printed above in all your future correspondences.
d) After completing the project, 2 to 3 page write-up (synopsis) needs to be uploaded on to the following Google Forms link https://forms.gle/YMn9K7XETu96i8KbA. The synopsis should include following:
   1) Project Reference Number
   2) Title of the project
   3) Name of the College & Department
   4) Name of the students & Guide(s)
   5) Keywords
   6) Introduction / background (with specific reference to the project, work done earlier, etc) - about 20 lines
   7) Objectives (about 10 lines)

CHILDREN'S EDUCATION SOCIETY (Regd.)
THE OXFORD COLLEGE OF ENGINEERING
(Recognised by the Govt. of Karnataka, Affiliated to Visvesvaraya Technological University, Belagavi &
amp; Approved by A.I.C.T.E. New Delhi, Accredited by NAAC &
NBA New Delhi and Recognised by UGC Under Section 2(f))
Bommanahalli, Hosur Road, Bangalore – 560 068.
Ph: 080 -61754601/602, Fax: 080 – 25730551
E-mail: engprincipal@theoxford.edu Web: www.theoxford.edu

8) Methodology (about 20 lines on materials, methods, details of work carried out, including drawings, diagrams etc)

9) Results and Conclusions (about 20 lines with specific reference to work carried out)

10) Scope for future work (about 20 lines).

e) In case of incompeted projects, the sanctioned amount shall be returned to KSCST.

f) The sanctioned amount will be transferred by NEFT to the bank account provided by the College/Institute.

g) The sponsored projects evaluation will be held in the Nodal Centre/Online Mode and the details of the same will be intimated shortly by email / Website announcement.

h) After completion of the project, soft copy of the project report duly signed by the Principal, the HoD, Guide(s) and studetn(s) shall be uploaded in the following Google Forms Link https://forms.gle/PciAaAVisn6bn8AM7. The report should be prepared in the format prescribed by the university.

Please visit our website for further announcements / information and for any clarifications please email to spp@kscst.org.in

Thanking you and with best regards,

Yours sincerely,

(H. Hemanth Kumar)

Copy to:

1) The HoD
COMPUTER SCIENCE AND ENGINEERING
THE OXFORD COLLEGE OF ENGINEERING, BENGALURU

2) Dr. P. BINDHU MADHAVI
COMPUTER SCIENCE AND ENGINEERING
THE OXFORD COLLEGE OF ENGINEERING, BENGALURU

3) THE ACCOUNTS OFFICER
KSCST, BENGALURU

CHILDREN'S EDUCATION SOCIETY (Regd.)
THE OXFORD COLLEGE OF ENGINEERING
(Recognised by the Govt. of Karnataka, Affiliated to Visvesvaraya Technological University, Belagavi &
amp; Approved by A.I.C.T.E. New Delhi, Accredited by NAAC &
NBA New Delhi and Recognised by UGC Under Section 2(f))
Bommanahalli, Hosur Road, Bangalore – 560 068.
Ph: 080 -61754601/602, Fax: 080 – 25730551
E-mail: engprincipal@theoxford.edu Web: www.theoxford.edu

Karnataka State Council for Science and Technology
(An autonomous organisation under the Dept. of Science & Technology, Govt. of Karnataka)
Indian Institute of Science Campus, Bengaluru – 560 012
Telephone: 080-23341652, 23348848, 23348849, 23348840
Email: office.kscst@iisc.ac.in, office@kscst.org.in ♦ **Website:** www.kscst.iisc.ernet.in, www.kscst.org.in

Mr. H. Hemanth Kumar
Executive Secretary

11th May, 2022

Ref: 7.1.01/SPP/91

The Principal,
The Oxford College of Engineering,
Bommanahalli Hosur Road,
Bengaluru – 560 068

Dear Sir/Madam,

Sub : Sanction of Student Project - 45th Series: Year 2021-2022

Project Proposal Reference No. : **45S_BE_4353**
Ref : Project Proposal entitled **SMART BLIND STICK WITH OBJECT DETECTION AND ASSISTANCE**

We are pleased to inform that your student project proposal referred above, has been approved by the Council under "Student Project Programme - 45th Series". The project details are as below:

Student(s)	Mr. ANAND THEERTHA V	**Department**	INFORMATION SCIENCE AND ENGINEERING
	Mr. ABHISHEK N		
	Ms. ANUHYA Y		
	Ms. NAGAVARSHITHA C H	**Sanctioned Amount (in Rs.)**	5,000.00
Guide(s)	Mr. YADHUKRISHNA M R		
	Dr. R KANAGAVALLI		

Instructions:

a) The project should be performed based on the objectives of the proposal submitted.
b) Any changes in the project title,objectives or students team is liable for rejection of the project and your institution shall return the sanctioned funds to KSCST.
c) Please quote your project reference number printed above in all your future correspondences.
d) After completing the project, 2 to 3 page write-up (synopsis) needs to be uploaded on to the following Google Forms link https://forms.gle/YMn9K7XETu96i8KbA. The synopsis should include following:
   1) Project Reference Number
   2) Title of the project
   3) Name of the College & Department
   4) Name of the students & Guide(s)
   5) Keywords
   6) Introduction / background (with specific reference to the project, work done earlier, etc) - about 20 lines
   7) Objectives (about 10 lines)

CHILDREN'S EDUCATION SOCIETY (Regd.)
THE OXFORD COLLEGE OF ENGINEERING
(Recognised by the Govt. of Karnataka, Affiliated to Visvesvaraya Technological University, Belagavi &
amp; Approved by A.I.C.T.E. New Delhi, Accredited by NAAC &
NBA New Delhi and Recognised by UGC Under Section 2(f))
Bommanahalli, Hosur Road, Bangalore – 560 068.
Ph: 080 -61754601/602, Fax: 080 – 25730551
E-mail: engprincipal@theoxford.edu Web: www.theoxford.edu

45S_BE_4353

8) Methodology (about 20 lines on materials, methods, details of work carried out, including drawings, diagrams etc)
9) Results and Conclusions (about 20 lines with specific reference to work carried out)
10) Scope for future work (about 20 lines).

e) In case of incompeted projects, the sanctioned amount shall be returned to KSCST.
f) The sanctioned amount will be transferred by NEFT to the bank account provided by the College/Institute.
g) The sponsored projects evaluation will be held in the Nodal Centre/Online Mode and the details of the same will be intimated shortly by email / Website announcement.
h) After completion of the project, soft copy of the project report duly signed by the Principal, the HoD, Guide(s) and studetn(s) shall be uploaded in the following Google Forms Link https://forms.gle/PciAaAVisn6bn8AM7. The report should be prepared in the format prescribed by the university.

Please visit our website for further announcements / information and for any clarifications please email to spp@kscst.org.in

Thanking you and with best regards,

Yours sincerely,

(H. Hemanth Kumar)

Copy to:

1) The HoD
INFORMATION SCIENCE AND ENGINEERING
THE OXFORD COLLEGE OF ENGINEERING, BENGALURU

2) Mr. YADHUKRISHNA M R Dr. R KANAGAVALLI
INFORMATION SCIENCE AND ENGINEERING
THE OXFORD COLLEGE OF ENGINEERING, BENGALURU

3) THE ACCOUNTS OFFICER
KSCST, BENGALURU

CHILDREN'S EDUCATION SOCIETY (Regd.)
THE OXFORD COLLEGE OF ENGINEERING
(Recognised by the Govt. of Karnataka, Affiliated to Visvesvaraya Technological University, Belagavi &
amp; Approved by A.I.C.T.E. New Delhi, Accredited by NAAC &
NBA New Delhi and Recognised by UGC Under Section 2(f))
Bommanahalli, Hosur Road, Bangalore – 560 068.
Ph: 080 -61754601/602, Fax: 080 – 25730551
E-mail: engprincipal@theoxford.edu Web: www.theoxford.edu

Karnataka State Council for Science and Technology
(An autonomous organisation under the Dept. of Science & Technology, Govt. of Karnataka)
Indian Institute of Science Campus, Bengaluru – 560 012
Telephone: 080-23341652, 23348848, 23348849, 23348840
Email: office.kscst@iisc.ac.in, office@kscst.org.in ♦ **Website:** www.kscst.iisc.ernet.in, www.kscst.org.in

Mr. H. Hemanth Kumar
Executive Secretary

11th May, 2022

Ref: 7.1.01/SPP/91

The Principal,
The Oxford College of Engineering,
Bommanahalli Hosur Road,
Bengaluru – 560 068

Dear Sir/Madam,

Sub : Sanction of Student Project - 45th Series: Year 2021-2022

Project Proposal Reference No. : **45S_BE_3464**
Ref : Project Proposal entitled **COMPACT NN BASED SMART PEN**

We are pleased to inform that your student project proposal referred above, has been approved by the Council under "Student Project Programme - 45th Series". The project details are as below:

Student(s)	Mr. N S DHANUSH	**Department**	INFORMATION SCIENCE AND ENGINEERING
	Ms. AISHWARYA		
	Ms. JYOTHI G		
	Mr. POLICEPATIL SOWMYA	**Sanctioned Amount (in Rs.)**	5,000.00
Guide(s)	Mrs. S VIDHYA		

Instructions:

a) The project should be performed based on the objectives of the proposal submitted.
b) Any changes in the project title,objectives or students team is liable for rejection of the project and your institution shall return the sanctioned funds to KSCST.
c) Please quote your project reference number printed above in all your future correspondences.
d) After completing the project, 2 to 3 page write-up (synopsis) needs to be uploaded on to the following Google Forms link https://forms.gle/YMn9K7XETu96i8KbA. The synopsis should include following:
   1) Project Reference Number
   2) Title of the project
   3) Name of the College & Department
   4) Name of the students & Guide(s)
   5) Keywords
   6) Introduction / background (with specific reference to the project, work done earlier, etc) - about 20 lines
   7) Objectives (about 10 lines)

CHILDREN'S EDUCATION SOCIETY (Regd.)
THE OXFORD COLLEGE OF ENGINEERING
(Recognised by the Govt. of Karnataka, Affiliated to Visvesvaraya Technological University, Belagavi &
amp; Approved by A.I.C.T.E. New Delhi, Accredited by NAAC &
NBA New Delhi and Recognised by UGC Under Section 2(f))
Bommanahalli, Hosur Road, Bangalore – 560 068.
Ph: 080 -61754601/602, Fax: 080 – 25730551
E-mail: engprincipal@theoxford.edu Web: www.theoxford.edu

8) Methodology (about 20 lines on materials, methods, details of work carried out, including drawings, diagrams etc)
9) Results and Conclusions (about 20 lines with specific reference to work carried out)
10) Scope for future work (about 20 lines).

e) In case of incompeted projects, the sanctioned amount shall be returned to KSCST.
f) The sanctioned amount will be transferred by NEFT to the bank account provided by the College/Institute.
g) The sponsored projects evaluation will be held in the Nodal Centre/Online Mode and the details of the same will be intimated shortly by email / Website announcement.
h) After completion of the project, soft copy of the project report duly signed by the Principal, the HoD, Guide(s) and studetn(s) shall be uploaded in the following Google Forms Link https://forms.gle/PciAaAVisn6bn8AM7. The report should be prepared in the format prescribed by the university.

Please visit our website for further announcements / information and for any clarifications please email to spp@kscst.org.in

Thanking you and with best regards,

Yours sincerely,

(H. Hemanth Kumar)

Copy to:

1) The HoD
INFORMATION SCIENCE AND ENGINEERING
THE OXFORD COLLEGE OF ENGINEERING, BENGALURU

2) Mrs. S VIDHYA
INFORMATION SCIENCE AND ENGINEERING
THE OXFORD COLLEGE OF ENGINEERING, BENGALURU

3) THE ACCOUNTS OFFICER
KSCST, BENGALURU

CHILDREN'S EDUCATION SOCIETY (Regd.)
THE OXFORD COLLEGE OF ENGINEERING
(Recognised by the Govt. of Karnataka, Affiliated to Visvesvaraya Technological University, Belagavi &
amp; Approved by A.I.C.T.E. New Delhi, Accredited by NAAC &
NBA New Delhi and Recognised by UGC Under Section 2(f))
Bommanahalli, Hosur Road, Bangalore – 560 068.
Ph: 080 -61754601/602, Fax: 080 – 25730551
E-mail: engprincipal@theoxford.edu Web: www.theoxford.edu

Karnataka State Council for Science and Technology
(An autonomous organisation under the Dept. of Science & Technology, Govt. of Karnataka)
Indian Institute of Science Campus, Bengaluru – 560 012
Telephone: 080-23341652, 23348848, 23348849, 23348840
Email: office.kscst@iisc.ac.in, office@kscst.org.in • **Website:** www.kscst.iisc.ernet.in, www.kscst.org.in

Mr. H. Hemanth Kumar
Executive Secretary

11th May, 2022

Ref: 7.1.01/SPP/91

The Principal,
The Oxford College of Engineering,
Bommanahalli Hosur Road,
Bengaluru – 560 068

Dear Sir/Madam,

Sub : Sanction of Student Project - 45th Series: Year 2021-2022

Project Proposal Reference No. : **45S_BE_3444**
Ref : Project Proposal entitled **SMART PORTABLE BIO-MECHANICAL PATIENT MONITORING VENTILATOR**

We are pleased to inform that your student project proposal referred above, has been approved by the Council under "Student Project Programme - 45th Series". The project details are as below:

Student(s)	Mr. SANDEEP H	**Department**	MECHATRONICS
	Ms. RANJITHA V		
		Sanctioned Amount (in Rs.)	7,000.00
Guide(s)	Prof. ANNAIAH C SHETTER		

Instructions:

a) The project should be performed based on the objectives of the proposal submitted.
b) Any changes in the project title,objectives or students team is liable for rejection of the project and your institution shall return the sanctioned funds to KSCST.
c) Please quote your project reference number printed above in all your future correspondences.
d) After completing the project, 2 to 3 page write-up (synopsis) needs to be uploaded on to the following Google Forms link https://forms.gle/YMn9K7XETu96i8KbA. The synopsis should include following:
   1) Project Reference Number
   2) Title of the project
   3) Name of the College & Department
   4) Name of the students & Guide(s)
   5) Keywords
   6) Introduction / background (with specific reference to the project, work done earlier, etc) - about 20 lines
   7) Objectives (about 10 lines)

CHILDREN'S EDUCATION SOCIETY (Regd.)
THE OXFORD COLLEGE OF ENGINEERING
(Recognised by the Govt. of Karnataka, Affiliated to Visvesvaraya Technological University, Belagavi &
amp; Approved by A.I.C.T.E. New Delhi, Accredited by NAAC &
NBA New Delhi and Recognised by UGC Under Section 2(f))
Bommanahalli, Hosur Road, Bangalore – 560 068.
Ph: 080 -61754601/602, Fax: 080 – 25730551
E-mail: engprincipal@theoxford.edu Web: www.theoxford.edu

45S_BE_3444

8) Methodology (about 20 lines on materials, methods, details of work carried out, including drawings, diagrams etc)
9) Results and Conclusions (about 20 lines with specific reference to work carried out)
10) Scope for future work (about 20 lines).

e) In case of incompeted projects, the sanctioned amount shall be returned to KSCST.
f) The sanctioned amount will be transferred by NEFT to the bank account provided by the College/Institute.
g) The sponsored projects evaluation will be held in the Nodal Centre/Online Mode and the details of the same will be intimated shortly by email / Website announcement.
h) After completion of the project, soft copy of the project report duly signed by the Principal, the HoD, Guide(s) and studetn(s) shall be uploaded in the following Google Forms Link https://forms.gle/PciAaAVisn6bn8AM7. The report should be prepared in the format prescribed by the university.

Please visit our website for further announcements / information and for any clarifications please email to spp@kscst.org.in

Thanking you and with best regards,

Yours sincerely,

(H. Hemanth Kumar)

Copy to:

1) The HoD
MECHATRONICS
THE OXFORD COLLEGE OF ENGINEERING, BENGALURU

2) Prof. ANNAIAH C SHETTER
MECHATRONICS
THE OXFORD COLLEGE OF ENGINEERING, BENGALURU

3) THE ACCOUNTS OFFICER
KSCST, BENGALURU

CHILDREN'S EDUCATION SOCIETY (Regd.)
THE OXFORD COLLEGE OF ENGINEERING
(Recognised by the Govt. of Karnataka, Affiliated to Visvesvaraya Technological University, Belagavi &
amp; Approved by A.I.C.T.E. New Delhi, Accredited by NAAC &
NBA New Delhi and Recognised by UGC Under Section 2(f))
Bommanahalli, Hosur Road, Bangalore – 560 068.
Ph: 080 -61754601/602, Fax: 080 – 25730551
E-mail: engprincipal@theoxford.edu Web: www.theoxford.edu

Karnataka State Council for Science and Technology
(An autonomous organisation under the Dept. of Science & Technology, Govt. of Karnataka)
Indian Institute of Science Campus, Bengaluru – 560 012
Telephone: 080-23341652, 23348848, 23348849, 23348840
Email: office.kscst@iisc.ac.in, office@kscst.org.in ♦ **Website:** www.kscst.iisc.ernet.in, www.kscst.org.in

Mr. H. Hemanth Kumar
Executive Secretary

11th May, 2022

Ref: 7.1.01/SPP/91

The Principal,
The Oxford College of Engineering,
Bommanahalli Hosur Road,
Bengaluru – 560 068.

Dear Sir/Madam,

Sub : Sanction of Student Project - 45th Series: Year 2021-2022

Project Proposal Reference No. : **45S_BE_3574**
Ref : Project Proposal entitled **DESIGN, FABRICATION and PERFORMANCE EVALUATION of HYBRID MOTOR CYCLE**

We are pleased to inform that your student project proposal referred above, has been approved by the Council under "Student Project Programme - 45th Series". The project details are as below:

Student(s)	Mr. TEJA M H	**Department**	AUTOMOBILE ENGINEERING
	Mr. MOHAMMAD WAEIZ AHEMD MANAAM		
	Mr. MAYANK RAJPUT		
	Mr. MOHAMMED IMADUDDIN	**Sanctioned Amount (in Rs.)**	10,000.00
Guide(s)	Dr. RAJU B R		
	Mr. PRADEEP C		

Comments / Suggestions of the Experts

Make a physical unit

Instructions:

a) The project should be performed based on the objectives of the proposal submitted.
b) Any changes in the project title,objectives or students team is liable for rejection of the project and your institution shall return the sanctioned funds to KSCST.
c) Please quote your project reference number printed above in all your future correspondences.
d) After completing the project, 2 to 3 page write-up (synopsis) needs to be uploaded on to the following Google Forms link https://forms.gle/YMn9K7XETu96i8KbA. The synopsis should include following:
   1) Project Reference Number
   2) Title of the project
   3) Name of the College & Department

CHILDREN'S EDUCATION SOCIETY (Regd.)
THE OXFORD COLLEGE OF ENGINEERING
(Recognised by the Govt. of Karnataka, Affiliated to Visvesvaraya Technological University, Belagavi &
amp; Approved by A.I.C.T.E. New Delhi, Accredited by NAAC &
NBA New Delhi and Recognised by UGC Under Section 2(f))
Bommanahalli, Hosur Road, Bangalore – 560 068.
Ph: 080 -61754601/602, Fax: 080 – 25730551
E-mail: engprincipal@theoxford.edu Web: www.theoxford.edu

45S_BE_3574

4) Name of the students & Guide(s)
5) Keywords
6) Introduction / background (with specific reference to the project, work done earlier, etc) - about 20 lines
7) Objectives (about 10 lines)
8) Methodology (about 20 lines on materials, methods, details of work carried out, including drawings, diagrams etc)
9) Results and Conclusions (about 20 lines with specific reference to work carried out)
10) Scope for future work (about 20 lines).

e) In case of incompeted projects, the sanctioned amount shall be returned to KSCST.
f) The sanctioned amount will be transferred by NEFT to the bank account provided by the College/Institute.
g) The sponsored projects evaluation will be held in the Nodal Centre/Online Mode and the details of the same will be intimated shortly by email / Website announcement.
h) After completion of the project, soft copy of the project report duly signed by the Principal, the HoD, Guide(s) and studetn(s) shall be uploaded in the following Google Forms Link https://forms.gle/PciAaAVisn6bn8AM7. The report should be prepared in the format prescribed by the university.

Please visit our website for further announcements / information and for any clarifications please email to spp@kscst.org.in

Thanking you and with best regards,

Yours sincerely,

(H. Hemanth Kumar)

Copy to:

1) The HoD
AUTOMOBILE ENGINEERING
THE OXFORD COLLEGE OF ENGINEERING, BENGALURU

2) Dr. RAJU B R Mr. PRADEEP C
AUTOMOBILE ENGINEERING
THE OXFORD COLLEGE OF ENGINEERING, BENGALURU

3) THE ACCOUNTS OFFICER
KSCST, BENGALURU

CHILDREN'S EDUCATION SOCIETY (Regd.)
THE OXFORD COLLEGE OF ENGINEERING
(Recognised by the Govt. of Karnataka, Affiliated to Visvesvaraya Technological University, Belagavi &
amp; Approved by A.I.C.T.E. New Delhi, Accredited by NAAC &
NBA New Delhi and Recognised by UGC Under Section 2(f))
Bommanahalli, Hosur Road, Bangalore – 560 068.
Ph: 080 -61754601/602, Fax: 080 – 25730551
E-mail: engprincipal@theoxford.edu Web: www.theoxford.edu

Karnataka State Council for Science and Technology
(An autonomous organisation under the Dept. of Science & Technology, Govt. of Karnataka)
Indian Institute of Science Campus, Bengaluru – 560 012
Telephone: 080-23341652, 23348848, 23348849, 23348840
Email: office.kscst@iisc.ac.in, office@kscst.org.in ♦ **Website:** www.kscst.iisc.ernet.in, www.kscst.org.in

Mr. H. Hemanth Kumar
Executive Secretary

11th May, 2022

Ref: 7.1.01/SPP/91

The Principal,
The Oxford College of Engineering,
Bommanahalli Hosur Road,
Bengaluru – 560 068

Dear Sir/Madam,

Sub : Sanction of Student Project - 45th Series: Year 2021-2022

Project Proposal Reference No. : **45S_BE_4546**
Ref : Project Proposal entitled **BIOREMEDIATION OF CARCINOGENIC POLYCYCLIC AROMATIC HYDROCARBONS(PAHS) RICH EFFLUENT FROM PETROCHEMICAL INDUSTRIES**

We are pleased to inform that your student project proposal referred above, has been approved by the Council under "Student Project Programme - 45th Series". The project details are as below:

Student(s)	Mr. PAVAN D N	**Department**	BIOTECHNOLOGY
	Mr. HEMAMALINI R M		
	Mr. SAI SHRUTI KANNAN		
	Mr. VILAS RAO SHINDE	**Sanctioned Amount (in Rs.)**	12,000.00
Guide(s)	Dr. B K MANJUNATHA		
	Prof. DIVAKARA R		

Instructions:

a) The project should be performed based on the objectives of the proposal submitted.
b) Any changes in the project title,objectives or students team is liable for rejection of the project and your institution shall return the sanctioned funds to KSCST.
c) Please quote your project reference number printed above in all your future correspondences.
d) After completing the project, 2 to 3 page write-up (synopsis) needs to be uploaded on to the following Google Forms link https://forms.gle/YMn9K7XETu96i8KbA. The synopsis should include following:
   1) Project Reference Number
   2) Title of the project
   3) Name of the College & Department
   4) Name of the students & Guide(s)
   5) Keywords
   6) Introduction / background (with specific reference to the project, work done earlier, etc) - about 20 lines
   7) Objectives (about 10 lines)

CHILDREN'S EDUCATION SOCIETY (Regd.)
THE OXFORD COLLEGE OF ENGINEERING
(Recognised by the Govt. of Karnataka, Affiliated to Visvesvaraya Technological University, Belagavi &
amp; Approved by A.I.C.T.E. New Delhi, Accredited by NAAC &
NBA New Delhi and Recognised by UGC Under Section 2(f))
Bommanahalli, Hosur Road, Bangalore – 560 068.
Ph: 080 -61754601/602, Fax: 080 – 25730551
E-mail: engprincipal@theoxford.edu Web: www.theoxford.edu

45S_BE_4546

8) Methodology (about 20 lines on materials, methods, details of work carried out, including drawings, diagrams etc)
9) Results and Conclusions (about 20 lines with specific reference to work carried out)
10) Scope for future work (about 20 lines).

e) In case of incompeted projects, the sanctioned amount shall be returned to KSCST.
f) The sanctioned amount will be transferred by NEFT to the bank account provided by the College/Institute.
g) The sponsored projects evaluation will be held in the Nodal Centre/Online Mode and the details of the same will be intimated shortly by email / Website announcement.
h) After completion of the project, soft copy of the project report duly signed by the Principal, the HoD, Guide(s) and studetn(s) shall be uploaded in the following Google Forms Link https://forms.gle/PciAaAVisn6bn8AM7. The report should be prepared in the format prescribed by the university.

Please visit our website for further announcements / information and for any clarifications please email to spp@kscst.org.in

Thanking you and with best regards,

Yours sincerely,

(H. Hemanth Kumar)

Copy to:

1) The HoD
BIOTECHNOLOGY
THE OXFORD COLLEGE OF ENGINEERING, BENGALURU

2) Dr. B K MANJUNATHA Prof. DIVAKARA R
BIOTECHNOLOGY
THE OXFORD COLLEGE OF ENGINEERING, BENGALURU

3) THE ACCOUNTS OFFICER
KSCST, BENGALURU

CHILDREN'S EDUCATION SOCIETY (Regd.)
THE OXFORD COLLEGE OF ENGINEERING
(Recognised by the Govt. of Karnataka, Affiliated to Visvesvaraya Technological University, Belagavi &
amp; Approved by A.I.C.T.E. New Delhi, Accredited by NAAC &
NBA New Delhi and Recognised by UGC Under Section 2(f))
Bommanahalli, Hosur Road, Bangalore – 560 068.
Ph: 080 -61754601/602, Fax: 080 – 25730551
E-mail: engprincipal@theoxford.edu Web: www.theoxford.edu

All India Council for Technical Education
(A Statutory body under Ministry of HRD, Govt. of India)
Nelson Mandela Marg, Vasant Kunj, New Delhi-110070 Website: www.aicte-india.org

SPICES - Sanction Letter

F.No. 10-108/AICTE/IDC/SPICES/2020-21 Dated: 05.03.2021

To

The Drawing and Disbursing Officer
All India Council for Technical Education
Nelson Mandela Marg, Vasant Kunj,
New Delhi-110070.

Subject: Release of a sum of Rs. **1,00,000/-** (Rupees One lakh only) as Grant-in-Aid under **AICTE-SPICES** for the year 2021-22 payable during the current financial year 2020-21-reg.

Madam/Sir,

With reference to the proposal submitted by the institute, this is to convey the sanction of the Council for payment of Rs. **1,00,000/-** (Rupees One lakh only) to support the student club/chapter/society **(hereinafter referred to as 'Club')** under the **"Scheme for Promoting Interests, Creativity and Ethics among Students (SPICES)"**, as per details given below:

1.	Name and address of the Beneficiary Institute:	**THE OXFORD COLLEGE OF ENGINEERING -(MCA), HOSUR ROAD, BOMMANAHALLI, BANGALORE, 560068, BANGALORE URBAN, Karnataka**
2.	Permanent ID of Institute:	1-14327361
3.	Name of student club:	ABHILASH ("ATMANIRBHAR BHARATH FOR HIGHLY INNOVATIVE LEVEL OF ACQUIRING STUDENTS HARMONY")
4.	Name of Coordinator:	**Dr. Shashidhara M S**
5.	Name of Co-coordinator	Sreevani Tapila
6.	Grant-in-aid Sanctioned:	Rs. **1,00,000**/- (Rupees One Lakh only)
7.	Amount to be released during the year 2020-21	Rs. **1,00,000**/- (Rupees One Lakh only)
8.	Sanctioned grant-in-aid is debitable to:	**Major Head 602.22 (a) General (Non-Plan Head)**

- The amount of the grant shall be drawn by the Drawing and Disbursing Officer, All India Council for Technical Education, New Delhi on the Grant-in-aid bill and shall be disbursed to and credited to the account of Registrar/ Director/ Principal of the institute through RTGS.
- This grant-in-aid is being released in conformity with the terms & conditions as well as norms of the Scheme as already communicated and also being communicated in this letter.

The instructions/ guidelines to be followed by college/institution

I. Release of funds

a. The Principal/ Director of the institute and the Coordinator of the student club is hereby requested to verify the correctness of the undermentioned bank account/ RTGS details submitted by them alongwith the proposal, against which the grant is being released:

Institute PAN No.	Bank Name	Bank Branch Name	Bank Branch Address	Account Holder Name	Account Type	Account Number	IFSC Code
AAATC1553A	BANK OF BARODA	Oxford Dentle College Branch	Bommanhalli, Bangalore - 560068	Principal The Oxford College of Engineering	Saving Account	67590100005036	BARB0VJOXDC

In case of any omission the same should be reported to AICTE within 7 (Seven) days.

b. The full amount of the grant sanctioned is being released as advance to the College/ Institute.
c. This sanction is issued in exercise of the powers delegated to the Council and other terms and condition laid down in the guidelines of the Scheme.

II. Limit of Funding

a. The grant from AICTE will be Rs. **1,00,000/-** (Rupees One lakh only) and the institute is required to make a contribution of **Rs. (100001 to 200000)** to the club (as committed by the institute in the proposal), non-compliance of which shall invite penal action.

III. Utilization of funds

a. Funds once released/sanctioned for supporting the particular student club cannot be utilized for any other programme/ student club.
b. Students on roll in the institute shall be the member of the club.
c. The grant can be utilized for supporting Interests/Hobbies, Creativity/ Imagination/ Innovation and Ethics/ Value through a range of student activities and meeting the cost of registration and travel (up to 40% of the total grant) of students of the beneficiary club, participating in outstation activities.
d. Ex-students and ex- faculty members and other officials of the institute shall not be the member of club.
e. The clubs must be encouraged to reach out alumni and industries for fund-raising for their events.
f. Coordinator will maintain an electronic record of activities, participants etc..

IV. Maintenance of accounts

a. The institute shall strictly follow the provisions laid down in the Scheme document and this sanction letter. All correspondence related to the project must contain the number of this letter alongwith year of sanction of the project failing which correspondence will not be entertained.
b. The institute shall maintain proper accounts of the expenditure out of the grant and the Council or its nominee shall have the right to check/verify the account to satisfy that the fund has been utilized for the purpose for it was sanctioned.
c. Funds covered by this grant shall be kept separately and would not be mixed up with other funds, so as to know the amount of interest accrued on the grant.

V. Refund of grant to AICTE (by way of a demand draft in favour of Member Secretary, AICTE, New Delhi)

a. The grant shall be refunded to AICTE if the Letter of Approval (LOA) or Extension of Approval is not issued by AICTE to the institute for the academic year 2021-22.
b. Interest accrued on the grant released, shall be refunded to AICTE.
c. No payment is permissible against the activities **already conducted** by club
d. As AICTE needs adequate time for depositing the Demand Draft in the bank, the same be immediately dispatched to avoid any lapse of the validity period.

VI. Documents to be uploaded on AICTE Dashboard/ Portal

a. On receipt of grant:

i. The Acceptance Letter within 7 days from the date of receipt of the Sanction Letter duly signed and seal affixed by Coordinator and Head of the Institutions.

b. After completion of every quarter (from the date of receipt of grant)

i. Upload the list of activities /events /participation date-wise brief description, achievement and 4–5 pictures.

c. After completion of the project (after one year):

Institute has to fill up and update information on AICTE Dashboard/ Portal and upload following documents:

i. Photographs showing various activities, events organized by club.
ii. Feed-back of members of the club.
iii. Identify 3 other clubs which the institution proposes to develop on the lines of club benefited under SPICES.

VII. Submission of documents by institute for project closure (after one year)

The following documents must be submitted to AICTE within a period of one month, after completion of one year, to stay eligible for receiving further grants from AICTE:

a. Utilization Certificate and Statement of Accounts in prescribed format duly audited by the Chartered Accountant in the case of a private institution and by the Finance Officer/Account Officer in respect of government/government- aided institution.
b. Supporting bills/documents on account of expenses incurred for the purpose duly attested by the Head of the Institute.
c. Proof of the amount made available by the institution approved by the Council/ University/ State Government and other sources.
d. Soft copy of final report submitted on AICTE Dashboard/ Portal as mentioned above (in section VI).

VIII. General instructions

a. The assets acquired wholly or substantially of the grants from AICTE shall not be disposed or encumbered or utilized for the purposes other than those for which it was given without proper sanction of the Council and should, at any time the Institution ceased to function, such assets shall revert to the AICTE.

b. The beneficiary institute will make best efforts to promote the scheme by mentioning the sponsorship/ support from AICTE, carrying the Logo of AICTE in club activities and other means.

c. The beneficiary institution shall observe all financial norms and guidelines as prescribed by the AICTE/ Government of India from time to time. GOI GFR rules (@https://doe.gov.in/order-circular/general-financial-*rules2017-0) should be followed during* utilization of grant.

d. This Sanction Letter may be treated as Offer Letter for all purposes.

Yours sincerely

9/3/21

(Dr. Neeraj Saxena)
Adviser (IDC)

Copy forwarded for information and necessary action to:

1. **Dr. Shashidhara M S,**
   THE OXFORD COLLEGE OF ENGINEERING -(MCA),
   HOSUR ROAD, BOMMANAHALLI, BANGALORE,
   560068, BANGALORE URBAN, Karnataka.
2. **The Registrar / Director / Principal,**
   THE OXFORD COLLEGE OF ENGINEERING -(MCA), HOSUR ROAD, BOMMANAHALLI, BANGALORE, 560068, BANGALORE URBAN, Karnataka.
3. **Guard File.**

CHILDREN'S EDUCATION SOCIETY (Regd.)
THE OXFORD COLLEGE OF ENGINEERING
(Recognised by the Govt. of Karnataka, Affiliated to Visvesvaraya Technological University, Belagavi.
Approved by A.I.C.T.E. New Delhi.
Recognised by UGC Under Section 2(f)
Bommanahalli, Hosur Road, Bangalore - 560 068.
Ph: 080-61754601/602, Fax: 080 - 25730551
E-mail: engprincipal@theoxford.edu Web: www.theoxfordengg.org

3.2.1

Doc – 2

List of ongoing & completed projects funded by Institution

Index

PRINCIPAL
The Oxford College of Engineering
Bommanahalli, Hosur Road
Bengaluru-560 068

CHILDREN'S EDUCATION SOCIETY (Regd.)
THE OXFORD COLLEGE OF ENGINEERING
(Recognised by the Govt. of Karnataka, Affiliated to Visvesvaraya Technological University, Belagavi.
Approved by A.I.C.T.E. New Delhi.
Recognised by UGC Under Section 2(f)
Bommanahalli, Hosur Road, Bangalore - 560 068.
Ph: 080-61754601/602, Fax: 080 - 25730551
E-mail: engprincipal@theoxford.edu Web: www.theoxfordengg.org

List of Completed Projects Funded by Institution

2017 - 2021

Sl.No	USN	Name of the Project Members	Project Title	Duration of the Study	Funding Agency
1	1OX17IS006 1OX17IS042 1OX17IS052 1OX17IS055	BASAVARAJ RAKESH SAYEESH C NAIK SHUKIL R	ACCIDENT DETECTION USING ML	2017-2021	The Oxford College of Engineering
2	1OX17IS009 1OX17IS022 1OX17IS029 1OX17IS036	CHAITRA B U MANASA B R MEGHANA CHANDRA POOJA K	DETECTION OF ENEMY AND PREDICT THE DIRECTION OF GUN SHT USING IOT & IMAGE PROCESSING	2017-2021	The Oxford College of Engineering
3	1OX17IS010 1OX17IS018 1OX17IS067	CHANDANA T KEERTHI RAJ SR SHIVAM SHARMA	CAMOUFLAGE ARMY ROBOT	2017-2021	The Oxford College of Engineering
4	1OX17IS012 1OX17IS028 1OX17IS051 1OX16IS115	DEEPAK MAYANK NEGI SANTHOSH VINAY MADHUSUDHAN	FINGERSPELLING-A SIGN LANGUAGE LEARNING TOOL WITH AUDIO	2017-2021	The Oxford College of Engineering
5	1OX17IS020 1OX17IS021 1OX17IS023 1OX17IS031	LATEEFULLA KHAN LEANDER JOSEPH MANISHA M SHAJU MOHAMMAD ABDUL BASITH	DESIGN AND DEVELOPMENT OF LAKE CLEANING MACHINE USING ARTIFICIAL INTELLIGENCE	2017-2021	The Oxford College of Engineering
6	1OX17CV062, 1OX18CV435, 1OX18CV444, 1OX17CV053	H M TILAK GOWDA, SHARATHKUMAR M S, YATISH KUMAR M, SUPRIYA M P	EXPERIMENTAL INVESTIGATION ON COMPRESSIVE STRENGTH OF CONCRETE WITH PARTIAL REPLACEMENT OF FINE AGGREGATE BY RECYCLED CONCRETE WASTE	2017-2021	The Oxford College of Engineering

7	1OX17CV039, 033,050, 1OX18CV427	RAKSHITHA Y N, POOJA N, SOWMYA U, PRAGATHI K	Study on Reverse Osmosis rejected water and its reuse	2017-2021	The Oxford College of Engineering
8	1OX17CV054, 1OX18CV426	SUSHMA G, PAVAN S	Eco-Friendly Petrichor block	2017-2021	The Oxford College of Engineering
9	1OX16CV043,054, 1OX17CV061	MADHUSHREE D, POOJA B M, YOGANANDA S	Study on Pervious Concrete	2017-2021	The Oxford College of Engineering
10	1OX17CV032, 019,006, 1OX18CV411	PAVANESH S, Gurubasava Shetkar, Akarsh T, Divya V P	Mivan Construction Technology	2017-2021	The Oxford College of Engineering
11	1OX17CS015 1OX17CS030 1OX17CS031 1OX17CS041	ARFA TASKEEN HARSHITHA B U HARSHITHA G V KEERTHANA B	Garbage and Drainage Detection Drone	2017-2021	The Oxford College of Engineering
12	1OX17CS016 1OX17CS040 1OX17CS047 1OX17CS059	ARUN REDDY S KARTHIK K MANOJ K MUSAVIR ARAFATH	Vitrual Trial Room	2017-2021	The Oxford College of Engineering
13	1OX17CS057 1OX17CS058 1OX17CS042 1OX16CS103	MONISHA M MOUNASHREE KS LAVANYA P VIJAYALAKSHMI	Covid 19 future forecasting using supervised machine learning models	2017-2021	The Oxford College of Engineering
14	1OX17CS009 1OX17CS033 1OX17CS045 1OX17CS051	ANJALI YADAV IBRAHIM ASKARY MAJID MOHIDEEN R MERIN PHILIP	Design and Implementation of an IOT based Forest Monitoring System	2017-2021	The Oxford College of Engineering
15	1OX17ME038,1OX15ME096,1OX16ME080,1OX17ME072	Pavan M, Vamshith v, Sankar narayan .N, Yashwanth K P	Design and vibration analysis of impeller of submersible pump for septic tank		The Oxford College of Engineering
16	1OX17ME062,1OX17ME060,1OX17ME074,1OX16ME056	Shrikant, Sharanabasappa Patil, Srinivas Kulkarni, Naveen Kumar G B	"Design and fabrication of andriod operated waste collecting vehicle from water sources using solar energy"	2017-2021	The Oxford College of Engineering
17	1OX17ME051,1OX17ME047,1OX17ME054,1OX17ME057	Rakshith Varun A K, Puneeth R , Sampath Roshan Dsouza, Santhosh R	Design & fabrication of three wheeled solar electric vehicle	2017-2021	The Oxford College of Engineering
18	1OX17ME001,1OX17ME010, 1OX17ME011,1OX17ME020	Abhay Prasan Gowda, Avinash S Chandavar, C H Shashikumar, Karan B	synthesis and mechanical properties of aluminium based metal matrix composites	2017-2021	The Oxford College of Engineering

19	1OX17ME021, 1OX17ME027, 1OX17ME009, 1OX17ME012	Kiran K S, Martand Rao, Avanieshsrijiith, Chandan M	Real time pressure monitoring system based on FBG sensor for sports and rehabilitation application	2017-2021	The Oxford College of Engineering
20	1OX18MCA55	ANUP THAKUR	Advance Data Sharing Through Cloud With Two Factor Authentication	2017-2021	The Oxford College of Engineering
21	1OX17MCA08	SUMAIYA	Advanced Recognition of Automobiles using Machine Learning	2017-2021	The Oxford College of Engineering
22	1OX18MCA89	SINGALA UGANDHAR	Business Management Application for Aviation Management System	2017-2021	The Oxford College of Engineering
23	1OX18MCA73	NARENDRA REDDY S	Hosted Management Tool with Effective Analysis	2017-2021	The Oxford College of Engineering
24	1OX16MCA21	RAJA PAUL	Property Swipes	2017-2021	The Oxford College of Engineering
24	1OX17EC053 1OX16EC087 1OX17EC410 1OX17EC405	Sanjay SN Venu prasad KM Vijay Kumar DB SharanaBasava	Contact less door and doorbell security system for pandemic	2017-2021	The Oxford College of Engineering
25	1OX17EC057 1OX17EC063 1OX17EC060 1OX17EC058	Sharan A Sumeet Kulkarni SibinBinu Sharan S Patil	Development of Hand Grip Monitoring Device using a Optical FBG	2017-2021	The Oxford College of Engineering
26	1OX17EC065 1OX17EC067 1OX17EC0575	Sushma P Kamath Tharunya M Yasgaswini L	Health monitoring System of Rail –Wheel	2017-2021	The Oxford College of Engineering
27	1OX17EC006 1OX17EC026 1OX17EC007 1OX17EC023	Archana K ManasaL Ashwini Jha Komala J	Low cost Density based Traffic light controller system with real time air quality monitoring and intergrated surveillance camera	2017-2021	The Oxford College of Engineering
28	1OX17EC046 1OX17EC047 1OX17EC070 1OX17EC040	Rashmi S RuchithaV Vanishree P Padmavathi K	Humanoid Skull	2017-2021	The Oxford College of Engineering

CHILDREN'S EDUCATION SOCIETY (Regd.)
THE OXFORD COLLEGE OF ENGINEERING
(Recognised by the Govt. of Karnataka, Affiliated to Visvesvaraya Technological University, Belagavi.
Approved by A.I.C.T.E. New Delhi.
Recognised by UGC Under Section 2(f)
Bommanahalli, Hosur Road, Bangalore - 560 068.
Ph: 080-61754601/602, Fax: 080 - 25730551
E-mail: engprincipal@theoxford.edu Web: www.theoxfordengg.org

29	1OX17BT042 1OX17BT029 1OX17BT022	Sushma Bhandarkar M Noor Tuba Kunalika M	Development of antimicrobial flavored water	2017-2021	The Oxford College of Engineering
30	1OX17BT033 1OX17BT016 1OX17BT020 1OX17BT024	Preetham A Ishwarya A Komalesh S Mala N	Biochemical characterization and in vitro study of phytoconstituents extracted from Lecuas aspera	2017-2021	The Oxford College of Engineering
31	1OX17BT005 1OX17BT017 1OX17BT008 1OX17BT036	Ardrha Anil Jasmine veronica Azra Taskeen S. Kushmitha Jadhav	Antifungal Ointment Production from plant source	2017-2021	The Oxford College of Engineering
32	1OX17BT004 1OX17BT041	Anusha.S Sumalatha.M	Development of herbal product with anti oxidant properties	2017-2021	The Oxford College of Engineering
33	1OX17BT007 1OX17BT015 1OX17BT021 1OX17BT023	Atul Anand Gupta Harshitha S Thodkar Krishnadev Nair M Purushotham Rao	Discovery of phytochemical based btk inhibitor for immunological disorder	2017-2021	The Oxford College of Engineering
34	1OX17MT007 1OX17MT017 1OX17MT033 1OX17MT046	Aman Raj K Vishnu Sanjay R Vishnu S Kumar	solar powered self sustaininghydrophonics system	2017-2021	The Oxford College of Engineering
35	1OX17MT014 1OX17MT042	Deshna MOHANTY Vijayalakshmi S	Robotic fish for under water surveillance(ROFUS)	2017-2021	The Oxford College of Engineering

36	1OX17MT008 1OX17MT010 1OX17MT035 1OX17MT039	Anniesh Brundha J Shreya Biradar.G VarshaDhare.K	Humanoid Robot with three Gripper End Effector	2017-2021	The Oxford College of Engineering
37	1OX17MT045 1OX17MT018 1OX17MT032	Vishnu Manohar Kiran S Sanjay J	Sign language interpreter using Labview and Raspberrypi	2017-2021	The Oxford College of Engineering
38	1OX17MT025 1OX17MT013 1OX17MT027 1OX17MT011	Muruli Krishna Deeksith g s Nikhil Srinivas K R Chethan m	Voice controlled fork lift with photo sensor	2017-2021	The Oxford College of Engineering
39	1OX17EE006 1OX17EE036 1OX17EE048 1OX17EE053	Aishwarya P Megha M Preethi P Ruzaina	Fully Automated Driverless Metro Train System	2017-2021	The Oxford College of Engineering
40	1OX16EE044 1OX17EE022 1OX17EE025 1OX17EE031	Pavan M Lianzamuna H Janarthanan R Lingala Chandra Shekar Reddy	Wireless Power Transmission for Electrical Vehicle Batteries Charging using Inductive Coupling	2017-2021	The Oxford College of Engineering
41	1OX17EE001 1OX17EE023 1OX17EE024 1OX17EE027	Aadil Bashir Harshitha M R Ivana Merlin Kavya G S	The Prospectivity of Bio sensing in Environmental Monitoring For Biosecurity	2017-2021	The Oxford College of Engineering
42	1OX17EE045 1OX17EE052 1OX18EE402 1OX18EE404	Prabhath S Ruthik Gowda N Manohara M Prem B	Hybrid Smart Power Generation Using Vertical Axis Wind Turbine & Sola	2017-2021	The Oxford College of Engineering

CHILDREN'S EDUCATION SOCIETY (Regd.)
THE OXFORD COLLEGE OF ENGINEERING
(Recognised by the Govt. of Karnataka, Affiliated to Visvesvaraya Technological University, Belagavi.
Approved by A.I.C.T.E. New Delhi.
Recognised by UGC Under Section 2(f)
Bommanahalli, Hosur Road, Bangalore - 560 068.
Ph: 080-61754601/602, Fax: 080 - 25730551
E-mail: engprincipal@theoxford.edu Web: www.theoxfordengg.org

43	1OX17EE040 1OX17EE055 1OX17EE068 1OX17EE069	Nagaraja H S Sagar D Sushmitha K Thanuja K H	Arduino Based Load Monitoring and overload Protection System	2017-2021	The Oxford College of Engineering

CHILDREN'S EDUCATION SOCIETY (Regd.)
THE OXFORD COLLEGE OF ENGINEERING
(Recognised by the Govt. of Karnataka, Affiliated to Visvesvaraya Technological University, Belagavi.
Approved by A.I.C.T.E. New Delhi.
Recognised by UGC Under Section 2(f)
Bommanahalli, Hosur Road, Bangalore - 560 068.
Ph: 080-61754601/602, Fax: 080 - 25730551
E-mail: engprincipal@theoxford.edu Web: www.theoxfordengg.org

List of Ongoing Projects Funded by Institution

Sl.No	USN	Name of the Project Members	Project Title	Duration of the Study	Funding Agency
1	1OX18IS066 1OX18IS063 1OX18IS080 1OX18IS084	Sanjay R Sandeep hegde Syed Imaaduddin Y G Prateek	Navigation Robot	2018-2022	The Oxford College of Engineering
2	1OX18IS012 1OX18IS029 1OX18IS030	Aradhana M K Inchara T Ishita Soni	Sign Language Translator	2018-2022	The Oxford College of Engineering
3	1OX18IS037 1OX19IS400 1OX18IS032	MD Asif AimaanSharieff KosukondaChethan Kumar	Real Time assistive shoe for visually impaired people	2018-2022	The Oxford College of Engineering
4	1OX18IS027 1OX18IS044 1OX18IS054 1OX18IS083	Govinda C V Naveen G Ganapa MullaiVendhan R M VijeyAdhithyan S K	AI based smart combat helmet	2018-2022	The Oxford College of Engineering
5	1OX18IS009 1OX18IS039 1OX18IS053 1OX18IS056	Ambika T Meghana MR Punyashree G Rida Fathima	Anti-sleep alarm for drivers	2018-2022	The Oxford College of Engineering
6	1OX18CS009 1OX18CS010 1OX18CS023 1OX18CS041	Ashwini L Asma Sultana E Bharath Reddy Margaret V	Smart Stick for the Trammels	2018-2022	The Oxford College of Engineering
7	1OX18CS078	SivakamaSundari K	Smart Wrist Pulse Oximeter	2018-2022	The Oxford College of Engineering

	1OX18CS111	Vishal S SSindhe			
	1OX18CS070	Salim Khan			
	1OX18CS071	SatarupaNaskar			
8	1OX18CS063	Ruksar Khanum	Medical Assistance for Alzheimers patients	2018-2022	The Oxford College of Engineering
	1OX18CS064	Ruzaina Anjum			
	1OX18CS079	Sneha Manjunath			
	1OX18CS086	Suriya Jan			
9	1OX18CS069	Sai Supriya G S	Diagnosing CORONA Virus using Chest X-Ray Images	2018-2022	The Oxford College of Engineering
	1OX18CS076	Shwetha Shree			
	1OX18CS087	Suvarchana			
	1OX18CS088	Swarnashree S			
10	1OX18CS095	Merline Mary S	Mental and physical health care management system using ML computer vision and IOT sensor network	2018-2022	The Oxford College of Engineering
	1OX19CS410	Sneha S			
	1OX19CS402	Jasmine A			
	1OX19CS412	Tasmiya Tabassum			
11	1OX18CV002, 022, 006, 1OX19CV413	AIMAN ZEHRA, NISHAT FATHIMA, MYSAR JAN, AMJID SHOWKAT	GREEN BUILDING FOR QUALITY	2018-2022	The Oxford College of Engineering

12	1OX18CV040,044, 025, 020	Shashank K, Tarunkumar M, Priyanka A H, Nisarga G	COMPARATIVE STUDY OF WATER PURIFICATION USING BAMBOO CHARCOAL AND COCONUT-SHELL CHARCOAL	2018-2022	The Oxford College of Engineering
13	1OX19CV424,427, 406, 408	Suryaprakash A, Ullas K, Ganesha P, Hariharan V S	DETERMINATION OF TENSILE PROPERTY OF BAMBOO AND BAMBOO TWING AND STUDY OF ITS BEHAVIOUR AS A REINFORCED CONCRETE BEAM	2018-2022	The Oxford College of Engineering
14	1OX18CV052, 023, 038,051	Vishak L V, P JAHNAVI, SATYANARAYANA V, VINODRICHARD	CONSTRUCTION OF A SMALL-SCALE BIOGAS REACTOR FROM ORGANIC SOLID WASTE	2018-2022	The Oxford College of Engineering
15	1OX18CV048,031,027,003	Vamsikrishna H K, S Basaveshwara, Rahul Arun Patil	Ajay EXPERIMENTAL STUDY ON CELLULAR FORM CONCRETE AND SAW DUST CONCRETE	2018-2022	The Oxford College of Engineering
16	10X17ME41, 10X17ME48, 10X17ME035, 10X17ME015	PRAJWALPRAVEENJIT, RAHUL, NIDITH K. BALLAl, GIDEON SUJITH	Air ambulance and aerial rescue vehcile	2018-2022	The Oxford College of Engineering
17	10X18ME021,110X18ME016,10X18ME005,10X18ME013	SUPREET K,HARSHIT M,AKSHAY B.,DARSHAN D	Design and fabrication of electrical vehicle chagrin station using hybrid, wind and solar energy	2018-2022	The Oxford College of Engineering
18	10X18ME038, 10X18ME009, 10X18ME015, 10X18ME020	V. RANJITKUMA, BHARAT KUMAR S, HARSHIT , JACKSON J	Designa and realization of 3D prinited pulse Monitoring Probes	2018-2022	The Oxford College of Engineering
19	10X18ME008, 10X18ME025, 10X18ME035, 10X18ME051	AVINASH, MANOJKUMAR N, NIRANJAN, TARUNKUMAR K	Fabrication of waste segregation using smart dustbin	2018-2022	The Oxford College of Engineering
20	10X18ME018, 10X18ME048, 10X18ME014, 10X18ME024	HEMANTH KUMAR J,SUSHANTHSHETTY,GURUDATT K.S.MANOJ H.C.	Fabrication and design of mechanical ventilator	2018-2022	The Oxford College of Engineering
21	1OX18EC004,1OX18EC007,1OX18EC019,1OX18EC062	Achsah Mary Ben, AfraTasleem, BrindithaRavi,Sheikh Roshni	Palm Pressure Monitoring Sensor	2018-2022	The Oxford College of Engineering

22	1OX18EC055, 1OX18EC053, 1OX18EC075, 1OX19EC404	Ranjitha R Ramya G, Vidya K V, Nandini H S	DEVELOPMENT OF GRIPPER DEVICE FOR HAND USING FBG SENSOR	2018-2022	The Oxford College of Engineering
23	1OX18EC008, 1OX18EC023, 1OX18EC035, 1OX18EC037	Ajith J, Dhanya N, Manoj L, Navya S	Measurement of foot pressure distribution using FBG sensors	2018-2022	The Oxford College of Engineering
25	1OX18BT001 1OX18BT009 1OX18BT015 1OX18BT020	Afrah Raihan Debleena Bose Jemima saji Mohasina Anjum P	Aromatic Hydrocarbons removal by immobilized bacteria in fluidized bed reactor.	2018-2022	The Oxford College of Engineering
26	1OX18BT013 1OX18BT023 1OX18BT032 1OX18BT046	Hemamalini.R.M Pavan DN Sai Shruti Kannan Vilas Rao Shinde	Establishing biodegradation pathway of carcinogenic PAHs	2018-2022	The Oxford College of Engineering
27	1OX18BT004 1OX18BT005 1OX18BT022 1OX18BT024	Ans Mersa Jasmine P Aparna R Nandini V Pavithra P	Chemical synthesis of Morpholine derivatives of 1,3,4 oxadiazole for evaluation of its biological activities	2018-2022	The Oxford College of Engineering
28	1OX18BT008 1OX18BT017 1OX18BT018 1OX18BT025	ChaithraMuniyoor Kruthika KB M Nithyashri Poojaswini T	Preparation of natural cleansing agent enriched with aromatic oil/herbal extract with special reference to skin care.	2018-2022	The Oxford College of Engineering
29	1OX18BT034 1OX18BT035 1OX18BT042 1OX18BT043	Samuel Prince Sanjay B R Tejas H N Tejas M	In vitro and insilico evaluation of anti-quorum sensing of genistein on MDR Pseudomonas aeruginosa	2018-2022	The Oxford College of Engineering
30	1OX20MC051	MOHAMMED ALAIF H	Data Poison detection in Distributed System	2018-2022	The Oxford College of Engineering
31	1OX20MC011	ANUSHKA V	Modern Approach for Loan Sanctioning In Banks Using Machine Learning	2018-2022	The Oxford College of Engineering
32	1OX20MC088	SANGEETHA S	Business Technological unit Project	2018-2022	The Oxford College of Engineering

33	1OX20MC068	POOJA PATEL	A blockchain based Reward Mechanism for Mobile Crowdsensing Platform	2018-2022	The Oxford College of Engineering
34	1OX20MC084	RAVI KUMAR	Handling Big Data Using aware HDFS and Evolutionary Clustering Technique	2018-2022	The Oxford College of Engineering
35	1OX18EE058 1OX18EE059 1OX18EE065 1OX19EE405	SingamsettiJayahari Sneha V Sushma S Mamatha G	Battery Management System For Electric Vehicles	2018-2022	The Oxford College of Engineering
36	1OX18EE009 1OX18EE013 1OX18EE043 1OX18EE046	BRM Thriguneswari Deepa Kiran Pooja Prabhu Rakshitha S	Smart Security System	2018-2022	The Oxford College of Engineering
37	1OX18EE042 1OX18EE044 1OX18EE047 1OX18EE067	Pooja M Preethi B Rishika S R Vidya shree J	Foot Step Power Generation System	2018-2022	The Oxford College of Engineering
38	1OX18EE023 1OX18EE027 1OX18EE034 1OX18EE063	Karthik Kushal R S Naveen C Suraj R	Solid State Circuit Breaker based smart distribution Board with IoT Integration	2018-2022	The Oxford College of Engineering
39	1OX18EE026 1OX18EE032 1OX18EE041 1OX18EE061	Kumar P Manoj R Pavithra S Sudharshan Bhat	Smart Hand Gesture Gloves with Audio Outputs	2018-2022	The Oxford College of Engineering
40	1OX18MT029 1OX18MT011 1OX18MT006 1OX19MT423	Skanda Narayan J Deon Gomes Arvind M S V Dheeraj	Smart Walking Stick	2018-2022	The Oxford College of Engineering
41	1OX19MT416 1OX18MT025 1OX19MT426 1OX19MT409	Rakesh N R Sahana S R Yugal Kishore R N Mahesh P S	Portable device to detect skin cancer and skin related disease using machine learning	2018-2022	The Oxford College of Engineering
42	1OX18MT026 1OX18MT024	Sandeep H Ranjitha V	Smart portable bio-mechanical patient monitoring ventilator	2018-2022	The Oxford College of Engineering

43	1OX18MT015 1OX18MT018 1OX18MT001 1OX18MT017	M Kiridhar Mohammed Fahad Aftaab Ali Khan Mohammed Anas Pasha	Smart Farming Robot	2018-2022	The Oxford College of Engineering
44	1OX18MT004 1OX18MT010 1OX18MT020 1OX18MT022	Anirudh K R Dhanush D Mohammed Ubaidulla P L Prashanth C	Real time health monitoring band using IOT	2018-2022	The Oxford College of Engineering

CHILDREN'S EDUCATION SOCIETY (Regd.)
THE OXFORD COLLEGE OF ENGINEERING
(Recognised by the Govt. of Karnataka, Affiliated to Visvesvaraya Technological University, Belagavi.
Approved by A.I.C.T.E. New Delhi.
Recognised by UGC Under Section 2(f)
Bommanahalli, Hosur Road, Bangalore - 560 068.
Ph: 080-61754601/602, Fax: 080 - 25730551
E-mail: engprincipal@theoxford.edu Web: www.theoxfordengg.org

Academic Year: 2020-2021

CHILDREN'S EDUCATION SOCIETY (Regd.)
THE OXFORD COLLEGE OF ENGINEERING
(Recognised by the Govt. of Karnataka, Affiliated to Visvesvaraya Technological University, Belagavi.
Approved by A.I.C.T.E. New Delhi.
Recognised by UGC Under Section 2(f)
Bommanahalli, Hosur Road, Bangalore - 560 068.
Ph: 080-61754601/602, Fax: 080 - 25730551
E-mail: engprincipal@theoxford.edu Web: www.theoxfordengg.org

Department of Computer Science and Engineering

Sl.No	Name of the Inventor	Department	Title of the Patent	Patent No	Applied Date	Published Date
1	Ms. Seema Patil Ms. Shobha T Ms. Sowmya HK Ms Jesy Janet Kumari J	CSE	New method for user authentication using artificial intelligence and machine learning approaches	202041053730	10-12-2020	21/12/2020
2	Dr.E.Saravana Kumar	CSE	Delicate Vibratory Instrument for Neonates Oral Motor Simulation	2021101385	17/03/2021	13/05/2021

CHILDREN'S EDUCATION SOCIETY (Regd.)
THE OXFORD COLLEGE OF ENGINEERING
(Recognised by the Govt. of Karnataka, Affiliated to Visvesvaraya Technological University, Belagavi.
Approved by A.I.C.T.E. New Delhi.
Recognised by UGC Under Section 2(f)
Bommanahalli, Hosur Road, Bangalore - 560 068.
Ph: 080-61754601/602, Fax: 080 - 25730551
E-mail: engprincipal@theoxford.edu Web: www.theoxfordengg.org

Department of Electronics & Communication Engineering

Sl.No	Name of the Inventor	Department	Title of the Patent	Patent No	Applied Date	Published Date
1	Dr.Preetha Sharan	ECE	PHOTONIC CRYSTAL BASED OPTICAL SENSOR FOR DETECTION OF PESTICIDES IN LIQUID	.201941010905 A	20/3/19	25/09/2020
2	Dr. Bhargava Rama Gowd	ECE	Efficient Bandwidth Allocation For Routing And Restoration In Optical Networks For Multimedia Applications	202041016069	14/04/2020	19/06/2020
3	Dr.Preetha Sharan	ECE	EFFICIENT BANDWIDTH ALLOCATION FOR ROUTING AND RESTORATION IN OPTICAL NETWORKS FOR MULTIMEDIA APPLICATIONS	202041016069 A19/06/2020	14/04/2020	19/06/2020
4	Dr.Preetha Sharan	ECE	Wireless Keyboard and Mouse for Handicapped	201811032829	31/08/18	14/08/2020
5	Dr.Preetha Sharan	ECE	Hand Exercising Device	20211106120	16/4/2021	16/4/2021
6	Dr.Preetha Sharan	ECE	PHOTONIC CRYSTAL BASED OPTICAL SENSOR FOR DETECTION OF PESTICIDES IN LIQUID	201941010905 A	20/3/19	25/09/2020
7	Dr.Manju Devi	ECE	Bidirectional multipurpose locking pin	202041042484	30/09/2020	-
8	Dr. A Chrispin Jiji	ECE	A New Model for Investigation of marine world using Optical Simulation Extended Depth of Field Platform	202041041346	24/09/2020	09-10-2020
9	Dr.Manju Devi	ECE	Microstrip patch antennas with double wide slots for wireless communication using direct contact probe feed excitation with broadsided radiation	202041046850	27/10/2020	6-11-2020
10	Dr.Manju Devi	ECE	Micromechanical Based Optical Resonator Sensor for Chemical Analysis	202121001531	13/01/2021	-
11	Dr. A Chrispin Jiji	ECE	LCD Screen Cleaning Machine	202041036434	24/08/2020	

CHILDREN'S EDUCATION SOCIETY (Regd.)
THE OXFORD COLLEGE OF ENGINEERING
(Recognised by the Govt. of Karnataka, Affiliated to Visvesvaraya Technological University, Belagavi.
Approved by A.I.C.T.E. New Delhi.
Recognised by UGC Under Section 2(f)
Bommanahalli, Hosur Road, Bangalore - 560 068.
Ph: 080-61754601/602, Fax: 080 - 25730551
E-mail: engprincipal@theoxford.edu Web: www.theoxfordengg.org

Department of Mechanical Engineering

Sl.No	Name of the Inventor	Department	Title of the Patent	Patent No	Applied Date	Published Date
1	Mr Anup M Upadhyaya	Mechanical	Hand Exercising Device	20211106120	16/4/2021	16/4/2021

CHILDREN'S EDUCATION SOCIETY (Regd.)
THE OXFORD COLLEGE OF ENGINEERING
(Recognised by the Govt. of Karnataka, Affiliated to Visvesvaraya Technological University, Belagavi.
Approved by A.I.C.T.E. New Delhi.
Recognised by UGC Under Section 2(f)
Bommanahalli, Hosur Road, Bangalore - 560 068.
Ph: 080-61754601/602, Fax: 080 - 25730551
E-mail: engprincipal@theoxford.edu Web: www.theoxfordengg.org

Department of Electrical & Electronics Engineering

Sl.No	Name of the Inventor	Department	Title of the Patent	Patent No	Applied Date	Published Date
1	Mr. Jayakumar. N , Dr.B.DeviVighneshwari, Mrs. Nisha C Rani	EEE	IoT BASED PROPORTIONAL-INTEGRAL SLIDING MODE DIRECT POWER CONTROL OF DOUBLE FED INDUCTION GENERATOR WIND TURBINE	202141003295 A	25/01/2021	29/01/2021
2	Mrs. Sumitha T L, Mrs. Resna S R, Mrs. M. Raichel Ruby, Mrs. Someswari T, Mrs. Sandhya Rai	EEE	SMART VEHICLE PARKING SYSTEM USING ANDROID APPLICATION	`	17/01/2021	22/01/2021
3	Mr. Jayakumar. N &Dr.B.DeviVighneshwari	EEE	IoT BASED ADVANCED TRAFFIC MANAGEMENT SYSTEM INTEGRATED WITH IMAGE PROCESSING TECHNIQUE	202041032370 A	28/07/2020	21/08/2020
4	Mr. Jayakumar. N ,Dr.B.DeviVighneshwari, Mrs. Nisha C Rani	EEE	Artificial Intelligence Based Smart Surveillance System for Real Time Pedestrian Crossing	202041053074 A	05-12-2020	11-12-2020
5	Mrs. Prakruthi Parthasarathy	EEE	Intelligent battery swapping technology for E-vehicle	202141023431	26/05/2021	-

CHILDREN'S EDUCATION SOCIETY (Regd.)
THE OXFORD COLLEGE OF ENGINEERING
(Recognised by the Govt. of Karnataka, Affiliated to Visvesvaraya Technological University, Belagavi.
Approved by A.I.C.T.E. New Delhi.
Recognised by UGC Under Section 2(f)
Bommanahalli, Hosur Road, Bangalore - 560 068.
Ph: 080-61754601/602, Fax: 080 - 25730551
E-mail: engprincipal@theoxford.edu Web: www.theoxfordengg.org

Department of Humanities & Science

Sl.No	Name of the Inventor	Department	Title of the Patent	Patent No	Applied Date	Published Date
1	Dr.H.N.Gayathri	Chemistry	COST EFFECTIVE WATER FILTRATION SYSTEM AND TREATMENT METHOD THEREOF	2021101309	2021-03-12	21 April 2021,
2	Dr.H.N.Gayathri	Chemistry	A CRITICAL EVALUATIVE PROCESS FOR THE GROUNDWATER STABILITY INDICES	2021101301	2021-03-12	21 April 2021,

CHILDREN'S EDUCATION SOCIETY (Regd.)
THE OXFORD COLLEGE OF ENGINEERING
(Recognised by the Govt. of Karnataka, Affiliated to Visvesvaraya Technological University, Belagavi.
Approved by A.I.C.T.E. New Delhi.
Recognised by UGC Under Section 2(f)
Bommanahalli, Hosur Road, Bangalore - 560 068.
Ph: 080-61754601/602, Fax: 080 - 25730551
E-mail: engprincipal@theoxford.edu Web: www.theoxfordengg.org

Department of MCA

Sl.No	Name of the Inventor	Department	Title of the Patent	Patent No	Applied Date	Published Date
1	Dharamvir	MCA	ACCIDENT PREDICTION SYSTEM FOR ELECTRIC VEHICLE USING AI	20211110158118A	03-04-2021	23-04-2021

CHILDREN'S EDUCATION SOCIETY (Regd.)
THE OXFORD COLLEGE OF ENGINEERING
(Recognised by the Govt. of Karnataka, Affiliated to Visvesvaraya Technological University, Belagavi.
Approved by A.I.C.T.E. New Delhi.
Recognised by UGC Under Section 2(f)
Bommanahalli, Hosur Road, Bangalore - 560 068.
Ph: 080-61754601/602, Fax: 080 - 25730551
E-mail: engprincipal@theoxford.edu Web: www.theoxfordengg.org

Academic Year: 2021-2022

CHILDREN'S EDUCATION SOCIETY (Regd.)
THE OXFORD COLLEGE OF ENGINEERING
(Recognised by the Govt. of Karnataka, Affiliated to Visvesvaraya Technological University, Belagavi.
Approved by A.I.C.T.E. New Delhi.
Recognised by UGC Under Section 2(f)
Bommanahalli, Hosur Road, Bangalore - 560 068.
Ph: 080-61754601/602, Fax: 080 - 25730551
E-mail: engprincipal@theoxford.edu Web: www.theoxfordengg.org

Department of Computer Science and Engineering

Sl.No	Name of the Inventor	Department	Title of the Patent	Patent No	Applied Date	Published Date
1	Dr Buddesab	CSE	DEVELOPMENT OF MULTI-SENSOR SMART ROBOT FOR INTELLIGENT BORDER SECURITY SURVEILLANCE SYSTEMS	202141033795	27/7/2021	6-8-2021
2	Dr.E.Saravana Kumar	CSE	Sustainable remote assisted & transportable neonatal care device for jaundice treatment	2021101143	11-04-2021	11-08-2021
3	Dr Nirmala	CSE	A VIRTUAL REALITY BASED PERSONALIZED VIRTUAL ROOM FOR IMPROVING QUALITY OF LIFE FOR THE BEDRIDDEN PATIENT	202141031084	11-07-2021	16/07/2021
4	Dr Buddesab	CSE	IOT BASED SMART ENERGY THEFT DETECTION AND POWER MONITORING SYSTEM FOR SMART HOMES	202141035598	06-08-2021	13/08/2021

CHILDREN'S EDUCATION SOCIETY (Regd.)
THE OXFORD COLLEGE OF ENGINEERING
(Recognised by the Govt. of Karnataka, Affiliated to Visvesvaraya Technological University, Belagavi.
Approved by A.I.C.T.E. New Delhi.
Recognised by UGC Under Section 2(f)
Bommanahalli, Hosur Road, Bangalore - 560 068.
Ph: 080-61754601/602, Fax: 080 - 25730551
E-mail: engprincipal@theoxford.edu Web: www.theoxfordengg.org

Department of Electronics & Communication Engineering

Sl.No	Name of the Inventor	Department	Title of the Patent	Patent No	Applied Date	Published Date
1	Dr.Preetha Sharan	ECE	WEARABLE HEALTH MONITORING AND CURING DEVICE	202111025557 A	08-06-2021	18/06/2021
2	Dr.Manju Devi	ECE	A Novel classical Error control codes system using design and verification of Verilog HDL	202141061632	29/12/2021	07-01-2022
3	Dr.Manju Devi	ECE	Micromechanical Based Optical Resonator Sensor for Chemical Analysis	202121001531	13/01/2021	-
4	Dr.Preetha Sharan	ECE	A DIGITAL SIGNAL PROCESSING SYSTEM USING QUANTUM COMPUTATION TECHNOLOGY	202111048167	22/10/21	-
5	Dr.Manju Devi	ECE	Design of VLSI System to detect abnormal behaviour of heart beat.	202141020972	09-05-2021	25/06/2021
6	Dr. Bhargava Rama Gowd	ECE	Predicting the user preferences on ecommerce sites using Machine Learning		24.01.2022	

CHILDREN'S EDUCATION SOCIETY (Regd.)
THE OXFORD COLLEGE OF ENGINEERING
(Recognised by the Govt. of Karnataka, Affiliated to Visvesvaraya Technological University, Belagavi.
Approved by A.I.C.T.E. New Delhi.
Recognised by UGC Under Section 2(f)
Bommanahalli, Hosur Road, Bangalore - 560 068.
Ph: 080-61754601/602, Fax: 080 - 25730551
E-mail: engprincipal@theoxford.edu Web: www.theoxfordengg.org

Department of Mechanical Engineering

Sl.No	Name of the Inventor	Department	Title of the Patent	Patent No	Applied Date	Published Date
1	Dr Madhu Sudana Reddy G	Mechanical	Design and development of automatic gear changing model ising electromagnetic valves	202141031663	14-07-2021	13-08-2021

CHILDREN'S EDUCATION SOCIETY (Regd.)
THE OXFORD COLLEGE OF ENGINEERING
(Recognised by the Govt. of Karnataka, Affiliated to Visvesvaraya Technological University, Belagavi.
Approved by A.I.C.T.E. New Delhi.
Recognised by UGC Under Section 2(f)
Bommanahalli, Hosur Road, Bangalore - 560 068.
Ph: 080-61754601/602, Fax: 080 - 25730551
E-mail: engprincipal@theoxford.edu Web: www.theoxfordengg.org

Department of Electrical & Electronics Engineering

Sl.No	Name of the Inventor	Department	Title of the Patent	Patent No	Applied Date	Published Date
1	Mr. Jayakumar. N , Dr.B.DeviVighneshwari, Mrs. Nisha C Rani	EEE	MOBILE SOLAR POWERED SEWING MACHINE CART	202141025388 A	08-06-2021	25/06/2021

CHILDREN'S EDUCATION SOCIETY (Regd.)
THE OXFORD COLLEGE OF ENGINEERING
(Recognised by the Govt. of Karnataka, Affiliated to Visvesvaraya Technological University, Belagavi.
Approved by A.I.C.T.E. New Delhi.
Recognised by UGC Under Section 2(f)
Bommanahalli, Hosur Road, Bangalore - 560 068.
Ph: 080-61754601/602, Fax: 080 - 25730551
E-mail: engprincipal@theoxford.edu Web: www.theoxfordengg.org

Department of Bio Technology

Sl.No	Name of the Inventor	Department	Title of the Patent	Patent No	Applied Date	Published Date
1	Dr.B.K.Manjunath Dr.K.Valarmathy BT	Bio Technology	AN INTEGRATED SYSTEM OF IMAGE RECOGNITION ALONG WITH ARTIFICIAL INTELLIGENCE FOR ACCURATE PREDICTION OF LUNG CANCER USING VARIOUS MEDICAL MODALITIES	202241020244	04-04-2022	13/05/2022

CHILDREN'S EDUCATION SOCIETY (Regd.)
THE OXFORD COLLEGE OF ENGINEERING
(Recognised by the Govt. of Karnataka, Affiliated to Visvesvaraya Technological University, Belagavi.
Approved by A.I.C.T.E. New Delhi.
Recognised by UGC Under Section 2(f)
Bommanahalli, Hosur Road, Bangalore - 560 068.
Ph: 080-61754601/602, Fax: 080 - 25730551
E-mail: engprincipal@theoxford.edu Web: www.theoxfordengg.org

Department of Humanities & Science

Sl.No	Name of the Inventor	Department	Title of the Patent	Patent No	Applied Date	Published Date
1	Dr.H.N.Gayathri	Chemistry	A SYSTEM FOR DEVELOPING AN ACTIVATED CARBON FOR BIOSORPTION OF CADMIUM IONS FROM AQUEOUS SOLUTION	CO1B32/312	2021-12-02	12 Jan 2022

CHILDREN'S EDUCATION SOCIETY (Regd.)
THE OXFORD COLLEGE OF ENGINEERING
(Recognised by the Govt. of Karnataka, Affiliated to Visvesvaraya Technological University, Belagavi.
Approved by A.I.C.T.E. New Delhi.
Recognised by UGC Under Section 2(f)
Bommanahalli, Hosur Road, Bangalore - 560 068.
Ph: 080-61754601/602, Fax: 080 - 25730551
E-mail: engprincipal@theoxford.edu Web: www.theoxfordengg.org

Department of MCA

Sl.No	Name of the Inventor	Department	Title of the Patent	Patent No	Applied Date	Published Date
1	Dr. M S Shashidhara	MCA	AI BASED PREDICTING AND OPTIMIZING TRAFFIC FLOW AT TOLL PLAZA	202141031902A	15-07-2021	13-08-2021
2	Dharamvir	MCA	AI BASED ENERGY SUSTAINABILITY IN SMART CITIES	20214103479A	02-08-2021	06-08-2021
3	J C Achutha	MCA	LITHIUM-ION BATTERY AGEING MANAGEMENT FOR ELECTRIC VEHICLE	20211110158118A	29-07-2021	20-08-2021
4	Kalpana K	MCA	A CHATBOT CLASSIFICATION USING MACHINE LEARNING APPROACH	202241002510A	17-01-2022	28-01-2022
5	Divyashree Nayak	MCA	A FIREWALL SYSTEM IN THE ARCHITECTURE OF IoT TO AVOID CYBER ATTACK	202211002430A	17-01-2022	28-01-2022
6	Dr. M S Shashidhara	MCA	AI BASED TECHNIQUES TO DECIDE AND GUIDE PILOT FOR LANDING OF AIRCRAFTS	2022410084A	10-01-2022	21-01-2022
7	Dharamvir	MCA	A MACHINE LEARNING BASED APPROACH TO ANALYZE THE NETWORK SECURITY OF MEDICAL DATA USING BLOCKCHAIN	202241001101A	08-01-2022	21-01-2022
8	Mridula Shukla	MCA	MACHINE LEARNING ANALYTICS FOR SPECIALISED STOCK TRADING	202211002430A	15-01-2022	28-01-2022
9	Ashok B P	MCA	MACHINE LEARNING BASED APPROACH TO ANALYSIS THE HEART DISESES	202231002221A	14-01-2022	04-02-2022

Academic year 2019-20

Name of the Project/ Endowments, Chairs	Name of the Principal Investigator/Co-investivator	Department of Principal Investigator	Year of Award	Amount Sanctioned	Duration of the project	Name of the Funding Agency	Type (Government/non-Government)
Efficient bioremediation tool for hydrocarbon contaminanation management .scale up and pilot scale study	Dr.B.K.Manjunatha	BT	2019	40,00,000	2019-2021	BIRAC	Government
Nanotization of potential indigenious herbal medications in treatment of high blood pressure	Dr.B.K.Manjunatha	BT	2020	4,41,331	2020-21	NIF	Government

birac
Ignite Innovate Incubate

Biotechnology Industry Research Assistance Council
(A Government of India Enterprise)

Dated: 1-5-2019

To,
Dr. Manjunatha Bukkambudhi Krishnaswamy
Professor & Head,
The Oxford College of Engineering
10th Milestone,
Bommanahalli, Hosur Road,
Bangalore - 560068,
Karnataka
Email: dr.manjunath.tocc@gmail.com

Ref: PACE Project Title *"Efficient bioremediation tool for hydrocarbon contamination management. Scale-Up and Pilot Scale Study"*

Dear Dr. Krishnaswamy,

With reference to your above, mentioned PACE proposal, we are pleased to inform that your proposal has been approved by BIRAC at a total cost of **Rs. 40.00 Lakhs** (Rupees Forty Lakhs only). The contribution of BIRAC is **Rs. 40.00 Lakhs** (Rupees Forty Lakhs only) as Grant-in-aid to the **The Oxford College of Engineering, Bangalore** for **18 Months** as per the terms of the Grant in Aid Letter Agreement (GLA) enclosed.

If you are in acceptance with the terms of funding support as mentioned in the GLA, the following documents should be executed within a time period of ***TWO WEEKS*** from the date of issue of this communication

- Grant-in-aid Letter Agreement (GLA) including all the Schedules: All pages to be clearly initialled by the Fund Recipient.
- Letter of Authorization from the institute in the prescribed format of BIRAC
- Bank Details

The Grant-in-Aid Letter agreement has been executed by BIRAC, kindly take a colour printout of this GLA and the schedules; and execute the same from your end.

The first instalment of fund release will be made only after completion of all these formalities and upon submission of above mentioned documents as per norms.

For Biotechnology Industry Research Assistance Council

Dr. Sanjay Saxena
(GM & Head - Investment)

Oxford College of Engineering, Bommanahalli, Hosur Road

राष्ट्रीय नवप्रवर्तन प्रतिष्ठान - भारत
विज्ञान और प्रौद्योगिकी विभाग, भारत सरकार का स्वायत्तशासी संस्थान
National Innovation Foundation - India
Autonomous Body of Department of Science & Technology, Govt. of India

Date: 01/05/2020
NIF/VARD-Vet/2020/125990

SANCTION ORDER

Subject: Research project for Nanotization of potential indigenous herbal medications for reducing blood pressure - reg.
Ref. No.: TOCE/EST/2019-20 dated 19.03.2020

Dear Dr. B.K.Manjunath,

A sanction not exceeding of Rs. 4,41,331/- (Rupees Four Lakhs Forty-one Thousand Three Hundred and Thirty-one only) is hereby accorded for the project titled "Nanotization of potential indigenous herbal medications in treatment of high blood pressure". The objectives and processing of the program will be according to the proposal submitted to NIF.

The items of expenditure for which total allocation of Rs. 4,41,331/- has been approved and released are given below as:

S. No.	Particulars	Amount (Rs.)
	Source drug - herbal formulation/major lead molecule:	
1.	β-Sitosterol (25 grams)	31,600/-
2.	Cucurbitacin B (10 mg)	45,110/-
3.	β-amyrin (10 mg)	49,500/-
4.	Functionalized nanoparticles - 10 mg	50,000/-
5.	Preliminary characterization	50,000/-
6.	Consumables - Stabilizers/reducing agents / Buffers/Solvents	50,000/-
7.	Contingency	25,000/-
8.	Travel	25,000/-
9.	Outsourcing cost for SEM/TEM/XRD/GC-MS/DLS - studies	75,000/-
	Total	**4,01,210/-**
	Overhear [10% of total cost]	40,121/-
	Grand Total	**4,41,331/-**

The amount of Rs. 2,20,666/- (Rupees Two Lakhs Twenty Thousand Six Hundred and Sixty-six only) has been released as first installment and transferred through NEFT Transaction ID: S61181292 on 27.04.2020 to the account of TOCE-BT-NIF, TOCE-BT-NIF, The Oxford College of Engineering/Dental College and Hospital, Acc. No: 181801011002534, Vijaya Bank. IFSC Code: VIJB0001818.

The University will furnish to the NIF, Utilization Certificate and audited statement of accounts pertaining to the program immediately after completion of project. The Oxford College of Engineering will maintain separate audited accounts for the project. If it is found expedient to keep a part or whole of the grant in a bank account earning interest, then the interest earned should be reported to the NIF. The interest thus earned will be treated as a credit to the university to be adjusted.

The grant sanctioned and released is for the specific program and portion of grant, which the grantee fails to utilize for the purpose for which the grant is sanctioned will be recovered along with interest.

It will be mandatory to submit interim and final reports to NIF.

Please acknowledge the receipt of the sanction order and sanctioned amount for the program.

With kind regards,

[Ravikumar]
ravikumar@nifindia.org

To,
Dr.B.K.Manjunath
Professor and Head
Department of Biotechnology
The Oxford College of Engineering
10th Milestone, Bommanahalli, Hosur Road, Bangalore - 560 068

Copy to:
Principal
The Oxford College of Engineering
10th Milestone, Bommanahalli, Hosur Road, Bangalore - 560 068

From: Dr. Swati Verma Sood
Address: 503, A1 Gulmohar City
Kharadi, Pune - 411014

GSTIN: 27AERPV5469D1ZS

INVOICE

INVOICE NO : SWA/INV-38/NOV-2021
DATE: 01/12/2021

To:
The Oxford college of Engineering,
10th Mile stone, Bommanahalli,
Hosur Road, Bangalore - 560068.

GSTIN: 29AAATC1553A1Z9

Training Conducted for "GRE training"
Training Date: 20th Sep-2021 to 10th Nov-2021

DESCRIPTION	Total Days of Training	RATE/hour	AMOUNT (INR)
Professional Charges for Online training on 'GRE Preparation' (Quant + Verbal Ability + Mock test) for TOCE Students	17 days		35593/-
	IGST	18%	6406.7/-
	SGST		
	CGST		
Amount in Words: Fourty Two Thousand, Only		**TOTAL(INR)**	**42,000/-**

Thanking you,

TRAINER'S CLUB ★ PUNE-411014 ★

Yours truly,
(Dr. Swati Verma)

Bank Details for payment remittance:
Cheque in the name of : Dr. Swati Verma
A/c Name: Trainers Club
A/c Number: 1332102000008587
Bank Name: IDBI Bank
IFSC Code : IBKL0001332
Branch: Sakore Nagar Society, Pune-14
Pan No: AERPV5469D

PRINCIPAL
The Oxford College of Engineering
Bommanahalli, Hosur Road
Bengaluru-560 068.

From: Dr. Swati Verma Sood
Address: 503, A1 Gulmohar City
Kharadi, Pune - 411014

GSTIN: 27AERPV5469D1ZS

INVOICE

INVOICE NO : SWA/INV-26/AUG-2021
DATE: 11/08/2021

To:
The Oxford college of Engineering,
10th Mile stone, Bommanahalli,
Hosur Road, Bangalore - 560068.

GSTIN: 29AAATC1553A1Z9

Training Conducted for "IELTS training"
Training Date: 5th July-2021 to 6th Aug-2021

DESCRIPTION	Total Days of Training	RATE/hour	AMOUNT (INR)
Professional Charges for Online training on 'IELTS Preparation' 30 hours for TOCE Students	24 days (17 days preparation 'LSRW' + 7 days Mock test)		35593/-
	IGST	18%	6406.7/-
	SGST		
	CGST		
Amount in Words: Fourty Two Thousand, Only		**TOTAL(INR)**	**42,000/-**

Thanking you,

Bank Details for payment remittance:
Cheque in the name of : Dr. Swati Verma
A/c Name: Trainers Club
A/c Number: 1332102000008587
Bank Name: IDBI Bank
IFSC Code : IBKL0001332
Branch: Sakore Nagar Society, Pune-14
Pan No: AERPV5469D

TRAINER'S CLUB ★ PUNE-411014 ★

Yours truly,
(Dr. Swati Verma)

PRINCIPAL
The Oxford College of Engineering
Bommanahalli, Hosur Road
Bengaluru-560 068.

ALL INDIA COUNCIL FOR TECHNICAL EDUCATION

Nelson Mandela Marg, Vasant Kunj, New Delhi-110070.
www.aicte-india.org

Ref. No. 65-24/RIFD/SPDP/Policy-1/2016-17 Dated: 27.11.2020

The Drawing and Disbursing Officer
All India Council for Technical Education
(AICTE), Nelson Mandela Marg, Vasant Kunj,
New Delhi-110070.

Sub: Release of 3rd installment of Grant-in-Aid under Skill and Personality Development Programme Centre for SC/ST Students (SPDC) scheme for the year 2016-17 payable during the current financial year 2020-21.

Sir,

I am directed to convey the sanction of the Council for payment of **Rs. 5,73,101/-** (Rupees Five lakh seventy-three thousand one hundred one only) for the year 2016-17 out of the total approved grant-in-aid of Rs.22,98,824/- (Rupees Twenty-two lakh ninety-eight thousand eight hundred twenty-four only) under the Skill and Personality Development Programme Centre for SC/ST Students (SPDC) scheme to The Oxford College of Engineering, Hosur Road, Bommanahalli, Bangalore Rural, Bangalore – 560068, Karnataka as 3rd installment for meeting the expenditure for implementing the scheme as per details given below:

1.	Name of the Beneficiary Institution	:	**The Oxford College of Engineering**, Hosur Road, Bommanahalli, Bangalore Rural, Bangalore – 560068, Karnataka		
2.	Permanent ID of Institute	:	1-5770711		
3.	Scheme under which grant is to be released	:	Skill and Personality Development Programme Centre for SC/ST Students (SPDC) scheme		
4.	Name of Coordinator	:	**Dr. E. Saravana Kumar**		
5.	Sanction Order No. & date	:	65-24/RIFD/SPDP/Policy-1/2016-17 dated 06.11.2020		
6.	Amount Sanctioned	:	Rs. 22,98,824/-		
			Non-Recurring	**Recurring**	
			1st Year 9,77,000/-	**Rs. 1,72,412/-**	
			2nd Year 4,88,500/-	**Rs. 86,206/-**	
			3rd Year 4,88,500/-	**Rs. 86,206/-**	
7.	**Amount to be Released** The remaining amount 25% each in 2nd & 3rd Year.	:	Rs. 5,74,706/- (25% of the total recommended amount)		
	Particulars of release		**Non-Recurring**	**Recurring**	**Total**
	1. Grant released as 2nd installment		Rs. 4,88,500/-	Rs 4,768/-	**Rs. 4,93,268/-**
	2. Expenditure incurred	:	Rs.4,88,282/-	Rs.4,768/-	**Rs. 4,93,250/-**
	3. Amount incurred in excess of release from institute own resources/Unspent amount available	:	Rs.218/- ***(Unspent)**	Nil	**Rs. 218/-**
	4. Interest	:	Rs. 30,859/-	*Rs. 29,472/- (Refunded by the institute)	**Rs. 1,387/-** (Interest available with the institute)
	5. Amount of 3rd installment being the 25% of the total grant of Rs. 22,98,824/-	:	Rs. 4,88,500/-	Rs.86,206/-	**Rs. 5,74,706/-**
	6. Amount to release as 3rd installment after deduction of [3+4] Rs. 1,605/-	:	Rs. 4,88,500/-	Rs.84,601/-	**Rs. 5,73,101/-**
8.	Duration	:	1 Year (Amount to be spent during the approved duration on purchase of approved items only)		

1. The sanctioned grant-in-aid is debitable to the major Head 601.1.b. **"SPDC Scheme" "Plan Head"** grant and is valid for payment during the financial year 2020-21.

2. The grant-in-aid of the grant shall be drawn by the Drawing and Disbursing Officer (DDO), All India Council for Technical Education, New Delhi on the Grants-in-aid bill and shall be disbursed to and credited to the account of the Principal, The Oxford College of Engineering, Hosur Road, Bommanahalli, Bangalore Rural, Bangalore – 560068, Karnataka through RTGS.

Contd...2/-

Ref. No. 65-24/RIFD/SPDP/Policy-1/2016-17

3. The Institute is requested to verify the correctness of the under mentioned bank account/ RTGS submitted by them along with the proposals, in which the grant is being released. In case of any omission the same should be reported to AICTE immediately along with refund of entire grant.

Bank Name	Bank Branch and Address	Account Holder's name	Account Number	Type of Account	IFSC Code	Type of Institution	Institution's PAN No.
Bank of Baroda	Oxford Dental College Branch & VJOXDC, Oxford College Campus, Hosur Road, Bommanahalli-560068	M/S Principal TOCE – AICTE (SPDP) Grant A/C	67590100004867	Saving Account	BARB0VJOXDC	Self Finance	AAATC1553A

4. The date of release of the grant by AICTE shall be taken as the date of commencement of the project. The Principal shall intimate about the receipt of the grant to AICTE. Any expenditure incurred prior to the issuance of the approval letter will not be allowed to be adjusted in the grant and if the Institution/ University do not take the project within 6 months of the receipt of the grant, the approval shall ipso facto lapse.

5. Each project sanctioned by AICTE is assigned a specific Ref. No. given on the pre-page. All correspondences related to the project must contain this number along with year of sanction of the project; failing which correspondence will not be entertained.

6. The accounts of the grantee which are liable to be audited by the Council or Comptroller and Audited General of India or by any Officer designated for the purpose.

7. The institute/University shall not charge any overheads on this project and will provide all the administrative support for completion of the project.

8. The grantee shall utilize grants on only approved items of expenditure (list enclosed). However, in case the grantee wishes to recast the project, approval of the Council must be obtained for the revised item of expenditure and they will maintain proper accounts of the expenditure as per the norms/procedures of AICTE/Government of India.

9. The assets acquired wholly or substantially out of All India Council for Technical Education's grant shall not be disposed or encumbered or utilize for the purpose other than those for which the Grant was given without proper sanction of the All India Council for Technical Education and should at any time the institution cease to function, such assets shall revert to the All India Council for Technical Education.

10. The grantee shall maintain an audited record of assets acquired wholly or substantially out of the grant-in-aid and a register or assets shall be maintained by the Institute in the prescribed form i.e. GFR-19.

11. The Amount of interest accrued on the grant should be treated as part of the grant to be utilized for that particular project. However, the interest amount accrued along with grant disbursed should not exceed the total grant sanctioned for the project. The Institute receiving the grant should reflect the same in the audited statement of accounts/ Utilization Certificate and may either refund the interest amount to AICTE or AICTE should adjust the same in the next installment of grant before releasing.

12. The Annual Progress Report in the prescribed format along with Statement of Expenditure and Audited Utilization Certificate shall be submitted to AICTE not later than one month after completion.

13. Project Completion Report (PCR) in the prescribed format along with the Audited Statement of Expenditure indicating expenditure incurred in the total duration of the project in the prescribed format, utilization in the format and GFR-19 shall be submitted to the Council.

14. The Utilization Certificate (UC) supported by Audited Statement of Expenditure to the effect that the grant has been utilized for the purpose for which it has been sanctioned shall be furnished to the All India Council for Technical Education immediately after completion of the project. It should contain the head-wise break up of expenditure made from the grant-in-aid provided by the Council.

Contd...3/-

15. The grantee shall follow the terms and conditions of Skill and Personality Development Programme Centre for SC/ST Students (SPDC) as laid down by the council from time to time.

16. The Grantee shall fully implement the official language policy of Union Government and comply with the official language Act, 1963 and official language (use of official purposes of the Union Rules, 1976 etc.)

17. The University/Institute receiving grant under SPDP is expected to put up a plaque at the main entrance of the Lab/Department, which has been modernized using the grant. All the equipment procured through the project should be superscribed with AICTE project file number.

18. The funds to the extent are available under the scheme.

19. The sanction issues in exercise of the powers delegated to the Council. It is also certified that grant-in-aid is being released in conformity with the Rules and Regulation of the scheme.

Yours Sincerely,

(Dr. Neeraj Saxena)
Adviser (IDC)

Copy forwarded for information and necessary action to:

1. **The Principal,**
   The Oxford College of Engineering,
   Hosur Road, Bommanahalli, Bangalore Rural,
   Bangalore – 560068, Karnataka

2. **Dr. E. Saravana Kumar,**
   Dept. of CSE,
   The Oxford College of Engineering,
   Hosur Road, Bommanahalli, Bangalore Rural,
   Bangalore – 560068, Karnataka

3. **Office of Director General of Audit,**
   (Central Revenues)
   AGCR Building, I.P. Estate,
   New Delhi-110002.

4. Guard File.

Cartel Infosystems

Together we grow.....

Cartel Infosystems Private Limited.

TAX INVOICE

e-Invoice

IRN : 98354d6e54956aa2b11498bae0137a90c5a2eb1a1cc791169a48-f641dd4643cd
Ack No. : 112111795278434
Ack Date : 11-Oct-21

Cartel Infosystems Pvt Ltd #48, 1st Floor, 3rd Cross SBM Colony, BSK 1st Stage Bangalore - 560 050 CIN: U72900KA2011PTC058896 GSTIN/UIN: 29AAECC4270H1ZM State Name : Karnataka, Code : 29	Invoice No. **CISPL/2579/21-22**	Dated **11-Oct-21**
		Mode/Terms of Payment 243788/- Advance and Balnce Against Delivery
	Reference No. & Date.	Other References
	Buyer's Order No. SPDP For Students for the year 2021-20222	Dated **17-Sep-21**
Buyer (Bill to) **The Principal** **The Oxford College of Engineering,** 10th Milestone, Hosur road, Bommanahalli Bangalore - 560068 GSTIN/UIN : 29AAATC1553A1Z9	Terms of Delivery **KS**	

Sl No.	Description of Goods	HSN/SAC	Quantity	Rate	per	Amount
1	**Dell OptiPlex 3080 Tower XCTO** *Dell 20" Monitor -E2020H* *S/n: BSRGSH3 CSRGSH3 DSRGSH3* *FSRGSH3 6SRGSH3 7SRGSH3* *8SRGSH3 9SRGSH3*	8471	**8 No**	51,650.00	No	**4,13,200.00**
	Central Output Tax @ 9%				9 %	37,188.00
	State Output Tax @ 9%				9 %	37,188.00
	Total		**8 No**			**₹ 4,87,576.00**

E. & O.E

PRINCIPAL
The Oxford College of Engineering
Bommanahalli, Hosur Road
Bengaluru-560 068.

Amount Chargeable (in words)
Indian Rupees Four Lakh Eighty Seven Thousand Five Hundred Seventy Six Only

Company's PAN : AAECC4270H

Declaration
We declare that this Invoice shows the actual price of the goods described & that all the perticulars are true & correct & incase of delay in payment interest will be charged @ 2.5% P.M from the due date. The Product once sold is not returnable and non exchangeable. All Cheques/DD should be in favor of "CARTEL INFOSYSTEMS PRIVATE LIMITED" payable at Bangalore.

Company's Bank Details
Bank Name : Axis Bank
A/c No. : 911020034897194
Branch & IFS Code : Srinivas Nagar & UTIB0001856

for Cartel Infosystems Pvt Ltd

Authorised Signatory

This is a Computer Generated Invoice

GOVERNMENT OF KARNATAKA

VISION GROUP ON SCIENCE AND TECHNOLOGY

Karnataka Science and Technology Promotion Society
Department of Information Technology, Biotechnology and Science & Technology

Annexure-III

A. GENERAL INFORMATION

1.	**Scheme Applied** (CESEM, CISEE, K-FIST L1 & L2 and RGS/F)	:	CISEE
2.	**About the project**		
a)	Title of the project	:	Design and Development of Fiber Bragg Grating Sensing system for monitoring handgrip muscle fatigue
b)	Subject area as per instruction (Please refer serial No.26 under Annexure-II)	:	Electronics and Communication Engineering
3.	**Details of Principal Investigator**		
a)	Name	:	Dr. Preeta Sharan
b)	Date of Birth & Gender (Age as on 30/10/2019)	:	M [ ] F [√]
c)	Qualification	:	PhD, Post Doctorate
d)	Designation	:	Professor
e)	Department	:	Dept. of Electronics and Communication Engg
f)	Years of teaching/research experience	:	24 (Teaching),15 (Research)
g)	Email ID	:	sharanpreeta@gmail.com

h)	Cell Number	:	+91 9449612666
i)	Residential Address	:	#340, D Block, Mahaveer Marwel Apt, Kodichikanhalli, Bangalore- 560 076.
4.	**Details of Co-Principal Investigator -I**		
a)	Name	:	Dr. Manju Devi
b)	Date of Birth & Gender (Age as on 30/10/2019)	:	M [ ] F [√]
c)	Qualification	:	Ph.D
d)	Designation	:	Professor & Head
e)	Department	:	Dept. Electronics and communication engineering
f)	Year of teaching/research experience	:	23 Years (Teaching), 13 (Research)
g)	Email ID	:	manju3devi@gmail.com
h)	Cell Number	:	+91 9448761979
i)	Residential Address	:	#610, Park Golden Aura, Hosur Main Road, Chandapura
5	**Details of Co-Principal Investigator -II**		
a)	Name	:	Anup M Upadhyaya
b)	Date of Birth & Gender (Age as on 30/10/2019)	:	30-06-1989 M [√] F [ ]
c)	Qualification	:	M.Tech
d)	Designation	:	Assistant Professor
e)	Department	:	Mechanical Engineering
f)	Year of teaching/research experience	:	5 Years
g)	Email ID	:	Upadhyayaanup74@gmail.com
h)	Cell Number	:	+91 9481213596
i)	Residential Address	:	No.28/1,Madwapati Nilaya, Kalappa Block, Srinagara, 25th Main , 1sta Cross, Pin:560065
6.	**Details of the Head of the Department**		
a)	Name of the Head of the Department		Dr Manju Devi

b)	Email ID	:	manju3devi@gmail.com
c)	Cell Number	:	+91 9448761979
7.	**Details of the Institution**		
a)	Name of the College/Institution with address	:	The Oxford College of Engineering 10th Milestone, Bommanahalli, Hosur Road, Bangalore - 560 068
b)	Type of the Institution (as per the instruction in Sl.No.29)	:	MIN
c)	Accredited year by NAAC/NBA	:	NAAC-2015 NBA - 2018
d)	Name of the Head of the Institution	:	Dr A S Aravind
e)	Designation of the Head of the Institution	:	Principal
f)	Phone Number (Landline) and college website	:	Ph: 080 - 3021 9601 / 602 / 604
g)	Cell Number	:	+91 9886852161
h)	Email ID	:	engprincipal@theoxford.edu
8.	**If your proposal is selected,**		
a)	Cheque/DD to be written in favour of	:	The Oxford College of Engineering
8.	**If, amount to be credited to your bank**		
a)	Name of the Account holder	:	The Oxford College of Engineering
b)	Name of the Bank and Branch	:	Vijaya Bank (Now Bank of Baroda)
c)	IFS Code	:	VIJB0001818
d)	SB A/c Number	:	181801011000015
e)	Address of the bank		The Oxford College of Engineering, Bangalore

e)	Address of the Bank	:	

* Plea ...heet to provide mo...

Signature of the Principal Investigator

Signature of Co-Principal Investigators

Signature of Head of the Department (with seal)

Signature of the Head of the Institution (with seal)

PRINCIPAL
The Oxford College of Engineering
Bommanahalli, Hosur Road
Bengaluru-560 068.

GOVERNMENT OF KARNATAKA

VISION GROUP ON SCIENCE AND TECHNOLOGY

Karnataka Science and Technology Promotion Society

Department of Information Technology, Biotechnology and Science & Technology

A. DETAILS OF THE PROJECT PROPOSAL

1.	Title of the Project Proposal	:	Design and Development of Fiber Brag Grating Sensing system for monitoring handgrip muscle fatigue
2.	Project Keywords	:	Fibre Brag grating, Muscle Fatigue, Forearm, Radial tunnel syndrome, Radial nerve, Handgrip
3.	Objectives of the proposal (Not more than six points)		1. Design of FBG sensing system for measuring handgrip muscle fatigue. 2. Design of handgrip holder for embedding FBG sensor. 3. Design analogy with experimental grip force and realization of FBG sensor for various handgrip pressure and temperature. 4. Optimization of pressure and temperature transmission from each individual finger to grip holder by finite element methodology. 5. Real time implementation, Testing and calibration of device.
4.	Background of the project	:	Handgrip strength has been used extensively as a measure to monitor and evaluate different physical and functional disorders related to health care. It is rated as one of the top ten fitness tests. It is used as a tool to evaluate an individual's capacity to perform physically

			demanding work tasks. The performance of hand and arm function has also been used to identify various physiological disabilities. The handgrip test is an easy and inexpensive tool to identify elderly people at risk of disability. Handgrip-strength measurement is included in many rehabilitation programs to monitor the patient progress. Many factors or physiological conditions are associated with handgrip strength and are thus studied in terms of grip strength. The current handgrip-testing methods includes the use of a hydraulic or electronic dynamometer. The hydraulic dynamometer utilizes the measurement of pressure change developed on a suitable fluid due to the gripping force. The pressure change is monitored by a hydraulic-pressure gauge. In the case of an electronic dynamometer, the gripping force changes the impedance of an electronic circuit attached to the grip holder, and the handgrip strength can be calculated by measuring this resistance change. These mechanical instruments are too rugged and do not offer comfortable measurements, especially in rehabilitation programs. Moreover, these instruments cannot provide individual finger strengths apart from measuring the hand strength. Therefore, we propose a simple, low-cost optical technique to measure the individual finger strengths.
5.	Methodology (Please include flowsheet, if required)	:	Appendix - 1
6.	Milestones with time schedule & work plan	:	Appendix - 1
7.	List of equipment available in your Institute/College for the project implementation	:	Appendix - 1
8.	List of equipment required for Phase-I & Phase-II for Project Implementation (as per the instruction Sl.No.27 under Annexure-II)		Appendix - 1

9.	Relevance, importance & application of the project	:	If our grip and forearm muscles are not conditioned with mobility, strength and endurance, then the result winds up being the frustrating chronic repetitive motion injuries that plague all type of people. For example, without adequate grip and forearm strength, tennis players develop tennis elbow (lateral epicondylitis), which is debilitating and disabling pain on the outside of the elbow. Golfers, climbers, Cross Fitters and obstacle racers who don't have adequate grip and forearm training often develop the opposite issue, a problem known as golfer's elbow, climbers elbow and medial epicondylitis, which is basically pain anywhere on the inside of the elbow and forearm. People who work on a computer often get one or both of these same issues. And we can undergo all the deep tissue work, injections, massage, and anti-inflammatory remedies on the face of the planet, but until we address the underlying issue of grip and forearm conditioning, these problems will continue to plague us. Often over looked or taken for granted, the strength of one's grip plays a key role in injury prevention and overall strength development. The Proposed research work here method of assessment can provide the patient with a cost effective, non-invasive screening tool to evaluate health.
10.	Novelty/Uniqueness of the project proposal	:	Many daily functions and sporting events require high activity levels of the flexor musculature of the forearms and hands. These are the muscles involved in gripping strength. From sports like wrestling, tennis, football, basketball, and baseball to daily activities such as carrying laundry, turning a doorknob, and vacuuming, some degree of grip strength is necessary to be successful. For example, without adequate grip and forearm strength, tennis players may run the risk of developing lateral epicondylitis, otherwise known as tennis elbow. Proposed research work is design and development of optical sensor based handgrip strength monitoring system having benefits of increased sensitivity by encapsulation of fiber bragg grating sensor in suitable holder material.

			Device to be developed will be insensitive to electromagnetic interference. High mechanical stability of device with embedded FBG sensor, since FBG sensor will be in micron size, embedding the FBG sensor in Handgrip holder will not alter the properties of holder material.
11.	Whether this project leads to innovations and patents, if yes explain	:	Yes, Existing handgrip monitoring system and IP generated so far is based on electronic and hydraulic dynamometer. Proposed handgrip strength monitoring system will based on Fiber Bragg Grating based sensing system.
12.	Whether this project leads to a Startup, if yes explain	:	Yes. Developed device will be innovative in the field of biomechanics hand rehabilitation. Device developed will be benefitted for large number of community, those people suffering from neuromuscular diseases. Developed device can fabricated in bulk with cost effective.
13.	Whether this project leads to cost effective Technology, if yes explain	:	Yes. Developed device can be made cost effective by bulk production.
14.	Additional details about the Project, if any	:	-NA-
15.	Deliverables of the project (Precise and in bullet form)	:	➢ Design of Handgrip Holder ➢ FBG Encapsulated handgrip holder ➢ Handgrip force investigation with FBG ➢ Handgrip Strength Monitoring Device
16.	Whether the project involves collaboration with research Institution/Industry: If yes, please enclose a letter to this effect	:	No
17. **a)**	Other additional information: Principal Investigator & Co-Principal Investigator	:	

	List of Publications (For the last 5 years) i) Journal Publications listed in SCImago Journal Rank (Rating … Q1 OR Q2 OR Q3 OR Q4). Specify rating referring to the website: https://www.scimagojr.com/journalsearch.php ii) Journal publications -Not listed in SCImago Journal rating rank iii) Google Impact factor of journal iv) Conference Presentations	:	Appendix- 2 Appendix - 2 Appendix - 2 Appendix - 2
b)	Books published/chapter contributed with details	:	1. Lab. Manual for "Advanced Communication Lab Manual", published in University Science Press, Laxmi Publications, Delhi and by in International Firewall Publications. 2. Lab. Manual for "Analog Communication" for 5thSemster of VTU in Star Publications, Bangalore. 3. Lab. Manual for "Advanced Communication" for M. Tech DEC/DCN by CBS, Publications, Delhi. 4.Advanced Mobile Technologies for Secure Transaction Processing by IGI Global, USA.
c)	Patent (s) filed/granted with details	:	1) Indian Patent "Photonic crystal based Biosensor for Detection of Glucose Concentration in Urine and in Blood" published on 19/12/2014, Application No. 6398/CHE/2014. 2) Indian Patent "Efficient Quantum Dots Based Computing Element" published on24/07/2015, Application No. 3809/CHE/2015 India Published. 3) Indian Patent "Photonic Crystal based Piston

			Type Micro Pressure Sensor" published on 2018, Application No. E-101/29979/2017-CHE. 4) Indian Patent "Ultrasensitive array accelerometer sensor based on Optical Nano cavity for Automotive of Application" filed on 8/10/18, Application No. 101/23714/2018-CHE/201841038029. 5) Indian Patent "A Method, System and Apparatus for detection of skin cancer" filed on 1/5/2018 E-101/9961/2018-CHE India In Process. 6) Indian Patent and PCT has been filed for the "Wireless Mouse and Keyboard for Handicapped" on 31/08/2018, Application No. 201811032829
d)	Details of commercialization status for the granted patents	:	Patent of project titled "Wireless Mouse and Keyboard for handicapped" available in funding agency website ICMR for commercialization purpose. https://www.icmr.nic.in/technology
e)	Industrial consultation (given/undertaken): provide details	:	Appendix - 2
f)	Please state willingness of your Institute to give partial financial support to this proposal. If yes, state percentage of the total cost that will be supported by your Institute. Include a signed letter from the head of the institute assuring the said support	:	-NA-
g)	Highlight reasons in FIVE sentences or less, what is special, unique or novel in your project that makes it an attractive proposition	:	1. Research is basically focused on humanity and mankind 2. This is mainly applicable for neurological disorder. 3. Proposed device development is photonic in nature which is ultra-sensitive.

Appendix - I

1. Methodology (Please include flowsheet, if required)

Step1: FBG Design and Principle:

The strain dependence of the center wavelength of the FBG is utilized for measuring grip strength. Five FBGs, written at different center wavelengths on a single photosensitive fiber, can be utilized to get a response from individual fingers. The fiber containing the gratings is attached to a suitable grip holder, which can effectively transfer the grip force to the FBGs. The strain dependence of the Bragg center wavelength is given as

$$\frac{\Delta\lambda_b}{\lambda_b} = \varepsilon_z - \frac{n_{\text{eff}}^2}{2}[\varepsilon_r(P_{11}+P_{12}) + P_{12}\varepsilon_z],$$

where $\Delta\lambda_b/\lambda$ is the relative shift in the center wavelength, ε_z is the axial strain, ε_r is the strain in the radial direction, n_{eff} is the effective refractive index, and P_{11} and P_{12} are the photo elastic coefficients of silica fiber in the axial and radial directions, respectively.

Step 2: Handgrip design and device instrumentation with FBG sensor

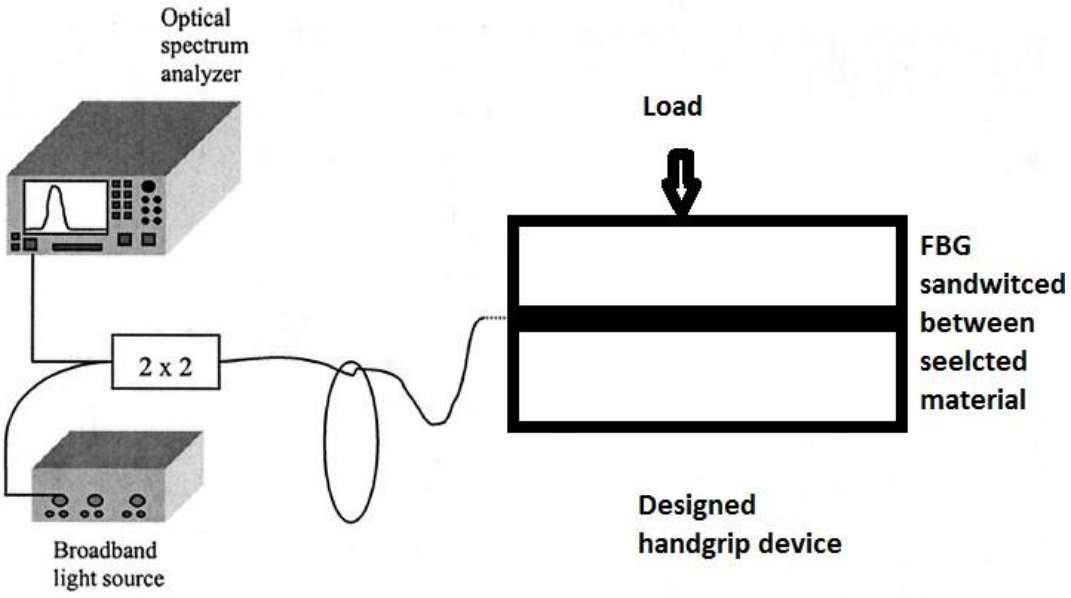

Figure 1. FBG Instrumentation System Setup

Appendix - I

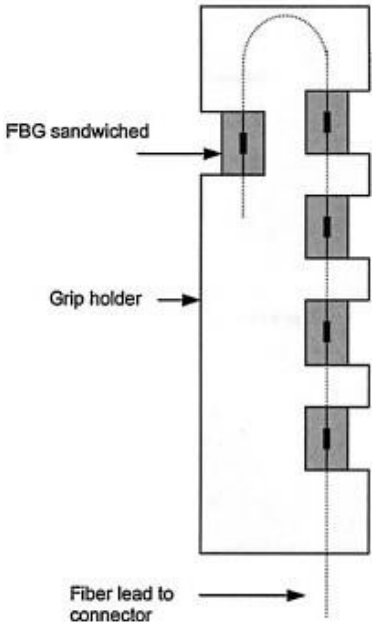

Figure 2: Schematic Handgrip design

Figure 2 shows the schematic handgrip design and FBG sensor encapsulated. In the testing period handgrip holder will be designed with the help of available 3D printer in the research lab. Bushing material for designed handgrip need to select based ability to withstand maximum force, mean time sensitive to smaller forces, Thickness of holder, mechanical strength for different applied pressure under controlled temperature conditions will be monitored during the experimentation.

Step 3: Sensitivity optimization of handgrip by optimizing the pressure transmission from fingers to FBG embedded handgrip.

Achieving the high sensitivity and tuning the wavelength for handgrip requires the optimization of the handgrip device based type of materials coated in FBG sensor material for handgrip. Radial and axial stress has to calculated. Experiment of handgrip monitoring is conducted for children, adults and old age people. During the experimentation force from each finger is monitored and required optimization has to be carried with FBG sensor design. For each individual finger different FBG sensor has to incorporated in the device. Figure 3 shows the schematic diagram of FBG sensor for individual finger.

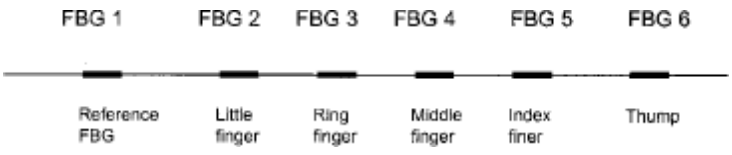

Appendix - I

Figure 3. FBG sensor system for individual fingers of human hand

Step 5: Testing, real time implementation, calibration of device

Hangrip holder designed will be tested in real time on different age group of people during the experimentation process, since the method of test to used will be non-invasive. Device has to be calibrated for sensitivity for each individual finger force on holder. Accuracy of device developed will be calibrated in this stage.

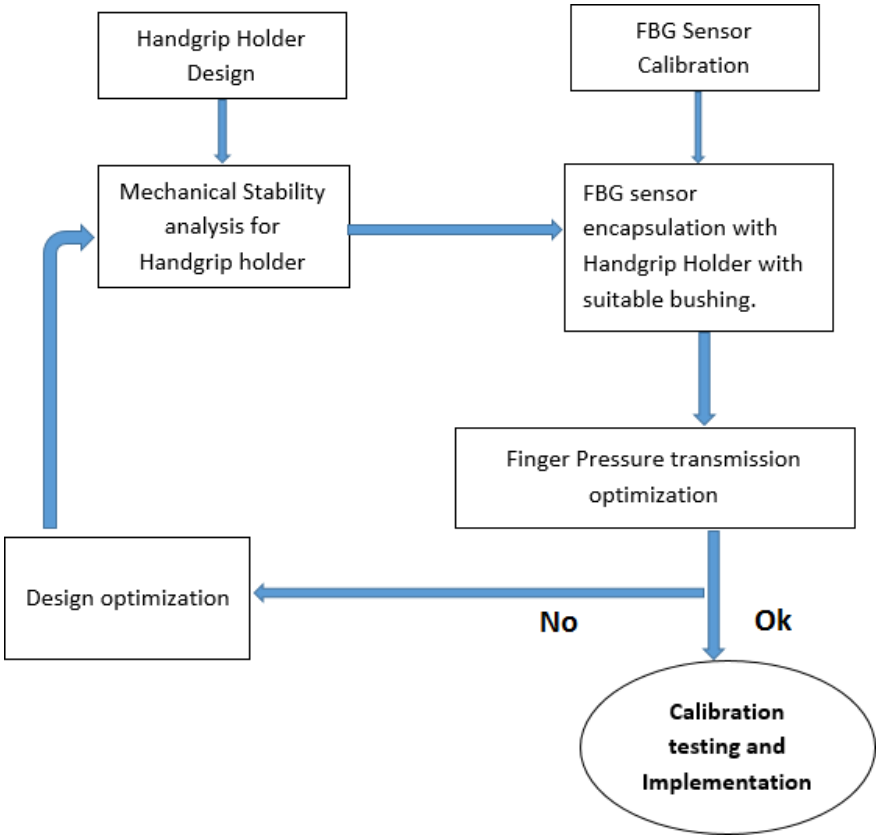

Figure 4. Flowchart of proposed research work

2. Milestones with time schedule & work plan

BAR CHART/PERT CHART INDICATING MAJOR MILESTONES

S.N	ACTIVITY	Year 1											
		1	2	3	4	5	6	7	8	9	10	11	12
1	Task-1	■	■	■	■								
2	Task-2					■	■	■	■				
3	Task-3									■	■	■	■

Appendix - I

S.N	ACTIVITY	Year 2											
		1	2	3	4	5	6	7	8	9	10	11	12
1	Task-1												
2	Task-2												
3	Task-3												

Year 1

Task1: Design of Handgrip Holder and model generation by 3D printer

Task 2: FBG Sensing system design and encapsulation for Handgrip holder

Task 3: Finite Element Analysis of handgrip holder for mechanical stability

Year 2

Task1: Pressure and Temperature sensitivity optimization of handgrip holder with FBG sensor

Task 2: Testing of device for accuracy and sensitivity for each individual finger force on handgrip holder

Task 3: Real time implantation, Testing, documentation, Patent process.

3. List of equipment available in your Institute/College for the project implementation

Sl.No	Item	Justification of Usage
1	3D Printer	3D model of Handgrip holder model.
2	Comsol Multiphysics	FBG design and simulation
3	Ansys Workbench	FEA optimization analysis

Appendix - I

4. List of equipment required for Phase-I & Phase-II for Project Implementation (as per the instruction Sl.No.27 under Annexure-II)

Sl.No.		Specification	Estimated cost	Justification
a) Non-recurring expenditure				
I Year				
1	Item 1	FBG Interrogator,8 CH Weight: 0.3 kg/pcs	**9,40,000 Rs**	This amount will be utilized for purchase of FBG interrogator. An FBG interrogator, also known as measurement unit or data acquisition system, is an optoelectronic instrument, which allows the reading of optical fiber Bragg grating (FBG) sensors in static and dynamic monitoring applications. An interrogator can measure a large sensing network composed by various types of sensors (such as strain, temperature, displacement, acceleration, tilt…) connected along multiple fibers, by acquiring data simultaneously and at different sampling rates. During data acquisition, the interrogator measures the wavelength associated with the light reflected by the optical sensors and then converts it into engineering units.
2	Item 2	Desktop - Personal computer (i7 processor)	**60,000 Rs**	This amount will be utilized for purchase of Desktop. Desktop with Intel i7 processor, allows memory sharing that can accelerate some operations. Dual RAM channeling capabilities speed up the memory access and can also greatly improve performance.
	Others	Nil	Nil	Nil

Appendix - I

II Year (if necessary)				
1	Item 1	Optical Spectrum Analyzer	**4,27,550 Rs**	This amount will be utilized for purchas optical spectrum analyzer. An Optical Spectrum Analyzer (or OSA) is a precision instrument designed to measure and display the distribution of power of an optical source over a specified wavelength span. An OSA trace displays power in the vertical scale and the wavelength in the horizontal scale.
2	Item 2	Fibre optic laser source	**5,52,450 Rs**	This amount will be utilized for purchase of laser source. A broadband light source is supplied to FBG sensor through a three port optical circulator. Conversion between the intensity of lig and voltage signal by a photodetector (PD) after the reflected light passed through the filter signal acquisition
3	Item 3	Fibre bragg grating sensors	**20,000 Rs**	This amount will be utilized for purchase of FBG sensors. It is a single FBG centered in a two meter length of polyimide coated optical fiber. It may be used individually or can be spliced into an array of many FBGs.
b) Recurring expenditure				
I Year				
1	Moulding	Enclosure Development (Moulding)	**80,000 Rs**	This amount will be utilized for development of enclosure to the cad model printed for Handgrip holder.
2	Calibration	Hardware calibration and Testing	**60,000 Rs**	Amount will be utilized for testing of handgrip holder device for accuracy of results
3.	Others	Travel	**60,000 Rs**	The amount will be utilized for visiting foundry, labs & institutions in India &

Appendix - I

				in the free panel review meetings.
4	Others	Training material preparation and Misc. Expenses	**50,000 Rs**	The amount asked is very nominal is required for contingency expenditure such as consumables & stationary, , books, Tale-printing including escalation charges connected with the project.
II Year (if necessary)				
1	Expenses 1	Workshop, conference, patent, publication	**2,00,000 Rs**	The amount will be utilized for conducti workshop for attending conferences, patent process & publications
2	Expenses 2	Training material preparation and Misc. Expenses	**50,000 Rs**	The amount asked is very nominal is required for contingency expenditure such as consumables & stationary, , books, Tale-printing including escalation charges connected with the project.
Total Amount : Rs 25,00,000/-				

Appendix -II

i) Journal Publications Dr Preeta Sharan – Principal Investigator- listed in SCImago Journal Rank (Rating … Q1 OR Q2 OR Q3 OR Q4). Specify rating referring to the website: https://www.scimagojr.com/journalsearch.php

(i) SCImago Journal Rank: Rating Q1

1. Design of Photonic Crystal Based Biosensor for Detection of Glucose Concentration in Urine, IEEE Sensors Journal, vol: PP, Issue: 99, 23-Sep-14, ISSN: 1530437X, DOI: 10.1109/SEN.2014.2359799.
2. An Analysis and Design of Photonic Crystal-Based Biochip for Detection of Glycosuria, IEEE Sensor Journal, VOL. 15, NO. 10, OCTOBER 2015
3. Design of photonic crystal based ring resonator for detection of different blood constituents, P Sharma, P Sharan, Optics Communications 348, 19-23, 4, 2015

SCImago Journal Rank: Rating Q2

4. Photonic crystal ring resonator structure for temperature measurement, CS Mallika, I Bahaddur, PC Srikanth, P Sharan, Optik, 126 (20), 2252-2255,3,2015
5. Photonic crystal ring resonator structure for temperature measurement, CS Mallika, I Bahaddur, PC Srikanth, P Sharan, Optik, 126 (20), 2252-2255,3,2015
6. A novel quantum dot cellular automaton for 4-bit code converters, OptiK 127(2016)4246-4249

7. Lab-on-chip based optical biosensors for the application of dental fluorosis, DL Girijamba, P Sharan, PC Srikanth, Optik-International Journal for Light and Electron Optics 127 (6), 3480-3483, 2016

SCImago Journal Rank: Rating Q3

8. Application of machine learning for real-time evaluation of salinity (or TDS) in drinking water using photonic sensors, Journal of Drinking Water Engineering and Science, 9, 37–45, 2016.
9. "Photonic Crystal Based Sensor for DNA Analysis of Cancer Detection". In: Mishra A., Basu A., Tyagi V. (eds) Silicon Photonics & High-Performance Computing. Advances in Intelligent Systems and Computing, vol 718, 2018, Springer, Singapore

SCImago Journal Rank: Rating Q4

10. Structure Design of Photonic crystal Based MOEMS accelerometer sensor for supplemental restraint system in automobile passenger safety' Indian Journal of Science and Technology, Volume 10, Issue 29, August 2017 .
11. "Photonic Crystal Based Micro Interferometer Biochip (PC-IMRR) for Early Stage Detection of Melanoma", Pertanika J. Sci. & Technol. 26 (3): 1505 - 1512, 2018, Malaysia

Appendix -II

12. "Optical Biosensor Design to Detect Mycobacterium Tuberculosis Bacteria", Journal of Advanced Research in Dynamical and Control Systems,100-11302-Special Issue, 2017

13. MOEMS based Displacement Sensor in Nano Bio-photonics Platform, Journal of advanced research in dynamical and control system. ISSN 1943-023X, Volume 9, issue 4, page no 28-35.

14. Real-Time QoS Performance Analysis for Multimedia Traffic in an Optical Network, Advances in Intelligent Systems and Computing, vol 718. Springer, Singapore 2018, First Online24 December 2017

15. Photonic Crystal Based Micro Mechanical Sensor in SOI Platform" ISSN: 0128-7680 © 2018 Universiti Putra Malaysia Press.Pertanika J. Sci. & Technol. 26 (3): 1481 - 1488 (June 2018)

16. Adaptive MOEMS Based Micro Pressure Sensor Using Photonic Crystal, Pertanika Journal of Science & Technology. Jul2018, Vol. 26 Issue 3, p1489-1504. 15p.

17. Wavelength Selectivity Using Adaptive Shortest Path Algorithm for Optical Network. Pertanika Journal of Science & Technology. Jul2018, Vol. 26 Issue 3, P1527-1538. 11p

18. Modeling and Simulation of Pressure Sensitivity of Bragg Grating sensor for Structural health monitoring Application, International Journal of Advanced Computer Research, pp2249-7277, vol:4(1), Issue:14, 2014. Peer reviewed/Refereed Journal

19. A Comprehensive Digital Cross Connect (DCS) for Buffered and Unbuffered Switching Applications, International Journal of Control Theory and Applications (IJCTA), Volume 9, Issue 17, 2016

Appendix - II

1. Research Publications of Dr. Preeta Sharan – Principal Investigator- For the last 5 years - Not listed in SCImago Journal rating rank Google Impact factor of journal and Conference Presentations

2014

International Conferences

1. Design and simulation of biosensors for detection of different blood components,IEEE TENSYMP (2014 IEEE Region 10 IEEE Symposium: TENCON SPRING),Kuala Lumpur ,Malaysia, p175, 14-16 April, 2014, 171-176, ISBN: 978-1-4799-2027-3
2. An Optical Sensor for Propagation Analysis of Lymphocyte Cell for Cancer Cell Detection, 2014 IEEE Global Humanitarian Technology Conference - South Asia Satellite (GHTCSAS), Trivandrum, Kerala, India, GHTC-SAS_2014_064, 26-27 September 2014.
3. An Analysis of Quality Factor for Different Bio-analytes by Using Photonic Crystal Based Sensor, IEEE ICACCCT- 2014, Ramnathpuram, (57-875), 8th to 10th May, 2014, 924-928
4. Photonic Crystal Based Sensor for Detection of High Glucose Concentration in Urine,IEEE INDICON 2014, Pune, 204, 11-13, December 2014.
5. An analysis of quality factor for different bio-analytes by using photonic crystal based sensor, IEEE international conference on advanced communication control and computing technologies (ICACCCT) ISBN no: 978-1-4799-3914-5/14.
6. Design and modeling of Photonic sensor for cancer cell detection, IEEE international conference on IMpact of E-Technology on US (IC-IMPETUS) Digital Object Identifier: 10.1109/IMPETUSUS.2014.6775872.
7. Early stage detection of breast cancer using hybrid photonic crystal ring resonator, IEEE International Conference on Advanced Communication Control and Computing Technologies[ICACCCT], 8-October 2014, ISBN: 978-1-4799-3914-5/14.
8. MOEMS Based Photonic Crystal sensor for structural /health Monitorng System, IEEE International Conference on Advanced Communication Control and Computing Technologies[ICACCCT], 8-October 2014, ISBN: 978-1-4799-3914-5/14.
9. An analysis of quality factor for different bio-analyser by using photonic crystal based sensor, IEEE International Conference on Advanced Communication Control and Computing Technologies[ICACCCT], 8-October 2014, ISBN: 978-1-4799-3914-5/14.
10. A Nano-Platform Based Optical Sensor for the Detection of Breast Cancer at DNA Level, IONS Asia 6 Kharagpur Conference,2014 at IIT Kharagpur.
11. Ultra Compact Photonic Crystal Based Sensor for Detecting Bioterrorism, communicated with photonics 2014, 12th international conference on fiber optics and photonics, IIT Kharagpur 2014.
12. Early stage detection of breast cancer using hybrid photonic crystal ring resonator, IEEE international conference on advanced communication control and computing technologies (ICACCCT). ISBN no: 978-1-4799-3914-5/14.
13. A nano-platform based optical sensor for the detection of breast cancer at DNA level,The Optical Society [OSA]- IONS ASIA-6 Conference, IIT :Kharagpur WB,10-12 December 2014.

Appendix - II

14. An optical sensor for propagation analysis of Lymphocyte cell for cancer cell detection, P Sharma, P Sharan, Global Humanitarian Technology Conference-South Asia Satellite (GHTC-SAS),2014.

Journal Publications

1. Performance Analysis of Configuration IPV6 Networks Communicating Over IPV4, IJECSE, December 2014 International, ISSN-2277-1956 V4 N1-11-18. peer reviewed /Refereed journal
2. Photonic Crystal Based Ring Resonator Sensor for Detection of Glucose Concentration for Biomedical Applications, International Journal of Emerging Technology and Advanced Engineering (IJETAE), Impact Factor= 1.932, vol:4, Issue:3, Mar-14, ISSN. 2250-2459. UGC listed Journal No.44256/63196
3. Measurement of environmental Parameters (i.e. Humidity) by using Bragg Grating Sensor for Structural Health Monitoring Application, International Journal of Advanced Computer Technology (IJACT), vol:3, Issue:2, 2014, ISSN: 2319-7900. Peer reviewed/Refereed Journal
4. Performance analysis of configuring IPv6 network communicating over IPv4, International Journal of Electronics and Computer Science Engineering, vol:4, Issue:1, 2014, ISSN: 2277- 1956. Peer reviewed/Refereed Journal
5. Modelling and Simulation of Optical Pressure Sensors For Detection of Acoustic Signals In Sub-Micron Range, International journal of emerging technology and advanced engineering, Volume 4, issue 4, April 2014 (ISSN 2250 – 2459). UGC listed Journal No.44256/63196

National conferences:

1. Modelling and Simulation of Temperature Sensitivity of FBG sensor for Structural health monitoring Application, National Conference on Technological advances in electronic system design [NCTAESD-2014], Vemana Institute of Engineering, Bangalore, 26th April 2014.
2. Design of Optical Sensor for the Detection of Harmful Chemicals in Air, National Conference on Technological advances in electronic system design [NCTAESD-2014], Vemana Institute of Engineering, Bangalore, 26th April 2014.
3. Photonic crystal based bio-sensor, National Conference on Technological advances in electronic system design [NCTAESD-2014], Vemana Institute of Engineering, Bangalore, 26th April 2014.
4. Design and Modeling of Photonic sensor for cancer detection, International Conference on the IMpact of E-Technology on US, PES Institute of Technology, 10-11 Jan 2014Applications of MOMES in Submicron Displacement Detection, National Level conference on Convergence in Operational and Computational Technology –COCT-2K14, Garden City College, Bangalore, 28th March 2014.

2015

International Conferences

1. Gallium arsenide based surface plasmon resonance for glucose monitoring, H Patil, V Sane, G Sriram, TS Indumathi, P Sharan, International Conference on Optical and Photonic Engineering (icOPEN2015),2 2015

Appendix - II

2. Analysis and Detection of Oncological Cells Using Nano-Photonics, International Conference on Micro-electronics, Communication and Computation- ICMCC, SAN DIEGO, USA, 27th & 28th February 2015.
3. Photonic Crystal based detection of cancer cells, 1st International Conference on Opto Electronics and Photonic materials-ICOPMA 15, SASTRA University, Tanjavur, 27-28 Feb 2015.
4. 2-D Photonic crystal based Bio-chip for DNA analysis of breast cancer, IEEE International conference on pervasive computing, 8th -10th January 2015.
5. DNA analysis for the detection of Lung cancer using a photonic crystal bio-chip, ICOMPA, TANJORE, 27th -28th February 2015.
6. Hexagonal ring resonator lab-on-chip sensor for DNA analysis of lung cancer, International Conference on Networks, Electronics, Communication and Control"- ICONECC 2015, Cape Institute of technology at Levengipuram, Kanyakumari on 5th & 6th of March 2015.
7. Hybrid Photonic crystal based Lab-on-chip sensor for DNA analysis of lung cancer, CCEEDS.
8. Liquid Crystal based bio-chip for DNA analysis of cancer using Photonic Crystal, ICOPENSPIE, 14-17th April 15, Singapore.
9. Photonic Crystal Based Biosensor for The Detection of Biological Agents Causing Biowar, International conference on computing, communication, electrical, electronics, devices and signal processing March-2015, Vijayawada.
10. Photonic Crystal Based Nano Scaled for The Detection of Agent Causing Typhoid In Water, International conference on computing and signal processing, April 2015, Kanchipuram.
11. Ultra Compact Photonic Crystal Based Sensor for Detecting Bioterrorism, 2015 IEEE International conference on engineering and technology, March 20 Coimbatore.
12. A Photonic crystal based optical sensor for the detection of sulfate in seawater, IEEE ICETECH 20-Mar-15, Coimbatore.
13. A Novel-Platform for the Detection of Magnesium in Sea Water using Photonic crystal based ring resonator", International conference on computing, Communication, electrical, Electronics, Devices, Signal processing, Communication and Control(CCEEDS) 28-30th March, 2015 at Vijayawada, Andhra Pradesh.
14. High sensitive Photonic crystal based sensor for detection of anaemia, IEEE ICETECH, Coimbatore, 20-Mar-15.
15. A Novel-Platform for the Detection of Magnesium in Sea Water using Photonics, International conference on Networks, Electronics, Communication and Control(ICONECC), 5-6th march,2015 at Levengipuram, Tamilnadu.
16. A Novel Design of High Speed Frequency Divider Using Various Flipflop In Quantum-Dot Cellular Automata, International conference on computing, communication, electrical, electronics, devices and signal processing March-2015, Vijayawada.
17. Comparative Analysis on Protocols of Quantum Cryptography: A Literature Survey, 1st International Conference on Opto-Electronics and Photonic Materials (ICOPMA 2015), SASTRA University, Thanjavur, Tamilnadu, February 2015. Comparative Study of Half Adder and Subtractor Circuits based on Quantum-Dot Cellular Automata (QCA), International Journal of Innovative Research in Computer and Communication Engineering (IJIRCCE), ISSN(Online): 2320-9801, Vol.3, Special Issue 5, May 2015.
18. Surface Plasma Resonance Based Non-Invasive Optical Sensor for Glucose Monitoring, ICMCC SAN DIEGO, USA, 27 and 28 February 2015.
19. Gallium Arsenide Based Surface Plasmon Resonance for Glucose Monitoring, icOPEN (SPIE) Singapore

Appendix - II

20. A Non Invasive Technique for glucose monitoring, International Conference on Networks, Electronics, Communication and Control"- ICONECC 2015, Cape Institute of technology at Levengipuram, Kanyakumari on 5th & 6th of March 2015.

21. Photonic Crystal based SPR Technique for Detection of Glucose Concentration for Diabetic, IEEE-1st International Conference on Computing, Communication, Electrical, Electronics, Devices and Signals Processing – CCEEDS 2015, Vijayawada 28th- 30th March 2015.

22. A Novel Approach to Non-Invasive Monitoring for Diabetes Using Surface Plasmon Resonance Sensor, ICOMPA, Tanjore, 27th – 28th February 2015.

23. The Surface Plasmon Resonance based optical biosensor for the diagnosis of kidney failure, ICOMPA, TANJORE, 27 -28 February 2015.

24. Design and Simulation of Micro Displacement Sensor Based on MOEMS for Detection of acoustic signals, International Conference on Micro-electronics, Communication and Computation-ICMCC, SAN DIEGO, USA, 27th & 28th February 2015.

25. Photonic Crystal MOEMS Based Micro Displacement Sensor for the Detection of the Acoustic Signals, IEEE-1st International Conference on Computing, Communication, Electrical, Electronics, Devices and Signals Processing – CCEEDS 2015, Vijayawada 28th- 30th Mar 2015.

26. MOEMS Based Ultrasensitive Micro Displacement Sensors for the Membrane applications, IEEE International Conference On Smart Technologies And Management For Computing, Communication, Controls, Energy & Materials - ICSTM 2015, VEL TECH Technical University Chennai 6th – 8th May 2015, 978-1-4799-9853-1/15/$31.00 ©2015 IEEE.

27. Micro Displacement Sensitive Photonic Crystal Based MOEMS Structure for the Detection of the Acoustic Signals, 5th IEEE International Advanced Computing Conference IACC 2015 BMSCE, 12th & 13th June 2015, 978-1-4799-8047-5/15/$31.00 © 2015 IEEE.

28. Detection of the Acoustic Signals Using MOEMS Based Micro Displacement Sensors in Nanophotonics, International Conference on Networks, Electronics, Communication and Control"- ICONECC 2015, Cape Institute of technology at Levengipuram, Kanyakumari, 5th & 6th of March 2015.

29. Displacement Sensitive Photonic Crystal Based MOEMS Structure for the Detection of the Acoustic Signals, International Conference on Developments in Engineering Research"- ICDER-2015, IAETSD held on 5th April at Bangalore, India, ISBN: 978-1511486-493.

30. Design and Simulation of Photonic Crystal Based Bio-Sensor for Early Stage Detection of Cervical Cancer, ICOMPA, TANJORE, 27 -28 February 2015.

31. Spectral Analysis of photonic crystal based Bio-sensor using Adaboost Algorithm, IEEE - ICCSP, Melmaruvathur.

32. Analysis of Photonic Crystal Based Double Hexagonal Ring Resonator Using AdaBoost Algorithm, IEEE - ICCT – Kanyakumari.

33. Analysis of Photonic Crystal Based Sensor Using AdaBoost Algorithm for Diabetic Application, IEEE-1st International Conference on Computing, Communication, Electrical, Electronics, Devices and Signals Processing – CCEEDS 2015, Vijayawada 28th- 30th March 2015.

34. Spectrum Analysis of Photonic Crystal based Optical Sensor using Adaptive Boosting Algorithm, International Conference on Networks, Electronics, Communication and Control"- ICONECC 2015, Cape Institute of technology at Levengipuram, Kanyakumari on 5th & 6th of March 2015.

35. Performance Analysis Implementation of IPV4-IPV6 Communication Network, International Conference on Networks, Electronics, Communication and Control"- ICONECC 2015, Cape Institute of technology at Levengipuram, Kanyakumari on 5th & 6th of March 2015.

36. Multimedia Data Transfer from Ipv4-Ipv6 in an Optical network by Using Routing table, IEEE International Advance Computing Conference (IACC), June 12, 13th 2015, ISBN 978-14799-8047-5

Appendix - II

37. An efficient design of serial and parallel memory using Quantum dot cellular automata, IEEE TENCON, MACAU, CHINA, 1-4 Nov. 2015.
38. Multimedia data transfer from IPV4–IPV6 in an optical network by using routing table, P Piruthiviraj, P Sharan, R Nagaraj, Advance Computing Conference (IACC), 2015 IEEE International, 1044-1049,2015
39. Micro displacement sensor design based on photonic crystal emulating MOEMS for detection of acoustic signals, KV Ullal, P Sharan,Advance Computing Conference (IACC), 2015 IEEE International, 1236-1241,2015
40. A photonic crystal sensor for analysis and detection of cancer cells, P Sharma, P Sharan, P Deshmukh, Pervasive Computing (ICPC), 2015 International Conference on, 1-5
41. Liquid sensor based bio-chip for DNA analysis of cancer using photonic crystal, H Patil, R Nischitha, TS Indumathi, P Sharan, International Conference on Optical and Photonic Engineering (icOPEN2015)
42. "A Novel-Platform for the Detection of Magnesium in Seawater using Photonic Crystal based Ring Resonator", Discovery, 47(216), 18-21, 2015 ISI (Thomson Reuters) & Scopus

National Conferences

1. Blood pressure measurement of the Neonatal Baby by using Photonic Crystal based MOEMS Sensors, 7th Annual KSTA Conference -A Means for Growth, The Oxford Science College, 5th & 6th of Feb 2015.
2. Design and Simulation for the Detection of Acoustic Signals by Micro Displacement Sensor Based on MOEMS, 4th National Conference on "Emerging Trends in Engineering Technologies"- ETET 2015, Jyothy Institute of Technology, Bengaluru, 20th & 21th of Feb 2015.
3. Cancer analysis using Nano-photonics, 7th Annual KSTA Conference -A Means for Growth, The Oxford Science College, 5th & 6th of Feb 2015.
4. DNA analysis for diagnosis of cancer at early stage using photonic crystal Lab-on-chip, 7th Annual KSTA National Conference, Oxford Science College, Bangalore, 5th -6th February 2015.
5. Cancer detection using Photonic Crystal Lab-on-chip bio sensor, RISE(National), 2-3 May 2015, PESIT, Bangalore, Karnataka
6. Photonic Crystal Based Biosensor For Biosecurity, National conference on emerging trends in science, engineering and management, K S school of engg, may 2015, BENGALURU.
7. Photonic crystal based sensor for detection of Ischeamia, 7th Annual KSTA national Conference, Bengaluru, Feb 2015.
8. DESIGN OF OPTICAL MEMORY CELL USING QUANTUM DOTS, KSTA national conference, Bangalore.
9. Design And Analysis Of Counters using Quantum Dots Cellular Automata, National conference on recent innovations in science and engineering. May-2015, PESIT, BENGALURU.
10. Detection of Glucose Levels Based on Optical Sensors Using Surface Plasma Resonance, 4th National Conference on "Emerging Trends in Engineering Technologies"- ETET 2015, Jyothy Institute of Technology, Bengaluru, 20th & 21th of Feb 2015.
11. Interferometric sensor for the diagnosis of kidney failure using surface Plasmon Resonance, 7th Annual KSTA Conference -A Means for Growth, The Oxford Science College, 5th & 6th of Feb 2015.
12. An optical biosensor based on the surface Plasmon Resonance for the diagnosis of Kidney Failure, 4th National Conference on "Emerging Trends in Engineering Technologies"- ETET 2015, Jyothy Institute of Technology, Bengaluru, 20th & 21th of Feb 2015.

Appendix - II

13. Design and Simulation of Micro Displacement Sensor based on MOEMS for Detection of Acoustic Signals, National Conference on Innovations in Electronics, Instrumentation, Biomedical and Computing Technologies- IEIBCT-15 Adhiyamaan College of Engineering, Tamil Nadu, 23rd & 24th of Mar 2015.
14. Implementation of Mixed Network using Optical Communication for Real Time, The National Conference on Advanced Communication, VLSI Design & Signal Processing (NCCVS), April 29 2015.

Journals:

1. An Efficient Design Of 4:1 Multiplexer In Quantum-Dot Cellular Automata, International Journal Of Emerging Technology And Advanced Engineering, ISSN 2250-2459. UGC listed Journal No.44256/63196
2. Photonic Crystal MOEMS Based Micro Displacement Sensor for the Detection of the Acoustic Signals Publication History Received: 02 September 2015 Accepted: 04 October 2015 Published: 02 November 2015, The international Discovery Journal. ISSN 2278-5469 Peer reviewed/Refereed Journal,
3. A Novel MOEMS Sensor Design Simulation and Analysis with MEEP, published in IJETSR www.ijetsr.com ISSN 2394 – 3386, Volume 2, Issue 8, August 2015, UGC listed Journal.No.44431
4. Design and Simulation of Micro Displacement Sensor Based on MOEMS for Structural Health Monitoring System, International Journal of Innovative Research in Computer and Communication Engineering (IJIRCCE), ISSN (Online): 2320-9801, Vol.3, Special Issue 5, May 2015. Peer reviewed/Refereed Journal
5. Layout Design of Photonic Crystal Based Liquid Refractive Index Based Sensor, International Journal of Advancements in Research and Technology, Volume 4, Issue-1, January 2015 Page no 42-45. ISSN 2278-7763, Peer reviewed/Refereed Journal

2016

International Conferences:

1 A digital Cross Connect (DCS) switch for multicast and broadcast traffic,G Thakur, P Sharan, M Sarvagya, India Conference (INDICON), 2016 IEEE Annual, 1-5

2 Application of machine learning for real-time evaluation of salinity (or TDS) in drinking water using photonic sensors,SK Roy, P Sharan,Drinking Water Engineering and Science 9 (2), 37, 2016. (UGC list #10065), Nederland, Indexed in Scopus

3 An area efficient multiplexer for crossbar arbiter design using quantum dot cellular automata G Thakur, A Gumpe, M Sarvagya, P Sharan, Recent Trends in Electronics, Information & Communication Technology, (RTEICT), IEEE International Conference, 2016

4 Detection of oncological cell for breast cancer by using SPR technology, KS Rao, P Sharan, Computing for Sustainable Global Development (INDIACom), IEEE International Conference2016

5 Wireless digital cross connect SOC for optical networks using FPGA, GT Vemana, M Sarvagya, P Sharan, Computing for Sustainable Global Development (INDIACom), Scopus Indexed, IEEE International Conference 2016.

6 An optical storage device by surface plasmon resonance, HA Navyashree, P Sharan
Computing for Sustainable Global Development (INDIACom), 2016

Appendix - II

7 A comparative study of saline and non-saline water in application of tomato yield by using photonic sensor,SK Roy, M Harshitha, P Sharan,Computing for Sustainable Global Development (INDIACom), 2016

8 A photonic crystal based pressure sensor, I Bahaddur, PC Srikanth, P Sharan, Electrical, Electronics, and Optimization Techniques (ICEEOT), International ... 2016

9 "Surface Plasmon Resonance (SPR) Based Dual Channel Optical Waveguide for Biosensing Application", Recent Trends in Sensor Research and Technology, 3(2), 2016. (UGC list #47092).

10 "A comparative study of saline and non-saline water in application of tomato yield by using photonic sensor," 2016 3rd International Conference on Computing for Sustainable Global Development (INDIACom 2016), New Delhi, 2016, pp. 2733-2735.

11 Sensor based photonic crystal, Indira Bahaddur1, P.C.Srikanth Ponnathapur , Preeta Sharan ; PHOTONICS-2016,XIIIth International Conference on Fiber Optics and Photonics Indian Institute of Technology Kanpur,Dec 04-08,2016.

12 An efficient design of QCA based memory SK Pratibha, TNV Kumar, P Sharan, Computing for Sustainable Global Development (INDIACom), 2016

13 Low power quantum gates for the implementation of reversible memory elements using quantum dot cellular automata, SA Hassan, P Sharan, Computing for Sustainable Global Development (INDIACom), 2016

2017

International Conference:

1 Automated cervical cancer detection using photonic crystal based bio-sensor, P Sharan et al. Advance Computing Conference (IACC), 2015 IEEE International, 1174-1178.

2 'Design of Ultra-High Sensitive Biosensor to Detect E. Coli in Water IEEE 11th INDIACom-2017.

3 "Photonic Crystal Based Sensor for Human Blood Group Analysis", IEEE 11th INDIACom-2017

Journals:

1. Rapid Detection of Drugs Abuse by Adapting Surface Plasmonic Micro Ring Resonator", International Journal of Signal Processing, Image Processing and Pattern Recognition. 10, No. 8 (2017), pp.111-124, Indexed in Scopus/DOAJ, SJR = 0.11

2. Automated cervical cancer detection using photonic crystal based bio-sensor, P Sharan et al.), 2015 International Journal of Signal Processing, Image Processing and Pattern IEEE International, 1174-117, Indexed in Scopus/DOAJ, SJR = 0.11

3. Design and implementation of crossbar scheduler for system-on-chip network in quantum dot cellular automata technology. Volume1, Issue6, https://doi.org/10.1002/itl2.26

2018

Journals:

1. "Design and analysis of high sensitive phc based sensor for methane gas detection" j Fundam Appl Sci. 2018, 10(6S), 2137-2144 2138 (Scopus Index journal)

Appendix - II

2019

Journals:

1. Design of ultra-high sensitive biosensor to detect E. Coli in water, International Journal of Information Technology, Springer, July 2019, P. No,1-6, https://doi.org/10.1007/s41870-019-00327-5.

2. Interpretation of Photonic Crystals with Hexagonal Symmetry, Advances in Intelligent Systems and Computing, Springer, pp 902-912|, https://doi.org/10.1007/978-3-030-22263-5_86 , 2019.

3. An Innovative Low Power Reversible ALU for Quantum Processor using QCA, (IJITEE) ISSN: 2278-3075, Volume-8 Issue-12, October 2019. (Scopus).

International Conference:

1. Performance Analysis of Optical MEMS Based Pressure Sensor Using Ring Resonators Structure on Circular Diaphragm, TENCON, Oct. 2019.

2. Industrial consultation (given/undertaken): provide details

Name of Funding Agency	Project Title	Year	Amount
Naval Research Board - DRDO, India	Modelling and Simulation of Optical Sensor on Naval Platform	**May 2011**	**₹ 25 Lacs/-**
	Conceptualization of GPS/INS Integration for FPGA Platform	**Sept. 2011**	**₹ 28 Lacs/-**
Vision Group of Science and Technology (VGST), Gov. of Karnataka	"Center of Excellence in PHOTONICS", on optical networking	**2012**	**₹ 20 Lacs/-**
Institute of Electrical and Electronics Engineers (IEEE USA)	Wireless Mouse Control	**May 2012**	**$ 980/-**
	Smart Health Monitoring System Using GSM Technology for Pregnant Lady in Rural Area with Audio Interaction	**May 2013**	**$ 980/-**
Indian council of Medical Research (ICMR)	Wireless mouse and keyboard for handicapped	**March 2017**	**₹ 9,32,940**
KSCST	Photonic crystal based biosensor on mobile application for cancer cell detection	**2017**	**₹ 6500**
KSCST	The smart wrist band based human interface for PWD (person with disability)	**2017**	**₹ 6500**
	Pitch Based Human Computer Interface quadriplegic and speech impaired	**2018**	**₹ 8000**

Appendix - II

	Biosensor for detection of various stages of malignant Tumour cells	**2018**	**₹ 7000**
KSCST	Bionic Hand for basic need	**2019**	**₹ 7000**
		Total	**84,05,940/-**

Appendix -II

1. Research Publications of Co-Principal Investigator – I, Dr. Manju Devi For the last 5 years - Not listed in SCImago Journal rating rank Google Impact factor of journal and Conference Presentations

1. "Highly sensitive lab-on-chip with deep learning AI for detection of bacteria in water" International Journal of Information Technology, Springer, with ISSN 2511-2104 ,DOI 10.1007/s41870-019-00363-1
2.
3. "Highly Secure Advanced Encryption Standard using Vedic Mathematics and Visual Cryptography" Journal of Emerging Technologies and Innovative Research, volume 6, issue-5, Pg.No.30-32, May2019. Impact factor 5.87

4. "A Novel Low Power MUX based Dynamic Barrel Shifter using Footed Diode Domino Logic" International Journal of Innovative Technology and Exploring Engineering (IJITEE), ISSN:2278-3075, Vol-8, Issue-6S3, Pg. No-34-36 ,April2019 .DOI:10.1109/CTCEEC.2017.8455194, Impact factor 5.54

5. "Design and Implementation of Secure Cryptographic Algorithm Using Vedic Mathematics", *pices*, vol. 3, no. 2, pp. 30-32, Jul. 2019.

6. Design and Fabrication of Animatronic Skull using 3D Printer, International Journal Of Engineering Research & Technology (IJERT) Volume 08, Issue 06 (June 2019). Impact factor 7.86

7. "Design and Development of Mach Zehnder Interferometer based Optical Sensors to Detection of Arsenic compound in Drinking Water" International Journal of Engineering & Technology(IJET), 7 (4.38) Pg. No-880-884(2018),(Scopus indexed). DOI: 10.14419/ijet.v7i4.38.27599

8. " Design and Performance Analysis of Differential Amplifier for Various Applications "Journal of Computational and Theoretical Nanoscience , Volume 15, Numbers 11-12, pp. 3501-3508(8) , November 2018. **DOI:** https://doi.org/10.1166/jctn.2018.7652

9. "Design and Smart steering in Automobiles for safe driving" International Journal of Advance Research, Ideas and Innovations in Technology Engineering & Technology(IJARIIT), ISSN: 2454-132X, Volume-5, Issue-3, Pg. No-476-478, May2019.

10. "Implementation of Area and Memory Efficient Combined ByteSub and InvByteSub Transformation For AES Algorithm" International journal of Engineering Research in Electronics and Communication Engineering (IJERECE) ISSN:2394–6849, Volume:5; Issue:5; Pg. No78-83May-2018.). Impact factor 4.135

Appendix -II

11. "A Novel Method of Brain Tumor Detection and the Classification Using FCM AND SVM" the International Journal of Combined Research & Development (IJCRD), eISSN:2321-225X; pISSN:2321-2241 Volume: 7; Issue: 1; Pg. No-823-828 January - 2018.

12. "De-Noising Image Based On Epitome Modify Domain" International Journal of Combined Research & Development (IJCRD), eISSN:2321-225X; pISSN:2321-2241Volume:7; Issue:1; Pg.No.813-817; January-2018.

13. "An Efficient Fingerprint Compression Algorithm Using Sparse Coding" International Journal of Combined Research & Development (IJCRD), 7(1), PP 818-821, 2018.

14. "Implementation of Data Transfer in Micro grid and HEMS using ZigBee" International journal of Engineering Research and Technology(IJERT), ISSN:2278-0181, Volume-1, Issue-21, Page no.213-216, April2016.

15. Electronic aid based Assistive Text and Product Label Reading from Hand-Held Objects for Especially Abled Persons, International Journal of Engineering Research & Technology (IJERT) ICRET (Volume 4 – Issue 21), – 2016.

16. Hybrid Cars, International Journal of Engineering Research & Technology (Inert) (Volume 4 – Issue 21), 2016.

17. "Smart Security Framework Using GSM-GPS Technologies Indication of Digital Fuel" in the International journal of Engineering Research and Technology(IJERT), ISSN:2278-0181, Volume-1, issue-21, Page no. 246-249, April 2016.

18. "Stock Price Prediction Using Artificial Neural Network" International Journal of Engineering Research and Technology(IJERT), ISSN:2278-0181, Volume-1, issue-21, Page no. 41-45, April 2016.

19. "Monitoring and Detecting Vehicle based on Accident Sensor using GPS and GSM Technologies" International Journal of innovative Research in Technology(IJIRT), ISSN:2349-6002, Volume-1, issue-12, Pg. No1219-1223, May2015.

20. "Design of 1st order sigma Delta ADC for non-uniform quantization" in International Journal of innovative Research in Technology(IJIRT), ISSN:2349-6002, Volume-1,issue-12, Pg.No1224-1229,May2015,

Appendix -II

21. "A Novel Design of 9-bit Pipeline ADC," in the International Journal of Science and Engineering Research (IJSER),5(10), PP.358-362, 2014. Impact factor 4.4

22. A 9-bit, 200MS/s low power CMOS Pipeline ADC," International Journal of Engineering and Advanced Technology (IJEAT), 3(6), PP.180-183,2014.

23. "A 1.5V 3bit, 500MS/s LOW POWER CMOS Flash ADC", ijecs, vol. 3, no. 03, Mar. 2014.

24. "A 1.5-V, 10-bit, 200MS/s CMOS Pipeline Analog to Digital Converter," in the International Journal of Computer Applications (IJCA), 88 (7), PP 35-38, 2014.

25. "The Driving Analysis System through Wireless Network" IOSR Journal of Computer Engineering (IOSR-JCE),12(4), PP 94-100, 2013.

26. "Removal of Impulse Noise Using Eodt with Pipeline ADC," International Journal of Computational Engineering Research (IJCER).2 (4),PP 991-996,2012 .Impact factor 6.41

International conferences:

1. **"**Design and Development of Mach Zehnder Interferometer based Optical Sensors to Detection of Arsenic compound in Drinking Water at International Conference On Recent Trends In Computer Science and Electronics (RTCSE), on 03rd -06th Jan2019 in University of Hawaii (Manoa campus) in Honolulu, Hawaii, USA .

2. **"**Highly Sensitive Lab-On-Chip with Deep learning AI for detection of bacteria in water at International Conference On Recent Trends In Computer Science and Electronics (RTCSE), on 03rd -06th Jan2019 in University of Hawaii(Manoa campus) in Honolulu, Hawaii, USA .

3. **"**Design and performance analysis of differential amplifier for various applications" in the International Conference on topical transcends in Science, Technology and Management(ICTTSTM2018) organised by Sai Vidya Institute of Technology(SVIT), Bengalure on 17th and 18th August2018.

4. **"**Implementation of Area and Memory Efficient Combined ByteSub and InvByteSub Transformation For AES Algorithm" in the 5th International Conference on Applied Science, Engineering and Technology(ICASEC-18) held in Sri SaiRam College of Engineering, Anekal ,Bengaluru on 17th and 18th May2018.

5. **"**Design Of S-Box And INVS-Box Using Composite Field Arithmetic For AES ALGORITHM**"** at the 3rd national level conference on "Electronics, Signals and Communication (NCESC-2018)"in

association with IEEE Bangalore section on 17th May2018 at GSSS Institute of Engineering and Technology for Women, Mysuru and published in international journal of Engineering Research and Technology(IJERT) with ISSN: 2278-0181.

6. "Heuristic approach for optimal energy usage by selection of relay node" in IEEE International Conference On Recent Trends In Electronics Information Communication Technology, 0n May 19-20, 2017, India at Sri Venkateswara College of Engg. 978-1-5090-3774-9/17 © 2017 IEEE pg. No.1-5.

7. "Synthesis of A Thinned Planar Antenna Array With Maximum Reduction In Peak Side Lobe Level Using Modified Binary Coded Genetic Algorithm at" International Conference on Signal, Image Processing Communication and Automation - ICSIPCA- 2017 on 6th-7th July 2017at JSS Academy of Technical Education, Bangaluru.Pg No. 482-488.

8. "Synthesis of A Thinned Planar Antenna Array With Maximum Reduction In Peak Side Lobe Level Using Modified Binary Coded Genetic Algorithm(MB-BCG)" at" IEEE second International Conference on circuits,controls and Communication CCUBE2017 on 15th-16th Dec- 2017 at RNSIT, Bangaluru, and published in the proceedings with Pg. No.Pg No. 11-13.

9. "Implementation of Data Transfer in Microgrid and HEMS using Zigbee" in the International Conference on Research in Engineering, Technology and Management organized by BTL Institute of Technology, Bengalure on 16TH April 2016.
10. "Electronic aid based assistive text and product label reading from Hand-Held Objects for especially abled persons" in the International Conference on Research in Engineering, Technology and Management organized by BTL Institute of Technology, Bengalure on 16TH April 2016.

2. Research Publications of Co-Principal Investigator – II, Mr. Anup M Upadhyaya For the last 5 years - Not listed in SCImago Journal rating rank Google Impact factor of journal and Conference Presentations

[1] Grating based pressure monitoring system for subaquatic application (Accepted for publication in International Journal of information technology, Springer Publication); https://doi.org/10.1007/s41870-018-0128-x, 2017 *

[2] Design and Analysis of Pipeline Leakage Detection Using Fibre Bragg Grating Sensor, 2018, IEEE Explorer, DOI: 10.1109/CESYS.2018.8724113*

Appendix -II

[3] Sensitivity improvement and Optomechanical analysis of composite material using Fiber Bragg Grating sensor (International Journal of Engineering and Technology (UAE); Scopus Indexed, 2018, DOI: 10.14419/ijet.v7i4.36.23777 *

[4] MOEMS based sensor for tire carcass deflection monitoring in automobile using photonic crystal (Accepted for Publication in IEEE Explorer), 2017; DOI:10.1109/icaecc.2018.8479484. *

[5] Structure Design of Photonic Crystal Based MOEMS accelerometer sensor for supplemental restraint system in automobile passenger safety, Thomson Reuters, Indian Journal of Science and Technology. DOI: 10.17485/ijst/2017/v10i29/117327 ;2017

[6] MOEMS based Micro displacement sensor in antitheft device in vehicle security system, Tat McGraw-Hill Publication, Grenze International Journal. 2017. ISSN: 2455-1694

[7] "Fatigue and fretting studies of gas compressor blade roots", IJIRSET V5, Issue 9, September 2016. DOI:10.15680/IJIRSET.2016.0509018.

[8] Analysis on Mechanical Characteristics of Hybrid Composite with Silicon Carbide Filler, IJSRD,2019, Volume 7, Issue 7, Pg. No 74-76

(a) Papers accepted for publication

[1] Performance Analysis of Optical MEMS Based Pressure Sensor Using Ring Resonators Structure on Circular Diaphragm, IEEE TENCON, 2019 (Accepted for publication).

[2] Design and Simulation of micro displacement sensor based on MOEMS using acoustic signal, NCSEM Proceeding, The oxford college of Engineering", Bangalore.

conferences.

[1] Performance Analysis of Optical MEMS Based Pressure Sensor Using Ring Resonators Structure on Circular Diaphragm, **IEEE TENCON**, 2019.

[2] Micro mechanical deformation sensor based on ultra-sensitive photonic crystal membrane, **IEEE WRAP**, 2019.

[3] Optical MEMS Based Micro Displacement Sensor Using Photonic Crystal for Crank Positioning in Automobile (Accepted for Publication in IEEE Explorer), Indiacom 2017, New Delhi

Appendix -II

[4] Photonic Crystal Quadruple Ring Resonator (PCQRR) For Carcinogenic Sensing. (Accepted for Publication in IEEE Explorer), Indiacom 2017, New Delhi

[5] Design and Analysis of MOEMS Based Displacement Sensor for Detection of Muscle Activity in Human Body. (Accepted for Publication in IEEE Explorer), Indiacom 2017, New Delhi.

Patents

[1] Photonic crystal based piston type micro pressure sensor; No: 201741047023, (Published), 05/07/2019

[2] Wireless Mouse and Keyboard for Handicapped – Spectacle Design and Features (Patent with Government of India) (Filed for Spectacle Design) patent app. no.; 201811032829

[3] Wireless Mouse and Keyboard for Handicapped – Spectacle Design and Features (Filed PCT) Indian patent app. 201811040235

Please provide student strength of College/Institution.

Student strength		
Details	**UG**	**PG**
Corresponding Department	**10**	**10**
College (Total)	**1080**	**180**

A. UNDERTAKING FROM THE PRINCIPAL INVESTIGATOR AND CO-PRINCIPAL INVESTIGATOR

Project Title:

Design and Development of Fiber Brag Grating Sensing system for monitoring handgrip muscle fatigue

VGST Scheme: CISEE

1) We have carefully read the terms and conditions of VGST Scheme and we agree to abide by them and complete the project by fulfilling all the formalities.

2) We have not submitted or obtained any financial support for this or a similar project proposal.

3) We shall ensure that the equipment shown in the project proposal which will be procured under this project are not available in our institution/college.

4) The equipment procured under VGST Scheme will be made available to other faculty and students, as needed by them.

Preeta Sharan.
(Dr. PREETA SHARAN)

Name and Signature of the Principal Investigator

1. Dr. Manju Devi 4/12/19.
2. ANUP. MUDAGUNNAVAR 4/12/19

Name and Signature of Co-Principal Investigator

The Oxford College of Engineering
Bommanahalli
Hosur Road
Bengaluru-560 068

The Oxford College of Engineering
Bommanahalli
Hosur Road
Bengaluru-560 068

Date:

CHILDREN'S EDUCATION SOCIETY (Regd.)
Administrative Office :
1st Phase, J.P. Nagar, Bengaluru - 560 078. ✆ : 080 -30410501 - 502 Fax: 080 2654 8658

THE OXFORD COLLEGE OF ENGINEERING

(Recognized by the Govt. of Karnataka, Affiliated to Visvesvaraya Technological University, Belagavi &
Approved by A.I.C.T.E., New Delhi, Accrediated by NAAC & NBA New Delhi and Recognized by UGC under section 2(f))
Bommanahalli, Hosur Road, Bengaluru - 560 068.
✆ : 080 30219601 / 602 / 604 / 736 Fax: 25730551 / 30219629
E-mail: engprincipal@theoxford.edu Web: www.theoxford.edu

Estd. 1974

A. ENDORSEMENT FROM HEAD OF THE COLLEGE/INSTITUTION

Project Title:

Design and Development of Fiber Bragg Grating Sensing system for monitoring handgrip muscle fatigue

VGST Scheme: CISEE

1) Certify that the College/Institution welcomes the participation of Dr. Preeta Sharan as the Principal Investigator and Dr. Manju Devi,Mr. Anup M Upadhyaya as the Co-Principal Investigators for the project, and that in the unforseen and legitimate event of discontinuation by the Principal Investigator, the Co-Principal Investigator will accept/take full responsibility for completion of the project. Information to this effect, endorsed by me, will be promptly sent to VGST.

2) Certify that the Laboratory equipment and adminitrative facilities will be made available to the Investigators throughtout the duration of the project.

3) The College/Institution will take the responsibility of all the financial and purchase procedures as per the prevailing Government norms within the allocated and approved budget.

4) The College/Institution shall provide timely statements of expenditure and utilization certificates of the funds received under this project/scheme in the prescribed format.

Date: 04.12.2019

Signature of the Head of the Institution

PRINCIPAL
The Oxford College of Engineering
Bommanahalli, Hosur Road
Bengaluru-560 068.

CHILDREN'S EDUCATION SOCIETY (Regd.)
THE OXFORD COLLEGE OF ENGINEERING
(Recognised by the Govt. of Karnataka, Affiliated to Visvesvaraya Technological University, Belagavi
Approved by A.I.C.T.E. New Delhi.
Recognised by UGC Under Section 2(f)
Bommanahalli, Hosur Road, Bangalore - 560 068.
Ph: 080-61754601/602, Fax: 080 - 25730551
E-mail: engprincipal@theoxford.edu Web: www.theoxfordengg.org

Details of research papers published

Index

for PRINCIPAL
The Oxford College of Engineering
Bommanahalli, Hosur Road
Bengaluru-560 068

CHILDREN'S EDUCATION SOCIETY (Regd.)
THE OXFORD COLLEGE OF ENGINEERING
(Recognised by the Govt. of Karnataka, Affiliated to Visvesvaraya Technological University, Belagavi.
Approved by A.I.C.T.E. New Delhi.
Recognised by UGC Under Section 2(f)
Bommanahalli, Hosur Road, Bangalore - 560 068.
Ph: 080-61754601/602, Fax: 080 - 25730551
E-mail: engprincipal@theoxford.edu Web: www.theoxfordengg.org

Summary

In academic Year 2021-2022, the faculty of The Oxford College of Engineering has published papers in various International Journals. There are total 85 international publication in academic year 2021-2022. In that 56 Scopus indexed, 10 SCI Journals and 3 Web of Science Journals.

Sl. No	Year	International
5	2021-22	85

Sl. No	Year	Journal Indexing Type					
		Google Scholar	Web of Science	UGC	Scopus	SCI	Total
1	2021-2022	16	3	0	56	10	85

for PRINCIPAL
The Oxford College of Engineering
Bommanahalli, Hosur Road
Bengaluru-560 068

CHILDREN'S EDUCATION SOCIETY (Regd.)
THE OXFORD COLLEGE OF ENGINEERING
(Recognised by the Govt. of Karnataka, Affiliated to Visvesvaraya Technological University, Belagavi.
Approved by A.I.C.T.E. New Delhi.
Recognised by UGC Under Section 2(f)
Bommanahalli, Hosur Road, Bangalore - 560 068.
Ph: 080-61754601/602, Fax: 080 - 25730551
E-mail: engprincipal@theoxford.edu Web: www.theoxfordengg.org

‘

Sl.NO	Title of paper	Name of the author/s	Department of the teacher	Name of journal	Year of publication	ISSN number	Link to article/paper/abstract of the article
1	Data Access Control for Cloud Storage that is Secure and Expressive	Dr. M S Shashidhara	MCA	TELEMATIQUE	2022	1856-4194	https://www.provinciajournal.com/index.php/telematique/article/view/208
2	Implementation and Image Transformation for Ground Penetration Image Radar System	Dharamvir	MCA	Springer Nature	2022	DOI: 10.1007/978-981-19-1324-2_3	https://link.springer.com/chapter/10.1007/978-981-19-1324-2_3
3	Enhancing the Naïve Bayes Spam Filter through Intelligent Text Modification Detection	Mridula Shukla	MCA	TELEMATIQUE	2022	1856-4194	https://www.provinciajournal.com/index.php/telematique/article/view/211
4	Pre-current amplifier based transimpedance amplifier for biosensors	Dr Manju Devi	ECE	Scopus	2022	2089-4864	https://ijres.iaescore.com/index.php/IJRES/article/view/20442
5	IOT based Automatic Forest Fire Detection based on Machine Learning Approach	Dr. A Chrispin Jiji	ECE	Annals of Forest Research-Scopus	2022	18448135, 20652445	https://www.researchgate.net/publication/365264540_IOT_BASED_AUTOMATIC_FOREST_FIRE_DETECTION_BASED_ON_MACHINE_LEARNING_APPROACH
6	Improving Low Illumination Image	Dr. A Chrispin	ECE	Journal of Emerging	2021	ISSN2349-5162	https://www.jetir.org/view?paper=JETIR2109429

	Based on Multi-Scale Retinex Via Bilinear Interpolation	Jiji		Technologies and Innovative Research-UGC			
7	Soft-Switching Integrated Quasi Resonance Buck-Boost Converter for HHO Optimized Grid Connected PV System	Nisha C Rani, Dr N Amuthan	EEE	SSRG International Journal of Electrical and Electronics Engineering, vol. 9, no. 8, pp. 28-39, 2022	2022	2348 - 8379	https://doi.org/10.14445/23488379/IJEEE-V9I8P104
8	Closed Loop control of BLDC motor in Aircrafts for Flap angle Applications	Mrs.Resna S R	EEE	ijareeie	2022	2320-3765	http://www.ijareeie.com/upload/2022/july/7_Closed_HARD%20CERT.pdf
9	Smart security System	Mrs.Resna S R	EEE	International journal for research trends and innovation	2022	2456-3315	https://www.ijrti.org/viewpaperforall?paper=IJRTI2207295
10	Analysis and Design of Multistorey Building using E Tabs	Dr T S Malleshiah	civil	International Journal o0f Engineering and Technology	2022	2395-1303	http://www.ijetjournal.org/volume8/issue5/IJET-V8I5P12.pdf
11	Analysis and Design of Multistorey Building using E Tabs	Gayathri R	civil	International Journal o0f Engineering and Technology	2022	2395-1303	http://www.ijetjournal.org/volume8/issue5/IJET-V8I5P12.pdf
12	A Comparative Study of Framed Structure,	Shivanand C.G	civil	International Journal of	2022	2320-9364,	https://www.ijres.org/papers/Volume-10/Issue-4/Ser-

	Frame Tube and Tube In Tube Structures Subjected To Lateral Load Under Zone Iii And Zone V			Research in Engineering and Science (IJRES)			3/B10040713.pdf
13	Molecular Docking of Macelignan a polyphenolic derivative isolated ffrom L.aspera & L.cephalotes on colorectal cancer receptor and its ADMET prediction	Salma Kausar M, B.K. Manjunatha	BT	Paripex-Indian Journal of Research	2021	2250-1991	https://www.worldwidejournals.com/paripex/recent_issues_pdf/2021/December/molecular-docking-of-macelignan-a-polyphenolic-derivative-isolated-from-leucas-cephalotes-leucas-aspera-on-colorectal-cancer-receptor-protein-and-its-admet-prediction_December_2021_9375866101_7207180.pdf
14	Synthesis of Silver Nanoparticle Using Bioactive Phenolic Compound Extracts of Leucas aspera and Leucas cephalotes and Evaluation of its Antibacterial Activity	Salma Kausar M, B.K. Manjunatha	BT	Asian Journal of Organic & Medicinal Chemistry	2021	2456-8937	https://www.scilit.net/article/bc022bf58d133c80cd16aeffe8a6040b
15	In-vitro Study of Macelignan as a Potential Anticancer Drug against Colorectal Cancer using HCT116 Cell Line	Salma Kausar M, B.K. Manjunatha	BT	Journal of Clinical & Diagnostic research	2022	0973-709X	https://jcdr.net/articles/PDF/15787/53339_CE[Ra1]_F(KM)_PF1(SC_KM)_PFA(SC_KM)_PN(KM).pdf
16	"An empirical study on Employee	A. Sahana	MBA	Korea Review of International	2021	ISSN-1226-	https://kristudies.org/volume-15-issue-31-feb-2022/

	Engagement in Higher Educational Institutions"			Studies,		4741,	
17	Comprehensive analysis of cloud-based databases	E Saravana Kumar,	CSE	IOP Conference Series: Materials Science and Engineering	2021	1757-899X	https://iopscience.iop.org/article/10.1088/1757-899X/1131/1/012021/meta
18	Internet of things (IoT)-based unmanned intelligent street light using renewable energy	M. Ashwin Dinesh Kumar Anguraj, S. Balasubramaniyan, E. Saravana Kumar, J. Vakula Rani	CSE	International Journal of Intelligent Unmanned Systems	2021	2049-6427	https://doi.org/10.1108/IJIUS-10-2020-0060
19	Comprehensive analysis of cloud based databases	R Ch A Naidu	CSE	IOP Conference Series: Materials Science and Engineering	2021	1757-899X	https://iopscience.iop.org/article/10.1088/1757-899X/1131/1/012021/meta
20	An Enhanced Bio-Inspired Routing Algorithm for Vehicular Ad Hoc Networks.	Raghu Ramamoorthy, Menakadevi	CSE	Trends in Sciences	2022	2774-0226	https://doi.org/10.48048/tis.2022.4188

		Thangavelu					
21	OHAR: Optimized Human Action Recognition Paradigm using Optimized Type 2 Neuro-Fuzzy Classifier	J.A. SMITHA ,, Dr RAGHURAMAMOORTHY AND DR. R CHINAAPPALANAIDU	CSE	PERIODICO di MINERALOGIA	2022	0369-8963	https://doi.org/10.37896/pd91.4/91445
22	Energy efficient routing with correlation based data transmission reduction in energy efficient routing with correlation based data transmission reduction in uasn	BUDDESAB , REKHA .P, RAGHURAMAMOORTHY and SARAVANAKUMAR .E	CSE	Jilin Daxue Xuebao (Gongxueban)/ Journal of Jilin University (Engineering and Technology Edition)	2022	1671-5497	https://jilindaxuexuebao.com/details.php?id=DOI:10.17605/OSF.IO/6EA7S
23	scanning method for segmentation in Iris Biometric Authentication for security systems	Dr.Vanajaroselin E.Chirchi	ISE	GIS Science Journal	2022	1869-9391	https://drive.google.com/file/d/1ZPAiOUR-ByEd3s_awz9q-FGzWVtBUYmV/view

24	MonoLayer Graphene-Based Plasmonic Biosensor for Urine Glucose Detection	Dr Preeta Sharan	ECE	Springer	2022	978-981-16-8826-3	https://link.springer.com/chapter/10.1007/978-981-16-8826-3_39
25	An Optical Solution for High-Density Data Storage Using Plasmonic Based MZI Nano-Structures	Dr Preeta Sharan	ECE	Springer	2022	978-3-030-99329-0	https://link.springer.com/chapter/10.1007/978-3-030-99329-0_10
26	Design and Analysis of Outer Rotor Brushless DC Motor for Robotics Using Ansys Maxwell Software	Dr Preeta Sharan	ECE	Springer	2022	978-3-030-99329-0	https://link.springer.com/chapter/10.1007/978-3-030-99329-0_7
27	Theoretical investigation of Bragg Reflector optical sensor for the measurement of cryogenic temperatur	Dr Preeta Sharan	ECE	Elseveir	2022	2214785 3	https://www.sciencedirect.com/science/article/pii/S2214785322011397

28	Compactness measure of rail wheel rolling contact of the freight wagon	Dr Preeta Sharan	ECE	International Journal of Information Technology	2022	2511-2112	https://link.springer.com/article/10.1007/s41870-022-00977-y
29	Comparative analysis and design of high-performance photonic crystal add–drop filter for optical switching	Dr Preeta Sharan	ECE	Journal of Optics, Springer	2022	https://doi.org/10.1007/s12596-022-01004-w	https://link.springer.com/article/10.1007/s12596-022-01004-w
30	Compactness measure of rail wheel rolling contact of the freight wagon	Dr Preeta Sharan	ECE	International Journal of Information Technology	2022	2511-2112	https://link.springer.com/article/10.1007/s41870-022-00977-y
31	Cloud to cloud data migration using self sovereign identity for 5G and beyond	Dr Preeta Sharan	ECE	Cluster computing	2022	1386-7857	https://link.springer.com/article/10.1007/s10586-021-03461-7
32	Image Denoising Using Multi Scaling Aided Double Decker Convolutional Neural Network	Dr Manju Devi	ECE	Springer	2022		https://www.sciencedirect.com/science/article/abs/pii/S0030402622016084

33	Range-enhanced packet classification to improve computational performance on field programmable gate array.	Dr Manju Devi	ECE	IJECE	2022	2088-8708	https://ijece.iaescore.com/index.php/IJECE/article/view/28463/16104
34	Efficient Puncture and Non Puncture Architecture of Turbo Encoder on FPGA for Advanced Communication System	Dr Manju Devi	ECE	Mathematical statistician and engineering applications	2022	2094-0343 2326-9865	https://www.philstat.org.ph/special_issue/index.php/MSEA/article/view/355
35	Hybrid Technique for improving Underwater image	Dr. A Chrispin Jiji	ECE	3C Technologia-Scopus, Web of Science	2021	ISSN: 2254 – 4143	https://www.3ciencias.com/wp-content/uploads/2021/11/art.-39_3C-Tecnologi%CC%81a_Special_Issue_39-2_nov-1.pdf

36	UPQC Based Power Quality Improvement of Solar Photovoltaic Systems Using ANFIS and MFA"	Dr.Bharath.V.S, Madhavim	EEE	Journal of Neuroquantology	2022	1303-5150	https://www.neuroquantology.com/data-cms/articles/20221103125726pmNQ88071.pdf
37	A Novel Double Frequency SEPIC Converter with Improved Transient Characteristics and Efficiency	S.Vijayalakshmi, M.Marimuthu,N.Jayakumar, B.Devi Vighneshwari, B.Paranthagan, Nisha C Rani, R.Shenbagalakshmi	EEE	Journal of Electrical Engineering & Technology	2022	1039–1050	https://link.springer.com/article/10.1007/s42835-021-00906-2

38	Cascade H Bridge Multilevel Inverter with Pwm for Lower Thd, Emi & Rfi Reduction	,N.Jayakumar, B.Devi Vighneshwari, Monalisa Mohanty, Subash Ranjan Kabat,Bibhu Prasad Gantia,Nisha C Rani,L.Vadivel Kannan	EEE	Annals of R.S.C.B	2021	1039–1050	https://www.annalsofrscb.ro/index.php/journal/article/view/6013/4594
39	Novel soft-switching integrated various converter of ZVT-ZCT grid connected PV system	Nisha C Rani, Dr N Amuthan	EEE	Renewable Energy Focus Volume 42, September 2022, Pages 70-78	2022	1755-0084.	https://doi.org/10.1016/j.ref.2022.05.004

40	Effects of Polypropylene Waste Addition as Coarse Aggregates in Concrete: Experimental Characterization and Statistical Analysi	Madhu Sudana Reddy G,Naresh Kakur,Durga Prasad	Mechanical	Advances in Materials Science and Engineering	2022	: 1687-8434	https://www.hindawi.com/journals/amse/2022/7886722/
41	Solid Particle Erosion Behaviour of Plasma-Sprayed (WC–Co)/(Cr3C2–NiCr) Coatings	G Reddy, S Ramesh, Gajanan Anne, MR Ramesh, T Nageswara Rao, Pradeep Patil	Mechanical	Journal of Bio- and Tribo-Corrosion	2022	2198-4220	https://doi.org/10.1007/s40735-022-00629-5
42	Microstructural characterization and wear behavior of 12 wt% of boron carbide reinforced Al2030 alloy composites	VA Anjan Babu, R Saravanan, M Raviprakash, Madeva Nagaral, Nithin Kumar	Mechanical	Materials Today: Proceedings	2022	22147853	https://www.sciencedirect.com/science/article/pii/S2214785321058958

43	Synthesis of nanostructured ternary Ti based alloy for bio-medical applications	NB Pradeep, BK Venkatesha, S Parameshwara, R Raghavendra Rao, M Raviprakash	Mechanical	Materials Today: Proceedings	2022	22147853	https://www.sciencedirect.com/science/article/pii/S2214785321063458
44	Fabrication of Mg-Zn/Al and Mg-Zn/Anodized Al Multilayered Composites by Accumulative Roll Bonding, Investigation of Corrosion Behavior	MSRG Madhu Sudana Reddy G,Ramesh Sampath , Gajanan Anne , Gajanan Manjunath .	Mechanical	Materials International	2022	26685728	https://materials.international/wp-content/uploads/2022/03/Materials41.003.pdf

45	Renewable Energy based smart grid construction using hybrid design in control system with enhancing of energy efficiency of electronic converters for power electronic in electric vehicles	Dr.Manjula C	Mechatronics	International Transactions on Electrical Energy Systems, Wiley Hindawi	2022	2986605	https://doi.org/10.1155/2022/2986605
46	"Investigations on Microstructure and Tensile properties of as-cast ZA-27 Metal matrix Composite Reinforced with Zircon Sand "	Dr. Raju B R	Automobile Engineering	Materials Today ELSEVIER Journal	2021	2214-7853	https://doi.org/10.1016/j.matpr.2021.01.896
47	"Mechanical, Wear and Corrosion Properties of Micro Particulates Reinforced ZA-27 Hybrid MMC by Stir casting "	Dr. Raju B R	Automobile Engineering	Materials Today ELSEVIER Journal	2021	2214-7853	https://www.sciencedirect.com/science/article/pii/S2214785321009895?via%3Dihub

48	"Microstructure, Dislocation Density and Thermal Expansion Behavior Using Thermo Elastic Models of Zircon Sand Reinforced as Cast ZA-27 Composites"	Dr. Raju B R	Automobile Engineering	Journal of Minerals and Materials Characterization and Engineering (JMMCE)	2021	2327-4077	https://www.scirp.org/journal/paperinformation.aspx?paperid=106925
49	Immunomodulatory and radioprotective property of glucans isolated from lactobacillus species	B.K. Manjunatha	BT	Bioactive Carbohydrates and Dietary Fibre	2022	2212-6198	https://www.sciencedirect.com/science/article/abs/pii/S2212619821000449
50	Relationship between microbial biomass and extracellular enzymes: a study of Pachamalai forested streams,	K. Valarmathy,B. K. Manjunatha	BT	Natural Volatiles & Essential Oils	2021	2148-9637	https://www.nveo.org/index.php/journal/article/view/1108

51	Application Of RBNN Method For Identification Of Thyroid Disease Cases Using Electro Photonic Images	Dr. M S Shashidhara	*MCA*	NVEO – Natural Volatiles & Essential Oils	2022	2148-9637	https://www.nveo.org/index.php/journal/article/download/4577/3730/4654
52	Implementation and Image Transformation for Ground Penetration Image Radar System	Dharamvir ,Dr. M S Shashidhara	*MCA*	Springer Nature	2022	978-9811913235	https://link.springer.com/chapter/10.1007/978-981-19-1324-2_3
53	Handling Big Data Using a Data-Aware HDFS and Evolutionary Clustering Technique	Dr. M.S. Shashidhara*, Abhishek Madhusoodhanan, Monish N, Namratha T K & Subash N	MCA	Yantu Gongcheng Xuebao/Chinese Journal of Geotechnical Engineering	2022	10004548	http://ytgcxb.periodicales.com/index.php/CJGE/article/view/147
54	Analysis of Adversarial Attacks against Speaker Recognition System	Dr. Ms Shashidhara*, Akshath, Akashh D, Abhilash	MCA	Yantu Gongcheng Xuebao/Chinese Journal of Geotechnical Engineering	2022	10004548	http://ytgcxb.periodicales.com/index.php/CJGE/article/view/147

		mv & Thanujas N					
55	A Semantically Improved Marginalization Denoising Auto Encoder is Used to Detect Cyberbullying	JC Achutha	MCA	Chinese Journal of Geotechnical Engineering (Scopus-Q2); Volume 44 Issue 8 Year 2022.	2022	1000454 8	http://ytgcxb.periodicales.com/index.php/CJGE/article/view/148
56	Operational Efficiency Improvement of Power Grid by Improving MPPT Charge Controller	JC Achutha	MCA	Chinese Journal of Geotechnical Engineering Volume 44 Issue 8 Year 2022	2022	1000454 8	http://ytgcxb.periodicales.com/index.php/CJGE/article/view/138
57	REAL-TIME MOVIE TICKET BOOKING CHATBOT BASED ON NLP AND RASA FRAMEWORK	JC Achutha	MCA	Neuroquantology	2022	DOI: 10.14704/nq.2022.20.8.NQ44532	https://www.neuroquantology.com/issue.php?volume=28&issue=130&page=53
58	A comprehensive Review on power Consumption with Applied deep Analytics	JC Achutha	MCA	Journal of Optoelectronics Laser/Volume 41, Issue 6,Page no.496-	2022	2022-06-15	http://www.gdzjg.org/index.php/JOL/article/view/548

				506			
59	Anti-fake Technology of Commodity by Using the QR Code Application	Dharamvir	MCA	Int. Journal of Neuroquantology	2022	1303-5150	https://www.neuroquantology.com/article.php?id=5535
60	Fake news detection using Python	Dharamvir	MCA	International Journal of Health Sciences	2022	ISSN 2550-696X	https://sciencescholar.us/journal/index.php/ijhs/article/view/9537/6458
61	Transformational Perceptive of Data Recorder for UAV Flight Automation Control System using Image Processing Techniques	Dharamvir	MCA	Journal of Physics: Conference Series 2335 (2022)	2022	1742-6596	https://iopscience.iop.org/article/10.1088/1742-6596/2335/1/012016/pdf
62	Carrying Out Indian Repealed Farm Regulations to a Web-Based Entrance	Mridula Shukla	MCA	Chinese Journal of Geotechnical Engineering (Scopus-Q2); Volume 44 Issue 8	2022	10004548	http://ytgcxb.periodicales.com/index.php/CJGE/article/view/152

63	Farmers Trade Marketing-Agriculture Marketing Information System	Mridula Shukla	MCA	Chinese Journal of Geotechnical Engineering (Scopus-Q2); Volume 44 Issue 8	2022	10004548	http://ytgcxb.periodicales.com/index.php/CJGE/article/view/151
64	Fake Review Detection on Yelp	Ashok B P	MCA	Journal of Geotechnical Engineering	2022	ISSN: 1000-4548	http://ytgcxb.periodicales.com/index.php/CJGE/article/view/145
65	Forecasting Modern Mortgage Acceptance Methodology Derived from Machine Learning Approach	Ashok B P	MCA	Journal of Geotechnical Engineering	2022	ISSN: 1000-4548	http://ytgcxb.periodicales.com/index.php/CJGE/article/view/145
66	Development of an Evaluation Model for Measuring the Competencies of Business School Faculty Members	Sahana A and Tharaka Rami Reddy	MBA	Journal of Positive Psychology & Wellbeing	2021	ISSN: 2587-0130	https://www.journalppw.com/index.php/jppw/article/view/437

67	Artificial Intelligence in Healthcare:21 Century ages of Rifles – A Bibliometric Analysis	M Kathiravan	MBA	Asia Pacific Journal of Health Management	2021	ISSN 2204-3136	https://journal.achsm.org.au/index.php/achsm/article/view/1327
68	High-performance 2D photonics MOEMS pressure sensors	Yashaswini,Dr.H.N.Gayathri,Sreekanth	Chemistry	Springer International Journal of Information Technology	2022	ISSN: 2511-2104	https://doi.org/10.1007/s41870-022-00986-x
69	Theoretical investigation of Bragg Reflector optical sensor for the measurement of cryogenic temperature	DR.H.N. GAYATHRI	Chemistry	Elseveir, Materials Today: Proceedings	2022	ISSN: 2214-7853	https://www.sciencedirect.com/science/article/pii/S2214785322011397
70	Enhancement of Meta Verse Capabilities by IoT Integration	Vivek Veeraiah, Dr. Gangavathi P,Dr. Gangavathi P	CSE, Matheamtics, CSE	2022 2nd International Conference on Advance Computing and Innovative Technologies in Engineering	2022	978-1-6654-3789-9/22/	Enhancement of Meta Verse Capabilities by IoT Integration | IEEE Conference Publication

71	Influence of Nanomaterial Coated Condensing Surface on the Productivity of Evacuated Tube Assisted Solar Still	P.GangavathiaG.RamyabM.S.Karunac	Mathematics, Mechanical, Chemical engg	sciencedirect.com, Materials today	2022	https://doi.org/10.1016/j.matpr.2022.07.285	https://doi.org/10.1016/j.matpr.2022.07.285
72	An improved watermarking algorithm for robustness and imperceptibility of data protection in the perception layer of internet of things	Nazmus Shaker Nafi Mohammad Kamrul Hsan, Samar Kamil, Muhammad Shafiq,Yuvaraj S,E. Saravana Kumar, Rajiv Vincent	CSE	Pattern Recognition Letters	2021	0167-8655	An improved watermarking algorithm for robustness and imperceptibility of data protection in the perception layer of internet of things - ScienceDirect

73	An enhanced distance and residual energy-based congestion aware ant colony optimization routing for vehicular ad hoc networks	Raghu Ramamoorthy, Menakadevi Thangavelu	CSE	International Journal of Communication Systems	2022	1099-1131	https://doi.org/10.1002/dac.5179
74	Real time implementation of fiber Bragg grating sensor in monitoring flat wheel detection for railways	Dr Preeta Sharan	ECE	Engineering Failure Analysis	2022	13506307	https://doi.org/10.1016/j.engfailanal.2022.106376
75	Sensitivity enhancement of a plasmonic biosensor for urine glucose detection by employing black phosphorous	Dr Preeta Sharan	ECE	Optical Society of America	2022	1520-8540	https://opg.optica.org/josab/abstract.cfm?uri=josab-39-1-200

76	Real time implementation of fiber Bragg grating sensor in monitoring flat wheel detection for railways	Suchandana ishra	ECE	Engineering Failure Analysis	2022	13506307	https://doi.org/10.1016/j.engfailanal.2022.106376
77	Design and analysis of photonic MEMS based micro ring resonators for pressure sensing application	Prajwal P Patil, Sushma P Kamath, Anup M Upadhyaya and Preeta Sharan	Mechanical	Journal of Micromechanics and Micro Engineering	2021	0960-1317	https://iopscience.iop.org/article/10.1088/1361-6439/ac2bb1/meta
78	High-temperature oxidation behavior of plasma-sprayed NiCrAlY/TiO2 and NiCrAlY/Cr2O3/YSZ coatings on titanium alloy	G Reddy, C Durga Prasad, Gagan Shetty, MR Ramesh, T Nageswara Rao, Pradeep Patil	Mechanical	Welding in the world	2022	0043-2288	https://doi.org/10.1007/s40194-022-01268-7

79	Elevated Temperature Erosion Performance of Plasma Sprayed NiCrAlY/TiO2 Coating on MDN 420 Steel Substrate	C Durga Prasad, Pradeep Patil, Naresh Kakur, MR Ramesh	Mechanical	Surface Topography: Metrology and Properties	2022	2051-672X	https://iopscience.iop.org/article/10.1088/2051-672X/ac6a6e/meta
80	Investigation of thermally sprayed NiCrAlY/TiO2 and NiCrAlY/Cr2O3/YSZ cermet composite coatings on titanium alloys	G Madhu Sudana Reddy, C Durga Prasad6, Pradeep Patil, Gagan Shetty, M R Ramesh and T Nageswara Rao	Mechanical	Engineering Research Express	2022	2631869 5	https://iopscience.iop.org/article/10.1088/2631-8695/ac7946/meta
81	Rational design of flavonoid based potential inhibitors targeting SARS-CoV 3CL protease for the treatment ofCOVID-19	Dr. Shipra Bhati	Chemistry	Journal of Molecular Structure	2021	0022-2860	Rational design of flavonoid based potential inhibitors targeting SARS-CoV 3CL protease for the treatment of COVID-19 - ScienceDirect80

82	Analysis and design of multi-storey building using etabs	Gayathri R	civil	International journal of Engineering and Technologies	2022	2395-1303	https://scholar.google.com/citations?view_op=view_citation&hl=en&user=ez3Lxf8AAAAJ&sortby=pubdate&citation_for_view=ez3Lxf8AAAAJ:ohFW0PAxsewC
83	A Face Recognition Method In Machine Learning (ML) For Enhancing Security In Smart Home	Dharamvir	MCA	IEEE	2022	978-1-6654-3790-5	A Face Recognition Method In Machine Learning (ML) For Enhancing Security In Smart Home | IEEE Conference Publication
84	Circumstantial Discussion on Security and Privacy Protection using Cloud Computing Technology	Dharamvir	MCA	IEEE	2022	978-1-6654-3790-5	https://ieeexplore.ieee.org/document/9823875
85	A Comprehensive Analysis of Internet of Things (IOT) Sustained Integrity System Services with Data Management Based ON Machine Learning	Dharamvir	MCA	IEEE	2022	978-1-6654-3790-5	https://ieeexplore.ieee.org/abstract/document/9823431

Data Access Control for Cloud Storage that is Secure and Expressive

PDF (https://www.provinciajournal.com/index.php/telematique/article/view/208/199)

Dr. M S Shashidhara
Prof. & HOD, Department of MCA, the Oxford College of Engineering, Bengaluru, Karnataka India – 560068

Ankur Pandey
MCA Final Year Department of MCA, the Oxford College of Engineering, Bengaluru, Karnataka India – 560068

Divyanshu Pandey
MCA Final Year Department of MCA, the Oxford College of Engineering, Bengaluru, Karnataka India – 560068

Harshit Srivastava
MCA Final Year Department of MCA, the Oxford College of Engineering, Bengaluru, Karnataka India – 560068

Ishita Mukand
MCA Final Year Department of MCA, the Oxford College of Engineering, Bengaluru, Karnataka India – 560068

Abstract

Secure appropriated dealing with, one farther pall association, that is anticipated to guard insurance that is redefined data while other than giving versatile data admission to pall guests whose data isn't impacted a huge aggregate by CP- ABE(among all the best elevating methods towards attracting assistance involves secret key particularity-based cryptography.Anyhow of this, the use of CP- ABE could achieve a certain security break known as abuse of access demand. Because of CP- inbuilt ABE's" go everything" loosening up part,(for case, unscrambling open galleries) We dissect two enormous events of access limit maltreatment in this paper bone for semi- trusted in power, and the other for pall guests. We introduce Crypt Cloud, the centrally appropriate capability and changeable CP- ABE based dispersion limited system with white-box definite build quality, to combat usage. We also give the security

examination and use appraisal to show the avail of our frame. Stable pall Hosting, Codeword Policy Attribute- predicated Encryption, Abuse of Access Credentials, Traceability and cancellation, Auditing are record terms.

Issue

Vol 21, No 1 (2022)
(https://www.provinciajournal.com/index.php/telematique/issue/view/44)

Section

Articles

Important Links

Home (http://provinciajournal.com/index.php/telematique)
Aims and Scope (http://provinciajournal.com/index.php/telematique/aims_and_scope)
Call for Papers (http://provinciajournal.com/index.php/telematique/call_for_papers)

Instructions for Authors (http://provinciajournal.com/index.php/telematique/instructions_for_authors)
Editorial Board (http://provinciajournal.com/index.php/telematique/about/editorialTeam)
Archive (http://provinciajournal.com/index.php/telematique/issue/archive)
Download (http://provinciajournal.com/index.php/telematique/downloads)
Ethics & Policies (http://provinciajournal.com/index.php/telematique/ethics_and_policies)
Publication Ethics and Publication Malpractice Statement (http://provinciajournal.com/index.php/telematique/publication_ethics)
Peer Review Policy (http://provinciajournal.com/index.php/telematique/peer_review_policy)
Plagiarism Policy (http://provinciajournal.com/index.php/telematique/plagiarism_policy)
Copyright, Grants and Ownership Declaration (http://provinciajournal.com/index.php/telematique/copyright_grants_ownership_declaration)
Refund Policy (http://provinciajournal.com/index.php/telematique/refund_policy)
Open Access Overview (http://provinciajournal.com/index.php/telematique/open_access_overview)
Open Access License (http://provinciajournal.com/index.php/telematique/open_access_license)
Permissions (http://provinciajournal.com/index.php/telematique/permissions)

Downloads

Copyright Transfer Form (http://provinciajournal.com/downloads/copyright_form.pdf)
Paper Template (http://provinciajournal.com/downloads/paper_template.docx)

Language

English (https://www.provinciajournal.com/index.php/telematique/user/setLocale/en_US?source=%2Findex.php%2Ftelematique%2Farticle%2Fview%2F208)

Español (España) (https://www.provinciajournal.com/index.php/telematique/user/setLocale/es_ES?source=%2Findex.php%2Ftelematique%2Farticle%2Fview%2F208)

Recent Trends in Communication and Intelligent Systems pp 13–19

Implementation and Image Transformation for Ground Penetration Image Radar System

Dharamvir & M. S. Shashidhara

Conference paper | First Online: 25 May 2022

Part of the Algorithms for Intelligent Systems book series (AIS)

Abstract

Ground Penetration Radar (GPR) detects buried detonatory objects. The data collection may be view with different source of information to make use of Ground Penetration Radar System. In the normal data gives hyperbolic effects, which make the analysis and detection of targets difficult. So a focusing algorithm, Kirchoff Migration has been used for a synthetically generated GPR data pattern, The task control behavior of assigned data performs with Stepped Frequency Continuous Wave Radar (SFCW). The data is migrated, simulated in Mat Lab. Architecture has been proposed for the FPGA Implementation of the same.

Keywords

GPR **Kirchoff migration** **Interpolation**

FPGA implementation

References

1. I.A. Ruthenberg, *Curve Fitting and Migration of GPR Data for the Detection*. (Department of Computer Science and Electrical Engineering, University of Queensland, IJMRT Journal, 2018) pp. 119–126

2. R. Gupta et al., Automation and aviation radar techniques. IEEE Trans. **29**(11), 219–231 (2018)

Pre-current amplifier based transimpedance amplifier for biosensors

Jyoti M. Roogi, Manju Devi

Abstract

In this paper, we present current amplifier based transimpedance amplifier (TIA) for biosensor applications. Proposed design has low-noise, high Transimpedance gain that can be used for low current measurement applications. The current amplifier based TIA is implemented in order to resolve the fabrication issues related to high value feedback resistor. In this design, the input block to TIA is a low amplitude current amplifier. The designed amplifier is implemented in 90 nm complementary metal-oxide semiconductor (CMOS) technology. The design achieves transimpedance gain of 800 kΩ with a bandwidth of 5 kHz and input referred current noise is of 0.152 pA/$\sqrt{HZ}$ for an input of 41 nA bypassed from current amplifier with input of 200 pA.

Keywords

Current amplifier; Fabrication; Noise; Resistor; Transimpedance amplifier

Full Text:

PDF

DOI: http://doi.org/10.11591/ijres.v11.i2.pp188-195

Refbacks

- There are currently no refbacks.

IOT BASED AUTOMATIC FOREST FIRE DETECTION BASED ON MACHINE LEARNING APPROACH

Article *in* Annals of Forest Research · November 2022

CITATIONS
0

READS
45

6 authors, including:

Chrispin Jiji
The Oxford Educational Institutions
12 PUBLICATIONS **26** CITATIONS
SEE PROFILE

Kdv PRASAD Xxx
Symbiosis Institute of Business Management
127 PUBLICATIONS **508** CITATIONS
SEE PROFILE

Ann. For. Res. 65(1): 1792-1809, 2022
ISSN: 18448135, 20652445

ANNALS OF FOREST RESEARCH
https://www.e-afr.org/

IOT BASED AUTOMATIC FOREST FIRE DETECTION BASED ON MACHINE LEARNING APPROACH

Dr. A Chrispin Jiji[1], Dr. KDV Prasad[2], Nagarajan Jeyaraman[3], Dillip Narayan Sahu[4*], Dr A.Yasmine begum[5], Nitin Jagannath Patil[6]

[1]Associate Professor, Department of ECE, The Oxford College of Engineering, Bangalore, Karnataka, India.

[2]Assistant Professor(Research), Symbiosis Institute Of Business Management, Hyderabad, Telangana, India.

[3]Assistant Professor, Department of EEE, Dr. Mahalingam College of Engineering and Technology, pollachi, Tamilnadu, India.

[4*]Assistant Professor, Department of MCA, Gangadhar Meher University, Odisha, India.

[5]Associate professor, department of EIE,sree Vidyanikethan Engineering College, A.rangampet, Andhra Pradesh, India.

[6]Professor, Instrumentation Engineering, D. N. Patel College of Engineering Shahada Maharashtra,India.

Corresponding Author Email-id: Dillip1seminar@gmail.com

Abstract

There are many applications for monitoring the environment thanks to the development of wireless sensor networks and the Internet of Things. As a possible use case for WSNs and the Internet of Things, we investigated the issue of monitoring and detecting forest fires in this paper. The current environmental damage is mostly caused by forest fires. The current forest fire monitoring system falls short in its ability to continuously provide real-time monitoring for every location within a target region and to facilitate early danger identification. Forest fires pose a significant hazard to the ecosystem as a whole, contributing to both global warming and ozone layer loss. The potential answer to decrease the cause or the danger of a fire occurrence by up to 95% is early detection. There are several strategies that may be used to keep woodlands fire-free. The technologies that may be helpful for the early identification of forest fires include satellite systems and unmanned aerial vehicles. Although these systems are capable of covering any geographical area, they are unable to provide real-time information on the full region of interest. Additionally, satellite-based and UAV-based systems are only suitable for monitoring and battling fires. Therefore, it is very vital to make accurate predictions of forest fires at an early stage.

Keywords: Forest, Fire, Internet of Things, Detection, Wireless Sensor Network and Actuator.

1. Introduction

An overview of the worldwide context for forest fires is provided in this section. Studying forest fires is crucial to understanding their causes and establishing the need for further research. The most uncontrolled occurrence that seriously disturbs the whole ecosystem is a forest fire, which must be dealt with by using WSN technology. The motivation for this research's endeavour is to

stop forest fires, and the following justification serves as that motivation. Because of these and other issues, human civilization severely degrades biological variety by negatively affecting biological resources. For the preservation of biological variety, it is crucial to plan forest management using effective instruments. India is a nation with a diverse array of plants and animals [1]. It has been a worry that the destruction of forests brought on by forest fires and other activities impacts animals and threatens their habitat. In order to guarantee the nation's biological and environmental security, a law (the Wildlife Protection Act, 1972) for the protection of wildlife, animals, birds, plants, and items related to wildlife has been established. Article 8 of the CBD addresses the creation and management of protected areas with a focus on resource conservation and ecological restoration (Convention on biological diversity). The value and importance of a nation's protected areas for the preservation of its natural and cultural riches cannot be overstated. Protected places that are well-maintained provide a variety of chances and advantages in terms of ecological, educational, economic, and social aspects. However, these protected areas in a nation are vulnerable to a number of dangers [2]. The most frequent risk in a forest is wildfire, which drastically disrupts and obliterates the environment and fauna. Every year, there are more wildfires on the planet, which poses a serious danger to the overall biodiversity. The phrases "fire risk" and "fire hazard" have been associated with forest fire control since the dawn of science. These two names have been used in several different ways, with numerous distinct meanings. The right interpretation of terminology used in fire management, such as fire hazard, danger, risk, susceptibility, etc., is crucial to avoid misunderstanding their intended meanings. The definition of fire risk is the sum of the probabilities of a fire occurring and the effects of a fire danger that has been recognised. It is used to calculate the damage and loss caused by a fire activity [3]. The likelihood of hazardous fire outcomes and anticipated loss for estimating damage in terms of human and natural property loss are determined by the concept of fire risk. For the use of a fire monitoring system, wireless sensor networks have unique characteristics that provide a number of benefits and several obstacles. Before developing a system for leveraging WSNs to detect fire events early, factors including restricted power, weak sensor nodes, and hostile environmental conditions must be taken into account. This section provides information about sensor nodes, different uses, and their deployment for locating forest fires and gathering data. Recent developments in wireless technology have drawn interest in several real-time application domains. Numerous wireless communication models have been created to support the real-time environment from various angles, such as data transmission, data availability, network security, and so forth [4]. The introduction of wireless sensor networks as a new kind of networking module resulted from the integration of integrated circuits with cutting-edge technology. The manufacturing of sensor devices is in line with communication technologies, ensuring quick and reliable information transmission modules. From the perspective of computational costs, the smaller the devices are, the lower the costs. These characteristics have made wireless sensor networks quite popular with both academics and industry. It facilitates a variety of applications and difficulties for the researchers. The hardware is also improving at the same time, which facilitates the implementation of sensor networks in a real-time context [5]. The potential of sensor networks in several types of

network modelling, such as routing, data analytics, task scheduling, network localisation, key management, and cryptography, has been extensively researched. These types of sensor network applications need the creation of low-cost, low-power, multifunctionality-supporting, and efficient communication capabilities. It has inspired the creation of a team-based workplace using various sensor networks. According to the needs of the application, a sensor network is a kind of ad-hoc network that includes a substantial number of sensor nodes. These sensor nodes have the capacity to sense the surrounding environment by using factors like temperature, humidity, light changes, and more [6]. The deployed sensor node has the ability to interpret data and perform computations despite perceiving its surroundings. It was observed that the nodes' sensing capabilities changed depending on the wireless communication connections' range. Since the sensors are powered by batteries, a long lifetime is anticipated; yet, in the hostile environment, it acts invisibly. The sensor nodes are reusable and provide mass deployment for monitoring an area at a minimal cost. Because it adheres to these qualities, it is appropriate for use in large-scale applications. As was previously said, a sensor network is made up of a number of sensor nodes that are very helpful to put within the forest. The modulation or pre-estimation of the sensor nodes' positions has not been done. At the interior of the forest, the sensor units are dispersed randomly. In order to protect the environment, Wireless Sensor Networks (WSNs) are used to identify forest fires early on.

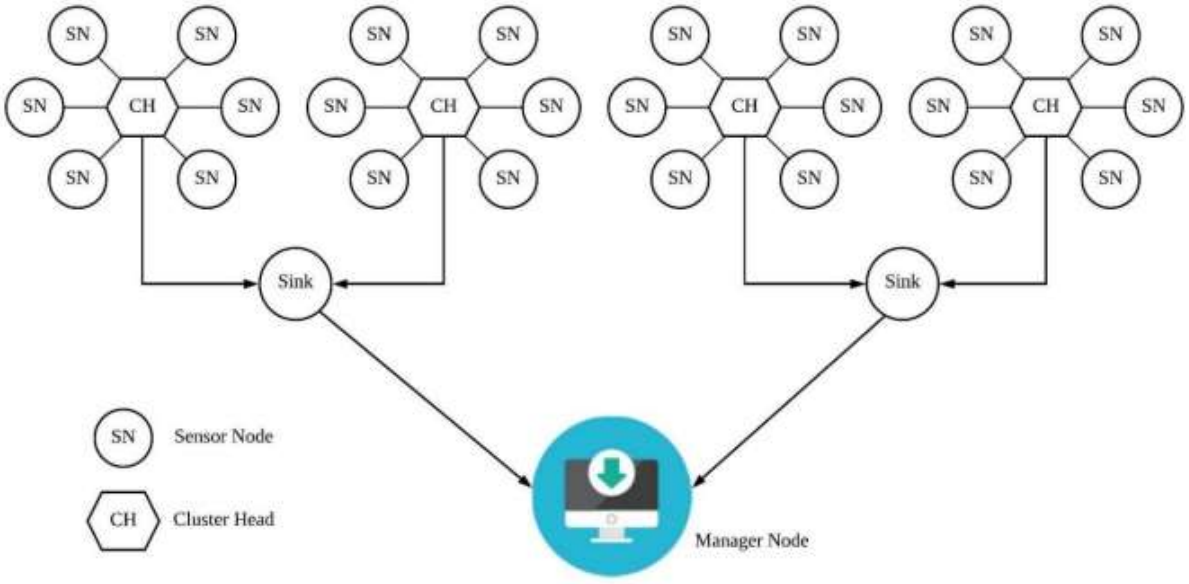

Figure.1: Architecture of the WSNs deployment in forest environment

The deployment architecture of WSNs in a forest setting is shown in Figure 1. It shows the hierarchical architecture of a wireless sensor network, where all sensor nodes are connected at the lowest level. By using the data from the sensor nodes in their individual neighbourhoods, the sensor nodes build clusters and choose a cluster head (CH). The selection of the cluster head is influenced by crucial factors such limited energy resources, the quantity of nearby nodes, and proximity to the base station [7]. The field data is gathered by each sensor node at the lowest level, and it is then sent to the appropriate cluster head. Information that has been detected is sent to the

sink node via the cluster heads. Every level of the hierarchy repeats the same data collecting procedure. It is the coordination node's responsibility to compile the necessary data and send it to the management node or base station for analysis. The implementation of sensor networks is made more difficult by the scarce energy resources and hostile forest environment [8]. Deploying sensor networks is primarily responsible for monitoring the environment for any unusual occurrences of events. In the context of forest applications, it is used to monitor the forest's terrain for any unforeseen environmental catastrophes like fires. By gathering the temperature or humidity of the region in the forest, it provides information to the relevant parties. In order to gather data on the woods, the sensor node uses wireless networks to connect with the forest fields [9]. Any forest area's acquired data is sent in many hops to the sink node. The gateway connects each sensor node to the other networks. The deployed sensor nodes in the forest are outfitted with wireless communication devices since they are unsure of where they will be placed. Due of the environmental flaws prevalent in the forest, there is a great likelihood that the nodes would malfunction.

2. Literature Review

In this specific area, "How to Protect our Environment from Degradation," much study is being conducted. Forest and rural area fires are the primary cause of the poor environment. There are several factors that contribute to forest fires, and for the longest time, the only way we can see the tragic events as they unfold is by reading about them in newspapers, magazines, or online. The goal of this body of research is to examine numerous methods for detecting forest fires in order to determine which method is most effective for use in real-time applications. Several research databases are retrieved for the current study due to the diversity of research publications in the field of forest fire detection [10]. In this research, we looked into six distinct databases to investigate the most current developments in the use of fire detection. This chapter provides a short overview of previous work in the field of forest fire detection that served as our inspiration for creating a reliable early fire detection system as well as a solution to the false alarm and localization problems. The efficacy of different techniques in terms of accurate and early detection of forest fires is evaluated after a thorough literature review that outlines the significance of forest fire detection systems. This chapter goes into depth about the initiatives done by several researchers in this application for monitoring, mapping burned areas, and early fire detection. Some research gaps have been found in this chapter based on the performed literature assessment, which has led to the beginning of the thesis research work's aim framing[11]. At the conclusion of this chapter, the contributions of the planned work in this thesis are also covered. Since the late 1990s, there have been several satellite systems that may be used to provide data and other operational capabilities for the application of forest fires. In the literature, there were several efforts by different researchers to monitor forest fires using satellite systems. Fire detection, monitoring, and area evaluation may all be done using satellite-based systems. The benefit of employing a satellite-based system is that it can cover any large region. The majority of satellite-based systems are used for tracking forest fire activity and assessing burned areas [12]. There are several satellite-based methods that may be used to detect fires via remote sensing. These strategies are described

in the literature and in this chapter's section. A remote sensing-based strategy to monitoring and predicting forest fire threat is presented in [13]. Monitoring forest fires with remote sensing is a way to describe the present situation. Four phases make up the remote sensing-based monitoring process: the acquisition of relevant data, calculation of resultant variables that correspond to danger situations, establishment of relationships between the resulting variables and risk indicators, and creation of risk maps. The variables collected from remote sensing include the vegetation state, meteorological factors, and surface conditions. Their study focuses on the drawbacks of systems that use remote sensing to track environmental threats and anticipate risk factors. The primary purpose of the remote sensing-based approaches is to calculate the indications of fire occurrence and compare the results with actual fire. Although the system has certain limits, there are numerous ways to improve it and get it to be dependable and acceptable. [8] reports another method for detecting fire via distant sensing that addresses the problems of accurate detection and lengthy calculation. Their detection system gathers pictures from sophisticated, extremely high-resolution radiometers for processing (AVHRR). The design has a number of benefits, including totally autonomous operation, consistently high data quality, and cost effectiveness, but one drawback is that the outcomes are not immediate. The technology exhibits false detection and has not been evaluated for consequences in real time. Forest fire detection methods based on IR cameras and image processing are helpful for confirming fire incidents. This section examines image processing-based fire detection systems that address the need for fire event confirmation in order to decrease false alarms. It has been noted that several researchers have made outstanding efforts to design effective systems for fire confirmation. A multi-feature analysis of smoke particles for the confirmation of forest fire is described in [11]. A method for image processing is suggested for video signal smoke detection. According to their system, the use of video in smoke detection has a number of advantages over earlier methods, including a wide coverage area and a quick reaction time. They have employed three distinct aspects in their study on the decrease of false alarms. To locate or describe the smoke area known as a candidate, colour is first filtered in YUV colour space. Next, spatial and temporal information are retrieved from the smoke candidates using spatio-temporal analysis and dynamic texture analysis, which are then submitted to SVM for classification. In compared to other strategies already in use, investigations based on their study demonstrate that their methodology has a high detection rate and speedy processing. An intelligent method for monitoring forest fires is provided in [12]. They have put up a system architecture for an image-processing-based platform. They want to create a system that can automatically detect fires. An intelligent system called iForestfire is based on the monitoring of video cameras that can be managed remotely and the integration of metrological stations with geolocational information systems. This data is originally evaluated in real time to identify fire. The technology is very accurate and compatible with a variety of tools, including Sony and Samsung cameras.

In [13], an algorithm for video analysis was created using VS2010 and Open CV2.1 to identify flame and smoke. The authors employ backdrop modelling to extract the area, followed by mixed colour space features to identify the flame, then threshold segmentation to detect smoke. The

outcome demonstrates the suggested system's accuracy in terms of precise detection. In [14], a real-time detection method that uses spatiotemporal analysis of video was presented. There are various phases in the suggested architecture's technique. Background removal is done in the first step, and then fire categorization using colour analysis is done. Following the computation of a few characteristics whenever fire is detected, the classification procedure then occurs. The scientists applied innovative characteristics to distinguish between actual fire pixels and fire-like pixels; as a consequence, there are fewer detection errors and the system performs better.

Using spatiotemporal modelling and texture analysis, [15] suggested an automated fire detection method based on video analysis. Filtering out the coloured, non-fire moving zones is the first stage. Because of its effectiveness and quickness, background removal comes first in the adaptive median algorithm's process of extracting features. The colour analysis is then carried out using the RGB colour distribution in the next phase. For each identified fire candidate, the six separate characteristics are calculated. The fire colour probability is the first feature to be identified, and then the spatial wavelet energy analysis, the spatio-temporal energy, and the last three characteristics to be calculated. Finally, categorization is completed in order to make decisions. The obtained findings show how well the technique performs for precise detection.

A wildfire colour segmentation system was given in [16]. For fire colour segmentation, they examined eleven methods. The YCbCr model is used in the suggested approach to minimise the impacts of light. According to the experimental findings, segmentation can detect fire in the daytime without smoke. [17] has developed an edge detection method for the image-processing-based identification of flame edges. They have provided a computational technique that can clearly and continuously describe flame and fire edges. The histogram is first normalised to modify the grey scale, and after that, background noise is eliminated to smooth the picture. After background noise has been eliminated, the basic edges are determined using a sobel operator, and then the higher and lower threshold values are adjusted. For the purpose of distinguishing between a preparatory picture with edges and the actual image, they built a least mean square algorithm, and in the final phase, the undesirable edges were deleted. The results of the experiment demonstrate how well-suited and reliable their algorithm is at identifying fire flames of various colours. The main benefit of their approach is that the fire edges are sensed clearly and continuously. A CCD camera-based fire detection system has been developed in [18]. The created method uses statistical parameters like standard deviation and mean values for the verification of fire pixels to forecast the fire pixels from grayscale frames of films. Real-time images are utilised in conjunction with the developed system's smoke detecting capabilities to validate fire and non-fire incidents. A system that employs the YUV space model for fire detection is reported in [19]. While the chrominance U, V are computerised for the categorization of fire and non-fire pixels, the design computes the luminance Y for the declaration of candidate area. Additionally, the study they propose computes motion vectors to understand the behaviour. The technology reduces the false alarm rate, according to the published experimental findings, although there are no tests for performance validation. The background noise in the system causes a significant number of false alerts. This section explores the use of machine learning and deep learning to build fire detection

systems that can satisfy the demands of high computing speed, energy efficiency, and accuracy. It has been discovered that several researchers have made outstanding attempts to construct effective fire detection systems utilising ML and DL approaches. Many research efforts have gone into developing fire confirmation methods, and the work that has been done in this area is detailed in the part that follows. Author shows a support vector machine fire detection. Although the technique is effective in terms of precise detection, calculation time is lengthy. A crucial factor in fire event modelling is the fire weather index. The FWI is a complete system that has been supported throughout North America for many years. A data aggregation strategy is given and put to the test for a wildfire detection application using the FWI system. Their data aggregation method's key benefit is that it only sends the data that the application is interested in. The experiment's findings demonstrate that the system provides trustworthy coverage. A fire event prediction algorithm based on ANN was created in [20]. The technology uses artificial neural networks to enable automated decision-making. Data is first gathered via sensors (Micaz mote), then passed to an ANN that has previously been trained, which then determines whether or not there is a fire. The results highlight the value of their architecture for detecting fire together with the understanding of fire development direction. Without any human oversight, the technology continually monitors the forest fire. The same model's potential for future development includes being expanded to precisely locate the position of the firing point. [21] suggested a cellular automata-based approach for simulating the incidence of forest fires and their propagation throughout a zone. The authors have enhanced the forest fire model and gone through computer algorithms in their study. They have integrated dynamic updating of tree clusters and are working on a breadth-first strategy, which reduces time. The outcome demonstrates how practical and very successful the design is. Their paper is realistically applicable to the majority of fire forecast and management applications. [8] discusses the significance of statistical data modelling for precise fire detection. The model was created with both indoor and outdoor contexts in mind. The design tackles the energy and delay problems and has been tested in a variety of environmental settings. In sensor networks, energy consumption is a crucial problem. A network's optimization problem lowers performance and raises energy use. For the purpose of optimising, a harmony search method is helpful in lowering intra-cluster distance [9]. The experimental finding demonstrates that employing HSACP increases network longevity compared to LEACH-C and FCMCP. [22] addresses the optimization problem and in WSNs during routing. The authors used the swarm intelligence method to create a routing algorithm for WSNs. An artificial bee colony algorithm is used to regularly gather environmental data. Ant colony optimization technique is used to extend network longevity. They combined the two algorithms, ABC and ACO, in their study and created the ABCACO method to address an optimization and finite issue in WSN. Three key elements make up their algorithm. The outcome demonstrates how effective their method is at watching for and identifying fire. When compared to Leache, their approach improves both stability and output. Using VS2010 and Open CV2.1, n [13] have created an algorithm for video analysis that recognises flame and smoke. The authors employ backdrop modelling to extract the area, followed by mixed colour space features to identify the flame, then threshold segmentation to detect smoke.

The outcome demonstrates the suggested system's accuracy in terms of precise detection. In [14], a real-time detection method that uses spatiotemporal analysis of video was presented. There are various phases in the suggested architecture's technique. Background removal is done in the first step, and then fire categorization using colour analysis is done. Following the computation of a few characteristics whenever fire is detected, the classification procedure then occurs. The scientists applied innovative characteristics to distinguish between actual fire pixels and fire-like pixels; as a consequence, there are fewer detection errors and the system performs better.

Using spatiotemporal modelling and texture analysis, [15] suggested an automated fire detection method based on video analysis. Filtering out the coloured, non-fire moving zones is the first stage. Because of its effectiveness and quickness, background removal comes first in the adaptive median algorithm's process of extracting features. The colour analysis is then carried out using the RGB colour distribution in the next phase. For each identified fire candidate, the six separate characteristics are calculated. The fire colour probability is the first feature to be identified, and then the spatial wavelet energy analysis, the spatio-temporal energy, and the last three characteristics to be calculated. Finally, categorization is completed in order to make decisions. The obtained findings show how well the technique performs for precise detection.

A wildfire colour segmentation system was given in [16]. For fire colour segmentation, they examined eleven methods. The YCbCr model is used in the suggested approach to minimise the impacts of light. According to the experimental findings, segmentation can detect fire in the daytime without smoke. [17] has developed an edge detection method for the image-processing-based identification of flame edges. They have provided a computational technique that can clearly and continuously describe flame and fire edges. The histogram is first normalised to modify the grey scale, and after that, background noise is eliminated to smooth the picture. After background noise has been eliminated, the basic edges are determined using a sobel operator, and then the higher and lower threshold values are adjusted. For the purpose of distinguishing between a preparatory picture with edges and the actual image, they built a least mean square algorithm, and in the final phase, the undesirable edges were deleted. The results of the experiment demonstrate how well-suited and reliable their algorithm is at identifying fire flames of various colours. The main benefit of their approach is that the fire edges are sensed clearly and continuously. A CCD camera-based fire detection system has been developed in [18]. The created method uses statistical parameters like standard deviation and mean values for the verification of fire pixels to forecast the fire pixels from grayscale frames of films. Real-time images are utilised in conjunction with the developed system's smoke detecting capabilities to validate fire and non-fire incidents. A system that employs the YUV space model for fire detection is reported in [19]. While the chrominance U, V are computerised for the categorization of fire and non-fire pixels, the design computes the luminance Y for the declaration of candidate area. Additionally, the study they propose computes motion vectors to understand the behaviour. The technology reduces the false alarm rate, according to the published experimental findings, although there are no tests for performance validation. The background noise in the system causes a significant number of false alerts. This section explores the use of machine learning and deep learning to build fire detection

systems that can satisfy the demands of high computing speed, energy efficiency, and accuracy. It has been discovered that several researchers have made outstanding attempts to construct effective fire detection systems utilising ML and DL approaches. Many research efforts have gone into developing fire confirmation methods, and the work that has been done in this area is detailed in the part that follows. Author shows a support vector machine fire detection. Although the technique is effective in terms of precise detection, calculation time is lengthy. A crucial factor in fire event modelling is the fire weather index. The FWI is a complete system that has been supported throughout North America for many years. A data aggregation strategy is given and put to the test for a wildfire detection application using the FWI system. Their data aggregation method's key benefit is that it only sends the data that the application is interested in. The experiment's findings demonstrate that the system provides trustworthy coverage. A fire event prediction algorithm based on ANN was created in [20]. The technology uses artificial neural networks to enable automated decision-making. Data is first gathered via sensors (Micaz mote), then passed to an ANN that has previously been trained, which then determines whether or not there is a fire. The results highlight the value of their architecture for detecting fire together with the understanding of fire development direction. Without any human oversight, the technology continually monitors the forest fire.

3. Proposed Forest Fire Detection System

Our research tries to provide a paradigm that takes into account three fundamental objectives of forest fire detection. 1) Constant environmental monitoring at all times; 2) Reduced power usage; 3) Adaptability to harsh conditions; and 4) Early fire event detection. Early forest fire detection is important for environmental preservation. The use of image processing or other approaches to anticipate forest fires is well-documented in the literature. Although several studies have used satellite systems for fire monitoring, the adoption of these approaches is currently unfavourable in part due to high costs, poor resolution, and lengthy procedures. As far as early feasible detection of the forest fire is concerned, real-time execution of these technologies is not conceivable. IR cameras and Unmanned Aerial Vehicles (UAVs) [8,9] were used for the detection procedure in the deep analysis. However, line of sight vision is initiated by the IR cameras, which degrades the collection of fire events that are not located in the LOS region [23,24]. The usage of UAVs is rapidly increasing, as well [25]. As a result, the process of sensor measurement is essential to the process of finding forest fires. As a result, this part shows how to install sensor nodes effectively to gather sensor data. In WSNs, there are typically two kinds of sensor nodes: mobile and stationary nodes. With regard to sensor node size, proper sensor node placement inside the forest coverage area becomes crucial. With the aid of sink nodes, the deployed sensor module collects data and then exchanges it with the base station. The selected approach for the forest fire detection procedure is shown in Figure.2 below.

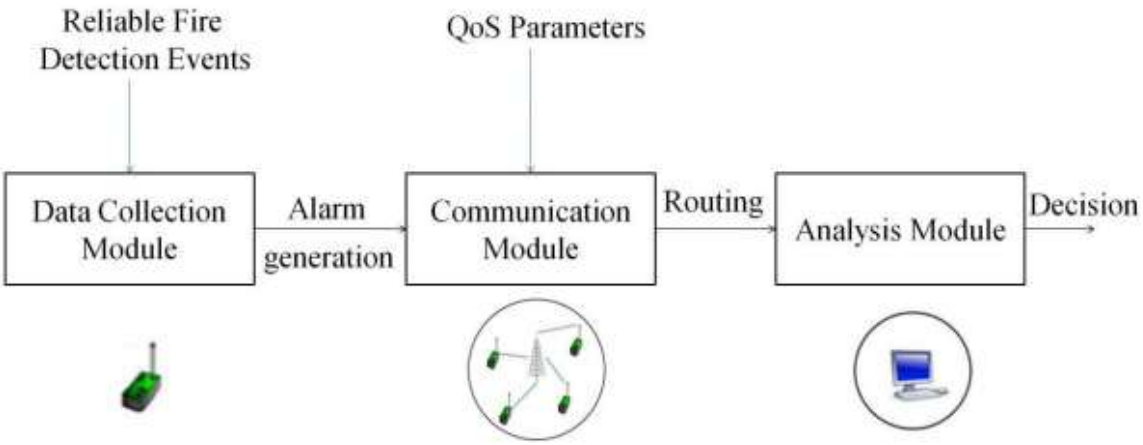

Figure.2. Adopted methodology of the forest fire detection process

The approach used for the WSN-based forest fire systems is shown in the above graphic. Three distinct stages make up the system's operation. In the first stage, sensor modules are positioned in the desired region to continuously monitor the environment. The sensor will continue to function normally up until a fire occurs. The sensor nodes monitor things like temperature, humidity, light intensity, and gases. The communication module, which is part of the second phase, is in charge of sending essential information, such as alerts, events, or any detected data, to the analysis module while taking specific quality of service characteristics into account. Reliability (an event must reach the coordinate node securely), temporal constraint (an event must take sufficient time to reach the destination), and security are among the QoS characteristics that are taken into account (the path must be secure from any attack). The analysis module, which is in charge of looking over the received alerts, is in charge of functioning in the third phase. The decision-making centre then processes the detected data and determines whether or not an alert is false. By removing the overhead present throughout the transmission process, the sensor node has the capacity to identify nearby woods. The sensor node that is capable of picking up on fire occurrences will function as active sensors. This makes an attempt to deliver the data via the cluster head and gateway to the sink node.

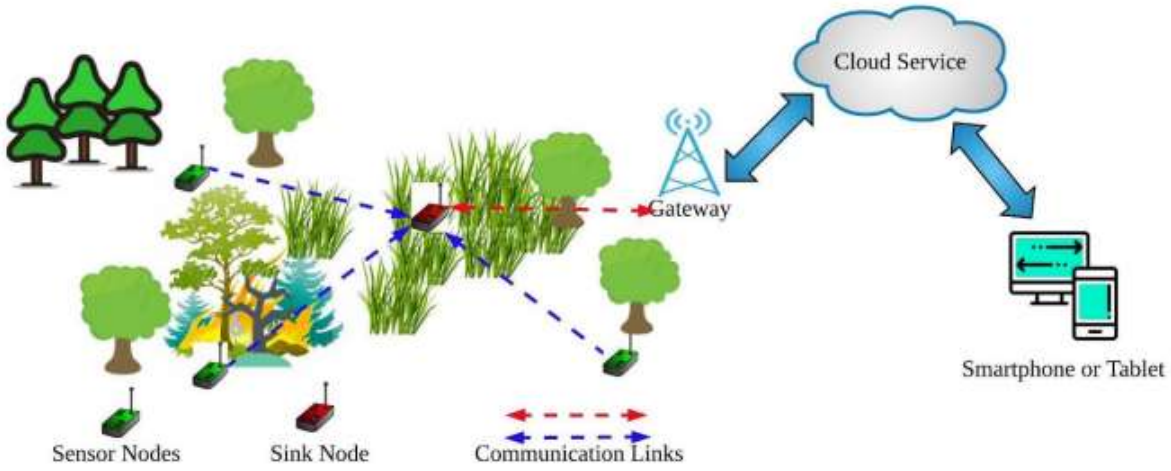

Figure.3: Sensor deployment and information transmission

The Figure.3 above top. explains the process of information transfer and sensor deployment. The sensor nodes, sink nodes, gateway, and smartphone with cloud-assisted services make up this system. The number of sensor modules is distributed randomly, and the forest's sensing field is established. The following section contains information about the sensor node's hardware. The deployed sensor node gathers the data and uses a gateway to interact with the sink nodes. Then, the activities taking place in the forest are watched over using cloud-assisted gadgets. A characteristic that characterises the forest has a significant value, I. It emphasises how crucial it is to save the forest from fire. Think of a situation where a forest is better protected because it is near a cultural heritage monument. The protection's perimeter is determined by the value of I. It stores the value on a scale of 1 to 10, with 1 denoting "not significant" and 10 denoting "very essential."

4. Data Collection and Communication Module

The factors of the forest environment, including humidity, light intensity, gases, and ambient temperature, are measured by the sensor nodes after they have been installed. Thinkspeak, an IoT-based cloud analytics solution that intends to store the sensed data under cloud channels, supports it. Figure. 4 depicts the data collection phase, during which field data is sent to the cloud server through a sink node for storage and real-time analysis. Field data is gathered, tracked, and stored in real time using the ThingSpeak cloud analytics platform. Data may be retrieved at any time and for any reason. Every two to three minutes, entries of environmental sensed variables are recorded in the cloud analytics platform ThingSpeak. The user at the control station may utilise algorithms to link the sensor network and controller by seeing the most current entries in graphical form. Each measurement's data is kept in a specific field, and the channel ID indicates different field attributes. Through the ThingSpeak channel on the Internet, the environment's real-time data is monitored. The user may at any time alter the field data and status depending on the analysis.

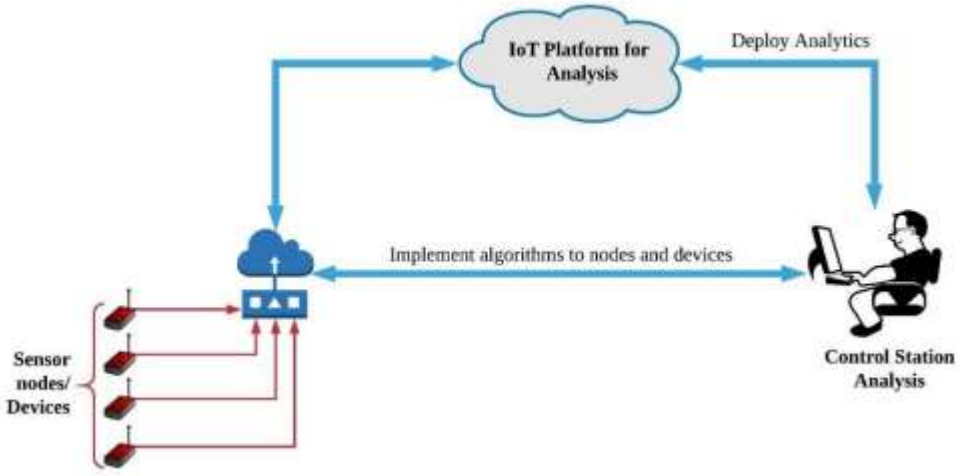

Figure.4: Data collection and storing using ThingSpeak cloud analytics platform

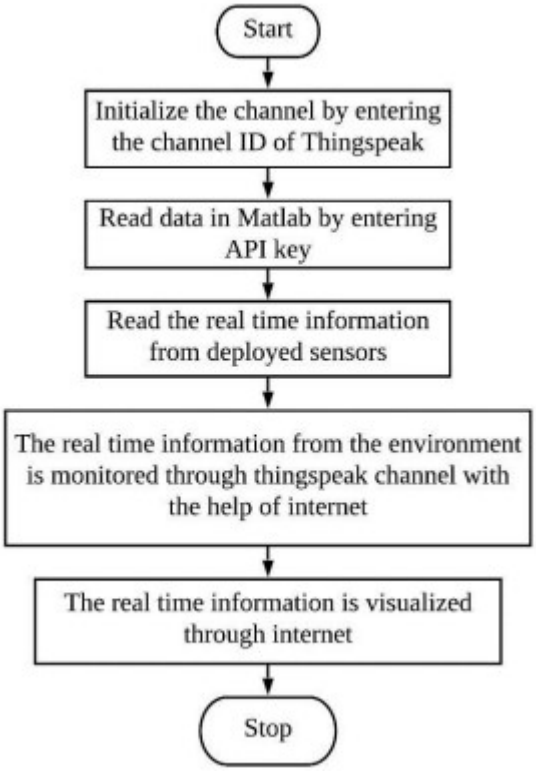

Figure.5: Flowchart of data collection and communication module

The workflow flowchart for data collecting using ThingSpeak analytics is shown in Figure.5. The reading of detected environmental factors comes after the channel startup, which creates the channel. The ThingSpeak platform's MATLAB interface enables real-time data reading and monitoring utilising Channel ID and API credentials. The newest items are updated in the cloud by the MATLAB code, which reads the channel ID. A MATLAB programme is used to run graphical plots of the real-time data. The last step is updating the channel with the field parameters and status. The acquired dataset must be configured in a way that reduces the anticipated fire

detection time. There are two states, namely regular states and abnormal states. The lack of data that differ from the default values, which indicates that the environment is safe, characterises normal circumstances. The other, however, is characterised by abnormal circumstances that mandate the existence of values that depart from the norm and indicate an unsafe setting. The Monitoring Centers take prompt action based on the Important value if any deviating values are discovered (I). The sensor nodes support the adaptive (or) external settings to do this. The sample rate of the sensing parameters is changed to improve the system's fidelity based on the environmental circumstances. An alert is created and sent through gateway to the monitoring module whenever any incident is discovered. The analysis step then verifies the warning that was produced.

5. Results and Discussion

Sensor nodes are placed in the forest area both randomly and deterministically to evaluate the effectiveness of the proposed model for detecting forest fires. Regular environmental monitoring is required to gauge the current condition of the area in order to make an early forecast of a fire outbreak. The deployed sensor modules gather ambient temperature, atmospheric gases, light intensity, humidity, and light intensity from the area of interest and send the data to a control centre for analysis. The only way to prevent the cause of wildfires and lessen their impact is via early fire event prediction. By continuously monitoring the environment, WSNs effectively forecast fire events in their earliest stages. The ground workers can get the timely notifications and act accordingly to avoid fires and put out other emergencies.

Figure.6: (a, b, c, d, e): Deployment of sensor nodes for collection of environmental parameters (a) Temperature & Humidity, (b) Smoke 1, (c) Light Intensity, (d) Smoke 2 and (e) Sink node

Figure 6 shows the placement of sensor modules to collect environmental data under typical atmospheric conditions. In Figure.6, (a) stands for the HTS-220 sensor node, which measures temperature and humidity, (b and d) for the MQ-2 sensor, which detects smoke particles in the environment, (c) for the TL sensor, which measures light intensity, and (e) for the sink node, which collects all sensed data. Each of these sensor nodes is placed in a distinct area that is within the sink node's transmission range and wirelessly transmits measured data to the coordinator node. The Fibocom G510 GPRS modules serve as the sink node, sending all detected data to a cloud platform for analysis and storage. The deployed sensor technology gathers environmental parameter information to identify potential enemies. The HTS-220 light sensor is a simple, affordably priced sensor that monitors light intensity. The examination of energy consumption and WSN lifetime is significantly impacted by the sink node, which is located in the centre of the area of interest. The sink node is configured to provide the cloud server the most current field data entries every two to five minutes. In the field, sensors and an intelligent sensor gateway module are used to track a variety of characteristics, including humidity, light intensity, gases, and ambient temperature. The data was collected using the deployed sensor nodes and saved in the cloud for processing. Using the ThingSpeak IoT Application, data gathered from these sensors is saved in the cloud. The measured values of humidity, light intensity, gases, and ambient temperature are shown in the table for each time occurrence. For data collection during the experiment in a live outside area, simulation is used. In order to gather and save data in a real-time context, the ThingSpeak IoT analytics is employed, and associated difficulties are noted. Several graphical charts for humidity, light intensity, gases, and ambient temperature have been created using the ThingSpeak IoT analytics on the basis of the observed information. Figure.7 depicts the analysis and verification of the sensor readings in ThingSpeak.

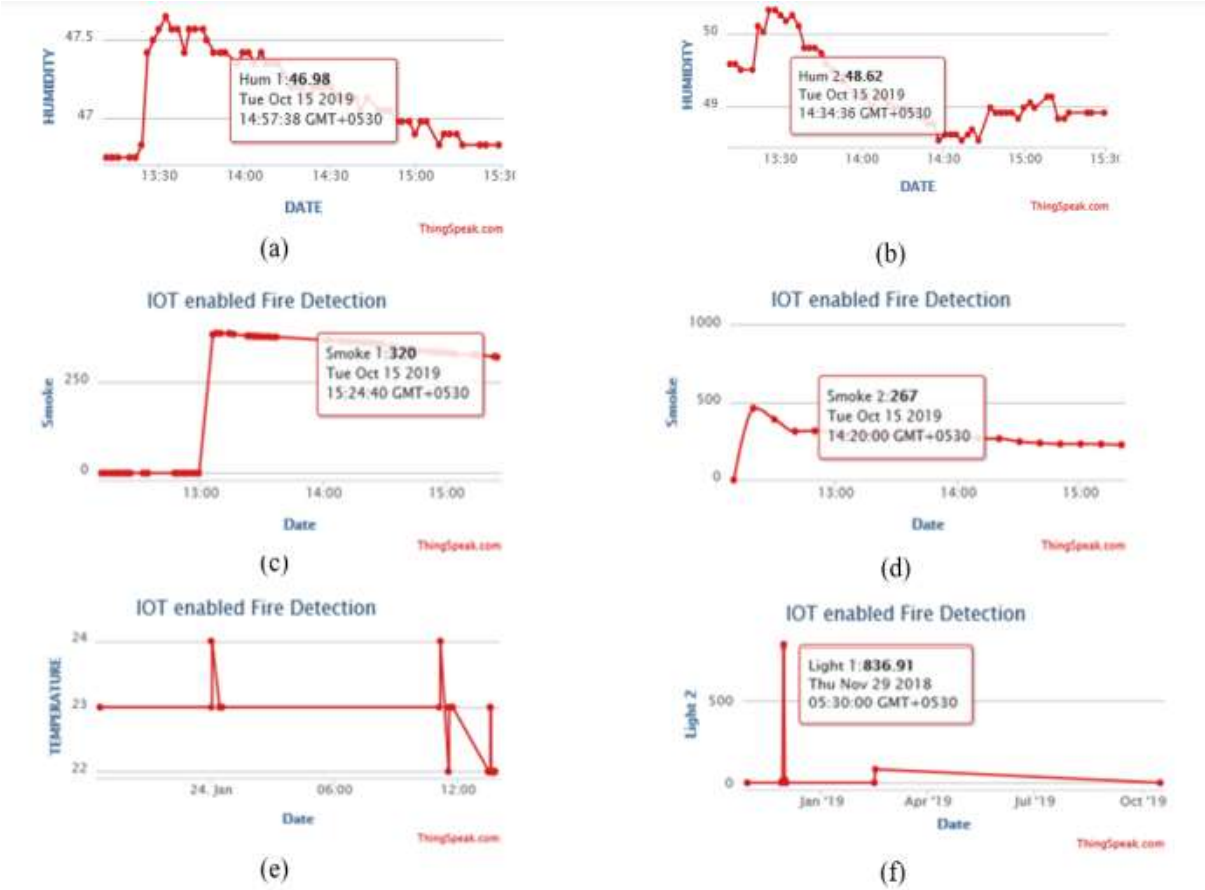

Figure.7: Obtained results from Thingspeak IoT analytics for various field set as (a & b): Humidity (in %), (c & d): Smoke (in ppm), (e): Temperature (in °C), (f): Light (in lux)

The graphical representation of several recorded environmental parameters is shown in the above image. It depicts the fluctuations of characteristics including humidity, light intensity, gases, and ambient temperature as well as the output results of the data gathered from the ThingSpeak cloud. Given that data updates on Think speak take a few seconds, it detects in almost real time. Figuring 7. The plot of recorded humidity values at two separate locations is shown in (a & b), the plot of recorded smoke values at two different locations is shown in (c & d), and the plot of temperature and light intensity from two different locations is shown in (e & f). When monitoring the status of the environment, the cloud platform offers a clear verification and analysis of all sensor information. By generating channel field sets, the MATLAB interface of cloud platforms enables real-time monitoring as well as the display of multiple sensor readings in graphical representation. The installed sensors gather data in real time, however there is a little lag before the data is updated on the ThinkSpeak cloud platform.

6. Conclusion

Researchers are paying a lot of attention to early forest fire detection. Recent years have seen an increase in awareness of the need to protect biodiversity, which has led to innovative planning techniques for controlling forest fires. Real-time applications should focus on creating an effective

nodes deployment method. This chapter explores efficient data collecting and real-time data processing since an efficient design will improve the performance of the systems. This study's major objective is to use WSNs to monitor the forest ecosystem. The detected information, such as humidity, light intensity, atmospheric gases, and ambient temperature from a real-time environment, is managed by Thingspeak, an IoT-based cloud analytics platform. This chapter explores how decisions are made in the case of a fire, including the collection, monitoring, and real-time analysis of measured data. The suggested system effectively monitors forest fires using sensors and the cloud-based IoT platform ThingSpeak. Real-time transmission to the ThingSpeak cloud of sensor data for temperature, humidity, light intensity, and gases. The system has the ability to gather, track, and analyse data for decision-making. The system provides an excellent solution for the early identification of fire incidents and is useful for the real-time study of environmental factors.

References

1. T. Zumbrunnen, G. B. Pezzatti, P. Menéndez, H. Bugmann, M. Bürgi, and M. Conedera, "Weather and human impacts on forest fires: 100 years of fire history in two climatic regions of Switzerland," Forest Ecology and Management, vol. 261, no. 12, pp. 2188-2199, 2011.
2. A. Nelson, and K. M. Chomitz, "Effectiveness of strict vs. multiple use protected areas in reducing tropical forest fires: a global analysis using matching methods," PloS one, vol. 6, no. 8, e22722, 2011. [10] M. D. Flannigan, B. J. Stocks, and B. M. Wotton, "Climate change and forest fires," Science of the total environment, vol. 262, no. 3, pp. 221-229, 2000.
3. M. E. Harrison, S. E. Page, and S. H. Limin, "The global impact of Indonesian forest fires," Biologist, vol. 56, no. 3, pp. 156-163, 2009.
4. V. Kafka, S. Gauthier, and Y. Bergeron, "Fire impacts and crowning in the boreal forest: study of a large wildfire in western Quebec," International Journal of Wildland Fire, vol. 10, no. 2, pp. 119-127, 2001.
5. E. Den Breejen, M. Breuers, F. Cremer, R. Kemp, M. Roos, K. Schutte, and J. S. De Vries, "Autonomous forest fire detection," Coimbra, Portugal: ADAIAssociacao para o Desenvolvimento da Aerodinamica Industrial, pp. 2003- 2012,1998.
6. A. B. Utkin, A. Fernandes, F. Simoes, A. Lavrov, and R. Vilar, "Feasibility of forest-fire smoke detection using lidar," International Journal of Wildland Fire, vol. 12, no. 2, pp. 159-166, 2003.
7. C. Yuan, Y. Zhang, and Z. Liu, "A survey on technologies for automatic forest fire monitoring, detection, and fighting using unmanned aerial vehicles and remote sensing techniques," Canadian journal of forest research, 45(7), 783-792, 2015.
8. K. Graham, and D. Spennemann, "Disaster management and cultural heritage: An investigation of knowledge and perceptions of New South Wales Rural fire service brigade captains," Australasian Journal of Disaster and Trauma Studies, vol. 1, pp. 5-31, 2006.

9. R. Lanorte, R. Lasaponara, F. De Santis, A. Aromando, and G. Nole, G. "Daily estimates of fire danger using multitemporal satellite MODIS data: the experience of FIRE-SAT in the Basilicata Region (Italy)" EGUGA, 14064, 2012.
10. R. S. Gautam, D. Singh, and D. Mittal, "An efficient contextual algorithm to detect subsurface fires with NOAA/AVHRR data," IEEE Transactions on Geoscience and Remote Sensing, vol. 46, no. 7, pp. 2005-2015, 2008.
11. N. Von Wahl, S. Heinen, H. Essen, W. Kruell, R. Tobera, and I. Willms, "An integrated approach for early forest fire detection and verification using optical smoke, gas and microwave sensors," WIT Transactions on Ecology and the Environment, vol. 137, pp. 97-106, 2010.
12. V. Sherstjuk, M. Zharikova, and I. Sokol, "Forest fire monitoring system based on UAV team, remote sensing, and image processing," In IEEE Second International Conference on Data Stream Mining & Processing (DSMP), pp. 590-594, 2018.
13. K. M. Modieginyane, B. B. Letswamotse, R. Malekian, and A. M. Abu-Mahfouz, "Software defined wireless sensor networks application opportunities for efficient network management: A survey," Computers & Electrical Engineering, vol. 66, pp. 274-287, 2018.
14. P. Bellavista, G. Cardone, A. Corradi, and L. Foschini, "Convergence of MANET and WSN in IoT urban scenarios," IEEE Sensors Journal, vol. 13, no. 10, pp. 3558- 3567, 2013.
15. R. N. Duche, and N. P. Sarwade, "Sensor node failure detection based on round trip delay and paths in WSNs," IEEE Sensors journal, vol. 14, no. 2, pp. 455-464, 2013.
16. H. Y. Zhou, D. Y. Luo, Y. Gao, and D. C. Zuo, "Modeling of node energy consumption for wireless sensor networks," Wireless Sensor Network, vol. 3, no. 1, 18, 2011.
17. I. Al-Anbagi, M. Erol-Kantarci, and H. T. Mouftah, "A survey on cross-layer quality-of-service approaches in WSNs for delay and reliability-aware applications," IEEE Communications Surveys & Tutorials, vol. 18, no. 1, pp. 525- 552, 2014.
18. M. Kuorilehto, M. Hännikäinen, and T. D. Hämäläinen, "A survey of application distribution in wireless sensor networks," EURASIP Journal on Wireless Communications and Networking, vol. 5, 859712, 2005.
19. M. Bedo, G. Blanco, W. Oliveira, M. Cazzolato, A. Costa, J. Rodrigues, and C. Traina Jr, "Techniques for effective and efficient fire detection from social media images," arXiv preprint arXiv:1506.03844, 2015.
20. T. Toulouse, L. Rossi, A. Campana, T. Celik, and M. A. Akhloufi, "Computer vision for wildfire research: An evolving image dataset for processing and analysis," Fire Safety Journal, vol. 92, pp. 188-194, 2017.
21. A. P. Gabriel Henrique de, A. M. Fusioka, B. T. Nassu, R. Minetto, "A Large-Scale Dataset for Active Fire Detection/Segmentation (Landsat-8)," IEEE Dataport. http://dx.doi.org/10.21227/t9gn-y009, 2020.
22. E. H. Chowdhury, and Q. K. Hassan, "Operational perspective of remote sensingbased forest fire danger forecasting systems," ISPRS Journal of Photogrammetry and Remote Sensing, vol. 104, pp. 224-236, 2015.

23. Z. Li, S. Nadon, and J. Cihlar, "Satellite-based detection of Canadian boreal forest fires: Development and application of the algorithm," International Journal of Remote Sensing, vol. 21, no. 16, pp. 3057-3069, 2000.
24. A. Prakash, K. Schaefer, W. K. Witte, K. Collins, R. Gens, and M. P. Goyette, "A remote sensing and GIS based investigation of a boreal forest coal fire," International Journal of Coal Geology, vol. 86, no. 1, pp. 79-86, 2011.
25. M. S. Guettouche, A. Derias, M. Boutiba, M. Guendouz, and A. Boudella, "A fire risk modelling and spatialization by GIS," Journal of Geographic Information System, vol. 3, no. 3, 254, 2011.

Journal of Emerging Technologies and Innovative Research

(An International Scholarly Open Access Journal, Peer-reviewed, Refereed Journal)

UGC Approved Journal no 63975

ISSN: 2349-5162 | ESTD Year : 2014

Call for Paper

Volume 10 | Issue 2 | February 2023

Multidisciplinary, Monthly, Multilanguage Journal

Published in:

Volume 8 Issue 9
September-2021
eISSN: 2349-5162

UGC and ISSN approved 7.95 impact factor UGC Approved Journal no 63975

7.95 impact factor calculated by Google scholar

Unique Identifier

Published Paper ID:
JETIR2109429

Registration ID:
315422

Page Number

e248-e252

Title

Improving Low Illumination image based on Multi-Scale Retinex via Bilinear Interpolation

Authors

Dr. A Chrispin Jiji

Abstract

Images taken at night in low-light situations are more likely to have poor visibility, which can affect future processing for outdoor computer vision applications. As a result, we recommend a retinex upgrade for nighttime image enhancement. Retinex is one of the most widely used techniques. It's used on photographs with non-uniform brightness in terms of colour or lightness, and it gets the job done in terms of colour consistency and dynamic range compression. Few studies have looked into retinex's performance on night-time photos, especially those taken in challenging conditions (i.e., images with over- or under-lit areas, or images with noisy speckles), where the technique can fall short. The original multi-scale retinex via Bilinear Interpolation (MSRBI) is particularly sensitive to camera noise speckles in low light, and it has a poor effect on areas with ordinary or irradiated light. In low-light circumstances, the original MSR is particularly sensitive to noise speckles produced by cameras, and it performs poorly in areas with normal or bright lighting. In addition, the original MSR used a gain-offset technique for pre-display processing, which could result in visible data loss on night-time images. This study replaces MSR's logarithm function with a customised sigmoid function to prevent data loss, and adapts MSRBI to night-time photography by combining sigmoid-MSR findings with original images.

Key Words

Multi-scale retinex, Bilinear interpolation, sigmoid function, high-light preserving

Cite This Article

"Improving Low Illumination image based on Multi-Scale Retinex via Bilinear Interpolation", International Journal of Emerging Technologies and Innovative Research (www.jetir.org), ISSN:2349-5162, Vol.8, Issue 9, page no.e248-e252, September-2021, Available :http://www.jetir.org/papers/JETIR2109429.pdf

ISSN

2349-5162 | Impact Factor 7.95 Calculate by Google Scholar

An International Scholarly Open Access Journal, Peer-Reviewed, Refereed Journal Impact Factor 7.95 Calculate by Google Scholar and Semantic Scholar | AI-Powered Research Tool, Multidisciplinary, Monthly, Multilanguage Journal Indexing in All Major Database & Metadata, Citation Generator

Cite This Article

"Improving Low Illumination image based on Multi-Scale Retinex via Bilinear Interpolation", International Journal of Emerging Technologies and Innovative Research (www.jetir.org | UGC and issn Approved), ISSN:2349-5162, Vol.8, Issue 9, page no. ppe248-e252, September-2021, Available at : http://www.jetir.org/papers/JETIR2109429.pdf

Publication Details

Published Paper ID: JETIR2109429

Registration ID: 315422

Published In: Volume 8 | Issue 9 | Year September-2021

DOI (Digital Object Identifier):

Page No: e248-e252

Country: The Oxford College of Engineering Bangalore, KARNATAKA, India .

Area: Engineering

ISSN Number: 2349-5162

Publisher: IJ Publication

Published Paper URL :: https://www.jetir.org/view?paper=JETIR2109429

Published Paper PDF: https://www.jetir.org/papers/JETIR2109429

Call for Paper February 2023
(https://www.internationaljournalssrg.org/cal-for-paper.html)

(https://www.internationaljournalssrg.org/cal-for-paper.html)
(https://www.internationaljournalssrg.org/cal-for-paper.html)
(https://www.internationaljournalssrg.org/cal-for-paper.html)

(https://www.internationaljournalssrg.org/cal-for-paper.html)
(https://www.internationaljournalssrg.org/cal-for-paper.html)

(https://www.internationaljournalssrg.org/cal-for-paper.html)
(https://www.internationaljournalssrg.org/cal-for-paper.html)
(https://www.internationaljournalssrg.org/cal-for-paper.html)
(https://www.internationaljournalssrg.org/cal-for-paper.html)
(https://www.internationaljournalssrg.org/cal-for-paper.html)

(https://www.internationaljournalssrg.org/cal-for-paper.html)

IJEEE

(https://www.internationaljournalssrg.org/cal-for-paper.html)
(https://www.internationaljournalssrg.org/cal-for-paper.html)

Soft-Switching Integrated Quasi Resonance Buck-Boost Converter for HHO Optimized Grid Connected PV System

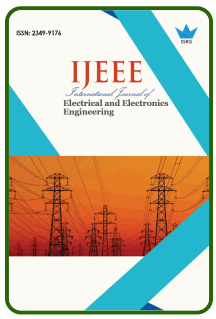

International Journal of Electrical and Electronics Engineering

Volume 9 Issue 8

Year of Publication : 2022

Authors : Nisha C. Rani, N Amuthan

doi 10.14445/23488379/IJEEE-V9I8P104 (https://doi.org/10.14445/23488379/IJEEE-V9I8P104)

(https://www.internationaljournalssrg.org/IJEEE/2022/Volume9-Issue8/IJEEE-V9I8P104.pdf)

How to Cite?

Nisha C. Rani, N Amuthan, "Soft-Switching Integrated Quasi Resonance Buck-Boost Converter for HHO Optimized Grid Connected PV System," *SSRG International Journal of Electrical and Electronics Engineering*, vol. 9, no. 8, pp. 28-39, 2022. *Crossref,* https://doi.org/10.14445/23488379/IJEEE-V9I8P104

(https://doi.org/10.14445/23488379/IJEEE-V9I8P104)

Abstract:

The most economical and ecologically beneficial electrical energy worldwide results from solar photovoltaic systems. However, switching action under normal operation undergoes stress since the voltage or current may not be zero at the changeover time. Here, we suggested the ZVT-ZCT Quasi Resonance Buck-Boost converter (QRBB), which introduces L-C dynamics and induces a forced oscillation, allowing the primary switch (IGBT) to turn off at zero current transition and turn on at zero voltage transition, thereby reducing stress on switching device. Furthermore, the VSI is controlled by the Harris Hawks Optimization Algorithm (HHO) optimized proportional-integral (PI) controller. The proposed dc-dc converter can deliver pure sinusoidal output current and voltage waveforms with better output voltage enhancement. The suggested QRBB Converter's performance and efficiency are tested through simulation using the Matlab Simulink software. The result shows that the PI-HHO controller provides a better steady and dynamic state response and delivers quality power to the grid than the conventional PI controller.

Keywords:

Global Warming, Solar Photovoltaic Systems, Electrical Energy, Output Voltage, Matlab.

References:

[1] S. S. Kumar, A. K. Panda, and T. Ramesh, "A Zvt–Zct Pwm Synchronous Buck Converter with a Simple Passive Auxiliary Circuit for Reduction of Losses and Efficiency Enhancement", Ain Shams Engineering Journal., vol.6, no.2, pp.491-500, 2015.

[2] Mohammed. S. Mohammed, Khaled. M. Al-Awasa, Husssein. D. Al-Majali, "Energy Management and Control in Micro Grid with Hybrid Energy Storage Systems By Using Pi and Flatness Theory," International Journal of Engineering Trends and Technology, vol.69, no.11, pp.227-235, 2021, Crossef, Https://Doi.Org/10.14445/22315381/IJETT-V69I11P229.

[3] Khodabandeh, M., Afshari, E. and Amirabadi, M., "A Family of Ćuk, Zeta, and Sepic Based Soft-Switching Dc-Dc Converters," IEEE Transactions on Power Electronics, vol.34, no.10, pp.9503-9519, 2019.

[4] Nourieh, N., Adib, E. and Wheeler, P., Zvt High Step-Up Boost Converter with Wide Input Voltage and Wide Output Power for Renewable Energy Applications, 2022.

[5] Yau, Y.T., Hwu, K.I. and Shieh, J.J, "Soft Switching of Non-Isolated Buck-Type Converter with Common-Ground Switch," Energies, vol.14, no.17, pp.5290, 2021.

[6] Mageshwari, S. and Kumar, J.V, "Implementation of Pso Algorithm in Novel Sepic Converter with Pv Fed Source," in Interdisciplinary Research in Technology and Management, Crc Press, pp.160-167, 2021.

[7] S. Jalilzadeh, and M. Pakdel, "A Soft Switched Dc-Dc Boost Converter for Use in Grid Connected Inverters," Journal of Operation and Automation in Power Engineering, vol.5, no.1, pp.75-82, 2017.

[8] X. Wang, H. Xiao, Z. Wei, and C. Chen, "An Improved Transformerless Photovoltaic Grid-Connected Soft-Switching Inverter," in 14th IEEE Conference on Industrial Electronics and Applications (ICIEA), pp.2338-2343, 2019.

[9] Lee, H. J., Kim, and Y. H, "Analysis and Design of A Zvt Resonant Boost Converter Using An Auxiliary Resonant Circuit," Electronics, vol.8, no.4, pp.466, 2019.

[10] A. Marrekchi, S. Sallem, and M. B. Kammoun, "A New Soft Switching Algorithm for Active and Reactive Power Control in Three Phase Grid-Connected Pv Plant", In16th International Multi-Conference on Systems, Signals & Devices (Ssd), pp.578-582, IEEE, 2019.

[11] U. Khaled, H. Farh, S. Alissa, A. Abanmi, and O. Aldraimli, "Efficient Solution of the Dc-Link Hard Switching Inverter of the Pv System", Journal of King Saud University-Engineering Sciences, vol.32, no.7, pp.425-31, 2020.
[12] Appathurai, A., Carol, J. J., Raja, C., Kumar, S. N., Daniel, A. V., Malar, A. J. G., and Krishnamoorthy, S, "A Study on Ecg Signal Characterization and Practical Implementation of Some Ecg Characterization Techniques," Measurement, vol.147, pp.106384, 2019.
[13] M. Salem, A. Jusoh, N. R. Idris, H. S. Das, and I. Alhamrouni, "Resonant Power Converters with Respect To Passive Storage (Lc) Elements and Control Techniques–An Overview," Renewable and Sustainable Energy Reviews, vol.91, pp.504-20, 2018.
[14] Mr. Anem Apparo, Dr. G. Chandra Sekhar "A Grid Connected Hres Using Seven Level Inverter - A Hybrid Mfo-Rbfnn Technique," International Journal of Engineering Trends and Technology, vol.68, no.7, pp.56-68, 2020, Crossef, Https://Doi.Org/ 10.14445/22315381/IJETT-V68I7P209S.
[15] M. S. Ramkumar, A. Amudha, P. Nagaveni, G. Emayavaramban, S. Divyapriya, V. M. Mansoor, M. Sivaramkrishnan, D, and Kavitha, "Analysed Results of Dc-Dc Converters with Softswitching Techinques," Materials Today: Proceedings, vol.37, pp.2631-5, 2021.
[16] M. Rezvanyvardom, and A. Mirzaei, "High Gain Configuration of Modified Zvt Sepic-Boost Dc-Dc Converter with Coupled Inductors for Photovoltaic Applications", Solar Energy, vol.208, pp.357-67, 2020.
[17] Sivasankari, B., Ahilan, A., Jothin, R., and Malar, A. J. G, "Reliable N Sleep Shuffled Phase Damping Design for Ground Bouncing Noise Mitigation," Microelectronics Reliability, vol.88, pp.1316-1321, 2018.
[18] Malar, A. J. G., Kumar, C. A., and Saravanan, A. G, "Iot Based Sustainable Wind Green Energy for Smart Cites Using Fuzzy Logic Based Fractional Order Darwinian Particle Swarm Optimization," Measurement, vol.166, pp.108208, 2020.
[19] Ahmad Hamdan Ariffin, Zeittey Karmilla Kaman , "Review on Consumers' Privacy and Economic Value Acceptance in Smart Grid Implementation," International Journal of Engineering Trends and Technology , pp.16-20, 2020.
[20] Shenoy, K.L., Nayak, C.G. and Mandi, R.P., "Effect of Partial Shading in Grid Connected Solar Pv System with Fl Controller," International Journal of Power Electronics and Drive Systems, vol.12, no.1, pp.431, 2021.
[21] Nimita Gajjar, Tejas Zaveri, Naimish Zaveri, "Low-Cost Implementation of Pv-Statcom for Non-Linear Load Using Stm32f407vg Controller," International Journal of Engineering Trends and Technology, vol.69, no.9, pp.212-219, 2021, Crossef, Https://Doi.Org/10.14445/22315381/IJETT-V69I9P225.
[22] Malar, J. G., & Kumar, C. A. Implementation of Mppt Techniques for Wind Energy Conversion System," Internal Journal of Research and Analytical Reviews, vol.5, no.3, 2018.
[23] S. Ekinci, B. Hekimoğlu, A. Demirören, and S. Kaya, "Harris Hawks Optimization Approach for Tuning of Fopid Controller in Dc-Dc Buck Converter", in International Artificial Intelligence and Data Processing Symposium (Idap), IEEE, pp.1-9, 2019.
[24] Batarseh, A. Harb, "Power Electronics. Springer Nature", 2018.

Enhancing the Naïve Bayes Spam Filter through Intelligent Text Modification Detection

PDF (https://www.provinciajournal.com/index.php/telematique/article/view/211/202)

Keywords:
Naïve Bayes, leetspeak, ham, SpamAssassin, Bayesian Poisoning.

Mridula Shukla
Asst. Professor, Dept. of MCA, the Oxford College of Engineering, Bengaluru -560068

Santhosh Kumar Reddy E
MCA Final Year Dept. of MCA, The Oxford College of Engineering, Bengaluru -560068

Ragavendra G
MCA Final Year Dept. of MCA, The Oxford College of Engineering, Bengaluru -560068

Sathish S
MCA Final Year Dept. of MCA, The Oxford College of Engineering, Bengaluru -560068

Abstract

Spam messages have been a diligent issue in PC security. They are over the top financially and exceptionally risky for PCs and associations. Despite of the improvement of casual associations and other Internet based information exchange scenes, dependence on email correspondence has extended all through the long haul and this dependence has achieved a critical need to additionally foster junk mail. Yet many junk mail filters have been made to help with hindering these junk mail messages from incoming a client's inbox, there is a shortfall of assessment focusing in on message modifications. At this point, Naïve Bayes is one of the most notable procedures for spam classification considering its straightforwardness and efficiency. Naïve Bayes is also very exact; in any case, it can't precisely bunch messages once they cover lee speak or accents. Henceforth, in this proposes, we executed a smart estimation for redesigning the accuracy of the Naïve Bayes Spam Filter so it can perceive text modifications and precisely describe the email as spam or ham.

Issue

International Journal for Research Trends and Innovation
International Peer Reviewed & Refereed Journals, Open Access Journal
ISSN Approved Journal No: 2456-3315 | Impact factor: 8.14 | ESTD Year: 2016
Scholarly open access journals, Peer-reviewed, and Refereed Journals, Impact factor 8.14 (Calculate by google scholar and Semantic Scholar | AI-Powered Research Tool) , Multidisciplinary, Monthly, Indexing in all major database & Metadata, Citation Generator, Digital Object Identifier(DOI)

Call For Paper
Issue: February 2023
Volume 8 | Issue 2
Submit Paper Online
Review Result and Publication of Paper within : 2-3 days
Click Here For more Details

For Authors
Submit Paper Online
Publication Guidelines
Publication Charges
HardCopy and DOI Charges
Pay Publication Charges
Track Paper
Research Area
All Policy

Forms / Download
Copyright Form
Undertaking Form
Paper Format
Sample Certificate
Sample Publication Letter
Sample Hard Copy of Journal

Published Issue Details
Current Issue
Archive
Conference Proposal
Recent Conference Details

Editorial Board
Editorial Board
Join As A Referral/Reviewer
Benefits of Referral/Reviewer

Other IMP Links

Published Paper Details

Paper Title:	**Smart Security System**
Authors Name:	Bommanahal Ramagiri Mata Thrigunyeshwari , Deepa Kiran , Pooja Pabhu , Rakshitha S , Mrs Resna SR, Mrs Sandhya Rai
Download E-Certificate:	Download
Author Reg. ID:	IJRTI_183418
Published Paper Id:	IJRTI2207295
Published In:	Volume 7 Issue 7, July-2022
DOI:	
Abstract:	The present security system takes longer time for sending security alerts. It's reported that they are system which sends the alert message after a duration of the occurrence of security violation. This paper mainly focuses on development of system which works rapidly for short time period. The security is important to provide safety, therefore, a smart security system is being proposed in this paper which monitor and alert regarding the un-usual activities. This security system plays a vital role in securing the location. This remote security system which is used for detection of harmful gases or smoke, detection of fire, detection of theft, etc. It has been successfully completed, and this system send the notification to the owner's mobile phone regarding the problems in form of SMS alerts. This system also has an exhaust fan which works automatically when there is presence of harmful smoke or gas. The security system programmed in the Embedded C programming. The system is wireless therefore adaptable and greater efficiency. In this project we have developed an economically smart security system with fault-tolerant, secured, easy to install and use surveillance system through wireless connection using lower cost devices controlled by smart phones
Keywords:	
Cite Article:	**"Smart Security System"**, International Journal of Science & Engineering Development Research (www.ijrti.org), ISSN:2455-2631, Vol.7, Issue 7, page no.1711 - 1716, July-2022, Available :http://www.ijrti.org/papers/IJRTI2207295.pdf
Downloads:	000202352
ISSN:	2456-3315 | IMPACT FACTOR: 8.14 Calculated By Google Scholar| ESTD YEAR: 2016 An International Scholarly Open Access Journal, Peer-Reviewed, Refereed Journal Impact Factor 8.14 Calculate by Google Scholar and Semantic Scholar | AI-Powered Research Tool, Multidisciplinary, Monthly, Multilanguage Journal Indexing in All Major Database & Metadata, Citation Generator
Publication Details:	Published Paper ID: IJRTI2207295 Registration ID:183418 Published In: Volume 7 Issue 7, July-2022 DOI (Digital Object Identifier): Page No: 1711 - 1716 Country: Bangalore, Karnataka , India Research Area: Engineering Publisher : IJ Publication

Submit Paper Online
Check Paper Status
Call for Paper
Join As reviewer
All Policy

ISSN Details
INTERNATIONAL STANDARD SERIAL NUMBER
ISSN 2456-3315
OPEN ACCESS
WhatsApp Click Here
ISSN: 2456-3315
Impact Factor: 8.14 and ISSN APPROVED
Journal Starting Year (ESTD) : 2016

DOI (A digital object identifier)
DOIONE
Providing A digital object identifier by DOI.ONE
How to Get DOI?

Conference
Conference Proposal
Recent Conference Details

Facts & Figure

Impact Factor : 8.14

Issue per Year : 12

Volume Published : 8

Issue Published : 81

Article Submitted : 5965

Article Published : 3277

Total Authors : 8322

Total Reviewer : 541

Total Countries : 72

Indexing Partner

Published Paper URL : https://www.ijrti.org/viewpaperforall?paper=IJRTI2207295
Published Paper PDF: https://www.ijrti.org/papers/IJRTI2207295

- Undetaking Form
- Publication Charges
- FAQ
- Contact US

- Payment Refund Policy

ANALYSIS AND DESIGN OF MULTI-STOREY BUILDING USING ETABS

[1]GAYATHRI R, [2]HARSHITHA, [3]DR.T S MALLESHIAH
[1]Asst Professor, [2]Student, [3]Professor
[1,2,3]Department of civil Engineering,
[1,2,3]The Oxford College of Engineering, Bangalore, Karnataka, India

Abstract: A multi-storey building has several floors at different levels above the ground. Analysis and design of multi-storied building deals with economic factor, serviceability and durability of a building. The foremost basic in structural engineering is the design of simple basic components and members of the building i.e., beams, columns, slabs and footings.Thisproject work aims to analysis and design of a four storied building using ETABS.
ETABS stands for Extended Three-Dimensional Analysis of Building Systems. It is a stand-alone structural analysis programme with a special purpose features for structural design and analysis of building systems. It is simple to use and user friendly and it is unique in its ability to address the full spectrum of tasks involved in the process of structural analysis and design. The main purpose of this software is to design multi-storey building in a systematic process. This project accomplishes a typical design project which is designed as per Indian Codes IS1893-Part 2:2000 and IS456:2000. The design involves determining the most suitable proportions of a structure and dimensioning and detailing the structural elements. Once the structure is analysed and designed it must have sufficient strength to withstand the maximum stresses to which it is subjected. This paper discuss the analysis of a conventional building (G+4) under the effect of shear forces and bending moment of beams and columns.

Keywords: ETABS, analysis, structural design, shear force, bending moment

1. Introduction

This Project is based on the analysis and design of a four storied building. The determination of general shape, specific dimension and size of a building is known as structure analysis, so that it will perform the function for it and will safely withstand the influences which will act on throughout its useful life. In short, the specification of the required structure is the most important thing to decide many aspects of the structure, such as functional safety and economic aspects. The entire process of structural planning and designing requires not only imagination and calculations, but also science knowledge of Structural Engineer.In this Project, an effort made on planning, analysis and design of residential building using E-TABS. We have taken a plan of a building on the basis of which the analysis will be done for the whole structure. For the analysis of a building one has to consider all the possible loadings and see that the structure is safe against all possible loading conditions. The dead load and live loads are calculated and applied and the design for beams, columns, footing and slabs are obtained. Analysis of beams and columns has been done using E-TABS software.

2.Significance of The Study

Analysis of a building means the estimation of the response of structures towards variable external loads considering all the deviants that may occur. During the preliminary design-stage the estimated external load is used to design the size and geometry of the structures of interconnected members by using local building code and specifications of the area where the structure is located. Therefore, assuring the structural integrity, durability etc. Neglecting this crucial analysis and design stage or erring during the process will result in catastrophic failure within the building structure which can, in the worst-case scenario may lead to the loss of lives. Since this stage is the most important, the margin of error is required to be close to zero. We are making use of a software called ETABS, which is a highly efficient structural analysis and design programme consisting of modelling tools, code-based load prescriptions, analysis methods and solution techniques. Through this study we want to signify the importance of analysing and design of a multi - storey building to ensure that it satisfies the safety and serviceability requirements with help of the software ETABS.

3.Review Of Related Studies

Balaji.U and Selvarasan (2016) used ETABS to analyse and design a multi-storeyed building which was under static and dynamic loading. In the study a G+13 storey residential building was studies for earthquake loads using ETABS. Here they assumed that the material property to be linear, static and dynamic analysis were performed. The non-linear analysis was performed by considering severe seismic zones and the behaviour

[

was assessed by considering type II soil condition. Various results like displacements, base shear were plotted and studied.

Geethu (2016)carried out a comparative study on analysis and design of a multi-storeyed building by STAAD.Pro and ETABS software's. They concluded that while comparing both the results, ETABS software shows higher values of bending moment and axial force

Mr.Raghunandan M and Mrs. Suma Devi (2107)used ETABS non-linear software for simulation of adjacent multi-storeyed RC frame buildings of 15 storey and 10 storey. The provisions which may reduce the effects of pounding like the separation distance, addition of shear walls, lateral bracings and variation in storey height of the buildings have been considered for analysis. The results by considering both fixed and base isolated conditions were arrived.

Mr. Abhayguleria (2016) pointed out that ETABS is commonly used to analyse: skyscrapers, parking, garages, steel & concrete structures, low and high-rise buildings and portal frame structures. The case study in this paper mainly focuses on structural behaviour of a multi-storey building for different plan configurations like rectangular, C, L and I-shape. Modelling of 15- storey RC framed building is done on the ETABS software for analysis. Post analysis of the structure, maximum shear forces, bending moments, and maximum storey displacement are computed and then compared for all the analysed cases.

4.Objectives Of The Study

- To analyze the G+4 building using the software ETABS.
- To design the building for stability, serviceability and also it must be economical.

5.Hypotheses Of The Study

- Awareness on healthy dietary habits among prospective teachers are moderate.
- There is no significant difference between prospective teachers in their awareness on healthy dietary habits with reference to the following background variables.

(i)Gender (ii)Locality of residence (iii)Nature of college (iv)Type of family (v)Medium of Instruction

- There is no significant difference among prospective teachers in their healthy dietary habits with reference to father's and mother's educational qualification

6.Methodology

6.1 Project details

Safe bearing capacity of soil (SBC) = 200KN/mm^2

Total height of the building = 15.5m

An already existing G+4 building of plan 15m×20m is considered. It is situated in zone II. The soil condition is medium. The overall height of the building is 15.5m with basement height of 3.5m and the typical floor height is 3m. the building consists of columns of size 230mm×500mm and beams 230mm×450mm respectively. The plan of the layout of the column is as shown in the fig.6.1 and the corresponding elevation in fig.6.2

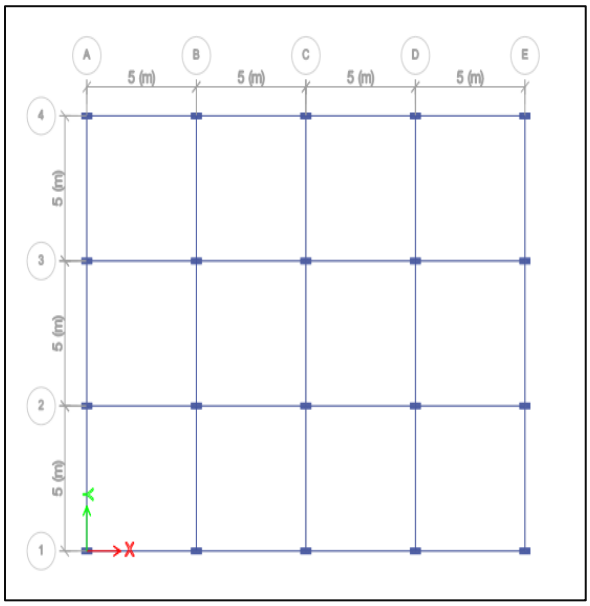

Fig 6.1.1 Column layout of the building(plan)

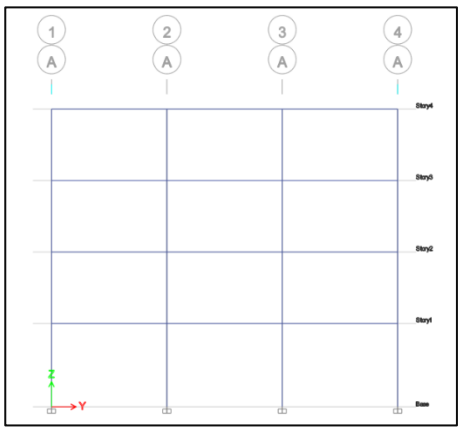

Fig 6.1.2 Building Frame

6.2 Modelling

Step 1: New Model

- Press (File and choose New Model)
- Choose the following settings.
- Design the (Grid Only) according to the plan of beams (Spacing method). Fill the Uniform grid spacing.

Step 2: Defining the Material Properties

- Defining the materials type like concrete, steel, rebar and masonry with their standard grade.

Step 3: Defining the Sectional Property

- Defining the column properties.

In this plan we take concrete grade as M25 for the ground floor as well as for the upper stories.

Step 4: Defining Beam Properties.

In this modelling we can take M25 concrete for the Ground Floor as well as for the upper stories.

Step 5: Defining the Slab Properties.

Step 6: Assigning all the elements to the model.

3D View of the Building

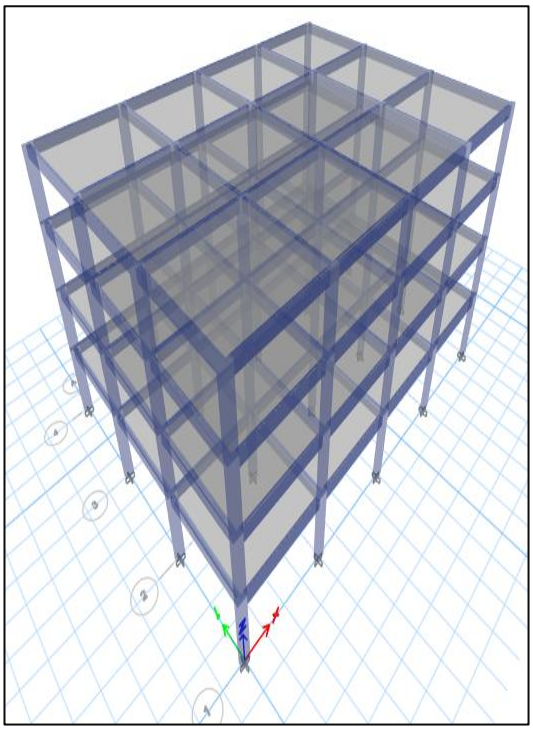

Fig 6.6 Three-dimensional view of the building

Step 7: Defining and assigning the loads

We can define the various load according to IS codes specified.

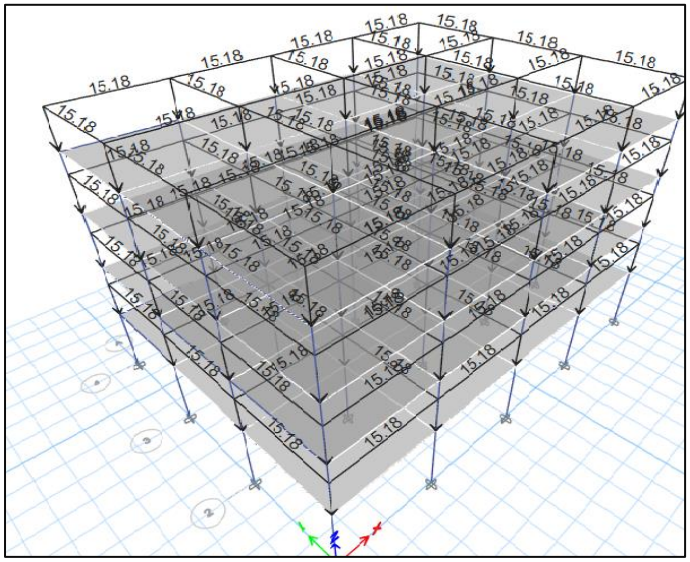

Fig7.4(c) 3-Dimensional View

Step 8: After assigning all the loads replicate the floors(G+4). We did diaphragm for the plan.

Step 9: Analyze the building.

- After the load application, we analyze the structure.
- The bending moment of the whole building is shown in

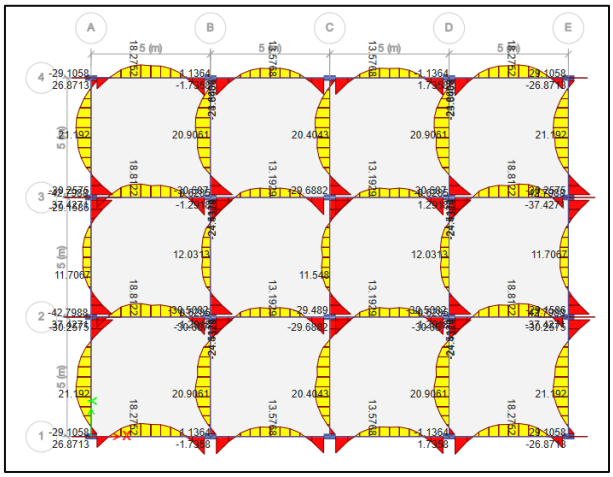

Max Bending Moment for Beams and column

Maximum bending moment value for beams and column

	Bending moment values KN-m	
Frames	Column	Beam
X-Direction		
A and E	30.25	29.192
B and D	31.89	20.91
C	30.57	20.4
Y-Direction		
1 and 4	24.73	18.27
2 and 3	25.86	18.81

Based on the above BM values we designed manually for Beams and Columns.

As per the design, the dimensions of Beams and columns are safe

Designing

During the preliminary design-stage the estimated external load is used to design the size and geometry of the structures of interconnected members by using local building code and specifications of the area where the structure is located. Therefore, assuring the structural integrity, durability etc. Neglecting this crucial design stage or erring during the process will result in catastrophic failure within the building structure which can, in the worst-case scenario may lead to the loss of lives. Since this stage is the most important, the margin of error is required to be close to zero.

CONCLUSION:

Analysis of a building ensures safety, serviceability, longevity and economic efficiency.

It can be done either by manually or with the help of automated computer software's.

The manual method of analyzing a building is time consuming and may result in various errors.

For this reason, we make use of computer software "E-TABS" which is efficient, reliable and precise.

With this study we like to conclude that through careful and precise analysis of buildings with the help of powerful computer software's the margin of error, the stability of the structure and an overall safe environment can be achieved.

Reference:

- **(A)** Ravi Kiran Sachin Metre,Shivanand C ghule(2017)," Comparitive study of Different types of bracing system by placing at different locations." International Research Journal of Engineering & Technology (IRJET), Vol. 4 Issue 8, May-2017
- **(A)** IS:875-1987 (part 1 to 5), "Code of practice for Design Loads in Buildings and Structures", Bureau of Indian Standards, New Delhi
- **(B)** IS:456-2000 "Indian Standard code of practice for plain and reinforced Cement Concrete", Bureau of Indian Standards, New Delhi
- **(C)** Abhay Guleria (2014): Structural Analysis of a Multi-Storeyed Building Using ETABS for different Plan Configurations". International Journal of Engineering Research & Technology (IJERT), Vol. 3 Issue 5, May-2104
- **(D)** Raghunandan MH and Suma (2015): Seismic Pounding between Adjacent RC Buildings with and without Base Isolation System, International Journal of Research in Engineering and Technology, Volume: 04 Issue: 06, June- 2015
- **(E)** Balaji and Selvarasan (2016): "Design and Analysis of multi-storeyed building under static and dynamic loading conditions using ETABS", International Journal of Technical Research and Applications.

ANALYSIS AND DESIGN OF MULTI-STOREY BUILDING USING ETABS

[1]GAYATHRI R, [2]HARSHITHA, [3]DR.T S MALLESHIAH
[1]Asst Professor, [2]Student, [3]Professor
[1,2,3]Department of civil Engineering,
[1,2,3]The Oxford College of Engineering, Bangalore, Karnataka, India

Abstract: A multi-storey building has several floors at different levels above the ground. Analysis and design of multi-storied building deals with economic factor, serviceability and durability of a building. The foremost basic in structural engineering is the design of simple basic components and members of the building i.e., beams, columns, slabs and footings.Thisproject work aims to analysis and design of a four storied building using ETABS.
ETABS stands for Extended Three-Dimensional Analysis of Building Systems. It is a stand-alone structural analysis programme with a special purpose features for structural design and analysis of building systems. It is simple to use and user friendly and it is unique in its ability to address the full spectrum of tasks involved in the process of structural analysis and design. The main purpose of this software is to design multi-storey building in a systematic process. This project accomplishes a typical design project which is designed as per Indian Codes IS1893-Part 2:2000 and IS456:2000. The design involves determining the most suitable proportions of a structure and dimensioning and detailing the structural elements. Once the structure is analysed and designed it must have sufficient strength to withstand the maximum stresses to which it is subjected. This paper discuss the analysis of a conventional building (G+4) under the effect of shear forces and bending moment of beams and columns.

Keywords: ETABS, analysis, structural design, shear force, bending moment

1. Introduction

This Project is based on the analysis and design of a four storied building. The determination of general shape, specific dimension and size of a building is known as structure analysis, so that it will perform the function for it and will safely withstand the influences which will act on throughout its useful life. In short, the specification of the required structure is the most important thing to decide many aspects of the structure, such as functional safety and economic aspects. The entire process of structural planning and designing requires not only imagination and calculations, but also science knowledge of Structural Engineer.In this Project, an effort made on planning, analysis and design of residential building using E-TABS. We have taken a plan of a building on the basis of which the analysis will be done for the whole structure. For the analysis of a building one has to consider all the possible loadings and see that the structure is safe against all possible loading conditions. The dead load and live loads are calculated and applied and the design for beams, columns, footing and slabs are obtained. Analysis of beams and columns has been done using E-TABS software.

2.Significance of The Study

Analysis of a building means the estimation of the response of structures towards variable external loads considering all the deviants that may occur. During the preliminary design-stage the estimated external load is used to design the size and geometry of the structures of interconnected members by using local building code and specifications of the area where the structure is located. Therefore, assuring the structural integrity, durability etc. Neglecting this crucial analysis and design stage or erring during the process will result in catastrophic failure within the building structure which can, in the worst-case scenario may lead to the loss of lives. Since this stage is the most important, the margin of error is required to be close to zero. We are making use of a software called ETABS, which is a highly efficient structural analysis and design programme consisting of modelling tools, code-based load prescriptions, analysis methods and solution techniques. Through this study we want to signify the importance of analysing and design of a multi - storey building to ensure that it satisfies the safety and serviceability requirements with help of the software ETABS.

3.Review Of Related Studies

Balaji.U and Selvarasan (2016) used ETABS to analyse and design a multi-storeyed building which was under static and dynamic loading. In the study a G+13 storey residential building was studies for earthquake loads using ETABS. Here they assumed that the material property to be linear, static and dynamic analysis were performed. The non-linear analysis was performed by considering severe seismic zones and the behaviour

[

was assessed by considering type II soil condition. Various results like displacements, base shear were plotted and studied.

Geethu (2016)carried out a comparative study on analysis and design of a multi-storeyed building by STAAD.Pro and ETABS software's. They concluded that while comparing both the results, ETABS software shows higher values of bending moment and axial force

Mr.Raghunandan M and Mrs. Suma Devi (2107)used ETABS non-linear software for simulation of adjacent multi-storeyed RC frame buildings of 15 storey and 10 storey. The provisions which may reduce the effects of pounding like the separation distance, addition of shear walls, lateral bracings and variation in storey height of the buildings have been considered for analysis. The results by considering both fixed and base isolated conditions were arrived.

Mr. Abhayguleria (2016) pointed out that ETABS is commonly used to analyse: skyscrapers, parking, garages, steel & concrete structures, low and high-rise buildings and portal frame structures. The case study in this paper mainly focuses on structural behaviour of a multi-storey building for different plan configurations like rectangular, C, L and I-shape. Modelling of 15- storey RC framed building is done on the ETABS software for analysis. Post analysis of the structure, maximum shear forces, bending moments, and maximum storey displacement are computed and then compared for all the analysed cases.

4.Objectives Of The Study

- To analyze the G+4 building using the software ETABS.
- To design the building for stability, serviceability and also it must be economical.

5.Hypotheses Of The Study

- Awareness on healthy dietary habits among prospective teachers are moderate.
- There is no significant difference between prospective teachers in their awareness on healthy dietary habits with reference to the following background variables.

(i)Gender (ii)Locality of residence (iii)Nature of college (iv)Type of family (v)Medium of Instruction

- There is no significant difference among prospective teachers in their healthy dietary habits with reference to father's and mother's educational qualification

6.Methodology

6.1 Project details

Safe bearing capacity of soil (SBC) = 200KN/mm^2

Total height of the building = 15.5m

An already existing G+4 building of plan 15m×20m is considered. It is situated in zone II. The soil condition is medium. The overall height of the building is 15.5m with basement height of 3.5m and the typical floor height is 3m. the building consists of columns of size 230mm×500mm and beams 230mm×450mm respectively. The plan of the layout of the column is as shown in the fig.6.1 and the corresponding elevation in fig.6.2

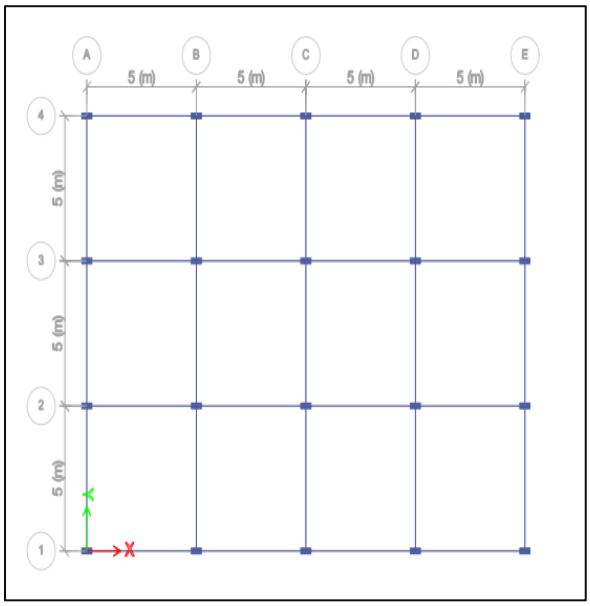

Fig 6.1.1 Column layout of the building(plan)

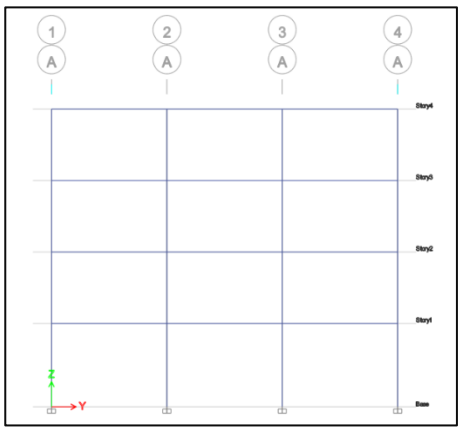

Fig 6.1.2 Building Frame

6.2 Modelling

Step 1: New Model

- Press (File and choose New Model)
- Choose the following settings.
- Design the (Grid Only) according to the plan of beams (Spacing method). Fill the Uniform grid spacing.

Step 2: Defining the Material Properties

- Defining the materials type like concrete, steel, rebar and masonry with their standard grade.

Step 3: Defining the Sectional Property

- Defining the column properties.

In this plan we take concrete grade as M25 for the ground floor as well as for the upper stories.

Step 4: Defining Beam Properties.

In this modelling we can take M25 concrete for the Ground Floor as well as for the upper stories.

Step 5: Defining the Slab Properties.

Step 6: Assigning all the elements to the model.

3D View of the Building

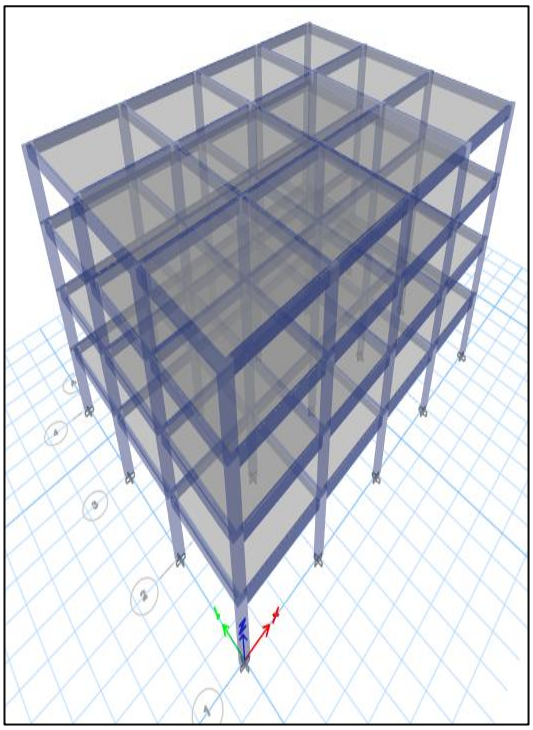

Fig 6.6 Three-dimensional view of the building

Step 7: Defining and assigning the loads

We can define the various load according to IS codes specified.

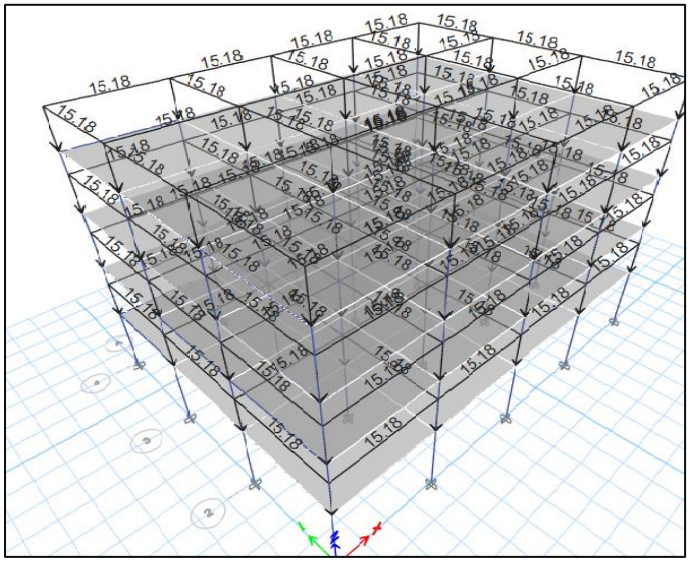

Fig7.4(c) 3-Dimensional View

Step 8: After assigning all the loads replicate the floors(G+4). We did diaphragm for the plan.

Step 9: Analyze the building.

- After the load application, we analyze the structure.
- The bending moment of the whole building is shown in

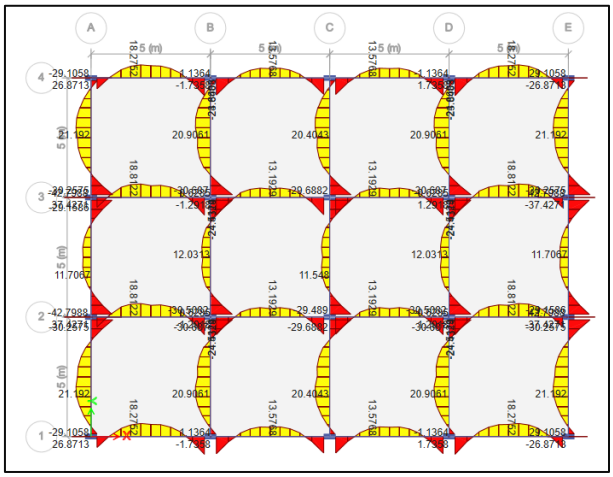

Max Bending Moment for Beams and column

Maximum bending moment value for beams and column

	Bending moment values KN-m	
Frames	Column	Beam
X-Direction		
A and E	30.25	29.192
B and D	31.89	20.91
C	30.57	20.4
Y-Direction		
1 and 4	24.73	18.27
2 and 3	25.86	18.81

Based on the above BM values we designed manually for Beams and Columns.

As per the design, the dimensions of Beams and columns are safe

Designing

During the preliminary design-stage the estimated external load is used to design the size and geometry of the structures of interconnected members by using local building code and specifications of the area where the structure is located. Therefore, assuring the structural integrity, durability etc. Neglecting this crucial design stage or erring during the process will result in catastrophic failure within the building structure which can, in the worst-case scenario may lead to the loss of lives. Since this stage is the most important, the margin of error is required to be close to zero.

CONCLUSION:

Analysis of a building ensures safety, serviceability, longevity and economic efficiency.

It can be done either by manually or with the help of automated computer software's.

The manual method of analyzing a building is time consuming and may result in various errors.

For this reason, we make use of computer software "E-TABS" which is efficient, reliable and precise.

With this study we like to conclude that through careful and precise analysis of buildings with the help of powerful computer software's the margin of error, the stability of the structure and an overall safe environment can be achieved.

Reference:

- **(A)** Ravi Kiran Sachin Metre,Shivanand C ghule(2017)," Comparitive study of Different types of bracing system by placing at different locations." International Research Journal of Engineering & Technology (IRJET), Vol. 4 Issue 8, May-2017
- **(A)** IS:875-1987 (part 1 to 5), "Code of practice for Design Loads in Buildings and Structures", Bureau of Indian Standards, New Delhi
- **(B)** IS:456-2000 "Indian Standard code of practice for plain and reinforced Cement Concrete", Bureau of Indian Standards, New Delhi
- **(C)** Abhay Guleria (2014): Structural Analysis of a Multi-Storeyed Building Using ETABS for different Plan Configurations". International Journal of Engineering Research & Technology (IJERT), Vol. 3 Issue 5, May-2104
- **(D)** Raghunandan MH and Suma (2015): Seismic Pounding between Adjacent RC Buildings with and without Base Isolation System, International Journal of Research in Engineering and Technology, Volume: 04 Issue: 06, June- 2015
- **(E)** Balaji and Selvarasan (2016): "Design and Analysis of multi-storeyed building under static and dynamic loading conditions using ETABS", International Journal of Technical Research and Applications.

International Journal of Research in Engineering and Science (IJRES)
ISSN (Online): 2320-9364, ISSN (Print): 2320-9356
www.ijres.org Volume 10 Issue 4 ǁ 2022 ǁ PP. 07-13

A Comparative Study of Framed Structure, Frame Tube and Tube In Tube Structures Subjected To Lateral Load Under Zone Iii And Zone V

Priyanka[1], Shivanand C.G[2], Dr. P. Prakash[3], Geetha L[4]
[1] *MTECH. In Structural Engineering, Department of Civil Engineering, The Oxford College of Engineering Bangalore- 56006, India.*
[2]*Assistant professor, Department of Civil Engineering, The Oxford College of Engineering Bangalore- 560068, India.*
Professor, Department of Construction Technology and Management, DSCE, Bangalore- 560068, India.
Assistant professor, Department of Construction Technology and Management, DSCE, Bangalore- 560068, India.

Abstract - *This study aims to understand the effect of the earthquake on framed structure, frame tube and tube in tube structures. The main objective of the study is to understand the behavior of structure with respect to story drift, story shear and story displacement. The G+39 and G+29 storied Structure are acquired for dynamic analysis. Method adopted was Response spectrum method. For the purposes of analysis software used is ETAB'S. After analysis the results are compared between framed structure, frame tube and tube in tube structures. The comparative study of frame tube structure, tube in tube structure, framed structure under Zone III and Zone V and is to be done to find most efficient structure in order to resist the lateral loads of the combined system.*

Key Word: Framed structure, Frame tube, Tube in tube, ETABS.

Date of Submission: 01-04-2022 Date of acceptance: 14-04-2022

I. INTRODUCTION

Development of the country can be accomplished through proper planning and economic development as they are the vital reasons that encourage technological progress by dogging the use of the latest materials and technological systems. The main concept of tubular structures is to design the tall structure as a vacant cantilever vertical to the surface of ground which can resist the lateral loads. These structures consist of ring of columns at the edge of the structure are closely spaced columns and these columns are connected to each other by deep spandrel beams through moment connections. In this tube at the exterior of the building a very stiff moment resisting frame i.e. a tube is formed which provides the lateral resistance to the building or structures.
The tubular structures of much type have been developed to resist the lateral loads.

- **Frame tube**
- **Tube in tube**

1.1 Framed Tube

In this tube at the exterior of the building a very stiff moment resisting frame i.e. a tube is formed which provides the lateral resistance to the building or structures. This exterior framed tube consists of closely spaced columns at a distance of 6-12 ft between centers; these columns are connected to each other by deep spandrel beams. The peripheral framed tube and core columns or walls resist gravity or vertically downward loads while the lateral loads acts, at the face of the framed tube formed by closely set apart columns which acts as the webs, when aligned along the loading direction, and act as the flanges when the loading direction is normal to the tube surface .

Fig. 1.1 Chestnut Dewitt Apartments, Chicago, 1965

1.2 Tube In Tube

Tube in Tube structure is new technology with advancement to the framed tube structure in these structures along with an outer frame tube which is called as the Hull there is an additional internal elevator and service core frame tube called as Core. Both gravity and lateral loads are resisted by the Hull and Core together. In these types of structures outer framed tube hull acts as shear component and the inner core acts as the flexural component. In these structures generally high governing role of the structural tube is because of its abundantly greater structural depth.

Fig. 1.3 World Trade Centre, USA, 1972

II. METHODOLOGY

A high-rise building of G+39 and G+29 stories with framed structure, frame tube and tube in tube considered for analysis. Modal analysis and response spectrum analysis is carried out using the ETABS 2015 software. Seismic analysis of framed structure, frame tube and tube in tube structures considered for study.

2.1 Response spectrum analysis:

Response spectrum analysis is most widely used in seismic analysis of a structure. A response spectrum is a graphical representation of the peak or steady-state response (displacement, velocity or acceleration) of a series of oscillators of varying natural frequency. Response spectrum analysis is more optimistic for design purpose compared to static analysis. Typical Response spectrum curve as shown below.

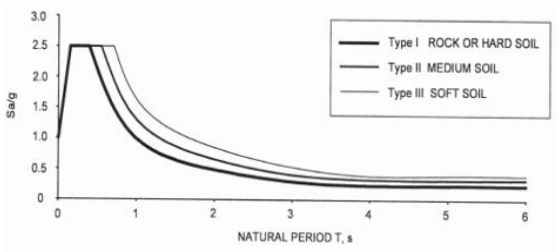

Fig:1.1.Response Spectrum analysis

2.2. BUILDING SPECIFICATIONS

2.2.1. Plan details

- (G+39) and (G+29) story building
- No. of bays along x direction - 8
- No. of bays along y direction - 8
- Spacing between two bays – 7.5m
- Story height - 3.5m
- Soil type - I (hard)
- Location – Zone III and Zone V
- Grade of concrete - M25
- Grade of steel - Fe415
- Response reduction factor – 5
- Impedance factor - 1.5

2.3. Modelling:

A high-rise building of G+39 and G+29 story with framed structure, frame tube and tube in tube analyzed using ETABS software. Model consists of G+39 and G+29 story with a typical floor height of 3.5 m. The building plan consists of 8 bays along the direction x and 8 bays along the direction y direction.

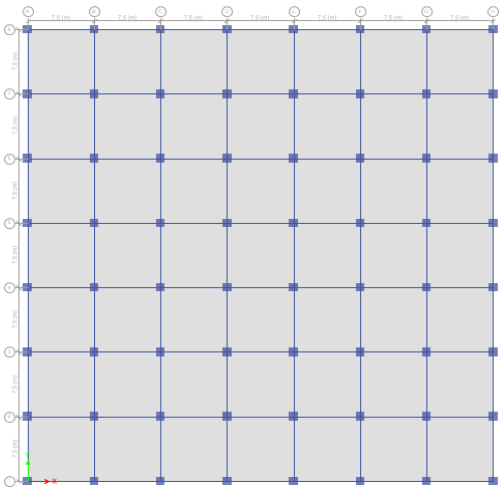

Fig: 1.2. Plan of a framed structure

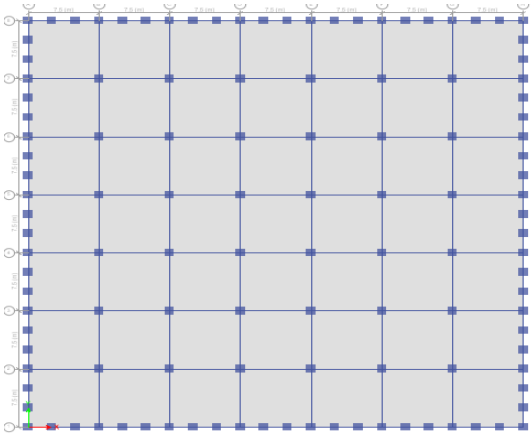

Fig: 1.3. Plan of a frame tube

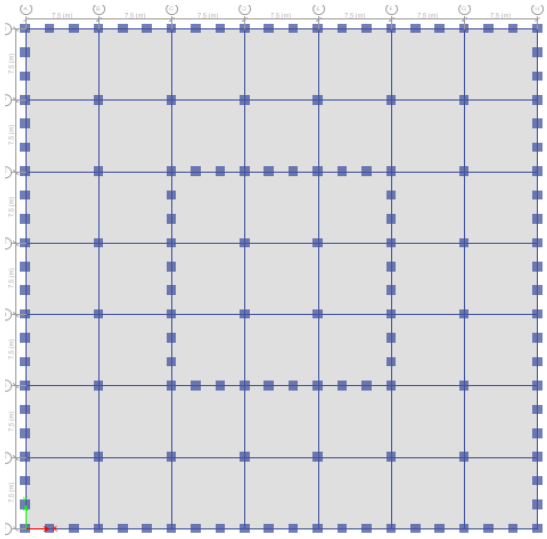

Fig: 1.3. Plane of tube in tube

2.4. Loads and dynamic parameters considered for study:

Dead loads and live loads are considered as per IS 875 Part III. The structural elements were designed in compliance with IS 456-2000 and IS 1893-2002, with regard to grades M 25 of concrete and Fe 415 of steel. The complex parameters considered for the study of the response spectrum method. Designed building dimensions are shown in Table.

Table-1. Details of Load

Dead load	Self Weight of Building
Live load	4 kN/m^2
Floor Finish	1 kN/m^2
Young's modulus of concrete	25X10^6 kN/m^2
Density of steel	76.59kN/m^3
Density of concrete	25kN/m^3

Dynamic parameters considered as per code IS 1893:2002 for analysis is shown below table. Seismic zone consider as III and zone V. Soil type considered as type 1 (it's a hard soil). Importance factor considered as 1.5 (commercial building). Response reduction factor is 5.

Table-2: Details of dynamic parameters.

Seimic zone	**III and V**
Soil type	**I (hard)**
Importance Factor	**1.5**
Response reduction factor	**5**

Table-3: Dimensions of Building Components

Column (G+39)	C1 – 1000mm x 1000mm (Ground to 10th floor) C2 – 800mm x 800mm (11th to 20th floor) C3 – 600mm x 600mm (21st to 30th floor) C4 – 500mm x 500mm (31st to 40th floor)
Column (G+29)	C1 – 1000mm x 1000mm (Ground to 10th floor) C2 – 800mm x 800mm (11th to 20th floor) C3 – 600mm x 600mm (21st to 30th floor)
Beam	300mm x 450mm
Slab	150mm thick

3. Modelling procedure of response spectrum analysis:

Step 1: Defining a response spectrum function

Define – function – Response spectrum functions – select code - add new function

Step 2: Defining the load cases of RSA

Define – load cases - Add new case
Load case 1 – RSX
Load case 2 – RSY
scale factor = Ig /2R
Step 3: Run analysis
Step 4: Scaling up of base reactions of seismic analysis and response spectrum analysis After analysis, the base reaction of EQX and RSX load case are not same, by using below formula can make base reaction same.
Scale factor = BASE REACTION OF EQX/ BASE REACTION OF RSX x I_g /2R

III. RESULTS AND DISCUSSION

General:
Earthquake load are considered for the analysis of all the models. ETABs software is used for the analysis of all the models. The results such as displacement, storey drift and base shear are considered for analysis.

4.1 Storey wise displacements due to seismic loads for Framed structure, Frame tube and Tube in tube in Zone III AND Zone V (G+39) along X-direction (Response spectrum method).

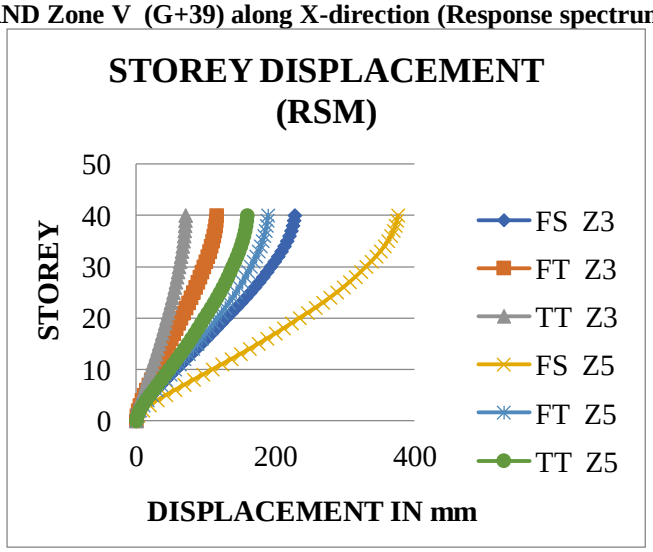

4.2 Storey wise displacements due to seismic loads for Framed structure, Frame tube and Tube in tube in Zone III AND Zone V (G+29) along X-direction (Response spectrum method).

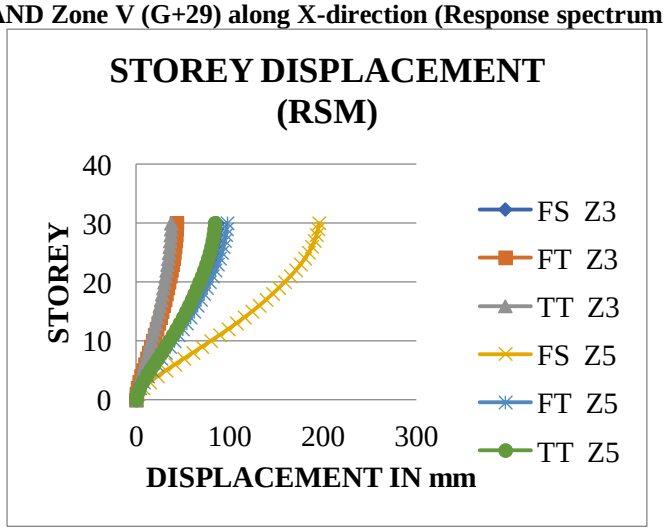

4.3 Storey wise displacements due to seismic loads for Framed structure, Frame tube and Tube in tube in Zone III (G+39) and (G+29) along X-direction (Response spectrum method).

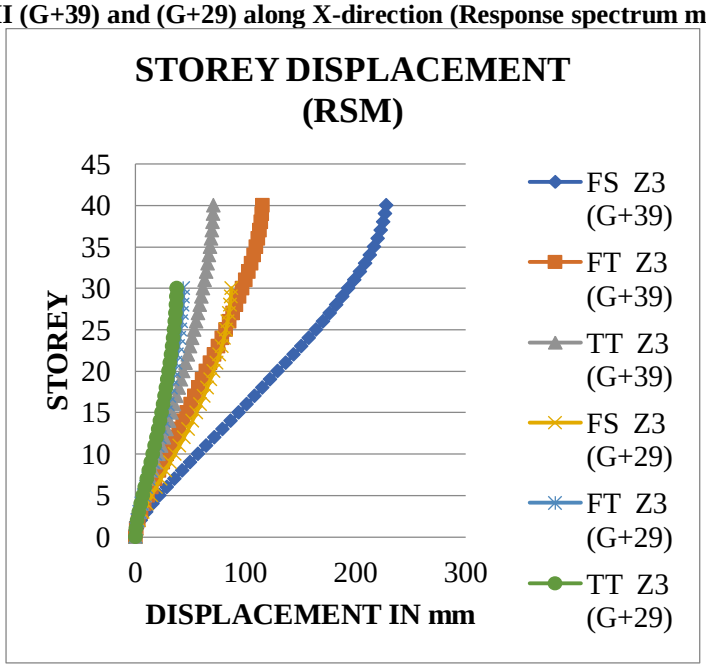

4.4 Storey wise displacements due to seismic loads for Framed structure, Frame tube and Tube in tube in Zone V (G+39) and (G+29) along X-direction (Response spectrum method).

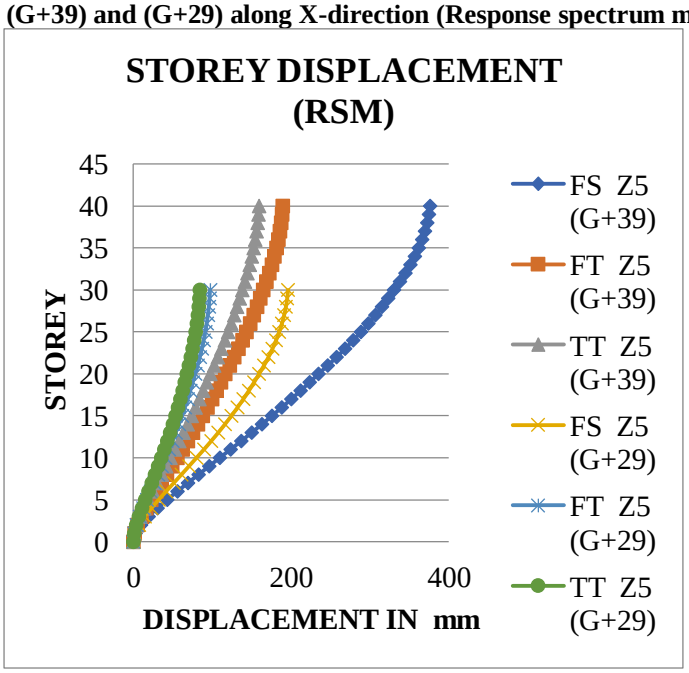

4.5 Storey wise drifts due to seismic loads for Framed structure, Frame tube and Tube in tube in Zone III AND Zone V (G+39) along X-direction (Response spectrum method).

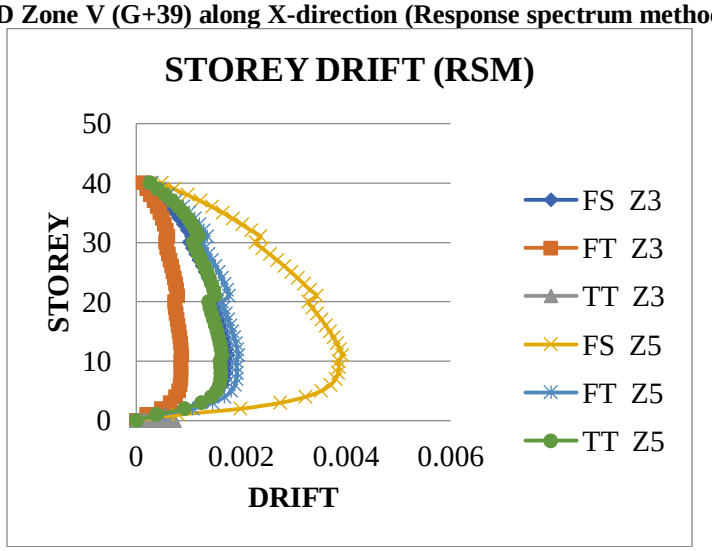

4.6 Storey wise drifts due to seismic loads for Framed structure, Frame tube and Tube in tube in Zone III AND Zone V (G+29) along X-direction (Response spectrum method).

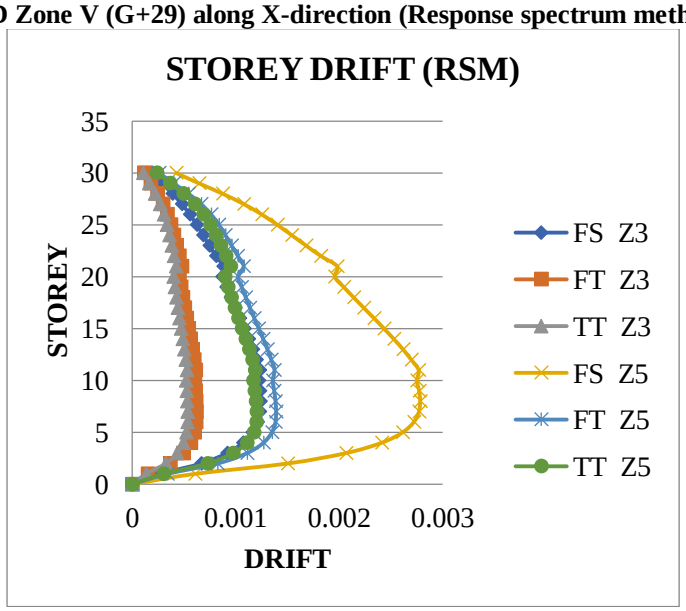

4.7 Storey wise drifts due to seismic loads for Framed structure, Frame tube and Tube in tube in Zone III (G+39) and (G+29) along X-direction (Response spectrum method).

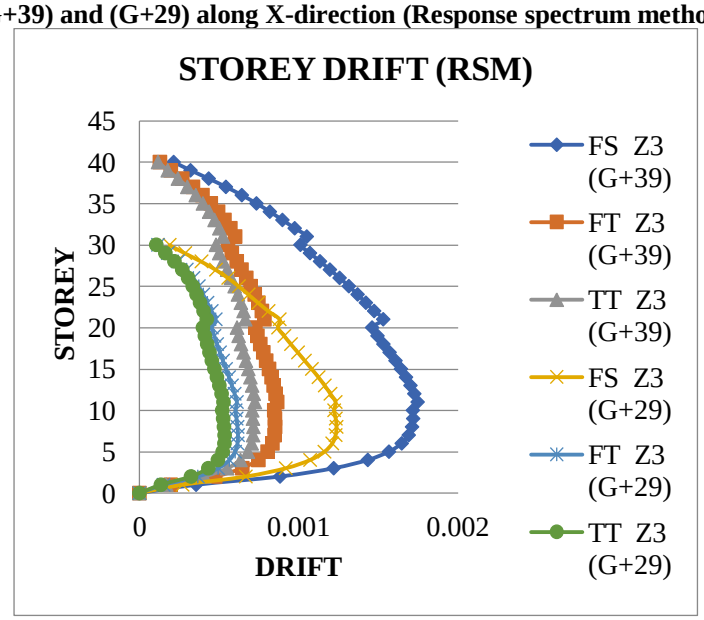

4.8 Storey wise drifts due to seismic loads for Framed structure, Frame tube and Tube in tube in Zone V (G+39) and (G+29) along X-direction (Response spectrum method).

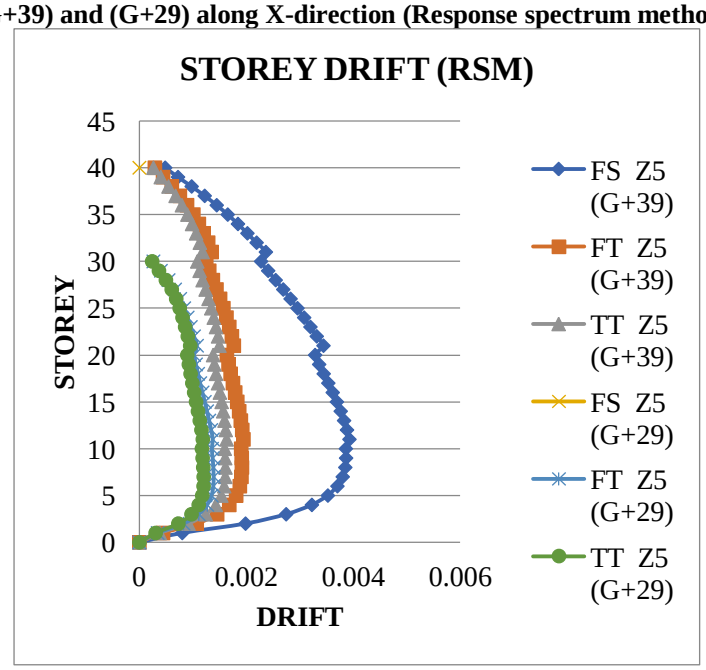

4.9 Comparison of maximum displacements of Frame structure, frame tube and tube in tube models due to seismic loads in Z0NE III and ZONE V (Response spectrum Method)

Table 4 : Maximum displacements for FS FT,TT (G+39)

MODELS	STOREY DISPLACEMENT (mm)	PERCENTAGE (%) CHANGE (COMPARED TO FS Z3)
FS Z3	227.751	0
FT Z3	115.316	49.37% (Decrease)
TT Z3	70.826	68.91% (Decrease)
FS Z5	376.165	39.46% (Increase)

FT Z5	189.341	16.87% (Decrease)
TT Z5	159.358	30.01% (Decrease)

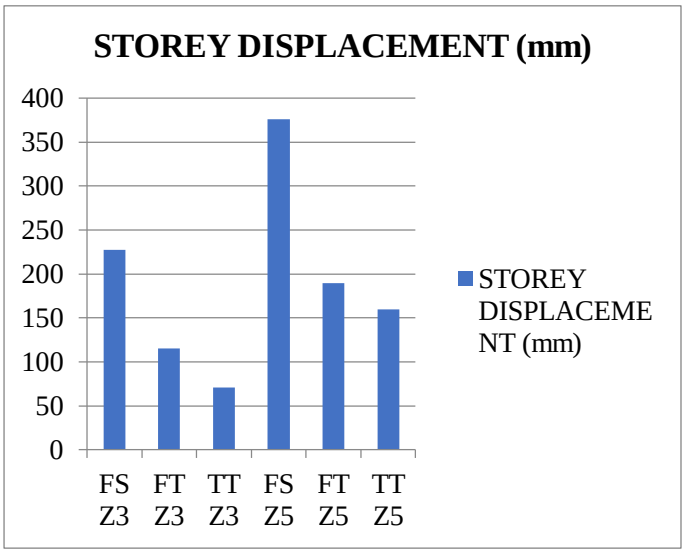

Fig 1: Maximum displacements for FS FT,TT (G+39)

The maximum storey displacements for seismic analysis from Response spectrum method is tabulated above. According to the results it can be seen that the frame structure at zone V model will have more displacements which is 376.165mm along X direction and the minimum displacements are obtained in tube in tube at zone III i.e. is 70.826mm.

Table 5: Maximum displacements for FS FT,TT (G+29)

MODELS	STOREY DISPLACEMENT (mm)	PERCENTAGE(%) CHANGE(COMPARED TO FS Z3)
FS Z3	87.112	0
FT Z3	43.385	50.20% (Decrease)
TT Z3	37.455	57.01%(Decrease)
FS Z5	196.002	55.56 (increase)
FT Z5	97.615	13.84 (increase)
TT Z5	84.274	3.26%(Decrease)

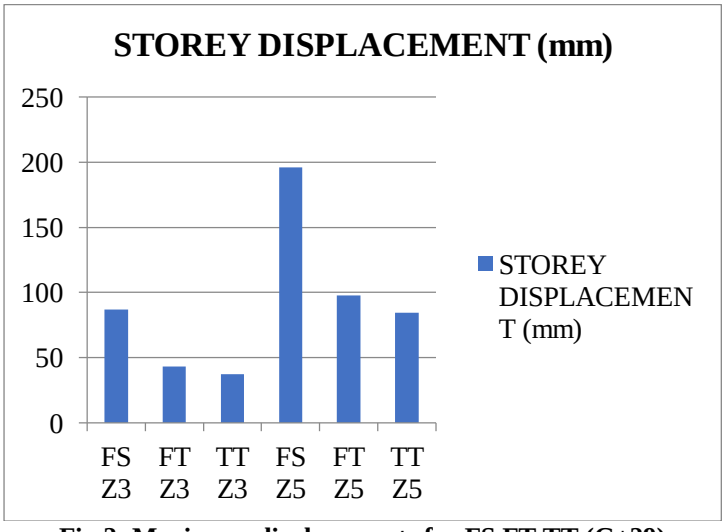

Fig 2: Maximum displacements for FS FT,TT (G+29)

Similarly, the maximum storey displacements for seismic analysis from Response spectrum method is tabulated above. According to the results it can be seen that the frame structure at zone V model will have more displacements which is 196.002mm along X direction and the minimum displacements are obtained in tube in tube at zone III i.e. is 37.455mm.

4.10 Comparison of maximum drifts of Frame structure, frame tube and tube in tube models due to seismic loads in Z0NE III and ZONE V (Response spectrum Method).

Table 6: Maximum drifts for FS FT,TT (G+39)

MODELS	STOREY DRIFT	PERCENTAGE (%) CHANGE (COMPARED TO FS Z3)
FS Z3	0.001747	0
FT Z3	0.000865	49.51%(Decrease)
TT Z3	0.000725	41.49%(Decrease)
FS Z5	0.00393	44.44% (Increase)
FT Z5	0.001946	10.23% (Increase)
TT Z5	0.001632	93.41% (Decrease)

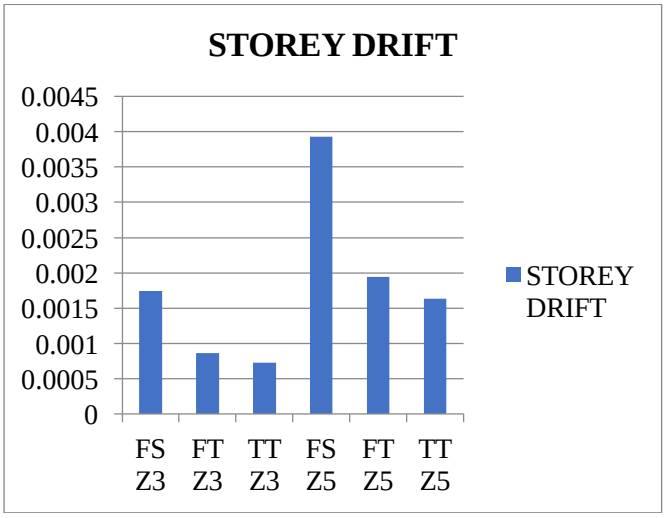

Fig 3: Maximum drifts for FS FT,TT (G+39)

The maximum storey drifts for seismic analysis from Response spectrum method is tabulated above. According to the results it can be seen that the frame structure at zone V model will have more drifts which is 0.00393 along X direction and the minimum drift ts are obtained in tube in tube at zone III i.e. is 0.000725.

Table 7: Maximum drifts for FS FT,TT (G+29)

MODELS	STOREY DRIFT	PERCENTAGE (%) CHANGE (COMPARED TO FS Z3)
FS Z3	0.001232	0
FT Z3	0.000619	50.24%(Decrease)
TT Z3	0.000532	43.18%(Decrease)
FS Z5	0.002785	22.6%(Increase)
FT Z5	0.001392	11.5%(Increase)
TT Z5	0.001176	95.45% (Decrease)

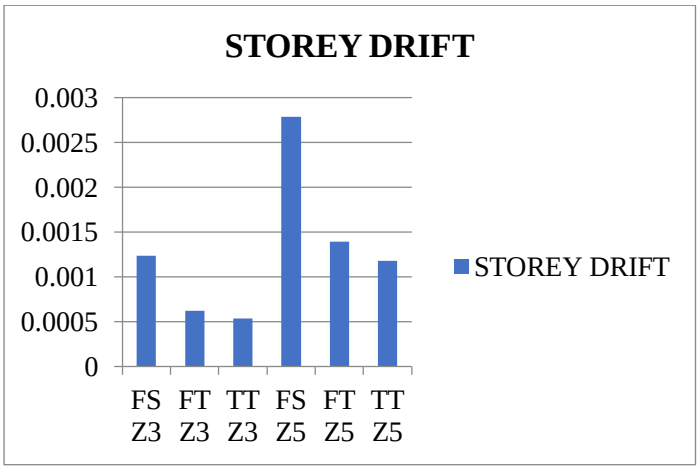

Fig 4: Maximum drifts for FS FT,TT (G+29)

The maximum storey drifts for seismic analysis from Response spectrum method is tabulated above. According to the results it can be seen that the frame structure at zone V model will have more drifts which is 0.002785 along X direction and the minimum drifts are obtained in tube in tube at zone III i.e. is 0.000532.

7.6 Comparison of base shear of Frame structure, frame tube and tube in tube models due to seismic loads in Z0NE III and ZONE V (Response spectrum Method).

Table 8: Base shear for FS FT,TT (G+39)

MODELS	BASE SHEAR (kN)	PERCENTAGE INCREASE COMPARED TO FS Z3
FS Z3	3833.32	0
FT Z3	4479.92	14.44%
TT Z3	4757.04	19.42%
FS Z5	8624.97	55.56%
FT Z5	10015.37	61.73%
TT Z5	10656.74	64.03%

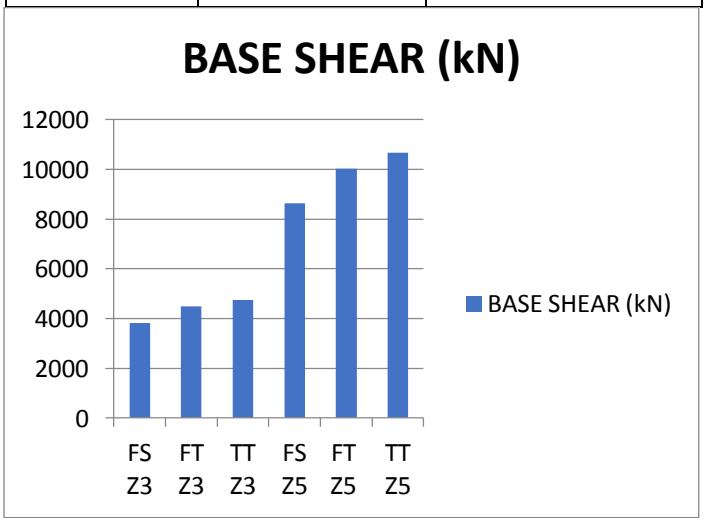

Fig 5: Base shear for FS FT,TT (G+39)

The base shear for seismic analysis from Response spectrum method is tabulated above. According to the results it can be seen that the tube in tube structure at zone V model will have more base shear which is 10656.74 along X direction and the minimum base shear obtained in framed structure i.e 3833.32 at zone III.

Table 9: Base shear for FS FT,TT (G+29)

MODELS	BASE SHEAR (kN)	PERCENTAGE INCREASE COMPARED TO FS Z3
FS Z3	2947.32	0
FT Z3	3543.79	16.84%
TT Z3	3862.62	23.7%
FS Z5	6683.98	55.91%
FT Z5	7918.61	62.78%
TT Z5	8685.86	66.07%

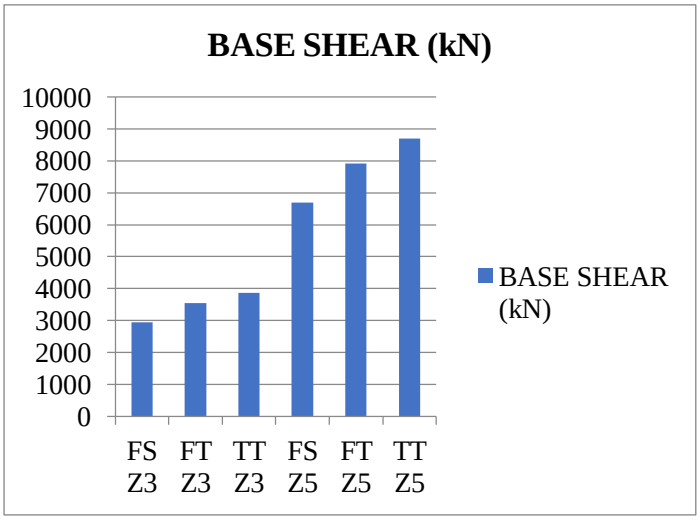

Fig 6: Base shear for FS FT,TT (G+29)

The base shear for seismic analysis from Response spectrum method is tabulated above. According to the results it can be seen that the tube in tube structure at zone V model will have more base shear which is 8685.86 along X direction and the minimum base shear obtained in framed structure i.e 2947.32 at zone III.

IV. CONCLUSION:

1. Framed structure, frame tube and tube in tube structures were compared by using parameters such as storey displacement, storey drift and base shear.
2. The results showed that the displacement values due to seismic loads for Framed structure zone V values are maximum i.e. 39.46% increases when compared to frame structure zone III at (G+39) .
3. Similarly, the results showed that the displacement values due to seismic loads for Framed structure zone V values are maximum i.e. 56.56% increases when compared to framed structure zone III at (G+29).
4. The results showed that the drift values due to seismic loads for Framed structure zone V values are maximum i.e. 44.44% increases when compared to framed structure zone III at (G+39).
5. Similarly, the results showed that the drift values due to seismic loads for Framed structure zone V values are maximum i.e. 22.6% increases when compared to framed structure zone III at (G+29).
6. The results showed that the base shear values due to seismic loads f tube in tube zone V values are maximum 64.03% more when compared to framed structure zone III (G+39).
7. Similarly, the results showed that the base shear values due to seismic loads for Tube in tube zone V values are maximum i.e. 66.07% when compared to framed structure zone III (G+29).
8. This study concludes that storey displacement, storey drift and base shear values are more in zone V as compared to zone III at (G+39) and (G+29).
9. This study also concludes that framed structure is having more displacement and drift compared to frame tube and tube in tube and tube in tube structure is having more base shear compared to framed structure and frame tube.

ORIGINAL RESEARCH PAPER

Biotechnology

MOLECULAR DOCKING OF MACELIGNAN A POLYPHENOLIC DERIVATIVE ISOLATED FROM LEUCAS CEPHALOTES &LEUCAS ASPERA ON COLORECTAL CANCER RECEPTOR PROTEIN AND ITS ADMET PREDICTION.

KEY WORDS: Macelignan, vascular endothelial growth factor – 2, cytochrome P450, caspase-3, epidermal growth factor receptor

Salma Kausar M Assistant professor, Department of Biotechnology, The Oxford College of Engineering, Bangalore, India.

Manjunatha B.K.* Professor, Department of Biotechnology, The Oxford College of Engineering, Bangalore, India. *Corresponding Author

ABSTRACT

The aim of the present study is to analyze the molecular aspects of the lignan macelignan, against colorectal cancer receptors, namely vascular endothelial growth factor 2(VEGF-2), cytochrome P450(CYP), caspase-3, BAX, BCl -2, CDK – 2 and epidermal growth factor receptor (EGFR). Macelignan identified as lignan, a polyphenolic phytocompound that has been successfully isolated from *Leucas cephalotes* & *Leucas aspera* is traditionally identified as a medicinal herb and several studies have shown that they exert antimicrobial, anticarcinogenic and antiaging property. The docking studies have proven to be an essential tool for opening up the structural diversity of natural products to be used in an orderly manner. Molecular docking was effectively done with Schrodinger Glide software version 2020-4. The binding affinity was found to be in the range of -7.8 to -6.3 kcalmol^{-1}. From the toxicity assessment, which was carried out with pkCSM online server, it was found that the macelignan had no show skin sensitization, hepatotoxicity and AMES toxicity and that the ADMET behavior was within the acceptable limits of the drug behavior.

1. INTRODUCTION

Colorectal cancer (CRC) is the 3rd most rampant cancer witnessed in both males and females and the second most common in terms of mortality rate. Globally 10% and 9.2% of men and women are diagnosed with CRD and has caused over 500,000 deaths annually.[1]. CRC results from the atypical division and progressive growth of colon cells. This abnormal cell division forms polyps, which may be benign or cancerous. The cause of these abnormal divisions is yet to be fully understood[2].

Like most cancers, CRC does not show any significant symptoms in infancy, which makes it difficult to detect early. However, the commonly associated symptoms include changes in stool frequency, rectal bleeding, abdominal pains, weakness, and weight loss[3]. CRC is detected by sigmoidoscopy or colonoscopy while treatment proceudres include surgery, radiation therapy and drug treatments, viz; chemotherapy, targeted therapy, and immunotherapy [4], [5]. The apoptosis suppression is often associated with an increased expression of anti-apoptotic proteins and a decreased countenance of pro-apoptotic proteins [6], [7]. Few important examples of carcinogenic macromolecules are B-cell lymphoma 2 (Bcl-2), vascular endothelial growth factor receptor 2 (VEGFR-2), cyclin-dependent protein kinase 6 (CDK-6), CDK-2, [8], Bcl-2 associated X protein(BAX) [9], EGFR [10], Caspase-3[11], cytochrome P450[12]. All of these receptors/proteins can be used as potential therapeutic targets for cancer therapy.

Macelignan also termed as Anwulignan is classified as a polyphenolic belongs to the class of lignans compound. Macelignan found in the nutmeg mace of Myristica fragrans is gaining importance as a new source in treating various diseases. Macelignan has been shown to hold a variety of pharmacological activities, including antibacterial, antiinflammatory, anticancer, antidiabetic, and hepatoprotective activities; Recently, studies have also reported neuroprotective activities [13].

Various invitro, *Invivo*, and *Insilco* methods were employed to evaluate the anticancer potential of drugs molecules. Among these methods, docking has been widely used as a tool in drug discovery and designing for cancer [14], [15]. Molecular docking is used as a striking framework to understand biomolecular interactions of drug for drug design and discovery as well as for mechanistic investigation by placing a ligand mainly at the preferred binding site of the target specific region of the receptor (DNA/protein) primarily in a non-covalent manner to form a constant composite of potential efficacy and specificity. The core objective of molecular docking is to obtain ligand-receptor complex with optimized conformation and with the purpose of having reduced binding free energy[16], [17]. An insilico analysis is performed by docking a molecule to envisage its action with the selected target cell. Docking is an effort to complement the ligand, a small molecule within the receptor that is a large protein molecule[18]. In addition, evaluating docking activity which is one of the principal stages in drug design, is the evaluation of the pharmacokinetic attributes of a compound under study. ADMET analysis using an animal model is expensive, therefore molecular modelling is used to predict the chemical properties, pharmacokinetic properties (ADME), and compound toxicity [19], [20].

In the present study macelignan was screened for its binding affinity for colorectal receptor molecules through *Insilico* approach towards finding the best lead that can be a novel antagonist in inhibiting the progression of CRC.

MATERIALS AND METHODOLOGY

I. Insilco study

a. Ligand preparation

PDB file of macelignan was given as an input to SCFBio software to interpret the drug-likeness of macelignan. The 3D crystallographic structure of macelignan was obtained from PUBCHEM in sdf format. The ligand structure was prepared by LigPrep wizard of Maestro. OPLS3e force field was selected. pH 5-9 was set to generate states, possible tautomers were generated and specified chiralities were retained. The output format was set to maestro [21].

b. Receptor Preparation

Protein preparation wizard of Maestro software was used for protein preparation. The receptor structures namely 4SO0 (BAX), 2O2F (BCl-2), 5I9B (Caspase-3), 4NZ2 (CDK-2), 1M17 (EGFR), 2OH4 (VEGFR), were taken from Protein Data bank [22]. Bond orders were assigned, zero-bond orders to metals and sulphide bridges were created, missing side chains and loops were filled using Prime, water molecules beyond 5 Å were deleted and hetero states at 7 +/- 2 were generated. H-bonds assignment was optimised based on sample water orientations using PROPKA. Finally, the protein structure was minimized in the OPLS3E force field to the default Root Mean Square Deviation (RMSD) value of 0.30 [23].

c. Site prediction

The possible binding sites on the receptor were predicted using SiteMap from the system tray. The option for potential high ranked receptor binding sites was checked and partial input charges were also used. The ligand binds to the receptor

Synthesis of Silver Nanoparticle Using Bioactive Phenolic Compound Extracts of Leucas aspera and Leucas cephalotes and Evaluation of its Antibacterial Activity

M. Salma Kausar, B.K. Manjunatha, C. Purvika, Mizba Farkana

Published: 31 December 2021 by Asian Journal of Chemistry (/publisher/1620) in Special Issue Iv (/wcg/container_group/48609)

Special Issue Iv (/wcg/container_group/48609) , Volume 6, pp 310-314; https://doi.org/10.14233/ajomc.2021.ajomc-p355 (https://doi.org/10.14233/ajomc.2021.ajomc-p355)

Publisher Website (https://doi.org/10.14233/ajomc.2021.ajomc-p355)

Google Scholar (https://scholar.google.com/scholar_lookup?title=Synthesis+of+Silver+Nanoparticle+Using+Bioactive+Phenolic+Compound+Extracts+of+Leucas+aspera+and+Leucas+cephalotes+and+Evaluation+of+its+Antibacterial+Activity&publicatio p355&journal=Special+Issue+Iv&pages=310-314)

Show/hide abstract

Abstract: The present study was carried out to investigate the antibacterial activity of the bioactive phenolic extract from Leucas aspera and Leucas cephalotes. The phenolic compounds were extracted using water: ethanol (1:3, v/v) by hydroethanolic extraction method. The hydroethanolic extracts were subjected to qualitative and FTIR analysis as a confirmatory step for the presence of phenolics. Synthesis of silver nanoparticle from both plants was carried out by acid hydrolysis method and subjected to UV-visible spectrophotometry, SEM, TEM and XRD analysis, for confirmation of tagged bioactive compound to AgNO3. The nanoparticle size distribution ranged between 50-94 nm in L. aspera and 40-67 nm in L. cephalotes. The antibacterial study was carried out using both crude phenolic extract and synthesized nanoparticles and tested against 5 pathogens namely Escherichia coli (ATCC® 8739™), Pseudomonas aeruginosa (ATCC® 25619™), Staphylococcus aureus (ATCC® 6538™), Bacillus subtilis (ATCC® 11774™) and Klebsiella pneumonia (ATCC® 13882™) for their antibacterial activity. From present study, the crude extract of L. cephalotes showed good antibacterial effect against test pathogen species wherein highest inhibition was observed in, P. aeruginosa, followed by B. subtilis and S. aureus with an average zone of inhibition of 23, 14 and 12 mm, E. coli and K. pneumonia measured 9 and 7 mm. The crude extract of L. aspera showed the highest inhibition in P. aeruginosa followed by S. aureus and E. coli with an average zone of inhibition of 12,11 and 10 mm B. subtilis and K. pneumonia measured 8 and 7 mm. Statistical analysis was calculated using One way ANOVA and was found to be statistically significant with $p < 0.05$.

Keywords: antibacterial / phenolic / ATCC / Leucas aspera / nanoparticle / extract / cephalotes

(https://www.altmetric.com/details.php?domain=www.scilit.net&doi=10.14233%2Fajomc.2021.ajomc-p355)

Click here to see the statistics on "*Special Issue Iv" (/wcg/container_group/48609)* .

References (*12*)

Show/hide references

DOI: 10.7860/JCDR/2022/53339.15787

Original Article

Biotechnology Section

In-vitro Study of Macelignan as a Potential Anticancer Drug against Colorectal Cancer using HCT116 Cell Line

M SALMA KAUSAR[1], BK MANJUNATH[2]

ABSTRACT

Introduction: Many recent studies have shown that lignans from many plant sources have an effective impact on cancer treatment and it is evident that many medicinal plants are rich in lignans. Genus *Leucas* is known for its medicinal use and is rich in lignans. Macelignan a polyphenolic derivative might play significant roles as clinically useful anticancer agents in treating Colorectal Cancer (CRC).

Aim: Isolation, characterisation and pharmacological profiling of bioactive compound lignan from *Leucas aspera* and *Leucas cephalotes* and to assess the anticancer potential using in-vitro methods using Human Colorectal Cancer (HCT116) cell lines.

Materials and Methods: This in-vitro study was conducted from August 2018 to January 2020 at The Oxford College of Engineering in Bengaluru, Karnataka, India. Anticancer potential of Macelignan was evaluated through 3-(4,5-Dimethylthiazol-2-yl)-2,5-diphenyltetrazolium bromide (MTT) assay, Reactive Oxygen Species (ROS) measurement, cell cycle study, apoptosis analysis, and gene expression studies. One-way Analysis of Variance (ANOVA) was performed for the total phenolic content estimation and the results were expressed as mean±SD with n=3 trials.

Results: The MTT assay result indicated that macelignan has an IC50 value of 22.8 µM with 73% of cells showing inhibition, ROS production was enhanced 2.5-fold at a maximum concentration at 100 µM. Macelignan (12.5 µM and 25 µM) significantly prevented cell growth in G0/G1 and G2 phases of the cell cycle, while the apoptotic study showed that 12.5 µM and 25 µM macelignan induced early and late apoptosis in HCT116 cells with 21.28% and 19.17%, 21.54 % and 29.02% apoptosis at cellular level, respectively. This set of tests sought to examine the effect of macelignan on the *Caspase 3* gene expression in HCT116 cells by semi-quantitative Polymerase Chain Reaction (PCR). The study showed that *Caspase 3* expression was upregulated up to 1.98 and 2.87 folds when treated with macelignan.

Conclusion: The macelignan could serve as a potent drug derivative for the treatment of colon cancer with further study on the mechanism of action, structure-activity relation, toxicity profiling, bioavailability.

Keywords: Apoptosis, *Caspase 3*, Cell growth, Cytotoxicity, Human colorectal cancer, Reactive oxygen species production

INTRODUCTION

Cancer is one of the most serious health issues affecting the length and quality of human life and has been classified as one of the deadliest diseases affecting mankind worldwide. Limited success has been witnessed even with enormous effort put to cope with the disease. Since conventional therapeutic strategies do not meet the essential requirements for successful cancer therapy, the use of natural bioactive compounds isolated from medicinal plants such as *Leucas aspera* as anticancer agents has emerged as an alternative safe, inexpensive, and convenient method. Four of the most common cancers are lung, breast, prostate, and colon cancer [1].

Colorectal Cancer (CRC) is predominantly the 2nd most fatal cancer and the 3rd most widespread malignant tumour globally. A 2018 survey reported 1.8 million new CRC cases and 881,000 deaths, accounting for nearly 10% of new cancer cases and deaths on the global death scale [2]. Generally, CRC is characterised as an uncharacteristic growth on the internal lining of colon epithelial cells that are surgically removed upon early diagnosis [3]. The existing treatment for CRC consists of chemotherapy with solo drug fluoropyrimidine and numerous agent regimes including capecitabine, oxaliplatin, and irinotecan [4].

Leucas aspera Linn. (*L.aspera*) is a widely distributed herbaceous plant across the Indian subcontinent, which belongs to the family *Lamiaceae* and is an annual, branched plant. The taxonomic classification and anatomy of this plant are well documented through many research studies [5-8]. The plant is known to contain many potent metabolites like triterpenoids, oleanolic acid, urosolic acid, β-sitosterol, nicotine, sterols, glucoside, diterpenes, and phenolic compounds [8]. Indian traditional medicines Ayurveda and Siddha use this plant. The plant is reported to have pharmacologic activities like carminative, antihistaminic, antipyretic, and antiseptic. It is used to treat diseases like jaundice, anorexia, dyspepsia, fever, helminthic infestation, respiratory and skin diseases [9].

From the study on green synthesis of silver nanoparticles of *L.aspera*, it has been reported that these plants serve as potent herbs [10], and have been reported to contain many phytotoxic components [11].

Leucas cephalotes another species commonly called "Dronapushpi" in Sanskrit belonging to the family *Lamiaceae* as *L.aspera*, is a weed and grows in monsoon. Reportedly, two protostane-type triterpenoids named leucastrins A and B and oleanolic acid were isolated from *L.cephalotes* [12]. Triterpenoids β-sitosterol [13], stigmasterol [14], lupeol [15,16], labellinic acid isolated were also reported from *L.cephalotes* [17]. Aliphatic esters [18], essential oils [19,20], flavones [20] were other metabolites that have been successfully isolated from *L.cephalotes.*

Macelignan, a class of secondary metabolite classified as phytolignan, a polyphenolic derivative might offer new anticancer therapeutic ability and play significant roles as clinically useful anticancer agents in treating CRC [21]. In this context, the present study was undertaken to evaluate the anticancer efficacy of the macelignan isolated from *L.aspera* and *L.cephalotes* on CRC cell line HCT116, and a sincere attempt was made to provide scientific validation for the role of macelignan as a therapeutic lead molecule in treating CRC.

MATERIALS AND METHODS

This in-vitro study was conducted from August 2018 to January 2020 at the Oxford College of Engineering, Bengaluru, Karnataka, India. The experiment was carried out under a controlled laboratory environment, at the approved research centre and, this does not require ethical approval from regulatory committees.

Study Procedure

Collection of plant sample: The plants of *L.aspera* and *L.cephalotes* were collected from the Western Ghats region and Turahalli Forest of Karnataka, India. Taxonomical identification was performed and the samples were deposited with the Research and Development Centre, Department of Biotechnology, Oxford College of Engineering.

Preparation of plant extracts: Whole plants of *L.aspera* and *L.cephalotes* were washed, dried in shade, and pulverised with a blender. 100 gm of defatted plant residues were subjected to cold hydroethanolic extraction in ethanol: water (ratio 3:1), the samples were left to stand overnight and the extract was collected by vacuum filtration. The extract was concentrated and vacuum dried using a rotary flash evaporator (IKA, Germany).

Column chromatography: The polyphenols of both samples were separated using Sephadex LH-20 column chromatography. The column was mobilised by adding homogenised gel with a methanol solution concentration of 99.9%. Fractions containing polyphenols were pooled and subjected to High Performance Liquid Chromatography (HPLC) for purity [22].

Estimation of total phenolic content by Folin-Ciocalteu (FC) method: Phenolic content present in the extract reacts with the phosphomolybdic acid present in the FC reagent and forms a blue complex (molybdenum blue). Aliquots of the gallic acid standard (0.2-1.0 mL) and simultaneously 0.1 mL of crude extract and a sample eluted from column chromatography were taken and methanol was added to all tubes to increase the volume to 3.0 mL. Total 0.5 mL of Folin-Ciocalteu reagent was added to tubes and incubated for six minutes at Retention Time (RT) and 1.0 mL of 20% Na_2CO_3 was added and incubated for 1 hour in the dark. The developed blue colour was read at 650 nm. Gallic acid was used as the standard and total phenolics were expressed in Gallic Acid Equivalent (GAE)/100 mg [23,24].

High Performance Liquid Chromatography (HPLC): Sephadex LH-20 Column chromatography was used to separate polyphenols. The column was mobilised by adding homogenised gel at a concentration using 99.9% methanol solution. Polyphenol-containing fractions were combined and submitted to phenolic content estimate and HPLC purity testing (Pharmacia Corporation) to obtain pure lignan using the ODS-reverse phase column [25].

Gas Chromatography-Mass Spectrometry (GCMS) analysis: Gas Chromatography (GC) analysis was carried out using Agilent 6890N GC equipped with photon multiplier tube as detector coupled to front injector type 1079. The chromatograph was fitted with HP 5 MS capillary column (30 m×0.25 mm i.d., film thickness 0.25 mm). The injector temperature was set at 250°C, and the oven temperature was initially set at 70°C, held for 4 minutes then programmed to 200°C at the rate of 10°C/min and finally held at 200°C for 13 minutes. Helium was used as a carrier gas with a flow rate of 1.5 mL/min. 0.2 µL of the sample (diluted with methanol 1:10) was injected in the splitless mode. The mass spectrometer was operated in the electron impact mode at 70 eV. Ion source and transfer line temperature were kept at 250°C. The mass spectra were obtained by centroid scan of the mass range from 50-600 amu. The compounds were identified based on the comparison of their Retention Indices (RI), Retention Time (RT), mass spectra of WILEY, NIST library data of the GC-MS system, and literature data (Robert A, 2005), [25].

Cell lines and culture medium: Stock cells of HCT116 cell lines obtained from American Type Culture Collection (ATCC), were grown in modified Roswell Park Memorial Institute (RPMI) 1640 media with 10% inactivated fetal bovine serum (FBS), penicillin (100 IU/ml), and streptomycin (100 µg/ml) to confluent in CO_2 incubator at 37°C. The dissociation solution {0.2% trypsin, 0.02% EDTA, 0.05% glucose in Phosphate Buffered Saline (PBS)} was used to dissociate cell. The cellular viability was checked [26,27].

Cytotoxicity assay: The cytotoxicity activity of crude extract and purified bioactive macelignan was studied by 3-(4,5-dimethylthiazol-2-yl)-2,5-diphenyl tetrazolium bromide (MTT) assay. HCT116 cell lines cultured at a concentration of 10^5 cells/well were seeded in a 96 well plate and incubated for 24 hours at 37°C. Doxorubicin and Dimethyl Sulfoxide (DMSO) were used as positive and negative controls. Further, the MTT assay kit (Himedia) guidelines were followed. The absorbance was read using a microplate reader at 590 nm [28]. Half maximal inhibitory concentration (IC_{50}) values were generated from the dose-response curves for different concentrations of test drugs [28].

Reactive Oxygen Species (ROS) measurement: Intracellular levels of ROS were determined using the 2', 7'- Dichlorofluorescein Diacetate (DCFDA) method. DCFDA is a ROS-sensitive fluorescence indicator. HCT116 cells at a concentration of 5×10^5 cells/well were seeded in a 96-well titer plate and after 24 hour of incubation 100 µL of test compound with varying concentrations were added and incubated for 24 hour. Treated samples were removed from the plates and washed with 1X PBS to which 100 µL of 25 µM DCFDA solution was added and incubated at 37°C for 30 minutes. The fluorescence was measured using a microplate reader at 485/535 nm [29].

Apoptosis analysis: Apoptosis is a cell death process with morphological and biochemical characteristics that appear at different stages. Apoptosis begins with varying kinetics depending on the cell type and ends with cell disintegration and the creation of apoptotic bodies. Several alterations on the surface of apoptotic cells have previously been identified, including the expression of thrombospondin binding sites, the removal of sialic acid residues, and the exposure of phospholipid-like phosphatidylserine (PS) [30,31]. Annexin V, a member of the annexins family of anticoagulant proteins, has shown to be a valuable tool in detecting apoptotic cells since it preferentially attaches to negatively charged phospholipids such as PS in the presence of Ca^{2+} and has a low affinity to phosphatidylcholine and sphingomyelin [32].

The HCT116 cells were subjected to Flow cytometry by Annexin V- Fluorescein Isothiocyanate (FITC) staining to determine the apoptotic cell distribution. A 1×10^5 cells per well were seeded in a 96 well plate. After 18 hours, the cells were treated with different concentrations of the test sample to induce apoptosis. After 24 hours of incubation, cells were pelleted. The pellet was rinsed in cold PBS and resuspended in 1 mL 1X binding buffer. A 500 µL of cell suspension was aliquoted with 5 µL Annexin V and 10 µL of Propidium Iodide (PI), 15 minutes of incubation was done at RT in dark, followed by flow cytometric analysis [31-33].

Cell cycle analysis: Cell cycle distribution was analysed by flow cytometry using PI staining. Briefly, 1×10^6 cells were seeded and cultured for 24 hours in a 96-well plate with 2 mL serum-free media. Cells were later treated with different concentrations of test compound and incubated for 24 hours. Cells were pelleted and washed in 2 mL of 1X PBS and were fixed in 300 µL of sheath fluid and 1 mL of chilled 70% ethanol was added. Cell pellets were stained with PI (20 µg/mL) in presence of RNase A (0.05 mg/mL) and incubated for 15 minutes in the dark. Determination of percentage of cells in various stages of the cell cycle in treated and untreated populations was done using Fluorescence-Activated Cell Sorter (FACS) Caliber (BD Biosciences, San Jose, CA) [34].

Gene expression studies: About 1×10^6 cells cultured with P35 were subjected to test sample followed with RNA isolation with TRIzol™ Reagent (In-vitro gen,) according to the manufacturer's instructions, and the extracted mRNA was further subjected to Reverse Transcription- PCR (RT-PCR). RT-PCR was carried out (Thermo Fischer VERITI Scientific system) to determine the levels of β-Actin mRNA and *caspase 3* expressions. The cDNA was synthesised from 2 µg of RNA using the Verso cDNA synthesis kit (Thermo Fischer Scientific) with oligo dT primer and the assay was performed as per the manufacturer's instructions [29]. The optimal cycles were selected for amplification of these genes experimentally such that it was in the exponential range and would not reach a plateau. Results were measured quantitatively using the optical density of the bands (computerised imaging program Image J). The values were normalised to β-Actin intensity levels.

STATISTICAL ANALYSIS

One-way Analysis of Variance (ANOVA) was performed for the total phenolic content estimation and the results are expressed as mean±SD with n=3 trials. And non linear regression analysis using Graph Pad Prism 6 software was performed for the cytotoxicity study and graphical representation of the same has been incorporated in the results.

RESULTS

1. Total Phenolic Content

In the present study, on the total phenolic content of *L.aspera* and *L.cephalotes*, *L.cephalotes* showed the highest phenolic content of 7400±152.75 mg of GAE/100 g of plant extract in comparison to *L.aspera* which recorded 7133±152.75 mg of GAE/100 gm of plant extract [Table/Fig-1a,b]. The results of this study reveal that both plants possess a considerable amount of phenolic content that offers potential radical scavenging ability.

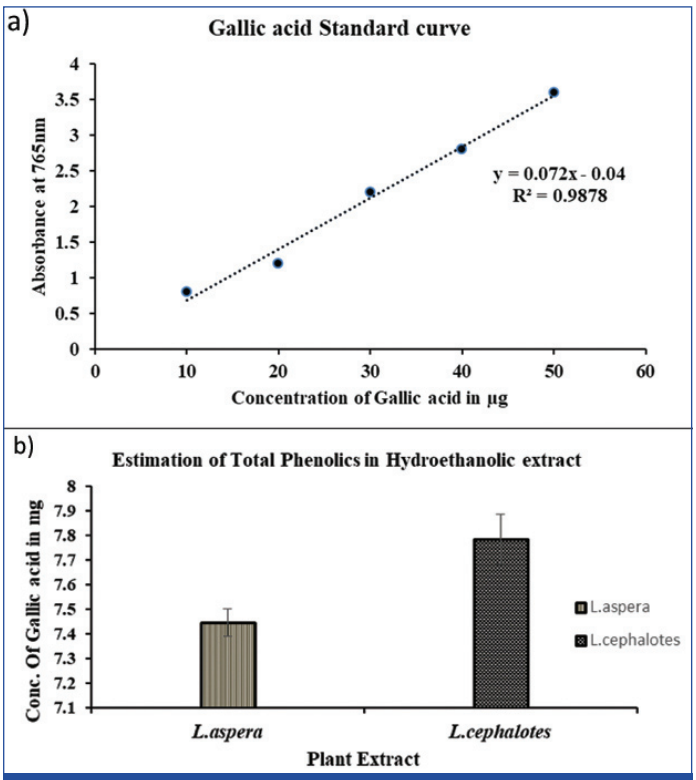

[Table/Fig-1]: a) Gallic acid standard curve for estimation of total phenolic content. b) The total phenolic content by FC method for hydroethanolic plant extract is statistically significant with p-value <0.05 and data expressed in mean±SD of 3 trials.

2. High Performance Liquid Chromatography

This analysis spectra of an eluted fraction of *L.aspera* and *L.cephalotes* showed the bioactive compound with different RTs as shown in [Table/Fig-2,3]. Various fractions were eluted by column chromatography and based on the chromatogram pattern the fractions were collected with similar Rf values and evaluated by GCMS. The hydroethanolic fraction of *L.aspera* and *L.cephalotes* yielded bioactive compounds when eluted with ethanol:water (3:1). The compounds obtained were fatty acid esters and phenolic derivatives which belong to various classes of flavonoids and lignans [Table/Fig-4-7]. One of the common compounds found in both the samples was Macelignan belonging to the lignan family of polyphenolics which has previously not been reported as isolated from *L.cephalotes* whereas the other compounds have been reported to be isolated from another family of *L.amiaceae*. As macelignan though isolated is the novel compound isolated from *L.cephalotes* which has not formed part of any previous anticancer study, an attempt to purify it was done, and its anticancer properties were evaluated against CRC using the HCT116 cell line.

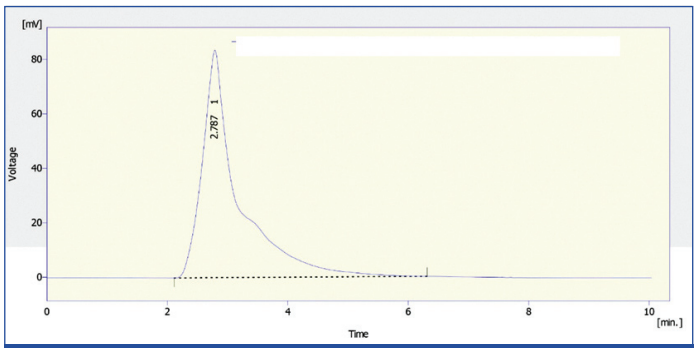

[Table/Fig-2]: Chromatogram of *L.aspera* peak showing measurement of voltage (mV) vs time (min).

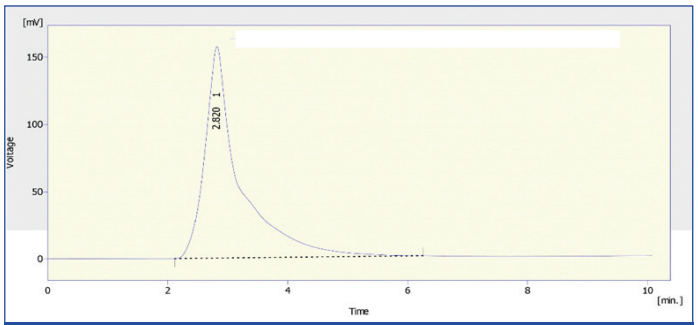

[Table/Fig-3]: Chromatogram of *L.cephalotes* peak showing measurement of voltage (mV) vs time (min).

Compound	Molecular Formula (MF)	Molecular Weight (MW) (gm/mol)	Retention Time (RT) (min)	Peak Area (PA) (%)
1,1-Cyclobutanedicarboxamide, 2-phenyl-N,N'-bis (1-phenylethyl)-	$C_{28}H_{30}N_2O_2$	426.3131	20.62	9.3
Di-(1,3,2)-oxazino (6,5-f:5',6'-H) quinoxaline, 2,3,4,5,6,7- hexahydro-3,6-bis (2-diethylaminoethyl)-10,11-diphenyl-	$C_{36}H_{46}N_6O_2$	86.00	16.17	43.6
Macelignan	$C_{20}H_{24}O_4$	328.00	17.85	21.3
Corynan-17-ol, 18,19-didehydro-10-methoxy-, acetate (ester)	$C_{22}H_{28}N_2O_3$	368.47	19.34	8.4
Cyclopentanepropanoic acid, 3,5-bis (acetyloxy)-2-(3,8-bis (acetyloxy) octyl)-, methyl ester	$C_{25}H_4O_{10}$	500.6	22.18	8.0
4-(4-Diethylamino-1-methylbutylamino)-1,2-dimethoxy-6-bromonaphthalene	$C_{21}H_{31}BrN_2O_2$	423.4	14.28	5.4

[Table/Fig-4]: Compounds detected in Gas Chromatography-Mass Spectrometry (GCMS) analysis of *L.cephalotes*.

3. Cytotoxicity Test

The cytotoxicity of the isolated compound on HCT116 cells was evaluated using the MTT test. The IC_{50} of a drug was ascertained by building a dose-response curve and an examination of the effect of

Compound	Molecular Formula (MF)	Molecular Weight (MW) (gm/mol)	Retention Time (RT) (min)	Peak Area (PA) (%)
Oxirane-2-carboxylic acid,3-(3,4,5 trimethoxyphenyl)-,methyl ester	$C_{13}H_{16}O_6$	268.26	22.55	23.1
Pentadecanoic acid methyl ester	$C_{16}H_{32}O_2$	256.4	16.63	100
Octadec-9-enoic acid	$C_{18}H_{34}O_2$	282.5	18.22	100
Macelignan	$C_{20}H_{24}O_4$	328.4	17.57	21.3
9-hexadecenoic acid	$C_{16}H_{30}O_2$	254.414	20.2	14.9

[Table/Fig-5]: Compounds detected in Gas Chromatography-Mass Spectrometry (GCMS) analysis of *L.aspera*.

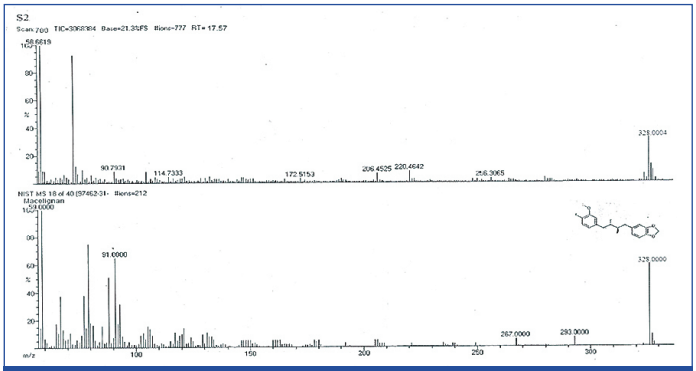

[Table/Fig-6]: Gas Chromatography Mass Spectrometry (GCMS) chromatogram of *L. aspera* hydroethanolic extract showing six major peaks of active compounds and a peak at 17.57 indicate macelignan content.

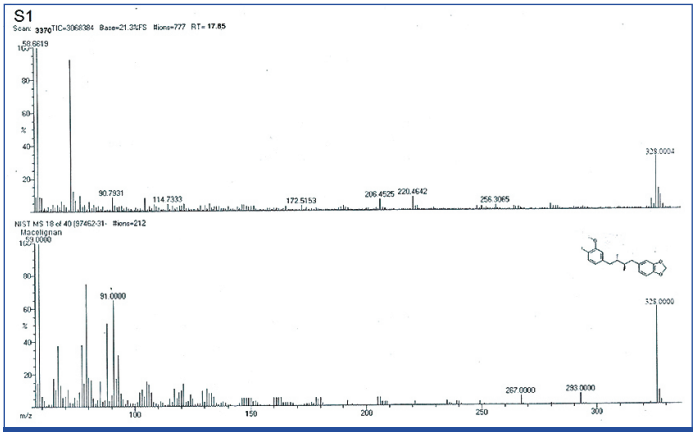

[Table/Fig-7]: Gas Chromatography-Mass Spectrometry (GCMS) chromatogram of *L. cephalotes* hydroethanolic extract showing 5 major peaks of active compounds and a peak at 17.85 indicate macelignan content.

different concentrations of antagonists on reversing agonist activity was made. The IC_{50} value of macelignan was found to be 22.83 µM while that of doxorubicin was 15 µM. From a non linear regression analysis based on the sigmoid dose-response curve (variable), IC_{50} values for cytotoxicity tests were obtained. Statistically, a non linear regression graph obtained using Graph Pad Prism 6 (Graph pad, San Diego, CA, USA) revealed that [Table/Fig-8a,b] about 73% of the cells were inhibited at a maximum concentration (100 µM) by macelignan against doxorubicin which showed 79% inhibition. Therefore, it can be considered that macelignan exhibited a cytotoxicity property as good as the standard drug.

4. Macelignan Exhibited Better Apoptosis Effect and Reactive Oxygen Species (ROS) Measurement

Flow cytometry was used for quantitative measurement of cellular apoptosis following annexin V-FITC/PI double staining. Annexin V was used as a marker to detect early apoptosis and PI to late apoptosis and necrosis. The cells treated with 25 µM of doxorubicin, induced early and late apoptosis in HCT116 cells with 48.43% and 3.71%, respectively as 12.5 µM and 25 µM of macelignan induced early and late apoptosis in HCT116 cells with 21.28% and

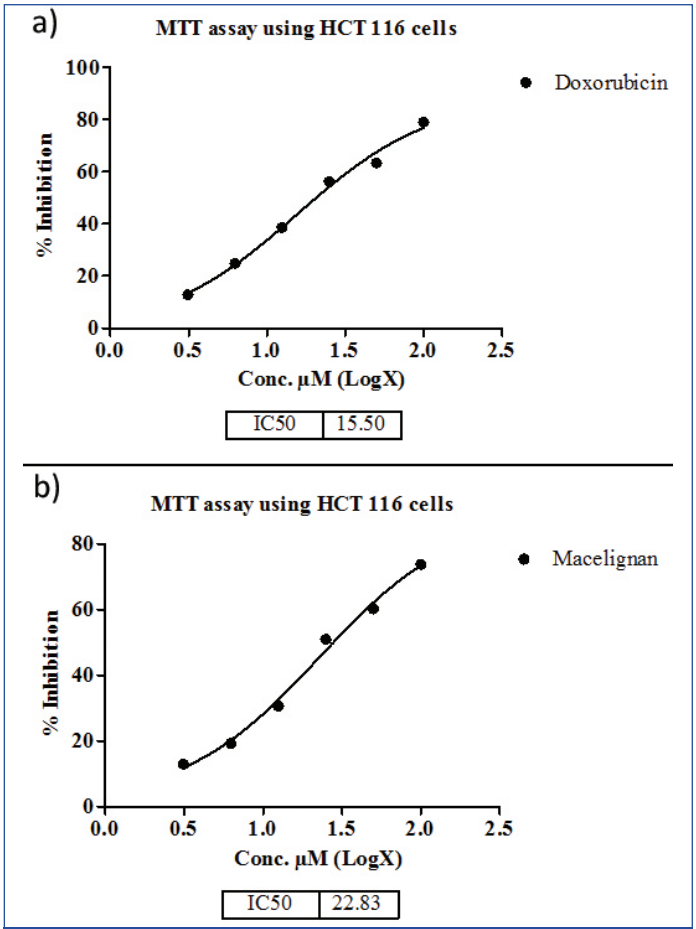

[Table/Fig-8]: Non linear regression schematic of cytotoxic effect of: (a) doxorubicin; (b) Macelignan, on the HCT116 cell line treated with varying µM concentrations.

19.17%, 21.54% and 29.02% apoptotic cells respectively. These conclusions are drawn upon observation indicated in the form of the cells scattered in the lower right and upper right region of the quadrant presented in the X-axis, as shown in [Table/Fig-9].

Sample	Percentage of cells at different apoptotic phases			
	Viable cells	Early apoptotic	Late apoptotic	Necrotic cells
Control	98.42	1.16	0.24	0.18
Macelignan 12.5 µM	58.35	21.28	19.17	1.20
Macelignan 25 µM	48.10	21.54	29.02	1.34
Doxorubicin 25 µM	46.20	48.43	3.71	1.66

[Table/Fig-9]: Percentage of the cells that has undergone apoptosis in untreated, standard and test samples treated HCT116 cells.

The results clearly show the programmed cell death-induced effect of macelignan was comparatively stronger than the control.

Intracellular ROS plays an important role in mediating cell death. The intracellular ROS levels in the HCT116 cells were measured using the DCFDA method. Measuring the fluorescence in terms of Relative Fluorescence Unit (RFU) at 485/535 nm, revealed macelignan enhanced the ROS production up to 2.5 folds at its maximum concentration (100 µM) in HCT116 cells [Table/Fig-10]. The results obtained indicate elevated levels of ROS which generally is a result of greater mitochondrial membrane potential. From our study, we infer that the 2.5-fold increase of ROS production strongly supports the cancer cell death through ROS dependent mechanism [Table/Fig-11].

5. Cell Cycle Arrest and Gene Expression Studies

The effect of macelignan on cell cycle distribution was calculated using flow cytometry. Macelignan (12.5 µM and 25 µM) stimulated arrest in G0/G1 phase and G2 phase. The percentage of cells arrested at different stages in comparison to standard doxorubicin

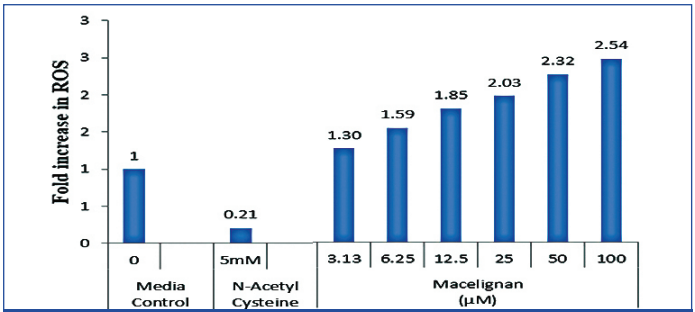

[Table/Fig-10]: ROS detection by DCFDA method, the graph illustrates the concentration of Macelignan vs. fold increase in ROS in the cells; culture media and N-Acetyl Cysteine was taken as control.

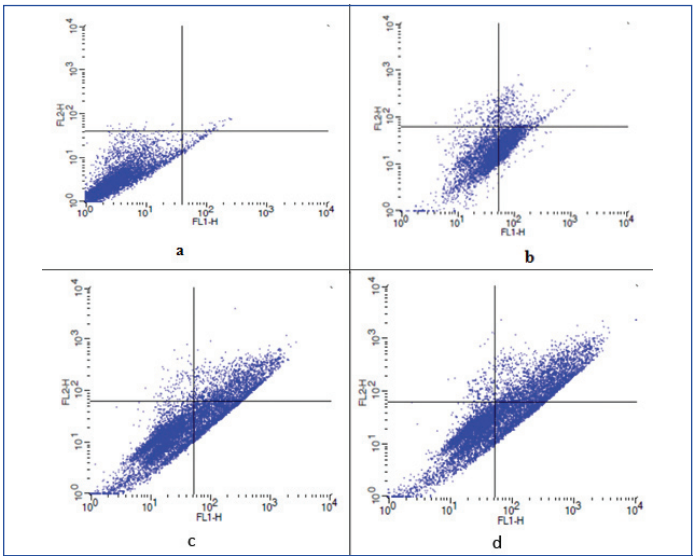

[Table/Fig-11]: Dot plots of HCT116 cells distribution due to apoptosis: (a) untreated cells; (b) treatment with doxorubicin 25 µM; (c) treatment with macelignan 12.5 µM; (d) treatment with macelignan 25 µM.

is shown in [Table/Fig-12]. A schematic of overlay representing cell cycle arrest with different concentrations of macelignan along with doxorubicin is indicated in [Table/Fig-13]. There is no direct study investigating the effect of the compound on *caspase 3* gene expression on HCT116, hence the effectiveness of cells was determined by semiquantitative PCR. β-Actin was used as a control to normalise the gene expression. The study revealed that the *caspase 3* expression was upregulated up to 1.98 and 2.87 folds in the treatment of macelignan [Table/Fig-14,15].

Samples	Percentage of cells arrested			
	Sub G0 Phase	G0/G1 Phase	S Phase	G2/M Phase
Control	0.10	86.51	6.53	7.18
Macelignan 12.5 µM	1.06	66.66	5.69	26.83
Macelignan 25 µM	1.68	59.34	12.65	26.70
Doxorubicin	3.07	43.47	38.40	16.83

[Table/Fig-12]: Percentage of cells arrested in HCT116 cells at different stages of cell cycle.

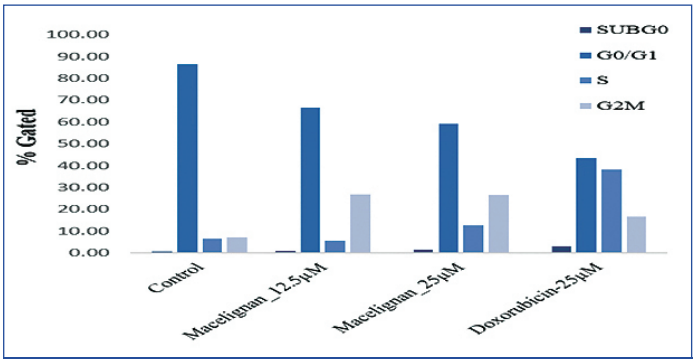

[Table/Fig-13]: Percentage of cells arrested in HCT116 cells at different stages of cell cycle.

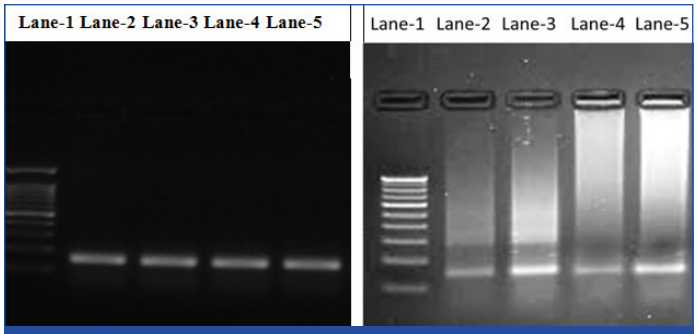

[Table/Fig-14]: (i) Amplification of β-Actin gene in HCT-116 cells; (ii) Amplification of *Caspase 3* gene in HCT-116 cells. (Images from left to right).

Samples	Concentrations	Beta-Actin expression	*Caspase 3* expression
		Lane number	
DNA Ladder		1	1
Control	0	2	2
Doxorubicin	25 µM	3	3
Macelignan	12.5 µM	4	4
	25 µM	5	5

[Table/Fig-15]: Samples details in Lane.

DISCUSSION

Since ancient times, plants and their bioactive compounds such as phenols, terpenoids, flavonoids, sterols, and coumarins are in medicinal practices and several phytoconstituents from medicinal plants species inhibit the progression and development of cancer. Several isolated phytochemicals such as flavonoids, lignans, terpenes, saponins, vitamins, etc., play a significant role in inhibiting cancer cell-activating proteins, enzymes, and signalling pathways [35]. These phytoconstituents work on various mechanisms of signaling pathways such as apoptosis and cell cycle arrest at G2/M phase, anti apoptotic proteins *c-IAP* and *Bcl-2*, activation of pro-apoptotic protein such as p21, p53, *caspases 3*, and *caspase 9*, induction of ROS, inhibition of topoisomerase-1 and cyclooxygenase, etc., [36,37]. Novel anticancer drugs could, therefore, be useful in ameliorating damage with less severe side effects than the synthetic drugs currently available.

In the present study, a systematic screening approach has been followed to isolate and purify macelignan from *L.cephalotes* and *L.aspera*. The obtained compound thus may behave in a way as to induce apoptosis in cancer cells. Another study looked into the effect of macelignan on P-gp and cytochrome P450 enzyme (CYP3A4)-mediated drug metabolism, with the goal of finding a way to improve the bioavailability of paclitaxel, an anti-neoplastic medicine with anti-tumoural properties [38]. Several researchers have reported that macelignan could possess therapeutic properties and its subsequent isolation and screening from nutmeg have shown it to work as a potent biomolecule against obesity, diabetes and also as an antiaging molecule [39].

Studies by Lee KE et al., have reported macelignan, a natural lignan compound isolated from *Myristica fragrans* Houtt. (nutmeg), to possess antioxidant and anti-inflammatory activities when investigated on mechanisms of action in UV-irradiated human skin fibroblasts (Hs68) by RT-PCR, DCFDA assay, and ELISA [40]. A review summarised by Paul S et al., suggests, that macelignan has been shown to possess a spectrum of pharmacological activities, including anti-bacterial, anti-inflammatory, anti-cancer, anti-diabetes, and hepatoprotective activities; recent studies have also suggested that it could have neuroprotective activities [21].

This study was aimed at isolating and screening macelignan as a potential anticancer drug molecule. The results obtained on the cytotoxic effect of macelignan against HCT116 showed good effect with 73% of the cancer cell inhibition at a maximum concentration of 100 µM, which was significantly compared with standard doxorubicin which showed inhibition of 79%. The effect of macelignan on apoptosis and ROS measurement are also suggestive that, this molecule could potentially induce programmed cell death at 12.5 µM and 25 µM concentrations, which was found to be better than the standard drug. The present study also infers a 2.5 fold increase in ROS production which makes macelignan a favorable bioactive molecule. The present study showed that macelignan at concentrations of 12.5 µM and 25 µM induced cell cycle arrest in the G0/G1 phase and G2 phase, and upregulation of *caspase 3* gene up to 1.98 and 2.87 folds was observed.

Limitation(s)

Though the present study suggests that macelignan could be a lead derivative, as anticancer drug molecule for CRC type. However, further investigations such as in-vivo studies, detection of its bioavailability, preclinical and clinical studies and mechanism of action at molecular level are required to authenticate the claims. Furthermore, the plant under study should be mass produced and macelignan expression has to be enhanced for increased yield.

CONCLUSION(S)

The present study concluded that the isolated natural bioactive compound from the hydroethanolic extraction method from *L.cephalotes* was identified as macelignan based on the gas chromatography mass spectrometry characterisation. Based on the findings of this investigation, it is clear that the medicinal plant in question has a secondary metabolite with therapeutic potential. These plant's phytoconstituent and antioxidant profiles indicate that they can scavenge free radicals generated in the system and so can be utilised in the development of herbal formulations. The pure compound's anticancer potential could be regarded as a novel source for obtaining the lead and developing a new herbal medicine formulation. However, more clinical research on its safety profile, dose, and absorption is needed to aid in the development of natural anticancer medication.

Acknowledgement

The authors would like to acknowledge the Management, Principal and R and D centre, Department of Biotechnology for the support extended to carry out the research work. The authors would like to acknowledge the financial assistance given by the Vision group of Science and Technology (VGST), Governement of Karnataka towards the research work.

REFERENCES

[1] Siegel RL, Miller KD, Jemal A. Cancer statistics, 2020. CA Cancer J Clin. 2020;70(1):07-30.
[2] Bray F, Ferlay J, Soerjomataram I, Siegel RL, Torre LA, Jemal A. Global cancer statistics 2018: GLOBOCAN estimates of incidence and mortality worldwide for 36 cancers in 185 countries. CA Cancer J Clin. 2018;68(6):394-424.
[3] Gothai S, Muniandy K, Mohd Esa N, Subbiah S, Arulselvan P. Anticancer potential of Alternanthera sessilis extract on HT-29 human colon cancer cells. Asian Pac J Trop Biomed. 2018;8(8):394.
[4] Xie YH, Chen YX, Fang JY. Comprehensive review of targeted therapy for colorectal cancer. Signal Transduct Target Ther. 2020;5(1):22.
[5] Kumar GV DN. An update of leucas aspera– a medicinal plant. Int J Sci Res Methodol. 2016;5(1):485-503.
[6] Sabri G, Vimala Y MP. Leucas aspera: Medicinal plant review. Int Res J multidiscip Stud. 2015;1(3):01-08.
[7] Srinivasan R, Ravali B, Suvarchala P, Honey A, Tejaswini A, Neeraja P. Leucas aspera medicinal plant: Review. Int J Pharma Bio Sci. 2011;2(2):153-59.
[8] Prajapati MS, Patel JB, Modi K, Shah MB. Leucas aspera: A review. Pharmacogn Rev. 2010;4(7):85-87.
[9] Khare CP. Indian Medicinal Plants-An Illustrated Dictionary. First Indian Reprint, Springer (India) Pvt. Ltd., New Delhi, 2007;717-18.
[10] Antony JJ, Nivedheetha M, Siva D, Pradeepha G, Kokilavani P, Kalaiselvi S, et al. Antimicrobial activity of Leucas aspera engineered silver nanoparticles against Aeromonas hydrophila in infected Catla catla. Colloids Surf B Biointerfaces. 2013;109:20-24.
[11] Islam AKMM, Ohno O, Suenaga K, Kato-Noguchi H. Two novel phytotoxic substances from Leucas aspera. J Plant Physiol. 2014;171(11):877-83.
[12] Chouhan HS, Singh SK. A review of plants of genus Leucas. Journal of Pharmacognosy and Phytotherapy. 2011;3(2):13-26.
[13] Bhandari P, Patel NK, Bhutani KK. Synthesis of new heterocyclic lupeol derivatives as nitric oxide and pro-inflammatory cytokine inhibitors. Bioorg Med Chem Lett. 2014;24(15):3596-99.
[14] Katsui N, Matsue H, Hirata T, Masamune T. Phytosterols and triterpenes in the roots of the "kidney bean" (Phaseolus vulgaris L.). Bulletin of the Chemical Society of Japan. 1972;45(1):223-26.
[15] Bhandari P, Patel NK, Gangwal RP, Sangamwar AT, Bhutani KK. Oleanolic acid analogs as NO, TNF-α and IL-1β inhibitors: Synthesis, biological evaluation and docking studies. Bioorg Med Chem Lett. 2014;24(17):4114-19.
[16] Galipalli S, Patel NK, Prasanna K, Bhutani KK. Activity-guided investigation of Carissa carandas (L.) roots for anti-inflammatory constituents. Nat Prod Res. 2015;29(17):1670-72.
[17] Bagby MO, Smith CR, Wolff IA. Laballenic Acid. A new allenic acid from leonotis nepetaefolia seed oil 1. J Org Chem. 1965;30(12):4227-29.
[18] Patel NK, Shahid Khan KKB. Investigations on leucas cephalotes (roth.) Spreng. For inhibition of lps-induced pro-inflammatory mediators in murine macrophages and in rat model. Excli J. 2015;14:508-16.
[19] Singh N, Nath R, Singh DR, Gupta ML, Kohli RP. An experimental evaluation of protective effects of some indigenous drugs on carbon tetrachloride-induced hepatotoxicity in mice and rats. Q J Crude Drug Res. 1978;16(1):08-16.
[20] Kamat M, Singh TP. Preliminary chemical examination of some Compounds in the different parts of the Genus Leucas R. Br. GEOBIOS-JODHPUR. 1994;21:31.
[21] Paul S, Hwang JK, Kim HY, Jeon WK, Chung C, Han JS. Multiple biological properties of macelignan and its pharmacological implications. Arch Pharm Res. 2013;36(3):264-72.
[22] Gini TG, Jeya Jothi G. Column chromatography and HPLC analysis of phenolic compounds in the fractions of Salvinia molesta mitchell. Egypt J Basic Appl Sci. 2018;5(3):197-203.
[23] Singleton, VL, Rossi JA. Colorimetry of total phenolics with phosphomolybdic-phosphotungstic acid reagent. Am J Enol Vitic. 1965;16:144-58.
[24] Tasioula-Margari M, Tsabolatidou E. Extraction, separation, and identification of phenolic compounds in virgin olive oil by HPLC-DAD and HPLC-MS. Antioxidants (Basel, Switzerland). 2015;4(3):548-62.
[25] Robert A. Identification of essential oil components by gas chromatography/ quadrupole mass spectroscopy. Carol Stream. 2005;16:65-120.
[26] Crouch SP, Kozlowski R, Slater KJ, Fletcher J. The use of ATP bioluminescence as a measure of cell proliferation and cytotoxicity. J Immunol Methods. 1993;160(1):81-88.
[27] Lundin A, Hasenson M, Persson J, Pousette A. Estimation of biomass in growing cell lines by adenosine triphosphate assay. Methods Enzymol. 1986;133:27-42.
[28] Denizot F, Lang R. Rapid colorimetric assay for cell growth and survival. Modifications to the tetrazolium dye procedure giving improved sensitivity and reliability. J Immunol Methods. 1986;89(2):271-77.
[29] Shin HJ, Han JM, Choi YS, Jung HJ. Pterostilbene suppresses both cancer cells and cancer stem-like cells in cervical cancer with superior bioavailability to resveratrol. Molecules. 2020;25(1).
[30] Casciola-Rosen L, Rosen A, Petri M, Schlissel M. Surface blebs on apoptotic cells are sites of enhanced procoagulant activity: Implications for coagulation events and antigenic spread in systemic lupus erythematosus. Proc Nat Acad Sci USA. 1996;93:1624-29.
[31] Van Engeland M, Ramaekers FC, Schutte B, Reutelingsperger CPM. A novel assay to measure loss of plasma membrane asymmetry during apoptosis of adherent cells in culture. Cytometry. 1996;24:131-39.
[32] Homburg C, de Haas M, von dem Borne A, Verhoeven A, Reutelingsperger C, Roos D. Human neutrophils lose their surface Fc gamma RIII and acquire Annexin V binding sites during apoptosis in vitro. Blood. 1995;85(2):532-40.
[33] Martin SJ, Reutelingsperger CP, McGahon AJ, Rader JA, van Schie RC, LaFace DM, et al. Early redistribution of plasma membrane phosphatidylserine is a general feature of apoptosis regardless of the initiating stimulus: Inhibition by overexpression of Bcl-2 and Abl. J Exp Med. 1995;182(5):1545-56.
[34] Vermes I, Haanen C, Steffens-Nakken H, Reutelingsperger C. A novel assay for apoptosis. Flow cytometric detection of phosphatidylserine expression on early apoptotic cells using fluorescein labelled Annexin V. J Immunol Methods. 1995;184(1):39-51.
[35] Iqbal J, Abbasi BA, Mahmood T, Kanwal S, Ai B, Shah SA, et al. Plant derived anticancer agents: A green anticancer approach. Asian Pac. J. Trop. BioMed. 2017;7(12):1129-50.
[36] Millimouno FM, Dong J, Yang L, Li J, Li X. Targeting apoptosis pathways in cancer and prospective with natural compounds from mother nature. Cancer Prev Rev. 2014;7(11):1081-107.
[37] Middleton E. Effect of plant flavonoids on immune and inflammatory cell function. In flavonoids in the living system. Springer. 1998;175-98.

[38] Qiang F, Lee BJ, Ha I, Kang KW, Woo ER, Han HK. Effect of maceligan on the systemic exposure of Biological activities of macelignan paclitaxel: In vitro and in vivo evaluation. European Journal of Pharmaceutical Sciences. 2010;41:226-31.
[39] Itharat A, Houghton PJ, Eno-Amooquaye E, Burke P, Sampson JH, Raman A. In vitro cytotoxic activity of Thai medicinal plants used traditionally to treat cancer. J Ethnopharmacol. 2004;90(1):33-38.
[40] Lee KE, Mun S, Pyun HB, Kim MS, Hwang JK. Effects of macelignan isolated from Myristica fragrans (Nutmeg) on expression of matrix metalloproteinase-1 and type I procollagen in UVB-irradiated human skin fibroblasts. Biol Pharm Bull. 2012;35(10):1669-75.

PARTICULARS OF CONTRIBUTORS:
1. Assistant Professor, Department of Biotechnology, The Oxford College of Engineering, Bengaluru, Karnataka, India.
2. Professor, Department of Biotechnology, The Oxford College of Engineering, Bengaluru, Karnataka, India.

NAME, ADDRESS, E-MAIL ID OF THE CORRESPONDING AUTHOR:
BK Manjunath,
10th Mile Stone, Bommanahalli, Hosur Road, Bengaluru, Karnataka, India.
E-mail: dr.manjunath.toce@gmail.com

PLAGIARISM CHECKING METHODS: [Jain H et al.]
- Plagiarism X-checker: Nov 19, 2021
- Manual Googling: Dec 16, 2021
- iThenticate Software: Dec 18, 2021 (20%)

ETYMOLOGY: Author Origin

AUTHOR DECLARATION:
- Financial or Other Competing Interests: None
- Was Ethics Committee Approval obtained for this study? NA
- Was informed consent obtained from the subjects involved in the study? NA
- For any images presented appropriate consent has been obtained from the subjects. NA

Date of Submission: **Nov 18, 2021**
Date of Peer Review: **Dec 05, 2021**
Date of Acceptance: **Dec 22, 2021**
Date of Publishing: **Jan 01, 2022**

KOREA REVIEW OF INTERNATIONAL STUDIES

Monthly Publication / Volume 15 Issue 31 Feb 2022

Cyber Forensic and Issues Related to Evidence
Md. Baharul Islam

KOREA REVIEW OF INTERNATIONAL STUDIES

ISSN : 1226-4741

Home

Call for Paper

Editorial board

Issues

Contact us

Address : 145, Anam-ro, Seongbuk-gu, Seoul 02841,
Republic of Korea.
Email : editor@kristudies.org

International Journal of Computers and Applications ›
Volume 43, 2021 - Issue 5

Sustainable Computing for Intelligent Systems

An investigation on adaptive HTTP media streaming Quality-of-Experience (QoE) and agility using cloud media services

Selvaraj Kesavan, E. Saravana Kumar, Abhishek Kumar

K. Vengatesan

d Department of Computer Engineering, Sanjivani College of Engineering, Kopargaon, India

https://orcid.org/0000-0002-8896-4925

View further author information

Pages 431-444 | Received 15 Nov 2018, Accepted 23 Jan 2019, Published online: 06 Feb 2019

Download citation https://doi.org/10.1080/1206212X.2019.1575034

ABSTRACT

Web services is software entity allows machine to machine communication, operates as standalone unit and interoperability over network using standard web technologies such as Hypertext transfer protocol (HTTP) and eXtensible markup language (XML). With the rapid growth of cloud platform, infrastructure and emergence of multiple Digital transformation technologies, more and more conventional applications are transformed into web-based services. Service-based approach creates tremendous impact on multimedia content storage, retrieval, delivery and communication. With cloud infrastructure and service, get economically viable, real time, high resolution multimedia content on-the-go anywhere and everywhere using adaptive http streaming approach. This paper presents convergence of adaptive http streaming from conventional infrastructure to cloud enabled model and presents the advancement and architecture of adaptive http streaming delivery as a web-based service delivery approach. The detailed performance evaluation of conventional and cloud enabled service-based approaches were presented, and the metrics were compared from real-time experiment. By analyzing performance indices and characteristics, cloud enabled multimedia service delivery approach poses advantages, gives promising result and better user experience compare to the conventional adaptive HTTP streaming approach.

KEYWORDS: Adaptive HTTP streaming conventional media service REST web service

Disclosure statement

No potential conflict of interest was reported by the authors.

ORCID

E. Saravana Kumar http://orcid.org/0000-0003-4839-9025

Abhishek Kumar http://orcid.org/0000-0002-9925-8137

K. Vengatesan http://orcid.org/0000-0002-8896-4925

Additional information

Notes on contributors

Selvaraj Kesavan

Dr Selvaraj Kesavan is currently working as technical architect in Accenture Digital, India. He received B.E. Electronics and communication from Bharathiar University in 2000, M.E communication Systems from Madurai Kamaraj University in 2002 and Ph.D. from Karunya University in 2017. He has immense experience in architecting end-to-end solutions for Cloud, IoT, Multimedia and embedded systems. He involved in design and development of many state-of-art next-generation IoT, Cloud and mobile technologies. He has published multiple papers in reputed international journals and conferences. His research interests include next generation IoT architecture, digital Transformation architecture, multimedia cloud computing, mobile multimedia and multimedia communications.

E. Saravana Kumar

Dr E. Saravana Kumar is currently working as Associate Professor in the Department of Computer Science and Engineering, The Oxford College of Engineering Bengaluru, Karnataka. He received Doctor of Philosophy Degree in Information and Communication Engineering from Anna University-Chennai, Master of Engineering Degree in Computer Science and Engineering from Annamalai University - Chidambaram and Bachelor of Engineering Degree in Electronics and Communicati Engineering from Bharatiar University-Coimbatore. He has 17 years of teaching experience. He is the author of two text books. He has two patents and a good number of publications in peer-reviewed reputed journals and conferences. His research interest includes grid computing, Cloud Computing, IoT, Image processing and Data Mining. He is a member of ISTE, Institution of Engineers India and International Association of Engineers.

Abhishek Kumar

Dr Abhishek Kumar is Assistant Professor in Computer Science at Banaras Hindu University. He is Apple Certified Associate and Autodesk Certified & Adobe Certified

Educator. His research area is Stereoscopy, 3D Animation, Image Processing, VR & AR, Multimedia, Game Technology, MOOCs, Graphics and Visual Effects.

K. Vengatesan

Dr K. Vengatesan is Associate Professor at the Department of Computer Engineering, Sanjivani College of Engineering. His research area is in data mining, bioinformatics, clustering correlation and bi-clustering.

Internet of things (IoT)-based unmanned intelligent street light using renewable energy

Dinesh Kumar Anguraj, S. Balasubramaniyan, E. Saravana Kumar, J. Vakula Rani, M. Ashwin

International Journal of Intelligent Unmanned Systems

ISSN: 2049-6427 (International Standard Serial Number.)

Article publication date: 12 January 2021

Issue publication date: 7 January 2022

Abstract

Purpose

The purpose of the research is to concentrate on the most important smart metropolitan applications which are smart living, smart security and smart maintainable. In that, Power management and security is a most important problem in the current metropolitan situation.

Design/methodology/approach

A smart metropolitan area utilizes recent innovative technologies to improve its living, security and maintainable. The aim of this study is to recognize and resolve the difficulties in metropolitan area applications.

Findings

The main aim of this study is to reduce the metropolitan foremost energy consumption, to recharge the electric vehicles and to increase the lifetime of smart street lights.

Originality/value

The hybrid renewable energy street light applies smart resolutions to substructure and facilities in rural and metropolitan areas to create them well. This study will be applying smart metropolitan solar and wind turbine street light using renewable energy for existing areas. In future, the smart street light work will be implemented everywhere else.

Keywords

Wi-Fi | LED lights | Micro-wind turbine | Internet of things (IoT)

Citation
Anguraj, D.K., Balasubramaniyan, S., Saravana Kumar, E., Vakula Rani, J. and Ashwin, M. (2022), "Internet of things (IoT)-based unmanned intelligent street light using renewable energy", *International Journal of Intelligent Unmanned Systems*, Vol. 10 No. 1, pp. 34-47. https://doi.org/10.1108/IJIUS-10-2020-0060

Download as .RIS

Publisher: Emerald Publishing Limited

PAPER • OPEN ACCESS

Comprehensive Analysis of Cloud based Databases

E. Saravana Kumar[1], Selvaraj Kesavan[2], R. Ch. A Naidu[3], Senthil Kumar R[4] and Latha[5]

Published under licence by IOP Publishing Ltd

IOP Conference Series: Materials Science and Engineering, Volume 1131, 4th International Conference on Emerging Technologies in Computer Engineering: Data Science & Blockchain Technology (ICETCE 2021) 3rd-4th February 2021, Jaipur, India

Citation E. Saravana Kumar *et al* 2021 *IOP Conf. Ser.: Mater. Sci. Eng.* **1131** 012021

DOI 10.1088/1757-899X/1131/1/012021

saraninfo@gmail.com
selvarajkesavan@gmail.com
chanr789@gmail.com
senkr.raj@gmail.com
latha.shreeram@gmail.com

[1] Associate Professor, Dept. of CSE, The Oxford College of Engineering, Bommanahalli, Bangalore-560068

[2] Advisor Solution Architect in DXC Technology, India

[3] Professor & H.O.D, Dept. of CSE, The Oxford College of Engineering, Bommanahalli, Bangalore-560068

[4] Associate Profesor, Dept. of CSE, The Oxford College of Engineering, Bommanahalli, Bangalore-560068

[5] Assistant Professor, Dept. of CSE, The Oxford College of Engineering, Bommanahalli, Bangalore-560068

Abstract

With standard change in the computing architecture and distributed, wide range processing approach leverage the large data to be analyzed and extract the content. The recent advancement in Web technology enables the user to produce process and ingest content of any structure. Cloud computing helps to provide computing infrastructure, centralized storage and seamless services for organizations and users. In a digital world, data is core aspect of the economy, become part of government, enterprise, social sectors and every individual in a day to day life. Data analysis is gathering of strength in both research and production communities. There are many social networking sites, web, enterprise and IoT data require being stored in secured, centralized data store. It also demands data to be stored without any predefined schema and able to retrieve in near real time. When demand goes up application needs to be scaled to sustain for the demand. Similarly, data store should support scalability to support applications demand. Cloud providers and third-party organization offers numerous data storage, database options. This article highlights various available data storage options, suitability and limitations.

Search for Multimessenger Sources of Gravitational Waves and High-energy Neutrinos with Advanced LIGO during Its First Observing Run, ANTARES, and IceCube

OBSERVATION AND CHARACTERIZATION OF A COSMIC MUON NEUTRINO FLUX FROM THE NORTHERN HEMISPHERE USING SIX YEARS OF ICECUBE DATA

THE SEARCH FOR TRANSIENT ASTROPHYSICAL NEUTRINO EMISSION WITH ICECUBE-DEEPCORE

PDF

Help

Trends in Sciences

HOME / ARCHIVES /
VOL. 19 NO. 10 (2022): TRENDS IN SCIENCES, VOLUME 19, NUMBER 10, 15 MAY 2022 /
Research Articles

An Enhanced Bio-Inspired Routing Algorithm for Vehicular Ad Hoc Networks

Raghu Ramamoorthy
Department of Computer Science and Engineering, The Oxford College of Engineering, Karnataka, India

Menakadevi Thangavelu
Department of Electronics and Communication Engineering, Adhiyamaan College of Engineering, Tamilnadu, India

DOI: https://doi.org/10.48048/tis.2022.4188

Keywords: VANETs, Routing, Pheromone count, Optimal path, Reliable communication

ABSTRACT

Vehicular ad hoc networks (VANETs) demands reliable communication mechanisms for time-critical communication between vehicles. In VANETs, communication links between vehicles are prone to frequent breaks due to high mobility and topology changes. In this context, this work presents an enhanced bio-inspired routing algorithm (EBIRA) to provide reliable communication. In EBIRA, enhanced ant colony optimization (EACO) finds the optimal long-life short-distance routes with the minimum hops based on distance, received signal strength metric, hop count, and evaporation rate. In EBIRA, the selected path has a short distance and a high level of connectivity at the link level with minimum hops. Choosing the shortest path through minimum hops with high connectivity level links improves route lifetime and reduces frequent link breaks between vehicles. Simulation results show that the performance of EBIRA is better than reliable route discovery by using ant colony optimization (RDACO) and road-aware geographic routing protocol (RAGR) in terms of packet delivery ratio, throughput, and latency. Furthermore, variations of the received signal strength based on vehicle density and speed are evaluated, and the EBIRA route discovery success ratio is estimated and shown based on vehicle density at speed.

HIGHLIGHTS

- Vehicular ad hoc networks (VANETs) demands reliable communication mechanisms for time-critical communication between vehicles. In VANETs, communication links between vehicles are prone to frequent breaks due to high mobility and topology changes
- VANET routing faces various challenges due to its unique characteristics such as high mobility, dynamic topology, unlimited network size, no infrastructure, and wireless communication
- Choosing the shortest path through minimum hops with high connectivity level links improves route lifetime and reduces frequent link breaks between vehicles
- The Less complexity, adaptability and self-organizing characteristics of ACO can cope with frequent topology changes, high mobility, absence of infrastructure, and wireless communication. The robustness feature of the ACO often helps to overcome network interruptions in the form of disconnections

GRAPHICAL ABSTRACT

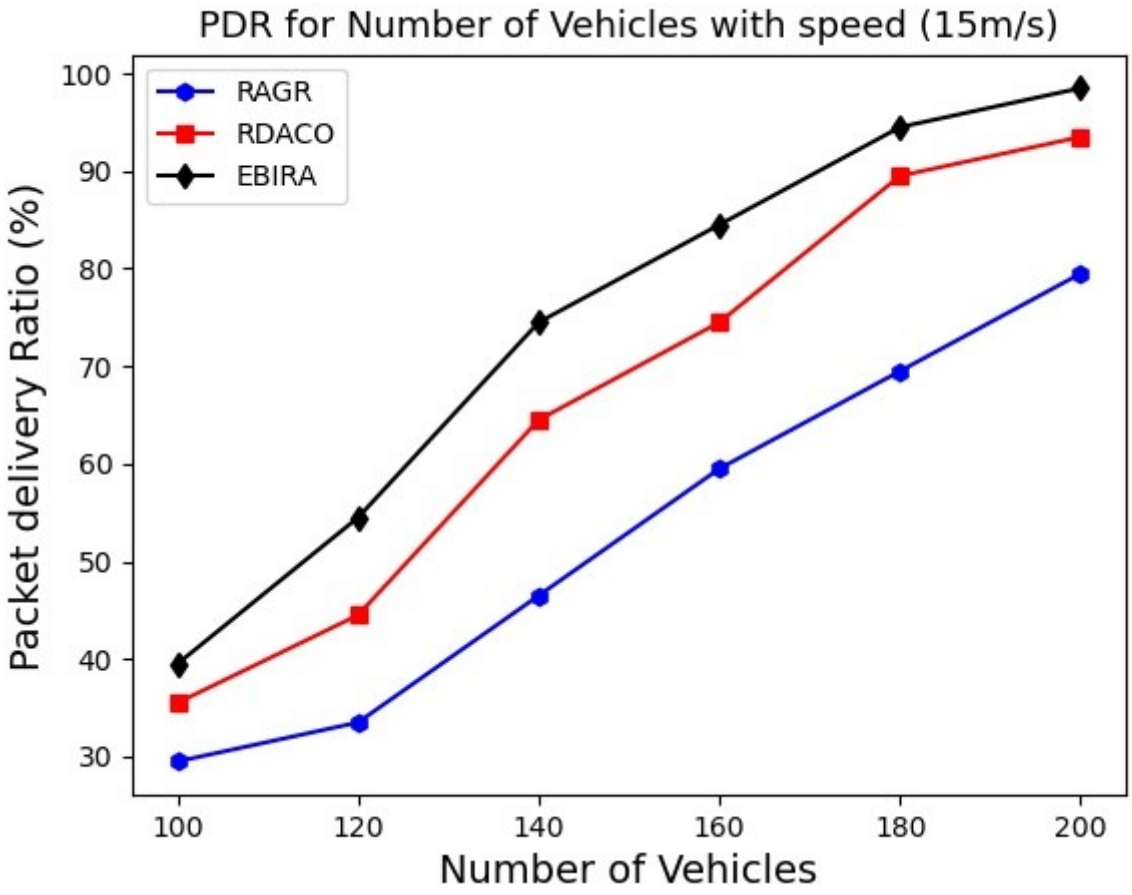

DOWNLOADS

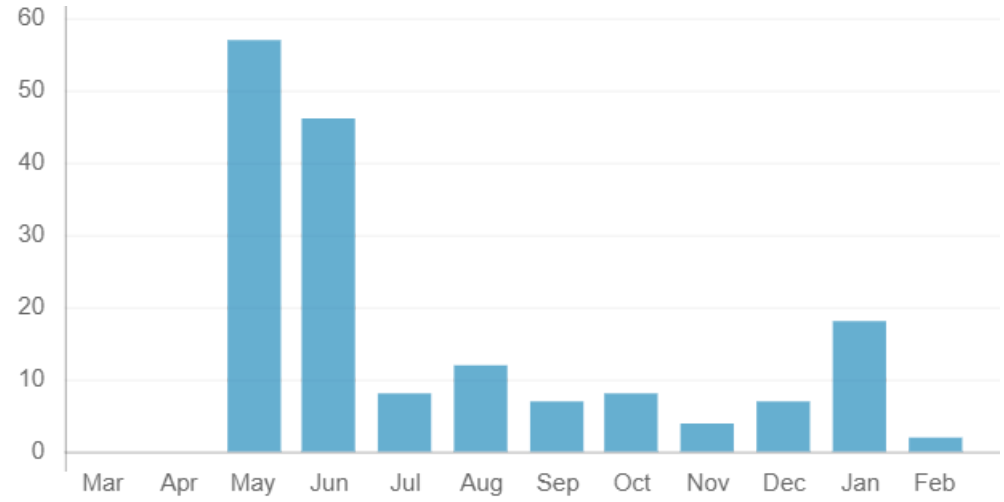

METRICS

Metrics Loading ...

REFERENCES

K Renuka, DS Roy and KHK Reddy. An SDN empowered location aware routing for energy efficient next generation vehicular networks. IET Intell. Transport syst. 2021; 15, 308-19.

S Al-Sultan, MM Al-Doori, AH Al-Bayatti and H Zedan. A comprehensive survey on vehicular Ad Hoc network. J. Netw. Comput. Appl. 2014; 37, 380-92.

H Bello-Salau, A Aibinu, Z Wang, A Onumanyi, E Onwuka and J Dukiya. An optimized routing algorithm for vehicle ad-hoc networks. Eng. Sci. Tech. Int. J. 2019; 22, 754-66.

Y Azzoug and A Boukra. Bio-inspired VANET routing optimization: An overview. Artif. Intell. Rev. 2021; 54, 1005-62.

J Sun, W Fang, X Wu, Z Xie and W Xu. QoS multicast routing using a quantum-behaved particle swarm optimization algorithm. Eng. Appl. Artif. Intell. 2011; 24, 123-31.

R Ramamoorthy and M Thangavelu. Group based dual mode key management scheme for secure

communication in vehicular ad hoc networks. Wireless Pers. Comm. 2021; 120, 949-73.

W Deng, J Xu and H Zhao. An improved ant colony optimization algorithm based on hybrid strategies for scheduling problem. IEEE Access 2019; 7, 20281-92.

G Li and L Boukhatem. An intersection-based delay sensitive routing for vanets using aco algorithm. In: Proceedings of the 23rd International Conference on Computer Communication and

Networks, Shanghai, China. 2014, p. 750-7.

S Bitam, A Mellouk and S Zeadally. Bio-inspired routing algorithms survey for vehicular ad hoc networks. IEEE Comm. Surv. Tutorials 2015; 17, 843-67.

F Dressler and O Akan. Bio-inspired networking: From theory to practice. IEEE Comm. Mag. 2010; 48, 176-83.

Y Lin, J Zhang, HS Chung, WH Ip, Y Li and Shi. An ant colony optimization approach for maximizing the lifetime of heterogeneous wireless sensor networks. IEEE Trans. Syst. Man Cybern. C 2012; 42, 408-20.

R Ramamoorthy and M Thangavelu. An improved distance-based ant colony optimization routing for vehicular ad hoc networks. Int. J. Comm. Syst. 2020; 33, e4502.

B Kazemi, S Ahmadi and Talebi. Optimum and reliable routing in VANETs: An opposition based ant colony algorithm scheme. In: Proceedings of the 2013 International Conference on Connected Vehicles and Expo, Las Vegas NV, United States. 2013, p. 926-30.

D Sinwar, N Sharma, SK Maakar and S Kumar. Analysis and comparison of ant colony optimization algorithm with DSDV, AODV, and AOMDV based on shortest path in MANET. J. Inform. Optim. Sci. 2020; 41, 621-32.

H Rana, P Thulasiraman and RK Thulasiram. MAZACORNET: Mobility aware zone-based ant colony optimization routing for VANET. In: Proceedings of the 2013 IEEE Congress on Evolutionary Computation, Cancun, Mexico. 2013, p. 2948-55.

O Chakroun, S Cherkaoui and J Rezgui. MUDDS: Multi-metric unicast data dissemination scheme for 802.11p VANETs. In: Proceedings of the 8th International Wireless Communications and Mobile Computing Conference, Yogyakarta, Indonesia. 2012, p. 1074-9.

SM Basavaraj and RM Jyoti. Reliable traffic and mobility aware position based vehicular ad hoc network routing using ACO. Int. J. Adv. Sci. Tech. 2020; 29, 645-69.

T Jeyaprakash and R Mukesh. An optimized node selection routing protocol for vehicular ad-hoc networks a hybrid model. J. Comm. Software Syst. 2015; 11, 80-5.

N Sallom Kadhim, MN Mohammed, M Abdul Majid, SQ Mohamd and H Tao. An efficient route selection based on AODV algorithm for VANET. Indian J. Sci. Tech. 2016; 9, 1-6.

S Zhang, X Liu and M Wang. A novel ant colony optimization algorithm for the shortest-path problem in traffic networks. Filomat 2018; 32, 1619-28.

N Melaouene and R Romadi. An enhanced routing algorithm using ant colony optimization and VANET infrastructure. In: Proceedings of the 6th International Conference on Traffic and Logistic Engineering, Bangkok, Thailand. 2019, p. 1-5.

SLO Correia, J Celestino and O Cherkaoui. Mobility-aware ant colony optimization routing for vehicular ad hoc networks. In: Proceedings of the 2011 IEEE wireless communications and networking conference, Cancun, Mexico. 2011, p. 1125-30.

A Mohammadnia, R Rahmani, S Mohammadnia and M Bekravi. A load balancing routing mechanism based on ant colony optimization algorithm for vehicular adhoc network. Int. J. Netw. Comput. Eng. 2016; 7, 1-10.

R Kumar and SK Routray. Ant colony based dynamic source routing for VANET. In: Proceedings of the 2nd International Conference on Applied and Theoretical Computing and Communication Technology, Bangalore, India. 2016, p. 279-82.

R Silva, HS Lopes and W Godoy. A heuristic algorithm based on ant colony optimization for multi-objective routing in vehicle ad hoc networks. In: Proceedings of the 2013 BRICS Congress on Computational Intelligence and 11th Brazilian Congress on Computational Intelligence, Ipojuca, Brazil. 2013, p. 435-40.

P Vijayalakshmi, SAJ Francis and JA Dinakaran. A robust energy efficient ant colony optimization routing algorithm for multi-hop ad hoc networks in MANETs. Wireless Netw. 2016; 22, 2081-100.

H Dong, X Zhao, L Qu, X Chi and X Cui. Multi-hop routing optimization method based on improved ant algorithm for vehicle to roadside network. J. Bionic Eng. 2014; 11, 490-6.

E Khoza, C Tu and PA Owolawi. Decreasing traffic congestion in VANETs using an improved hybrid ant colony optimization algorithm. J. Comm. 2020; 15, 676-86.

A Datta, C Chowdhury and S Neogy. Ant-AODV-VANET: A bio-inspired routing protocol for VANET. In: Proceedings of the International Conference on Emerging Research in Computing, Information, Communication and Applications Springer, Singapore. 2016, p. 251-61.

AM Oranj, RM Alguliev, F Yusifov and S Jamali. Routing algorithm for vehicular ad hoc network based on dynamic ant colony optimization. Int. J. Electron. Electr. Eng. 2016; 4, 79-83.

R Ramamoorthy and M Thangavelu. An enhanced hybrid ant colony optimization routing protocol for vehicular ad-hoc networks. J. Ambient Intell. Hum. Comput. 2021, https://doi.org/10.1007/s12652-021-03176-y.

KN Qureshi, F Bashir and AH Abdullah. Distance and signal quality aware next hop selection routing protocol for vehicular ad hoc networks. Neural Comput. Appl. 2020; 32, 2351-64.

WH Kuo, S Dong and JS Huang. Pheromone-based V2V unicast routing scheme in VANETs. In: Proceedings of the 2013 International Conference on Connected Vehicles and Expo, Las Vegas NV, United States. 2013, p. 783-4.

Z Ding, P Ren and Q Du. Ant colony optimization based delay-sensitive routing protocol in vehicular ad hoc networks. B Li, M Yang, H Yuan and Z Yan (Eds.). IoTaaS 2018: IoT as a service. Springer, Cham, Switzerland, 2018, p. 138-48.

JC Dias, P Machado, DC Silva and PH Abreu. An inverted ant colony optimization approach to traffic. Eng. Appl. Artif. Intell. 2014; 36,122-33.

R Raghu, Prabhushankar R, Rajaram J, Vaiyapuri M. Efficient dead reckoning approach for localization prediction in VANETs. J Appl Sci Comput. 2019; 6, 2093-2099.

R Raghu, M. Hema, and J. Jency Priya. Efficient Cluster Based Algorithm for Structured Wireless Sensor Networks. CIKITUSI Journal for Multidisciplinary Research. 2019; 6, 282-288.

SR Yahiabadi, B Barekatain and K Raahemifar. TIHOO: An enhanced hybrid routing protocol in vehicular ad-hoc networks. J. Wireless Comm. Netw. 2019; 1, 1-19.

S Chatterjee and S Das. Ant colony optimization based enhanced dynamic source routing algorithm for mobile Ad-hoc network. Inform. Sci. 2015; 295, 67-90.

R Raghu and T Menakadevi. A survey on anonymous secure on-demand routing protocols in MANETs. Middle East J. Sci. Res. 2016; 24, 3869-80.

A Srivastava, A Prakash and R Tripathi. Quality-of-service based reliable route discovery using ant colony optimization for VANET. In: Proceedings of the IEEE Conference on Information and Communication Technology, Allahabad, India. 2019, p. 1-6.

KN Qureshi, AH Abdullah and A Altameem. Road aware geographical routing protocol coupled with distance, direction and traffic density metrics for urban vehicular ad hoc networks. Wireless Pers. Comm. 2017; 92, 1251-70.

R Ramamoorthy and Thangavelu. An enhanced distance and residual energy-based congestion aware ant colony optimization routing for vehicular ad hoc networks. Int J Commun Syst. 2022, e5179, https://doi:10.1002/dac.5179.

Volume 19, Number 10, MAY, 2022

TiS
http://tis.wu.ac.th

Trends in Sciences
Formerly: Walailak Journal of Science and Technology

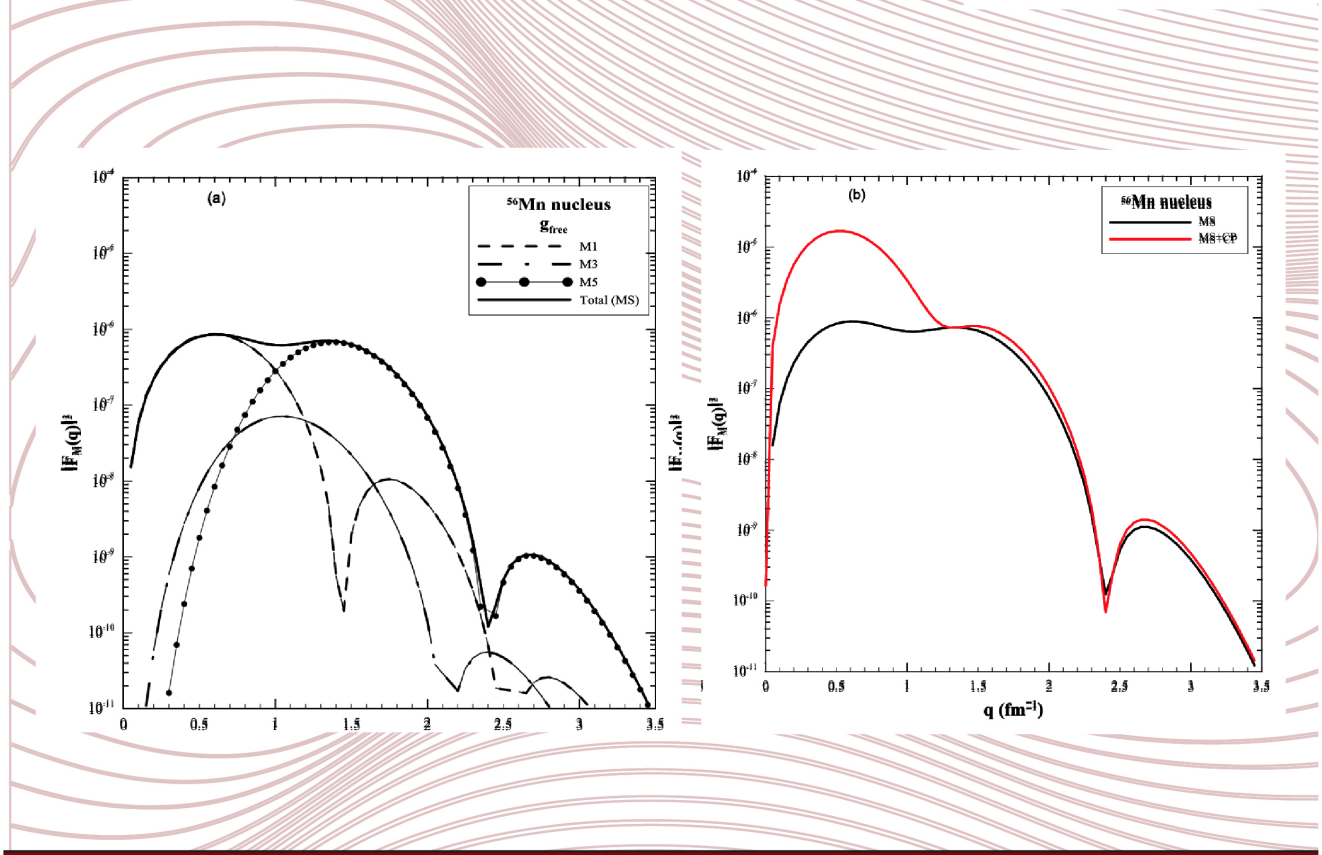

COVER : Magnetic Dipole Moments, Occupation Numbers and Magnetic Form Factors of Some Neutron Rich Nuclei in *sdpf*-shell Hameed *et al.*

E-ISSN: 2774-0226 (Online)

INDEXES & ABSTRACTS

Trends in Sciences is indexed in the Thai-Journal Citation Index Centre (TCI), Google Scholar, CAB Abstracts, EBSCOhost, JournalSeek, ASEAN Citation Index (ACI), ROAD: the Directory of Open Access scholarly Resources and SCOPUS.

PDF

PUBLISHED

2022-05-13

HOW TO CITE

Ramamoorthy, R. ., & Thangavelu, M. . (2022). An Enhanced Bio-Inspired Routing Algorithm for Vehicular Ad Hoc Networks. *Trends in Sciences*, *19*(10), 4188. https://doi.org/10.48048/tis.2022.4188

More Citation Formats

ISSUE

Vol. 19 No. 10 (2022): Trends in Sciences, Volume 19, Number 10, 15 May 2022

SECTION

Research Articles

0

MAKE A SUBMISSION

SCIMAGO JOURNAL RANK

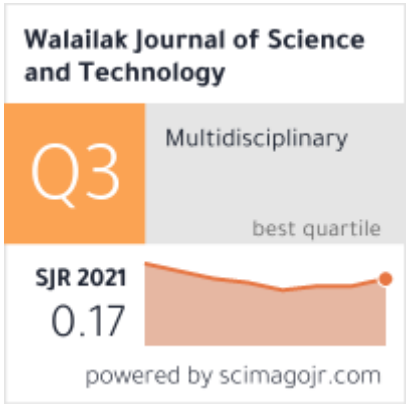

0.7 2020 CiteScore

37th percentile

CITESCORE Powered by Scopus

PLAGIARISM CHECKER turnitin Dupli Checker

JOURNAL METRICS 2022

Acceptance Rate:	**9%**
Review Speed:	**40 days**
Issue per Year:	**24**
Number of Volumes:	**19**
Number of Submissions:	**3,601**
Number of Published:	**360**
Number of Reviewers:	**823**
No. of Scopus Citations:	**3,083**
No. of Google Citations:	**6,583**
Google h-index:	**34**
Google i10-index:	**188**

2021 SJR (Scimago):	**0.166 (Q3)**
2021 Percentile (CiteScore):	**37th (Q3)**

Last updated: Jan 15, 2023 NEW

VISITORS

Counter Installed 30 Sep 2021

SCHOLARSHIPS

WU Graduate Programs

WU Scholarships

INFORMATION

For Readers

For Authors

For Librarians

ISSN 2774-0226 (Online)

PERIODICO di MINERALOGIA Volume 91, No. 4, 2022
ISSN: 0369-8963

OHAR: Optimized Human Action Recognition Paradigm using Optimized Type 2 Neuro-Fuzzy Classifier

DR. J.A. SMITHA[1,*], RAGHU RAMAMOORTHY[2] AND DR. R CHINA APPALA NAIDU[3]

[1]Professor, Department of Computer Science and Engineering, Sri Sairam College of Engineering, Bengaluru, Karnataka, India, (smithajeyakumar37@gmail.com)

[2]Assistant Professor, Department of Computer Science and Engineering, The Oxford College of Engineering, Bengaluru, Karnataka, India, 560 068. (raghuace85@gmail.com)

[3]Professor and Head, Department of Computer Science and Engineering, The Oxford College of Engineering, Bengaluru, Karnataka, India, 560 068 (chanr789@gmail.com).

[*] Corresponding author: DR. J.A. SMITHA

Abstract

Human activity recognition (HAR) is made to identify actions and goals of persons one or more from the images which contain sequence of actions related on environments and actions. However, different issues and challenges are increased in the applications of human activity recognition for improving detection accuracy with different activities. Hence, Optimized Human Action Recognition Paradigm (OHAR) is developed. In the paper, optimized type 2 fuzzy classifier is designed to classify human actions from the image database. The input video is transformed into multiple region in the initial stage. The collected frames are sent to the pre-processing stage for removing noise from frames. After that, the key frame is selected from the image frames by using the Structural Similarity Index (SSIM). Once key frames are selected, the three feature extraction methods are utilized like Space-Time Interest (STI) points, grid shape feature, and coverage factor. Finally, the proposed classifier is proceeding to human activity recognition with selected features set. Here, an optimized type 2 neuro-fuzzy classifier is used for detecting human action. The proposed classifier is enhanced Rider optimization algorithm (ROA). The presentation of proposed method is evaluated based on statistical computations such as accuracy, sensitivity, specificity, recall, and F_Score.

Key Words: *Human actions, Fuzzy classifier, Actions, Fuzzy rules, Riders and Membership functions.*

Introduction

Human activity recognition is fascinated research from together industry and researchers in human-computer interaction, human behaviour analysis, and ubiquitous computing. Human activity recognition is used in different real-time applications like indoor navigation, military, tactical, gaming, and healthcare to personal fitness [1]. Two major types are available in human activity detection such as wearable sensors and systems. In sensor-based detection, wearable sensors can be connected to human body, and human activity is interpreted into exact sensor signal designs that is identified as well as segmented [2]. In major cases, environmental devices needed an installation device in addition human activity translated like cameras can be utilized as invasive devices particularly through ageing people. Due to the reasons, human activity recognition has been considered important research with the utilization of wearable sensors [3].

 https://doi.org/10.37896/pd91.4/91445

ISSN: 0369-8963

There are many ways to achieve recognition of human activities from video frames. But that exiting methods are not attained the better results. The HAR database may contain events known as triplets that can easily identify human activity [4, 5]. Similarly, some databases contain video frames without very hard labels. Also, large data sets make it difficult to classify objects and humans in video frames. The shortcomings mentioned above are motivated by the need for machine learning and in-depth learning structure. Human activities are identified using machine learning techniques like Neural Network (NN) [6], Bayesian Network AND Support Vector Machine (SVM) [7]. However, machine learning techniques fails in providing better results. So today, in-depth learning is concentrated on recognizing human activities through video. Deep learning can manage a large number of databases to identify human activities.

In depth machine learning techniques such as Deep Neural Network (DNN) [8], Deep Belief Neural Network (DPNN) and Conventional Neural Network (CNN) [9] are used to identify human activities using videos. In-depth learning methods are widely used in variety of applications. Among all, CNN image-based processing methods are particularly suitable for detection and authentication. But CNN can suffer because of the undefined structure for identifying objects from humans and images. Algorithms like particle swarm optimization (PSO), cuckoo search algorithm (CA) and genetic algorithm (GA) [10] are used to improve the performance of CNN architecture, respectively. Each optimization algorithm captures the concentration. Therefore, an upgraded version of in-depth learning is needed to employ optimal human function detection from video frames.

Literature Review

HAR identification is processed using various methods. Among them few works are analysed here;

Mohammad Mehdi Hassan *et al.,* [11] have introduced a system based on cell phone passive sensors for human movement approval. Efficient highlights are first derived from initial information. Features extraction includes autoregressive coefficients, average and medium. For further processing the extracted features are given to DNN classifier. The approach introduced was different and conventional pronunciation approval approaches, for example, the conventional multiclass SVM and ANN overcame them.

Ignatov Andrey *et al.,* [12] Here, it introduces the use of CNN for HAR, with direct factual features that store data about the global type arrangement. Besides, researching the effect of time arrangement length on the accuracy of approval and pointing it up to a second creates a continuous static operating sequence. The accuracy of the introduced approach is estimated in two commonly used WISDM and UCI databases, which contain individually marked accelerometer information from 36 and 30 clients, and analyze in cross database. The results showed that proposed model is better in class operation, while low computational cost and manual component design are not required.

Abdulmajit Murad *et al.,* [13] have introduced Deep Recurrent Neural Networks (DRNNs) to generate detection models adapted to capture long-distance conditions in factor length input heirs. Here, long short-term memory (LSDM) can provide unilateral, bilateral, and degraded formats based on DRNs and evaluate their reliability across various benchmark datasets. Study

 https://doi.org/10.37896/pd91.4/91445

ISSN: 0369-8963

results show that our presented models have overcome techniques that use conventional methods.

Seokong Zhao *et al.*, [14] have introduced human movement endorsement that enhances deep learning in IoT conditions. A semi-directed in-deep learning framework was planned to provide most accurate HAR, which productively uses and breaks the labeled sensor information to produce categorized learning model. To make the problem of less marked example easier totake care of a brilliant auto-naming scheme based on Deep Q-Network (DQN) was recently developed with a planned distance-based award rule that can improve learning performance in IoT conditions.

Nafiul Rashid *et al.*, [15] have introduced Adaptive convolutional neural network (CNN) is an energy-productive Human Activity Recognition (AHAR) appropriate for low-power edge gadgets. AHAR utilizes a versatile engineering that chooses a part of pattern design to use during the induction stage. Here, approves the introduced strategy in characterizing velocity exercises from two different datasets like Opportunity and w-HAR.

Design of the proposed methodology

Recently, human activity recognition is as considered one of the most essential study areas in computer vision technology. Human activity recognition is used in different applications like multimedia industry, consumer agencies, robotics, sports, content-based image retrieval, human-computer interaction, smart technologies, video indexing, video surveillance, and security. Hence, in this paper, the Optimized Type 2 Neuro-Fuzzy Classifier to identify human actions from the images. The proposed method is proceeding related to five phases as video to frame conversion, pre-processing, keyframe extraction, feature extraction, and classification. The complete block diagram of proposed method is illustrated in Figure 1.

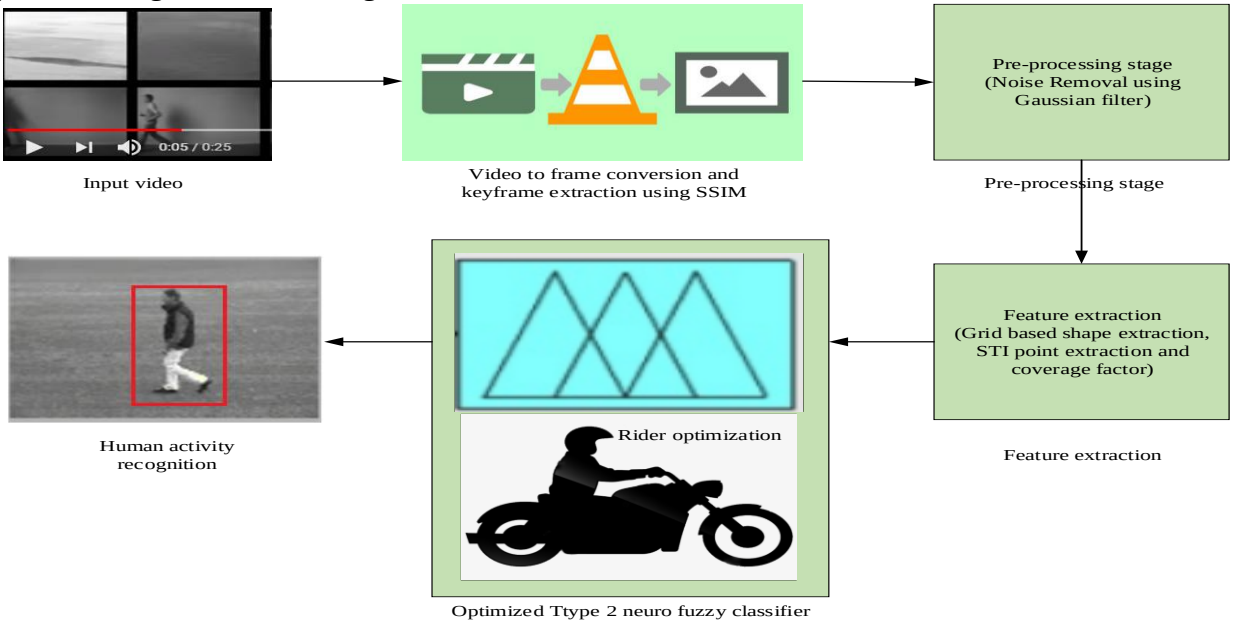

Figure 1. Block diagram of proposed methodology

https://doi.org/10.37896/pd91.4/91445

ISSN: 0369-8963

At the beginning, video dataset is collected from internet. After collection, video is converted into frame. The frame is used for further processing. Before, processing, pre-processing is applied for each frame. Because, the frames may contains noise and unwanted information. In this paper, pre-processing step includes background subtraction, Gaussian model, and noise removal. The pre-processed image is sent to keyframe extraction. The keyframe extraction is proceeding with the SSIM index which is utilized to compute similarity among the frames. The similarity value is compared with the threshold value which has a larger value it is designated as the keyframes. After that, the features are selected by different methods such as coverage factor, STI points and grid-based shape. Finally, extracted features are sent to proposed classifier for human activity recognition.

(i) Video to frame conversion

For human action recognition, the input video is converted into different frames. Using single frame, we cannot able to find the human action. Each and every frame are analysed for recognition process. The extracted frames are used for further processing.

(ii) Pre-processing stage

Pre-processing is performed in order to reduce the noise frames in video and to enhance image contrast. Human mobility changed in every frame of the video. So we process all the frames. Due to noise, the detection may fail to achieve best results. For noise removal and enhancement Gaussian filter is utilized. The Gaussian filters works, based on the pixel strength [16]. The intensity of a Gaussian action's probability and a frame's size are combined to form pixel strength. The Gaussian model can be created as follows:

$$M(f) = \frac{1}{\sqrt{2\pi\sigma^2}} e^{-\frac{f^2}{2\sigma^2}} \quad (1)$$

Where σ represent the standard deviation and f represent the inter-frame distance. The benefits of Gaussian filter includes reducing noise, blurring the edges from images and reduces hassle.

(iii) Key frame extraction

Frames are containing the major information of the images, but some of the frames are provided repeat information of actions. These frames have occupied the spaces and also increase the burden of the classifier. Hence, the keyframes are selected based on SSIM index values [17]. The keyframe extraction is essential requirement for effective human activity recognition. The sequence of video frames is mathematically formulated as follows,

$$F = \{f_1, f_2, \dots, f_j, \dots, f_m\} \quad (2)$$

Where, f_j can be represented as a jt^h frame of the video, m is described as several frames in the video. From the number of frames, the keyframes are selected based on SSIM which formulated as follows,

$$SSIM(f_j, f_{j+1}) = \frac{(2\mu_j\mu_{j+1} + S_1)(2\sigma_{jj+1} + S_1)}{(\mu_j^2 + \mu_{j+1}^2 + S_1)(\sigma_j^2 + \sigma_{j+1}^2 + S_2)'} \quad (3)$$

Where, S_1, S_2 can be described as two variables, σ_{jj+1} can be described as the covariance of f_j and f_{j+1}, σ_{j+1}^2 can be described as a variance of f_{j+1}, σ_j^2 can be described as a variance of f_j, μ_{j+1} can be described as an average of f_{j+1} and μ_j can be described as an average of f_j respectively. From the frames, the keyframes are selected

 https://doi.org/10.37896/pd91.4/91445

ISSN: 0369-8963

which are utilized to compute the features for human activity recognition.

(iv) Feature extraction

Once, the keyframes are selected, feature extraction procedure is initialized. The projected method is extracting the features like STI points, coverage factor, and shape features. The grid-based method is used to extract shape features from selected keyframes. The feature extraction process is mathematically formulated as follows,

Grid-based shape extraction

The shape of human activity is an essential feature extraction, utilized by grid method for human activity detection. In a grid-based method, the human body shape is extracted. The grid-based method is a pixel-oriented, in which the shape is planned to a grid of ideal measurement. In proposed methodology, 4*4 grid size is selected and the human shape in every keyframe is split into a cell with specified measurements. After that, the grid is skimmed from the top to bottom and left to the right frame. This process is initiated from the top left corner. In the keyframes, every cell is fixed as a binary parameter is 1, if the cell is changed into a human shape and 0 for the remaining cases [18]. Hence, the binary sequence of 0 and 1 with a matrix, it constructed as a matrix element. With the consideration of matrix parameter, the shape and thereby, the human activity is detected.

STI point extraction

To analyse spatiotemporal measures in video, local structure in space and time-based features are essential. This feature of image values is changing in combined domains [19]. The image noted that have a local change of strengths incline to be information which named as 'interest points'. To compute local features of the frame, the scale-space symbol is formulated as follows,

$$k(.,\eta^2,\tau^2) = k * U(.,\eta^2,\tau^2) \quad (4)$$

Where U can be described as Gaussian kernel, η,τ can be represented as spatial and temporal parameters. The Gaussian kernel is mathematically formulated as,

$$U = \frac{\exp\left(-\frac{b^2+c^2}{2\eta_x^2} - n^2/2\tau_x^2\right)}{\sqrt{(2\pi)^3\eta_x^4\tau_x^2}} \quad (5)$$

Where n can be described as a total number of frames. After that, a second-moment matrix can be computed by utilizing the spatiotemporal image gradients which formulated as follows,

$$\mu(.,\eta^2,\tau^2) = k * U(.,\eta^2,\tau^2) * (\nabla k(\nabla k)^T) \quad (6)$$

The local maxima feature is computed by defining the feature position which formulated as follows,

$$h^s = det(\mu) - trace^3(\mu) \quad (7)$$

In the feature extraction process, the spatiotemporal extent of the frame is utilized to calculate the feature size of the frame by choosing parameters. The spatiotemporal neighbor is formulated as follows,

$$X = (k^a, k^b, k^n, k^{aa}, \dots, k^{nnn}) \quad (8)$$

This feature extraction process is finding out the center of features with the consideration of normalized derivatives which can be computed related on the specified parameters. The velocity is computed, the neighborhood features also attuned to calculate the invariance related to the camera gestures. Hence, the STI point is extracted from the frames, a vector of measurement 1*40 is achieved.

(v) Coverage factor

This feature is utilized to compute the coverage factor-related to the coverage or

 https://doi.org/10.37896/pd91.4/91445

shape of the human activity from the images. To achieve human activity, the mean of the interesting point is extracted. Related to the mean value, the center opinion of human activity can be achieved. Additionally, the location of the human activity is identified with the basis of vertical length and horizontal length. Hence, the coverage of the human activity, the vector size is fixed as 1*2. So, in the feature extraction procedure, the feature vector is achieved. The collected vector is sent to the classification phase [20].

Proposed Optimized Type 2 Neuro-Fuzzy Classifier

In the proposed classifier, a combination of type-2 neuro-fuzzy classifier and ROA is utilized to recognize human activity from the images. The ROA is utilized to empower the type 2 neuro-fuzzy classifier efficiency in human activity recognition. The membership function of fuzzy classifier is improved with the help of the ROA algorithm. The process of type 2 neuro-fuzzy classifier and ROA is presented in this section.

(i) Type 2 neuro-fuzzy classifier

This method is used to make human activity recognition systems intelligent. Additionally, it reduces the burden of humans and it does not consider rigid distance metrics to decide the image similarity for activity recognition. To achieve efficient HAR, fuzzy logic is an efficient tool. It is a most efficient and flexible technique to manage the combination of measurements with their degree of uncertainty in HAR. In this study, an attempt is made to model the uncertainty of the similarity of image features with the help of Type 2 ambiguous model [21]. The Type 2 fuzzy model features a pacifier, rule-based operation, fuzzy inference engine and output processor, and includes a type reducer and diffuser. FL is again characterized by IF-THEN rules but not its effect or precursor packages. Obscure packages are processed by an uncertainty trail (FOU), which is characterized by their boundaries such as bottom and top member functions. In general, type 2 is more severe and computationally more severe due to type-reduction. In the Type-2 ambiguous classifier, the secondary member is either one or zero. The type 2 fuzzy classifier is mathematically formulated as follows,

$$\tilde{S} = \int_{x\in X}\int_{U\in J^X\sqsubseteq[0,1]^{1/(x,u)}} = \int_{x\in X}\int_{U\in J^X\sqsubseteq[0,1]^{(1/u)/6}} \quad (9)$$

Where, $\tilde{S}$ can be described as a union of all primary memberships, J^X can be described as the primary membership of x, U is the second variable and X is the second variable. The uncertainty of $\tilde{S}$ is considered as equal to one value. The union of the primary membership function is named FOU which presented as follows,

$$FOU(\tilde{S}) = U_{x\in X}J_x \quad (10)$$

$$\tilde{\mu}^{\tilde{A}}(x) = \overline{FOU(\tilde{A})\forall_x}\,\epsilon X \quad (11)$$

Where, $\tilde{\mu}^{\tilde{A}}(x)$ can be represented as upper membership function. For a continuous universe of distance U and X, the embedded interval of the primary membership function is denoted as follows,

$$\tilde{S}_e = \int_{x\in X}\left[\frac{1}{\theta}\right]x \quad \theta\epsilon J_x \sqsubseteq U = [0,1] \quad (12)$$

$$S_e = \int_{x\in X}\left[\frac{\theta}{x}\right] \quad \theta\epsilon J_x \sqsubseteq U = [0,1] \quad (13)$$

Where, $\tilde{S}_e$ can be described as a union of all primary memberships of the set, which is considered as embedded set and S_e can be described as the domain of fuzzy sets. In type 2 fuzzy set theory, the symmetric set is formulated as follows,

 https://doi.org/10.37896/pd91.4/91445

ISSN: 0369-8963

$$\tilde{\mu}^{\tilde{A}}(m+x) = \tilde{\mu}^{\tilde{A}}(x)(m - x) \quad (14)$$

After that, input and output of the system are fuzzified. The input image is A and the image from database is B. The similarity distance $L1, L2, L3$ among A and I are three inputs of the human activity recognition. Three types of fuzzy variables are considered to enable the optimal human activity recognition such as "Similar", "Very Similar" and "not similar" respectively. These fuzzy variables are utilized to describe the feature differences and the output of the system. From the description, the similar action of the images and characterize. In this proposed classifier, the trapezoidal MF is utilized which formulated as follows,

$$\tilde{\mu}^{\tilde{A}}(x) = \begin{cases} \dfrac{(x+b)}{b-d}, & if -b \le x \le -d \\ 1, & if -d \le x \le d \\ \dfrac{b-x}{b-d}, & if\ d \le x \le -b \\ 0, & otherwise \end{cases} \quad (15)$$

Based on the membership functions, human activity is recognized with related feature differences of images. The fuzzy descriptions are utilized to analysis the feature distance enabled by the rules of the fuzzy inference system. The fuzzy interference system is built by fuzzy IF-THEN rules which presents a degree of absence or presence of interaction or association among the elements of two or more sets. The fuzzy rules can be designed explicitly through the expert itself as is the case in the system. Additionally, Mandeni fuzzy interface method is utilized. In the proposed method, human activity recognition is achieved with the help of rules. the different objects have similar feature variance scopes, the rule is detected the human activity recognition. After that, the fuzzy values are defuzzifier to create a crisp value for the output variable [22]. The proposed type 2 fuzzy system, is proceeding with two steps such as type reduction and defuzzification. Different types of methods are available to type reduction in fuzzy sets, in this method, a center of sets are utilized which formulated as follows,

$$Y_{cos}(X) = \left[C_l(\tilde{A}) C_r C_l(\tilde{A})\right] \quad (16)$$

$$C_l(\tilde{A}) = \frac{\sum_{i=1}^{M} \mu_l^i C_l^i}{\sum_{i=1}^{M} \mu_l^i} \quad (17)$$

$$C_r(\tilde{A}) = \frac{\sum_{i=1}^{M} \mu_r^i C_r^i}{\sum_{i=1}^{M} \mu_r^i} \quad (18)$$

Where M can be represented as several rules. From the consideration of type reduction, the interval set is computed. After that, this interval set is defuzzified in type 2 fuzzy set which formulated as follows,

$$y = \frac{C_l(\tilde{A}) + C_r(\tilde{A})}{2} \quad (19)$$

At last, the human activity is recognized with type 2 fuzzy classifier. The test image is sent to the proposed classifier which computes the similarity index through the rules with the consideration of the feature set. The possible similarity is compared with the image's features. With the help of features and proposed classifier, human activity recognition is achieved. In the fuzzy classifier, ROA algorithm is used in selecting membership function variables. A detailed ROA description is presented below in this section.

(ii) Rider Optimization Algorithm

ROA algorithm is utilized to optimize the fuzzy membership function which empowers the recognition the human activity from the images. The general description of the ROA is presented in this The ROA algorithm is used to improve the ambiguous membership

 https://doi.org/10.37896/pd91.4/91445

ISSN: 0369-8963

function, which helps to recognize human activity from images. A general description of the ROA is provided in this section. Rider optimization is developed based on rider behaviours. The ROA consists of two riding punches that travel to the common objective space for the winner of the race. In calculation, all four meetings are considered, usually the size of riders at each meeting is selected similarly from full number of riders [23]. Side Step Rider, Devotee, Overtaker and Occupier are the 4 groups of riders. These four meetings followed a different strategy to achieve the goal introduced as follows,

- ❖ Side ride thinking process comes to the last part except the policy course.
- ❖ The follower follows the main riding devotion of the centre of devotion.
- ❖ The boss can follow his situation to get to the last area identified with the main ride stop area.
- ❖ The Extreme Occupier will come to the last part thinking of the riding situation too fast.

The pseudo-code of ROA is illustrated in Figure 2. The step by step process is explained below;

Algorithm 1: Pseudocode of ROA for membership function variable selection

Input: Random membership function variables.

Output: Optimal membership function variables.

Begin

Initialize the population with random membership function variables

Initialize the rider parameters, brake, accelerator, gear, steering angle

Find success rate

Evaluate the fitness function

While t< off time

For i=1 to R

Update the position of bypass rider

Update the position of bypass rider

Update the position of bypass rider

Rank the riders

Select the maximum leading rider

 https://doi.org/10.37896/pd91.4/91445

ISSN: 0369-8963

Update the parameters

Save the results of optimal membership function parameters.

Step 1: Initialization: The ROA is created by four-rider clusters which are denoted as G whose locations are generalized randomly. The generalization process can be mathematically formulated as follows,

$$X^t = \{X^t(i,j)\}; \quad 1 \le i \le R; 1 \le j \le Q \tag{20}$$

Where, $X^t(i,j)$ can be represented as a location of i^{th} rider at a time instant t, the dimension of number of coordinates is denoted by G,number of riders and Q is denoted by R which is equivalent to G. The number of riders computed, is related based on the number of riders in every group are formulated as follows,

$$R = B + F + O + A \tag{21}$$

Where, A can be represented as several attackers, O can be represented as several over-takers, F can be represented as several followers and B can be represented as several bypass riders. The relation among the aforesaid parameters is computed below,

$$B = F = O = A = \frac{R}{4} \tag{22}$$

Related on the above conditions, the rider locations are computed. The attacker position, overtaker position, follower position, and bypass rider positions are presented in the ranges $\left[X^{\frac{3R}{4}+1}, X^R\right]$ $\left[X^{\frac{R}{2}+1}, X^{3R/4}\right]$, $\left[X^{\frac{3R}{4}+1}, X^{R/2}\right]$ and $\left[X^1, X^{R/4}\right]$ respectively. Once completed the group initialization, the rider value is initialized like brake, accelerator, gear, in addition steering. The steering angle (T) of the rider vehicle at the time is presented as follows,

$$T^t = \left\{T_{i,j}^t\right\}: \ 1 \le i \le R; \ \ 1 \le j \le Q \tag{23}$$

Where, $T_{i,j}^t$ is represented as the steering angle of i^{th} rider vehicle. The starting point of steering angle at the starting time which formulated as follows,

$$T_{i,j}^t = \begin{cases} \theta^i & if\ j = 1 \\ T^{i,j-1} + \varphi & if\ j \ne 1 \& T^{i,j-1} + \varphi \le 360 \\ T^{i,j-1} + \varphi - 360; & otherwise \end{cases} \tag{24}$$

Where, φ can be described as coordinate angle, θ^i can be represented as the position angle of the i^{th} rider vehicle. The position angle of i^{th} rider can be computed based on maximum angle of 360^0 and the number of riders, which is formulated as follows,

$$\theta^i = i * \frac{360^0}{R} \tag{25}$$

Where R can be represented as several riders. The coordinate angle utilized to compute the steering angle is formulated as,

$$\varphi = \frac{360}{Q} \tag{26}$$

Step 2: Finding the success rate and fitness function evaluation: The parameters and rider groups are generalized, the success rate of every ride can be calculated. The success rate can be mathematically formulated related to the distance that can be computed based on the below equation,

$$r^i = \frac{1}{\|X^i - L^T\|} \tag{27}$$

https://doi.org/10.37896/pd91.4/91445

ISSN: 0369-8963

Where, L^T can be represented as final location position, X^i can be described as the position of i^{th} rider. To empower success rate, the distance of final location is reduced. Hence, the reciprocal of distance calculation provides the success rate of rider. The ROA is utilized to select optimal membership functions of the type 2 neuro-fuzzy classifier. The fitness evaluation of the ROA is formulated as follows,

$$FF = Min\,(M^E) \quad (28)$$

$$M^E = \frac{M^r}{T^r} \quad (29)$$

Where, M^E is described as classification error, M^r as classification records and T^r is described as total number of records. This fitness evaluation is proceeding by selecting the optimal membership function values.

Step 3: Position update: The location of each set of rider is updated periodically to compute the leading rider in addition, which is considered as the winner [24]. The rider positions are updated based on the characteristics. The bypass rider position updating process is presented as follows,

$$X_{t+1}^{i,j}(i,j) = \delta\left[X^t(\eta,j) * \beta(j) + X^t(\xi,j) * [1-\beta(j)]\right] \quad (30)$$

Where, β can be represented as a random value, this value takes among 0 and 1 but size $1 \times Q$, ξ can be described as random value 1 and R, η can be described as a random value which ranges from 1 to R and δ can be represented as a random number and parameter ranges from 0 and 1 respectively. The follower position is also updated based on the leading rider because it reaches target quickly and effectively. In the ROA algorithm, the follower position is updated based on the below equation,

$$X_{t+1}^F(i,k) = X^L(L,K) + \left[cos\left(T_{i,k}^t\right) * X^L(L,k) * D_i^t\right] \quad (31)$$

Where, D_i^t can be described as distance traveled by the i^{th} rider, $T_{i,k}^t$ can be described as the steering angle of i^{th} rider in the k^{th} coordinate, L can be described as leading rider index, X^L can be described as leading rider position and K can be described as coordinate selectors respectively. The travel distance is computed by multiplying the rider velocity with the rate of off time. The position update of overtaker is computed based on the below equation,

$$X_{t+1}^F(i,k) = X^t(i,K) + [D_t^I(i) * X^L(L,K)] \quad (32)$$

Where, $D_t^I(i)$ can be described as the direction indicator of i^{th} rider at the time t, position of i^{th} a rider can be denoted by $X^t(i,K)$ respectively. The direction indicator calculates, direction of relative success rate which formulated follows,

$$D_i^I(i) = \left[\frac{2}{1-log(S_t^R(i))}\right] - 1 \quad (33)$$

Where, $D_i^I(i)$ can be described as indicator of direction which presented in the range [-1,1], S_t^R can be described as interval time [0,1] and $S_t^R(i)$ can be described as the success rate of i^{th} rider respectively. The updating process of the attacker is mathematically formulated as follows,

$$X_{t+1}^A(i,k) = X^L(L,j) + \left[cos\left(T_{i,j}^t\right) * X^L(L,j) * D_i^t\right] \quad (34)$$

Where, D_i^t can be described as distance calculation of i^{th} rider, $T_{i,k}^t$ can be described as steering angle of i^{th} rider in k^{th} coordinate and $X^L(L,j)$ as the position of leading rider respectively.

 https://doi.org/10.37896/pd91.4/91445

ISSN: 0369-8963

Step 4: Calculate success rate: **T**he achievement pace of every rider can be Figured, on fruition of position update measure. The situation of rider can be refreshed with the main race up until now. The pioneer position is supplanted with another rider position to such an extent that the achievement pace of the new rider is in the greatest reach [25]. Consequently, the rider, who gave the greatest achievement rate which considered as a main rider.

Step 5: Rider parameter update: The rider parameters are required to compute an efficient optimal solution. The rider value updating proceeds with consideration of additional parameters such as the activity counter. The steering angle and gear are examined related to the activity count which can be updated following the success rate. The activity count is mathematically formulated as follows,

$$A_c^{t+1}(i) = \begin{cases} 1; & if r^{t+1}(i) > r^t(i) \\ 0; & otherwise \end{cases} \quad (35)$$

Similarly, the steering angle can be updated related on the activity counter which formulated as follows,

$$T_{i,j}^{t+1} = \begin{cases} T_{i+1,j}^t; & if A_c^{t+1}(i) = 1 \\ T_{i-1,j}^t; & if A_c^{t+1}(i) = 0 \end{cases} \quad (36)$$

The vehicle gear is upgraded based on maximum value of the gear a rider and activity counter can take as follows,

$$e_I^{T+1} = \begin{cases} e_I^T + 1; & if A_c^{t+1}(i) = 1 \ \& \ e_i^T \neq |e| \\ e_I^T - 1; & if A_c^{t+1}(i) = 0 \ \& \ e_i^T \neq 0 \\ e_I^T; & otherwise \end{cases} \quad (37)$$

The vehicle accelerator can be updated based on the vehicle gear which formulated as follows,

$$e_I^{T+1} = \frac{e_I^{T+1}}{|e|} \quad (38)$$

Where, $|e|$ can be described as a number of gears.

The brake of the vehicle can be updated based on the below equation,

$$k_i^{T+1} = \left[1 - \frac{e_i^{T+1}}{|e|}\right] \quad (39)$$

Step 6: Riding off time: The above process is recurrent continuously, till the time moves the off time, withing that leading rider can be computed. In the final process, the leading rider can be considered a winner. Thus, with the help of proposed classifier, human activity is recognized efficiently.

Results and discussion

The experimental results of proposed approach are analysed in this section. The proposed approach is analysed based on the efficiency of specificity, precision, accuracy, recall, sensitivity and F_Measure respectively. Comparison is made between proposed approach performance and the existing methods like ANN, DNN, and FLC-PSO respectively. The validation is performed for projected method using the databases. In the proposed methodology, the KTH dataset is considered to authenticate the performance of the projected methodology. The KTH dataset consists of six classes like boxing, hand waving, clapping, running, walking and jogging. The 25 person activity are collected with six classes. This database contains 2391 sequences that are taken by utilizing the fixed camera with a 25fps frame rate and down samples to pixel resolution of $160 * 120$ which is an average length of four seconds. The KTH database is collected from [26]. In table 1, the simulation parameter is presented. The KTH dataset and human

 https://doi.org/10.37896/pd91.4/91445

ISSN: 0369-8963

activity recognition outputs are illustrated in Figure 2.

Table 1: Paramter used in this work

S. No	Method	Description	Values
1	Proposed method	FIS type	Mamdani
2		Defuzzification method	Centroid
3		Population size	200
4		Number of iterations	100
5		Random vectors	0,1
6		Coefficient vector	0,2
7	ANN	Architecture	Normal feedforward MLP
8		Hidden layer	1
9		Training algorithm	Backpropagation
10		Number of an input layer	3
11		Number of hidden layers	7
12		Number of the output layer	1
13		Transfer function	Sigmoid

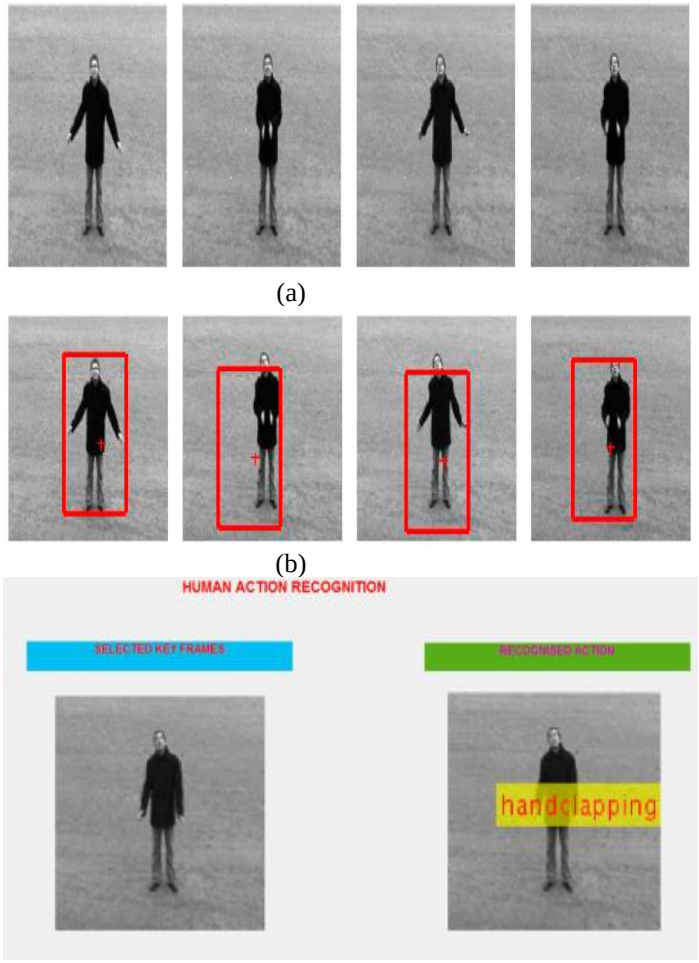

Figure 2. Analysis of (a) databases, (b) feature extraction, and (c) classification phase

https://doi.org/10.37896/pd91.4/91445

The dataset can be used to diagnosis human activity from the images. The proposed method is validated with the help of statistical measurements. The measures are given below;

Accuracy: The ratio of number of true patterns to the sum of all patterns is known as accuracy. The given formula is described for accuracy in equation 40,

$$Accuracy = \frac{TP + TN}{TP + FN + FP + TN} \quad (40)$$

Sensitivity: The two essential proportions of evaluating symptomatic precision of a test are affectability and explicitness. The affectability of a symptomatic test measures its capacity to accurately recognize subjects with human movement. It is the extent of genuine positives that are accurately recognized by the test, given by the condition 41,

$$sensitivity = \frac{TP}{TP + FN} \quad (41)$$

Specificity: The explicitness is the capacity of a test to effectively recognize subjects without condition. It is the extent of genuine negatives that are accurately recognized by the test. Tee formula for sensitivity is described in equation (42)

$$specificity = \frac{TN}{FP + TN} \quad (42)$$

Recall: Recall is the function of correctly classified error (TPs) and incorrectly classified error (FNs). The recall calculation is given in equation 1.

$$Recall = \frac{TP}{TP + FN} \quad (43)$$

F_Score: F_Score measure calculated based on precision and recall measure. It is defined by Equation (44) as

$$F_{Score} = 2.\frac{Precision \times recall}{Precision + recall} \quad (44)$$

The projected method is classified the human activity with six activities which are presented in Table 2.

Table 2: Confusion matrix with proposed classifier

	Clapping	Running	Hand waving	Walking	Jogging	Boxing
Clapping	97	1	0	0	0	1
Running	0	95	0	0	1	0
Hand waving	0	0	97	1	0	1
Walking	0	1	1	98	0	0
Jogging	3	3	0	1	99	1
Boxing	0	0	2	0	0	97

The comparison analysis is essential to validate the proposed methodology. The suggested approach is compared using conventional methods, such as FLC-PSO, DNN, and ANN respectively. The comparison of specificity measure is demonstrated in Figure 3. The specificity of suggested approach is 0.95 at the first class. Similarly, the existing methods attains the specificity values of 0.7, 0.68, and 0.71 respectively. From the contrast analysis of specificity measures, the suggested approach has been attained the best results in HAR. The comparison analysis of accuracy measure is presented in Figure 4. The accuracy of projected method is 0.97 at first class. Similarly, the existing methods attained accuracy values are 0.84, 0.82, and 0.85 respectively. The comparison analysis of sensitivity measure is presented in Figure 5.

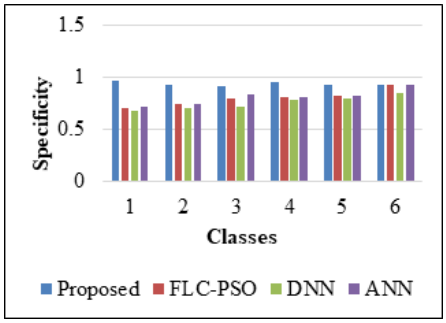

Figure 3: Specificity Analysis

https://doi.org/10.37896/pd91.4/91445

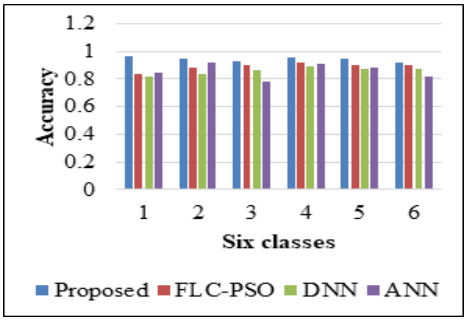

Figure 4: Accuracy Analysis

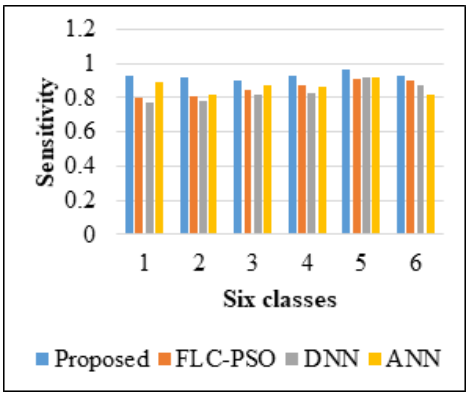

Figure 5: Precision Analysis

Figure 6**:** Recall Analysis

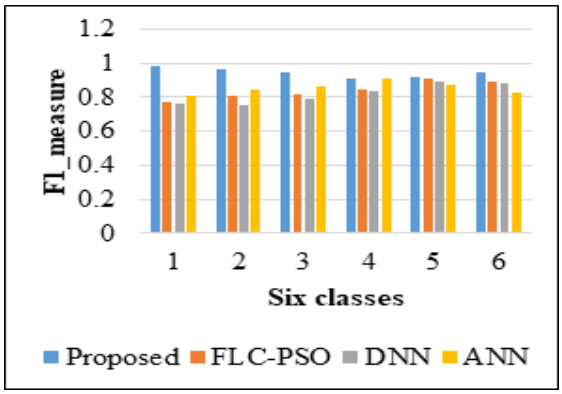

Figure 6: F1_Measure Analysis

The sensitivity of the suggested approach is 0.93 at the first class. Similarly, the existing methods are attained sensitivity values of 0.8, 0.77, and 0.89 respectively. From contrast analysis of sensitivity measures, the projected method has been achieved optimal results in human activity recognition. A comparative analysis of the recall measurement is given in Figure 6. The recall of the planned system is 0.98 in the first class. Similarly, the current methods achieve memory values of 0.79, 0.72 and 0.87, respectively. From diverse analysis of recall measures, the proposed method has reached best results in human activity recognition. A comparative analysis of F_Measure is demonstrated in Figure 7. The F_Measure of proposed work is 0.98 in the first class. Similarly, the current methods achieve F_Measure values of 0.77, 0.76 and 0.81, respectively. From the different analysis of F_Measure, the planned method has attained optimal results in human activity recognition.

Conclusion

In the proposed work, OHAR is established to identify human activity from images. The proposed method is a combination of type 2 fuzzy classifier and ROA algorithm. The type 2 fuzzy classifier process is enhanced with utilization of ROA and it is utilized to classify the human actions from the databases. In this approach, initially, the KTH databases are collected from the internet. The collected video databases are converted into frames. After that, in pre-processing stage all unnecessary features and noise are completely removed from images. From the pre-processing frames, essential frames are selected by using SSIM index values. The selected keyframes are considered for the feature extraction phase. Three different feature extraction methods are considered in the proposed method such as grid shape features, STI points, and coverage factor. Finally, extracted features are sent to the classifier for human activity recognition. The suggested approach has been validated using different metrics. The suggested approach has been contrasted with the

https://doi.org/10.37896/pd91.4/91445

conventional methods such as ANN, DNN, FLC-PSO respectively. From the contrast analysis, the projected technique has achieved the optimal solutions in terms of accuracy is 97%.

References

[1] Henry Friday Nweke, Ying Wah Teh, Mohammed Ali Al-Garadi, and Uzoma Rita Alo. (2018) - Deep learning algorithms for human activity recognition using mobile and wearable sensor networks: State of the art and research challenges. *Expert Systems with Applications*, 105, 233-261.

[2] Elnaz Soleimani, and Ehsan Nazerfard. (2021) - Cross-subject transfer learning in human activity recognition systems using generative adversarial networks. *Neurocomputing* 426 26-34.

[3] Raffaele Gravina, Congcong Ma, Pasquale Pace, Gianluca Aloi, Wilma Russo, Wenfeng Li, and Giancarlo Fortino. (2017) - Cloud-based Activity-aaService cyber–physical framework for human activity monitoring in mobility. *Future Generation Computer Systems*, 75, 158-171.

[4] Lukas Koping, Kimiaki Shirahama, and Marcin Grzegorzek. (2018) - A general framework for sensor-based human activity recognition. *Computers in biology and medicine*, 95, 248-260.

[5] K.S.Gayathri, K. S. Easwarakumar, and Susan Elias. (2017) - Probabilistic ontology-based activity recognition in smart homes using Markov Logic Network. *Knowledge-Based Systems*, 121, 173-184.

[6] Haihua Liu, Na Shu, Qiling Tang, and Wensheng Zhang. (2017) - Computational model based on neural network of visual cortex for human action recognition. *IEEE transactions on neural networks and learning systems*, 29 (5), 1427-1440.

[7] Majd Latah, (2017) - Human action recognition using support vector machines and 3D convolutional neural networks. *International Journal of Advances in Intelligent Informatics*, 3 (1) 47-55.

[8] Lei Wang, Yangyang Xu, Jun Cheng, Haiying Xia, Jianqin Yin, and Jiaji Wu. (2018) - Human action recognition by learning spatio-temporal features with deep neural networks. *IEEE access*, 6, 17913-17922.

[9] Aouaidjia Kamel, Bin Sheng, Po Yang, Ping Li, Ruimin Shen and David Dagan Feng. (2018) - Deep convolutional neural networks for human action recognition using depth maps and postures. *IEEE Transactions on Systems, Man, and Cybernetics: Systems*, 49 (9), 1806-1819.

[10] Alaa Tharwat, Hani Mahdi, Mohamed Elhoseny, and Aboul Ella Hassanien. (2018) - Recognizing human activity in mobile crowdsensing environment using optimized k-NN algorithm. *Expert Systems with Applications*, 107, 32-44.

[11] Mohammed Mehedi Hassan, Md Zia Uddin, Amr Mohamed, and Ahmad Almogren. (2018) - A robust human activity recognition system using smartphone sensors and deep learning. *Future Generation Computer Systems*, 81, 307-313.

[12] Andrey Ignatov, (2018) - Real-time human activity recognition from accelerometer data using Convolutional Neural Networks. *Applied Soft Computing*, 62, 915-922.

[13] Abdulmajid Murad, and Jae-Young Pyun. (2017) - Deep recurrent neural networks for human activity recognition. *Sensors*, 17 (11) 2556.

 https://doi.org/10.37896/pd91.4/91445

[14] Xiaokang Zhou, Wei Liang, I. Kevin, Kai Wang, Hao Wang, Laurence T. Yang, and Qun Jin. (2020) - Deep-learning-enhanced human activity recognition for Internet of healthcare things. *IEEE Internet of Things Journal*, 7 (7), 6429-6438.

[15] Nafiul Rashid, Berken Utku Demirel, and Mohammad Abdullah Al Faruque. (2021) - AHAR: Adaptive CNN for Energy-efficient Human Activity Recognition in Low-power Edge Devices. arXiv preprint arXiv: 2102.01875

[16] Ken Cai, Rongqian Yang, Huazhou Chen, Lihua Li, Jing Zhou, Shanxing Ou, and Feng Liu. (2017) - A framework combining window width-level adjustment and Gaussian filter-based multi-resolution for automatic whole heart segmentation. *Neurocomputing*, 220 138-150.

[17] Yiming Tang, Fuji Ren, and Witold Pedrycz. (2020) - Fuzzy C-means clustering through SSIM and patch for image segmentation. *Applied Soft Computing*, 87, 105928.

[18] Shouji Du, Yunsheng Zhang, Zhengrong Zou, Shenghua Xu, Xue He, and Siyang Chen. (2017) - Automatic building extraction from LiDAR data fusion of point and grid-based features. *ISPRS journal of photogrammetry and remote sensing*, 130, 294-307.

[19] Paul T Sheeba and S. Murugan. (2018) - Hybrid features-enabled dragon deep belief neural network for activity recognition. *The Imaging Science Journal* 66 (6), 355-371.

[20] Gellért Máttyus, Wenjie Luo, and Raquel Urtasun. (2017) - Deeproadmapper: Extracting road topology from aerial images. *In Proceedings of the IEEE International Conference on Computer Vision*, 3438-3446.

[21] Saad M Darwish, and Raad A. Ali. (2015) - Observations on Using Type-2 Fuzzy Logic for Reducing Semantic Gap in Content–Based Image Retrieval System. *International Journal of Computer Theory and Engineering*, 7 (1), 12015.

[22] Xiaomei Li, and Yang Chen. (2021) - Discrete Non-iterative Centroid Type-Reduction Algorithms on General Type-2 Fuzzy Logic Systems. *International Journal of Fuzzy Systems*, 1-12.

[23] D.Binu, and B. S. Kariyappa. RideNN: (2018) - A new rider optimization algorithm-based neural network for fault diagnosis in analog circuits. *IEEE Transactions on Instrumentation and Measurement*, 68 (1), 2-26.

[24] Guohu Wang, Yongliang Yuan, and Wenwen Guo. (2019) - An improved rider optimization algorithm for solving engineering optimization problems. *IEEE Access*, 7, 80570-80576.

[25] Ambaji S Jadhav, Pushpa B. Patil, and Sunil Biradar. (2020) - Optimal feature selection-based diabetic retinopathy detection using improved rider optimization algorithm enabled with deep learning. *Evolutionary Intelligence*, 1-18.

[26] https://www.csc.kth.se/cvap/actions/

 https://doi.org/10.37896/pd91.4/91445

Manuscript Title:

ENERGY EFFICIENT ROUTING WITH CORRELATION BASED DATA TRANSMISSION REDUCTION IN UASN

Author:

BUDDESAB, REKHA .P, RAGHU RAMAMOORTHY, SARAVANA KUMAR .E

DOI Number:

DOI:10.17605/OSF.IO/6EA7S

Published : 2022-08-10

About the author(s)

1. BUDDESAB - Department of Computer Science and Engineering, The Oxford College of Engineering, Bangalore, Karnataka, India.
2. REKHA .P - Department of Computer Science and Engineering, The Oxford College of Engineering, Bangalore, Karnataka, India.
3. RAGHU RAMAMOORTHY - Department of Computer Science and Engineering, The Oxford College of Engineering, Bangalore, Karnataka, India.
4. SARAVANA KUMAR .E - Department of Computer Science and Engineering, The Oxford College of Engineering, Bangalore, Karnataka, India.

Full Text : PDF

Abstract

Under water Acoustic Sensor Networks (UASN) is a kind of wireless sensor networks deployed inside water for various applications like pipe line monitoring, under water aquatic life monitoring. Energy efficiency and reliability are two important challenges in UASN. This work proposes a energy efficient routing in UASN based on the concept of 3D cubes. The proposed solution conserves energy using the concept of clustering and aggregation. Further as extension, we implement a correlation based avoidance of unnecessary forwards. Due to this energy consumption is further reduced in UASN.

Keywords

EGRCs, efficient scheduling, Autonomous Underwater Vehicles, UASN.

Scanning Method for segmentation in Iris Biometric Authentication for Security Systems

Dr.Vanajaroselin E.Chirchi
Professor,
The Oxford College of Engineering, Bangalore

Abstract—*Pupil detection and iris localisation using scanning method and feature extraction is performed with five level decomposition techniques, with these two proposed algorithm we could achieve efficient and fast person authentication in biometric security systems. Statistical performance evaluation is also performed using parameters False acceptance rate (FAR), False rejection rate (FRR), Correct recognition rate (CRR), Equal error rate (EER), Match ratio etc, using CASIA database.*

Index Terms—Feature extraction, haar wavelet transformation, FAR, FRR, Feature vector size, Computational time.

I. INTRODUCTION

Biometrics, which refers to authentication based on his or her physiological or behavioral characteristics, its capability to distinguish authorized person and an unauthorized. Since biometric characteristics are distinctive as it cannot be forgotten or lost, for identification person has to be present physically. Biometric is more reliable and capable than traditional knowledge based and token-based techniques. Biometric has drawback i.e., if compromised then it is difficult to replace. Among all biometrics such as fingerprint, facial thermogram, hand geometry, face, hand thermogram, iris, retina, voice, signature etc., Iris-based identification is one of the most mature and proven technique. Iris is colored part of eye and it is protected by eyelid and cornea as in Fig.1.Security with iris is more reliable as compared to other biometrics. Spoofing is very difficult with respect to iris pattern and thus cannot be compromised easily. In practical situation it is observed that iris part is occluded by interference of eyelids and eyelashes, improper eye opening, light reflection and image quality is degraded because of low contrast image and other artifact. Advantages of Iris is that it is not subject to the effects of aging which means it remains in a stable form from about age of one until death . Our experiment uses wavelets such as Haar, db2, db4 for feature extraction and Hamming distance classifier used for matching process.

The paper is organized in the following manner; section I Introduction to iris biometric system, section II Related work, section III System model with preprocessing steps such as image acquisition, iris localization, normalization, feature extraction and Matching. Experimental results and discussion in section IV, finally conclusion in section V.

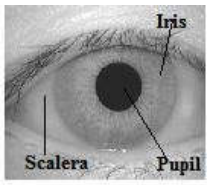

Figure.1: Structure of Iris

II. RELATED WORK

Various approaches exist in the past for iris recognition for person identification which includes John Daugman's Iriscode [4]. However proposed work uses Haar decomposition for iris feature extraction to get 348-bits iris code for effective iris recognition. Advantages of haar wavelet decomposition are its computational simplicity and speed. This method is less likely to be affected by environmental factors as compared to Gabor wavelet The Iris Recognition system's main work role is to provide compact and significant feature extraction algorithm for iris images with reduced false rejection rate. The extracted feature should have high discriminating capability and the segmented iris image should be free from artifacts. Daugman [4] used a multiscale quadrature two- dimentional(2-D) Gabor filter to demodulate phase information of an iris image to create an Iriscode for authentication by comparing the Iriscode stored in database. Li Ma et al. [14] extracted features using spatial filter, this technique first converts the round image of the iris into rectangular pattern by unwrapping the circular image. Wildes et al. [16] uses Laplacian pyramid for analysis of the Iris images. Boles and Boashash [19] uses zero-crossing method with dissimilarity functions of matching. Lim et al. [18] 2D Haar Transform for feature extraction and classifier used are initialization method of the weight vectors and a new winner selection method designed for iris recognition. A. Poursaberi and H. N. Araabi [1] [2] use wavelet Daubechies2 for feature extraction and two classifiers such as Minimum Hamming Distance and Harmonic mean.L. Ma et al., [11] class of 1-D wavelet i.e., 1-D Intensity signals for feature extraction and for feature matching they have used expanded binary feature vector with exclusive OR operations. In our proposed research work we will be using wavelet family i.e., Haar wavelet, db2 wavelet and db4 wavelet for feature extraction and perform comparison on the basis of their performance evaluation. We also use Hamming Distance classifier to matching binary strings with enrolled entity in the database. To fasten the matching speed, a lower number of 90 bits are used in composing the iris code, as compared with other methods such as 2048 bits in [1] [2].

III. SYSTEM MODEL

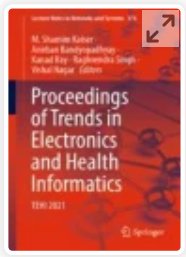

Proceedings of Trends in Electronics and Health Informatics pp 459–468

MonoLayer Graphene-Based Plasmonic Biosensor for Urine Glucose Detection

Archana Yadav, Anil Kumar & Preeta Sharan

Conference paper | First Online: 22 March 2022

Part of the Lecture Notes in Networks and Systems book series (LNNS,volume 376)

Abstract

In this proposed work, a plasmonic biosensor based on graphene has been presented to detect the biosample consisting of urine glucose. The proposed biosensor is comprised of five layers in the order of prism/Au/Si/graphene-sensing medium. P-polarized monochromatic light of 633 nm has been used for the excitation of the plasmons at the metal–semiconductor interface. This simulation study shows, by optimizing the thickness of gold (Au), silicon (Si), and graphene, the proposed biosensor can provide the sensitivity up to 219°/RIU (Refractive Index Unit) and gives the distinct shift in the resonance angle for a quite

small variation in the value of refractive indices (1.335, 1.336, 1.337, 1.338, 1.341, 1.347) corresponding to the glucose concentration level in non-diabetic person (0–15 mg/dl) and diabetic person (0.625 gm/dL, 1.25 gm/dL, 2.5 gm/dL, 5 gm/dL, and 10 gm/dL), respectively. A comparison is also made with, a bare gold (Au) layer and combination of gold–silicon (Au–Si) layer-based structure, and it is found that monolayer graphene plays a major role and enhances the sensitivity remarkably better than the other two structures which are having a sensitivity of 150°/RIU and 180°/RIU, respectively. We expect this novel work, which would be helpful in the diagnosis of the sugar concentration level with high sensitivity and high accuracy.

Keywords

SPR **Sensitivity** **Silicon** **Graphene**

Reflectance intensity

References

1. Oliver NS et al (2009) Glucose sensors: a review of current and emerging technology. Diabetic Med 26(3):197–210

2. World Health Organization (WHO). Diabetes. Available online: http://www.who.int/news-room/factsheets/detail/diabetes. Accessed on 3 Oct 2018

3. Karim MN, Anderson SR, Singh S, Ramanathan R, Bansal V (2018) Nanostructured silver fabric as a free-standing NanoZyme for colorimetric detection of glucose in urine. Biosens Bioelectron 110:8–15. https://doi.org/10.1016/j.bios.2018.03.025

4. Wild S, Roglic G, Green A, Sicree R, King H (2004) Global prevalence of diabetes: estimates for the year 2000 and projections for 2030. Diabetes Care 27:1047–1053

5. Zhang S, Wang N, Yu H, Niu Y, Sun C (2005) Covalent attachment of glucose oxidase to an Au electrode modified with gold nanoparticles for use as glucose biosensor. Bioelectrochemistry 67:15–22

6. Choi SH, Kim YL, Byun KM (2011) Graphene-on-silver substrates for sensitive surface plasmon resonance imaging biosensors. Opt Express 19:458–466

7. Kim M, Park K, Jeong E-J, Shin Y-B, Chung BH (2006) Surface plasmon resonance imaging analysis of protein–protein interactions using on-chip-expressed capture protein. Anal Biochem 351:298–304

8. Kretschmann E, Reather H (1968) Radiative decay of non-radiative surface plasmons excited by light. Zeitschrift fur Nature forschung 23:2135–2221

9. Hayashi S, Okamoto T (2012) Plasmonics: visit the past to know the future. J Phys D Appl Phys 45:433001. https://doi.org/10.1088/0022-3727/45/43/433001

10. Vibisha GA, Nayak JK, Maheswari P, Priyadharsini N, Nisha A, Jaroszewicz Z, Jha R (2020) Sensitivity enhancement of surface plasmon resonance sensor using hybrid configuration of 2D materials over bimetallic layer of Cu-Ni. Optics Comm 463:125337

11. Tabasi O, Falamaki C (2018) Recent advancements in the methodologies applied for the sensitivity enhancement of surface plasmon resonance sensors. Anal Methods 10:3906–3925. https://doi.org/10.1039/C8AY00948A

12. Wang J, Xiao Y, Cecen V, Shao C, Zhao Y, Qu L (2019) Tunable-deformed graphene layers for actuation. Front Chem 7:725. https://doi.org/10.3389/fchem.2019.00725

13. Lin Z, Jiang L, Wu L, Guo J, Dai X, Xiang Y, Fan D (2016) Tuning and sensitivity enhancement of surface plasmon resonance biosensor with graphene covered Au-MoS2-Au films. IEEE Photonics J 8(6):4803308

14. Rahman MM, Rana MM, Rahman MS, Anower MS, Mollah MA, Paul AK (2020) Sensitivity enhancement of SPR biosensors employing heterostructure of PtSe2 and 2D materials. Opt. Mater. **107**, 110123

15. Aspnes DE, Studna AA (1983) Dielectric functions and optical parameters of Si, Ge, GaP, GaAs, GaSb, InP, InAs, and InSb from 1.5 to 6.0 ev. Phys Rev B **27**(2):985

16. Prabowo BA, Alom A, Secario MK, Masim FCP, Lai HC, Hatanaka K et al (2016) Graphene-based portable SPR sensor for the detection of *Mycobacterium tuberculosis* DNA strain. Procedia Eng 168:541–545. https://doi.org/10.1016/j.proeng.2016.11.520

17. Wu L, Guo J, Wang Q, Lu S, Dai X, Xiang Y, Fan D (2017) Sensitivity enhancement by using few-layer black phosphorusgraphene/TMDCs heterostructure in surface plasmon resonance biochemical sensor. Sens. Actuators B 249:542–548

18. Markos P, Soukoulis C (2008) “Wave propagation,” in from electrons to photonic crystals and left-handed materials. Princeton University

19. Yadav A, Sharan P, Kumar A (2020) Surface plasmonic resonance based five layered structure-biosensor for sugar level measurement in human. Results in Optics 1:100002. https://doi.org/10.1016/j.rio.2020.100002

Author information

Authors and Affiliations

Department of ECE, ASET, Amity University, Uttar Pradesh, Noida, UP, 226010, India
Archana Yadav & Anil Kumar

Department of ECE, The Oxford College of Engineering, Bengaluru, 560068, India
Preeta Sharan

Editor information

Editors and Affiliations

Jahangirnagar University, Dhaka, Bangladesh
Dr. M. Shamim Kaiser

National Institute for Materials Science, Tsukuba, Japan
Dr. Anirban Bandyopadhyay

Amity University, Jaipur, India
Prof. Kanad Ray

Pranveer Singh Institute Of Technology, Kanpur, India

Dr. Raghvendra Singh

Pranveer Singh Institute Of Technology, Kanpur, India

Dr. Vishal Nagar

Rights and permissions

Copyright information

About this paper

Cite this paper

Yadav, A., Kumar, A., Sharan, P. (2022). MonoLayer Graphene-Based Plasmonic Biosensor for Urine Glucose Detection. In: Kaiser, M.S., Bandyopadhyay, A., Ray, K., Singh, R., Nagar, V. (eds) Proceedings of Trends in Electronics and Health Informatics. Lecture Notes in Networks and Systems, vol 376. Springer, Singapore. https://doi.org/10.1007/978-981-16-8826-3_39

.RIS .ENW .BIB

DOI
https://doi.org/10.1007/978-981-16-8826-3_39

Published	Publisher Name	Print ISBN
22 March 2022	Springer, Singapore	978-981-16-8825-6

Online ISBN	eBook Packages

978-981-16-8826-3

Engineering

Engineering (R0)

New Trends and Applications in Internet of Things (IoT) and Big Data Analytics pp 139–148

An Optical Solution for High-Density Data Storage Using Plasmonic Based MZI Nano-Structures

R. Srujana, Thangadurai Natarajan, Mohammad Kamrul Hasan, Preeta Sharan, Manpreet S. Manna & Shayla Islam

Chapter | First Online: 17 May 2022

Part of the Intelligent Systems Reference Library book series (ISRL,volume 221)

Abstract

The mounting demands for superior data processing and data storage due to the rapid growth in data analytics has led a new direction towards optical data computation and storage technology. Towards this endeavor, we have designed and simulated a Mach-Zhender interferometer based optical waveguide structure to store optical information. The simulated structure consists of Mach-Zhender cavity created on the metal layer which is placed on top of the layer-based optical waveguide structure. The

intensity difference exhibited by the Plasmonic Mach-Zhender Nanostructure can be comparable with the logic conditions 0 and 1 states which can be identified by the respective phase shifts. Each unit cell can transfer data at a speed of 73 MB/s, a figure significantly higher than what the existing technology could achieve, which is roughly 4.5 MB/s.

Keywords

Plasmons **Optical waveguides**

Phase shifting interferometry

Optical data storage

References

1. W.A. Bhat, “Bridging data-capacity gap in big data storage, Future Generation Computer Systems”. 2018.

2. Gu, M, Li, X. & Cao Y, “Optical storage arrays: a perspective for future big data storage”, Light Sci Appl 3. 2014.

3. Mansuripur, M., et al.: "Plasmonic Optical data storage, "Optical Data Storage Topical Meeting, pp. 43–45. Lake Buena Vista, FL, USA (2009)

4. Mansuripur, Masud; Zakharian et al., “structures for Optical Data Storage”, Optics express. 2009.

5. Tong, Quang et al., “Arbitrary Form Plasmonic Structures: Optical Realization, Numerical Analysis and Demonstration Applications”, 2018.

6. Hu Jinlian, Wang Cong, Yan Shikuan, Zhou Fei, Li Zhigang, Kan C, “Surface Plasmon Resonance in Periodic Hexagonal Lattice Arrays of Silver Nanodisks”, Journal of Nanomaterials, 2013.

7. Zhang Junxi, Zhang Lide, Xu Wei, “Surface plasmon polaritons: Physics and applications”, Journal of Physics D-applied Physics - J PHYS-D-APPL PHYS, 2012.

8. Davis, Timothy, Gómez, Daniel Roberts, Ann, "Plasmonic circuits for manipulating optical information", Nanophotonics, 2016.

9. Sorger Volke, Oulton Rupert, Ma, Ren-Min, Zhang Xiang, "Toward integrated plasmonic circuits", MRS Bulletin, Vol. no 37, 2012.

10. Wu y, C Liu, G Jhan, "All-optical switch based on the local nonlinear plasmonic Mach-Zehnder interferometer waveguides", International Conference on Numerical Simulation of Optoelectronic Devices (NUSOD), Taipei. pp. 51–52, 2015.

11. Fang Y, Sun M, "Nanoplasmonic waveguides: towards applications in integrated Nanophotonic circuits", Light Sci Appl 4. 2015.

12. Bozhevolnyi, Sergey, " Plasmonic Nano-Guides and Circuits", 2008. https://doi.org/10.1364/META_PLAS.2008.MWD3.

13. Nemova, Galina, Kabashin, Andrey.V, Kashyap, Raman, "Surface plasmon-polariton Mach-Zehnder refractive index sensor", J. Opt. Soc. Am. B 25; 1673–1677, 2008.

14. Bahrampour, Ali Reza; Tofighi, Sara; Bathaee, Marzieh; Farman, Farnaz, “Optical Fiber Interferometers and Their Applications, Interferometry”, Research and Applications in Science and Technology, 2016.

15. Fernandez, Luis; Torres, Pedro; Causado, Jesús; Betancur, Rafael. Development of a Mach-Zehnder interferometer based on a twin-core fiber and analysis of its thermal stability”, Proc. SPIE 7056, Photonic Fiber and Crystal Devices: Advances in Materials and Innovations in Device Applications II. 2008.

16. Ueli Koch et al., “A monolithic bipolar CMOS electronic–plasmonic high-speed transmitter”, Nature Electronics. 2020.

17. https://refractiveindex.info/

18. Sing P, Tripathi D.K, Jaiswal S, Dixit H.K. “Design and analysis of all-optical AND, XOR and OR gates basedon SOA-MZI configuration”, Optic Laser Technol.Vol no. 66, Pages 35–44, 2015

19. Singh Pallavi, Singh Ashutosh Kumar, Arun, Vanya Tripath, Devendra K, “Comparative study of all-optical INVERTER and BUFFER gates using MZI structure”, Journal of Optical Communications no. 2020.

Acknowledgements

Place your acknowledgments before References. Do not mention the sponsors and/or financial support obtained in this section. These specifications are to be included in an unnumbered footnote on the first page of the paper.

Author information

Authors and Affiliations

Department of ECE, Jain University, Bangalore, India

R. Srujana & Thangadurai Natarajan

Faculty of Information Science and Technology, Universiti Kebangsaan, Bangi, Malaysia

Mohammad Kamrul Hasan

Electronics and Communication Engineering, The Oxford College of Engineering, Bangalore, India

Preeta Sharan

Instrumentation and Control Engineering, Sant Longowal Institute for Engineering and Technology, Longowal, Punjab, India

Manpreet S. Manna

Institute of Computer Science and Digital Innovation, UCSI University, Bangi, Malaysia

Shayla Islam

Editor information

Editors and Affiliations

SRM Institute of Science and Technology, Ghaziabad, Uttar Pradesh, India

Dr. Rohit Sharma

Department of Computer Engineering & Applications, GLA University, Mathura, Uttar Pradesh, India

Prof. Dilip Sharma

Rights and permissions

Copyright information

About this chapter

Cite this chapter

Srujana, R., Natarajan, T., Hasan, M.K., Sharan, P., Manna, M.S., Islam, S. (2022). An Optical Solution for High-Density Data Storage Using Plasmonic Based MZI Nano-Structures. In: Sharma, R., Sharma, D. (eds) New Trends and Applications in Internet of Things (IoT) and Big Data Analytics. Intelligent Systems Reference Library, vol 221. Springer, Cham. https://doi.org/10.1007/978-3-030-99329-0_10

.RIS .ENW .BIB

DOI
https://doi.org/10.1007/978-3-030-99329-0_10

Published Publisher Name Print ISBN

17 May 2022 | Springer, Cham | 978-3-030-99328-3

Online ISBN 978-3-030-99329-0

eBook Packages
Intelligent Technologies and Robotics
Intelligent Technologies and Robotics (R0)

New Trends and Applications in Internet of Things (IoT) and Big Data Analytics pp 139–148

An Optical Solution for High-Density Data Storage Using Plasmonic Based MZI Nano-Structures

R. Srujana, Thangadurai Natarajan, Mohammad Kamrul Hasan, Preeta Sharan, Manpreet S. Manna & Shayla Islam

Chapter | First Online: 17 May 2022

Part of the Intelligent Systems Reference Library book series (ISRL,volume 221)

Abstract

The mounting demands for superior data processing and data storage due to the rapid growth in data analytics has led a new direction towards optical data computation and storage technology. Towards this endeavor, we have designed and simulated a Mach-Zhender interferometer based optical waveguide structure to store optical information. The simulated structure consists of Mach-Zhender cavity created on the metal layer which is placed on top of the layer-based optical waveguide structure. The

intensity difference exhibited by the Plasmonic Mach-Zhender Nanostructure can be comparable with the logic conditions 0 and 1 states which can be identified by the respective phase shifts. Each unit cell can transfer data at a speed of 73 MB/s, a figure significantly higher than what the existing technology could achieve, which is roughly 4.5 MB/s.

Keywords

Plasmons **Optical waveguides**

Phase shifting interferometry

Optical data storage

References

1. W.A. Bhat, “Bridging data-capacity gap in big data storage, Future Generation Computer Systems”. 2018.

2. Gu, M, Li, X. & Cao Y, “Optical storage arrays: a perspective for future big data storage”, Light Sci Appl 3. 2014.

3. Mansuripur, M., et al.: "Plasmonic Optical data storage, "Optical Data Storage Topical Meeting, pp. 43–45. Lake Buena Vista, FL, USA (2009)

4. Mansuripur, Masud; Zakharian et al., “structures for Optical Data Storage”, Optics express. 2009.

5. Tong, Quang et al., “Arbitrary Form Plasmonic Structures: Optical Realization, Numerical Analysis and Demonstration Applications”, 2018.

6. Hu Jinlian, Wang Cong, Yan Shikuan, Zhou Fei, Li Zhigang, Kan C, “Surface Plasmon Resonance in Periodic Hexagonal Lattice Arrays of Silver Nanodisks”, Journal of Nanomaterials, 2013.

7. Zhang Junxi, Zhang Lide, Xu Wei, “Surface plasmon polaritons: Physics and applications”, Journal of Physics D-applied Physics - J PHYS-D-APPL PHYS, 2012.

8. Davis, Timothy, Gómez, Daniel Roberts, Ann, “Plasmonic circuits for manipulating optical information”, Nanophotonics, 2016.

9. Sorger Volke, Oulton Rupert, Ma, Ren-Min, Zhang Xiang, “Toward integrated plasmonic circuits”, MRS Bulletin, Vol. no 37, 2012.

10. Wu y, C Liu, G Jhan, “All-optical switch based on the local nonlinear plasmonic Mach-Zehnder interferometer waveguides”, International Conference on Numerical Simulation of Optoelectronic Devices (NUSOD), Taipei. pp. 51–52, 2015.

11. Fang Y, Sun M, “Nanoplasmonic waveguides: towards applications in integrated Nanophotonic circuits”, Light Sci Appl 4. 2015.

12. Bozhevolnyi, Sergey, “ Plasmonic Nano-Guides and Circuits”, 2008. https://doi.org/10.1364/META_PLAS.2008.MWD3.

13. Nemova, Galina, Kabashin, Andrey.V, Kashyap, Raman, “Surface plasmon-polariton Mach-Zehnder refractive index sensor”, J. Opt. Soc. Am. B 25; 1673–1677, 2008.

14. Bahrampour, Ali Reza; Tofighi, Sara; Bathaee, Marzieh; Farman, Farnaz, “Optical Fiber Interferometers and Their Applications, Interferometry”, Research and Applications in Science and Technology, 2016.

15. Fernandez, Luis; Torres, Pedro; Causado, Jesús; Betancur, Rafael. Development of a Mach-Zehnder interferometer based on a twin-core fiber and analysis of its thermal stability”, Proc. SPIE 7056, Photonic Fiber and Crystal Devices: Advances in Materials and Innovations in Device Applications II. 2008.

16. Ueli Koch et al., “A monolithic bipolar CMOS electronic–plasmonic high-speed transmitter”, Nature Electronics. 2020.

17. https://refractiveindex.info/

18. Sing P, Tripathi D.K, Jaiswal S, Dixit H.K. "Design and analysis of all-optical AND, XOR and OR gates basedon SOA-MZI configuration", Optic Laser Technol.Vol no. 66, Pages 35–44, 2015

19. Singh Pallavi, Singh Ashutosh Kumar, Arun, Vanya Tripath, Devendra K, "Comparative study of all-optical INVERTER and BUFFER gates using MZI structure", Journal of Optical Communications no. 2020.

Acknowledgements

Place your acknowledgments before References. Do not mention the sponsors and/or financial support obtained in this section. These specifications are to be included in an unnumbered footnote on the first page of the paper.

Author information

Authors and Affiliations

Department of ECE, Jain University, Bangalore, India

R. Srujana & Thangadurai Natarajan

Faculty of Information Science and Technology, Universiti Kebangsaan, Bangi, Malaysia

Mohammad Kamrul Hasan

Electronics and Communication Engineering, The Oxford College of Engineering, Bangalore, India

Preeta Sharan

Instrumentation and Control Engineering, Sant Longowal Institute for Engineering and Technology, Longowal, Punjab, India

Manpreet S. Manna

Institute of Computer Science and Digital Innovation, UCSI University, Bangi, Malaysia

Shayla Islam

Editor information

Editors and Affiliations

SRM Institute of Science and Technology, Ghaziabad, Uttar Pradesh, India

Dr. Rohit Sharma

Department of Computer Engineering & Applications, GLA University, Mathura, Uttar Pradesh, India

Prof. Dilip Sharma

Rights and permissions

Copyright information

About this chapter

Cite this chapter

Srujana, R., Natarajan, T., Hasan, M.K., Sharan, P., Manna, M.S., Islam, S. (2022). An Optical Solution for High-Density Data Storage Using Plasmonic Based MZI Nano-Structures. In: Sharma, R., Sharma, D. (eds) New Trends and Applications in Internet of Things (IoT) and Big Data Analytics. Intelligent Systems Reference Library, vol 221. Springer, Cham. https://doi.org/10.1007/978-3-030-99329-0_10

.RIS .ENW .BIB

DOI
https://doi.org/10.1007/978-3-030-99329-0_10

Published	Publisher Name	Print ISBN
17 May 2022	Springer, Cham	978-3-030-99328-3

Online ISBN	eBook Packages
978-3-030-99329-0	Intelligent Technologies and Robotics Intelligent Technologies and Robotics (R0)

New Trends and Applications in Internet of Things (IoT) and Big Data Analytics pp 93–107

Design and Analysis of Outer Rotor Brushless DC Motor for Robotics Using Ansys Maxwell Software

Mohammad Kamrul Hasan, Yashu Verma, Preeta Sharan, Manpreet S. Manna & Shayla Islam

Chapter | First Online: 17 May 2022

Part of the Intelligent Systems Reference Library book series (ISRL,volume 221)

Abstract

Brushless DC (BLDC) Motors are attracting considerable interest from robotics industry for most of the last decade. They are highly durable and weightless than other devices with approximately equal power outputs, and they are ideal for high-speed robotic applications This chapter presents a design and performance analysis of two outer rotor BLDC motors of 1500 W rating for robotic application. The geometries of these BLDC motors having high slots and pole combination were designed by using RMxprt software and their efficiency and performance was

then analyzed. Further, its electromagnetic study was performed in Maxwell 2D environment. The results show the significant effect of high slots and pole configuration on the efficiency of the machines. The results obtained are found to be in good agreement.

Keywords

Brushless DC motor **Finite element method**

ANSYS Maxwell **Motor design**

References

1. Gandhi, S.U., Prasad, B.S.: Modelling and intelligent control of micro PMBLDC for surgical robotic applications. Proc. Comput. Sci. **171**, 745–754 (2020)

2. Patel, S.S., Botre, B.A., Krishan, K., Kaushal, K., Samarth, S., Akbar, S.A., Biradar, Y., Prabhu, K.R.: Modeling and implementation of intelligent commutation system for BLDC motor in underwater robotic applications. In: 2016 IEEE 1st International Conference on Power Electronics, Intelligent Control and Energy Systems (ICPEICES), pp. 1–4. IEEE (2016)

3. Seo, J.M., Rhyu, S.H., Kim, J.H., Choi, J.H., Jung, I.S.: Design of axial flux permanent magnet brushless DC motor for robot joint module. In: The 2010 International Power Electronics

Conference-ECCE ASIA, pp. 1336–1340. IEEE (2010)

4. Nguyen, P.T., Ha, D.H., Avand, M., Jaafari, A., Nguyen, H.D., Al-Ansari, N., Van Phong, T., Sharma, R., Kumar, R., Le, H.V., Ho, L.S., Prakash, I., Pham, B.T.: Soft computing ensemble models based on logistic regression for groundwater potential mapping. Appl. Sci. **10**, 2469 (2020)

5. Jha, S., et al.: Deep learning approach for software maintainability metrics prediction. IEEE Access **7**, 61840–61855 (2019)

6. Shrivastava, N., Brahmin, A.: Design of 3-phase BLDC motor for electric vehicle application by using finite element simulation. Int. J. Emerg. Technol. Adv. Eng. **4**(1), 140–145 (2014)

7. Sharma, R., Kumar, R., Sharma, D.K., Son, L.H., Priyadarshini, I., Pham, B.T., Bui, D.T., Rai, S.: Inferring air pollution from air quality index by different geographical areas: case study in India. Air Qual. Atmos. Health **12**, 1347–1357 (2019)

8. Sharma, R., Kumar, R., Singh, P.K., Raboaca, M.S., Felseghi, R.-A.: A Systematic study on the analysis of the emission of CO, CO2 and HC for four-wheelers and its impact on the sustainable ecosystem. Sustainability **12**, 6707 (2020)

9. Dansana, D., Kumar, R., Das Adhikari, J., Mohapatra, M., Sharma, R., Priyadarshini, I., Le, D.-N.: Global forecasting confirmed and fatal cases of COVID-19 outbreak using autoregressive integrated moving average model. Front. Public Health **8**, 580327 (2020). https://doi.org/10.3389/fpubh.2020.580327

10. Nekoubin, A.: Design a single-phase BLDC motor and finite-element analysis of stator slots structure effects on the efficiency. Int. J. Electr. Comput. Eng. **5**(5), 685–692 (2011)

11. Dusane, P.: Simulation of BLDC hub motor in ANSYS - Maxwell (2016). https://doi.org/10.13140/RG.2.1.2601.1764

12. Hendershot, J.R.: Brushless DC motor phase, pole and slot configurations. In: Proceedings of 9th International Symposium on Incremental Motion Control Systems and Devices, pp. 146–159 (1990)

13. Malik, P.K., Sharma, R., Singh, R., Gehlot, A., Satapathy, S.C., Alnumay, W.S., Pelusi, D., Ghosh, U., Nayak, J.: Industrial internet of things and its applications in industry 4.0: state of the art. Comput. Commun. 166, 125–139 (2021). https://doi.org/10.1016/j.comcom.2020.11.016, ISSN 0140-3664

14. Sharma, R., Kumar, R., Satapathy, S.C., Al-Ansari, N., Singh, K.K., Mahapatra, R.P., Agarwal, A.K., Le, H.V., Pham, B.T.: Analysis of water pollution using different physicochemical parameters: a study of Yamuna river. Front. Environ. Sci. **8**, 581591 (2020). https://doi.org/10.3389/fenvs.2020.581591

15. Waghmare, T., Choube, P.R., Dakre, A., Suryawanshi, A.M., Holambe, P.: Design of internal permanent magnet brushless DC motor using ANSYS. Int. J. Res. Publ. Eng. Technol. (4). ISSN: 2454–7875

16. Singh, V.K., Marwaha, S., Singh, A.K.: Design and analysis of permanent magnet brushless DC motor for solar vehicle using Ansys software. Int. J. Eng. Tech. Res. **6**, 4 (2017)

17. Dansana, D., Kumar, R., Parida, A., Sharma, R., Adhikari, J.D., et al.: Using susceptible-

exposed-infectious-recovered model to forecast coronavirus outbreak. Comput. Mater. Contin. **67**(2), 1595–1612 (2021)

18. Vo, M.T., Vo, A.H., Nguyen, T., Sharma, R., Le, T.: Dealing with the class imbalance problem in the detection of fake job descriptions. Comput. Mater. Contin. **68**(1), 521–535 (2021)

19. Sachan, S., Sharma, R., Sehgal, A.: Energy efficient scheme for better connectivity in sustainable mobile wireless sensor networks. Sustain. Comput. Inf. Syst. **30**, 100504 (2021)

20. Ghanem, S., Kanungo, P., Panda, G., et al.: Lane detection under artificial colored light in tunnels and on highways: an IoT-based framework for smart city infrastructure. Complex Intell. Syst. (2021). https://doi.org/10.1007/s40747-021-00381-2

21. Sachan, S., Sharma, R., Sehgal, A.: SINR based energy optimization schemes for 5G vehicular sensor networks. Wirel. Pers. Commun. (2021). https://doi.org/10.1007/s11277-021-08561-6

22. Priyadarshini, I., Mohanty, P., Kumar, R., et al.: A study on the sentiments and psychology of twitter users during COVID-19 lockdown

period. Multimed. Tools Appl. (2021). https://doi.org/10.1007/s11042-021-11004-w

23. Azad, C., Bhushan, B., Sharma, R., et al.: Prediction model using SMOTE, genetic algorithm and decision tree (PMSGD) for classification of diabetes mellitus. Multimed. Syst. (2021). https://doi.org/10.1007/s00530-021-00817-2

24. Priyadarshini, I., Kumar, R., Tuan, L.M., et al.: A new enhanced cyber security framework for medical cyber physical systems. SICS Softw.-Inensiv. Cyber-Phys. Syst. (2021). https://doi.org/10.1007/s00450-021-00427-3

25. Priyadarshini, I., Kumar, R., Sharma, R., Singh, P.K., Satapathy, S.C.: Identifying cyber insecurities in trustworthy space and energy sector for smart grids. Comput. Electr. Eng. **93**, 107204 (2021)

Acknowledgements

Place your acknowledgments before References. Do not mention the sponsors and/or financial support obtained in this section. These specifications are to be included in an unnumbered footnote on the first page of the paper.

Author information

Authors and Affiliations

Faculty of Information Science and Technology, Universiti Kebangsaan Malaysia, Bangi, Malaysia
Mohammad Kamrul Hasan

Instrumentation and Control Engineering, Sant Longowal Institute for Engineering and Technology, Longowal, Punjab, India
Yashu Verma

Electronics and Communication Engineering, The Oxford College of Engineering, Bangalore, India
Preeta Sharan

Instrumentation and Control Engineering, Sant Longowal Institute for Engineering and Technology, Longowal, Punjab, India
Manpreet S. Manna

Institute of Computer Science and Digital Innovation, UCSI University Malaysia, Kuala Lumpur, Malaysia
Shayla Islam

Editor information

Editors and Affiliations

SRM Institute of Science and Technology, Ghaziabad, Uttar Pradesh, India
Dr. Rohit Sharma

Department of Computer Engineering & Applications, GLA University, Mathura, Uttar Pradesh, India
Prof. Dilip Sharma

Rights and permissions

Reprints and Permissions

Copyright information

About this chapter

Cite this chapter

Hasan, M.K., Verma, Y., Sharan, P., Manna, M.S., Islam, S. (2022). Design and Analysis of Outer Rotor Brushless DC Motor for Robotics Using Ansys Maxwell Software. In: Sharma, R., Sharma, D. (eds) New Trends and Applications in Internet of Things (IoT) and Big Data Analytics. Intelligent Systems Reference Library, vol 221. Springer, Cham. https://doi.org/10.1007/978-3-030-99329-0_7

.RIS .ENW .BIB

DOI
https://doi.org/10.1007/978-3-030-99329-0_7

Published	Publisher Name	Print ISBN
17 May 2022	Springer, Cham	978-3-030-99328-3

Online ISBN	eBook Packages
978-3-030-99329-0	Intelligent Technologies and Robotics Intelligent Technologies and Robotics (R0)

ScienceDirect

Materials Today: Proceedings

Volume 58, Part 1, 2022, Pages 451-455

Theoretical investigation of Bragg Reflector optical sensor for the measurement of cryogenic temperature

Ranjith B. Gowda [a b], H.N. Gayathri [c], Preeta Sharan [d], K. Saara [a]

Show more

https://doi.org/10.1016/j.matpr.2022.02.482

Get rights and content

Abstract

The goal of the proposed work is to design and analyze a low temperature sensor to measure cryogenic temperature in the range of 0–120K. Proposed sensor design uses Distributed Bragg Reflector (DBR) multi-layer structure. DBR consists of high-low alternate dielectric materials arranged in one direction which acts as a one-dimensional photonic crystal (pc). Gallium Arsenide (GaAs) is used as high dielectric material and air as low dielectric material. GaAs dielectric constant is a function of the temperature and hence it can be used to detect any variation in the temperature. In this work, the number of alternate multi-layers (N) is chosen as 8 and the frequency of input electromagnetic wave is taken as 24THz. We achieved a high sensitivity of 1.525nm/K with a Q factor of 3534. The proposed sensor suits for the applications where critical low temperature measurement is needed.

Previous Next

Keywords

Photonic crystal; Cryogenic temperature; Distributed Bragg Reflector; Optical sensor; Gallium arsenide

Special issue articles Recommended articles

Cited by (3)

1-Dimensional silicon photonic crystal pressure sensor for the measurement of low pressure

2023, Results in Optics

Show abstract

Highly sensitive temperature sensor using one-dimensional Bragg Reflector for biomedical applications

2023, Biomedizinische Technik

One-dimensional optical Bragg grating sensor for the detection of urine glucose concentration

2022, Journal of Optics (India)

Original Research | Published: 22 May 2022

Compactness measure of rail wheel rolling contact of the freight wagon

Suchandana Mishra, Preeta Sharan & K. Saara

International Journal of Information Technology **14**, 2335–2342 (2022)

Abstract

This paper describes the measure of compactness using finite element analysis and stress–strain characteristics of freight wagon considering loaded and unloaded condition of wagon weight. Freight train wagons are used to carry various goods from one part to other parts of country. In terms of preserving the originality of the contact load transfer, the use of accurate finite element loading and boundary conditions has been a significant use. The main idea is to study the strain behaviour of goods wagon for empty and gross load condition. As the weight varies from low to high, that means from 22.47t to 88.47t, strain induced on rail increases linearly with the wagon load. This analysis is important as it determines the capacity to carry maximum load and to build weigh in motion system. By use of optical simulator, fiber

Bragg grating is designed to observe change in Bragg's wavelength with the wagon load.

References

1. Sasi D, Philip S, David R, Swathi J (2020) A review on structural health monitoring of railroad track structures using fiber optic sensors. Mater Today Proc 33:3787–3793. https://doi.org/10.1016/j.matpr.2020.06.217

2. Patrascu AI, Hadar A, Dan Pastrama S (2020) Structural analysis of a freight wagon with

composite walls. Mater Plast 57(2):140–151. https://doi.org/10.37358/MP.20.2.5360

3. Vinod P, Koteswara Rao U, Reddy CK (2014) Analysis of railway wheel to study the stress variations. Int J Eng Res Tech 3(2):1286–1291

4. Vendittozzi C et al (2020) Static and dynamic weighing of rolling stocks by mean of a customized FBG-sensorized-patch. Int J Saf Secur Eng 10(1):83–88. https://doi.org/10.18280/ijsse.100111

5. Kirushanth S, Kabaso B (2020) Design and development of weigh-in-motion using vehicular telematics. J Sensors. https://doi.org/10.1155/2020/7871215

6. Buchacz A, Płaczek M, Wróbel A (2016) Analysis of dynamical response of the freight wagon. Springer Proc Math Stat 181:117–129. https://doi.org/10.1007/978-3-319-42402-6_11

7. Wang H, Zhu Q, Li J, Mao J, Hu S, Zhao X (2019) Identification of moving train loads on railway bridge based on strain monitoring. Smart Struct Syst 23:263–278. https://doi.org/10.12989/sss.2019.23.3.263

8. Sharma SK, Kumar A (2016) Dynamic analysis of wheel/rail interaction using finite element method. Proc Eng 144:1119–1128

9. Du C, Dutta S, Kurup P, Yu T, Wang X (2020) "A review of railway infrastructure monitoring using fiber optic sensors. Sens Actuators A Phys 303:111728. https://doi.org/10.1016/j.sna.2019.111728

10. Wei CL et al (2010) A fiber Bragg grating sensor system for train axle counting. IEEE Sens J 10(12):1905–1912. https://doi.org/10.1109/JSEN.2010.2049199

11. Guta S, Tilahun D (2016) Stress analysis of rail joint under wheel load. Int J Innovative Sci Eng Technol 3(6):526–543

12. Zulkifli MA, Basaruddin KS, Abdul Rahim Y, Afendi M, Gurubaran P, Ibrahim I (2018) Three dimensional finite element analysis on railway rail. In: IOP Conf. Ser. Mater. Sci. Eng., vol 429(1). https://doi.org/10.1088/1757-899X/429/1/012010

13. Jagadeep B, Kiran Kumar P, Subbaiah KV (2018) Stress analysis on rail wheel contact. Int J Res Eng 1:47–52

14. Esen I, Eroglu M (2015) 3D finite element analysis of UIC 60 rail and UIC 515 wheel rolling contact and understanding starting mechanism of wear. 2nd International Iron and Steel Symposium (IISS'15)

15. Milne D, Masoudi A, Ferro E, Watson G, Le Pen L (2020) An analysis of railway track behaviour based on distributed optical fibre acoustic sensing. Mech Syst Signal Process 142:106769. https://doi.org/10.1016/j.ymssp.2020.106769

16. Mishra S, Sharan P, Kamath SP, Saara K (2021) Monitoring of rail wheel impact for various train speeds. In: Proc. 2021 8th Int. Conf. Comput. Sustain. Glob. Dev. INDIACom 2021, pp 714–719. https://doi.org/10.1109/INDIACom51348.2021.00127

17. Sharma R et al (2009) Design & simulation of optical fiber Bragg grating pressure sensor for minimum. J Theor Appl Inf Technol 515–530

18. Sharan P, Patil PP, Srivastava MC, Upadhyaya AM (2020) Nonlinear response of fiber Bragg grating for health monitoring of railway track. IEEE, India, pp 3–7

Acknowledgements

Authors would like to acknowledge the Faculty of ECE Department, Oxford College of Engineering, Bengaluru and Dayananda Sagar University, Bengaluru for providing lab facility and required software and guidance for completing the work.

Author information

Authors and Affiliations

Department of Electronics and Communication, School of Engineering, Dayananda Sagar University, Bangalore, 560068, Karnataka, India

Suchandana Mishra & K. Saara

Department of Electronics and Communication Engineering, The Oxford College of Engineering, Bangalore, 560068, Karnataka, India

Preeta Sharan

Corresponding author

Correspondence to Suchandana Mishra.

Rights and permissions

About this article

Cite this article

Mishra, S., Sharan, P. & Saara, K. Compactness measure of rail wheel rolling contact of the freight wagon. *Int. j. inf. tecnol.* **14**, 2335–2342 (2022). https://doi.org/10.1007/s41870-022-00977-y

Received	Accepted	Published
08 February 2022	28 April 2022	22 May 2022

Issue Date
August 2022

DOI
https://doi.org/10.1007/s41870-022-00977-y

Keywords

Freight wagon **Rail wheel** **Load analysis**

Optical sensor **Fiber Bragg grating**

Research Article | Published: 08 November 2022

Comparative analysis and design of high-performance photonic crystal add–drop filter for optical switching

Amita Asthana, Anil Kumar & Preeta Sharan

Journal of Optics (2022)

Abstract

Photonic crystal add–drop filter structures are promising technology for optical communication networks. This paper presents the design of H-shaped photonic crystal add–drop filter that consists of one straight waveguide and four arm waveguides. A ring resonator-based add–drop filter has been proposed with upper and lower waveguides for light propagation. A triangular-shaped add–drop filter has also been designed using two-dimensional photonic crystals (2D-PCs) also with high optical transmission capabilities. Numerical methods such as plane wave expansion and finite-difference time-domain method have been employed in the execution of this work. The proposed 1 × 4 H-shaped add–drop filter has shown an optimum quality factor (QF) and transmission

efficiency (TE) for the wavelength range of 1.465–1.50 μm. The ring resonator-based add–drop filter has been designed for the wavelength range from 1.48 to 1.495 μm to obtain better transmission potential. The triangular-shaped add–drop filter has been designed having a high QF with band gap ranging from 1.440 to 1.550 μm. From the results, it has been observed that the triangular-shaped filter has obtained a transmission efficiency of 90% and a QF of 7239 compared with other photonic crystal add–drop filters in the literature. The designed H-shaped add–drop filter and ring resonator have also obtained high QF values of 5853 and 6453, respectively. An extensive survey and comparison has been presented in the paper, and the related parameters have been compared to feature the obtained results. Photonic crystal structures presented in this paper have been redefined for different configurations with multiple ports for monitoring the power. The H-shaped and triangular-shaped add–drop filters for rod in air configuration have been designed, which has better visibility for simulation in micromachining domain with very less runtime.

Introduction

Integrated optical fibre technology has provided enormous resources in developing feasible fabrication systems onto a single chip. Numerous photonic or optical fields have been joined together to form integration for such devices [1]. While photons regulate the process of photonic integrated circuit (PIC) devices, electronic control of optical devices dictates the terminology of input and output via some conversion techniques between the two domains. Additionally, PIC is referred to as 'all-optical' technology since it does not involve any optoelectronic conversion of signals. An optical splitter built on a quartz substrate, which functions similarly to a coaxial cable transmission system, is an integrated waveguide optical power distribution component. Being customizable is one of an add–drop filter's most crucial properties which can be used for sensing applications. 2D-PCs with changing refractive indices are widely used for the bio-sensing applications [2, 3]. The best materials to create all optical components suited for integrated optical circuits right now are photonic crystals. Various parameters can be acquired to change the structure's spectral characteristics. In this work, high-performance add–drop filters have been proposed with silicon rods in air. H-shaped, ring-shaped and triangular-shaped add–drop filters have been investigated in terms of QF and TE. It is immensely required to construct the photonic crystal-based add–drop filter with an adjustable

and impressionable structure along with least no scattering and dispersion loss. The proposed structures are easy to simulate with very less runtime in micro-design environment. This paper presents a brief insight into the related works available in the literature. The time-domain mathematical modelling has been illustrated for a transverse electric mode. Structural details for the presented add–drop filters and simulation results have been presented in the paper. This paper also delineates the comparative analysis of the proposed add–drop filters with add–drop filters available in the literature.

Background work

The photonic band gap (PBG) is a crucial characteristic of photonic crystal lattices. High values of QF are the pivotal concern of the subject [4, 5]. A group of wavelengths known as the PBG are prohibited from moving through the crystal lattice. The linear defect created in the structure allows the light whose wavelength is within the PBG to flow readily without being scattered. The specified combination of waveguides with ring resonators can be selected for a broadband add–drop filter [6]. A one-dimensional thin-film stack, in which the thickness of the two distinct materials is on the order of a wavelength, reflects the embellished nucleation characteristics. Since thin-film stacks have been a thing for more than a century, the idea of two- or three-dimensional

photonic crystals did not come along until much later. In addition to the induction of 2D-PC, power separators have been designed by filling magnetic fluid in the selected rods of photonic crystal. These designs are able to differentiate the polarization modes as well by representing the photonic effects with magnetic properties [7]. A photonic crystal add–drop filter employing a photonic crystal ring resonator (PhCRR) within a two-dimensional (2D) square photonic crystal structure made of dielectric rods inserted in air has been proposed by Rakhshani and Mansouri Birjandi [8]. Optical filters provide the ability to transmit light selectively within a given wavelength window while blocking outliers. The filters can be created to pass some frequency bands of signals while attenuating others. The filters are often categorized based on their features in the frequency domain. These include low-pass, high-pass, band-pass, band-stop, all-pass and notch filters. A rounded square ring resonator and multi-channel square ring resonators with direct and non-direct dropping waveguides have been proposed [9, 10]. Besides wavelength selectivity, the photonic crystals are also being used for various sensing applications in various fields including medical applications. The bio-sensing applications are based conceptually on the pressures induced by the antibody (bio-molecules) chemical reactions. These pressures may be recorded by the micro-cantilevers containing photonic crystals in various shapes. The corresponding specific wavelengths detected or

sensed by the photonic crystals suggest the presence of the interrelated chemical acknowledgement [11,12,13,14]. Recently, numerous other types of photonic add–drop filters based on square and triangular lattices of a 2D-PC ring resonator have been presented. A quasi-square ring resonator in square-shaped photonic crystal, a hexagonal ring resonator in triangle-shaped photonic crystal and a circular ring resonator in 12 fastened quasi-photonic filters have been investigated in terms of QF and band tuning capability. It has been investigated that 2 × 2 and 3 × 3 PhCRRs theoretically offer high QF and the QF can also be increased by inducing line defects in the photonic crystals [15]. A photonics crystal filter with mirror cavities has been proposed by Djavid and Abrishamian [16]. Later, a dual-curved Fabry–Perot photonic crystal resonator was proposed. Since a high QF is always desirable for better optical communication in the given band gap, it has been stated that by inducing open-ended wave guides the QF can be improved [17]. By incorporating two distinct refractive indices into the two-dimensional photonic crystal with square lattices, a multi-channel drop filter can be created. A 3 × 3 input/output photonic crystal filter has been proposed, and the three different wavelengths were obtained with a greater efficiency in comparison with the other two ports [18]. Single- and dual-ring hexagonal-shaped photonic crystal add–drop filters were proposed in which a dual-ring filter with an open-end waveguide has shown a

better QF than a single-ring filter [19]. It has been further demonstrated that the resonant wavelength of the filter may be modified by adjusting structural factors such the dielectric constant of the inner, coupling, neighbouring and complete rods of the structure. For single and dual PhCRR, the filter properties such as dropping efficiency (DE), resonant wavelength and QF have been explored for evaluation of filter performance. The dielectric rods can also be used as scatters in the 2D-PC to correct the filter characteristics [20]. Nano-cavity resonator (NCR) and nano-ring resonator with hexagonal structures were examined and derived to be future technology for the sensing applications [21]. 45° PhCRRs have been designed in both serial and parallel configurations and compared with respect to QF and DE [22]. Us–Ls-type Fabry–Perot resonators were designed, where Us and Ls indicate the s number of air holes near to the drop waveguide and bus waveguide, respectively. Single-ring crossed, serial dual-ring crossed and diagonal dual-ring crossed PhCRRs were designed, and it has been proved that QF can be increased using dual ring on the cost of DE for such add–drop filters [24]. Other PhCRR forms that are employed for building optical channel drop filters include hexagonal PhCRRs, 45° PhCRRs and circular PhCRRs, and many more designs have been compared [25]. The refractive index of the dielectric rods, radius of the initial structure rods and radius of the quasi-crystal rods are ideal parameters for tuning the filter by examining the impact of various

factors on the resonant wavelength. A single H-shaped filter was designed and efficiency being compared with different values of refractive indices and rod's radius used for the conception of 2D-PCs [26]. Photonic crystal filters with ring defects have been introduced with varying internal and external radius defects. It has been observed that with an increase in external radius of the defect cavity, the wavelength drops along with the drop in QF and DE [27]. By supervisioning radii of the air holes in the cavity of 2D-PCs, coincidental profligacy of the frequency has been observed [28]. Photonic crystal filters with magnetic properties were also found to be unaffected from the waveguide defects [29]. A 3 × 3 wavelength division multiplexed system has been designed using super defect filter cells at input and output ports [30]. It has been observed that with increasing number of rings in the photonic crystal, the QF can be increased on the cost of transmission efficiency [31]. Hexagon ring resonators with a large hole showing a wavelength selective property have been proposed and analysed on the basis of QF and DE with respect to the increased number of holes for designed PhCRR [32]. An eight-shaped (adding more channels for wavelength dropping), diamond-shaped and quasi-fractal-shaped photonic ring resonators have been designed and investigated [33, 34, 36]. By considering the scatter effect, the transmission performance can be improved [35]. The one-dimensional, two-dimensional and three-dimensional photonic crystal-based ring resonators

with various structures have been proposed so far with the single objective to integrate the all-optical devices and support wavelength division multiplexing [37]. Various other properties of photonic crystals have also been investigated in optical domain such as a change in refractive index to be used in biological environment for detection of *Escherichia coli* [38]. By exhibiting the resonant wavelength shift, the photonic crystal-based bio-sensors can also detect the skin types, cancer and DNA analysis [39, 40]. The unique add–drop filter has been proposed by using yttrium-iron rods in the shape of a ring with two magnetic rods at each side [41]. The add–drop filter constructed by rods of refractive index of 3.59 in air has obtained the QF and TE values of 444 and 100%, respectively [42]. Other construction for the add–drop filter has been proposed by using two different layer slabs made up of silicon and silicon dioxide materials of approximately 2 micrometres thickness with embedded nano-cavities [43]. By using scattering and coupling rods, various shaped photonic crystal add–drop filters have been proposed to optimize the performance [44]. The add–drop filters can be used for constructing optical switch arrays and routers in fully optical environment for real applications.

Mathematical modelling

The time-varying Maxwell–Faraday's equation can be written as in Eq. (1), and the time-varying

Maxwell–Ampere's circuit law with position-varying constants, $\varepsilon(p)$, $\sigma(p)$ and $\mu(p)$, can be represented as in Eq. (2).

$$\frac{\partial \vec{H}}{\partial t} = -\frac{1}{\mu\,(p)}\left(\nabla \mathrm{X}\vec{E}\right)$$

(1)

$$\frac{\partial \vec{E}}{\partial t} = \frac{1}{\varepsilon\,(p)}\left(\nabla \mathrm{X}\vec{H}\right) - \frac{\sigma\,(p)}{\varepsilon\,(p)}\vec{E}$$

(2)

For the 2D-PC lattice structure, there may be two polarization modes as E-polarization and H-polarization. The finite-difference time-domain (FDTD) formulae for two-dimensional space with varying constants can be defined for TE polarization as in Eqs. (3, 4 and 5). $\mathrm{H_z}, \mathrm{E_x}$ and $\mathrm{E_y}$ are the components of magnetic and electric fields in x, y and z directions as in their respective subscripts. Since we have considered the two-dimensional structure, Δ_x and Δ_y are the non-equal changes in the respective directions.

$$\mathrm{H}_z\big|_{i+\frac{1}{2},j+\frac{1}{2}}^{n+\frac{1}{2}} = \frac{1-\frac{\sigma_i\Delta_t}{2\mu}}{1+\frac{\sigma_i\Delta_t}{2\mu}}\left[H_z\big|_{i+\frac{1}{2},j+\frac{1}{2}}^{n-\frac{1}{2}}\right] - \frac{1}{1+\frac{\sigma_i\Delta_t}{2\varepsilon}}\left[\frac{\Delta t}{\varepsilon\Delta_x}\left[\frac{\left(E_y\big|_{i+\frac{1}{2},j+1}^{n} - E_y\big|_{i,j+\frac{1}{2}}^{n}\right)}{\Delta_x}\right] - \frac{}{\mu}\right.$$

(3)

$$E_x\big|_{i+\frac{1}{2},j}^{n+1} = \frac{1-\frac{\sigma\Delta t}{2\varepsilon}}{1+\frac{\sigma\Delta t}{2\varepsilon}}\left[E_x\big|_{i+\frac{1}{2},j}^{n}\right] + \frac{1}{1+\frac{\sigma\Delta_t}{2\varepsilon}}\frac{\Delta t}{\varepsilon\Delta_y}\left[\left(H_z\big|_{i+\frac{1}{2},j+\frac{1}{2}}^{n+\frac{1}{2}} - H_z\big|_{i+\frac{1}{2},j-\frac{1}{2}}^{n+\frac{1}{2}}\right)\right]$$

(4)

$$E_y\big|_{i,j+\frac{1}{2}}^{n+1} = \frac{1-\frac{\sigma\Delta t}{2\varepsilon}}{1+\frac{\sigma\Delta t}{2\varepsilon}}\left[E_y\big|_{i,j+\frac{1}{2}}^{n}\right] - \frac{1}{1+\frac{\sigma\Delta_t}{2\varepsilon}}\frac{\Delta t}{\varepsilon\Delta_x}\left[\left(H_z\big|_{i+\frac{1}{2},j+\frac{1}{2}}^{n+\frac{1}{2}} - H_z\big|_{i-\frac{1}{2},j+\frac{1}{2}}^{n+\frac{1}{2}}\right)\right]$$

(5)

where n denotes the time and i, j are the axis units for the two-dimensional planes. The material parameter, μ, and magnetic conductivity, σ, are defined for the given specific position and are functions of p. Further, we can define the time step Δt as in Eq. (6),

$$\Delta t \leq \frac{1}{c\left(\frac{1}{\Delta(x_i)^2}+\frac{1}{\Delta(y_j)^2}\right)^{\frac{1}{2}}}$$

(6)

The QF can be calculated using Eq. (7),

$$\mathrm{QF} = \frac{\lambda_0}{\mathrm{FWHM}} = \frac{\lambda_0}{\text{Full width half maximum}}$$

(7)

where λ_0 is the resonant wavelength and full width half maximum (FWHM) is the spectral width. Here,

the lattice constant ‘a’ is defined as the distance between the two silicon rods, whereas the radius of each rod has been considered as ‘r’. For the analysis present here, the permittivity of 2D-PC has been varied in two principal directions.

$$\xi\left(x,y,z\right)=\left[\left[\begin{array}{ccc}\xi_{xx}^{2} & 0 & 0\\ 0 & \xi_{yy}^{2} & 0\\ 0 & 0 & \xi_{zz}^{2}\end{array}\right]\right]$$

(8)

The permittivity matrix vectors described in Eq. (8) satisfy the criteria ξ_{xx} and $\xi_{yy}=\xi_{zz}$, being the refractive index of silicon and air. For TE polarization, the magnetic field is parallel to the z-axis. According to the Bloch theorem, the periodic equation for boundaries is,

$$\vec{\phi}\left(\vec{p}+\overrightarrow{t1},t\right)=\vec{\phi}\left(\vec{p},t\right)e^{i\vec{k}\overrightarrow{t1}}$$

(9)

In Eq. (9), $\overrightarrow{\phi}$ represents any field component $\overrightarrow{E}$ or $\overrightarrow{H}$ (electric or magnetic field), $\overrightarrow{t1}$ is the period, $\overrightarrow{p}$ is the coordinate of any position and $\overrightarrow{k}$ is the wave vector of the first Brillouin zone.

For nonlinear dielectric medium, the energy density formula for oscillating rod/dipole having harmonic motion at position $\overrightarrow{p}$ and $\overrightarrow{D}$ ($\overrightarrow{p}$), being the electric displacement at any position $\overrightarrow{p}$ for a given time instant t, is given by Eq. (10),

$$W = \frac{1}{8\pi}\left[\vec{E}\left(\vec{p}\right)\cdot\vec{D}\left(\vec{p}\right) + \left|\vec{H}\left(\vec{p}\right)\right|^{2}\right]$$

(10)

Equation (11) calculates the energy density, *W*, using space discretization for TE polarization.

$$W = \frac{1}{8\pi}\sum_{i,j=0}^{ix,iy}$$

$$\left\{\begin{array}{l} \left[\left(E_x\left|\begin{matrix} i+\frac{1}{2} \\ j \end{matrix}\right.\right)\left(D_x\left|\begin{matrix} i+\frac{1}{2} \\ j \end{matrix}\right.\right)\right] + \left[\left(E_y\left|\begin{matrix} i \\ j+\frac{1}{2} \end{matrix}\right.\right) \\ + \left(H_z\left|\begin{matrix} i+\frac{1}{2} \\ j+\frac{1}{2} \end{matrix}\right.\right)^{2} \end{array}\right.$$

(11)

The coupled power, *P*, can also be calculated at the ports by incident magnetic and electric fields by integrating the multiplication of the Fourier transforms in fusing Eq. (12),

$$P = \frac{-1}{2}\left[Re\left\{\left(\int_{length}^{width\,of\,the\,surface} E_{y,\omega}H_{z,\omega}^{*}dx\right)\right\}\right]$$

(12)

Structural designs

A silicon photonic layer of size 17 μm × 17 μm in length and width, respectively, with micro-pillar

configuration has been chosen as represented in Table 1. A refractive index medium considered in the proposed structures is air. A Gaussian-modulated continuous light wave with circular pillars is considered in the analysis of the proposed structures. The proposed filters have square lattice configuration. Figures 1, 2 and 3 also show the different monitors to check the power. Each monitor will provide the power, absorption and transmission data. A way of propagation of light throughout the waveguide from input to output can be observed in a graphical representation form by using a monitor.

Table 1 2D Photonic Crystal Structural Parameters

Fig. 1

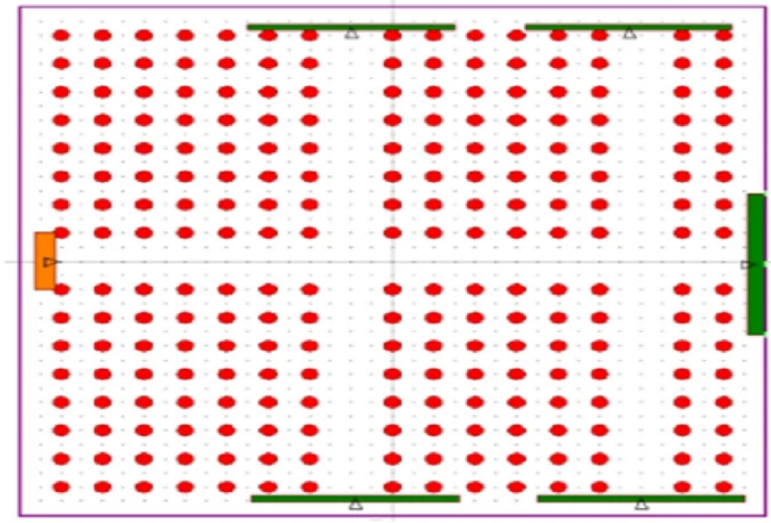

1 × 4 H-shaped splitter

Fig. 2

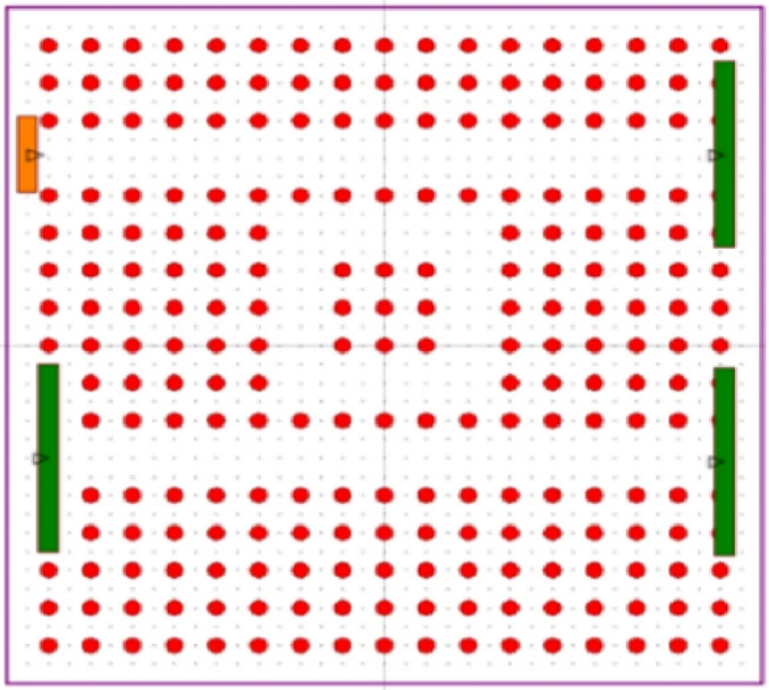

Add–drop filter with ring resonator

Fig. 3

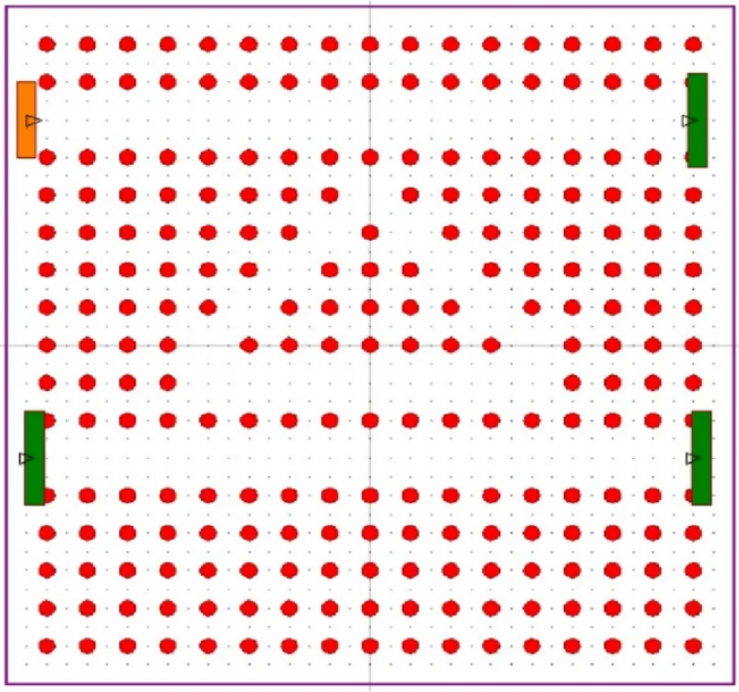

Add–drop filter with triangular resonator

A time-domain numerical method known as FDTD has been employed to analyse the simulation designs and also to simulate the propagation of electromagnetic waves in order to solve the Maxwell's equations. For the examination of the photonic crystal, it has been discovered that the FDTD technique is particularly exact and precise. The simulation has been carried out for TE mode. The TE-mode simulation can be carried out using the Brillouin zone by employing a 2D plane wave expansion method and FDTD. Anisotropic perfectly matched layer (APML) boundary conditions have been used for the simulation. The boundary conditions considered will analyse the critical photonic crystal structure, but computational resource can deal limit size of grid matrix in simulation region.

Distance between each lattice point is 1 μm. In this proposed work, three structures of add–drop filters have been designed and analysed using photonic crystal configuration.

The H-shaped filter with six ports, ring resonator-based filter with four ports and triangular-shaped filter with four ports have been used. Figures 1, 2 and 3 show the three different types of photonic add–drop filter structures and the ports under investigation, respectively.

To add or remove a channel from the multiplexed input/output signals, a ring resonator has been

sandwiched between two optical waveguides as a pertinent construction for designing an add–drop filter. Power from one waveguide is transmitted into the other through the resonance of the ring. Gaussian optical pulse is propagating through the waveguides, and power generated thorough each port has been analysed using photonic simulation tool Rsoft. The Gaussian pulse is used; Gaussian pulses are widely used in communications, as they show maximum steepness of transition with no overshoot and minimum group delay.

Results and discussion

Power distribution of the transmission spectrum obtained for structure1 and structure 2 has been analysed at various ports as assigned in the structures. The TE-mode simulation has been carried for both the structures. In the proposed structures, the laser source is input to the starting point of waveguides and monitors record the outputs. The FDTD technique which considered discrete Fourier transform has been used in generating the power distribution for each port designed.

Light is propagated through the H-shaped, ring-shaped and triangular-shaped structures as shown in Figs. 7a, 8a and 9a, respectively. Light outputs have been monitored at each port situated in the structures. PBG generated for the above structures has shown various regions of band gap available for

operative spectrum. Specific wavelengths and band gap range obtained at each port for structure 1, structure 2 and structure 3 have been analysed. Figures 7b, 8b and 9b represent the power outputs. Tables 2, 3 and 4 provide the details of wavelengths obtained at each port of all the photonic structures.

Table 2 Spectra data for structure 1

Table 3 Spectra data for structure 2

Table 4 Spectra data for structure 3

Port F in the H-shaped filter, port C in the ring resonator filter and port D in the triangular-shaped add–drop filter as represented in Figs. 7c, 8c and 9c, respectively, have indicated better monitor power compared with all other ports present in the structures. Input light is coupled with the waveguide during the propagation of light in the designed photonic structure. In ideal case, the ring resonator-based add–drop filter is sandwiched between two waveguides such as upper waveguide, i.e. bus waveguide and lower waveguide as dropping waveguides. In ring resonator-based structure, out of port C has shown better output power transmission compared with other two ports as shown in Fig. 5. The transmission spectrum and

efficiency of triangular resonator add–drop filter for port B, port C and port D are manifested in Fig. 6.

The transmission spectrum obtained for three different filter structures is shown in Figs. 4, 5 and 6, respectively. An amplitude obtained for each three figures has been above 75%, and port B in triangular resonator structure has shown less transmissive power compared with the other structures. Other two structures have shown consistently above 80% transmissive power, and 1 × 4 H splitter has shown transmissive power of above 90% (Table 5).

Fig. 4

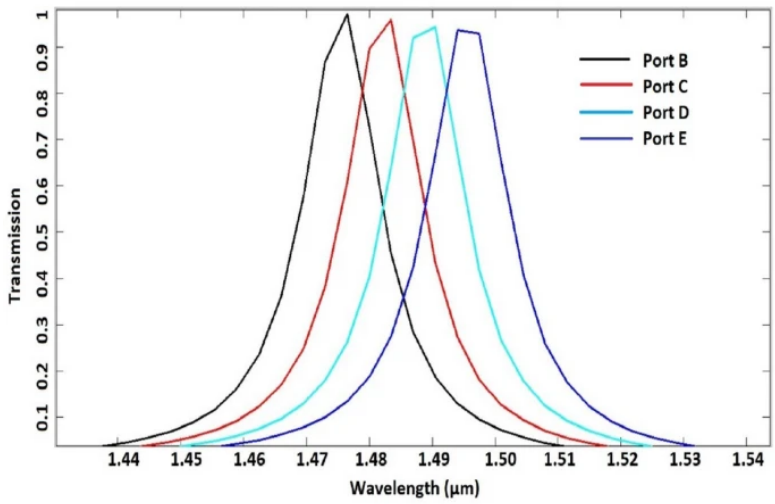

Transmission spectrum for 1 × 4 H-shaped splitter

Fig. 5

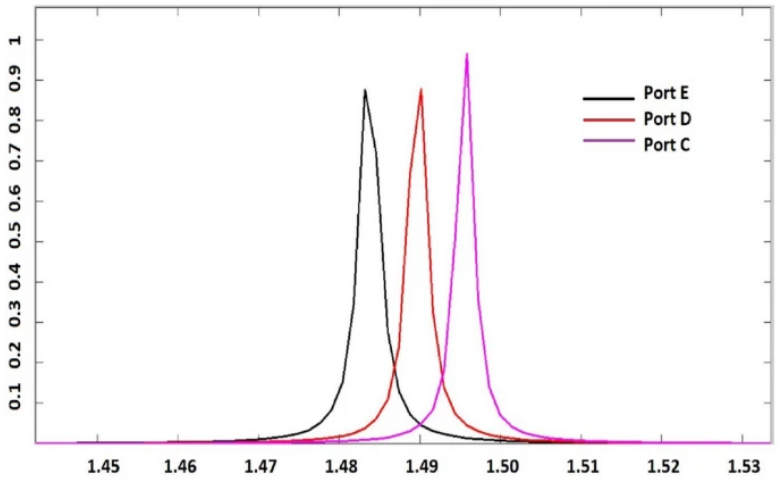

Transmission spectrum for ring resonator-based add–drop filter

Fig. 6

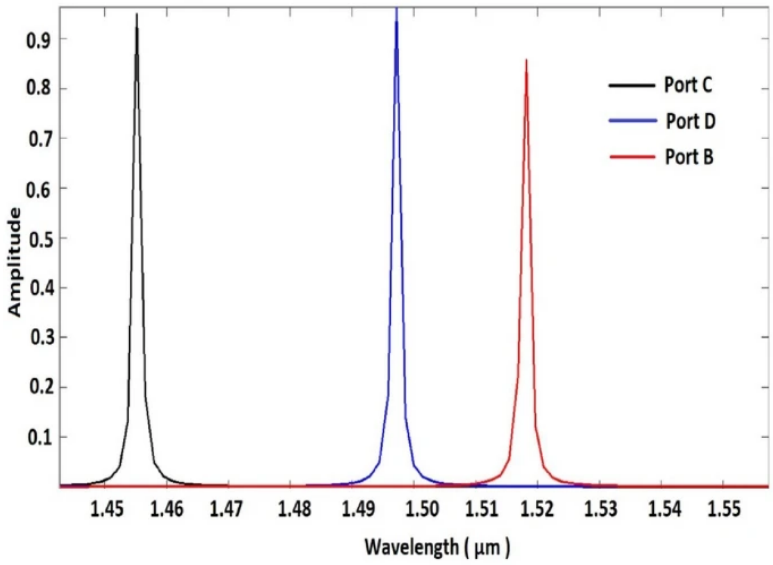

Transmission spectrum for triangular resonator-based add–drop filter

Table 5 Comparison of proposed structures with the reported structures

Figures 7, 8 and 9 show the light propagation for three different structures and monitor power

obtained for 1 × 4 H splitter, ring resonator add–drop filter and triangular-shaped add–drop filter, respectively. All the ports have shown approximately equal power transmission range with varying wavelength ranges.

Fig. 7

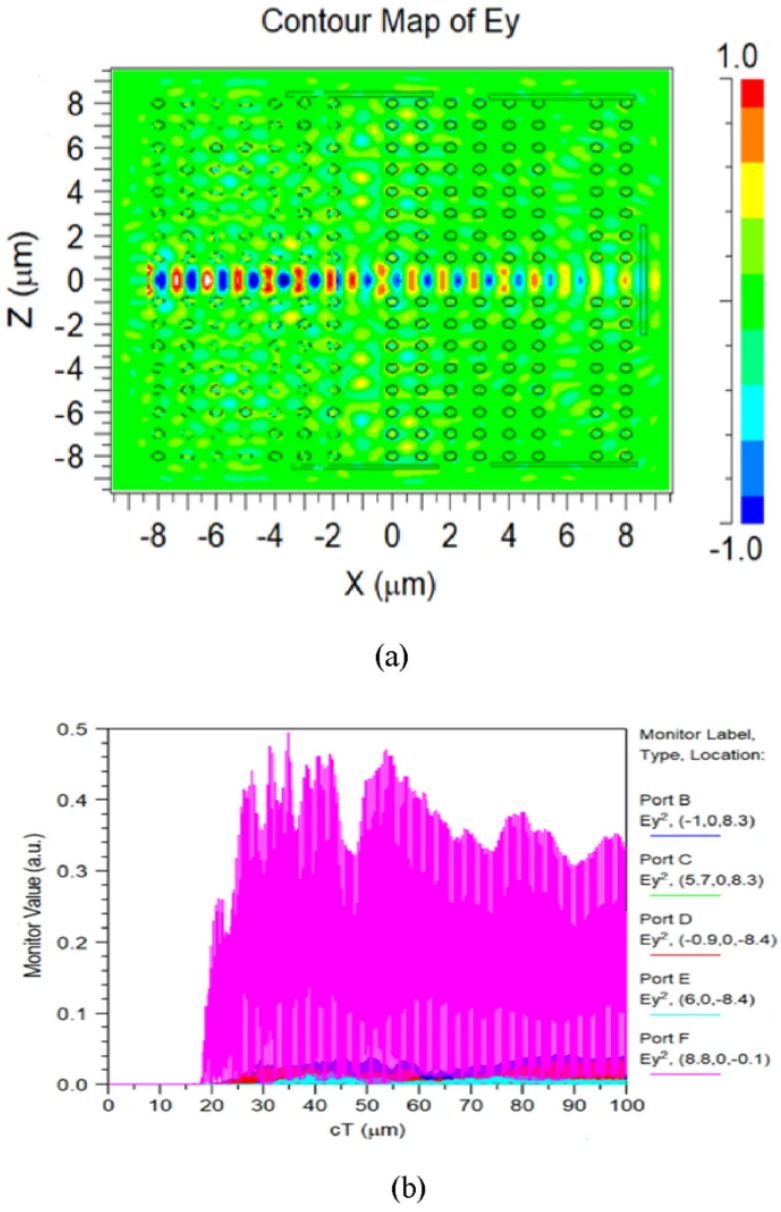

a Light propagation in H-shaped photonic crystal filter, **b** monitor power

Fig. 8

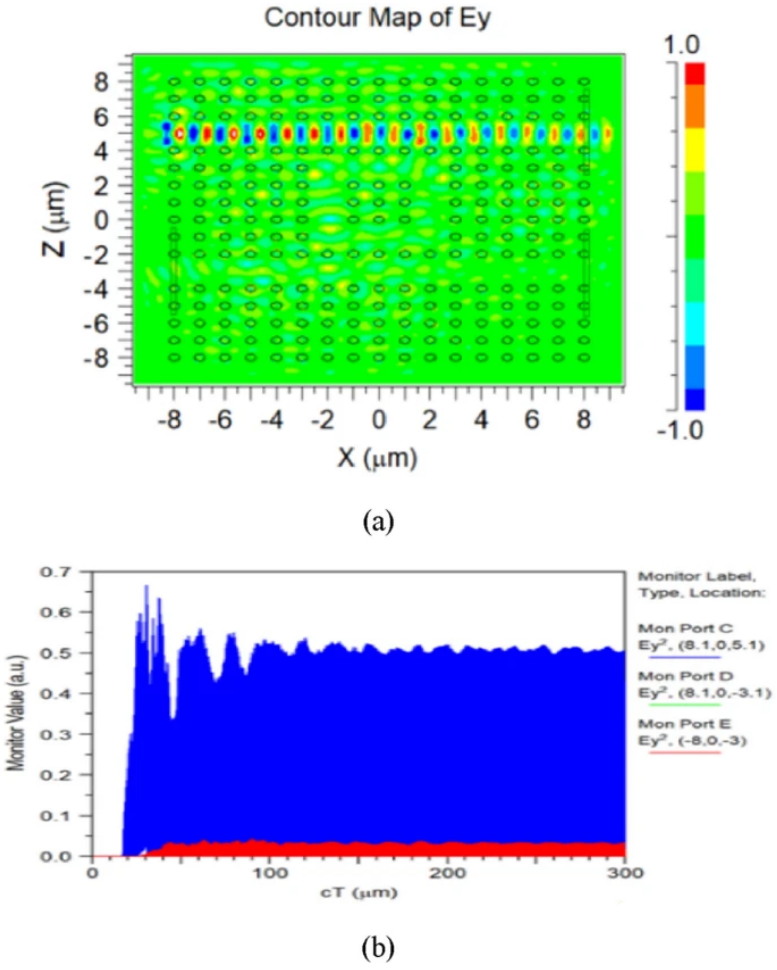

a Light propagation in ring-shaped photonic crystal, **b** monitor power

Fig. 9

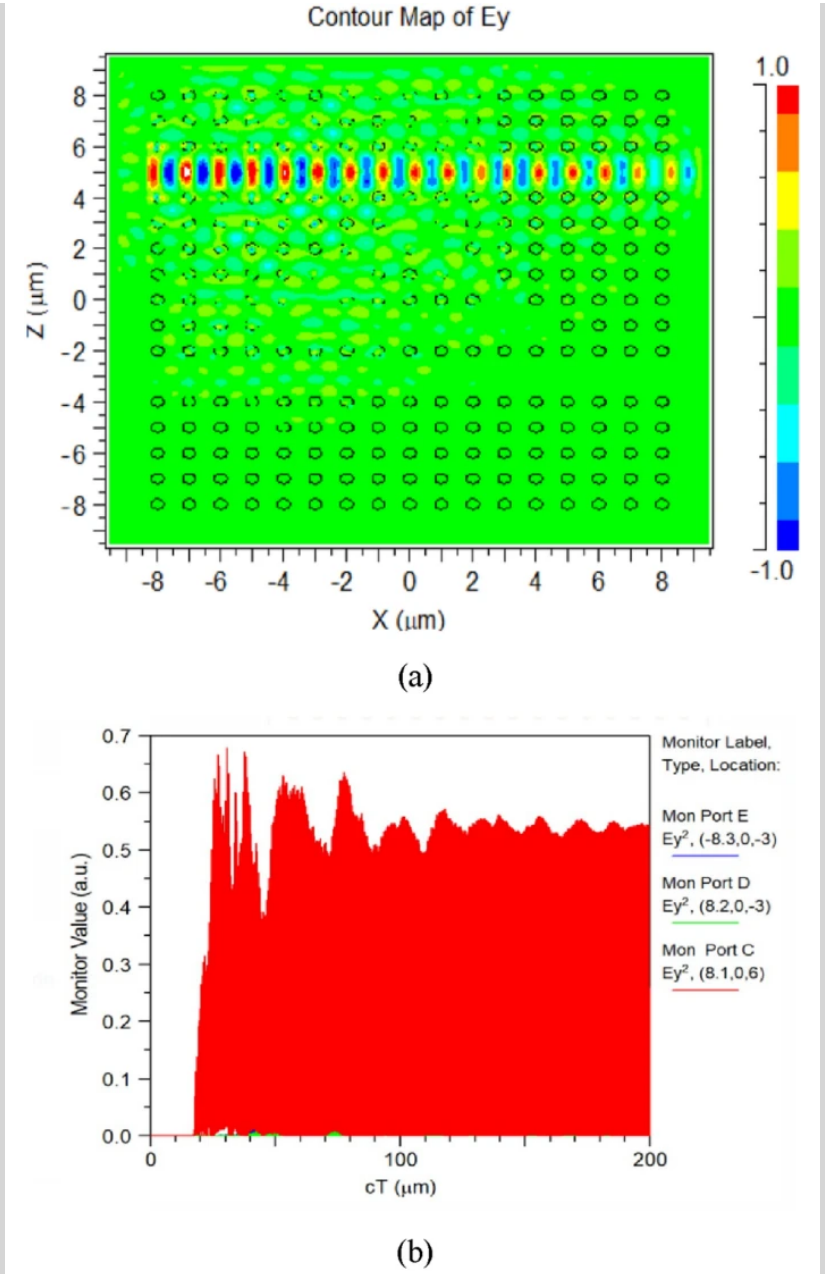

a Light propagation in triangular-shaped photonic crystal, **b** monitor power

Figures 4, 5, 6, 7, 8 and 9 represent the photonic designs and simulations of light transmission in the proposed structures using Rsoft photonic CAD suite. Peak resonant wavelengths in each port of add–drop filters are shown in Figs. 4, 5 and 6. The maximum Q factor and transmission efficiency have been achieved with the H-shaped add–drop filter, i.e. 5853 and above 90%, respectively. Quality of light propagation and QF in the ring resonator-

based structure is optimum. A larger wavelength shift has been observed for triangular resonator compared with the other structures. Port C and port D in triangular structure show the transmission efficiency above 90%. The optimum value of QF of 7239 for triangular-shaped filter has been achieved.

Comparative analysis

Conclusion

The proposed work consists of design and analysis of 1 × 4 H shape-, ring resonator- and triangular shape-based photonic crystal add–drop filters. The filters are designed in Rsoft CAD tool. Laser light has been allowed to propagate through structure for monitoring the power transmission. An optimum wavelength obtained for 1 × 4 H-shaped add–drop filter is ranged from 1.465 to 1.50 μm. A ring resonator-based add–drop filter has shown a wavelength range of 1.48–1.495 μm. The wavelength ranges for the designed triangular-shaped filter have been investigated from 1.4493 to 1.5625 μm. Photonic crystal-based add–drop filters are immune to rugged and conducting areas so these add–drop filters can be used with real-time applications of switching. The proposed work overcomes the requirement of multiple-port add–drop filter with different ranges of power splitting properties.

Future scope

The silicon rods have been utilized to construct the 2D-PC in the proposed rod in air structures, whereas different other materials can be utilized and investigated to obtain better wavelength dropping capability, transmission capability and optimum QF values.

References

1. M. Bazian, Photonic crystal add–drop filter: a review on principles and applications. Photon. Netw. Commun. **41**, 57–77 (2021). https://doi.org/10.1007/s11107-020-00907-7

2. Z. Qiang, W. Zhou, A. Richard, Optical add-drop filters based on photonic crystal ring resonators. Opt. Express **15**, 1823–1831 (2007). https://doi.org/10.1364/OE.15.001823

3. A. Kuzma, F. Uherek, J. Skriniarová, A. Kuzma, F. Uherek, Photonic crystal based add/drop filters for sensing. IEEE Conf. Photonics North (2016). https://doi.org/10.1109/PN.2016.7537913

4. S. Naznin, R. Mandal, S. Sarker, M. T. Alam, M. S. Ahsan, M. Y. Ali, Design and optimization of optical add-drop filter and sensor using 2D photonic crystal. in *3rd International Conference on Electrical Engineering and Information Communication Technology*

(ICEEICT), (2016), pp 1–5
https://doi.org/10.1109/CEEICT.2016.7873063

5. K. Tao, J. Xiao, X. Yin, Nonreciprocal photonic crystal add-drop filter. Appl. Phys. Lett. **105**(21), 1–5 (2014). https://doi.org/10.1063/1.4902868

6. F. Monifi, M. Djavid, A. Ghaffari, M.S. Abrishamian, A new broadband photonic crystal add drop filter. J. Appl. Scien. **8**(11), 2178–2182 (2008). https://doi.org/10.3923/jas.2008.2178.2182

7. M.R. Lebbal, F. Larioui, T. Bouchemat, M. Bouchemat, F. Kerrour, Power splitter and TE-TM polarization separator based on magneto-photonic crystal fiber. Phosphorus Sulfur Silicon Relat. Elem. **195**(11), 924–929 (2020). https://doi.org/10.1080/10426507.2020.1804163

8. Z. Rashki, B. Mansouri, M.R. Rakhshani, New design of optical add-drop filter based on triangular lattice photonic crystal ring resonator. Int. Res. J. Appl. Basic Sci. **4**(4), 985–989 (2013)

9. M. Radhouene, V. Balaji, M. Najjar, S. Robinson, V. Janyani, M. Murugan, Rounded square ring resonator based add drop filter for

WDM applications using two dimensional photonic crystals. Opt. Quant. Electron. **53**(5), 273 (2021). https://doi.org/10.1007/s11082-021-02924-w

10. V. Fallahi, M. Seifouri, Novel structure of optical add/drop filters and multi-channel filter based on photonic crystal for using in optical telecommunication devices. J. Opt. Electron. Nanostruct. **4**(2), 53–68 (2019). https://doi.org/10.1080/10426507.2020.1804163

11. M.A. Upadhyaya, P. Sharan, M.C. Srivastava, Micro-opto-electro-mechanical system based micro cantilever sensor for bio sensing applications. J. Opt. Soc. Am. B **39**(7), 1736–1742 (2022). https://doi.org/10.1364/JOSAB.455702

12. M.A. Upadhyaya, M.C. Srivastava, P. Sharan, S.K. Roy, Silicon nanostructure-based photonic MEMS sensor for bio sensing application. J. Nanophoton. **15**(2), 026001 (2021). https://doi.org/10.1117/1.JNP.15.026001

13. P. Patil, S.P. Kamath, A.M. Upadhyaya, P. Sharan, Design and analysis of photonic MEMS based micro ring resonators for pressure sensing application. J. Micromechan.

Micro. Eng. **31**(11), 115004 (2021). https://doi.org/10.1088/1361-6439/ac2bb1

14. A.M. Upadhyaya, M. Srivastava, P. Sharan, Integrated MOEMS based cantilever sensor for early detection of cancer. Optik **227**, 1–8 (2020). https://doi.org/10.1016/j.ijleo.2020.165321

15. Z. Qiang, W. Zhou, R.A. Soref, Optical add-drop filters based on photonic crystal ring resonators. Opt. Express **15**(4), 1823–1831 (2007). https://doi.org/10.1364/OE.15.001823

16. M. Djavid, M.S. Abrishanian, Photonic crystal channel drop filters with mirror cavities. Opt. Quant. Electro. **39**(14), 1183–1190 (2007). https://doi.org/10.1007/s11082-007-9168-3

17. P. Andalib, N. Granpayeh, Optical add/drop filter based on dual curved photonic crystal resonator. in *IEEE International Conference on Group IV Photonics*. (Freiburg, Germany, 2008) pp 249–250 https://doi.org/10.1109/GROUP4.2008.4638161

18. F. Monifi, A. Ghaffari, M. Djavid, M.S. Abrishamian, Three output port channel drop filter based on photonic crystals. Appl. Opt.

48(4), 804–809 (2009). https://doi.org/10.1364/AO.48.000804

19. F.L. Hsiao, C. Lee, A nano ring resonator based on 2D hexagonal lattice photonic crystals. in *IEEE International Conference on Optical MEMS and Nanophotonics*. (Clearwater, Florida, 2009),pp 107–108 https://doi.org/10.1109/OMEMS.2009.5338534

20. Y. Zheng, S. Li, J. Kang, Two dimensional photonic crystal channel filter based on ring resonator. in *IEEE International Conference* on Photonics and Optic electron. (Wuhan, China, 2009), pp 1–3 https://doi.org/10.1109/SOPO.2009.5230214

21. T. Thi, F.L. Hsiao, C. Lee, W. Xiang, C. Chen, W.K. Choi, Optimization and comparison of photonic crystal resonators for silicon micro cantilever sensors. Sens. Actuators A **165**(1), 16–25 (2011). https://doi.org/10.1016/j.sna.2010.01.006

22. J. Bai, J. Wang, X. Chen, J. Jiang, H. Li, Y. Qiu, Z. Qiang, Characteristics of 45° photonic crystal ring resonators based on square-lattice silicon rods. Optoelectron. Lett. **6**(3), 203–206 (2010). https://doi.org/10.1007/s11801-010-9263-8

23. Z. Ma, K. Ogusu, Channel drop filters using photonic crystal Fabry-Perot resonators. Opt. Commun. **284**(5), 1192–1196 (2011). https://doi.org/10.1016/j.optcom.2010.10.050

24. M. Youcef, G. Bassou, A. Taalbi, Z.M. Chekroun, Optical channel drop filters based on photonic crystal ring resonators. Opt. Commun. **285**(3), 368–372 (2011). https://doi.org/10.1016/j.optcom.2011.09.068

25. S. Robinson, N. Rangaswami, Photonic crystal ring resonator based add drop filters: a review. Opt. Eng. **52**(6), 1–12 (2022). https://doi.org/10.1117/1.OE.52.6.060901

26. S. Rezaee, M. Zavvari, H. Alipour-Banaei, A novel optical filter based on H-shape photonic crystal ring resonators. Optik **126**(20), 2535–2538 (2015). https://doi.org/10.1016/j.ijleo.2015.06.043

27. A. Dideban, H. Habibiyan, H. Ghafoorifard, Photonic crystal channel drop filter based on ring-shaped defects for DWDM systems. Phys. E Low-Dimen. Syst. Nanostruct. **87**, 77–83 (2017). https://doi.org/10.1016/j.physe.2016.11.022

28. M. Qiu, B. Jaskorzynska, Design of a channel drop filter in a two-dimensional triangular photonic crystal. Appl. Phys. Lett. **83**(6), 1074–1076 (2003). https://doi.org/10.1063/1.1599982

29. K. Tao, J. Xiao, X. Yin, K. Tao, J. Xiao, X. Yin, Nonreciprocal photonic crystal add-drop filter. Appl. Phys. Lett. **105**(21), 211105 (2014). https://doi.org/10.1063/1.4902868

30. S.M. Mirjalili, S.Z. Mirjalili, Single-objective optimization framework for designing photonic crystal filters. Neural. Comput. Appl. **28**, 1463–1469 (2017). https://doi.org/10.1007/s00521-015-2147-x

31. H. Alipour-Banaei, F. Mehdizadeh, M. Hassangholizadeh-Kashtiban, A new proposal for PCRR-based channel drop filter using elliptical rings. Phys. E Low-Dimen. Syst. Nanostruct. **56**, 211–215 (2014). https://doi.org/10.1016/j.physe.2013.07.018

32. J. Jiang, Z. Qiang, H. Zhang, Y. Zheng, Y. Qiu, A high-drop hole-type photonic crystal add-drop filter. Opt. Electron. Lett. **10**, 34–37 (2014). https://doi.org/10.1007/s11801-014-3180-1

33. M.R. Almasian, K. Abedi, Performance improvement of wavelength division multiplexing based on photonic crystal ring resonator. Optik **126**(20), 2612–2615 (2015). https://doi.org/10.1016/j.ijleo.2015.06.027

34. M.R. Almasian, K. Abedi, A proposal for optical WDM using embedded photonic crystal ring resonator with distributed coupling. Phys. E Low-Dimen. Syst. Nanostruct. **79**, 173–179 (2016). https://doi.org/10.1016/j.physe.2016.01.001

35. Y. Wu, T. Shih, J.J. Lee, High-quality-factor filter based on a photonic crystal ring resonator for wavelength division multiplexing applications. Appl. Opt. **48**(25), 24–30 (2009). https://doi.org/10.1364/AO.48.000F24

36. A. Dideban, H. Habibiyan, H. Ghafoorifard, Photonic crystal channel drop filters based on fractal structures. Phys. E Low-Dimen. Syst. Nanostruct. **63**, 304–310 (2014). https://doi.org/10.1016/j.physe.2014.06.009

37. S. Robinson, R. Nakkeeran, Characteristics of add drop filter using single and dual PCRR in square lattice. Optik **24**(23), 5918–5922 (2013). https://doi.org/10.1016/j.ijleo.2013.04.129

38. S.K. Roy, P. Sharan, Design of ultra-high sensitive biosensor to detect *E. Coli* in water. Int. J. Inform. Technol. **12**(3), 775–780 (2020). https://doi.org/10.1007/s41870-019-00327-5

39. V.L. Nandhini, K. Suresh Babu, S.K. Roy, P. Sharan, Multichannel biosensor for skin type analysis, in *Advances in Machine Learning and Computational Intelligence: Proceedings of ICMLCI 2019*. ed. by S. Patnaik, X.-S. Yang, I.K. Sethi (Springer Singapore, Singapore, 2021), pp.611–619. https://doi.org/10.1007/978-981-15-5243-4_57

40. S.K. Roy, P. Sharan, Photonic crystal based sensor for DNA analysis of cancer detection, in *Silicon Photonics & High Performance Computing*. ed. by A. Mishra, A. Basu, V. Tyagi (Springer, Singapore, 2017), p.79

41. T. Gangchao, H. Yuhao, J. Chen, Z.Y. Li, W. Liang, Controllable one-way add-drop filter

based on magneto-optical photonic crystal with ring resonator and microcavities. Opt. Express **30**, 28762–28773 (2022). https://doi.org/10.1364/OE.460271

42. P. Sharma, M. Gupta, N. Ghosh, S. Medhekar, 2D photonic crystal based all-optical add-drop filter consisting of square ring resonator. Mater. Today Proceed. **66**(7), 3344–3348 (2022). https://doi.org/10.1016/j.matpr.2022.07.062

43. P. Dong, C. Liu, L. Zhang, D. Dai, Y. Shi, Reconfigurable add-drop filter based on an antisymmetric multimode photonic crystal nanobeam cavity in a silicon waveguide. Opt. Express **30**(10), 17332–17339 (2022). https://doi.org/10.1364/OE.457883

44. M.K. Pandey, R. Sharma, M. Jangid, Design and simulation of a photonic crystal-based 2-D octagonal-shaped optical drop filter, in *Optical and Wireless Technologies: Proceedings of OWT 2020*. ed. by M. Tiwari, R.K. Maddila, A.K. Garg, A. Kumar, P. Yupapin (Springer Singapore, Singapore, 2022), pp.457–464. https://doi.org/10.1007/978-981-16-2818-4_49

2023, Results in Optics

Show abstract

Highly sensitive temperature sensor using one-dimensional Bragg Reflector for biomedical applications

2023, Biomedizinische Technik

One-dimensional optical Bragg grating sensor for the detection of urine glucose concentration

2022, Journal of Optics (India)

Original Research | Published: 22 May 2022

Compactness measure of rail wheel rolling contact of the freight wagon

Suchandana Mishra, Preeta Sharan & K. Saara

International Journal of Information Technology **14**, 2335–2342 (2022)

Abstract

This paper describes the measure of compactness using finite element analysis and stress–strain characteristics of freight wagon considering loaded and unloaded condition of wagon weight. Freight train wagons are used to carry various goods from one part to other parts of country. In terms of preserving the originality of the contact load transfer, the use of accurate finite element loading and boundary conditions has been a significant use. The main idea is to study the strain behaviour of goods wagon for empty and gross load condition. As the weight varies from low to high, that means from 22.47t to 88.47t, strain induced on rail increases linearly with the wagon load. This analysis is important as it determines the capacity to carry maximum load and to build weigh in motion system. By use of optical simulator, fiber

ScienceDirect

Optik

Available online 5 December 2022, 170350

In Press, Journal Pre-proof What's this?

Image Denoising Using Multi Scaling Aided Double Decker Convolutional Neural Network

Laya Tojo [a], Vivek Maik [b], Manju Devi [a]

Show more

Share Cite

https://doi.org/10.1016/j.ijleo.2022.170350

Get rights and content

Abstract

The digital image suffers from noise during transmission and reception. By preserving the qualities of the image, image denoising assists in the recovery of high-quality photos without noise (edge, corners, and sharp structures). Deep convolutional neural networks (CNNs) have been successfully employed for picture denoising due to their shifting topologies. Traditional approaches suffer from a number of drawbacks, such as a lack of adaptability when handling spatially invariant noise and the requirement for numerous models to denoise images. In this study, a novel approach that combines the advantages of various algorithms to achieve the objectives listed below. (1) Better performance (2) Faster processing (3) Less complexity in the denoiser (4) Extracting complementary characteristics to increase the denoiser's overall capacity. In terms of qualitative and quantitative analysis it has been evaluated and the simulation findings show that the Multi Scaling Aided Double Decker (MUS-ADD) convolutional neural network strategy is superior to other approaches.

Section snippets

INTRODUCTION

Due to the effect of the surroundings, channel, transmission, reflection and other variables, images are invariably tainted by noise during transmission, acquisition, and compression, resulting in distortion and loss of visual quality and information. Noise problem in image processing techniques including video processing, picture analysis, and tracking are crucial in today's image processing systems. Image denoising is a technique for removing noise from a noisy image and restoring the…

BACKGROUND LITERATURE

Denoising is a classic challenge that researchers are attempting to tackle. Denoising methods based on chrominance and luminance noise separation, linear and non-linear smoothing filters, Wavelet transform filters, Block matching algorithms, Deconvolution methods and others have been supplanted by deep learning algorithms in recent years. Deep learning architectures emerged as a result, suppressing standard denoising filters. The max-pooling strategy utilized in CNN was proposed by Weng et al. …

Proposed Multi Scaling Aided Double Decker (MUS-ADD) convolutional neural network Model

This section introduces the Multi-Resolution Dual CNN denoising model and shows how it may be used to solve picture denoising difficulties. To train the CNN model for a particular task, create network architecture and a model that learns from training data. The ideal depth for MUS-ADD is determined by the picture patch size.For model learning and data training, residual learning along with batch normalization is used.…

Training and testing datasets

The synthetic and real noisy images in our training dataset are separated into two categories. Gray and color level images are included in the 256×256 synthetic images. For synthetic noisy data, we used the same 400 photographs. Bicubic interpolation and the eight manipulations are the two basic approaches were used. The testing dataset include BSD68, Set 12 and CBSD68 in 256 ×256 patch size. Multi Scaling Aided Double Decker (MUS-ADD) CNN is a two-layer, 16-layer network that we created. It…

Conclusion

A novel Multi Scaling Aided Double Decker (MUS-ADD) CNN technique for image denoising was presented in this study using dual networks with a sparse mechanism. The compression block aids in the reduction of superfluous data and lowers computing costs. The performance parameters of the proposed technique are better when compared

to similar current learning-based and previous denoising techniques. This approach works for both colour and grayscale images because each convolutional layer has a…

Declaration of Competing Interest

The authors declare that they have no known competing financial interests or personal relationships that could have appeared to influence the work reported in this paper.…

Uncited references

[3], [27], [28], [29], [38], [39]…

References (39)

C. Tian *et al.*
"Deep Learning on Image denoising: an Overview"
Neural networks (2020)

Z.J. Wang *et al.*
"Images denoising with wiener filter in directionalet domain,"
Electronics Optics & Control (2007)

M. Diwakar *et al.*
"A review on CT image noise and itsdenoising"
Biomed Signal Process Control (2018)

D.L. Donoho *et al.*
Ideal spatial adaptation by wavelet shrinkage
Biometrika (1994)

D.H. Shin *et al.*
"Block-based noise estimation using adaptive gaussian filtering"
IEEE Trans Consum Electron (2005)

W. Liu *et al.*
Additive white Gaussian noise level estimation in SVD domain for images
IEEE Trans Image Process (2013)

G. Changlai
"Image-denoising method based on wavelet transform and mean filtering"
Opto-Electronic Engineering (2007)

Y. Ming *et al.*
"The application of an improved fast algorithm of median filter on removing image noise,"
Engineering ofSurveying and Mapping (2011)

Yao X.B. (2014) Image denoising research based on non-local sparse models with low-rank matrix decomposition....

M. Maggioni *et al.*
Nonlocal transform domain filter for volumetric data denoising and reconstruction
IEEE Tran Image Process (2013)

View more references

Cited by (0)

Recommended articles (6)

Research article

Microtactile Cantilever Resonators for Characterizing Surface Deposits
Procedia Engineering, Volume 120, 2015, pp. 861-864

Show abstract

Research article

Theoretical investigation of Bragg Reflector optical sensor for the measurement of cryogenic temperature
Materials Today: Proceedings, Volume 58, Part 1, 2022, pp. 451-455

Show abstract

Research article

Improving the quality of femtosecond laser processing micro-hole array by coated with aluminum film on fused silica sheet
Optik, Volume 128, 2017, pp. 178-184

Show abstract

Research article

Investigation & characterization of plasma sprayed cermet coatings on special steel alloy for gas turbine applications

Materials Today: Proceedings, Volume 47, Part 13, 2021, pp. 3720-3725

Show abstract

Research article

Dynamic Source Routing Protocol for Robust Path Reliability and Link Sustainability Aware Routing in Wireless Communication

Optik, 2022, Article 170036

Show abstract

Research article

Traffic Optimization Algorithms in Optical Networks For Real Time Traffic Analysis

Optik, 2022, Article 170418

Show abstract

View full text

programmable gate array.

- **Source:** International Journal of Electrical & Computer Engineering (2088-8708) . Dec2022, Vol. 12 Issue 6, p5840-5847. 8p.

- **Author(s):** Ponnuswamy, Anita; Devi, Manju

- **Abstract:** Multi-filed packet classification is a powerful classification engine that classifies input packets into different fields based on predefined rules. As the demand for the internet increases, efficient network routers can support many network features like quality of services (QoS), firewalls, security, multimedia communications, and virtual private networks. However, the traditional packet classification methods do not fulfill today's network functionality and requirements efficiently. In this article, an efficient range enhanced packet classification (REPC) module is designed using a range bit-vector encoding method, which provides a unique design to store the precomputed values in memory. In addition, the REPC supports range to prefix features to match the packets to the corresponding header fields. The synthesis and implementation results of REPC are analyzed and tabulated in detail. The REPC module utilizes 3% slices on Artix-7 field programmable gate array (FPGA), works at 99.87 Gbps throughput with a latency of 3 clock cycles. The proposed REPC is compared with existing packet classification approaches with better hardware constraints improvements.

MATHEMATICAL STATISTICIAN AND

Efficient Puncture and Non Puncture Architecture of Turbo Encoder on FPGA for Advanced Communication System

Rashmi R, Manju Devi

Keywords: no

Abstract

Abstract -This paper concentrates on plan and execution in-vehicle framework chip with the help of efficient turbo encoder. This module is fostered with the help of FPGA implementation. Both sequential and equal calculations for the encoding strategy are contemplated. Basically two Methodologies were implemented. Fostering the equal calculation technique utilizing convey skip snake, it is shown that both chip size and handling time are gotten to the next level. The rationale usage is improved by diminished region. The Turbo encoder module is planned, recreated, and integrated utilizing Xilinx apparatuses. Xilinx vertex low power is utilized

pdf

Issue
Vol. 71 No. 3s2 (2022): Special Issue on Mathematics Theory and its Contribution in Robotics and Computer Engineering

Section
Articles

Downloads

Copyright Transfer Form

Paper Template

Important Links

Home

Aims and Scope

Paper Topics

Call for Papers

Instructions for Authors

Archive

Download

Ethics & Policies

Publication Ethics and Publication Malpractice Statement

Peer Review Policy

Plagiarism Policy

Copyright, Grants and Ownership Declaration

Refund Policy

Open Access Overview

Open Access License

Permissions

Information

For Readers

For Authors

For Librarians

HYBRID TECHNIQUE FOR IMPROVING UNDERWATER IMAGE

A. Chrispin Jiji
Assistant Professor, Department of Electronics and Communication Engineering,
The Oxford College of Engineering, Bangalore, (India).
E-mail: chrispinjij@gmail.com
ORCID: https://orcid.org/0000-0001-5267-788x

Nagaraj Ramrao
Vice Chancellor, Kalasalingam University, Srivilliputtur, Tamilnadu, (India).
E-mail: Nagaraj.ramrao@gmail.com
ORCID: https://orcid.org/0000-0003-2542-5999

Recepción: 29/11/2019 **Aceptación:** 12/11/2020 **Publicación:** 30/11/2021

Citación sugerida:
Jiji, A. C., y Ramrao, N. (2021). Hybrid technique for improving underwater image. *3C Tecnología. Glosas de innovación aplicadas a la pyme, Edición Especial,* (noviembre, 2021), 645-665. https://doi.org/10.17993/3ctecno.2021.specialissue8.645-665

ABSTRACT

As light attenuate when disseminating in water, descriptions confined beneath water is generally corrupted towards varying degrees. An acquired image underneath water gets degraded due to optical properties of light in water. First, we describe optical behaviour of light in ocean due to which acquired images gets degraded. However, due to degradation of observed picture, conventional forms are not correct enough for faithful reconstruction. So, to improve the perception, we intend a Non-Locally Centralized Method (NLCM) for deblurring underwater descriptions. Later by considering characteristic of light propagation, we propose Gradient Guided Filter (GGF) method for improving the visibility of picture details. Finally, the image is well enhanced by Hybrid technique called Non-locally centralized gradient guided filter (NLCM-GGF). Tentative outcome demonstrates that proposed technique produces improved results than several conventional techniques together in quality metrics and visual evaluation.

KEYWORDS

Underwater Image Processing, Deblurring, Edge preserving filters.

https://doi.org/10.17993/3ctecno.2021.specialissue8.645-665

1. INTRODUCTION

Light always acts a significant task in oceanic explorer. Light transmission in sea is the base of ocular studies for describing light transmission procedure. Underwater image analysis attracts an increased level of attention as well as support of ocean application such as undersea exploration; see life in undersea, ocean rescue in Lebart *et al.* (2003) and species identification in Strachan (1993). Thus, it has been a challenging task to restore as well enhance underwater images reasons the variation in ocular property underneath. The main effect of degradation processes causes turbid, decreases visibility along with color distortion owing to ocular property. In particular, for severe absorption of light, confined picture is under exposed. In the meantime, altered wavelength of light has diverse absorbing characteristic in Seibert (1963), attained picture has cruel color distortion. Larger wavelength determines poorer attenuation in transmission medium. Shorter wavelength travel further, because of these undersea descriptions subject to blue or green color in Torres-Méndez and Dudek (2005). The water turbidity in Huimin *et al.* (2015) and organic element suspended on medium yields a hard restoration problem, since overall technique becomes highly dependent on environmental conditions.

Numerous works encompass to undertake those problems. For past decades, an extensive study has performed to build up a variety of reconstruction methods in Bertero and Boccacci (1998), and Chan *et al.* (2005). Based on ill-posed nature, several methods are widely employed to improve the restored picture. For effective process, it is very important to model earlier facts of natural descriptions. The classic models, such as quadratic Tikhonov as well as TV model in Oliveira, Bioucas-Dias, and Figueiredo (2009) are effective to decrease noise artefacts however have a tendency to over-smooth the descriptions based on piecewise steady statement. As a substitute, in modern era sparsity model in Daubechies, Defrise, and De Mol (2004) and Dong *et al.* (2011) shows the potential outcome for different reconstruction issues in Mairal, Elad, and Sapiro (2008) and Mairal *et al.* (2009).

In this paper, we intend hybrid technique for improving underwater image. Our contributions are two-fold: (1) Non-Locally Centralized Method (NLCM) for deblurring the images; (2) Gradient Guided Filter (GGF) method for enhancing the images. Finally, the proposed NLCM-GGF method better improve its quality than conventional technique.

https://doi.org/10.17993/3ctecno.2021.specialissue8.645-665

Tentative result shows that projected technique performs better than many conventional techniques together in quality metrics and visual evaluation. In the rest of the paper, we present short outline of earlier art and describe optical properties of light under water in section 2. Section 3 describes proposed hybrid technique. Section 4 describes tentative result; finally, section 5 brings to a close note.

2. MATERIALS AND METHODS

A variety of techniques has projected for getting better ocular excellence of degraded undersea descriptions, roughly classified into deblurring and enhancement process. Deblurring undersea picture is an ill-posed problem. As an essential issue in undersea description, reconstructions have widely considered in earlier years in Banham and Katsag (1997) and Bioucas-Dias and Figueiredo (2007). The ill-posed nature of IR is normally not exceptional. Past facts of typical descriptions employed to regularize such issues in reconstruction. The main model is total variation (TV) which lack flexibility for characterizing local picture structures but often generates over-smoothed results. To well keep up the picture boundaries, several methods have developed for improving TV model in Lysaker and Tai (2006), Beck and Teboulle (2009) and Chantas *et al.* (2010). The autoregressive (AR) modelling in Wu, Zhang, and Wang (2009) closely computes a primary representation which gives improved results than TV model to restore boundary formation, but have a tendency to generate ghost artefact.

In Buades, Coll, and Morel (2005) training-based adaptive scheme learns a better-quality learning pictures, to increase its accuracy. In modern era non-local (NL) in Kindermann, Osher, and Jones (2005) and Zhang *et al.* (2010) process has led a hopeful effect in several reconstruction schemes. The plan of NL process is straightforward: patch that contain related pattern be spatially distant and so we bring together in the image. In Dong *et al.* (2011) and Jiji and Vivek (2017), the edges are sharper than all the other process but there shows some ringing noise around edges and with different patches for reconstructing the images in Jiji and Ramrao (2017). With this aim, centralized NL method exploits NL redundancy to lower SCN noise.

https://doi.org/10.17993/3ctecno.2021.specialissue8.645-665

The NCSR method in Dong *et al.* (2013), use NL self-similarity for gaining fine approximation of sparse code coefficients, later integrate attained picture to those approximation. It is also characterized by training online sub-dictionaries by choosing most excellent online sub-dictionary for every patch. It employs Iterative Shrinkage-Threshold (IST) for solving l-norm trouble produced by model. Although the method achieved good, but never considers the statistical picture formation, therefore undergo artefact near boundaries.

Enhancement method does not rely on any picture formation, and enhances imagery by modifying scene pixel values. In Farbman *et al.* (2008) fine points in true description will smooth while keep boundaries to subtract smooth picture from true description for generating detailed picture. The mixture of range and domain filter in Tomasi and Manduchi (1998) keeps boundaries sharper, but experience gradient problems next to few boundaries. To avoid gradient reversal artifacts in He, Sun, and Tang (2013), picture elements in a window consider the structure of guidance image, but fail to signify close to a few boundaries. The boundary responsive factor in Li *et al.* (2015) lowers halo artifact which makes the edges better, but they cannot keep up edges well in some cases. The factors in Kou *et al.* (2015) signify the descriptions more correctly next to boundaries and keep up good boundaries. The work in Jiji and Ramrao (2019) is the extensive version primarily existed to improve the undersea imagery.

Here, we describe a hybrid technique for improving undersea descriptions which built upon the idea of NLCM exploit regulation limit determines the geometrical formation of image. A new method is particularly functional on boundaries of restored representation, so known as NLCM based Gradient guided filter (NLCM-GGF). Experimental results proved that the projected scheme gives much enhancement in both quality metrics and visual excellence than conventional technique.

2.1. OPTICAL PROPERTIES IN WATER

This section describes the behaviour of beam in undersea. Beam propagates in water medium is same as in air. Absorption denotes power reduction and scattering refers to deflection of propagation path. In underwater environment, beam also undergoes diffraction as well as refraction due to its wavelength and refractive index of water. Lambert-Beer empirical law states that the ocular property decay underneath material via exponential dependence:

https://doi.org/10.17993/3ctecno.2021.specialissue8.645-665

$$E_r = E_o e^{-cd} \tag{1}$$

where *c* denotes overall attenuation coefficient, *d* denotes the distance from an object. This model further decomposes in a form that openly expressed as

$$E_r = E_o e^{-ad} e^{-bd} \tag{2}$$

In order to deal with these effects another property volume scattering *B(θ)* as:

$$f = \frac{1}{2\pi} \int_0^{\pi} B(\theta) \sin(\theta) d\theta \tag{3}$$

The angle θ be integrated to get total scattering *f*. It theoretically considers all contributions coming from all directions. Modelling the backward scatter is more complicated than the forward one because it requires explicit volume scattering function. Four quantities *a*, *b*, *c*, *B(θ)* represents an ocular property of underneath medium. This resulting form used to predict ocular behaviour of light underneath.

For scattering, absorption as well as other optical properties always strictly related to specific medium composition. This fact justifies variability that we meet in dealing with them. Therefore, to concern picture arrangement process itself, direct, back-scattered as well as forward-scattered beam forms three additive total irradiance mechanisms, which mathematically expressed as:

$$E_T = E_D + E_B + E_F \tag{4}$$

Where light received by camera consists of three components: (i) object reflect beam with scattering, (ii) object reflect beam without scattering, (iii) back scatter part. For further details in Jaffe (1990) crucial quantities E_D, E_B and E_F as well analytical formulas that discussed in deep with definition of an expression for each part of whole irradiance.

https://doi.org/10.17993/3ctecno.2021.specialissue8.645-665

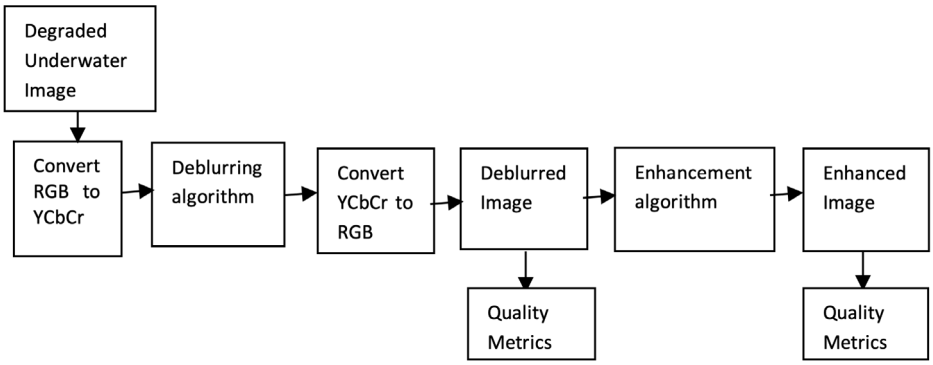

Figure 1. Block diagram of Proposed Method.
Source: own elaboration.

3. PROPOSED METHOD

The optical behaviour of beam in water will degrade the obtained pictures taken from underwater. In order to solve these issues, we intend a Hybrid technique that is able to deblur and enhance the underwater images depicted in Figure 1. Our hybrid approach consists of two main steps. In the first step, the Non-locally centralized method used for deblurring the scene. It mainly improves sparse restoration and suppresses the sparse coding noise. The main feature is to train online sub-dictionaries and choosing online sub-dictionary to each patch, using IST method for solving l1-minimization trouble created using such models. But it generates some ringing artefacts around the restored boundaries. In the second step, we introduce a Gradient guided filter (GGF) to improve edge sharpness. Finally, the output is well enhanced through Non-Locally Centralized Method via Gradient Guided Filter (NLCM-GGF). Experimental results proved that the projected scheme gives much enhancement in both quality metrics and visual excellence than conventional technique.

3.1. DEBLURRING ALGORITHM

The deblurring algorithm as depicted in Figure 2, blurred & noisy description *(b)* attained with blurring an ideal picture *(r)* with point spread function *(H)*, then imposing noise *(n)*, corresponding mathematical formula expressed as follows:

$$b = Hr + n \tag{5}$$

https://doi.org/10.17993/3ctecno.2021.specialissue8.645-665

In fact, some unknown quantities higher than known quantities; this problem becomes an ill-posed problem, which needs some other priori information.

To recover the reconstruction, first b is sparsely coded to solve minimization problem as:

$$\alpha_y = \arg\min\left\{\|b - H\phi\alpha\|_2^2 + \lambda\|\alpha\|_1\right\} \tag{6}$$

Conversely, reconstructing α_r from b is the very difficult task. For faithful reconstruction, we used in Dong *et al.* (2013) to reduce sparse coded image. The sparse coding noise stage represents

$$n_\alpha = \alpha_b - \alpha_r \tag{7}$$

By reducing n_α we can get better output. To suppress n_α, improve α_b, we propose the following model:

$$\alpha_b = \arg\min\left\{\|r - \phi\alpha\|_2^2 + \lambda\|\alpha_i\|_1 + \gamma\|\alpha_i - \beta_i\|_p\right\} \tag{8}$$

where β_i signify fine evaluation of α_i, γ signify regularize constraint and p will be 1 or 2.

To select dictionary, we cluster the patches by K-means clustering, then uses PCA in each cluster to find the sub dictionary. To code each patch, we enforce that particular patch by keeping sub-dictionaries as zero.

Hence sparse coding model as:

$$\alpha_b = \arg\min\left\{\|r - \phi\alpha\|_2^2 + \gamma\sum_i\|\alpha_i - \beta_i\|_p\right\} \tag{9}$$

Where β_i represents mass, average related by NL like patches

$$\beta_i = \sum_{t\in\Omega_i} m_{i,t}\alpha_{i,t} \tag{10}$$

where $m_{i,t}$ denotes weight. Related to NL means, we set weights as:

$$m_{i,t} = \frac{1}{w}\exp\left(-\left\|\hat{r}_i - \hat{r}_{i,t}\right\|_2^2 / h\right) \tag{11}$$

https://doi.org/10.17993/3ctecno.2021.specialissue8.645-665

where $\hat{r}_i$ and $\hat{r}_{i,t}$ denotes estimation of patch r_i and $r_{i,t}$ h represents predestined scalar and w denotes normalization part.

For each iteration, sparse vector represents:

$$\alpha_b^{(l)} = \arg\min\left\{\left\|r-\phi\alpha\right\|_2^2 + \gamma\sum_i\left\|\alpha_i-\beta_i^{(l)}\right\|_p\right\} \tag{12}$$

For IST process, learning patches updated by present description of reconstruction and update PCA bases as well as by repeating neighbourhood choice with reorganized learning information. For every iteration by updating learning set with PCA bases, current test patch updated by $y=\{y_j\}=\left\{\hat{r}_j\right\}_{j=1}^{M}$. The restored representation is then updated as $\hat{r}^{(l)}=\phi\circ\alpha_b^{(l)}$

3.2. GRADIENT GUIDED FILTER (GGF)

The deblurred output better reconstruct the image but it generates a few ring artefacts around the restored boundaries. With this aim, a Gradient guided filter (GGF) in Kou *et al.* (2015) is to improve edge sharpness. The filtered as well as guidance pictures are same for detailed output. The projected method gives an edge-preserved smooth picture. The difference among input with output gives detail layer, which is mainly for strengthening the output. In an edge, $a_{d'}$ denotes

$$a_{d'}=\frac{\sigma_{g,\xi_1}^2\left(d'\right)+\dfrac{\lambda}{\hat{\Gamma}\left(d'\right)}}{\sigma_{g,\xi_1}^2\left(d'\right)+\dfrac{\lambda}{\hat{\Gamma}\left(d'\right)}} \tag{13}$$

The rate of $a_{d'}$ is nearer to 1 if pixel $a_{d'}$ is in boundary, such that sharp boundaries are good in projected method than conventional technique.

In flat area, $a_{d'}$ is usually 0 and $\hat{\Gamma}(d')$ is smaller than 1 denoted as:

$$a_{d'}=\frac{\sigma_{g,\xi_1}^2\left(d'\right)}{\sigma_{g,\xi_1}^2\left(d'\right)+\dfrac{\lambda}{\hat{\Gamma}\left(d'\right)}} \tag{14}$$

https://doi.org/10.17993/3ctecno.2021.specialissue8.645-665

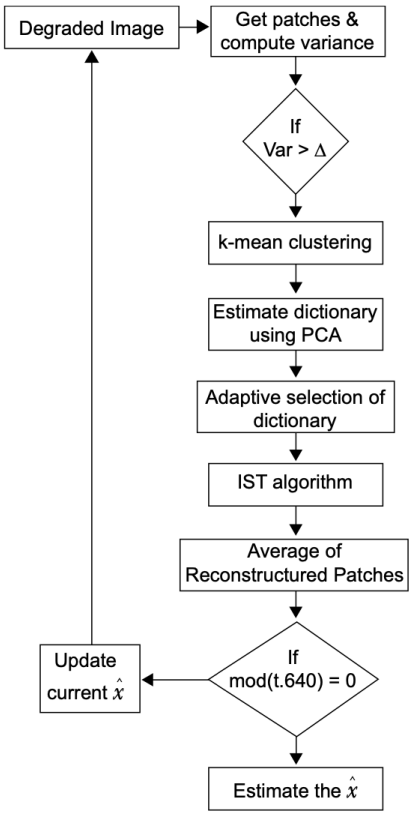

Figure 2. Flowchart of Deblurring algorithm.
Source: own elaboration.

In an edge, larger λ chooses for projected method than existing because choice will not affect edges. This means that projected method smooth flat area better than existing technique.

For these two cases the weighing function $\Gamma(d')$ denoted as:

$$\hat{\Gamma}\left(d^{'}\right)=\frac{1}{N}\sum_{d=1}^{N}\frac{\sigma_{g,\xi_1}^{2}\left(d^{'}\right)+\varepsilon}{\sigma_{g,\xi_1}^{2}\left(d\right)+\varepsilon} \tag{15}$$

Where ξ_1 signify filter window dimension. The projected method is sharper by way of increasing of λ. Though, it has fewer artefacts even by larger λ. So, we used larger λ in projected method exclusive of halo artefacts.

https://doi.org/10.17993/3ctecno.2021.specialissue8.645-665

3.3. ENHANCEMENT METHOD

After the process of NLCM and GGF, we joined both to improved eminence of representation. For better reconstruction we employed NLCM method which generate sharper boundaries and restore best descriptions, but it produces some ringing artefacts around the reconstructed edges. To avoid these effects, deblurred output takes advantage of GGF for edge-preservation. The projected NLCM-GGF offer enhanced outcome than existing techniques for both evaluation metrics and visual perception.

4. RESULTS

Our projected scheme compared by various conventional reconstruction methods: ASDSARNL in Dong *et al.* (2011), NCSR in Dong *et al.* (2013) and DCFGGF in Jiji and Ramrao (2019). Our method also combines with BF, GF, WGF and GGF. Consequently, it is obligatory for comparing different edge filters to better keep edges. Here we carried out performance of various techniques, image evaluations.

4.1. Subjective Performance Comparison

Various methods of reconstruction include: ASDSARNL in Dong *et al.* (2011), NCSM in Dong *et al.* (2013), DCFGGF in Jiji and Ramrao (2019), NLCM-BF, NLCM-GF, NLCM-WF and NLCM-GGF.

To make sure the fairness of each assessment system, all test underwater images are pre-processed at size 256×256 pixels and processed by evaluated schemes with default parameters. The results in Dong *et al.* (2011) generate better visual excellence and evaluation metrics, though lesser patch dimension produces few artefacts in smooth areas. The results in Dong *et al.* (2013) much outperform Dong *et al.* (2011), produce sharper boundaries and further restore its quality. The projected smoothing layer in Figure 3 yields improved results than conventional schemes. Similarly, detail enhancement in Figure 4 is also much clearer and better than conventional schemes but there exhibit fewer edges in WGF than others. In Figure 5 we present hybrid result of existing and projected means.

https://doi.org/10.17993/3ctecno.2021.specialissue8.645-665

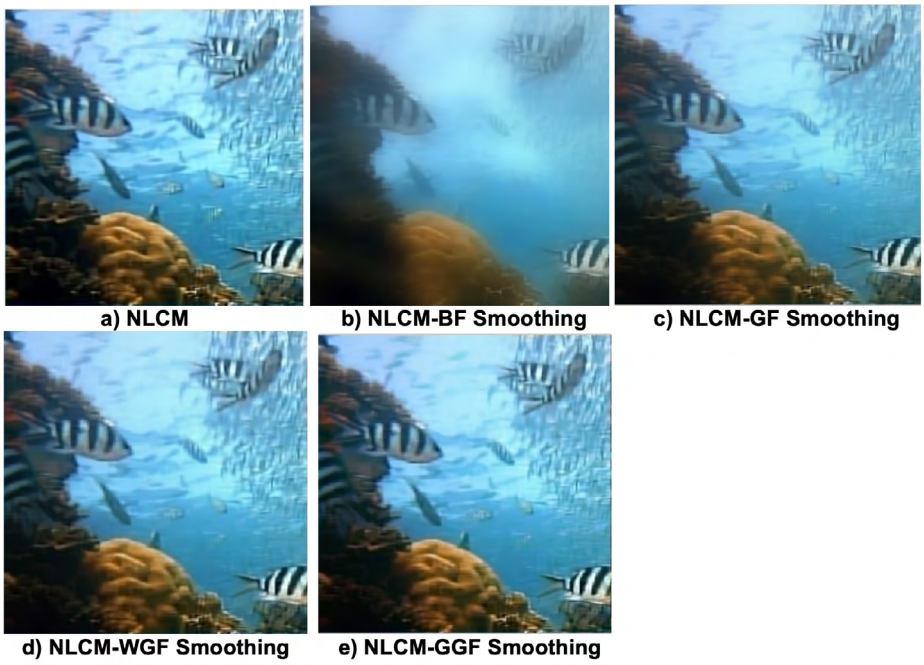

Figure 3. Edge smoothing results of Existing and Proposed Method.
Source: own elaboration.

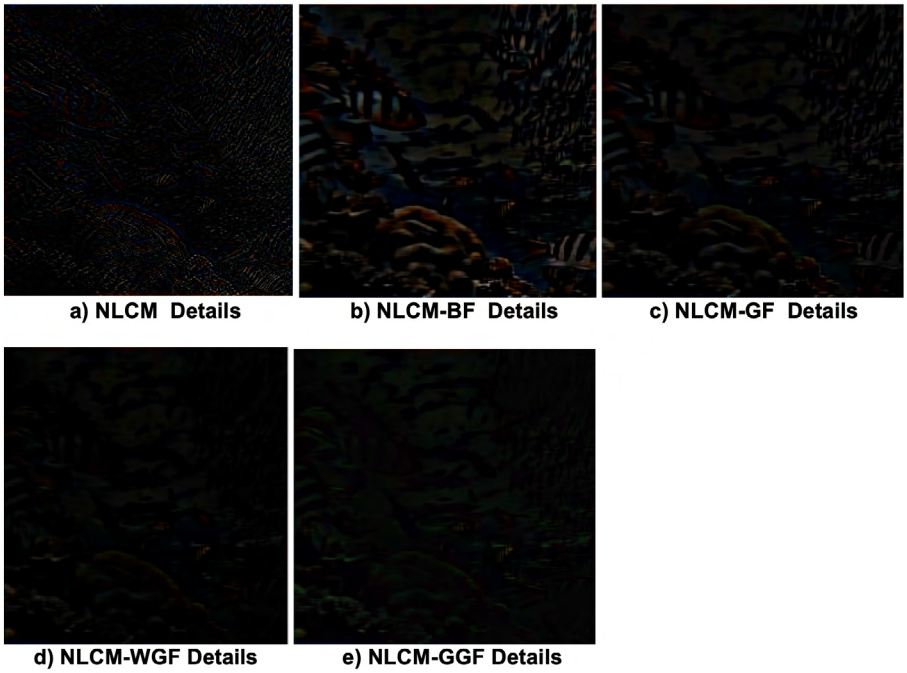

Figure 4. Detail Enhancement results of Existing and Proposed Method.
Source: own elaboration.

https://doi.org/10.17993/3ctecno.2021.specialissue8.645-665

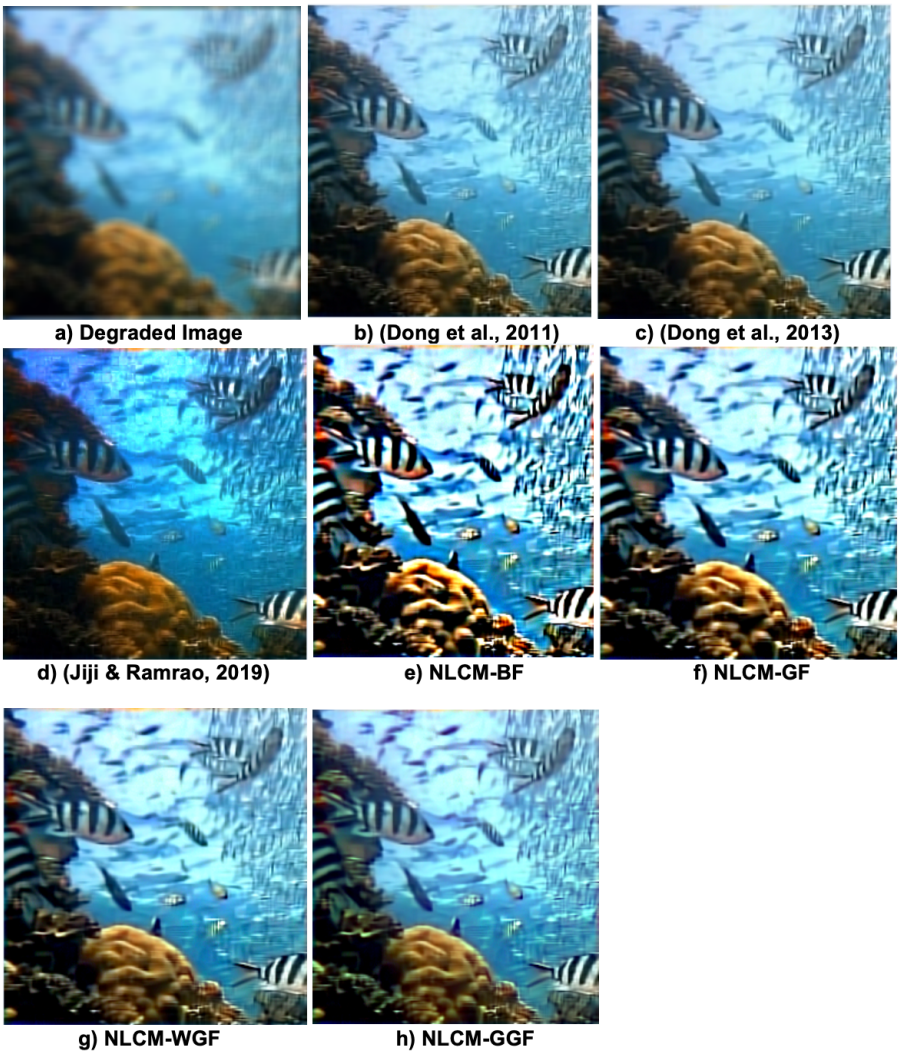

Figure 5. Enhancing performance evaluation of Underwater Imagery.
Source: own elaboration.

We observed that proposed process results much improved and enhanced details than conventional process.

4.2. OBJECTIVE PERFORMANCE COMPARISON

Image quality usually affected through imaging equipment, instrument noise, imaging conditions, image processing and other factors. Image Quality Assessment (IQA) is often

https://doi.org/10.17993/3ctecno.2021.specialissue8.645-665

separated into subjective qualitative assessment. Gray mean rate of picture reflects integral intensity and expressed as:

$$Mean = \frac{1}{RC}\sum_{r=1}^{R}\sum_{c=1}^{C} O(r,c) \tag{16}$$

Standard deviation reflects high frequency part that relates picture contrast. Higher values give better contrast.

$$SD = \frac{1}{RC}\sum_{r=1}^{R}\sum_{c=1}^{C}\{O(r,c), Mean\}^2 \tag{17}$$

Mean gradient reflects speed of changes in minor details of picture; it can represent description of grain transform and quantity of clearness well.

$$AG = \frac{1}{RC}\sum_{r=1}^{R}\sum_{c=1}^{C}\sqrt{\frac{\left[O(r,c)-O(r+1,c)\right]^2+\left[O(r,c)-O(r,c)+1\right]^2}{2}} \tag{18}$$

Entropy interprets as average uncertainty of data. When applied to images, it represents abundance data observed in picture. Higher entropy gives more uniform contrast

$$Entropy = -\sum_{r=1}^{L} P(O_r)\log_2 P(O_r) \tag{19}$$

Mean Square averages squared intensity differences of among distorted and reference representation as

$$RMSE = \sqrt{\frac{1}{RC}\sum_{r=1}^{R}\sum_{c=1}^{C}\left[O(r,c)-O'(r,c)\right]} \tag{20}$$

where *R, C* denotes row and column, *O(r,c)* remains original with *O'(r,c)* denotes deblurred picture. Peak SNR (PSNR) signify a key meant for signal alteration.

$$Peak\ SNR = 10\log\frac{O_{\max}^2}{MSE} \tag{21}$$

Where O_{max} represents maximum gray rate. Higher PSNR value represents lesser distortion. Generally, ocular view in Wang and Yuan (2017) and Wang *et al.* (2004) particularly adapted to extract picture information, thus process image excellence by three mechanism specifically; luminance *l(I,O)*, contrast *C(I,O)*, structure comparison *S(I,O)*. Thus, similarity computation represents

https://doi.org/10.17993/3ctecno.2021.specialissue8.645-665

$$S(r,c) = F\left(l(I,O), C(I,O), S(I,O)\right) \tag{22}$$

The similarity of two images has a rate among [0, 1]. When it is close to 1, two descriptions are more similar.

In Yang and Sowmya (2015) underwater color image quality evaluation (UCIQE) represents contrast, chroma and saturation expressed as:

$$UCIQE = c_1\sigma_c + c_2 con_l + c_3\mu_c \tag{23}$$

Where σ_c, con_l and μ_c represent standard deviation, contrast and mean, c_1, c_2, c_3 represent these three weights. Higher UCIQE metrics have improved results than conventional schemes. Similar to UCIQE, undersea image quality measure (UIQM) in Panetta, Gao, and Agaian (2016) constructed linear combination of UI colorfulness metric (UICM), UI sharpness metric (UISM) and UI contrast metric (UIConM). Thus, larger UCIQE and UIQM, improved undersea color image quality will be.

$$UIQM = \alpha UICM + \beta UISM + \gamma UIConM \tag{24}$$

Where α, β, γ signifies weight coefficients to organize each measure as well as balance their rates. Higher UICM value indicates improved color of undersea descriptions. Table 1 shows assessment metrics of conventional and projected technique.

Table 1. Comparison of quality metric with existing and proposed methods.

Methods / Quality metrics	DEBLURRED IMAGE		ENHANCED IMAGE				
	(Dong *et al.*, 2011)	(Dong *et al.*, 2013)	(Jiji & Ramrao, 2019)	NLCM-BF	NLCM-GF	NLCM-WGF	NLCM-GGF
Mean	127.34	127.36	96.639	126.81	126.73	127.22	127.29
SD	71.236	71.153	67.783	94.869	86.831	77.084	74.339
AG	9.226	8.065	10.194	23.761	18.507	12.988	11.681
Entropy	7.933	7.941	7.541	6.351	6.984	7.536	7.619
PSNR	24.10	26.231	65.843	66.916	70.956	72.255	72.417
RMSE	13.717	0.752	0.139	0.115	0.072	0.062	0.061
SSIM	0.619	12.443	0.9977	0.9990	0.9997	0.9998	0.9998
UICM	-45.558	-45.555	-62.107	-33.899	-39.299	-43.522	-44.177

https://doi.org/10.17993/3ctecno.2021.specialissue8.645-665

UIConM	0.736	0.728	0.785	0.305	0.583	0.701	0.681
UISM	6.906	7.007	7.105	7.827	7.289	7.057	7.073
UIQM	3.389	3.388	3.155	2.449	3.131	3.364	3.278
UCIQE	32.073	32.112	35.233	35.597	33.729	32.548	32.423

Source: own elaboration.

5. CONCLUSIONS

An acquired image underneath water gets degraded due to optical properties of light in water. However, due to degradation of observed picture, conventional forms are not correct enough for faithful reconstruction. In this paper, we proposed a hybrid technique for improving undersea descriptions. First, we used a Non locally centralized (NLCM) method for deblurring underwater descriptions, later gradient guided filter algorithm to improve the visibility of picture details and finally a Hybrid technique called non-locally centralized gradient guided filter (NLCM-GGF) gives improved results. Experimental results of proposed technique perform better than many conventional techniques together in quality metrics and visual evaluation. Nevertheless, when the illumination is very uneven, enhancement limits the local dark region, and it requires further research.

ACKNOWLEDGEMENT

We gratefully thank the Visvesvaraya Technological University, Jnana Sangama, Belagavi for their extended support to this Research work.

REFERENCES

Banham, M. R., & Katsag, A. K. (1997). Digital image restoration. *IEEE Signal Processing Magazine, 14*(2), 24-41. https://doi.org/10.1109/79.581363

Beck, A., & Teboulle, M. (2009). Fast Gradient-Based Algorithms for Constrained Total Variation Image Denoising and Deblurring Problems. *IEEE Transactions on Image Processing, 18*(11), 2419-2434. https://doi.org/10.1109/TIP.2009.2028250

Bertero, M., & Boccacci, P. (1998). *Introduction to Inverse Problems Imaging.* CRC Press.

Bioucas-Dias, J. M., & Figueiredo, M. A. T. (2007). A New TwIST: Two-Step Iterative Shrinkage/Thresholding Algorithms for Image Restoration. *IEEE Transactions on Image Processing, 16*(12), 2992-3004. https://doi.org/10.1109/TIP.2007.909319

Buades, A., Coll, B., & Morel, J.-M. (2005). A review of image denoising algorithms, with a new one. Multiscale Modeling and Simulation: *A SIAM Interdisciplinary Journal, Society for Industrial and Applied Mathematics, 4*(2), 490-530. ffhal-00271141f. https://hal.archives-ouvertes.fr/hal-00271141/document

Chan, T., Esedoglu, S., Park, F., & Yip A. (2005). *Recent developments in total variation image restoration*. http://vision.mas.ecp.fr/paragios-chen-faugeras/sample.pdf

Chantas, G., Galatsanos, N. P., Molina, R., & Katsaggelos, A. K. (2010). Variational Bayesian Image Restoration With a Product of Spatially Weighted Total Variation Image Priors. *IEEE Transactions on Image Processing, 19*(2), 351-362. https://doi.org/10.1109/TIP.2009.2033398

Daubechies, I., Defrise, M., & De Mol, C. (2004). An iterative thresholding algorithm for linear inverse problems with a sparsity constraint. *Communications on Pure and Applied Mathematics, 57*(11), 1413-1457. https://doi.org/10.1002/cpa.20042

Dong, W., Zhang, L., & Shi, S. (2011). Centralized sparse representation for image restoration. In *International Conference on Computer Vision,* 1259-1266. https://doi.org/10.1109/ICCV.2011.6126377

Dong, W., Zhang, L., Shi, G., & Li, X. (2013). Nonlocally Centralized Sparse Representation for Image Restoration. *IEEE Transactions on Image Processing, 22*(4), 1620-1630. https://doi.org/10.1109/TIP.2012.2235847

Dong, W., Zhang, L., Shi, G., & Wu, X. (2011). Image Deblurring and Super-Resolution by Adaptive Sparse Domain Selection and Adaptive Regularization. *IEEE Transactions on Image Processing, 20*(7), 1838-1857. https://doi.org/10.1109/TIP.2011.2108306

Farbman, Z., Fattal, R., Lischinski, D., & Szeliski, R. (2008). Edge-preserving decompositions for multi-scale tone and detail manipulation. *ACM Transactions on Graphics, 27*(3), 1-10. https://doi.org/10.1145/1360612.1360666

He, K., Sun, J., & Tang, X. (2013). *Guided image filtering.* http://kaiminghe.com/publications/eccv10guidedfilter.pdf

Huimin, L., Yujie, L., Lifeng, Z., & Seiichi, S. (2015). Contrast enhancement for images in turbid water. *Journal of the Optical Society of America A, 32*(5), 886-893. https://www.osapublishing.org/viewmedia.cfm?r=1&rwjcode=josaa&uri=josaa-32-5-886&html=true

Jaffe, J. S. (1990). Computer modeling and the design of optimal underwater imaging systems. *IEEE Journal of Oceanic Engineering, 15*(2), 101-111. https://doi.org/10.1109/48.50695

Jiji, A. C., & Ramrao, N. (2017). *Deblurring Underwater image degradations based on adaptive regularization*. ICICI.

Jiji, A. C., & Ramrao, N. (2019). A Novel Imaging System for Underwater Haze Enhancement. *International Journal of Information Technology, 12*, 85-90. https://link.springer.com/article/10.1007/s41870-019-00312-y

Jiji, A. C., & Vivek, M. (2017). Underwater turbidity removal through ill-posed optimization with sparse modelling. In *2017 IEEE International Conference on Power, Control, Signals and Instrumentation Engineering (ICPCSI)*, pp. 1865-1869. https://doi.org/10.1109/ICPCSI.2017.8392039

Kindermann, S., Osher, S., & Jones, P. W. (2005). Deblurring and denoising of images by nonlocal functional. *Multiscale Modeling & Simulation, 4*(4), 1091-1115. https://doi.org/10.1137/050622249

Kou, F., Chen, W., Wen, C., & Li, Z. (2015). Gradient Domain Guided Image Filtering. *IEEE Transactions on Image Processing, 24*(11), 4528-4539. https://doi.org/10.1109/TIP.2015.2468183

Lebart, K., Smith, C., Trucco, E., & Lane, D. (2003). Automatic indexing of underwater survey video: algorithm and benchmarking method. *IEEE Journal of Oceanic Engineering, 28*(4), 673-686. https://doi.org/10.1109/JOE.2003.819314

Li, Z., Zheng, J., Zhu, Z., Yao, W., & Wu, S. (2015). Weighted Guided Image Filtering. *IEEE Transactions on Image Processing, 24*(1), 120-129. https://doi.org/10.1109/TIP.2014.2371234

Lysaker, M., & Tai, X. C. (2006). Iterative Image Restoration Combining Total Variation Minimization and a Second-Order Functional. *International Journal of Computer Vision, 66*, 5–18. https://doi.org/10.1007/s11263-005-3219-7

Mairal, J., Bach, F., Ponce, J., Sapiro, G., & Zisserman, A. (2009). Non-local sparse models for image restoration. In *2009 IEEE 12th International Conference on Computer Vision*, pp. 2272-2279. https://doi.org/10.1109/ICCV.2009.5459452

Mairal, J., Elad, M., & Sapiro, G. (2008). Sparse Representation for Color Image Restoration. *IEEE Transactions on Image Processing, 17*(1), 53-69. https://doi.org/10.1109/TIP.2007.911828

Oliveira, P. J., Bioucas-Dias, J. M., & Figueiredo, M. A. T. (2009). Adaptive total variation image deblurring: A majorization-minimization approach. *Signal Processing, 89*(9), 1683-1693. https://doi.org/10.1016/j.sigpro.2009.03.018

Panetta, K., Gao, C., & Agaian, S. (2016). Human-Visual-System-Inspired Underwater Image Quality Measures. *IEEE Journal of Oceanic Engineering, 41*(3), 541-551. https://doi.org/10.1109/JOE.2015.2469915

Seibert, Q. (1963). Light in the sea. *Journal of the Optical Society of America, 53*(2), 214-233. https://doi.org/10.1364/JOSA.53.000214

Strachan, N. (1993). Recognition of fish species by color and shape. *Image and Vision Computing, 11*(1), 2-10. https://doi.org/10.1016/0262-8856(93)90027-E

Tomasi, C., & Manduchi, R. (1998). Bilateral filtering for gray and color images. *Proceedings of the 1998 IEEE International Conference on Computer Vision.* https://users.soe.ucsc.edu/~manduchi/Papers/ICCV98.pdf

Torres-Méndez, L. A., & Dudek, G. (2005) Color Correction of Underwater Images for Aquatic Robot Inspection. In: Rangarajan, A., Vemuri, B., & Yuille, A.L. (eds.),

Energy Minimization Methods in Computer Vision and Pattern Recognition. EMMCVPR 2005. Lecture Notes in Computer Science, vol. 3757. Springer, Berlin, Heidelberg. https://doi.org/10.1007/11585978_5

Wang, W., & Yuan, X. (2017). Recent advances in image dehazing. *IEEE/CAA Journal of Automatica Sinica, 4*(3), 410-436. https://doi.org/10.1109/JAS.2017.7510532

Wang, Z., Bovik, A. C., Sheikh, H. R., & Simoncelli, E. P. (2004). Image quality assessment: from error visibility to structural similarity. *IEEE Transactions on Image Processing, 13*(4), 600-612. https://doi.org/10.1109/TIP.2003.819861

Wu, X., Zhang, X., & Wang, J. (2009). Model-Guided Adaptive Recovery of Compressive Sensing. In *2009 Data Compression Conference*, pp. 123-132. https://doi.org/10.1109/DCC.2009.69

Yang, M., & Sowmya, A. (2015). An Underwater Color Image Quality Evaluation Metric. *IEEE Transactions on Image Processing, 24*(12), 6062-6071. https://doi.org/10.1109/TIP.2015.2491020

Zhang, X., Burger, M., Bresson, X., & Osher, S. (2010). Bregmanized nonlocal regularization for deconvolution and sparse reconstruction. *SIAM Journal on Imaging Sciences, 3*(3), 253-276. https://epubs.siam.org/doi/10.1137/090746379

https://doi.org/10.17993/3ctecno.2021.specialissue8.645-665

UPQC BASED POWER QUALITY IMPROVEMENT OF SOLAR PHOTOVOLTAIC SYSTEMS USING ANFIS AND MFA

MadhaviDasari[1] , Dr. V.S. Bharath[2], Dr.Madhu Palati[3], Dr D M Ganapathi[4]

[1]Assistant Professor, Dept. of EEE, R R Institute of Technology, VTU, Karnataka, India. E-mail: madhavi.81d@gmail.com

[2] Professor& HOD, Dept. of EEE, The Oxford College of Engineering, VTU, Karnataka, India, E-mail:bharathpg2002@gmail.com

[3]Assistant Professor, Dept. of EEE,BMS Institute of Technology & Management, VTU, Karnataka, India. E-mail: madhupalati@bmsit.in

[4]Professor& HOD, Dept. of EEE, East Point Institute of Technology, VTU, Karnataka, India

Abstract:

The ability of energy to reach consumer devices is determined by the quality of the power that was used to create it. Using a Unified Power Quality Conditioner (UPQC) improves the power quality on feeders in distribution system. The Unified Power Quality Conditioner is the most effective customized power equipment available in the market. An UPQC system with a three-phase bus that is fed by PV is modeled and tested. Sagging is caused by heavy loads, whereas swelling is caused by light loads. Solar arrays fed by UPQC are becoming increasingly popular as a means of reducing the severity of these power quality issues. The ANFIS–PSO basedMPPT method has no extra sensor requirement for measurement of irradiance and temperature variables. The employed methodology delivers remarkable driving control to enhance PV potential extraction.The Classical maximum power point tracking (MPPT) techniques, developed for uniform solar radiation on PV arrays such as P&O algorithm sometimes, are unable to discriminate between local and global maximum power points. Therefore, this research under partial shading condition (PSC) is aimed for enhancing the efficiency of the PV system by using modernistic techniques such as ANFIS-Particle Swarm Optimization (ANFIS-PSO), and ANFIS BASED Modified Firefly Algorithm (ANFIS- MFA). The main function of each algorithm is to find the optimal duty cycle for the DC-DC converter in order to increase the output power and efficiency. The P&O algorithm shows larger convergence time with high oscillation as compared with the other three algorithms which showed success in finding and tracking the GMPP, especially the last algorithm (MFA), as it was characterized by its speed, efficiency and convergence in finding the GMPP compared to the previous algorithms. The ripple in MFA in steady-state conditions is lower than P&O, PSO, and FA methods.

DOI Number: 10.14704/NQ.2022.20.14.NQ88071 **NeuroQuantology2022;20(14): 505-520**

Introduction

UPQC is a custom power device (CPD) utilized for eliminating the PQ problems such as harmonics [1] unbalance, sag and swell and phase-angle jump due to the extensive usage of electronically switched devices and non-linear load [2,3]. This CPD comprises of both shunt and series converters coupled through a common DClink voltage and deals with harmonics in load current and also imperfections in source voltage [4]. The shunt converter can eliminate current harmonics and unbalances from the nonlinear load so that perfect sinusoidal current flows through the power network, however series converter can compensate voltage sag/swell, voltage unbalance, voltage distortion and phase-angle jump present on the source side, so that perfect voltage regulation is maintained across the load [5]. Therefore, UPQC draws the consideration of power engineers to create active and adaptable solutions to PQ issues, which leads to the development of novel topologies and advanced control systems for UPQC. Control system plays an important part in the overall performance of a

eISSN 1303-5150

power conditioner. Power system uncertainty arises due to random variation of system loads, irregular fluctuations of system parameter such as capacity of distribution line and sudden failure of system component of the power line. To operate UPQC in the above uncertainty conditions, a fuzzy SMC based PWM technique is proposed for accurately tracking the reference signal, which provides better compensation capability of UPQC.

However, with the rising high of fossil fuels and ecological worry of their usage, there is raising interest in renewable energy sources especially photovoltaic (PV) sources that are used in many applications as they have the benefits of being clean and low maintenance [2][3]. To gain high PV efficiency, maximum power point tracking (MPPT) is a key technology because the PV power has low diversion efficiency of electric power. So, MPPT is employed to optimize the usage of PV systems and to extract the maximum power produced by the solar panels under alter climatic conditions [4].

There is a unique maximum power point (MPP) in the (P-V) curve when the radiations falling on PV are uniform, however, the P-V curve displayed many local MPP and there is only one-point appears the global MPP when one or further modules in the PV string are lower radiated than the other modules or cloudy [5, 6]. In order to recognize the global power point among the local maximum power points, different types of MPPT algorithms have been elaborated by researchers. Some of these MPPT algorithms are traditional MPPT techniques such as incremental conductance [7], perturbation and observation (P&O), and the other are the bio-inspired MPPT algorithms like particle swarm optimization (PSO) [8], firefly algorithm, and modified firefly algorithm [9] Under the impact of partial shading condition, the traditional techniques are highly futile for finding the GMPP, while the bio-inspired methods evidence many superior results in GMPP tracking. In this paper, P&O, PSO, FA, and MFA based MPPT are proposed. Moreover, a comparative study is executed between these algorithms at different patterns of partial shading and different irradiation along time. The results showed that the PSO and FA are powerful and reliable in tracking the GMPP. Furthermore, the MFA method is more reliable and more efficient than the PSO and FA methods.

I. Circuit Description

The PV-UPQC is a circuit with a combination of both the series and the shunt controller coupled with the DC-link that is powered by the photovoltaic panels [10]. The control of PV-UPQC is done by two separate controllers. The shunt controller is used for compensating the current. The series controller is used for compensating the voltage disturbances like voltage swell/voltage sag [11].

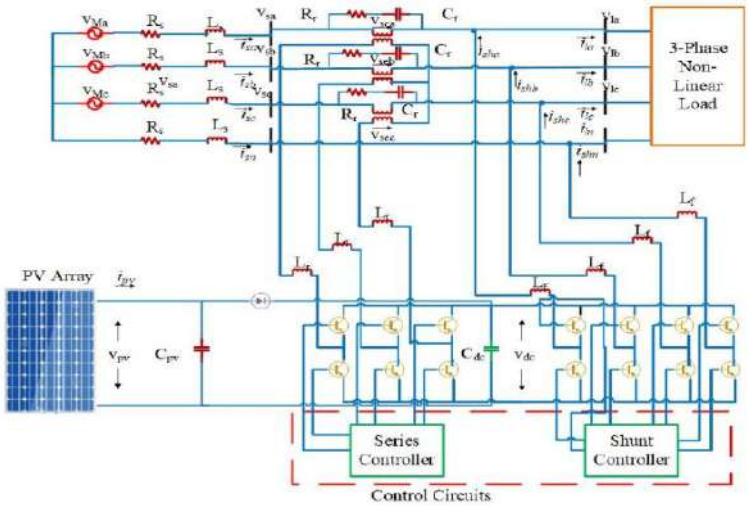

Fig. 1. Circuit diagram of PV-UPQC Three-phase four-wire system

eISSN 1303-5150

The photovoltaic panels harness the solar energy from the sun. The utilization and functionality of the UPQC can be increased by integrating with solar energy [12]. The photovoltaic system is modelled mathematically using MATLAB Simulink. The PV panel output is DC voltage. The output of the PV panel is boosted and fed to the common DC link capacitor. The MPPT controller like ANFIS BASED PSO is used to track the maximum power from the solar panels, and compare MFA MPPT [13].

II. UPQC power circuit configuration

The power circuit configuration of UPQC is shown in Fig. 2. It comprises of series converter and shunt converter. The series converter is a three phase PWM voltage source inverter, which mitigates voltage sag, swell, voltage distortion and voltage unbalance existing in the supply voltage. Subsequently, the LC filter consists of inductor L_{sef} and capacitor C_{ef} connected in output of series converter to prevent the flow of switching ripples [14]. Similarly, the transformers are connected at the output of the LC filter to provide isolation between series converter and the power line and also prevent the DC-link capacitor from being short circuited due to the operation of various switches. The power circuit of shunt converter consists of a three phase PWM voltage source inverter, which is connected through an interfacing inductor L_{shf} to provide isolation between the shunt converter and power line [15]. The purpose of shunt converter is to restrain the load current harmonics and to control the DC-link voltage. However, insulated gate bipolar transistors (IGBTs) with anti-parallel diodes are used as PWM voltage source inverter and a 3-phase diode-bridge rectifier employed with resistive RL as well as inductive LL are used as a nonlinear load [16].

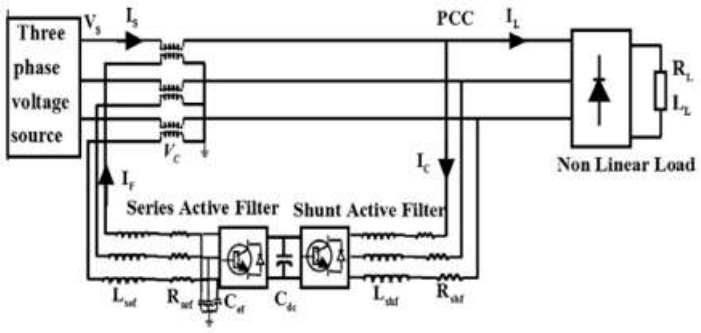

Fig. 2. Power Circuit Configuration for UPQC

III. Solar Cell

Sun based cells are intended to change over (something like a part of) accessible light into electrical energy, as their name recommends. They achieve this without depending on synthetic cycles or moving parts.

Characteristics of Solar Cells

The sun based cell, which is for the most part built of PV wafers, changes over sun oriented illumination's light energy straightforwardly into voltage and flow for load, and conveys power without the utilization of an electrolytic impact [17]. The electric energy is acquired from the PN interface of semiconductor straightforwardly; accordingly, the sun based cell is otherwise called PV cell .The same circuit of sun based cell as displayed in Fig 3.

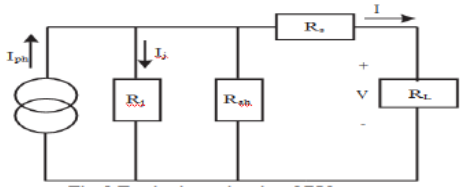

Fig.3. Equivalent circuit of PV array

eISSN 1303-5150

The latest source, photovoltaic cell current is addressed by I_{ph}, the nonlinear obstruction of the p-n intersection is addressed by R_j, and the natural shunt and series protections are addressed by R_{sh} and R_s, separately. Typically, the worth of R_{sh} is very high, though the worth of R_s is somewhat low. Therefore, the two of them may be disregarded to improve on the investigation. PV modules are comprised of PV cells that are assembled in bigger groupings [18].

They $I_{ph} = [I_{scr} + K_i(T - T_r)]\frac{S}{100}$ nnected in series-equal mix to shape PV clusters. The numerical model used to work on the PV exhibit is addressed by the condition.

$$I = n_p I_{ph} - n_p I_{rs}\left[e^{\left(\frac{q}{kTA}*\frac{V}{n_s}\right)} - 1\right]$$

Where I addresses the PV cluster yield current, V addresses the PV exhibit yield voltage, ns addresses the quantity of series cells, np addresses the quantity of equal cells, q addresses the charge of an electron, k addresses the Boltzman steady constant, addresses the p-n intersection ideality factor, T addresses the cell temperature, and I_{rs} addresses the cell invert immersion current. The sun powered cell's uniqueness from the best p-n intersection character is dictated by factor A chooses the deviation of sun oriented cell from the best p-n intersection attributes. It's worth reaches from one to five. The photograph current I_{ph} relies upon the sunlight based irradiance and cell temperature as below

Where I_{scr} is the cell short circuit current at reference temperature and radiation, K_i is the short circuit current temperature coefficient and S is the solar irradiance in mW/cm^2. The Simulink model of PV array is shown in Fig. 4. The model includes three subsystems. One subsystem to model PV module and two more subsystems to model I_{ph} and I_{rs} [19].

IV. Hybrid ANFIS–PSO Based MPPT Controller

The training and updation of ANFIS specifications are a challenging task for the designers nowadays. Compared to the gradient techniques, the PSO provides simpler and rapid updation convergence velocity [20]. Moreover, the PSO does not require initial parameter calculation and nor there is requirement of a learning rate. Fig. 4 depicts the architecture of the ANFIS controller and comprises antecedent and conclusions as a major component with five total layers [21].

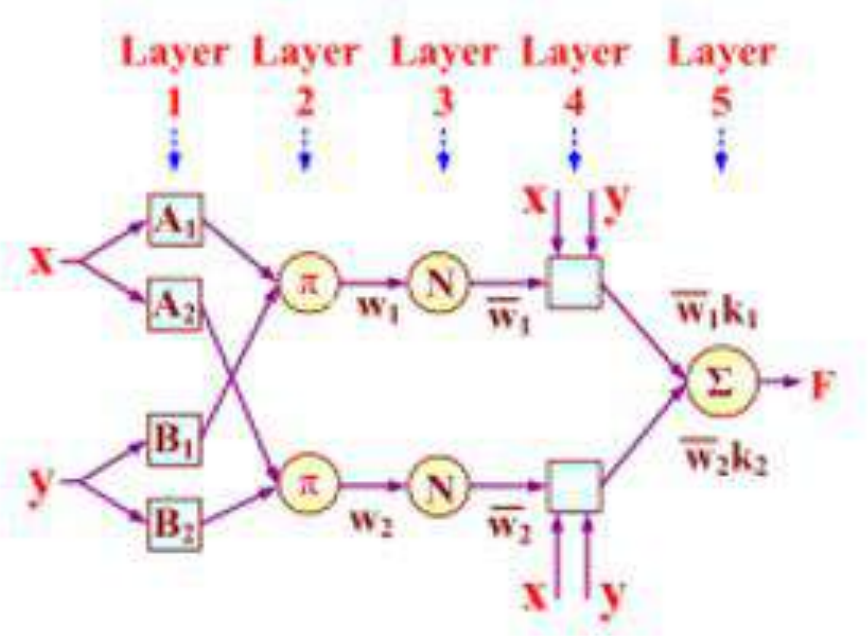

Fig.4. Architecture of an ANFIS Controller

eISSN 1303-5150

The mathematical equations associated with multilayer feedforward network are as follows:

$$W_j = \mu_{P_j}(x) * \mu_{Q_j}(y), \quad \bar{W}_j = \frac{W_j}{W_1 + W_2}, \quad j = 1, 2.$$

K_1, K_2, and K can be expressed as follows:

$$\left.\begin{aligned} K_1 &= A_1 x + B_1 y + R_1 z, \quad K_2 = A_2 x + B_2 y + R_2 z \\ K &= \frac{W_1 K_1 + W_2 K_2}{W_1 + W_2} = \bar{W}_1 K_1 + \bar{W}_2 K_2 \end{aligned}\right\}$$

The membership function (bell-shaped) lies between 0 and 1 and is evaluated mathematically as

$$\left.\begin{aligned} \mu_{P_j}(x) &= \frac{1}{1+\left[((x-r_j)p_j{}^{-1})^2\right]^{bj-3}} \\ \mu_{P_j}(x) &= \exp\left[-\left[\left(\frac{x-r_j}{p_j}\right)^2\right]^{bj}\right] \end{aligned}\right\}$$

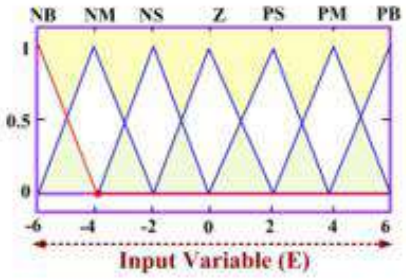

Fig. 5. Membership Functions Input Framework

INFERENCE FUZZY DECISION

E / dE	NB	NM	NS	Z	PS	PM	PB
NB	Z	PB	Z	Z	NS	PB	PB
NM	PS	Z	NS	Z	NS	Z	NM
NS	NB	Z	PB	PS	PS	PS	PS
Z	Z	PS	NM	Z	PS	Z	NS
PS	Z	NB	PB	NS	Z	Z	PS
PM	NS	NS	PS	Z	NS	PS	PB
PB	PS	PS	Z	NB	Z	PM	NB

Unlike traditional MPPT controllers, this control has peak maximum power tracking, fast dynamicity, the rapid velocity of convergence, and simpler contraption. Fuzzification, inference engine, and defuzzification are the premier process blocks of this algorithm. The MATLAB/Simulink model of an ANFIS– PSO methodology in the presence of an input parameter (PV voltage/current) yields duty ratio as pulse width modulation (PWM) generated signal [22] [23]. The detailed flowchart structure of an ANFIS–PSO-based MPPT control is described in Fig. 6. An advanced hybrid ANFIS technique gathers the fuzzy data with trained learning rules for proper adjustment of membership values before the error has been minimized to the merest amount. Whenever membership parameters are adapted, the learned system is equipped to work as a hybrid MPPT controller

eISSN 1303-5150

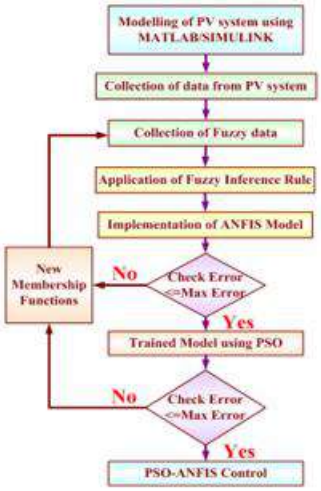

Fig. 6. Flowchart Structure of an ANFIS-PSO based MPPT Control

V. Modified Firefly Algorithm

In general, the population size for PSO and FA is constant. A larger population is beneficial to the global search process, but it increases tracking time. On the other hand, a low population decreases the tracking time of research, but might a trip to the local MPP instead of the global MPP. The modified firefly algorithm (MFA) is proposed , Where the main point behind this algorithm is an adaptation of population size , so, the coefficients of the algorithm (α, βo) are updated in each iteration, to obtain poise between convergence speed and the tracking efficiency. α and βo are defined as follows:

$$\alpha = \alpha_{max} + (\alpha_{min} - \alpha_{max})\frac{iter}{Max,iter}$$

$$\beta_o = \beta_{o_{max}} + (\beta_{o_{min}} - \beta_{o_{max}})\frac{iter}{Max,iter}$$

Where iter is the iteration number and Max,iter presents the maximum number of iterations. As can be seen in above Eq, the value of the parameter α is large at the first iteration, then, it is lowered in the next iterations for accelerating the convergence and decreasing the tracking time this lead to lower the chance of trapping in the local optimums. Furthermore, when βo reduced at each iteration, the convergence speed raises.

The steps of MFA algorithm to MPPT

1-Set the initial parameter of MFA such as randomization parameter and attractiveness.

2- Suppose population size.

3- Simulate the Simulink module.

4- extract the output power that's specified the brightness of the firefly.

5- Update the duty cycle value that's represented by the position of firefly depending on the optimization technique that's applied.

6- Check the restrictions and run the best solution

eISSN 1303-5150

VI. SIMULATION RESULTS

Case1: Hybrid ANFIS-PSO based MPPT Controller

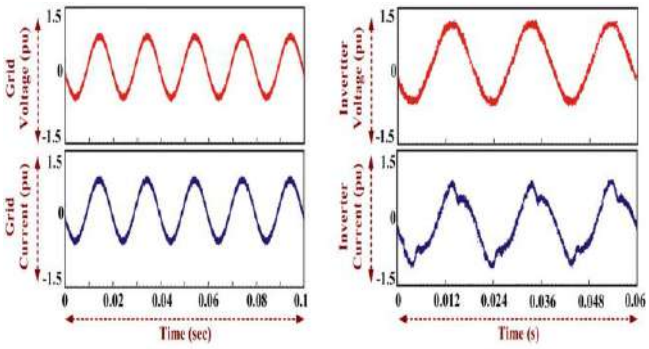

Fig.7.Behavior of grid and inverter.(a) Grid behavior at unity power factor. (b) Inverter pursuance under transient conditions

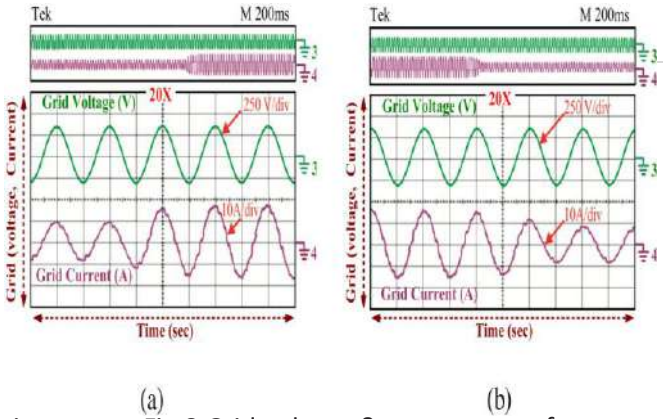

Fig.8.Grid voltage & current waveforms (a) Low to high insolation level (b) High to low insolation level

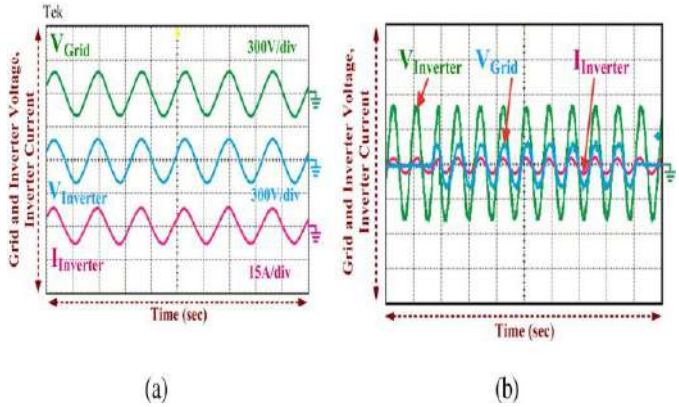

Fig. 9. Grid synchronization. (a) Inverter voltage, grid voltage and inverter current under steady-state conditions (b) Grid and inverter under dynamic operating conditions

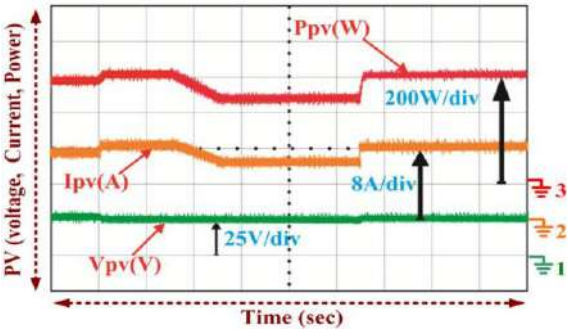

Fig.10. Performance of hybrid MPPT under changing solar insolation current under steady-state conditions

Case 2: Hybrid ANFIS-MFA based MPPT Controller with UPQC

eISSN 1303-5150

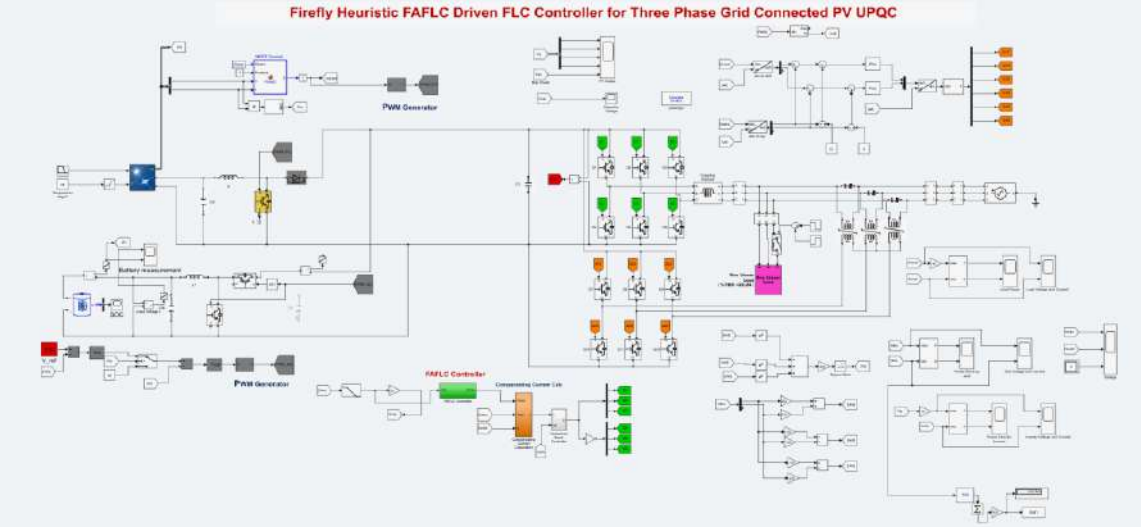

Fig. 11. Simulation of Hybrid ANFIS-MFA based MPPT Controller with UPQC

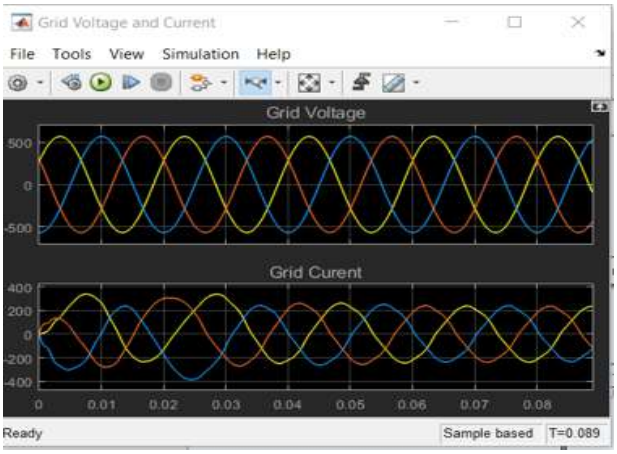

Fig. 12. Grid Voltage and Grid Current waveforms

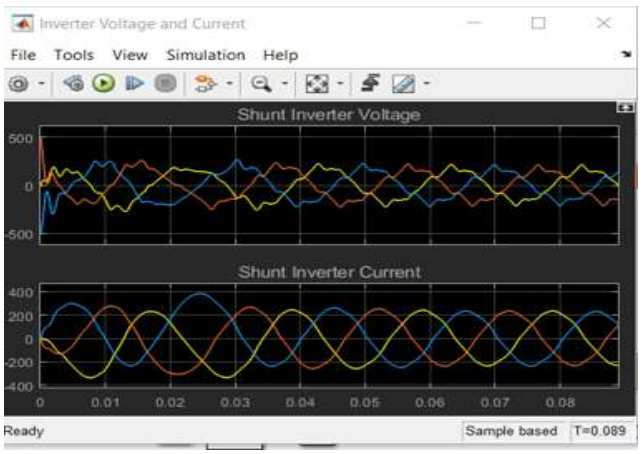

Fig. 13. Shunt Inverter Voltage and Shunt Inverter Current

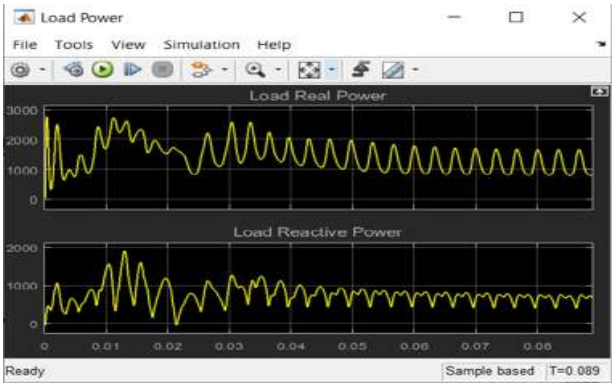

Fig. 14. Load Real Power and Reactive Power Waveforms

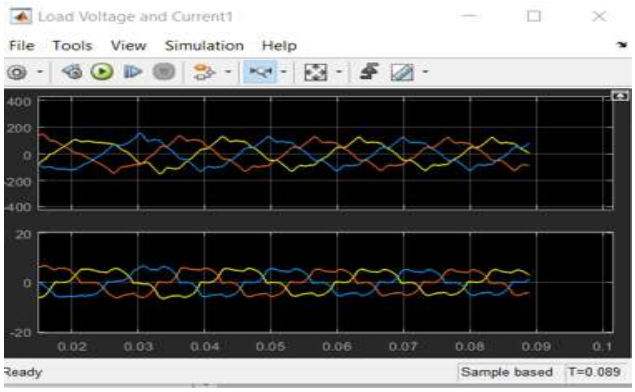

Fig. 15. Load Voltage and Current waveforms

eISSN 1303-5150

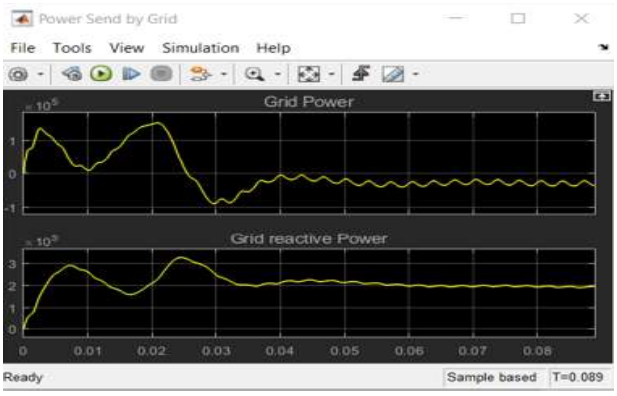

Fig. 16. Power send by Grid

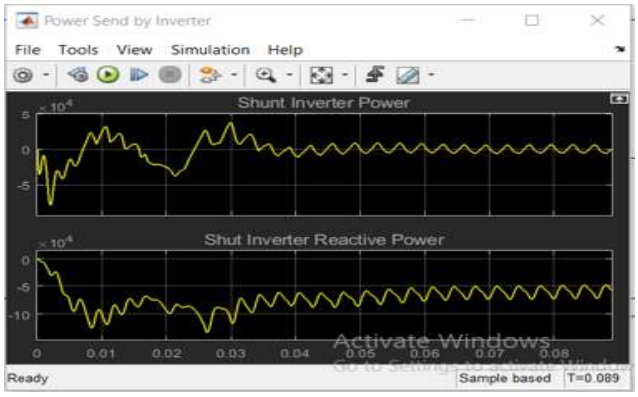

Fig. 17. Power send by Inverter

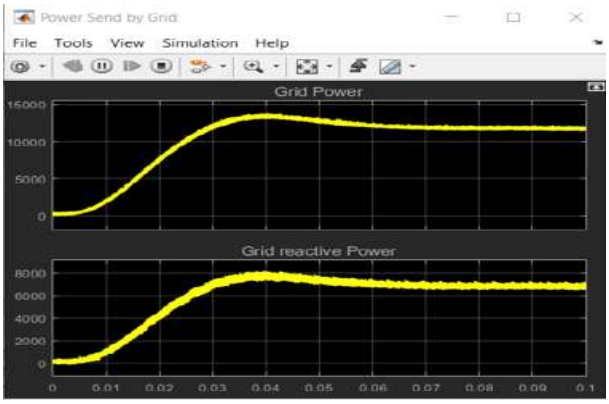

Fig. 18. Power send by Grid

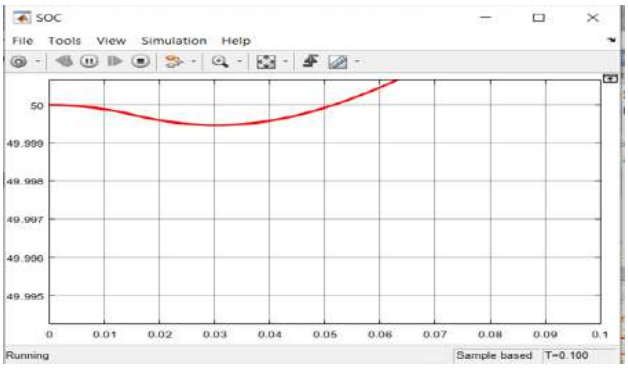

Fig.19. Battery State of Charge

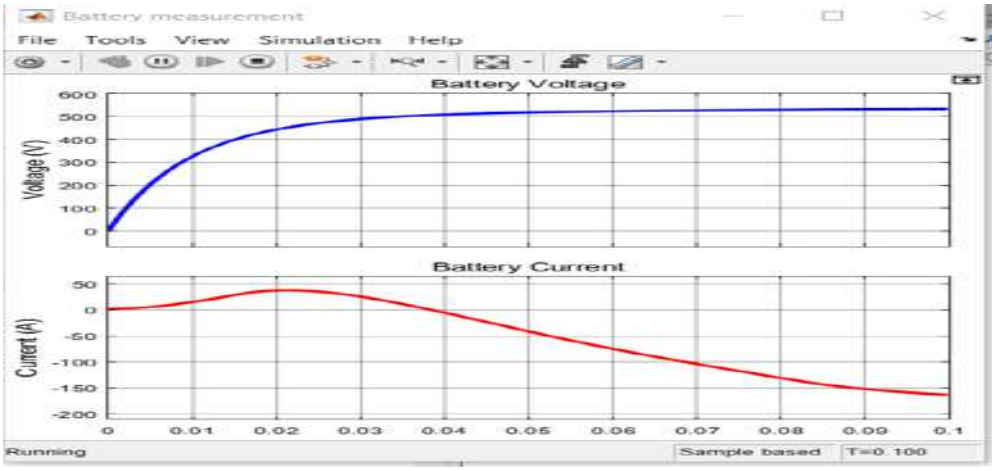

Fig. 20. Battery Management – Battery Voltage, Battery Current

eISSN 1303-5150

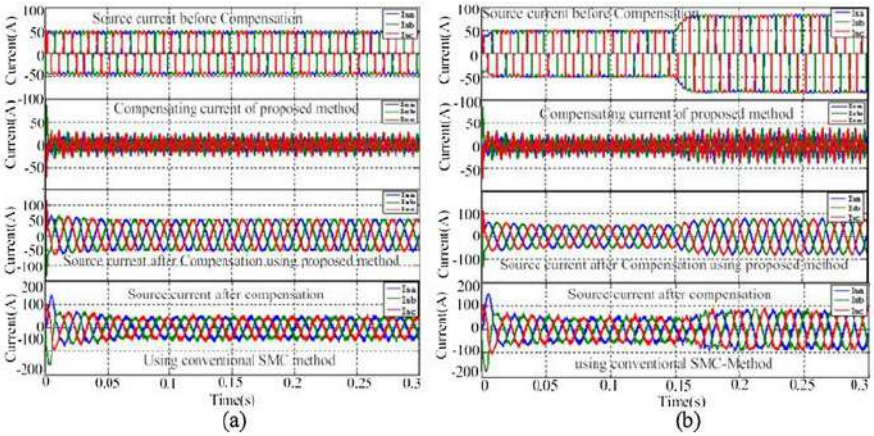

Fig.21.Simulation result of shunt converter, (a) shunt converter compensation waveforms during
Steady state condition and (b)shunt converter compensation waveforms during transient state condition.

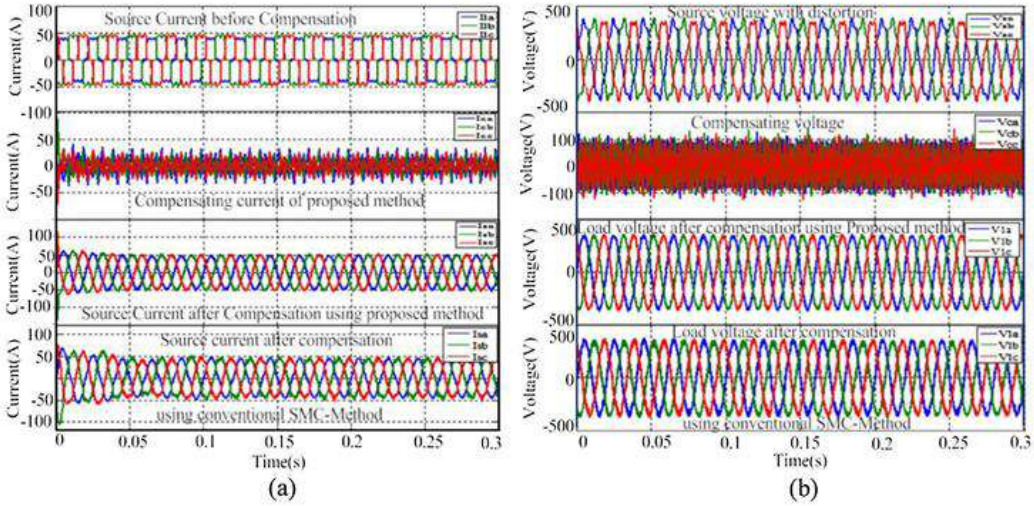

Fig. 22.Simulation result of shunt and series converter (a) shunt converter compensation waveform during load unbalance condition and (b)series converter compensation waveform during voltage distortion condition.

eISSN 1303-5150

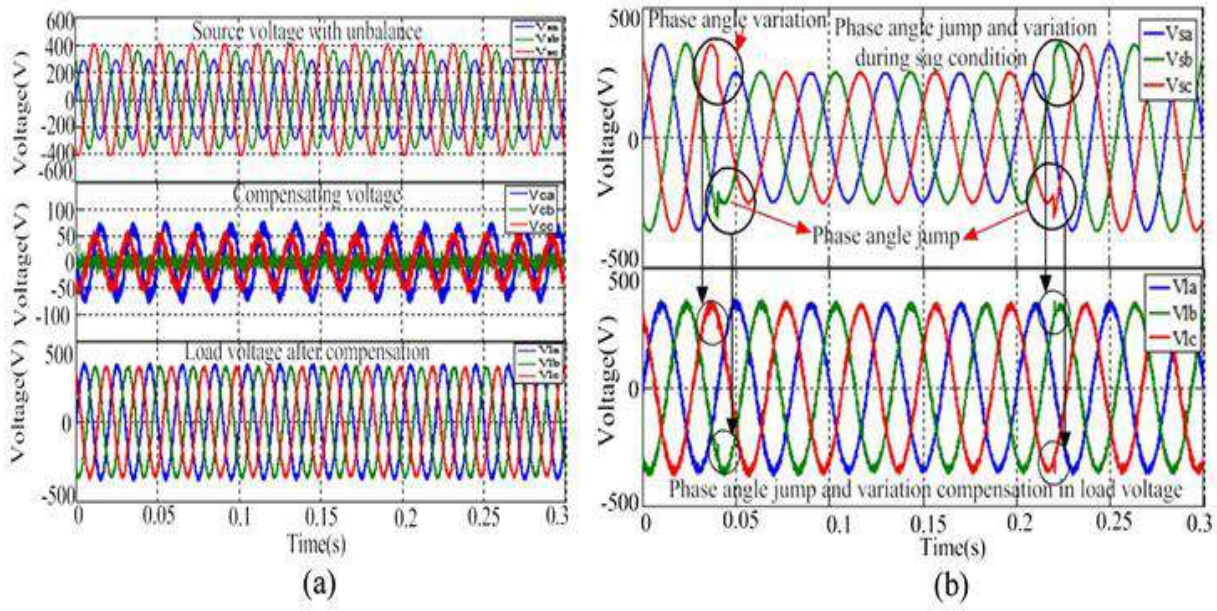

Fig. 23. Simulation results of unbalanced supply voltage and phase angle jump (a) supply voltage unbalance

Compensation waveform (b) Phase angle jump and variation compensation during sag condition

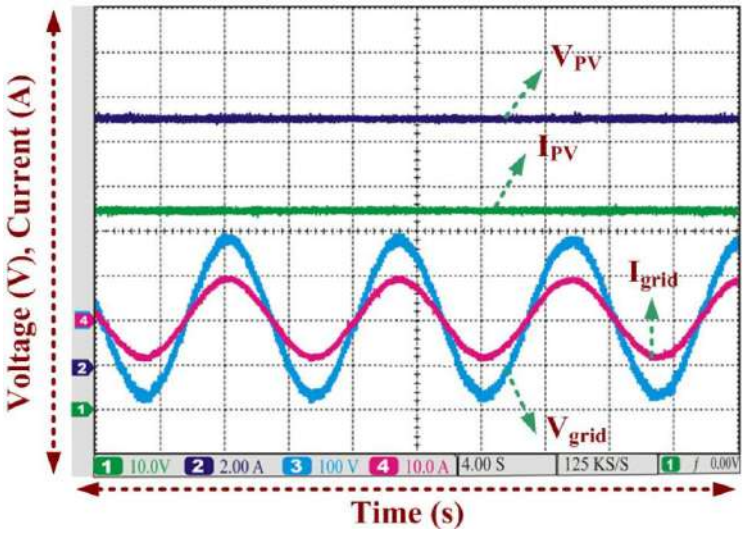

Fig.24. PV responses at Unity Power Factor

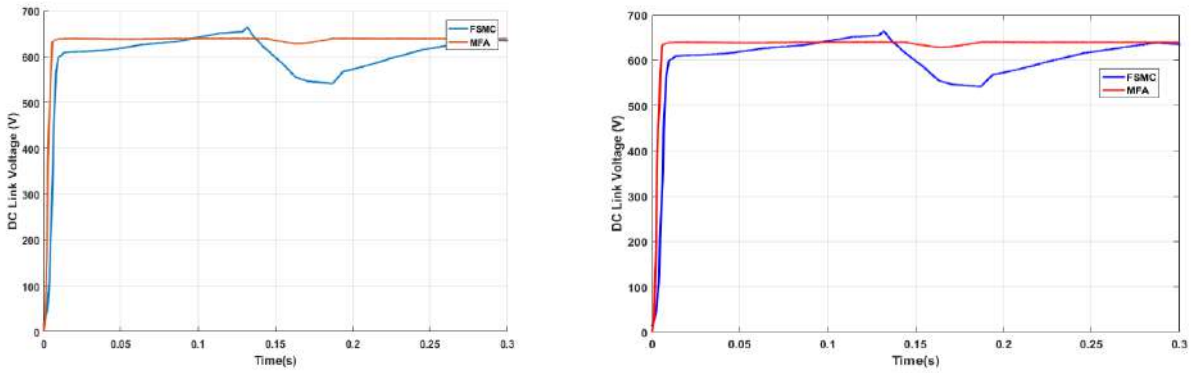

Fig. 25. (a) Voltage Swell V_{dc} (b) Voltage Sag V_{dc}

eISSN 1303-5150

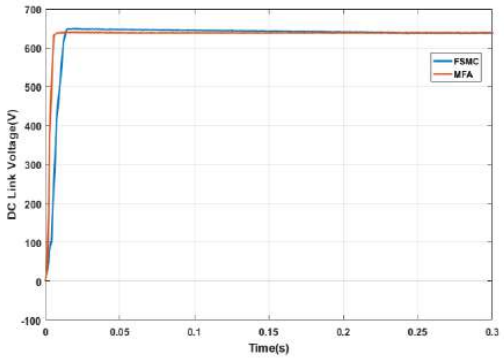

(c) Voltage distortion V_{dc}

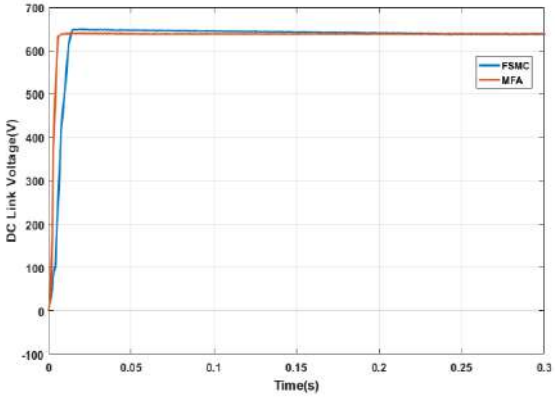

(d) Unbalanced nonlinear V_{dc}

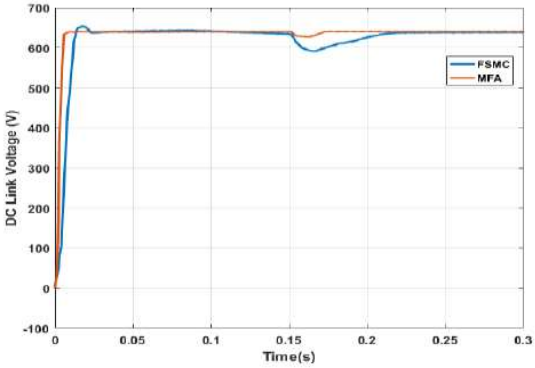

(e) Load change V_{dc} comp1

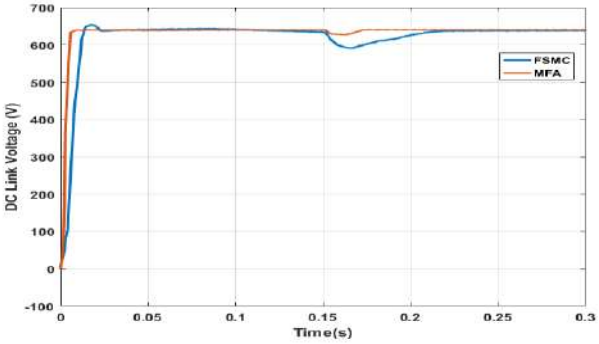

(f) Load change V_{dc} comp

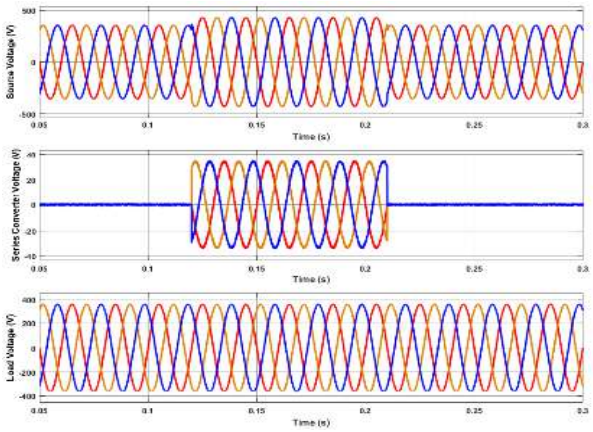

Fig.25 (a) Voltage swell

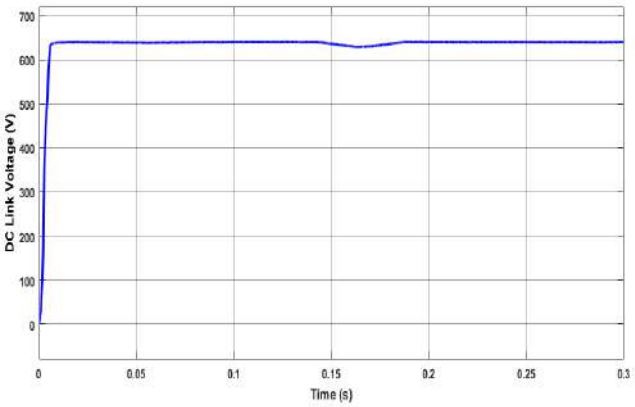

(b) Voltage swell V_{dc}

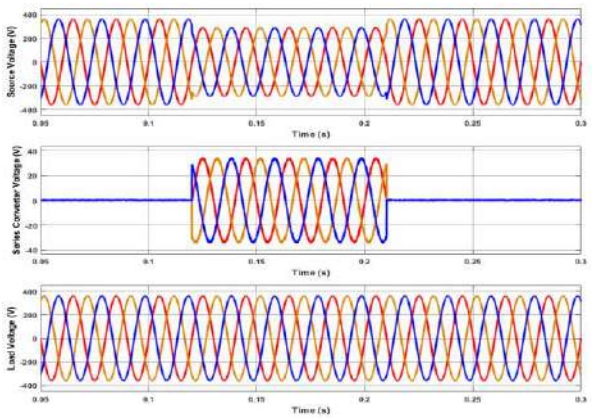

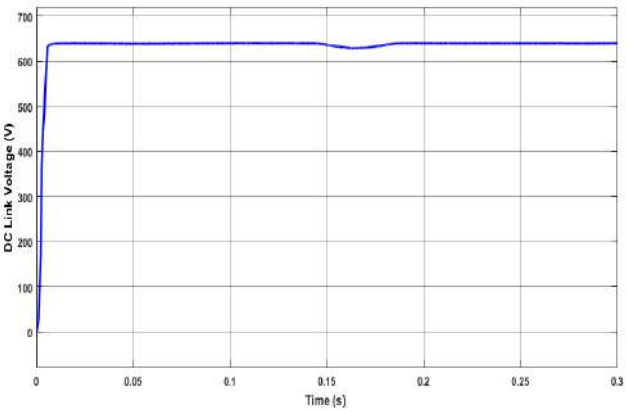

eISSN 1303-5150

(c) Voltage sag

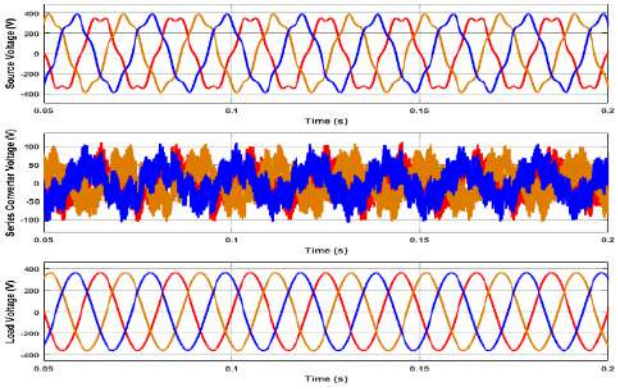

(d) Voltage sag V_{dc}

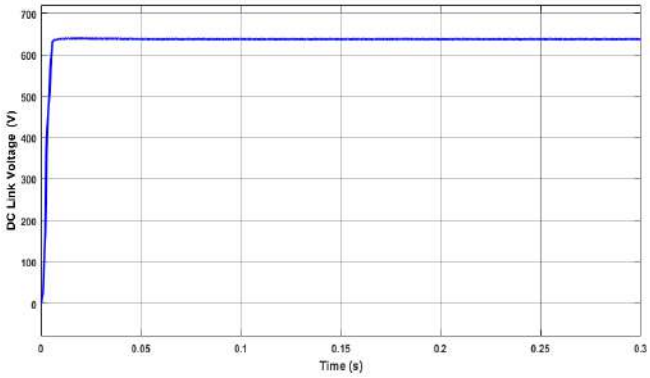

Fig. 26. (a) Voltage distortion

(b) Voltage distortion V_{dc}

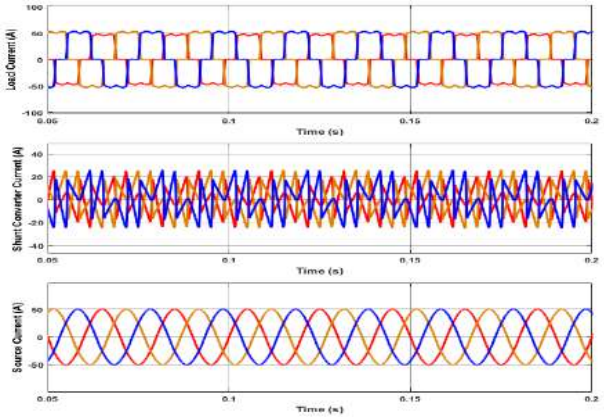

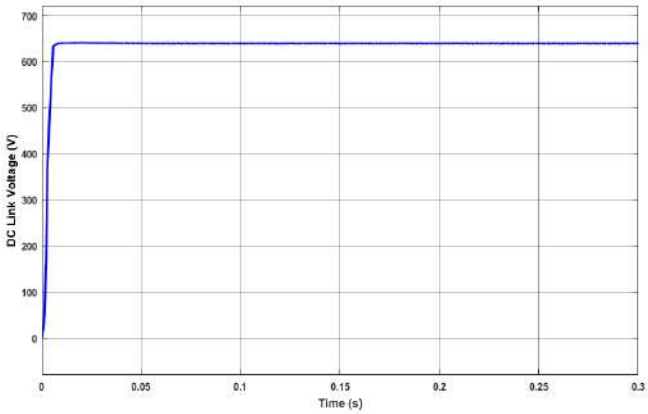

(c) Unbalanced nonlinear load

(d) Unbalanced voltage vdc

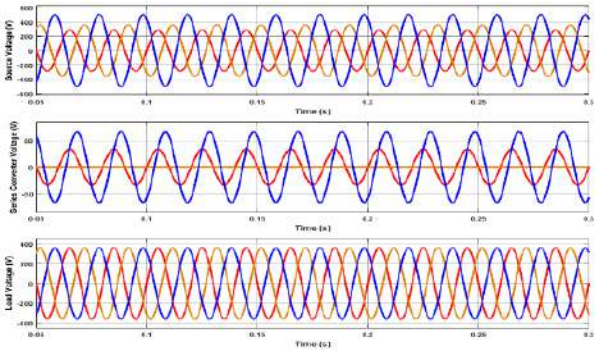

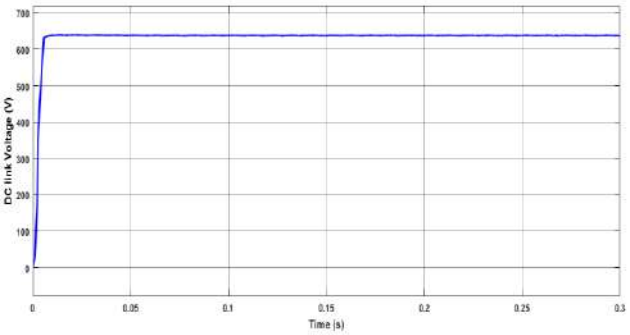

Fig.27 (a) Source Voltage Distortion

(b) Source voltage V_{dc}

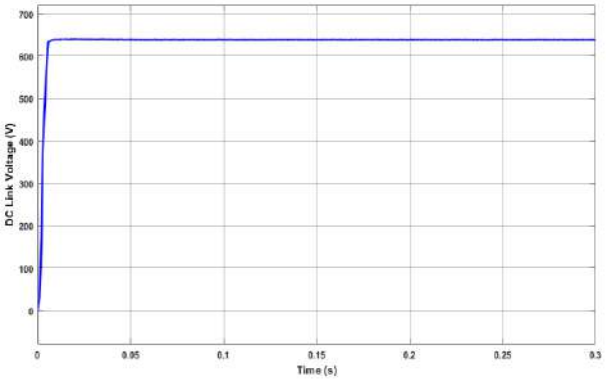

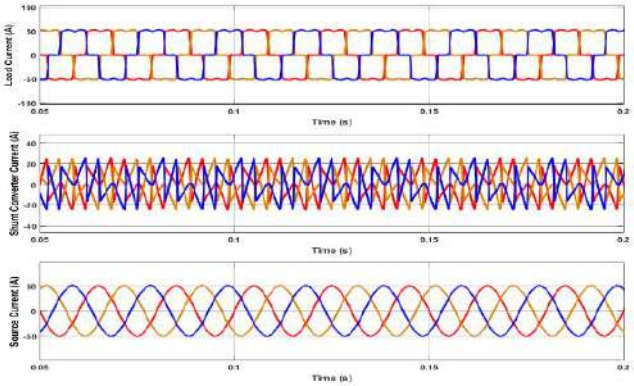

eISSN 1303-5150

(c) Load Constant V_{dc}

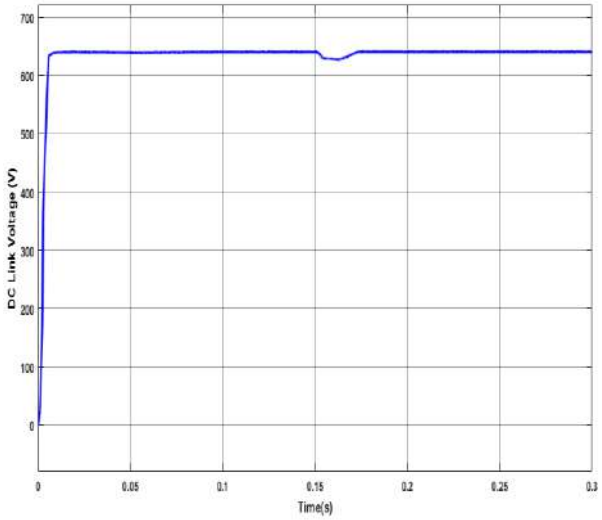

(d) Load constant current

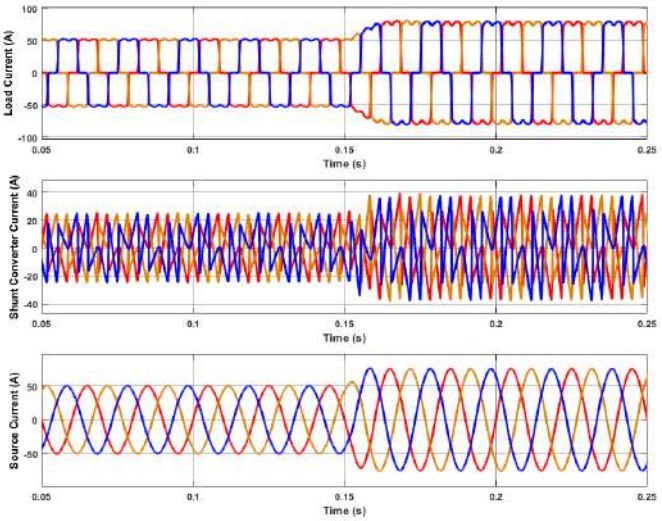

(e) Load change V_{dc}

(f) Load change current

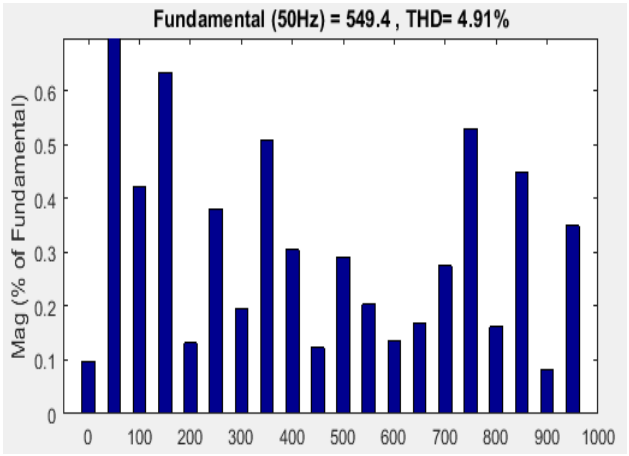

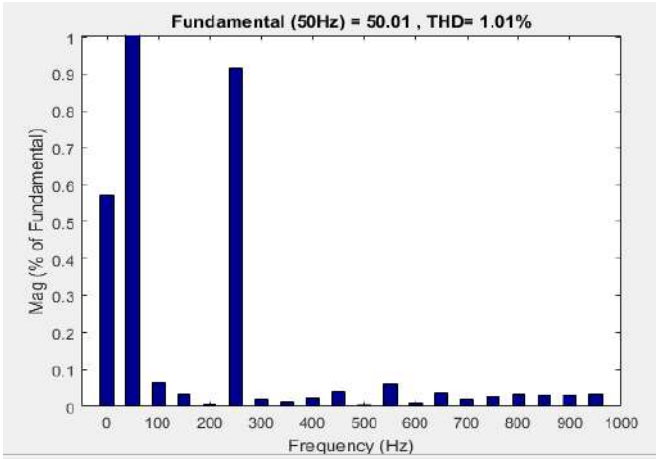

Fig. 28.Total Harmonic Distortion Analysis on Source side as well as Load side (a) Source Voltage THD

(b) Source Current THD

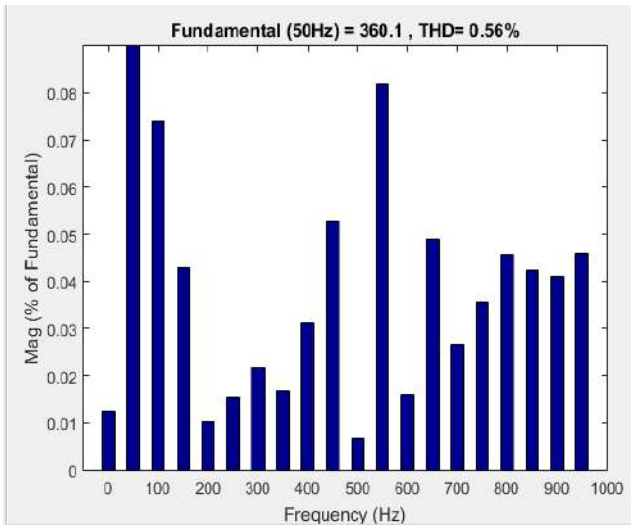

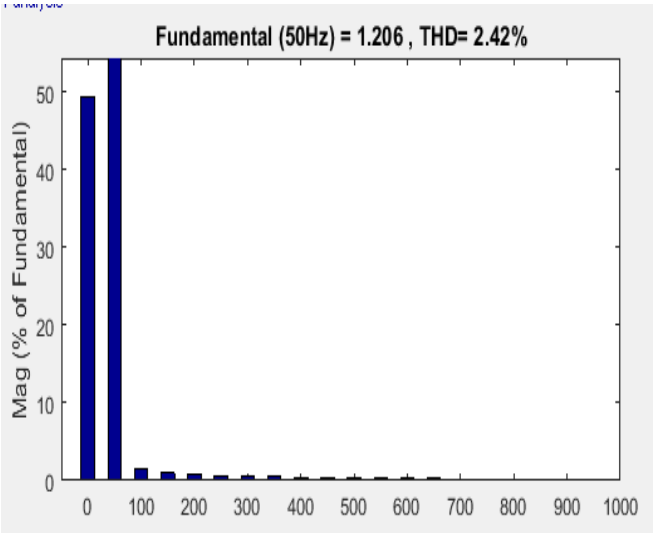

(c) Load Voltage THD

(d) Load current THD

eISSN 1303-5150

VII. Conclusion :

This paper emphasizes on design and performance analysis of photovoltaic array integrated unified power quality conditioner (PV-UPQC) and presents the idea of power quality enhancement along with the green energy transfer to the grid. PV array is integrated with UPQC by using maximum power point tracking (MPPT) circuit (boost converter and MPPT algorithm). PV-UPQC is dealing with power quality issues such as unbalanced current, harmonics, reactive power, dip and swell in the supply voltage. It will also transfer active power from the PV array to the load and/or grid depending upon solar radiation.

In this paper, a novel fixed frequency FSMPWM based control strategy is presented for UPQC. The proposed control methodology is responsible for fast and accurate tracking of the reference signal along with providing fixed switching frequency during power system perturbations and also eliminates the inherent chattering drawback of sliding mode control. The P&O algorithm is not efficient in finding the global maximum power point of the PV system, especially in the second scenario. Also the P&O algorithm shows larger convergence time with high oscillation as compared with the other three algorithms which showed success in finding and tracking the GMPP, especially the last algorithm (MFA), as it was characterized by its speed, efficiency and convergence in finding the GMPP compared to the previous algorithms. The MFA method proved to be the best MPPT tracking method compared to other three methods in all cases, Therefore, it successfully compensates several PQ problems such as current harmonics, load unbalance, voltage sag/swell, voltage unbalance, voltage distortion and phase-angle jump existing in the power distribution network and makes UPQC robust in comparison to the conventional SMC method during power system perturbations.

References

[1] Li P, Li Y, Yin Z. Realization of UPQC H1 coordinated control in Microgrid. Int J Electr Power Energy Syst 2015;65:443–52.

[2] Esfahani MT, Hosseinian SH, Vahidi B. A new optimal approach for improvement of active power filter using FPSO for enhancing power quality. Int J Electr Power Energy Syst 2015;69:188–99.

[3] Rahmani B, Li W, Liu G. An Advanced Universal Power Quality Conditioning System and MPPT method for grid integration of photovoltaic systems. Int J Electr Power Energy Syst 2015;69:76–84.

[4] Pal Y, Swarup A, Singh B. A comparative analysis of different magnetics supported three-phase four-wire unified power quality conditioners – a simulation study. Int J Electr Power Energy Syst 2013;47:436–47.

[5] Patjoshi RK, Mahapatr KK. Non-linear sliding mode control with SRF based method of UPQC for power quality enhancement. In: 9th International IEEE conference of industrial and information systems (ICIIS). p. 1–6.

[6] Kinhal VG, Agarwal P, Gupta HO. Performance investigation of neuralnetwork-based unified power-quality conditioner. IEEE Trans Power Delivery 2011;26(1):431–7.

[7] Patjoshi RK, Mahapatra KK. Resistive optimization with enhanced PLL based nonlinear variable gain fuzzy hysteresis control strategy for unified power quality conditioner. Int J Electr Power Energy Syst 2016;83:352–63.

[8] Karanki SB, Mishra MK, Kumar B. Particle swarm optimization-based feedback controller for unified power-quality conditioner. IEEE Trans Power Delivery 2010;25(4):2814–24.

[9] Patjoshi RK, Mahapatra KK. New control strategy of unified power quality conditioner with sliding mode approach. Mumbai: IEEE INDICON; 2013. p. 1–6.

[10] Rahman SA, Janakiraman PA, Somasundaram P. Voltage sag and swell mitigation based on modulated carrier PWM. Int J Electr Power Energy Syst 2015;66:78–85.

eISSN 1303-5150

[11] Khan JF, Bhuiyan SM, Rahman KM, Murphy GV. Space vector PWM for a twophase VSI. Int J Electr Power Energy Syst 2013;51:265–77.

[12] Monfared M, Rastegar H. Design and experimental verification of a dead beat power control strategy for low cost three phase PWM converters. Int J Electr Power Energy Syst 2012;42(1):418–25. [13] Monter AR, Bueno EJ, García-Cerrada A, Rodríguez FJ, Sánchez FM. Detailed analysis of the implementation of frequency-adaptive resonant and repetitive current controllers for grid-connected converters. Electric Power Syst Res 2014;116:231–42.

[14] Shieh CS. Fuzzy PWM based on Genetic Algorithm for battery charging. Applications of Soft Computing 2014;21:607–16.

[15] Venkataramanan G, Divan D. Discrete time integral sliding mode control for discrete pulse modulated converters. In: Power Electron Specialists Conf. p. 67–73 [21st Annual IEEE].

[16] Abrishamifar A, Ahmad AA, Mohamadian M. Fixed switching frequency sliding mode control for single-phase unipolar inverters. IEEE Trans Power Electron 2012;27(5):2507–14.

[17] Fang Y, Fei J, Mab K. Model reference adaptive sliding mode control using RBF neural network for active power filter. Int J Electr Power Energy Syst 2015;73:249–58.

[18] Yan W, Hu J, Utkin V, Xu L. Sliding mode pulsewidth modulation. IEEE Trans Power Electron 2008;23(2):619–26.

[19] Morris S, Dash PK, Basu KP. A fuzzy variable structure controller for STATCOM. Electric Power Syst Res 2003;65(1):23–34.

[20] Yu FM, Chung HY, Chen SY. Fuzzy sliding mode controller design for uncertain time-delayed systems with nonlinear input. Fuzzy Sets Syst 2003;140 (2):359–74.

[21] Yagiz N, Hacioglu Y, Taskin Y. Fuzzy sliding-mode control of active suspensions. IEEE Trans Ind Electron 2008;55(11):3883–90.

[22] Saetieo S, Devaraj R, Torrey DA. The design and implementation of a threephase active power filter based on sliding mode control. IEEE Trans Ind Appl 1995;31(5):993–1000.

[23] Ucar M, Ozdemir S. 3-Phase 4-leg unified series–parallel active filter system with ultracapacitor energy storage for unbalanced voltage sag mitigation. International Journal of Electrical Power Energy Systems 2013;49:149–59.

[24] JeraldineViji A, Aruldoss Albert Victoire T. Enhanced PLL based SRF control method for UPQC with fault protection under unbalanced load conditions. International Journal of Electrical Power Energy Systems 2014;58:319–2

Original Article | Published: 20 September 2021

A Novel Double Frequency SEPIC Converter with Improved Transient Characteristics and Efficiency

S. Vijayalakshmi, M. Marimuthu, N. Jayakumar, B. Devi Vighneshwari, B. Paranthagan, Nisha C. Rani & R. Shenbagalakshmi

Journal of Electrical Engineering & Technology **17**, 1039–1050 (2022)

Abstract

A novel double frequency SEPIC converter is discussed in this paper. Efficiency, static and dynamic characteristics of the dc to dc power converters are the concerned factors in power electronics. In order to improve the above factors, switching frequency play a vital role in converters. Hence, include High switching frequency in the converter can improve the dynamic characteristics, but it reduces the efficiency. In other words, put in low switching frequency in the converter may result in better efficiency but produces poor dynamic characteristic. In this concern double-frequency SEPIC converter is proposed. This SEPIC dc-dc converter consists of two SEPIC cells: one functions at high switching frequency, and other functions at

low switching frequency. The proposed SEPIC converter reveals enhanced steady state and transient characteristic than the other single frequency SEPIC converter and produces high efficiency also. The results of simulation and hardware prove that the anticipated converter extremely progresses the efficiency and displays more or less equal the same dynamics as the traditional high frequency SEPIC converter.

References

1. Usova M.A., Velkin, V.I.: 'Possibility to use renewable energy sources for increasing the reliability of the responsible energy consumers on the enterprise'. *IEEE Interanation Ural Conference on AC Electric Drives*, Mar 2018, pp. 1 – 4

2. Andre L. Schlingmann ; Roberto F. Coelho ; Denizar C. Martins.: 'A New dc-dc converter for Photo Voltaic application' .*IEEE International Symposium on Power Electronics for Distributed Generation Systems* (PEDG), August 2018

3. Verma, Mriduwani, Shiv Kumar, S.: 'Hardware design of SEPIC converter and its analysis'. *IEEEInternational Conference on Current Trends towards Converging Technologies (ICCTCT)*, Mar 2018, pp. 1 – 4.Charles Muranda ; Emre Ozsoy., et al: 'Modified SEPIC DC-to-DC boost converter with high output-gain configuration for renewable applications'. IEEE conference on Energy conversion, Oct 2017, 10, pp. 317–322

4. Moradpour, R., Ardi, H., Tavakoli, A.: 'Design and implementation of a new SEPIC-based high step-up DC/DC converter for renewable energy applications'. *IEEE transactions on industrial electronics*, July 2017, 28, 65(2), pp. 1290–1297

5. Geethalakshmi, B.: 'Design of a closed loop control scheme for a dc-dc SEPIC converter using loop shaping method'. *IEEE International Conference on Circuits, Power and Computing Technologies*, Mar 2015, 19, pp. 1 – 5

6. Hasanpour, S., Baghramian, A., Mojallali, H.: 'A new high-gain coupled-inductor SEPIC converter for a micro grid system'. *IEEE8th Power Electronics, Drive Systems & Technologies Conference*, Feb 2017, 14, pp. 294 – 299

7. Mriduwani Verma ; S. Shiv Kumar.: 'Hardware Design of SEPIC Converter and its Analysis', 18th IEEE International Conference on Current Trends towards Converging Technologies, Mar 2018, pp. 1002 – 1005

8. Cao Anh Tuan, Hirose Naoki, Takaharu Takeshita: 'Unidirectional Isolated High-Frequency-Link DC-DC Converter Using Soft-Switching Technique', IEEE 4th International Future Energy Electronics Conference (IFEEC), Feb 2020

9. Shalini NP, Dhanalakshmi R (2017) Soft switching based single switch integrated converter with high voltage gain for renewable energy conversion. IEEE International Conference on Smart Technologies for Smart Nation 17:40–45

10. Vijayalakshmi, S., Raja, T.S.R.: 'Development of robust discrete controller for double frequency buck converter'. *Automatika*, Jan 2015, 1, 56(3), pp. 303–317

11. Du X, Zhou L, Tai HM (2009) Double-frequency buck converter. IEEE Trans. Industrial Electro 56(5):1690–1698

12. Poornima, Rashmi: 'Design and simulation of interleaved SEPIC converter for photo voltaic applications'. 2017 International Conference on Computation of Power, Energy Information and Communication (ICCPEIC), Feb 2018

13. Pan, Z., Zhang, F., Peng, F.: 'Analysis and implementation of pulse-width modulated DC-DC converter for electric vehicles with improved efficiency'. *2016 IEEE conference on Power Electronics, Drives and Energy systems (PEDES),* May 2017

14. Shreelakshmi M. P. ; Moumita., et al.: 'Design and Development of a Novel High Voltage Gain, High-Efficiency Bidirectional DC–DC Converter for Storage Interface'. IEEE Transactions on Industrial Electronics, vol. 66, Issue. 6, Jun 2019, pp. 4490 – 4501

15. Amit Kumar ; Ravindra Kumar Singh.: 'Power loss calculation of diode assisted cascaded Quasi - Z-source converter with CCM and DCM operation'. 2016 IEEE 6th International Conference on Power Systems (ICPS), Oct 2016

16. Mohan N, Undeland TM, Robbins WP (2018) Power Electronics Converters Applications and Design, 6th edn. Wiley, New York

17. Erickson RW (2018) Fundamentals of power electronics, 6th edn. Kluwer, Secaucus, NJ

18. Chi-Wei Chen ; Hsin-Shu Chen ; Wen-Jong Wu.: 'A Fast-Transient Switched-Capacitor DC-DC Converter with a Current Sensing Control Technique'. *IEEE International Midwest Symposium on Circuits and Systems (MWSCAS)*, Aug 2019

19. Bhushan P. Mokal ; K. Vadirajacharya : 'Extensive modeling of DC-DC cuk converter operating in continuous conduction mode', International Conference on Circuit ,Power and Computing Technologies (ICCPCT), October 2017

20. P. K. C, S. K and R. J. N, "Soft Switching Hybrid Resonant Boost Converter for Energy Harvesting Application," 2020 3rd

International Conference on Intelligent Sustainable Systems (ICISS), 2020, pp. 1416–1422

Author information

Authors and Affiliations

Saranathan College of Engineering, Tiruchirapalli, Tamilnadu, India

S. Vijayalakshmi, M. Marimuthu & B. Paranthagan

The Oxford College of Engineering, Bangalore, Karnataka, India

N. Jayakumar, B. Devi Vighneshwari & Nisha C. Rani

Sinhgad Institute of Technology, Pune, Maharashtra, India

R. Shenbagalakshmi

Corresponding author

Correspondence to M. Marimuthu.

Additional information

Publisher's Note

Rights and permissions

About this article

Cite this article

Vijayalakshmi, S., Marimuthu, M., Jayakumar, N. *et al.* A Novel Double Frequency SEPIC Converter with Improved Transient Characteristics and Efficiency. *J. Electr. Eng. Technol.* **17**, 1039–1050 (2022). https://doi.org/10.1007/s42835-021-00906-2

Received	Revised	Accepted
12 June 2021	05 August 2021	05 September 2021

Published	Issue Date
20 September 2021	March 2022

DOI
https://doi.org/10.1007/s42835-021-00906-2

Keywords

SEPIC **Double frequency SEPIC**

Low frequency SEPIC **High frequency SEPIC**

Small signal model

Annals of R.S.C.B., ISSN:1583-6258, Vol. 25, Issue 6, 2021, Pages. 2972 - 2977
Received 25 April 2021; Accepted 08 May 2021.

Cascade H Bridge Multilevel Inverter with Pwm for Lower Thd, Emi & Rfi Reduction

Jayakumar N*[1], Dr.B. Devi Vighneshwari[2], Monalisa Mohanty[3],
Subash Ranjan Kabat[4], Bibhu Prasad Ganthia[5], Nisha C Rani [6], L Vadivel Kannan[7]
[1,2,6]*Associate Professor, Dept of EEE, The Oxford College of Engineering, India*
[3]*Teaching Associate, Dept of EEE, ITER, SOA University, India.*
[4]*Assistant Professor, Dept of EE, Radhakrishna Institute of Technology Engineering, India.*
[5] *Assistant Professor, Dept of EE, IGIT Sarang, Odisha, India*
[7]*Assistant Professor, Dept of Mechanical Engineering, PSNA College of Engineering and Technology, India.*
*jayakumar.kns@gmail.com**

Abstract— Solar inverter has entered the market, where it is a combination of multilevel, a multi monitoring transformer, and with a solar charger. Although most are single-level inverters, others are multi ported. This is the primary benefit of multilevel inverters as opposed to single level ones: minimum harmonic distortion, lower EMI/RFI the Multilevel inverters can be set to run on any voltage between 115 and 230VAC. Sinusoidal and trapezoidal implementations of active control have different waveforms, which can be implemented with different multi-stage inverters. by adding PWM power, we can optimize the benefit of the inverters. The most straightforward way to simulate multivalent DC sources with modulations is to intersect the modulating signal with a triangular-shaped carrier waveform. in this article, we are creating a microcontroller based Solar Multivel Pulse Width Modulator utilizing cascade H bridge topology. We are also implementing MPT to enhance our overall performance. We will use the capacity of the full duration of the day to capture the greatest amount of sunshine during the day.

Keywords-Multilevel inverter; Pulse-width modulation; H-brige; Stepper Motor; ATmega328 microcontroller; PIC16F877A micro- controller.

I. INTRODUCTION

The excessive usage of fossil energy is a significant contributor to global warming. Climate change is making it cheaper to look at renewable energy sources, which helps pave the path for fossil fuels. The SSI model is a combination of solar-charging multilevel.

In the coming years, the amount of power an inverters needed to be changed would be much greater than in the previous ones. An industry trend in recent years has been to upgrade the smart inverters. The most technical problem solved by the intelligent inverters is that of balance in the energy supply and demand. Because of the increased power demands, there is a need for improved inverter efficiency, and for this, solar power forecasts would also boost. multi-Diode topologies incorporate diode, flying capacitor, and H-bridge topologies.

Solar smart, also known as solar thermal, can be separated into two segments: absorbing sunlight and emitting steam. solar-tracking Multiver. When it comes to the use of solar panels, the process is twofold: panel movement and battery charging. The Multileader switch/section and Multiverse controller sections are the two central groups in the organization.

The sun would follow the physical movements of the vehicle over the course of the day in a solar panel mounted tracker. to switch to the original setting and switching the device off to save fuel. With the aid of a pause applied by the microcontroller, solar power can begin operating at sundown.

When on the topic of flipping, the case of the sun could appear in the field of common land. So, we will have to create a novel design to resolve the challenge of the level ground commonality dilemma. to be able to help, we must link to various times.

II. PROPOSED TOPOLOGY

We use cascaded H-bridge switching in our multi-level voltage regulator portion. 11 levels of alternating current (AC) are required for this circuit, and it is produced by a cascaded H-bridge.Fig.1 shows the proposed topology of cascade H-bridge.
Cascaded H-bridge in the Control section needs control. Electronic switching systems are many. We intend to only deal with Pulse Width Modulation (PWM) in this document.
In Solar Smart, the process starts with the design of multivolt tracking and creating alternating current from several inverters is the beginning of the energy flow. In addition, current is generated from batteries separate from the main

Annals of R.S.C.B., ISSN:1583-6258, Vol. 25, Issue 6, 2021, Pages. 2972 - 2977
Received 25 April 2021; Accepted 08 May 2021.

power supply.

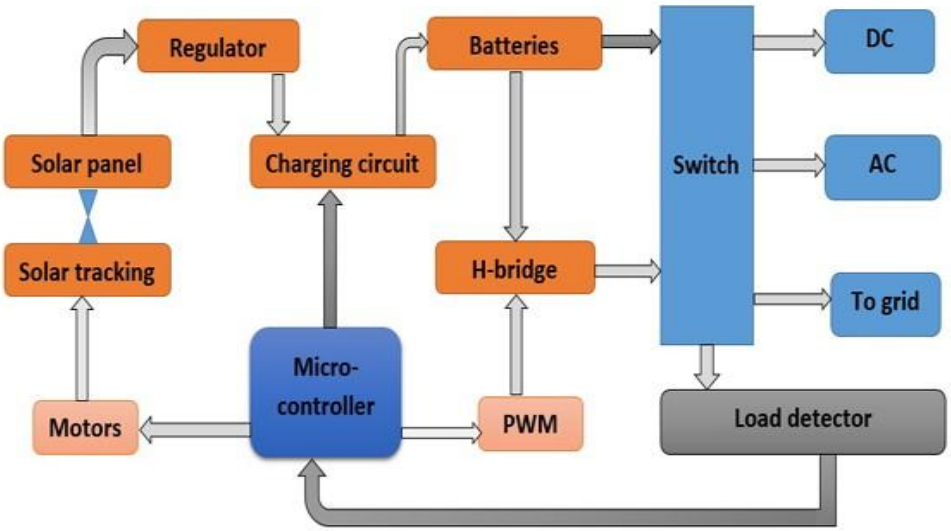

Figure.1 Proposed Topology.

III. SYSTEM DESIGN

3.1 Solar Tracking

As irradiance and temperature changes the output power obtained from photo-voltaic (PV) panel varies. In order to trap the maximum energy solar tracking is implemented using stepper motor. A stepper motor is an electromechanical device that divides a full rotation into a number of equal steps without any feedback. We can move and hold the motor position using microcontroller using desired control signal. The microcontroller used for this application is Atmega328p. We can divide a motor's fundamental step angle into micro steps by precisely controlling the current in each phase. The tracking is done by programmed time-delayed movement of the panel from dusk to dawn.Fig.2 shows the block diagram of solar tracking.

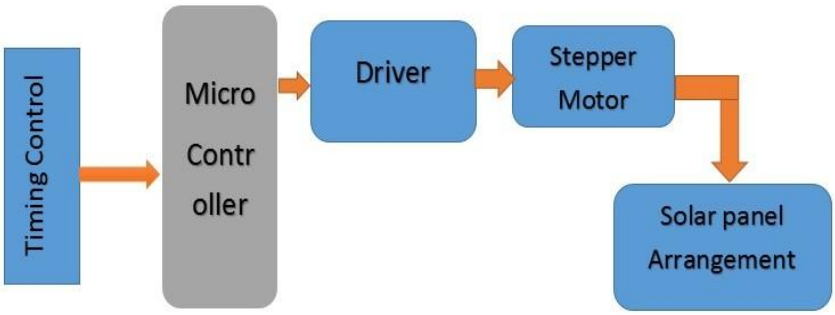

Figure 2. Block Diagram of Solar Tracking

3.2. Solar Charging

We cannot charge all batteries at a time because of common ground problem. Common ground problem arises when multilevel charging is employed. Multilevel charging needs separate ground for each battery. So, we opt relay switching for charging the batteries by eliminating common ground problem.Fig.3 shows the solar tracking simulation and Fig.4 shows the block diagram solar charging.

Annals of R.S.C.B., ISSN:1583-6258, Vol. 25, Issue 6, 2021, Pages. 2972 - 2977
Received 25 April 2021; Accepted 08 May 2021.

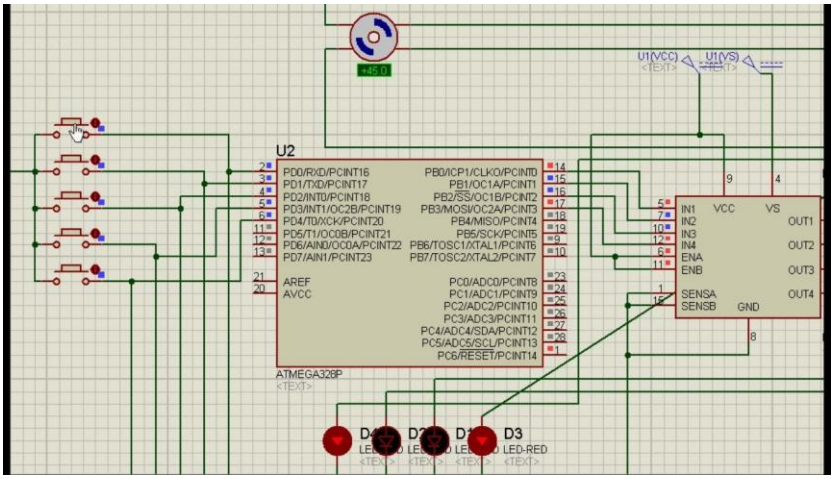

Figure 3. Solar Tracking- Simulation

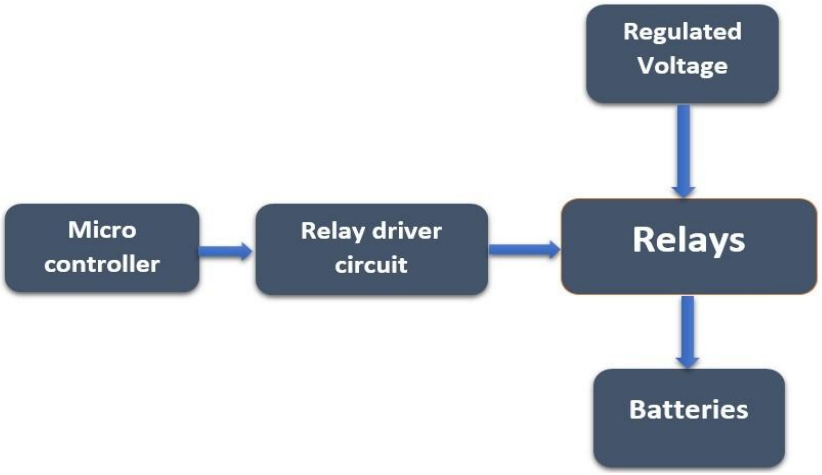

Figure 4. Block diagram of Solar Charging

3.3. Multilevel Inverter

Five H-bridge circuit to get eleven levels of AC voltage by PWM switching scheme powered by five separate DC source together constitute multilevel inverter.Fig.5 shows the Solar charging simulation.

A single-phase structure of an M-level cascaded inverter is illustrated in Figure 6[10]. Each separate dc source (SDCS) is connected to a single-phase full-bridge, or H- bridge, inverter. Each inverter level can generate three different voltage outputs, +V dc, 0, and −V dc by connecting the dc source to the ac output by different combinations of the four switches, S1, S2, S3, and S4. To obtain +V dc, switches S1 and S4 are turned on, whereas -Vdc can be obtained by turning on switches S2 and S3. By turning on S1 and S2 or S3 and S4, the output voltage is 0.

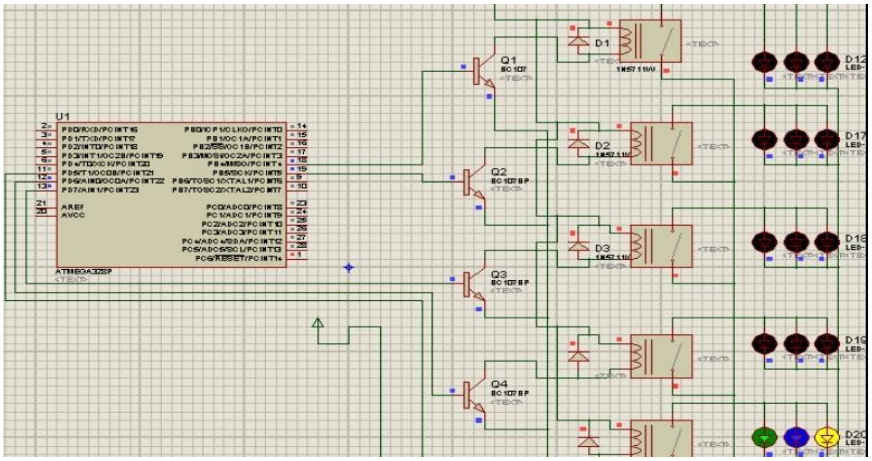

Figure 5. Solar Charging- Simulation

Annals of R.S.C.B., ISSN:1583-6258, Vol. 25, Issue 6, 2021, Pages. 2972 - 2977
Received 25 April 2021; Accepted 08 May 2021.

The components [as synthesized voltage is the combination of synthesized voltage, or to put it another way, synthesized voltage is the result of the individual waveforms in order, i.e.e. more than one full-bridge (A to A = V)] M is the number of voltage stages in a cascade inverter (separate DC sources), where m is 2 + 1 A theoretical voltage waveform for an eleven-stage cascaded H-bridge circuit (one H-level plus five D-level and five D-level SD stages) is depicted in Figure 7. It is expressed as van+van+van+van+van. To obtain the stepped waveform seen in Figure 7, the Fourier Transform was used.

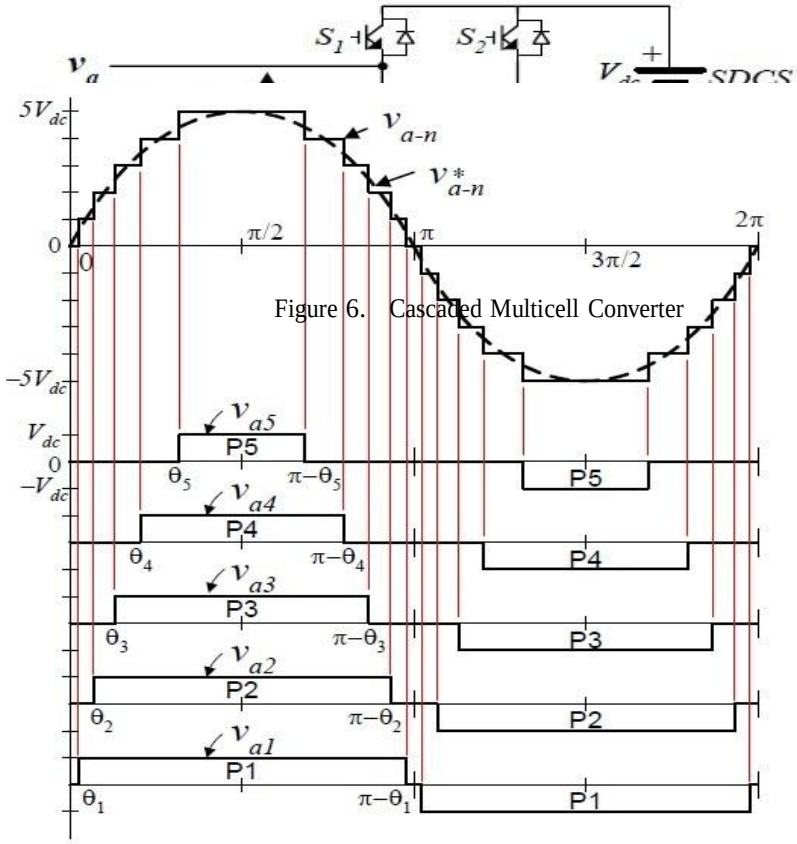

Figure 6. Cascaded Multicell Converter

Figure 7. Output Phase Voltage Waveform

The pulse-width modulation signal developed in the PIC16a. If you count the five H-bridge circuits, the first one uses a PWM scheme to regulate itself. There are numerous H-bridges which use normal signals to regulate them.

IV. EXPERIMENTAL RESULT

Binary Input	Designed Angle for Stepper Motor	Obtained Angle For Stepper Motor
1001	45^0	45^0
1000	90^0	90^0
1010	135^0	135^0
0010	180^0	180^0

Table 1. Experimental Results

A PIC and ATmega microcontroller dependent test are used to demonstrate the working of the solar inverter. This table describes the principal angles of rotation (Table.1). For convenience, we adopted a phase angle of 900 as the standard

Annals of R.S.C.B., ISSN:1583-6258, Vol. 25, Issue 6, 2021, Pages. 2972 - 2977
Received 25 April 2021; Accepted 08 May 2021.

angle of interest. For motors, Phase angle is normally ranges from 1.80 to 2.20 to 2.40.
Here is the primary example of a solar inverter in Figure 8. A single-phase solar inverter with a capacity of 250 watts and one (one) new stage has been built using PIC and microcontrollers. Figure.9 depicts the interconnected structure. As a result, the contribution from the solar cell/inverter is visually analysed and appears as a diagram. Eleven wave shapes in the output can be approximated as a sine wave, seen in the graph above. Figure .10 shows the output waveform of solar output.

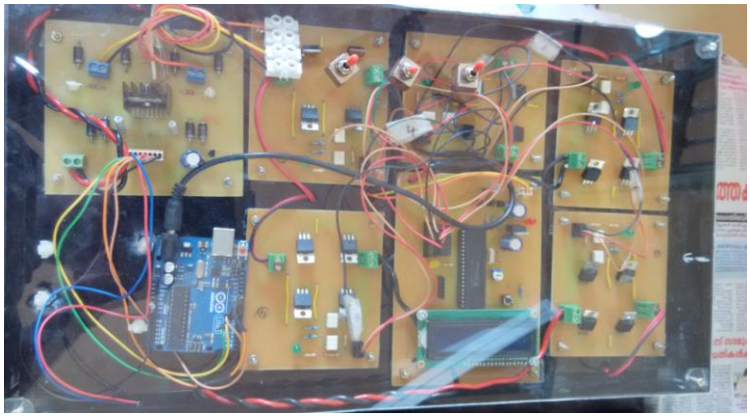

Figure 8. Prototype Test Platform

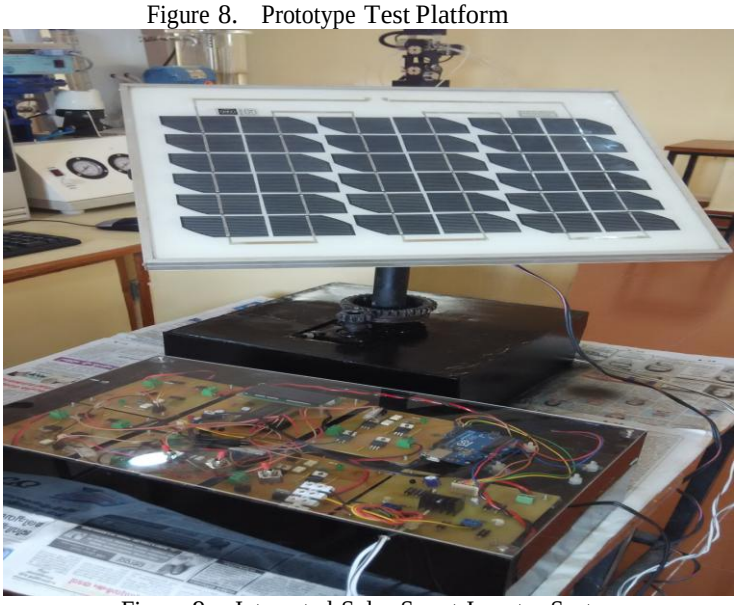

Figure 9. Integrated Solar Smart Inverter System

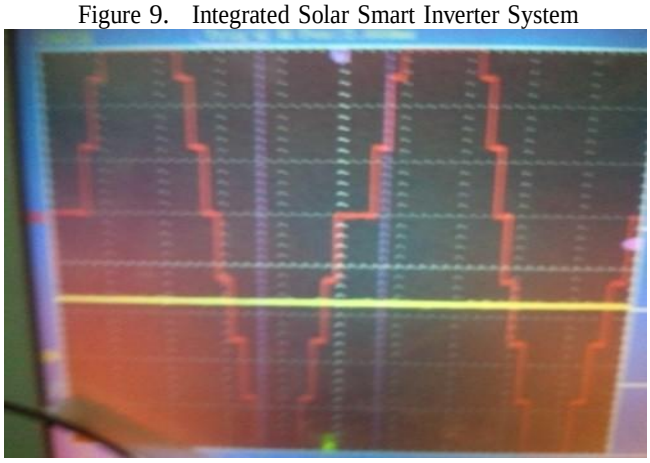

Figure 10. Output Waveform

V. CONCLUSION

In this article, a modern solar inverter device is introduced that incorporates power electronics as a major novel innovation in small-scale applications. To aid in battery storage, the panel is to switch from the east to

Annals of R.S.C.B., ISSN:1583-6258, Vol. 25, Issue 6, 2021, Pages. 2972 - 2977
Received 25 April 2021; Accepted 08 May 2021.

the west side of the roof during the day and then go back at night. For implementing solar charging, there are many considerations: the elimination of ground loops is one of the biggest advantages. The aim of this paper is to apply a minimal amount of signal-dependent distortion to sinusoidally shaped waveforms from different DC sources. However, in most of the cases, this book, the concept of a multivolt DC inverter will not be omitted, to highlight the other equally important topics. It has an exceptional electricity and service integration. It met with remarkable success; the findings were extremely close to those predicted by the simulation and the engineers." Present transformers are used to track variations in load current. When the current in the power transformer varies, so does the Arduino. a microcontroller is configured to cause the device to shut down if the load does not remain constant, we should reach out to the power grid and use weather forecasts to help us prevent disasters from occurring by using the information it provides. Furthermore, space vector pulse width modulation may provide increased switching power.

REFERENCES

[1] Ammar Masaoud, Hew Wooi Ping,Saad Mekhilef, Member, IEEE,New Three-Phase Multilevel Inverter With Reduced Number of Power Electronic Components,IEEE TRANSAC- TIONS ON POWER ELECTRONICS, VOL. 29, NO. 11, August 2014

[2] Meghdad Fazeli,Janaka B. Ekanayake,PaulM.Holland,Petar Igic, Member, IEEE,Exploiting PV Inverters to Support Local VoltageA Small-Signal Model,IEEE TRANSACTIONS ON ENERGY CONVERSION, VOL. 29, NO. 2, June 2014.

[3] Marcelo A. Perez,Steffen Bernet,Jose Rodriguez,Samir Kouro,Ricardo Lizana, Member, IEEE,Circuit Topologies, Modelling, Control Schemes and Applications of Modular Multilevel Converters,IEEE Transactions on Power Electronics,June 2014

[4] Md. Rabiul Islam, Youguang Guo,Jianguo Zhu, Senior Mem- ber, IEEE,A Multilevel Medium-Voltage Inverter for Step- Up-Transformer-Less Grid Connection of Photovoltaic Power Plants,IEEE Journal Of Photovoltaics, VOL. 4, NO. 3, May2014

[5] Nasrudin Abd. Rahim,Mohamad Fathi Mohamad Elias,Wooi Ping Hew, Member,IEEE,Transistor—Clamped H—Bridge Based Cascaded Multilevel Inverter With New Method of Capacitor Voltage Balancing,IEEE Transactions On Industrial Electronics, VOL. 60, NO. 8, August 2013

[6] Jia-Min Shen,Hurng-Liahng Jou,Jinn-Chang Wu, Member, IEEE,Five-Level Inverter for Renewable Power Generation System,IEEE Transactions On Energy Conversion, VOL. 28, NO. 2, June 2013

[7] R.Sakthivel, M.Murugesan, R.Senthilkumar,Selective Harmon- ics Elimination Pwm Based Multilevel Inverter With Reduced Number Of Switches, Quest International Multidisciplinary Research Journal,Volume II , Issue I June 2013

[8] Mohammad Farhadi Kangarlu, Ebrahim Babaei, Depart- ment of Electrical Engineering Tsinghua University Beijing,100084,China,A Generalized Cascaded Multilevel Inverter Us- ing Series Connection of Submultilevel Inverters,IEEE Trans- actions On Power Electronics, VOL. 28, NO. 2, February 2012

[9] Samir Kouro, Mariusz Malinowski, , K. Gopakumar,Josep Pou, Leopoldo Jose Rodriguez, Senior Members, IEEE,Recent Advances and Industrial Applications of Multilevel Convert- ers,IEEE Transactions On Industrial Electronics, Vol. 57, No.8, August 2010.

[10] Krishnan, M. S., Amudha, A., & Ramkumar, M. S. (2018). Execution Examination Of Three Phase Ac To Three Phase Ac Matrix Converter Using Distinctive Transporter Based Exchanging Algorithms. International journal of Pure and Applied Mathimatics, 118(11), 609-617.

[11] Krishnan, M. S., Dhevi, S. K., & Ramkumar, M. S. (2014). Power Quality Analysis in Hybrid Energy Generation System. International Journal, 2(1).

[12] Ramkumar, M. S., & Krishnan, M. S. (2014). Power Management of a Hybrid Solar-Wind Energy System. International Journal of Engineering Research & Technology, 3(2), 1988-1992.

ScienceDirect

Renewable Energy Focus
Volume 42, September 2022, Pages 70-78

Novel soft-switching integrated various converter of ZVT-ZCT grid connected PV system

Nisha C. Rani [a], N. Amuthan [b]

Show more

Share Cite

https://doi.org/10.1016/j.ref.2022.05.004
Get rights and content

Abstract

Solar photovoltaic systems contribute to the development of the world's most environmentally sustainable and cost-effective electrical energy. High-power inverters commonly use a technique known as three-level design to increase their performance by soft-switching. On the other hand, the switching action is stressed in normal operation because the current or voltage will not be zero at the time of the transition. For CUK, SEPIC, ZETA and CASCODE converters operating in critical switch mode, it has been proposed that a new type of DC-DC converters primarily formed on capacitive coupling DC-DC converters be developed. The proposed converters are zero-current-voltage-switching half-square-quarter-wave converters with a zero-current auxiliary circuit. LC-circuit resonance causes power switches to turn on at zero voltage, getting rid of the switching losses during turn on. The hybrid Incremental Conductance & Integral Regulator technique is used to track MPP available from PV system. The proposed converter's results and efficiency are compared to those of traditional semi-square-quarter-wave zero-current-converter converters. The proposed converters achieved power efficiencies of 98.7% in the step-up mode and 98.8% in the step-down mode for the rated load state, respectively. The proposed CUK, SEPIC, ZETA and CASCODE Converters Simulation are implemented in the MATLAB Simulink programme to validate its efficiency.

Introduction

Soft-switching approaches that offer Zero Current Transition (ZCT), Zero Voltage Transition (ZVT) or a combination of the two have been proposed to improve power conversion efficiency. A photovoltaic system is a power system that utilizes photovoltaic technology to generate usable solar energy. The suggested soft-switched DC-DC converter is compared to a normal DC-DC converter in terms of efficiency and a few topologies at different output powers.

Gurumurthy et al. [3] describes a new BDC (Bi-Directional Converter) design that uses a mix of quick turn off IGBTs and the implementation of a new control logic to attain switching losses to be zero utilising ZVT and ZCT approaches. The proposed topology has a drawback in that the optimum resonant component values are dependent on operational load conditions, which is a flaw in the design. Furthermore, this architecture is unsuited for applications with high frequencies. Reshma K R [10] has put forward the major advantage of the SEPIC converter is the constant input current, which can help with accurate PowerPoint monitoring of solar cells. The inductorless passive regenerative snubbed assists the converter in realizing zero current and zero voltage switching, improving performance of the converter.

K. Aravind, et. at [5] have proposed a high voltage gain improved converter, making it appropriate for applications such as solar systems. At full load, the machine had a high efficiency of 93.1 %. The proposed 80W updated SEPIC's experimental findings were in good agreement with the theoretical research. Annu Mary Zacharias [12] has done to reduce switching losses in the converter section of the system, hence improving its performance. SEPIC converters with soft switching have a non-inverted output and a 94 % reliability. In comparison to the current scheme, a 40% rise was discovered.

Antionio [1] has proposed, the Quadratic-Boost-ZETA converter. To test the feasibility, two 250W prototype circuits were installed and efficiency of the converter is discussed. Hosseini et al [6] suggested a topology that includes a new high voltage gain converter and a ZETA converter. In addition, the proposed structure has the benefit of lowering power electronic switches count and expenses, Ramkumar et al. [9]. Antonio et al [2], [4] have come up with the voltage static gain, as well as the voltage and current pressures on the converter's components and essential features.

Poorali et al [8] proposed the converter which is an improved topology of CUK converter. The proposed converter can be utilised as a substitute, and it has the advantage of being more effective. Lin B.R et al [7], the suggested converter's goal is to explore the CUK converter's expansion with coupled inductors and magnetic integration. Instead of

employing a single transformer, the suggested converter's main goals are parallel operation and balanced current sharing. Xiang et al [11] have named the most promising successor for Si MOSFETs in the future due to their superior performance in high-temperature, high-efficiency, and high-power-density converters.

Section snippets

Proposed System

The PI controller technique with the linearized PV array model is implemented in the proposed work, simulating the block diagram of various converter using ZVT-ZCT.

The proposed converters' block diagram shows a PV array that flows through an MPPT control and a filter. In the PI controller and converters, the filter is connected. The converter is powered by three-phase three-level voltage source inverter is powered by dc-dc converter. The VSI with a PI controller connected to the grid…

Experimental Results

MATLAB/Simulink software was used to create a grid-connected PV system. PV arrays are made up of strings of parallel connected PV modules.

Figure 2 gives waveform of the solar irradiance level of output current, output voltage, power, and the duty cycle of the PV panel. The sun’s irradiance is reduced from the solar panel is 100 kW when the irradiance level of 10000 W/m^2.The maximum power value of the SPR-305E-WHT-D sun power module is 305.226 W. MPPT is keeping track of the maximum power. The…

Conclusion

In this paper, a better circuit topology for conventional DC-DC converters with soft-switching operation is given, which has lower power losses and higher efficiency than the traditional. The active snubber of the buck-boost type is employed for limiting the voltage stress on the PI-main controller's switch. The auxiliary components prevent voltage ripples on all output switches, also provide a soft switch transition, which greatly improves the efficiency of the converter. So, soft switching…

Declaration of Competing Interest

The authors declare that they have no known competing financial interests or personal relationships that could have appeared to influence the work reported in this paper.…

References (13)

B.-R. Lin *et al.*

Analysis, design and implementation of an active snubber zero-voltage switching Cuk converter

IET Power Electron. (2008)

Andrade, António Manuel Santos Spencer, and MárioLȩcio da Silva Martins. “Quadratic-boost with stacked zeta converter...

António MSS, Luciano Schuch, and Mário L. da S. Martins. “Very high voltage step-up integrated quadratic-boost-zeta...

Salinamakki Ramabhatta Gurumurthy *et al.*

High-efficiency bidirectional converter for flywheel energy storage application

IEEE Trans. Ind. Electron. (2016)

G.P. Kannayeram

An elitist control scheme for power flow management in smart grid system: a hybrid optimization scheme

Energy Sources Part A (2021)

K. Aravind, et. at., “Photovoltaic Based Five Level Inverter with High Gain Dc-Dc Converter,” 2020 International...

There are more references available in the full text version of this article.

Cited by (0)

Recommended articles (6)

Research article

Integration of solar and flexible resources into expected security cost with dynamic optimal power flow problem using a Novel DE algorithm

Renewable Energy Focus, Volume 42, 2022, pp. 48-69

Show abstract

Research article

An analysis of statistical distributions of energy requirement in western part of India

Renewable Energy Focus, Volume 41, 2022, pp. 198-205

Show abstract

Research article

Prediction-optimization of the influence of 1-pentanol/jatropha oil blends on RCCI engine characteristics using multi-objective response surface methodology

Renewable Energy Focus, Volume 42, 2022, pp. 8-23

Show abstract

Research article

Economic-environmental operation of an unbalanced microgrid including energy storage systems via semidefinite relaxation

Renewable Energy Focus, Volume 42, 2022, pp. 129-145

Show abstract

Research article

A Bio inspired optimization with Reliable QoS Routing through Efficient Packet Transmission in Mobile ad-hoc Network

Renewable Energy Focus, Volume 41, 2022, pp. 188-197

Show abstract

Research article

Regional trade and expansion planning (RTEP) model: Model for regional power sector integration in Africa

Renewable Energy Focus, Volume 42, 2022, pp. 101-114

Show abstract

View full text

Hindawi

Advances in Materials Science and Engineering

Special Issue

Advanced Functional Graded Materials: Processing and Applications

View this Special Issue

Research Article | Open Access

Volume 2022 | Article ID 7886722 | https://doi.org/10.1155/2022/7886722

Show citation

Effects of Polypropylene Waste Addition as Coarse Aggregates in Concrete: Experimental Characterization and Statistical Analysis

D. C. Naveen,[1] **K. Naresh**,[2] B. S. Keerthi Gowda,[3] Madhu Sudana Reddy G,[4] C. Durga Prasad,[5] and Ragavanantham Shanmugam[6]

Show more

Academic Editor: Qian Chen

Published: 08 Nov 2022

Abstract

In recent times, thermoplastic waste materials are being extensively used as fine and coarse aggregates in the concrete mix as an environmentally friendly construction material. This study aims at utilizing polypropylene (PP) as a partial substitute for the conventional coarse aggregates in M30 grade concrete. The different replacement levels of coarse aggregates such as 0%, 20%, 40%, and 60% by weight were used in concrete. Sieve analysis, specific gravity, and water absorption tests were performed in all replacement levels of aggregates. The mechanical (compressive and split tensile tests) tests were conducted after 3, 14, and 28 days. The change in mechanical properties of concrete with the addition of different weight proportions of plastics was studied experimentally. Further, experimental values were predicted using the two-parameter Weibull distribution and artificial neural network (ANN)-based statistical approaches. The Levenberg–Marquardt algorithm was used in predicting the mechanical properties using the ANN. A good correlation was obtained between the experimental and predicted values with an error (%) of less than 10. The decrease in mechanical properties with the increase in replacement levels of coarse aggregates in concrete was observed in both experimental and predicted

Hindawi

Advances in Materials Science and Engineering

1. Introduction

In the past decades, the use of plastics has been widely increased in various applications such as automotive, medical, and housing applications [1–4]. More importantly, their use in packaging and distribution of food for daily usage is high; in that way a large quantity of plastic waste is accumulated all over the world [5, 6]. Larger areas of land are required for storing these several million tons of waste plastics. Even though plastic products are lightweight and easy to design and fabricate, they possess low- or nonbiodegradability. As a result, the disposal of plastic waste causes a considerable threat to humans and animals and is one of the major reasons for environmental pollution, [7]. Therefore, it is important to develop biodegradable plastics [8] or reuse plastic waste for the benefit of different perspectives. Most countries have already started to utilize plastic waste for various applications [9]. In particular, thermoplastic waste materials have been extensively used in energy applications [10] and the construction industry [11].

In recent years, many researchers studied the mechanical properties of thermoplastic waste materials incorporated in concrete structures [12, 13]. Almeshal et al. [14] used polyethylene terephthalate (PET) as a fine aggregate for the partial replacement of sand in concrete. They have investigated the compressive, flexural, and split tensile strength values for different weight substitution levels (0%, 10%, 20%, 30%, 40%, and 50%) of PET-incorporated concrete. A gradual decrease in compressive, flexural, and split tensile strength values with the increase of PET percentage in concrete was found. Ohemang and Ekolu [15] studied the compressive and flexural strength values of different volume fractions of low-density polyethylene (LDPE)-embedded cement mortar. These strength values were compared for different curing ages such as 7, 14, and 28 days. The decrease in strength values with the increase in various proportions of LDPE in cement mortar was found. Also, the increase in strength values with the increase of curing age was reported. In particular, the increase was reported to be higher from the age interval of 7 days to 14 days, compared to those at age intervals of 14 days to 28 days. The decrease in compressive strength with the increase in plastic waste contents and the enhancement in compressive strength with the increase of curing age were also found by several researchers [12, 16, 17].

Several researchers used analytical models to predict the flexural and split tensile strength values using compressive strength values [14, 18]. Moreover, many researchers are also used artificial neural network (ANN) methods to solve complex problems in the area of concrete technology [19–22]. Onyelow et al. [23] compared the compressive strength values of 28 days of post-cured Fly Ash-embedded concrete specimens using genetic programming (GP), evolutionary polynomial regression (EPR), and three different ANN (backpropagation, gradually reduced gradient, and genetic algorithm) methods. It was found that the compressive strength values of the GP model had the least accuracy of 81%, the EPR model had a moderate accuracy of 90%, and all ANN models had almost the same accuracy of approximately 94%. Rezazadeh Eidgahee et al. [24] employed different machine learning methods (ANN, GP, and group method of data handling (GMDH)) in predicting the dynamic modulus of hot mix asphalt. It was reported that the accuracy of the ANN model is higher based on higher correlation coefficient values greater than 0.98, compared with GP and GMDH models.

In general, there is a tendency for strength values to be scattered due to the possibility of operator and instrument errors. In particular, the occurrence of errors during the manufacturing of the component is high. Statistical studies are useful to capture the scatter in strength values [25, 26]. However, very limited researchers employed statistical approaches to predict the strength values for different weight proportions

Hindawi

Advances in Materials Science and Engineering

2. Materials and Methods

2.1. Materials

In this study, materials such as cement, sand as fine aggregate, and recycled polypropylene as coarse aggregate are used. The material specifications for cement, fine aggregate, coarse aggregate, and admixtures are discussed. Sieve analysis was done for sand and coarse aggregate to test their suitability for use in concrete.

2.1.1. Cement

In this study, ordinary Portland cement (OPC) of 53 grade was used for casting cubes and cylinders for all concrete mixes. The cement was of uniform color, i.e., grey with a light greenish shade and was free from any hard lumps. The specific gravity (SG) of cement was carried out as per IS 2386 (Part 3)-1963 using equation (1), as given in Table 1. The summary of the various tests conducted on cement is given in Table 2, and the obtained values are closer to standard values.

$$\frac{(W_2 - W_1)}{(W_2 - W_1) - (W_3 - W_4)\, x0.79}. \tag{1}$$

Table 1

Specific gravity of cement.

Table 2

Various tests conducted on cement.

2.1.2. Fine Aggregates

The sand used for the experimental program was locally procured and conformed to Indian Standard Specifications IS: 383–1970. The sand was first sieved through a 4.75 mm sieve to remove any particles greater than 4.75 mm and then was washed to remove the dust. The properties of the fine aggregate used in the experimental work are given in Table 3. The aggregates were sieved through a set of sieves as shown in Figure 1(a) to obtain the sieve analysis and the same is presented in Table 3. The fine aggregates belonged to grading zone III.

Hindawi

Advances in Materials Science and Engineering

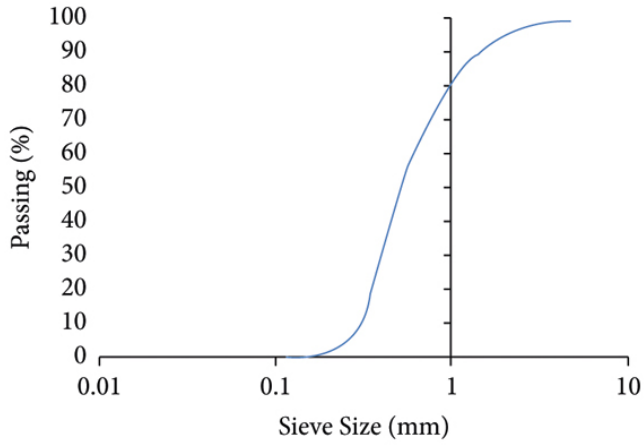

(a)

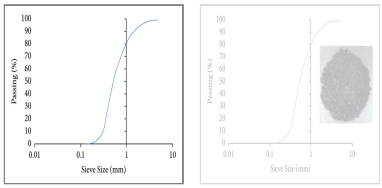

(a) (b)

Figure 1

Sieve analysis of fine (a) and coarse (b) aggregates.

2.1.3. Coarse Aggregates

The recycled polypropylene was used as coarse aggregate in this study. These aggregates were tested as per Indian Standard specifications IS: 383–1970. The results of the sieve analysis of recycled polypropylene are given in Table 4 and Figure 1(b).

Table 4

Sieve analysis of recycled polypropylene as coarse aggregates.

2.2. Specimen Fabrication

Hindawi

Advances in Materials Science and Engineering

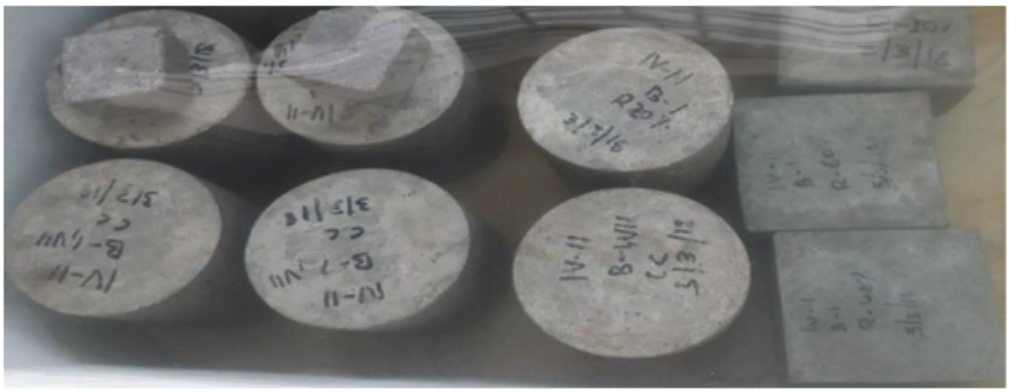

Figure 2

Fabricated cubic and cylindrical specimens.

2.3. Experimental Details

2.3.1. Compressive Strength of Concrete

Compression tests were performed as per IS 516–1999 standard on different weight proportions of polypropylene-embedded concrete cubic specimens. Three different specimens were tested in each combination. The dimensions of the specimens such as length, width, and thickness used for compression tests were $150\,\text{mm} \times 150\,\text{mm} \times 150\,\text{mm}$, respectively. The specimens were submerged in clean fresh water for the duration of 3, 14, and 28 days before testing and kept in a dry place so that the water is drained well to get better results. The compressive load is applied on the specimen using the universal testing machine, as shown in Figure 3(a). The load is gradually applied until it fails. The compressive strength of the specimen was calculated using equation (2), it is given by

$$F_c = \frac{P}{A}, \tag{2}$$

where F_c is the compressive strength, P is the ultimate load, and A is the area of the specimen which is $150\,\text{mm} \times 150\,\text{mm}$.

Hindawi

Advances in Materials Science and Engineering

(a)

(a)

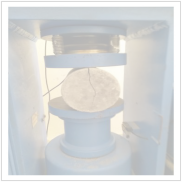

(b)

Figure 3

(a) Compression test setup. (b) Split tensile test setup.

2.3.2. Split Tensile Strength of Concrete

It is difficult to investigate the direct tensile strength of concrete; however, often, researchers are performed flexural or split tensile tests to estimate the direct tensile strength. A split tensile test for different weight proportions of polypropylene-embedded concrete specimens was performed as per IS 516–1999 standard. Three different specimens were tested in each combination. The dimensions of concrete cylindrical specimens such as a diameter of 150 mm and a length of 300 mm. The cylindrical specimens were placed horizontally between the loading surfaces of a compression testing machine, as shown in Figure 3(b) and the load is applied until the failure of the cylinder along the vertical diameter. The splitting tensile strength of specimens is calculated using equation (3), it is given by

$$F_t = \frac{2P}{\pi l d}, \tag{3}$$

where l and d are the length and diameter of the specimen, respectively.

3. Results and Discussion

3.1. Mechanical Properties

The average compressive and split strength values for different curing ages of concrete/polypropylene specimens are shown in Figures 3 and 4, respectively. It is clear from the figure that the strength values

Hindawi

Advances in Materials Science and Engineering

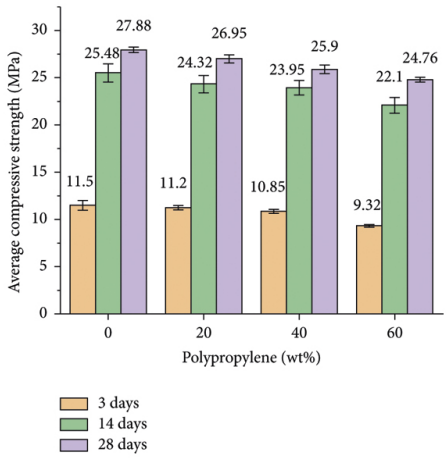

Figure 4

Effect of polypropylene addition in concrete on the compressive strength for different curing ages.

However, the decrease in strength values is observed with the increase in different weight percentages of polypropylene in the concrete. However, the strength values of 20% PP-embedded concrete specimens are closer to 0% PP-embedded concrete specimens. Therefore, specimens of 20% PP-embedded concrete specimens are recommended for primary load-bearing applications, whereas 40% and 60% PP-embedded concrete specimens are recommended for secondary load-bearing applications. The trend of the curves matches well with the literature [28–30]; in their studies, they have reported the decrease in compressive strength of concrete with the increase in plastic substitution. Thetwo main factors which restrict the improvement of compressive strength, at higher weight percentages (40% and 60%) of PP embedded in concrete specimens, are (i) poor bonding between PP aggregate and concrete due to the development of agglomerations, (ii) the hydrophobic nature of PP aggregate that decreases the rate of hydration [31]. A similar kind of decrease in strength values with the addition of higher weight percentages of waste materials in the concrete is found in these articles [9, 14, 32].

The trend of split tensile strength values seen in Figure 4 is similar to compressive strength values. Similar kinds of results are reported elsewhere [33]. As expected, from Figures 4 and 5, the compressive strength values are significantly higher in all specimens tested at different curing ages compared to split tensile strength values. A similar kind of trend is found elsewhere [34]. From equations (2) and (3), the applied direction of loading is the main reason for the difference between the values in these two tests [2 4]. The compressive strength of concrete is always higher for a concrete specimen as it withstands axially directed pushing force until it reaches its maximum force, after that the specimen is crushed, as shown in Figure 3(a). However, the failure response of the specimen subjected to the split tensile test is the transverse shear, as shown in Figure 3(b). Numerous researchers [35–37] have reported experimentally and theoretically that the compressive strength value of the cubic concrete specimen is several times higher than that of the split tensile strength.

Hindawi

Advances in Materials Science and Engineering

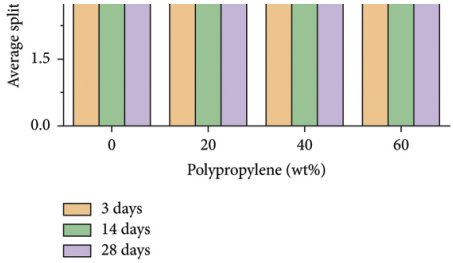

Figure 5

Effect of polypropylene addition in concrete on the split tensile strength for different curing ages.

3.2. Prediction of Compressive and Split Tensile Strength Values Using Two-Parameter Weibull Distribution

In this section, the procedure for predicting the compression and split tensile strength values are discussed using the two-parameter Weibull analysis. The compressive ($\overline{\sigma_C}$) and split tensile strength ($\overline{\sigma_{ST}}$) values can be written in terms of scale parameter (α), shape parameter (β), and gamma function (Γ) using equations (4) and (5), respectively [20, 38].

$$\overline{\sigma_C} = \alpha_C \Gamma_C \left(1 + \frac{1}{\beta_C}\right), \tag{4}$$

$$\overline{\sigma_{ST}} = \alpha_{ST} \Gamma_{ST} \left(1 + \frac{1}{\beta_{ST}}\right). \tag{5}$$

The subscript 'C' denotes the compressive strength and 'ST' denotes the split tensile strength. The scale parameter is the characteristic strength and the shape parameter is the Weibull modulus. These parameters can be determined by using equation (6) [39, 40].

$$\ln\left(\ln\left(\frac{1}{(1-F)}\right)\right) = \beta \ln(\overline{\sigma}) - \beta \ln(\alpha), \tag{6}$$

$$\ln\left(\ln\left(\frac{1}{(1-F)}\right)\right) = \beta \ln(\overline{\sigma}) - \beta \ln(\alpha), \tag{6}$$

where F is the cumulative failure probability $= (i - 0.3)/n + 0.4$ [41, 42]; i is the current test number which varies from 1 to 3 as three specimens are tested for each mixture of polypropylene-embedded concrete; n is the total number of specimens tested in each set which is equal to 3. $\overline{\sigma}$ is the experimental compressive or split tensile strength. $\Gamma(1 + (1/\beta))$ corresponding to β value is used in the gamma function data sheet.

The variability of compressive strength values for different curing ages such as 3, 14, and 28 days can be seen in Figures 6(a)–6(c), respectively. These are linear regression lines plotted using equation (6). Black, red, blue, and green color lines indicate the strength values for different weight contents of polypropylene

Hindawi

Advances in Materials Science and Engineering

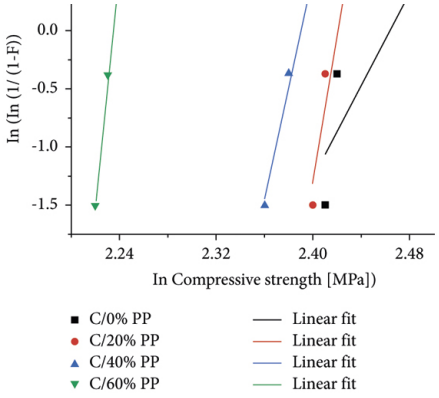

(a)

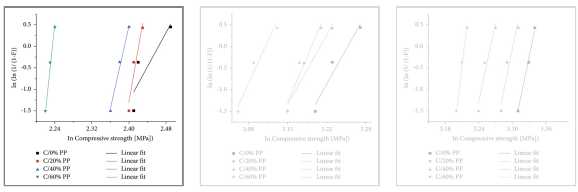

(a) (b) (c)

Figure 6

Compressive strength distributions for different curing ages of concrete specimens: (a) 3 days, (b) 14 days, and (c) 28 days.

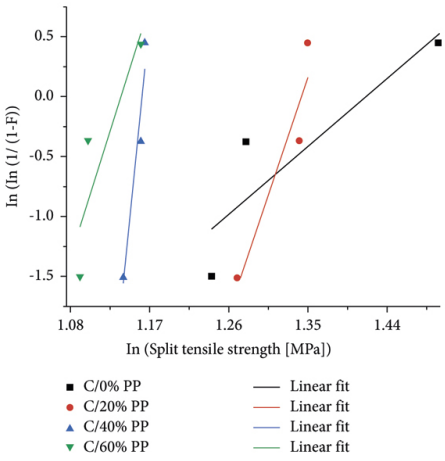

(a)

Hindawi

Advances in Materials Science and Engineering

(a) (b) (c)

Figure 7

Split tensile strength distributions for different curing ages of concrete specimens: (a) 3 days, (b) 14 days, and (c) 28 days.

Tables 5 and 6 show the scale parameter, shape parameter, and gamma function values for the compressive and split tensile strength values of PP-embedded concrete specimens for different curing ages, respectively. The comparison of the predicted and experimental compressive and split tensile strength values are given in Table 7. It is clear from the table that the percentage of deviation of the predicted strength values from the experimental results is less than 5%. The decrease in compressive and split tensile strength values with the increase in PP content in concrete is observed in both predicted and experimental results.

Table 5

Weibull parameters for compressive strength.

Table 6

Weibull parameters for split tensile strength.

Table 7

Comparison of experimental and predicted strength values.

3.3. Prediction of Compressive and Split Tensile Strength Values Using the ANN Model

The ANN is a family of massively parallel architectures that are capable of learning and predicting the results. The basic strategy for developing a neural network-based model for material behavior is to train a neural network on the results of a series of experiments using that material [43]. If the experimental results contain relevant information about the material behavior, then the trained neural network will contain sufficient information about the material's behavior to qualify a material for new values. Such a trained neural network not only could reproduce the experimental results but also could approximate the results in other experiments through its generalization capability [37].

The present study adopts a feed-forward supervised ANN model for the prediction of compression and split tensile strength values of different weight contents of PP-embedded concrete. The training

Hindawi

Advances in Materials Science and Engineering

number of input variables and the number of output or target variables. The number of hidden layers and neurons in the hidden layer is fixed during the training process.

Figure 8 depicts the ANN model adopted in this study to predict the compression and split tensile strength values for different weight contents of PP-embedded concrete specimens. Here, the Levenberg–Marquardt (LM) algorithm and the Log-Sigmoid transfer function are adopted for predicting the mechanical properties. Figure 9 shows the graphical representation of ANN predicted and experimental values. Here, all the data are convergent to the equity line. The correlation coefficient between the experimental and predicted data is 0.99. Table 8 shows the comparison of experimental and ANN predicted compressive and split tensile strength values and their respective percentage of errors. It is observed Table 8 that the deviation between the experimental and predicted results is less than 10%.

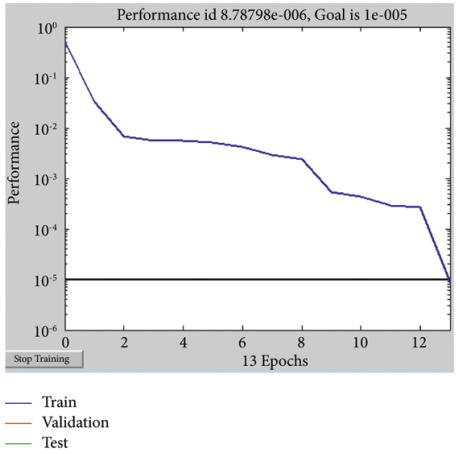

Figure 8

ANN training performance curve.

Hindawi

Advances in Materials Science and Engineering

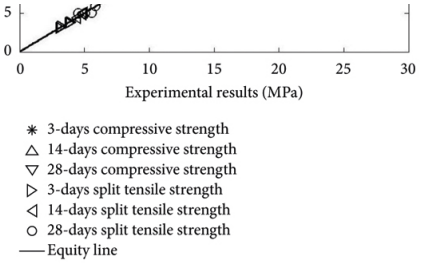

Figure 9

Predicted vs. experimental strength values using the ANN model.

Table 8

Comparison of experimental and ANN predicted strength values.

4. Conclusion

In the present work, mechanical properties for different weight percentages of polypropylene plastic wastes embedded in concrete specimens were studied. The mechanical properties were studied at different age intervals such as 3, 14, and 28 days. The compressive and split tensile strength values were predicted using two different theoretical models, the two-parameter Weibull distribution and ANN. The decrease in compressive and split tensile strengths was found in both predicted and experimental results, with the increase in polypropylene weight contents in the concrete specimens. However, the strength values for the specimens of 20% PP-embedded concrete specimens are closer to 0% PP-embedded concrete specimens. The mechanical properties were found to be increasing with the increase in the age duration from 3 to 28 days. This can be attributed to an increase in the bonding of the microstructure of the concrete specimen, which strengthens the specimen. However, the increase in mechanical properties is relatively less between 14 and 28 days compared to between 3 and 28 days, which indicate that the post-cure of the concrete specimen for a minimum of two weeks is essential. An excellent correlation is obtained between the predicted and experimental values. It can be concluded from this study that specimens of 20% PP-embedded concrete specimens can be used for primary load-bearing applications. This contributes to reduce the unit weight of the concrete.

Data Availability

This manuscript includes raw data recorded from the apparatus and processed data derived from raw data.

Hindawi

Advances in Materials Science and Engineering

References

1. P. O. Awoyera and A. Adesina, "Plastic wastes to construction products: status, limitations and future perspective," *Case Studies in Construction Materials*, vol. 12, Article ID e00330, 2020.
View at: Publisher Site | Google Scholar

2. R. Sundarakannan, V. Arumugaprabu, V. Manikandan, K. Arun Prasath, S. Vigneshwaran, and K. Naresh, "Effect of polyethylene terephthalate char on impact and erosion properties of polyester matrix composites," *Advances in Materials and Processing Technologies*, pp. 1–14, 2022.
View at: Google Scholar

3. S. Arun Karthick, T. Ragavi, K. Naresh, and P. Rama Sreekanth, "A study on collagen-PVA and chitosan-PVA nanofibrous matrix for wound dressing application," *Materials Today Proceedings*, vol. 56, pp. 1347–1350, 2022.
View at: Publisher Site | Google Scholar

4. M. Selva Priya, K. Naresh, R. Jayaganthan, and R. Velmurugan, "A comparative study between in-house 3D printed and injection molded ABS and PLA polymers for low-frequency applications," *Materials Research Express*, vol. 6, no. 8, Article ID 085345, 2019.
View at: Publisher Site | Google Scholar

5. A. Babafemi, B. Šavija, S. Paul, and V. Anggraini, "Engineering properties of concrete with waste recycled plastic: a review," *Sustainability*, vol. 10, no. 11, Article ID 3875, 2018.
View at: Publisher Site | Google Scholar

6. R. Olayil, V. Arumuga Prabu, S. DayaPrasad, K. Naresh, and P. S. Rama Sreekanth, "A review on the application of bio-nanocomposites for food packaging," *Materials Today Proceedings*, vol. 56, pp. 1302–1306, 2022.
View at: Publisher Site | Google Scholar

7. B. Jaivignesh and A. Sofi, "Study on mechanical properties of concrete using plastic waste as an aggregate," *IOP Conference Series: Earth and Environmental Science*, vol. 80, Article ID 012016, 2017.
View at: Publisher Site | Google Scholar

8. A. Serier and D. Aoufi, "Development of new biodegradable packaging," *Advances in Materials and Processing Technologies*, vol. 3, no. 2, pp. 155–163, 2017.
View at: Publisher Site | Google Scholar

9. L. Gu and T. Ozbakkaloglu, "Use of recycled plastics in concrete: a critical review," *Waste Management*, vol. 51, pp. 19–42, 2016.
View at: Publisher Site | Google Scholar

Hindawi

Advances in Materials Science and Engineering

11. F. Colangelo, R. Cioffi, B. Liguori, and F. Iucolano, "Recycled polyolefins waste as aggregates for lightweight concrete," *Composites Part B: Engineering*, vol. 106, pp. 234–241, 2016.
View at: Publisher Site | Google Scholar

12. A. M. Hameed and B. A. Fatah Ahmed, "Employment the plastic waste to produce the light weight concrete," *Energy Procedia*, vol. 157, pp. 30–38, 2019.
View at: Publisher Site | Google Scholar

13. I. Mercante, C. Alejandrino, J. P. Ojeda, J. Chini, C. Maroto, and N. Fajardo, "Mortar and concrete composites with recycled plastic: a review," *Science and Technology of Materials*, vol. 30, pp. 69–79, 2018.
View at: Publisher Site | Google Scholar

14. I. Almeshal, B. A. Tayeh, R. Alyousef, H. Alabduljabbar, and A. M. Mohamed, "Eco-friendly concrete containing recycled plastic as partial replacement for sand," *Journal of Materials Research and Technology*, vol. 9, no. 3, pp. 4631–4643, 2020.
View at: Publisher Site | Google Scholar

15. E. A. Ohemeng and S. O. Ekolu, "Strength prediction model for cement mortar made with waste LDPE plastic as fine aggregate," *Journal of Sustainable Cement-Based Materials*, vol. 8, no. 4, pp. 228–243, 2019.
View at: Publisher Site | Google Scholar

16. N. Saikia and J. d. Brito, "Waste polyethylene terephthalate as an aggregate in concrete," *Mathematical Research*, vol. 16, no. 2, pp. 341–350, 2013.
View at: Publisher Site | Google Scholar

17. Y. Adela, "Plastic Wastes as a Raw Material in the Concrete Mix," *An Alternative Approach to Manage Plastic Wastes in Developing Countries*, vol. 382, p. 7, 2020.
View at: Google Scholar

18. J. Wight, *Reinforced concrete: mechanics and design*, Pearson Education, England, 2016.

19. B. S. K. Keerthi Gowda and M. S. Dakshayini, "Application of FOSM and Chebyshev's theorem concept to predict compressive strength attributes of corncob ash embedded cement concrete," *Computational Engineering and Physical Modeling*, vol. 3, no. 1, pp. 16–24, 2020.
View at: Publisher Site | Google Scholar

20. B. S. K. Keerthi Gowda and G. L. Easwara Prasad, "Prognostication of concrete mix proportion by ANN approach," *Advanced Materials Research*, vol. 261–263, pp. 426–430, 2011.
View at: Publisher Site | Google Scholar

21. A. Bardhan, R. Biswas, N. Kardani et al., "A novel integrated approach of augmented grey wolf optimizer and ANN for estimating axial load carrying-capacity of concrete-filled steel tube columns," *Construction and Building Materials*, vol. 337, Article ID 127454, 2022.

23. K. C. Onyelowe, D. P. N. Kontoni, A. M. Ebid et al., "Multi-objective optimization of sustainable concrete containing fly ash based on environmental and mechanical considerations," *Buildings*, vol. 12, no. 7, p. 948, 2022.
View at: Publisher Site | Google Scholar

24. D. Rezazadeh Eidgahee, H. Jahangir, N. Solatifar, P. Fakharian, and M. Rezaeemanesh, "Data-driven estimation models of asphalt mixtures dynamic modulus using ANN, GP and combinatorial GMDH approaches," *Neural Computing & Applications*, vol. 34, no. 20, pp. 17289–17314, 2022.
View at: Publisher Site | Google Scholar

25. K. Naresh, K. Shankar, and R. Velmurugan, "Reliability analysis of tensile strengths using Weibull distribution in glass/epoxy and carbon/epoxy composites," *Composites Part B: Engineering*, vol. 133, pp. 129–144, 2018.
View at: Publisher Site | Google Scholar

26. K. Naresh, K. Shankar, R. Velmurugan, and N. K. Gupta, "Statistical analysis of the tensile strength of GFRP, CFRP and hybrid composites," *Thin-Walled Structures*, vol. 126, pp. 150–161, 2018.
View at: Publisher Site | Google Scholar

27. M. Shariati, M. S. Mafipour, P. Mehrabi et al., "Prediction of concrete strength in presence of furnace slag and fly ash using hybrid ANN-GA (artificial neural network-genetic algorithm)," *Smart Structures and Systems*, vol. 25, no. 2, pp. 183–195, 2020.
View at: Publisher Site | Google Scholar

28. N. Saikia and J. de Brito, "Use of plastic waste as aggregate in cement mortar and concrete preparation: a review," *Construction and Building Materials*, vol. 34, pp. 385–401, 2012.
View at: Publisher Site | Google Scholar

29. M. Batayneh, I. Marie, and I. Asi, "Use of selected waste materials in concrete mixes," *Waste Management*, vol. 27, no. 12, pp. 1870–1876, 2007.
View at: Publisher Site | Google Scholar

30. R. Siddique, J. Khatib, and I. Kaur, "Use of recycled plastic in concrete: a review," *Waste Management*, vol. 28, no. 10, pp. 1835–1852, 2008.
View at: Publisher Site | Google Scholar

31. B. Liguori, F. Iucolano, I. Capasso, M. Lavorgna, and L. Verdolotti, "The effect of recycled plastic aggregate on chemico-physical and functional properties of composite mortars," *Materials & Design*, vol. 57, pp. 578–584, 2014.
View at: Publisher Site | Google Scholar

32. A. Gupta, N. Gupta, and K. K. Saxena, "Experimental study of the mechanical and durability properties of Slag and Calcined Clay based geopolymer composite," *Advances in Materials and*

Hindawi

Advances in Materials Science and Engineering

Technologies, pp. 1–21, 2021.
View at: Publisher Site | Google Scholar

34. S. Jadhav and R. S. Patil, "Comparison of flexural, split tensile & compressive strength of HP-SCC using magnetized water," *International Journal of Emerging Trends in Engineering Research*, vol. 4, pp. 130–135, 2016.
View at: Google Scholar

35. M. A. Akinpelu, S. O. Odeyemi, O. S. Olafusi, and F. Z. Muhammed, "Evaluation of splitting tensile and compressive strength relationship of self-compacting concrete," *Journal of King Saud University - Engineering Sciences*, vol. 31, no. 1, pp. 19–25, 2019.
View at: Publisher Site | Google Scholar

36. A. Jaber, I. Gorgis, and M. Hassan, "Relationship between splitting tensile and compressive strengths for self-compacting concrete containing nano- and micro silica," *MATEC Web of Conferences*, vol. 162, Article ID 02013, 2018.
View at: Publisher Site | Google Scholar

37. G Zhang, N Hamzehkolaei, H Rashnoozadeh, and S Shahab, "Band & Amir Mosavi (2021) Reliability assessment of compressive and splitting tensile strength prediction of roller compacted concrete pavement: introducing MARS-Goa-MCS," *International Journal of Pavement Engineering*, 2021.
View at: Publisher Site | Google Scholar

38. A. Khalili and K. Kromp, "Statistical properties of Weibull estimators," *Journal of Materials Science*, vol. 26, no. 24, pp. 6741–6752, 1991.
View at: Publisher Site | Google Scholar

39. F. Wang and J. Shao, "Modified Weibull distribution for analyzing the tensile strength of bamboo fibers," *Polymers*, vol. 6, no. 12, pp. 3005–3018, 2014.
View at: Publisher Site | Google Scholar

40. L. Bazli, S. Eskandarinezhad, N. Kakur et al., "Electrical properties of polymer blend composites based on Silicone rubber/EPDM/clay for high voltage insulators," *Journal of Composites and Compounds*, vol. 2, no. 5, pp. 18–24, 2021.
View at: Publisher Site | Google Scholar

41. K. Naresh, K. Shankar, R. Velmurugan, and N. K. Gupta, "Probability-based studies on the tensile strength of GFRP, CFRP and hybrid composites," *Procedia Engineering*, vol. 173, pp. 763–770, 2017.
View at: Publisher Site | Google Scholar

42. S. Ilangovan, S. Senthil Kumaran, K. Naresh, K. Shankar, and R. Velmurugan, "Studies on glass/epoxy and basalt/epoxy thin-walled pressure vessels subjected to internal pressure using

Hindawi

Advances in Materials Science and Engineering

Materials and Processing Technologies, pp. 1–15, 2021.

View at: Publisher Site | Google Scholar

Copyright

More related articles

Determination of Optimized Mix Design of Reactive Powder Concrete

Abbas Moslehi | Mohammad Ali Dashti Rahmatabadi | Hosein Arman

Hindawi

Advances in Materials Science and Engineering

Use of Silica Fume, Bentonite, and Waste Tire Rubber as Impermeable Layer Construction Materials

Ahmet Şenol | Arzu Guner

Related articles

Prediction of the Mechanical Properties of Fibre-Reinforced Quarry Dust Concrete Using Response Surface and Artificial Neural Network Techniques

Jayaprakash Sridhar | Shanmugam Balaji | ... | Paul Awoyera

Evaluation of Mechanical and Durability Properties of Eco-Friendly Concrete Containing Silica Fume, Waste Glass Powder, and Ground Granulated Blast Furnace Slag

Mahdi Bameri | Soroush Rashidi | ... | Fereydoun Rahmani

Compressive and Flexural Strength of Concrete with Different Nanomaterials: A Critical Review

R. M. Ashwini | M. Potharaju | ... | Anish Paudel

Published: 11 February 2022

Solid Particle Erosion Behaviour of Plasma-Sprayed (WC–Co)/(Cr_3C_2–NiCr) Coatings

G. Madhu Sudana Reddy, S. Ramesh, Gajanan Anne, M. R. Ramesh, T. Nageswara Rao & Pradeep Patil

Journal of Bio- and Tribo-Corrosion **8**, Article number: 40 (2022)

Abstract

This study reports the high-temperature erosion behaviour of plasma-sprayed 35% (WC–Co)/65% (Cr_3C_2–NiCr) coating on MDN-420 alloy. Plasma spray coatings have always played a pivotal role in enabling industries to combat problems of premature degradation of components that operate in harsh environments. (WC–Co) + (Cr_3C_2–NiCr) coating is investigated for erosion under various laboratory-simulated conditions. Coating surface is characterized by using an optical microscope, scanning electron microscope (SEM), and X-ray diffraction (XRD). Porosity, microhardness, surface roughness, and adhesion strength of the coating are measured. The solid particle erosion test is conducted at the temperatures of 300 °C, 500 °C and 700 °C with the impact angles of 30° and 90°

by using Al_2O_3 as an erodent in the hot air jet erosion testing machine. The optical profilometer is used to evaluate the erosion volume loss of the coated and uncoated samples. It is observed that erosion resistance of the substrate is found to be higher than the coating at the different test temperatures. As the temperature increases, the erosion resistance of the coating is also increased at all the temperatures for both impact angles of 30° and 90°.The eroded coating surface morphology reveals that the generalized behaviour of the coating is ductile in nature.

References

1. Chawla V, Chawla A, Puri D, Prakash S, Gurbuxani PG, Sidhu BS (2011) Hot corrosion & erosion problems in coal based power plants in India and possible solutions—a review. J Miner Mater Charact Eng 10(04):367

2. Sundararajan G (1995) The solid particle erosion of metallic materials: the rationalization of the influence of material variables. Wear 186:129–144

3. Doddamani M, Mathapati M, Ramesh MR (2018) Microstructure and tribological behavior of plasma sprayed NiCrAlY/WC-Co/cenosphere/solid lubricants composite coatings. Surf Coat Technol 354:92–100

4. El Rayes MM, Abdo HS, Khalil KA (2013) Erosion-corrosion of cermet coating. Int J Electrochem Sci 8(1):1117–1137

5. Praveen AS, Sarangan J, Suresh S, Subramanian JS (2015) Erosion wear behaviour of plasma sprayed NiCrSiB/Al_2O_3 composite coating. Int J Refract Metal Hard Mater 52:209–218

6. Chatha SS, Sidhu HS, Sidhu BS (2012) Characterisation and corrosion-erosion behaviour of carbide based thermal spray

coatings. J Miner Mater Charact Eng 11(6):569–586

7. Chatha SS, Sidhu HS, Sidhu BS (2012) Characterisation and corrosion-erosion behaviour of carbide based thermal spray coatings. J Miner Mater Charact Eng 11(06):569

8. Di Girolamo G, Brentari A, Blasi C, Serra E (2014) Microstructure and mechanical properties of plasma sprayed alumina-based coatings. Ceram Int 40(8):12861–12867

9. Zavareh MA, Sarhan AADM, Zavareh PA, Abd Razak BB, Basirun WJ, Ismail MBC (2016) Development and protection evaluation of two new, advanced ceramic composite thermal spray coatings, Al_2O_3–40TiO_2 and Cr_3C_2–20NiCr on carbon steel petroleum oil piping. Ceram Int 42(4):5203–5210

10. Nithin HS, Desai V, Ramesh MR (2017) An investigation on high temperature erosion behaviour of plasma sprayed CoCrAlY/Al_2O_3/YSZ on Fe and Ni based alloys. Pertanika J Sci Technol 25(2):397–406

11. Reddy M, Prasad CD, Patil P, Ramesh MR, Rao N (2021) Hot corrosion behavior of plasma-sprayed NiCrAlY/TiO_2 and

NiCrAlY/Cr_2O_3/YSZ cermets coatings on alloy steel. Surf Interfaces 22:100810

12. Prasanna ND, Siddaraju C, Shetty G (2018) Studies on the role of HVOF coatings to combat erosion in turbine alloys. Mater Today 5(1):3130–3136

13. Madhu Sudana Reddy G, Ramesh MR, Rao N, Jegadeeswaran N (2018) Corrosion of metal construction structures. Int J Mech Prod Eng Res Dev 8(6):227–237

14. Wani TP, Raja R, Reddy G (2021) Synthesis and mechanical properties of HDPE based nano-clay polymer composites for industrial applications. Adv Mater Process Technol. https://doi.org/10.1080/2374068X.2021.1896864

15. Somasundaram B, Kadoli R, Ramesh MR, Ramesh CS (2016) High temperature corrosion behaviour of HVOF sprayed WC-CrC-Ni coatings. Int J Surf Sci Eng 10(4):400–413

16. Singh A, Goyal K, Goyal R, Krishan B (2021) Hot corrosion behaviour of different ceramics coatings on boiler tube steel at 800 °C temperature. J Bio-and Tribo-Corrosion 7(1):1–9

17. Levy AV, Buqian W (1988) Erosion of hard material coating systems. Wear 121(3):325–346

18. Wang Y, Yang Y, Yan MF (2007) Microstructures, hardness and erosion behavior of thermal sprayed and heat treated NiAl coatings with different ceria. Wear 263(1–6):371–378

19. Ramesh MR, Prakash S, Nath SK, Sapra PK, Venkataraman B (2010) Solid particle erosion of HVOF sprayed WC-Co/NiCrFeSiB coatings. Wear 269(3–4):197–205

20. Ramachandran CS, Balasubramanian V, Ananthapadmanabhan PV (2013) Erosion of atmospheric plasma sprayed rare earth oxide coatings under air suspended corundum particles. Ceram Int 39(1):649–672

21. Wang B-Q, Verstak A (1999) Elevated temperature erosion of HVOF Cr_3C_2/TiC–NiCrMo cermet coating. Wear 233–235:342–351

22. Yang GJ, Li CJ, Zhang SJ, Li CX (2008) High-temperature erosion of HVOF sprayed Cr_3C_2–NiCr coating and mild steel for boiler tubes. J Therm Spray Technol 17(5):782–787

23. Mathapati M, Ramesh MR, Doddamani M (2017) High temperature erosion behavior of plasma sprayed NiCrAlY/WC-Co/cenosphere coating. Surf Coat Technol 325:98–106

24. Ndumia JN, Kang M, Gbenontin BV, Lin J, Nyambura SM (2021) A review on the wear, corrosion and high-temperature resistant properties of wire arc-sprayed Fe-based coatings. Nanomaterials 11(10):2527

25. Hearley JA, Little JA, Sturgeon AJ (1999) The erosion behaviour of NiAl intermetallic coatings produced by high velocity oxy-fuel thermal spraying. Wear 233:328–333

26. Hussainova I, Kubarsepp J, Pirso J (2001) Mechanical properties and features of erosion of cermets. Wear 250(1–12):818–825

27. Mahesh RA, Jayaganthan R, Prakash S (2009) Microstructural characteristics and mechanical properties of HVOF sprayed NiCrAl coating on superalloys. J Alloy Compd 468(1–2):392–405

28. Mishra SB, Chandra K, Prakash S, Venkataraman B (2006) Erosion performance of coatings produced by shrouded plasma

spray process on a Co-based superalloy. Surf Coat Technol 201(3–4):1477–1487

Funding

This research received no specific grant from any funding agency.

Author information

Authors and Affiliations

Department of Mechanical Engineering, Oxford College of Engineering, Bangalore, 560068, India
G. Madhu Sudana Reddy

Department of Mechanical Engineering, RV Institute of Technology and Management, Bangalore, 560076, India
S. Ramesh

Department of Mechanical Engineering, Shri Madhwa Vadiraja Institute of Technology and Management, Udupi, 574115, India
Gajanan Anne

Department of Mechanical Engineering, National Institute of Technology Karnataka, Surathkal, 575025, India
M. R. Ramesh

Department of Mechanical Engineering, Gitam University, Bangalore, 560065, India

T. Nageswara Rao & Pradeep Patil

Corresponding author

Correspondence to S. Ramesh.

Ethics declarations

Conflict of interest

On behalf of all authors, the corresponding author states that there is no competing of interest.

Additional information

Publisher's Note

Springer Nature remains neutral with regard to jurisdictional claims in published maps and institutional affiliations.

Rights and permissions

Reprints and Permissions

About this article

Cite this article

Reddy, G.M.S., Ramesh, S., Anne, G. *et al.* Solid Particle Erosion Behaviour of Plasma-Sprayed (WC–Co)/(Cr_3C_2–NiCr) Coatings. *J Bio Tribo Corros* **8**, 40 (2022). https://doi.org/10.1007/s40735-022-00629-5

Received	Revised	Accepted
11 October 2021	24 November 2021	04 January 2022

Published

11 February 2022

DOI

https://doi.org/10.1007/s40735-022-00629-5

Keywords

MDN-420 alloy **Plasma spray**

(WC–Co)/Cr_3C_2–NiCr **Metal matrix composite**

Erosion

ScienceDirect

Materials Today: Proceedings

Volume 52, Part 3, 2022, Pages 439-444

Microstructural characterization and wear behavior of 12wt% of boron carbide reinforced Al2030 alloy composites

V.A. Anjan Babu [a b], R. Saravanan [a], M. Raviprakash [c], Madeva Nagaral [d 1], Nithin Kumar [e]

Show more

https://doi.org/10.1016/j.matpr.2021.09.098

Get rights and content

Abstract

In this study Al2030 alloy with 12wt% of B_4C particles reinforced composites were produced using stir cast method. Al2030 alloy with 12wt% of B_4C composites were studied for microstructural characteristics using SEM/EDS and XRD analysis. The prepared Al2030 alloy with 12wt% of B_4C composites were exhibited uniform distribution of parts in Al2030 alloy matrix as revealed by SEM micrographs. EDS and XRD patterns indicated presence of reinforcement in the form of B and C elements by EDS spectrum and B_4C phase by XRD patterns in the Al2030 alloy matrix. Further, wear behaviour of Al2030 alloy and composites were analysed using pin on disc machine by varying load and speed. The composites with B_4C particles were shown superior wear resistance properties as compared to base Al2030 material. Various wear mechanisms were studied with wear worn surface analysis obtained after wear tests.

Previous Next

Keywords

Al2030 Alloy; B_4C Particles; Microstructure; Wear; Worn Surface

Special issue articles Recommended articles

Cited by (0)

1 ORCID ID: 0000-0002-8248-7603.

ScienceDirect

Materials Today: Proceedings

Volume 54, Part 2, 2022, Pages 372-377

Synthesis of nanostructured ternary Ti based alloy for bio-medical applications

N.B. Pradeep [a], B.K. Venkatesha [b], S. Parameshwara [a], R. Raghavendra Rao [c], M. Raviprakash [d]

Show more

https://doi.org/10.1016/j.matpr.2021.09.429

Get rights and content

Abstract

This research article presents the preliminary findings of an investigation into the manufacturing and characterization of a Ti alloy powder utilizing a high-energetic ball milling process. To mechanically alloy elemental powders, a high-energetic Ball Mill used. Mechanically alloyed powders analysed by X-ray Diffraction (XRD), Scanning Electron Microscopy (SEM), and Transmission electron microscope to investigate structural, parameters. As indicated by XRay Diffraction data indicating crystallite size reduces to the nano scale regime, the elemental powders simultaneously alloyed with increasing ball milling duration. However, partial amorphization of elemental powders found during extended milling times. The results of transmission electron microscope (TEM) indicate a halo picture as well as crystalline rings, and also a shift from crystalline to partly amorphous structure during the ball milling process.

Previous Next

Keywords

Ti alloy; Ball milling; X-ray diffraction; Scanning electron microscopy

Special issue articles Recommended articles

Cited by (3)

Investigation of microstructure and mechanical properties of microwave consolidated TiMgSr alloy prepared by high energy ball milling
2022, Powder Technology

Show abstract

Investigation of Structural and Mechanical Properties of Nanostructured TiMgSr Alloy for Biomedical applications
2023, Biointerface Research in Applied Chemistry

FEA Analysis of TI-6AL-4V and 30% Collagen Reinforced PMC Used as Biomaterials for Ankle Implants
2023, Biointerface Research in Applied Chemistry

Materials International
Open Access Journal (ISSN: 2668-5728)

Article
Volume 4, Issue 1, 2022, 3
https://doi.org/10.33263/Materials41.003

Fabrication of Mg-Zn/Al and Mg-Zn/Anodized Al Multilayered Composites by Accumulative Roll Bonding, Investigation of Corrosion Behavior

Ramesh Sampath [1], Gajanan Anne [2,*], Gajanan Manjunath Naik [1], Shamanth Vasanth[3] Madhu Sudana Reddy [4]

[1] Department of Mechanical Engineering, RV Institute of Technology and Management, JP Nagar, Bengaluru, India – 560076; rameshs.rvitm@rvei.edu.in (R.S.); gajamnaik@gmail.com (G.M.N.);
[2] Department of Mechanical Engineering, Shri Madhwa Vadiraja Institute of Technology and Management, Udupi, India – 574115; gajanan.mech@sode-edu.in (G.A.);
[3] Department of Mechanical Engineering, REVA University, Banglore, India - 560024; shamanth053@yahoo.co.in (S.);
[4] Department of Mechanical Engineering, Oxford College of Engineering, Bangalore, India -560068; maddy_reddy@rocketmail.com (M.S.R.G.);
* Correspondence: gajanan.anne25@gmail.com (G.A.);

Scopus Author ID 57211503636
Received: 14.01.2022; Accepted: 15.02.2022; Published: 9.03.2022

Abstract: Mg-2%Zn/Al and anodized Mg-2%Zn/Al multilayered composites were developed from wrought Mg-2%Zn alloy with aluminum and anodized aluminum by accumulative roll bonding (ARB). The grain size was found to be 700-750 nm and the lowest density of 2122 kg/m^3 after roll bonding. The corrosion behavior of the multilayered composites has been examined using electrochemical polarization, zero resistance ammeter, and hydrogen evolution tests. Low corrosion current density, high induction time to passive film breakdown, and low hydrogen evolution are the significant features of multilayered Mg-2%Zn/Al and anodized Mg-2%Zn/Al composites. This feature is because of grain refinement, formation of additional β phases ($Al_{12}Mg_{17}$ and $AlMg_4Zn_{11}$), and presence of Al_2O_3.

Keywords: magnesium; accumulative roll bonding; ultrafine grain; multilayered composites; corrosion.

1. Introduction

Lightweight materials are the most demanding materials in aviation, transportation, electronics, and construction. They possess high strength and low weight, good damping capacity, thermal & electrical conductivity, and optimum corrosion resistance. Mg alloys are considered highly promising materials for lightweight applications [1-4]. However, the corrosion behavior of Mg alloy has been a major challenge due to the high electronegative potential of Mg metal which limits to use in many engineering applications [5]. Conventional methods used to enhance mechanical properties and corrosion behavior is either by an alloy design or severe plastic deformation (SPD) [6,7]. Accumulative roll bonding (ARB) is one of the SPD techniques to produce high strength as well as corrosion resistance by reducing the grain size. ARB is used to develop multilayered composites using similar and dissimilar materials with high productivity, low cost, and defect-free microstructure [8].

Corrosion behavior has been reported by many researchers, who have worked on various Mg alloys like AZ(Mg–Al– Zn), AM(Mg–Al–Mn), and ZK (Mg-Zn-Zr) series, and it

has been elucidated that corrosion resistance is directly affected by microstructures, surface finish and presence of secondary phases [9,10]. Nowadays, Mg-Zn alloys are the most widely used alloyed materials for a number of structural applications. Walter and Kannan [11] have found that corrosion current density and polarization resistance of AZ91 Mg alloy varied significantly with surface roughness. Aung and Zhou studied the effect of grain size of AZ31B on corrosion in the presence of 3.5 wt.% NaCl solution [12]. A significant corrosion rate reduction due to changes of grains from 250 to 65 μm was observed. Zhang *et al*. investigated AZ31 D Mg alloy for corrosion and the role of secondary phases (β phases) and its volume fractions on corrosion [13] and developed a relationship with corrosion current density and volume fractions of β phase.

In the present work, an effort was put to improve the corrosion behavior of Mg alloy by adopting alloy development, surface treatment (anodization), and bonding with Al through the accumulative roll bonding process. Paper deals with developing multilayered composites of wrought Mg-2%Zn alloy with Al and anodized Al using an accumulative roll bonding (ARB) process to examine the corrosion behavior of these newly developed newly developed multilayered composites using 0.1 M NaCl solution using potentiodynamic polarization, zero resistance ammeter, and hydrogen evolution tests.

2. Materials and Methods

2.1. Materials.

Binary alloys Mg-2%Zn and pure aluminum are used in the present study. Pure magnesium ingots and zinc granules are used to prepare Mg-2%Zn binary alloy by melting in the range of 750 - 800 ºC under the inert atmosphere of 99% CO_2 in an electrical resistance furnace and with the help of mechanical agitation, segregation of alloying elements was controlled. After casting, Mg-2% Zn binary alloy was homogenized at 400 °C for 24 h. Then Mg-2%Zn alloy slabs with the dimensions of 40mm × 30mm × 10mm thick were cut from the cast ingot. The process was subjected to rolling with 0.25% reduction per pass at a rolling temperature of 300 °C with an intermediate heating time of 10 min. Finally, Mg-2%Zn binary alloy was rolled into 1 mm thick for accumulative roll bonding. Similarly, pure cast aluminum is also rolled to 1 mm thick by the same technique.

2.2. Anodization.

Before ARB process, Al sheet was cleaned using NaOH and HNO_3 and followed by anodization treatment using 15 wt % H_2SO_4 solution at 18 ºC for 60 min at a voltage of 16 V. [14]. Anodization duration of one hour yields a uniform aluminum oxide film of about 10 μm, examined by scanning electron microscope (SEM).

2.3. ARB.

Figure 1 shows the ARB process, which involves four steps: surface preparation, stacking & furnace heating, rolling, and cutting for one complete cycle. Mg-2%Zn binary alloys and pure Al sheet were cleaned using acetone, wire-brushed, stacked together, and heated in the furnace for 10 min at 300 °C. Rolling was carried out immediately, with a thickness reduction of 50% using a laboratory rolling mill (⌀ 110 mm). The sheets are subjected to five ARB passes to obtain 32 layers (alternate) of Mg-2%Zn and Al. In the second material

system, anodized Al was roll bonded with the Mg-2%Zn to obtain 32 layered composites after sequentially performing five ARB passes. Sample codes for various processed conditions are tabulated in Table 1.

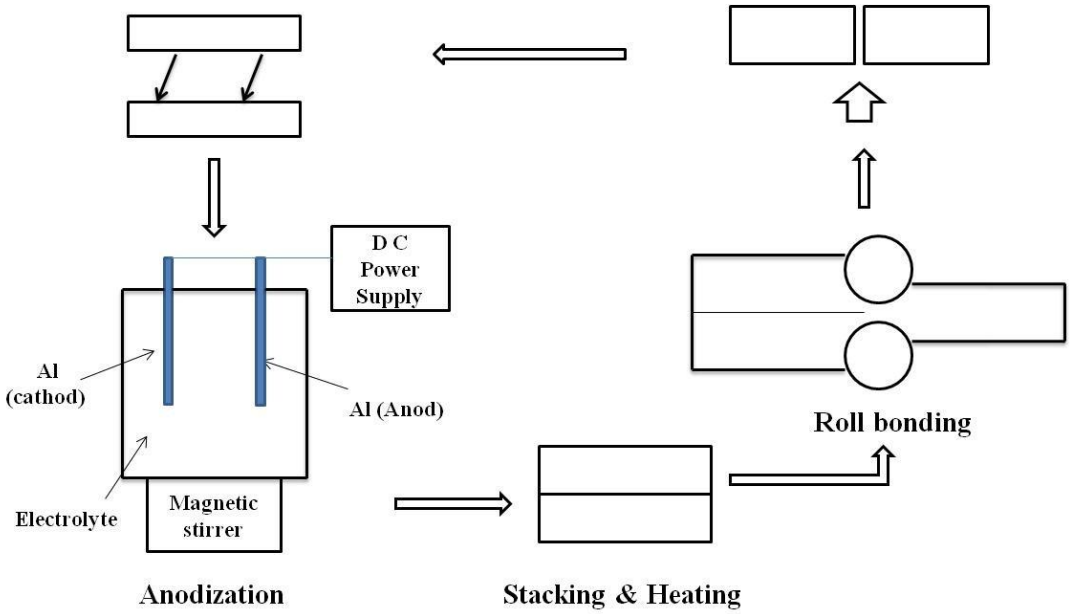

Figure 1. Schematic diagram of anodization and ARB process.

Table 1. Sample code.

S. No.	Processing condition	Sample code
1	Rolled Mg-2%Zn	R-1
2	Mg-2%Zn/Al multilayered composite	C-1
3	Anodized Mg-2%Zn/Al multilayered composite	AC-1

2.4. Characterization.

ARB processed samples were prepared for microstructural analysis using the following stages: polished using SiC paper and superfine diamond paste and etched with picral acetate solution. An optical microscope (OM) and Scanning Electron Microscope (SEM) were used to characterize the samples. Different phases in the roll bonded C-1 and AC-1 samples were identified by using X-ray diffraction (XRD) with Cu Kα radiation.

2.5. Electrochemical measurements.

Electrochemical corrosion measurements like potentiodynamic polarization and zero resistance ammeter tests were performed at room temperature using EC lab-Biologic SP-150 with a scan rate of 1 mV/s. The electrode was immersed in an electrochemical cell containing 200 ml of 0.1 M NaCl of 7.5 pH. 0.1 cm^2 area of the sample was exposed to the electrolyte solution, and the distance between electrodes was maintained at 30 mm. The corrosion potential (E_{corr}) and corrosion current density (i_{corr}) were calculated by extrapolating Tafel plots. The surface morphology of the composite was examined after electrochemical corrosion tests with the help of SEM.

In the ZRA test, galvanic coupling current density and galvanic potential between two identical electrodes were measured simultaneously every 0.5 s for 120 min. In addition, induction time for the passive film to break down under open-circuit conditions was measured. ZRA test results were plotted up to the first passivity breakdown, which was observed as a sudden fall in the Ecorr- ZRA values and an abrupt rise in the icorr-ZRA values. In ZRA test, fluctuation in current in the electrodes was measured. Further, fluctuations in the potential

difference between the reference electrode (SCE) and working electrodes were recorded without external voltage. At the beginning of corrosion, a decrease in potential and increase in current density was observed in the working electrodes. Theoretically, there should be no net current flow between the electrodes. However, in practice, change in the environmental condition leads to currents flow and electrochemical noise, resulting in statistical variation in the corrosion rate across the surface. ZRA test was carried out three times for each sample, and good reproducibility was observed.

2.6. Immersion corrosion.

An immersion corrosion test was carried out according to ASTM G31-72. The hydrogen evolution during the immersion test is proportional to the corrosion rate of the materials. For the immersion study, multilayered composites were cut normal to the rolling direction and were finely polished. The hydrogen evolution test was carried out in 0.1 M NaCl solution for 120 h at room temperature. At the beginning of the immersion test, the pH was adjusted to 7.5, and hydrogen evolution and pH were recorded throughout the process. The corrosion rate was calculated using the following equations [15].

$$P_H = 3.65\frac{\Delta w}{\rho} \qquad (1)$$

where PH = Corrosion rate through hydrogen evolution (mm/y)
ρ= Metal density (g/cm^3)
Δw = Weight loss rate (mg/cm^2/d)

$$\Delta w = 1.085 V_H \qquad (2)$$

where VH = Hydrogen evolution rate (ml/cm^2/d)

3. Results and Discussion

3.1. Microstructure analysis.

Figure 2 shows the SEM image of the R-1 sample revealed bimodal grain size distribution with an average grain size of 6 μm and deformed twins. During the ARB process, the original grains are divided into many lamellae by twining and dynamic recrystallization during the hot rolling process [16].

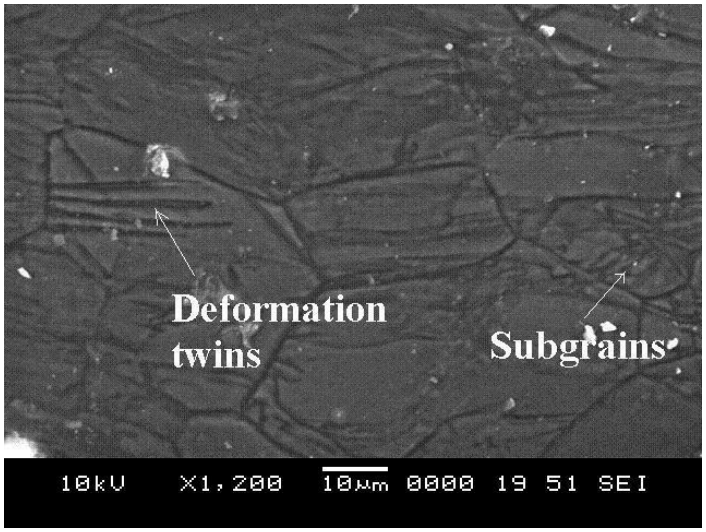

Figure 2. SEM micrographs of hot rolled Mg-2%Zn binary alloy.

3.2. ARB Microstructure.

Figure 3 shows the SEM micrographs of C-1 sample after five ARB passes. The average grain size in Mg-2%Zn and Al regions, after 5 ARB passes, was 750 nm and 700 nm, respectively (Figure 3c). Figure 3c shows alternate layers of thickness 35-40 μm of Al (region I) and Mg-2%Zn (region II) at the interface (region III). As the number of ARB passes increased, grain size reduced due to microstructure refinement because of dynamic recovery and recrystallization [17].

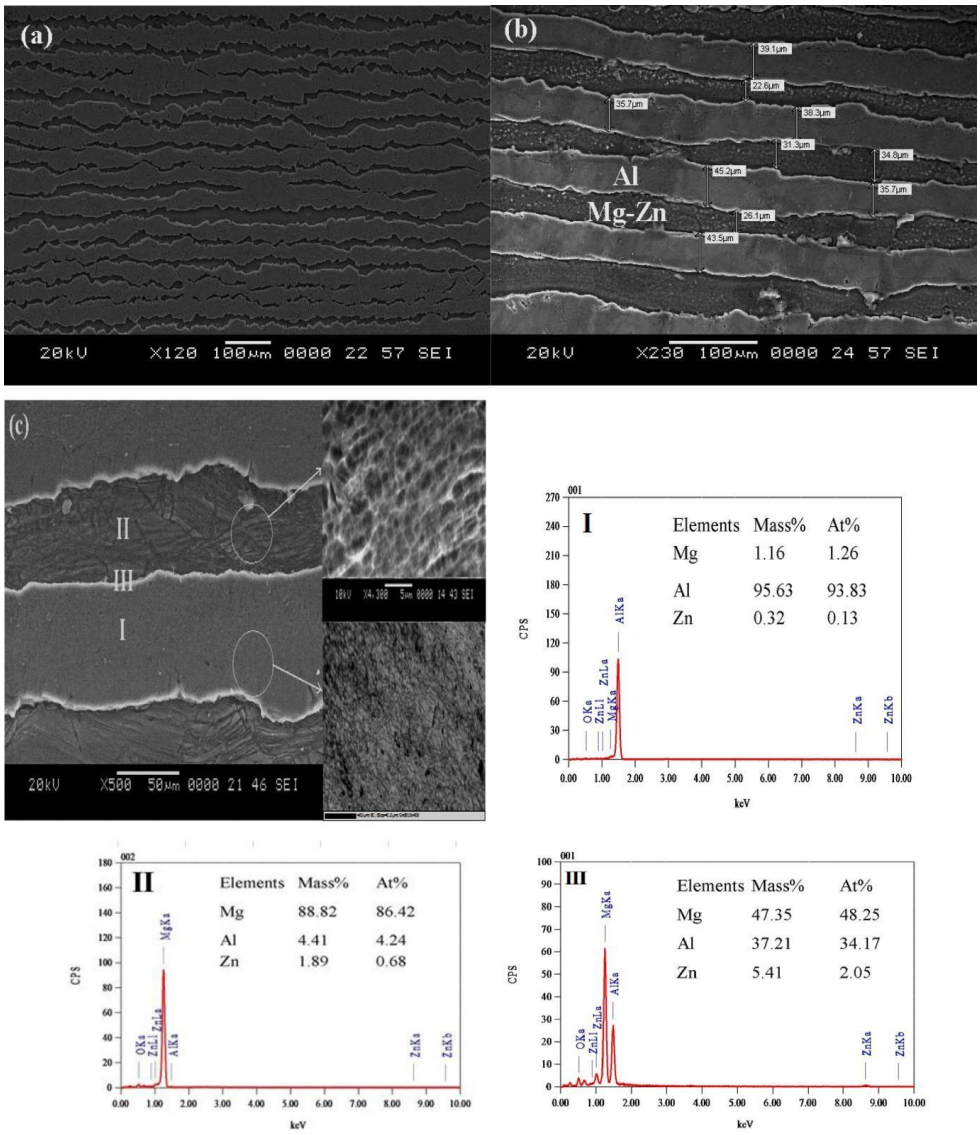

Figure 3. SEM micrographs of C-1sample processed by ARB. (**a**) C-1 sample after five ARB passes; (**b**) enlarged image with measured thickness; (**c**) composition of the different layers and its interface by EDX analysis.

3.3. X-ray diffraction analysis.

XRD patterns of the C-1 and AC-1 (Figure 4) revealed the peaks indexed to Al, αMg, Al17Mg12, and AlMg4Zn11, as intermetallic phases, along with Al_2O_3 peaks. The formation of intermetallic phases revealed in multilayered composites maybe because of the grain boundary area, dislocation density, and high rolling strain induced into the material during ARB at 300 ºC, which increases the bonding of different layers in the multilayered composite [18,19].

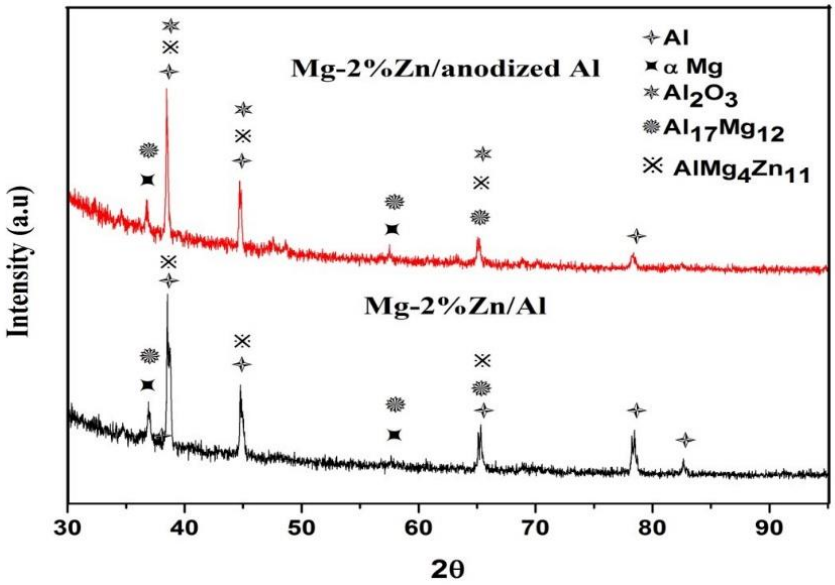

Figure 4. XRD patterns of the C-1 and AC-1 samples.

3.4. Potentiodynamic polarization studies.

Electrochemical corrosion plots of multilayered composites are shown in Figure 5, and electrochemical kinetics parameters are presented in Table 2. E_{corr} values of R-1, C-1 and AC-1 is -1.63, -1.40 and -1.36 VSCE, respectively. Shifting E_{corr} values towards the noble direction indicates lower corrosion current density (icorr) exhibited because of the ARB process. R-1 sample exhibits high evolution of H_2 as compared to ARB processed composites due to cathodic reduction reactions. To examine the stable passivation behavior of alloy and composite in exposed environments, passive current density provides a better representation of uniform and localized corrosion. Reduction in passive current density was observed in roll bonded composites compared to the R-1 sample. The corrosion resistance of ultrafine-grained multilayered composites increased due to decreased cathodic kinetics, passivation kinetics [20], and formation $Al_{12}Mg_{17}$ and $AlMg_4Zn_{11}$ [21].

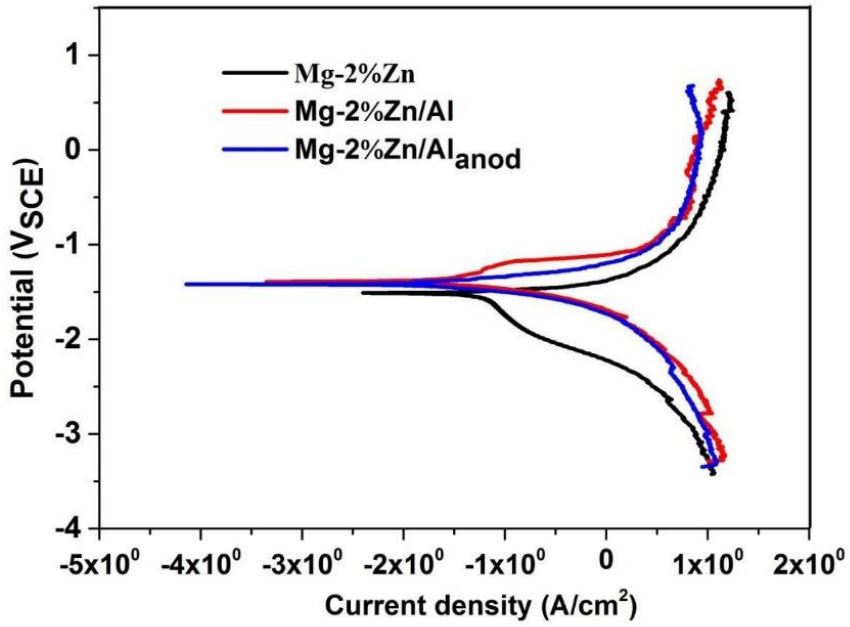

Figure 5. Potentiodynamic polarization curves of the R-1, C-1, and AC-1 samples.

Table 2. Electrochemical kinetic parameters.

Materials	*E*corr (VSCE)	*i*corr (μA/cm^2)	β_a (mV/decade)	β_c (mV/decade)	Corrosion rate (mm/y)
R-1	-1.63	77.96	238.1	- 882.2	2.38
C-1	-1.36	32.73	372.4	-180.8	1.69
AC-1	-1.40	30.14	119.2	-172.9	1.49

ARB has the advantage of breaking secondary phases with uniform distribution of ultrafine-grained microstructure. These intermetallic (β) phases act as an effective barrier and work as an active cathode concerning the active Mg matrix [22,23]. The corrosion resistance of the roll bonded AC-1 sample is high compared to C-1. The presence of rich Al2O3 on the surface of the anodized aluminum act as a barrier [24,25], a significant shift of Ecorr in a noble direction, and lower car values were noticed for the AC-1 sample. The icorr value of AC-1 sample is 0.00465 times the value of C-1 sample. Hence, the corrosion resistance of ultrafine-grained AC-1 has significantly improved by anodization treatment, where aluminum oxide particles were introduced in the multilayered with the network of intermetallic phases.

Significant dissolution of the Mg-Zn alloy layer was observed (Figure 6 a-c). It has also depicted those corrosion products from dissolved alloy slightly covered the pure Al layer. However, the roll bonded composite sample did not show any dissolution because of the anodization of Al before the ARB process. A cracking tendency of the anodized layer was found due to the high hardness of the surface (alumina).

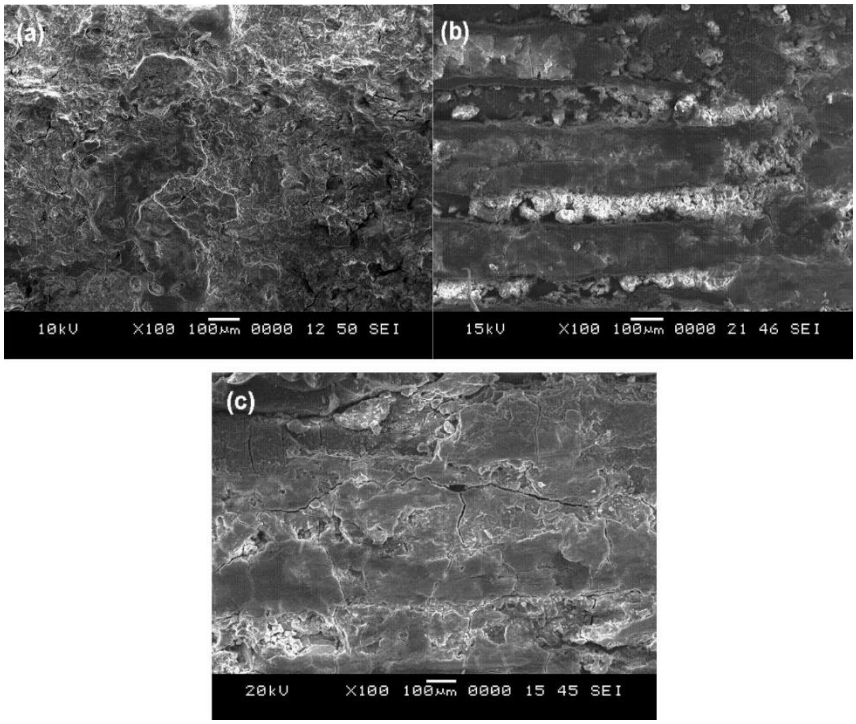

Figure 6. SEM micrographs of corroded (**a**) R-1; (**b**) C-1; (**c**) AC-1.

3.5. Zero Resistance Ammetry.

ZRA technique was used to represent the combined behavior of passivation and passivity break down with given time for Mg-Zn alloys and roll bonded composites in 0.1M NaCl for 5400 s (Figure 7). Icorr-ZRA was measured from the ZRA curves was found to be in the range of 1.29-0.77 mAcm^{-2}, and induction time to passivity breakdown increases from 1400, 1700, and 1800 s for the Mg-2%Zn alloy and roll bonded samples, respectively. It reveals that icorr-ZRA decreases as the Ecorr-ZRA increase with time. ZRA curves depict that higher

icorr-ZRA was observed in the R-1 sample as compared to C-1 and AC-1, which is also well justified with polarization curves (Figure 5).

The ZRA and polarization tests show a good agreement with their results, indicating that ARB processed multilayered composites show a reduction in corrosion current density was observed, and stability of passive film breakdown has been increased. Induction time to passive film breakdown gradually increased for C-1 and AC-1 samples compared to R-1, clearly indicated in the ZRA test due to high stable passive film formation due to ultra-fine grains after the ARB process.

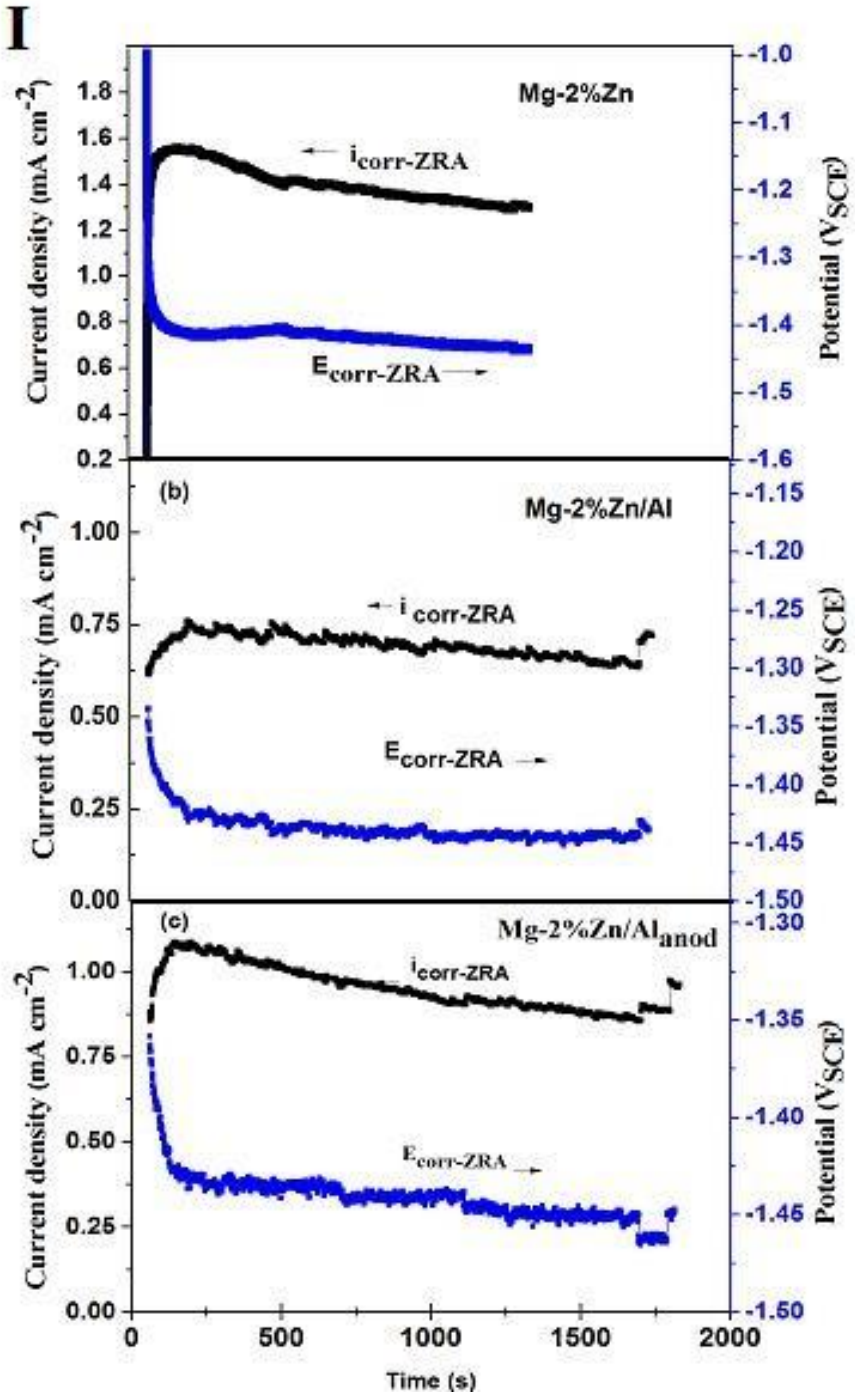

Figure 7. ZRA plots Mg-2%Zn alloys and their multilayered composites.

3.6. Immersion study.

Hydrogen evolution rate and corresponding corrosion rate of the R-1 and ARB processed multilayered composites are tabulated in Table 3. The hydrogen evolution drastically

reduced about 1.8 times and 2.4 times in C-1 and AC-1, respectively, compared with the R-1 sample. A similar trend of corrosion rate was observed in the potentiodynamic polarization (Table 2) and immersion tests (Table 3) in 0.1 M NaCl solution. The degradation of the C-1 composites is slower than R-1 due to refined microstructure and the presence of β phases ($Al_{12}Mg_{17}$ and $AlMg_4Zn_{11}$). Further, the AC-1 samples showed less hydrogen evolution than C-1 samples due to the presence of alumina (due to anodization before the ARB process).

Table 3. Immersion test results.

Materials	V_H (ml/cm^2/d)	P_H (mm/y)
R-1	1.15	2.55
C-1	0.75	1.40
AC-1	0.56	1.05

4. Conclusions

The multilayered composites of C-1 and AC-1 samples were developed successfully with an average grain size in the range of 700-750 nm. Corrosion current density (i_{corr}), cathodic kinetic (β_C), passive current density (i_{pass}), and hydrogen evolution have been significantly reduced for C-1 and AC-1 samples as compared to R-1 samples. The hydrogen evolution of the AC-1 samples reduced about 2.4 times compared with R-1 samples.The stability of the passive film was evaluated by the zero resistance ammetry, which revealed that the induction time taken for passive film breakdown got increased and icorr-ZRA decreased in multilayered composites. Formation of $Al_{17}Mg_{12}$, $AlMg_4Zn_{11}$ during ARB process, Al_2O_3 by anodization and passivation enhanced the corrosion resistance of the AC-1 samples.

Funding

This research received no external funding

Acknowledgments

The authors are thankful to the Mechanical Engineering department at the National Institute of Technology Karnataka, Suratkal, for providing the support in carrying out the present research work.

Conflict of interests

The authors declare no conflict of interest.

References

1. Song, D.; Ma, A.B.; Jiang, J.H.; Lin, P.H.; Yang, D.H.; Fan, J.F. Corrosion behaviour of bulk ultra-fine grained AZ91D magnesium alloy fabricated by equal-channel angular pressing. *Corros. Sci.* **2011**, *53*, 362-373, https://doi.org/10.1016/j.corsci.2010.09.044.
2. Clow, B.B. Magnesium industry overview. *Advanced materials & processes* **1996**, *150*, 33-35.
3. Ramesh, S.; Anne, G.; Nayaka, H. S.; Sahu, S.; Ramesh, M. R. Influence of multidirectional forging on microstructural, mechanical, and corrosion behavior of Mg-Zn alloy. *Journal of Materials Engineering and Performance* **2019**, *28*, 2053-2062.
4. Luo, A.A. Recent Magnesium Alloy Development for Automotive Powertrain Applications. *Mater. Sci. Forum* **2003**, *419-422*, 57-66, https://doi.org/10.4028/www.scientific.net/MSF.419-422.57.
5. Song, G.L.; Atrens, A. Corrosion Mechanisms of Magnesium Alloys. *Adv. Eng. Mater.* **1999**, *1*, 11-33, https://doi.org/10.1002/(SICI)1527-2648(199909)1:1<11::AID-ADEM11>3.0.CO;2-N.

6. Azushima, A.; Kopp, R.; Korhonen, A.; Yang, D.Y.; Micari, F.; Lahoti, G.D.; Groche, P.; Yanagimoto, J.; Tsuji, N.; Rosochowski, A.; et al. Severe plastic deformation (SPD) processes for metals. *CIRP Annals* **2008**, *57*, 716-735, https://doi.org/10.1016/j.cirp.2008.09.005.
7. Toth, L.S.; Gu, C. Ultrafine-grain metals by severe plastic deformation. *Mater. Charact.* **2014**, *92*, 1-14, https://doi.org/10.1016/j.matchar.2014.02.003.
8. Jinfeng, D.; Guangsheng, H.; Yanchun, Z.; Bei, W. Electrochemical Performance of AZ31 Magnesium Alloy under Different Processing Conditions. *Rare Metal Materials and Engineering* **2014**, *43*, 316-321, https://doi.org/10.1016/S1875-5372(14)60066-7.
9. Song, G.-L.; Xu, Z. The surface, microstructure and corrosion of magnesium alloy AZ31 sheet. *Electrochim. Acta* **2010**, *55*, 4148-4161, https://doi.org/10.1016/j.electacta.2010.02.068.
10. Wang, L.; Shinohara, T.; Zhang, B.-P. XPS study of the surface chemistry on AZ31 and AZ91 magnesium alloys in dilute NaCl solution. *Appl. Surf. Sci.* **2010**, *256*, 5807-5812, https://doi.org/10.1016/j.apsusc.2010.02.058.
11. Walter, R.; Kannan, M.B. Influence of surface roughness on the corrosion behaviour of magnesium alloy. *Materials & Design* **2011**, *32*, 2350-2354, https://doi.org/10.1016/j.matdes.2010.12.016.
12. Aung, N.N.; Zhou, W. Effect of grain size and twins on corrosion behaviour of AZ31B magnesium alloy. *Corros. Sci.* **2010**, *52*, 589-594, https://doi.org/10.1016/j.corsci.2009.10.018.
13. Zhang, T.; Li, Y.; Wang, F. Roles of β phase in the corrosion process of AZ91D magnesium alloy. *Corros. Sci.* **2006**, *48*, 1249-1264, https://doi.org/10.1016/j.corsci.2005.05.011.
14. Jamaati, R.; Toroghinejad, M.R. High-strength and highly-uniform composite produced by anodizing and accumulative roll bonding processes. *Materials & Design* **2010**, *31*, 4816-4822, https://doi.org/10.1016/j.matdes.2010.04.048.
15. Shi, Z.; Liu, M.; Atrens, A. Measurement of the corrosion rate of magnesium alloys using Tafel extrapolation. *Corros. Sci.* **2010**, *52*, 579-588, https://doi.org/10.1016/j.corsci.2009.10.016.
16. Zhang, S.; Zhang, X.; Zhao, C.; Li, J.; Song, Y.; Xie, C.; Tao, H.; Zhang, Y.; He, Y.; Jiang, Y.; et al. Research on an Mg–Zn alloy as a degradable biomaterial. *Acta Biomater.* **2010**, *6*, 626-640, https://doi.org/10.1016/j.actbio.2009.06.028.
17. Chen, Y.-j.; Wang, Q.-d.; Lin, J.-b.; Liu, M.-p.; Hjelen, J.; Roven, H.J. Grain refinement of magnesium alloys processed by severe plastic deformation. *Transactions of Nonferrous Metals Society of China* **2014**, *24*, 3747-3754, https://doi.org/10.1016/S1003-6326(14)63528-7.
18. Liu, C.Y.; Jing, R.; Wang, Q.; Zhang, B.; Jia, Y.Z.; Ma, M.Z.; Liu, R.P. Fabrication of Al/Al3Mg2 composite by vacuum annealing and accumulative roll-bonding process. *Materials Science and Engineering: A* **2012**, *558*, 510-516, https://doi.org/10.1016/j.msea.2012.08.037.
19. R.J. Hebert, J.H. Perepezko: Scr. Mater. 50 (2004) 807–812.
20. Zarebidaki, A.; Mahmoudikohani, H.; Aboutalebi, M.-R. Microstructure and corrosion behavior of electrodeposited nano-crystalline nickel coating on AZ91 Mg alloy. *J. Alloys Compd.* **2014**, *615*, 825-830, https://doi.org/10.1016/j.jallcom.2014.07.046.
21. Pardo, A.; Merino, M.C.; Coy, A.E.; Arrabal, R.; Viejo, F.; Matykina, E. Corrosion behaviour of magnesium/aluminium alloys in 3.5wt.% NaCl. *Corros. Sci.* **2008**, *50*, 823-834, https://doi.org/10.1016/j.corsci.2007.11.005.
22. Zhao, M.-C.; Liu, M.; Song, G.; Atrens, A. Influence of the β-phase morphology on the corrosion of the Mg alloy AZ91. *Corros. Sci.* **2008**, *50*, 1939-1953, https://doi.org/10.1016/j.corsci.2008.04.010.
23. Bakkar, A.; Neubert, V. Corrosion characterisation of alumina–magnesium metal matrix composites. *Corros. Sci.* **2007**, *49*, 1110-1130, https://doi.org/10.1016/j.corsci.2006.07.002.
24. Brace, A.W. The technology of anodizing aluminium. **2000.**
25. Jilani, O.; Njah, N.; Ponthiaux, P. Corrosion properties of anodized aluminum: Effects of equal channel angular pressing prior to anodization. *Corros. Sci.* **2014**, *89*, 163-170, https://doi.org/10.1016/j.corsci.2014.08.020.

Hindawi

International Transactions on Electrical Energy Systems

Special Issue

Federated Learning for Sustainable Power Management in Smart Grid Networks

View this Special Issue

Research Article | Open Access

Volume 2022 | Article ID 2986605 | https://doi.org/10.1155/2022/2986605

Show citation

Renewable Energy Based Smart Grid Construction Using Hybrid Design in Control System with Enhancing of Energy Efficiency of Electronic Converters for Power Electronic in Electric Vehicles

Suhasini Sodagudi,[1] C Manjula,[2] M. S. Vinmathi,[3] R. Shekhar,[4] José Luis Arias Gonzáles,[5] C. Ramesh Kumar,[6] Gaurav Dhiman ,[7,8,9] and **A. R. Murali Dharan** [1,10]

Show more

Academic Editor: R Sitharthan

Published: 04 Oct 2022

Abstract

The power electronic interface is critical in matching a distributed generation (DG) unit's characteristics to grid requirements as most DG technologies rely on renewable energy. Increased adoption of electric vehicles (EV) is seen as a positive step toward minimizing air pollution as well as carbon emissions. Rapid proliferation of electric vehicles as well as charging stations has exacerbated voltage quality as well as harmonic distortion difficulties, which harm the efficiency of combined renewable energy. This research proposes novel hybrid design techniques in control systems that enhance the energy efficiency of electronic converters for power electronics. The control system enhancement has been carried out using a hybrid energy storage electric convertor, and energy efficiency is improved using a synergetic battery reference adaptive controller. A plug-in hybrid electric vehicle (PHEV)'s internal combustion engine with a small photovoltaic (PV) module is utilised to assess a proposed control method which effectively regulates electric power on-grid by draining electricity from batteries during peak hours as well as then

Hindawi

International Transactions on Electrical Energy Systems

1. Introduction

Traditional power systems use enormous power producing units that are geographically scattered to produce the majority of power, which is then routed to large consumption centres as well as distributed to various clients. This composition has begun to shift toward new scenarios in which DG units are scattered across distribution networks [1]. Wind turbines, photovoltaics, fuel cells, biomass, tiny hydro-plants, and other renewable resources are used in these DGs [2]. Through quick and efficient PEs converters and sustainable are linked to the smart grid (SG) for the advanced data collection infrastructure [3]. Plug-in HEVs (PHEVs) have been offered as a possible alternative because the charging efficiency of CS mode is primarily dependent on regenerative braking and gasoline. Unlike HEVs, PHEVs can also be charged externally using power outlets [4]. The majority of power in a PHEV comes from an EM, which serves as the primary source of power, with ICE serving as a backup. When battery SOC reaches a certain level, the PHEV switches to a standard HEV mode, and ICE becomes the primary power source. PHEVs have extended all-electric range, better local air quality as well as ability to connect to the grid [5]. The efficient performance of EVs depends on perfect synchronisation between ESs as well as power electronic converters. The primary picture of an EV in Figure 1 helps to understand the application as well as the interfacing of ESs and power electronic converters in EVs.

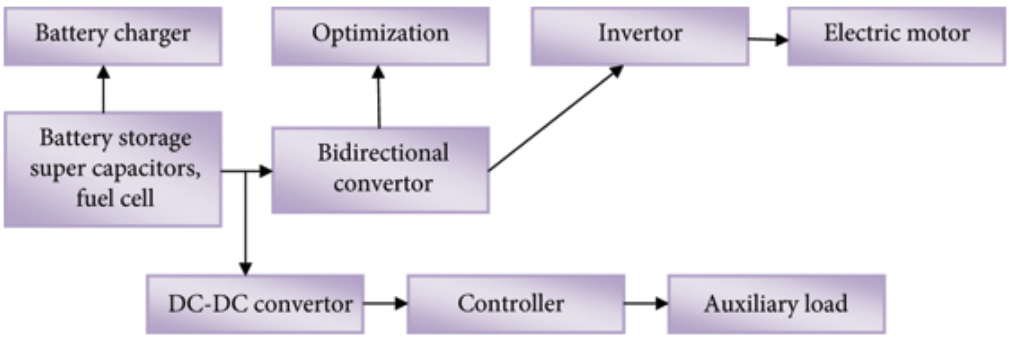

Figure 1

Architecture of interfacing and application of power electronic converters.

To build the internal structure of EVs, ESs types such as supercapacitors, batteries, and fuel cells, are combined with power electronic converters/inverters. ESs are protected from stray current harm by the inverter, which also functions as a motor controller as well as a filter. ESs delivers electricity with unstable characteristics and large voltage drops. It is efficiently addressed by DC-DC converters [6].

Contribution of this paper is as follows:

Hindawi

International Transactions on Electrical Energy Systems

(3) Designing a PHEV's internal combustion engine with a tiny photovoltaic (PV) module.

2. Related Works

HESS is primarily dependent on personal judgement and experience [7]. Researchers are experimenting with various combinations of energy sources to build an efficient HESS for HEVs. In HEVs, energy storage methods have primary and secondary energy sources [8]. The most prevalent fuel cell batteries are fuel cell-supercapacitor, battery-supercapacitor, and cell photovoltaic panels [9]. The primary energy source gives a long driving range, while the secondary energy source is only used when abrupt acceleration or braking is required [10]. The FC's high cost, as well as low power density, are two key drawbacks that prevent it from being utilised as an energy source. A supercapacitor (SC) is used as a supplementary energy source to balance the load from an FC [11]. SC's fundamental flaw is that it has a poor energy density [12]. [13] presented a battery-supercapacitor HESS; lithium-ion batteries' main drawbacks are their high cost as well as low energy density. Another stumbling block is that consumers must change batteries regularly, increasing the expense of HEVs. SC is utilised to capture energy loss as well as charge batteries in FC cars. A combined derived boost as well as a fly back converter design are presented [14] to achieve high voltage gain in fuel cell-based HEVs. A cascaded multiport converter for switching reluctance motors has been proposed for battery management as well as DC bus voltage adjustment [15]. A bidirectional DC-DC interleaved converter based on optimization is described [16] to minimize overshoots/undershoots in optimised switching functions. MIMO converters, as well as single bidirectional converter topologies, are introduced in HEVs. In the literature, numerous control methods for energy management as well as control of HEVs are proposed [17]. A GA-based fuzzy logic controller has been developed to increase the performance as well as fuel economy of fuel cell-based HEVs [18]. To manage power as well as maintain level of charge in battery, an adaptive fuzzy logic based controller for fuel energy management as well as battery-based HEVs was utilised [19]. To increase battery performance and prevent battery as well as fuel cell degradation, a predictive controller method has been introduced [20]. The energy management method in fuel cell vehicles includes a robust fuzzy model predictive controller [21, 22]. The most common type of main storage unit is lithium-ion batteries. Thermal runaway behaviour of lithium-ion batteries after overcharging is greatly influenced by diverse cell packaging configurations [23]. Furthermore, battery age prediction is required for the smooth as well as effective operation of coupled battery methods in electric cars. HESS's appropriate sizing is critical for increasing efficiency as well as extending the life of storage parts. The authors of [24] explore a multi-objective method for optimising overcharging aim as well as lowering the system's cost. Because UC has a higher power density than battery, a combination of battery as well as ultracapacitor (UC) may be a preferable solution [25]. The overall system performance will be cost-effective in a combined battery-UC-based HESS model, while battery life will be extended. Multiple control solutions are given in the literature; however, they all have localised control limits [26].

3. System Model

Environmental variables as well as load changes are studied to carry out renewable energy transmission on a transmission method. Environmental conditions, synchronisation and overloading are the main

Hindawi

International Transactions on Electrical Energy Systems

determines the flow of electrical energy based on the load demand.

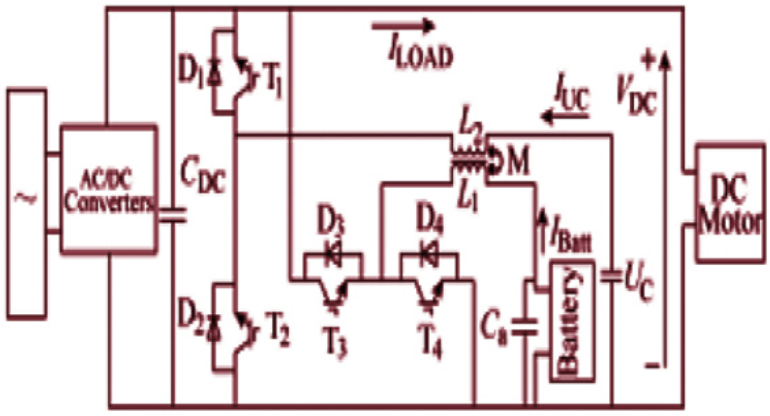

Figure 2

Topology of the hybrid energy storage structure.

Hybrid energy storage electric convertor (HESEC):

Physical, chemical, and EM energy storage devices are three types of energy storage devices. The essential speciation of most common energy storage devices is listed in Table 1.

Table 1

Main specifications of common energy storage.

Table 1 illustrates that a single energy storage device cannot unite power density and energy density and meet complex and variable power demands of electric vehicles. It is proposed that batteries as well as supercapacitors are employed to manage the EV power supply fluctuations. Te batterys high energy density ensures the EV range on a single charge, and the SCs can deliver a burst of high current to satisfy the peak power demands of electric vehicles, providing dynamic performance. The SC can absorb feedback energy more efficiently and quickly, improving the system's energy efficiency and protecting the battery from excessive current. A new power allocation approach is charging as well as discharging of the battery and SC.. The bidirectional DC/DC converter has a half-bridge architecture. A supercapacitor is an energy storage device that holds electric energy derived from various renewable energy sources. It's usually separated into two categories: piled and wound. The materials used in the electrodes have a significant impact on the energy storage capabilities of SCs. A spiral-wrapped SC with ordered mesoporous carbon electrodes was utilised in this investigation. The SC structure is depicted in Figure 3.

Hindawi

International Transactions on Electrical Energy Systems

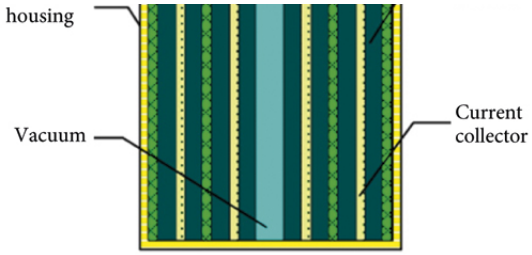

Figure 3

SC Structure diagram.

A cascade voltage as well as a current controller are chosen to maintain a consistent load voltage. Super-capacitors can respond more quickly and recycle braking energy when the DC side voltage rises significantly during braking. The supercapacitor controller's control structure is given in Figure 3.

V_{dc} and $V_{dc\text{-}sen}$ are actual as well as rated voltages of a DC motor, respectively; * UC I and * UC sen I are per unit actual and rated currents of a super-capacitor, respectively; fs is switching frequency, and $G_{1,2}$ are switching signals of T_1 and T_2. Duty cycle of the inductor current transfer function in boost mode is represented as :

$$\frac{I_{L2(s)}}{D(s)} \tag{1}$$

$$\frac{I_{L2(s)}}{D(s)} = \frac{V_{dc}R_{\text{Load}}C_{dc}s + 2V_{dc}}{R_{\text{Load}}L_2C_{dc}s^2 + L_2s + R_{\text{Load}}(1-D)^2}. = \frac{V_{dc}R_{\text{Load}}C_{dc}s + 2V_{dc}}{R_{\text{Load}}L_2C_{dc}s^2 + L_2s + R_{\text{Load}}(1-D)^2}. \tag{1}$$

The reference current of L_2 is IL2(s), the DC motor voltage is V_{dc}, the capacitor DC motor is C_{dc}, and the duty cycle is D.

In contrast to the nonisolated DC/DC converter used earlier, the DC/DC converter utilizes a composite converter with an isolated soft switch. Switching to an isolated converter during a rapid rise in current can protect the energy storage system from harm caused by direct electrical connections. Figure 4 shows how the DC/DC converter performs in the boost method during discharge as well as buck mode during energy feedback under normal working conditions.

Hindawi

International Transactions on Electrical Energy Systems

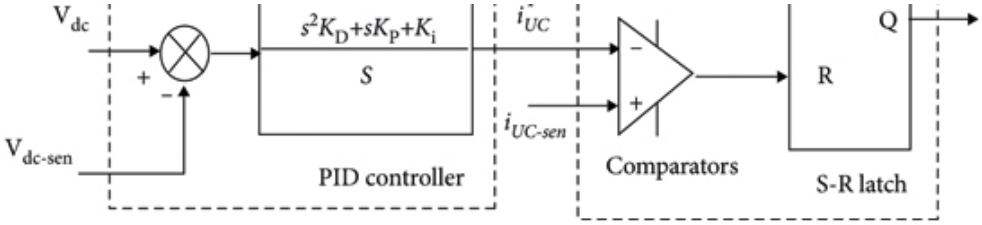

Figure 4

Topology of a DC/DC converter with an integrated magnetic structure.

This research utilizes an E-type magnetic core to achieve magnetic element integration. A coupling inductance (L_1 and L_2) is employed in this example. L_2 is output filter inductor, L_1 is external inductance, and Ca is the extra capacitance, as illustrated in Figure 5. Ca's voltage is identical to the output voltages of L_2 and L_1 in steady-state, regardless of the capacitor voltage ripple. Figure 4 shows a DC/DC converter with four IGBT switches (T_1~T_4) and four diodes (D_1~D_4). Two operating modes for a boost converter and three operational modes for a buck converter. Furthermore, output current ripple is minimized by using an integrated magnetic design.

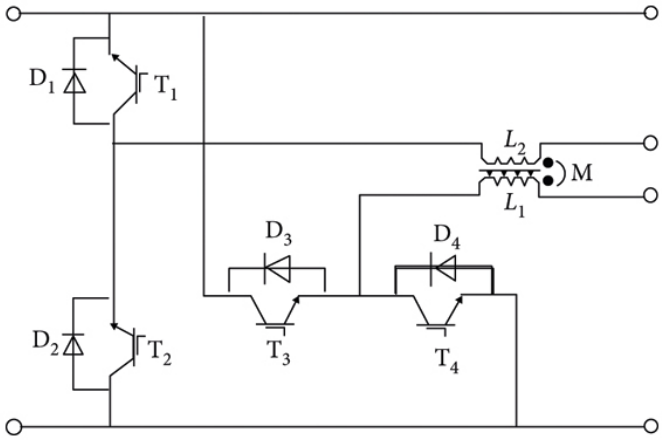

Figure 5

Block diagram of the supercapacitor voltage and current controller.

In order to highlight the operating principle of the proposed HESEC, reference should be made to overall DC-link voltage and energy time-variations. These can be achieved based on (2) and (3):

Hindawi

International Transactions on Electrical Energy Systems

link and the electrical drive, respectively. Referring to (5), CDC denotes equivalent DC-link series capacitance, whereas cH and cL are per unit capacitances in

$$C_{DC} = \frac{C_H C_L}{C_H + C_L}, c_H = \frac{C_H}{C_H + C_L}, c_L = \frac{C_L}{C_H + C_L}. \tag{4}$$

$$C_{DC} = \frac{C_H C_L}{C_H + C_L}, c_H = \frac{C_H}{C_H + C_L}, c_L = \frac{C_L}{C_H + C_L}. \tag{4}$$

Similarly, vH and vL reported in (5) represent the per unit capacitor voltages:

$$v_H = \frac{V_H}{V_H + V_L}, v_L = \frac{V_L}{V_H + V_L}. \tag{5}$$

Still referring to both (4) and (5), it can be stated that VDC and EDC can be varied independently if suitable combinations of (c_H, c_L) and (vH, vL) occur. As a result, the DC-link energy content can be changed without affecting the overall DC-link voltage: this is the fundamental concept based on which the proposed HESEC is developed. To corroborate the previous statement, DC-link energy base value can be introduced as

$$E'_{DC} = \frac{l}{2} C_L V_{DC}^2. \tag{6}$$

Therefore, dividing (4) by (6), per unit energy content of DC-link is easily attained as (7) where in which ζ denotes the unbalance capacitance factor (8):

$$e_{DC} = \zeta v_H^2 + (I - v_u)^2, \tag{7}$$

$$\zeta = \frac{C_H}{C_L}. \tag{8}$$

Hence, DC-link voltage unbalances can be usefully introduced by varying the UC voltage within a given range, thus varying the overall DC-link energy content without affecting its overall voltage. As a result, appropriate DC-link energy and voltage regulations enable optimal energy flow management among each HESEC component.

4. Synergetic Battery Reference Adaptive Controller (SBRAC)

The PHEV model was developed by ultilizing basic electric current as well as voltage rules across energy sources and power converters. The speed of an induction motor whose load torque is directly connected with rotor flux is controlled using a field oriented control technique. The circuit diagram of PHEV's unified method is represented in Figure 6.

Hindawi

International Transactions on Electrical Energy Systems

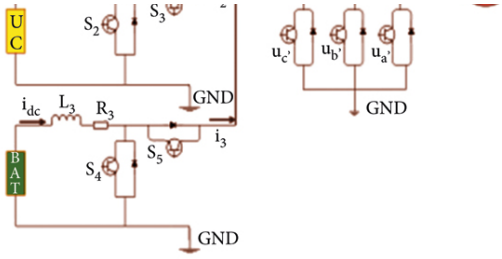

Figure 6

Electric circuit diagram of PHEV.

To overcome all of the difficulties above and achieve our desired response, an approach based on adaptive terminal sliding management of PHEV is provided. The general flow of PHEVs is depicted in Figure 7, which includes a charging unit, battery, mutual DC bus, UC bank, and load. An unregulated bridge rectifier and a DC-DC buck converter are connected to the mains supply to improve the charge of the battery using the charger. Bidirectional DC-DC buck-boost converters are utilised in the HESS model to connect the PHEV's power sources to the DC voltage line. The complete PHEV control system is split into two levels:

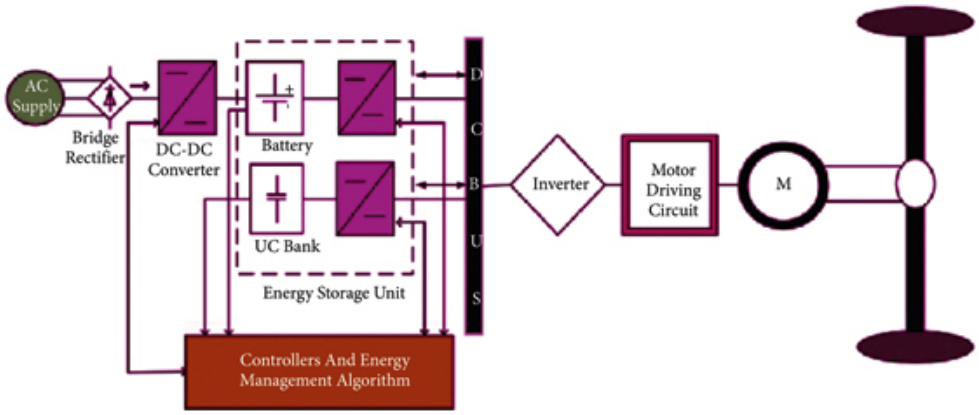

Figure 7

General block diagram of PHEV.

Low-level control: This entails controlling power converters to regulate the DC bus and allowing current to flow in both directions at a localised level.

Hindawi

International Transactions on Electrical Energy Systems

$$S = \frac{Ch}{Ch_{\text{nom}}}, \tag{9}$$

where S is SoC, Ch is the battery's absolute capacity in "A_h," and Chnom is the battery's nominal "A_h" capacity. Following (10) and (11) are utilised to detect fact of active and reactive grid powers during charging method of a PHEV.

$$P_{\text{grid}}(S) = VI \cos \phi(S), \tag{10}$$

$$P_{\text{grid}}(S) = VI \sin \phi(S), \tag{11}$$

where P_{grid} is the grid power, ϕ is the power factor, and V and I are grid voltage and current.Consider charging source's effectiveness, DC voltage is represented in AC power as

$$P_{ch}(S) = \eta \left[VI \cos \phi(S)\right], \tag{12}$$

where, η is the charging source's efficiency and P_{ch} is the charger's power. An integrated charging source has been modelled in this section, which comprises an AC supply linked with a boost converter and a regulated buck converter, as shown in Figure 8. Furthermore, an adaptive nonlinear controller was developed to manage charge flow and estimate unknown parameters (R_1, C_1). The charging source, as directed by the high level controller, provides instantaneous power to the battery linked in a HESS method of controlled buck converter is constructed, as shown in (13) and (14):

$$\frac{dx_1}{dt} = \frac{V_g}{L_1}u_1 - \frac{x_2}{L_1}, \tag{13}$$

$$\frac{dx_2}{dt} = \frac{x_1}{C_1} - \frac{V_g}{R_1 C_1}u_1, \tag{14}$$

where x_1 is average inductor current I_{L1}, x_2 is average output.

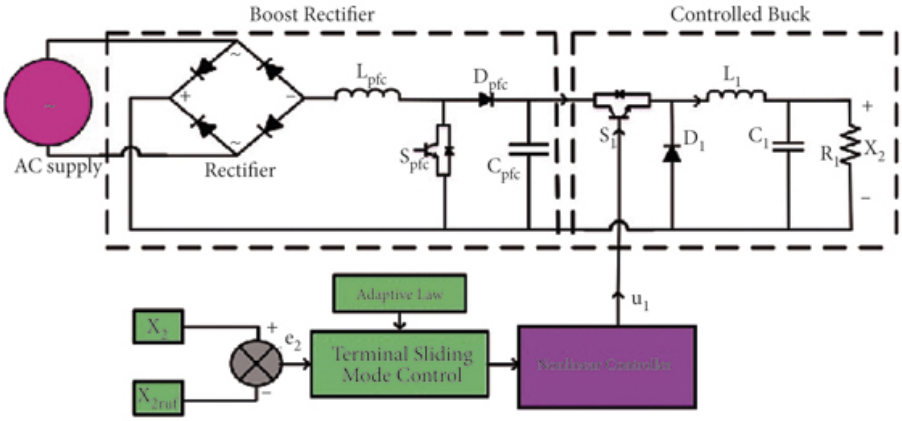

Figure 8

Hindawi

International Transactions on Electrical Energy Systems

Simulations on MATLAB/Simulink were used to test the validity of all of the suggested controllers, which were subjected to the normal European extra urban driving cycle to guarantee that the necessary control objectives were met. Tables 2–4 provide detailed information on energy sources, 3-phase induction, motors power converters and vehicle under consideration. Proposed controllers' design parameters were chosen using a hit-and-miss approach. Table 5 shows the parameters of the HESEC model.

Table 2

Energy sources data.

Table 3

Power converters data.

Table 4

Parameters of smart charging source.

Table 5

Parameters of HESEC model.

The above Table 6 shows comparative analysis based on constant acceleration and time-varying acceleration cases. Here the parameters compared are battery current, ultra-capacitor current, charging voltage, DC load current, and battery SOC. All the parameters have been analysed based on hybrid design in control systems enhancing the energy efficiency of electronic converters for power electronics.

Table 6

Comparative analysis is based on the constant acceleration case and the time varying acceleration case.

The above Figures 9 and 10 show comparative analysis of constant acceleration and time-varying acceleration case. Here for both cases, the proposed technique obtained optimal results in developing hybrid designs in control system while enhancing the energy efficiency of electronic converters for power electronics. The proposed technique in the constant acceleration case obtained a battery current of 92 Amps, ultracapacitor current of 89 Amps, charging voltage of 88 V, DC load current of 85 Amps, battery

Hindawi

International Transactions on Electrical Energy Systems

90 Amps, ultra-capacitor current of 85 Amps, charging voltage of 85 V, DC load current of 68 Amps, battery SOC of 74%; HEV obtained battery current of 92 Amps, ultra-capacitor current of 89 Amps, charging voltage of 89 V, DC load current of 78 Amps, battery SOC of 79%. From the above analysis, the proposed technique obtained optimal results in enhancing the energy efficiency of electronic converters for power electronics.

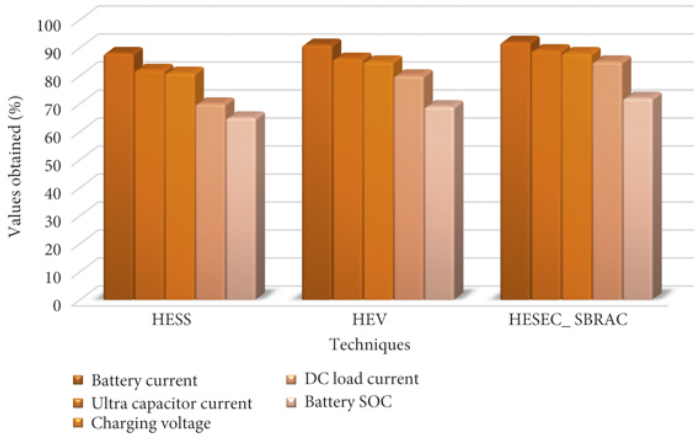

Figure 9

Comparative analysis of the constant acceleration case.

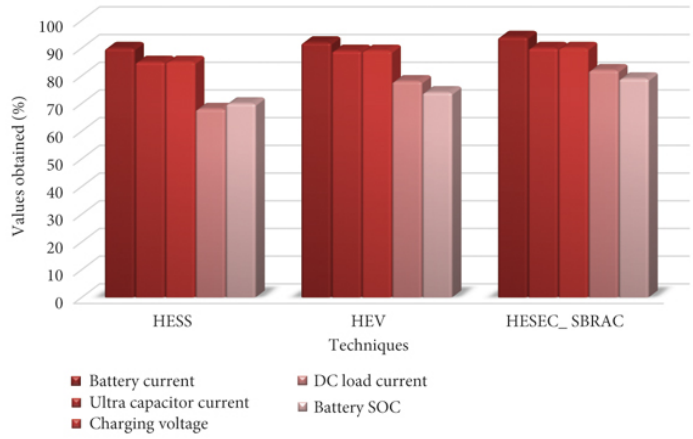

Figure 10

Comparative analysis of the constant acceleration case.

Hindawi

International Transactions on Electrical Energy Systems

synergetic battery reference adaptive controller. A PHEV's internal combustion engine with a small photovoltaic (PV) module is shown here. The effectiveness of the suggested control system's energy management is evaluated using simulations. By drawing power from batteries during peak hours and then recharging them during off-peak hours, the suggested method efficiently manages the grid's supply of electricity. This reduces the load on the converter and enables electric vehicles to charge more quickly. Regardless of changes in renewable energy supply and load, the system maintains a steady voltage. Experimental results show Constant acceleration case obtained battery current of 92 Amps, ultra-capacitor current of 89 Amps, charging voltage of 88 V, DC load current of 85 Amps, battery SOC of 72% and time-varying acceleration proposed technique obtained current of 94 Amps, ultracapacitor current of 90 Amps, charging voltage of 90 V, DC load current of 82 Amps, battery SOC of 79%.

Data Availability

The data will be avaible by corresponding author upon request.

Conflicts of Interest

The authors declare that they have no conflicts of interest.

References

1. D. Yuan, M. Sun, M. Zhao et al., "Persulfate promoted ZnIn2S4 visible light photocatalytic dye decomposition," *International Journal of Electrochemical Science*, vol. 15, pp. 8761–8770, 2020.
View at: Publisher Site | Google Scholar

2. X. Feng, Y. Zhang, L. Kang et al., "Integrated energy storage system based on triboelectric nanogenerator in electronic devices," *Frontiers of Chemical Science and Engineering*, vol. 15, no. 2, pp. 238–250, 2020.
View at: Publisher Site | Google Scholar

3. C. Y. Bu, F. J. Li, K. Yin, J. B. Pang, L. C. Wang, and K. Wang, "Research progress and prospect of triboelectric nanogenerators as self-powered human body sensors," *ACS Appl. Electron. Mater.*, vol. 2, no. 4, pp. 863–878, 2020.
View at: Publisher Site | Google Scholar

4. G. T. Xia, Y. N. Huang, F. J. Li et al., "A thermally flexible and multi-site tactile sensor for remote 3D dynamic sensing imaging," *Frontiers of Chemical Science and Engineering*, vol. 14, no. 6, pp. 1039–1051, 2020.
View at: Publisher Site | Google Scholar

5. W. L. Wang, Y. H. Li, L. W. Li, L. C. Wang, and K. Wang, "Nanoparticle structure for flexible quasi-solid-state lithium-ion batteries," *International Journal of Electrochemical Science*, vol. 15,

Hindawi

International Transactions on Electrical Energy Systems

lithium-ion batteries," *Energies*, vol. 14, no. 22, 2021.
View at: Publisher Site | Google Scholar

7. F. Mumtaz, N. Zaihar Yahaya, S. Tanzim Meraj, B. Singh, R. Kannan, and O. Ibrahim, "Review on non-isolated DC-DC converters and their control techniques for renewable energy applications," *Ain Shams Engineering Journal*, vol. 12, no. 4, pp. 3747–3763, 2021.
View at: Publisher Site | Google Scholar

8. C. Akkaldevi, S. D. Chitta, J. Jaidi, S. Panchal, M. Fowler, and R. Fraser, "Coupled electrochemical-thermal simulations and validation of minichannel cold-plate water-cooled prismatic 20 ah $LiFePO_4$ battery," *Electrochemistry (Tokyo, Japan)*, vol. 2, no. 4, pp. 643–663, 2021.
View at: Publisher Site | Google Scholar

9. K. Purohit, S. Srivastava, V. Nookala et al., "Soft sensors for state of charge, state of energy, and power loss in formula student electric vehicle," *Applied System Innovation*, vol. 4, pp. 78–85, 2021.
View at: Publisher Site | Google Scholar

10. V. G. Choudhari, A. S. Dhoble, S. Panchal, M. Fowler, and R. Fraser, "Numerical investigation on thermal behaviour of 5 × 5 cell configured battery pack using phase change material and fin structure layout," *Journal of Energy Storage*, vol. 43, Article ID 103234, 2021.
View at: Publisher Site | Google Scholar

11. K. Liu, Z. Yang, X. Tang, and W. Cao, "Automotive battery equalizers based on joint switched-capacitor and buck-boost converters," *IEEE Transactions on Vehicular Technology*, vol. 69, no. 11, pp. 12716–12724, 2020.
View at: Publisher Site | Google Scholar

12. Y. Shang, K. Liu, N. Cui, N. Wang, K. Li, and C. Zhang, "A compact resonant switched-capacitor heater for lithium-ion battery self-heating at low temperatures," *IEEE Transactions on Power Electronics*, vol. 35, no. 7, pp. 7134–7144, 2020.
View at: Publisher Site | Google Scholar

13. Y. Shang, K. Liu, N. Cui, Q. Zhang, and C. Zhang, "A sine-wave heating circuit for automotive battery self-heating at subzero temperatures," *IEEE Transactions on Industrial Informatics*, vol. 16, no. 5, pp. 3355–3365, 2020.
View at: Publisher Site | Google Scholar

14. K. Liu, X. Hu, H. Zhou, L. Tong, W. D. Widanage, and J. Marco, "Feature analyses and modeling of lithium-ion battery manufacturing based on random forest classification," *IEEE*, vol. 26, no. 6, pp. 2944–2955, 2021.
View at: Publisher Site | Google Scholar

Hindawi

International Transactions on Electrical Energy Systems

16. K. Wang, W. Wang, L. Wang, and L. Li, "An improved SOC control strategy for electric vehicle hybrid energy storage systems," *Energies*, vol. 13, no. 20, Article ID 5297, 2020.
View at: Publisher Site | Google Scholar

17. M. K. Azeem, H. Armghan, Z. e. Huma, I. Ahmad, and M. Hassan, "Multistage adaptive nonlinear control of battery-ultracapacitor based plugin hybrid electric vehicles," *Journal of Energy Storage*, vol. 32, Article ID 101813, 2020.
View at: Publisher Site | Google Scholar

18. M. S. Nazir, I. Ahmad, M. J. Khan, Y. Ayaz, and H. Armghan, "Adaptive control of fuel cell and supercapacitor based hybrid electric vehicles," *Energies*, vol. 13, no. 21, Article ID 5587, 2020.
View at: Publisher Site | Google Scholar

19. M. M. Islam, S. A. Siffat, I. Ahmad, M. Liaquat, and S. A. Khan, "Adaptive nonlinear control of unified model of fuel cell, battery, ultracapacitor and induction motor based hybrid electric vehicles," *IEEE Access*, vol. 9, pp. 57486–57509, 2021.
View at: Publisher Site | Google Scholar

20. F. Eroğlu, M. Kurtoğlu, and A. M. Vural, "Bidirectional DC–DC converter based multilevel battery storage systems for electric ˇ vehicle and large-scale grid applications a critical review considering different topologies, state-of-charge balancing and future trends," *IET Renewable Power Generation*, vol. 15, no. 5, pp. 915–938, 2021.
View at: Publisher Site | Google Scholar

21. M. Bortoluzzi, C. Correia de Souza, and M. Furlan, "Bibliometric analysis of renewable energy types using key performance indicators and multicriteria decision models," *Renewable and Sustainable Energy Reviews*, vol. 143, Article ID 110958, 2021.
View at: Publisher Site | Google Scholar

22. M. S. Miah, M. S. Hossain Lipu, S. T. Meraj et al., "Optimized energy management schemes for electric vehicle applications a bibliometric analysis towards future trends," *Sustainability*, vol. 13, no. 22, Article ID 12800, 2021.
View at: Publisher Site | Google Scholar

23. A. Katnapally, U. B. Manthati, A. Chirayarukil Raveendran, and S. Punna, "A predictive power management scheme for hybrid energy storage system in electric vehicle," *International Journal of Circuit Theory and Applications*, vol. 49, no. 11, pp. 3864–3878, 2021.
View at: Publisher Site | Google Scholar

24. J. Fang, H. Deng, N. Tashakor, F. Blaabjerg, and S. M. Goetz, "State-space modeling and control of grid-tied power converters with capacitive/battery energy storage and grid-supportive services," *IEEE Journal of Emerging and Selected Topics in Power Electronics*, vol. 19, pp. 1–17, 2021.
View at: Publisher Site | Google Scholar

Hindawi

International Transactions on Electrical Energy Systems

bidirectional DC-DC converter with intrinsic equal current sharing characteristic for electric vehicles," *IEEE Transactions on Industrial Electronics*, vol. 68, no. 2, pp. 1803–1813, 2021.
View at: Publisher Site | Google Scholar

Copyright

More related articles

High-Voltage Topological Architecture-Based Energy Management Strategy of the Plug-In Hybrid Powertrain System

Ziliang Zhao | Jun Zhao | ... | Rifei Lai

Hindawi

International Transactions on Electrical Energy Systems

DC/DC Modular Multilevel Converters for HVDC Interconnection: A Comprehensive Review

Hindawi

International Transactions on Electrical Energy Systems

Related articles

An Efficient Energy Management Scheme for an Islanded DC Microgrid with Hybrid VRFB System

S. Hameed | I. Prabhakar Reddy | ... | Aruna rai Vadde

Hybrid Renewable Power Generation for Modeling and Controlling the Battery Storage Photovoltaic System

Mohd Mustafa | G. Anandhakumar | ... | S. Arockia Jayadhas

Autonomous Multiport Solar Power Plant with Lithium Ion Battery Storage Using a Voltage Source Inverter for Automotive Applications

P. Vijayashankarganth | S. Sathish Kumar | ... | Martin Sankoh

Hindawi

International Transactions on Electrical Energy Systems

Hindawi

International Transactions on Electrical Energy Systems

Special Issue

Federated Learning for Sustainable Power Management in Smart Grid Networks

View this Special Issue

Research Article | Open Access

Volume 2022 | Article ID 2986605 | https://doi.org/10.1155/2022/2986605

Show citation

Renewable Energy Based Smart Grid Construction Using Hybrid Design in Control System with Enhancing of Energy Efficiency of Electronic Converters for Power Electronic in Electric Vehicles

Suhasini Sodagudi,[1] C Manjula,[2] M. S. Vinmathi,[3] R. Shekhar,[4] José Luis Arias Gonzáles,[5] C. Ramesh Kumar,[6] Gaurav Dhiman ,[7,8,9] and **A. R. Murali Dharan** [1,10]

Show more

Academic Editor: R Sitharthan

Published: 04 Oct 2022

Abstract

The power electronic interface is critical in matching a distributed generation (DG) unit's characteristics to grid requirements as most DG technologies rely on renewable energy. Increased adoption of electric vehicles (EV) is seen as a positive step toward minimizing air pollution as well as carbon emissions. Rapid proliferation of electric vehicles as well as charging stations has exacerbated voltage quality as well as harmonic distortion difficulties, which harm the efficiency of combined renewable energy. This research proposes novel hybrid design techniques in control systems that enhance the energy efficiency of electronic converters for power electronics. The control system enhancement has been carried out using a hybrid energy storage electric convertor, and energy efficiency is improved using a synergetic battery reference adaptive controller. A plug-in hybrid electric vehicle (PHEV)'s internal combustion engine with a small photovoltaic (PV) module is utilised to assess a proposed control method which effectively regulates electric power on-grid by draining electricity from batteries during peak hours as well as then

Hindawi

International Transactions on Electrical Energy Systems

1. Introduction

Traditional power systems use enormous power producing units that are geographically scattered to produce the majority of power, which is then routed to large consumption centres as well as distributed to various clients. This composition has begun to shift toward new scenarios in which DG units are scattered across distribution networks [1]. Wind turbines, photovoltaics, fuel cells, biomass, tiny hydro-plants, and other renewable resources are used in these DGs [2]. Through quick and efficient PEs converters and sustainable are linked to the smart grid (SG) for the advanced data collection infrastructure [3]. Plug-in HEVs (PHEVs) have been offered as a possible alternative because the charging efficiency of CS mode is primarily dependent on regenerative braking and gasoline. Unlike HEVs, PHEVs can also be charged externally using power outlets [4]. The majority of power in a PHEV comes from an EM, which serves as the primary source of power, with ICE serving as a backup. When battery SOC reaches a certain level, the PHEV switches to a standard HEV mode, and ICE becomes the primary power source. PHEVs have extended all-electric range, better local air quality as well as ability to connect to the grid [5]. The efficient performance of EVs depends on perfect synchronisation between ESs as well as power electronic converters. The primary picture of an EV in Figure 1 helps to understand the application as well as the interfacing of ESs and power electronic converters in EVs.

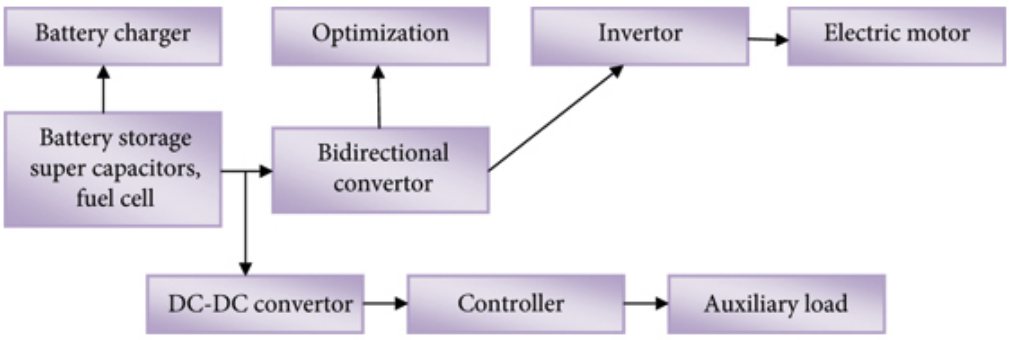

Figure 1

Architecture of interfacing and application of power electronic converters.

To build the internal structure of EVs, ESs types such as supercapacitors, batteries, and fuel cells, are combined with power electronic converters/inverters. ESs are protected from stray current harm by the inverter, which also functions as a motor controller as well as a filter. ESs delivers electricity with unstable characteristics and large voltage drops. It is efficiently addressed by DC-DC converters [6].

Contribution of this paper is as follows:

Hindawi

International Transactions on Electrical Energy Systems

(3) Designing a PHEV's internal combustion engine with a tiny photovoltaic (PV) module.

2. Related Works

HESS is primarily dependent on personal judgement and experience [7]. Researchers are experimenting with various combinations of energy sources to build an efficient HESS for HEVs. In HEVs, energy storage methods have primary and secondary energy sources [8]. The most prevalent fuel cell batteries are fuel cell-supercapacitor, battery-supercapacitor, and cell photovoltaic panels [9]. The primary energy source gives a long driving range, while the secondary energy source is only used when abrupt acceleration or braking is required [10]. The FC's high cost, as well as low power density, are two key drawbacks that prevent it from being utilised as an energy source. A supercapacitor (SC) is used as a supplementary energy source to balance the load from an FC [11]. SC's fundamental flaw is that it has a poor energy density [12]. [13] presented a battery-supercapacitor HESS; lithium-ion batteries' main drawbacks are their high cost as well as low energy density. Another stumbling block is that consumers must change batteries regularly, increasing the expense of HEVs. SC is utilised to capture energy loss as well as charge batteries in FC cars. A combined derived boost as well as a fly back converter design are presented [14] to achieve high voltage gain in fuel cell-based HEVs. A cascaded multiport converter for switching reluctance motors has been proposed for battery management as well as DC bus voltage adjustment [15]. A bidirectional DC-DC interleaved converter based on optimization is described [16] to minimize overshoots/undershoots in optimised switching functions. MIMO converters, as well as single bidirectional converter topologies, are introduced in HEVs. In the literature, numerous control methods for energy management as well as control of HEVs are proposed [17]. A GA-based fuzzy logic controller has been developed to increase the performance as well as fuel economy of fuel cell-based HEVs [18]. To manage power as well as maintain level of charge in battery, an adaptive fuzzy logic based controller for fuel energy management as well as battery-based HEVs was utilised [19]. To increase battery performance and prevent battery as well as fuel cell degradation, a predictive controller method has been introduced [20]. The energy management method in fuel cell vehicles includes a robust fuzzy model predictive controller [21, 22]. The most common type of main storage unit is lithium-ion batteries. Thermal runaway behaviour of lithium-ion batteries after overcharging is greatly influenced by diverse cell packaging configurations [23]. Furthermore, battery age prediction is required for the smooth as well as effective operation of coupled battery methods in electric cars. HESS's appropriate sizing is critical for increasing efficiency as well as extending the life of storage parts. The authors of [24] explore a multi-objective method for optimising overcharging aim as well as lowering the system's cost. Because UC has a higher power density than battery, a combination of battery as well as ultracapacitor (UC) may be a preferable solution [25]. The overall system performance will be cost-effective in a combined battery-UC-based HESS model, while battery life will be extended. Multiple control solutions are given in the literature; however, they all have localised control limits [26].

3. System Model

Environmental variables as well as load changes are studied to carry out renewable energy transmission on a transmission method. Environmental conditions, synchronisation and overloading are the main

Hindawi

International Transactions on Electrical Energy Systems

determines the flow of electrical energy based on the load demand.

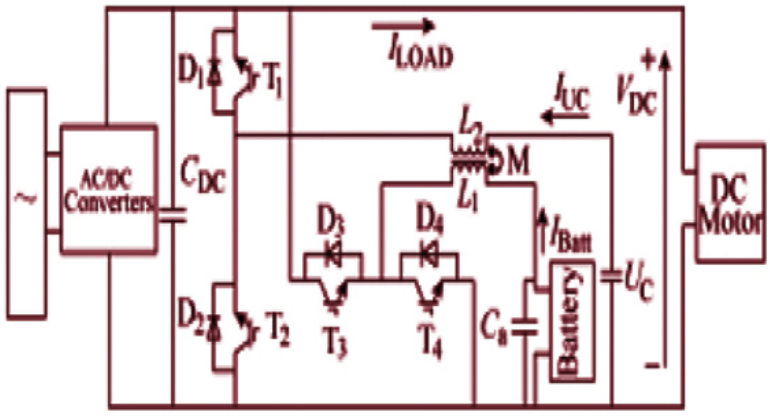

Figure 2

Topology of the hybrid energy storage structure.

Hybrid energy storage electric convertor (HESEC):

Physical, chemical, and EM energy storage devices are three types of energy storage devices. The essential speciation of most common energy storage devices is listed in Table 1.

Table 1

Main specifications of common energy storage.

Table 1 illustrates that a single energy storage device cannot unite power density and energy density and meet complex and variable power demands of electric vehicles. It is proposed that batteries as well as supercapacitors are employed to manage the EV power supply fluctuations. Te batterys high energy density ensures the EV range on a single charge, and the SCs can deliver a burst of high current to satisfy the peak power demands of electric vehicles, providing dynamic performance. The SC can absorb feedback energy more efficiently and quickly, improving the system's energy efficiency and protecting the battery from excessive current. A new power allocation approach is charging as well as discharging of the battery and SC.. The bidirectional DC/DC converter has a half-bridge architecture. A supercapacitor is an energy storage device that holds electric energy derived from various renewable energy sources. It's usually separated into two categories: piled and wound. The materials used in the electrodes have a significant impact on the energy storage capabilities of SCs. A spiral-wrapped SC with ordered mesoporous carbon electrodes was utilised in this investigation. The SC structure is depicted in Figure 3.

Hindawi

International Transactions on Electrical Energy Systems

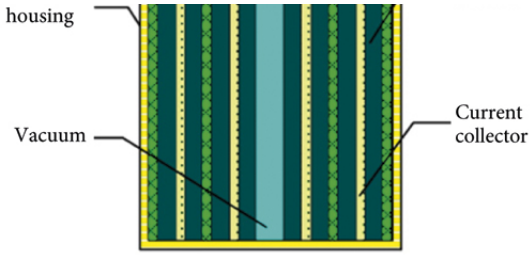

Figure 3

SC Structure diagram.

A cascade voltage as well as a current controller are chosen to maintain a consistent load voltage. Supercapacitors can respond more quickly and recycle braking energy when the DC side voltage rises significantly during braking. The supercapacitor controller's control structure is given in Figure 3.

V_{dc} and $V_{dc\text{-}sen}$ are actual as well as rated voltages of a DC motor, respectively; * UC I and * UC sen I are per unit actual and rated currents of a super-capacitor, respectively; fs is switching frequency, and $G_{1,2}$ are switching signals of T_1 and T_2. Duty cycle of the inductor current transfer function in boost mode is represented as :

$$\frac{I_{L2(s)}}{D(s)} \tag{1}$$

$$\frac{I_{L2(s)}}{D(s)} = \frac{V_{dc}R_{\text{Load}}C_{dc}s + 2V_{dc}}{R_{\text{Load}}L_2C_{dc}s^2 + L_2s + R_{\text{Load}}(1-D)^2}. = \frac{V_{dc}R_{\text{Load}}C_{dc}s + 2V_{dc}}{R_{\text{Load}}L_2C_{dc}s^2 + L_2s + R_{\text{Load}}(1-D)^2}. \tag{1}$$

The reference current of L_2 is IL2(s), the DC motor voltage is V_{dc}, the capacitor DC motor is C_{dc}, and the duty cycle is D.

In contrast to the nonisolated DC/DC converter used earlier, the DC/DC converter utilizes a composite converter with an isolated soft switch. Switching to an isolated converter during a rapid rise in current can protect the energy storage system from harm caused by direct electrical connections. Figure 4 shows how the DC/DC converter performs in the boost method during discharge as well as buck mode during energy feedback under normal working conditions.

Hindawi

International Transactions on Electrical Energy Systems

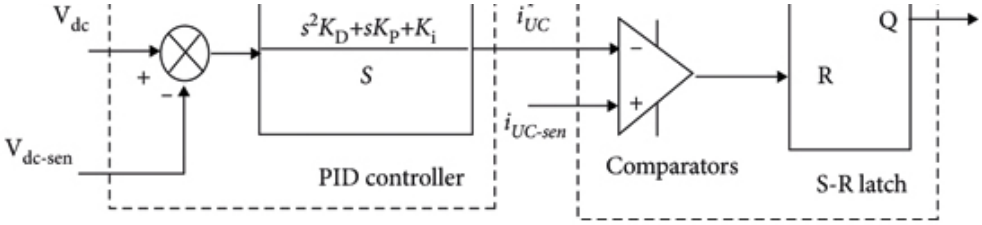

Figure 4

Topology of a DC/DC converter with an integrated magnetic structure.

This research utilizes an E-type magnetic core to achieve magnetic element integration. A coupling inductance (L_1 and L_2) is employed in this example. L_2 is output filter inductor, L_1 is external inductance, and Ca is the extra capacitance, as illustrated in Figure 5. Ca's voltage is identical to the output voltages of L_2 and L_1 in steady-state, regardless of the capacitor voltage ripple. Figure 4 shows a DC/DC converter with four IGBT switches (T_1~T_4) and four diodes (D_1~D_4). Two operating modes for a boost converter and three operational modes for a buck converter. Furthermore, output current ripple is minimized by using an integrated magnetic design.

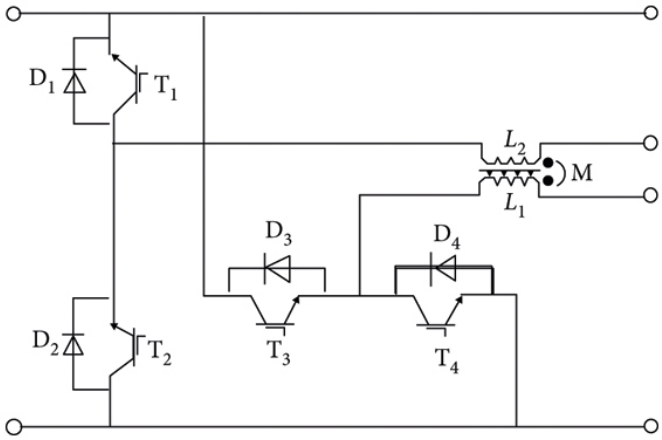

Figure 5

Block diagram of the supercapacitor voltage and current controller.

In order to highlight the operating principle of the proposed HESEC, reference should be made to overall DC-link voltage and energy time-variations. These can be achieved based on (2) and (3):

Hindawi

International Transactions on Electrical Energy Systems

link and the electrical drive, respectively. Referring to (5), CDC denotes equivalent DC-link series capacitance, whereas cH and cL are per unit capacitances in

$$C_{DC} = \frac{C_H C_L}{C_H + C_L}, c_H = \frac{C_H}{C_H + C_L}, c_L \quad (4)$$

$$C_{DC} = \frac{C_H C_L}{C_H + C_L}, c_H = \frac{C_H}{C_H + C_L}, c_L = \frac{C_L}{C_H + C_L}. \quad (4)$$

Similarly, vH and vL reported in (5) represent the per unit capacitor voltages:

$$v_H = \frac{V_H}{V_H + V_L}, v_L = \frac{V_L}{V_H + V_L}. \quad (5)$$

Still referring to both (4) and (5), it can be stated that VDC and EDC can be varied independently if suitable combinations of (c_H, c_L) and (vH, vL) occur. As a result, the DC-link energy content can be changed without affecting the overall DC-link voltage: this is the fundamental concept based on which the proposed HESEC is developed. To corroborate the previous statement, DC-link energy base value can be introduced as

$$E'_{DC} = \frac{l}{2} C_L V_{DC}^2. \quad (6)$$

Therefore, dividing (4) by (6), per unit energy content of DC-link is easily attained as (7) where in which ζ denotes the unbalance capacitance factor (8):

$$e_{DC} = \zeta v_H^2 + (I - v_u)^2, \quad (7)(8)$$

$$\zeta = \frac{C_H}{C_L}.$$

Hence, DC-link voltage unbalances can be usefully introduced by varying the UC voltage within a given range, thus varying the overall DC-link energy content without affecting its overall voltage. As a result, appropriate DC-link energy and voltage regulations enable optimal energy flow management among each HESEC component.

4. Synergetic Battery Reference Adaptive Controller (SBRAC)

The PHEV model was developed by ultilizing basic electric current as well as voltage rules across energy sources and power converters. The speed of an induction motor whose load torque is directly connected with rotor flux is controlled using a field oriented control technique. The circuit diagram of PHEV's unified method is represented in Figure 6.

Hindawi

International Transactions on Electrical Energy Systems

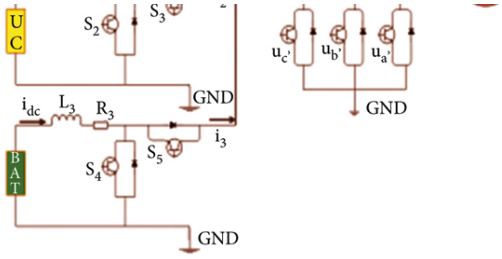

Figure 6

Electric circuit diagram of PHEV.

To overcome all of the difficulties above and achieve our desired response, an approach based on adaptive terminal sliding management of PHEV is provided. The general flow of PHEVs is depicted in Figure 7, which includes a charging unit, battery, mutual DC bus, UC bank, and load. An unregulated bridge rectifier and a DC-DC buck converter are connected to the mains supply to improve the charge of the battery using the charger. Bidirectional DC-DC buck-boost converters are utilised in the HESS model to connect the PHEV's power sources to the DC voltage line. The complete PHEV control system is split into two levels:

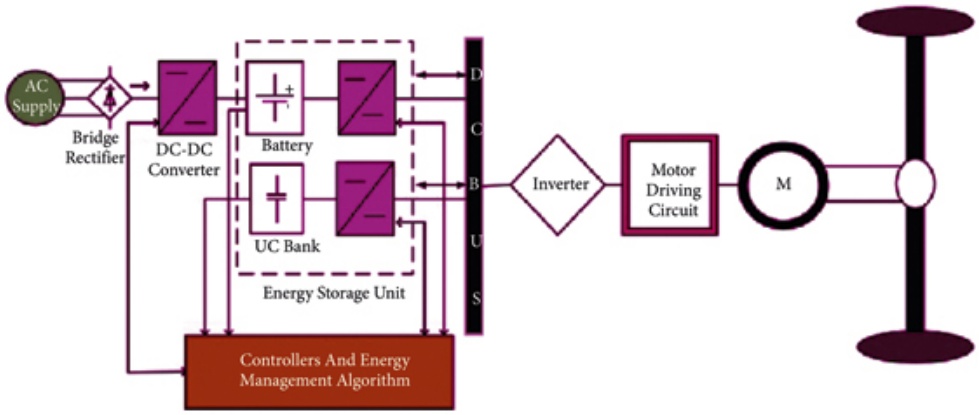

Figure 7

General block diagram of PHEV.

Low-level control: This entails controlling power converters to regulate the DC bus and allowing current to flow in both directions at a localised level.

Hindawi

International Transactions on Electrical Energy Systems

$$S = \frac{Ch}{Ch_{\text{nom}}}, \tag{9}$$

where S is SoC, Ch is the battery's absolute capacity in "A_h," and Chnom is the battery's nominal "A_h" capacity. Following (10) and (11) are utilised to detect fact of active and reactive grid powers during charging method of a PHEV.

$$P_{\text{grid}}(S) = VI \cos \phi(S), \tag{10}$$

$$P_{\text{grid}}(S) = VI \sin \phi(S), \tag{11}$$

where P_{grid} is the grid power, ϕ is the power factor, and V and I are grid voltage and current.Consider charging source's effectiveness, DC voltage is represented in AC power as

$$P_{ch}(S) = \eta \left[VI \cos \phi(S)\right], \tag{12}$$

where, η is the charging source's efficiency and P_{ch} is the charger's power. An integrated charging source has been modelled in this section, which comprises an AC supply linked with a boost converter and a regulated buck converter, as shown in Figure 8. Furthermore, an adaptive nonlinear controller was developed to manage charge flow and estimate unknown parameters (R_1, C_1). The charging source, as directed by the high level controller, provides instantaneous power to the battery linked in a HESS method of controlled buck converter is constructed, as shown in (13) and (14):

$$\frac{dx_1}{dt} = \frac{V_g}{L_1}u_1 - \frac{x_2}{L_1}, \tag{13}$$

$$\frac{dx_2}{dt} = \frac{x_1}{C_1} - \frac{V_g}{R_1 C_1}u_1, \tag{14}$$

where x_1 is average inductor current I_{L1}, x_2 is average output.

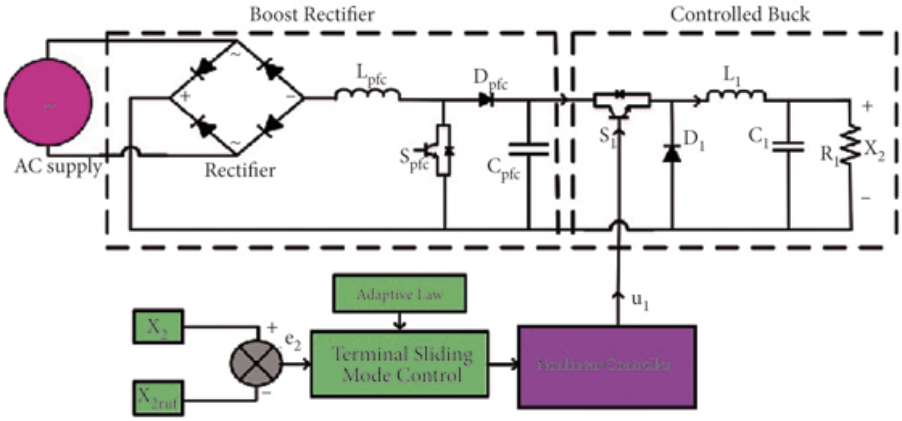

Figure 8

Hindawi

International Transactions on Electrical Energy Systems

Simulations on MATLAB/Simulink were used to test the validity of all of the suggested controllers, which were subjected to the normal European extra urban driving cycle to guarantee that the necessary control objectives were met. Tables 2–4 provide detailed information on energy sources, 3-phase induction, motors power converters and vehicle under consideration. Proposed controllers' design parameters were chosen using a hit-and-miss approach. Table 5 shows the parameters of the HESEC model.

Table 2

Energy sources data.

Table 3

Power converters data.

Table 4

Parameters of smart charging source.

Table 5

Parameters of HESEC model.

The above Table 6 shows comparative analysis based on constant acceleration and time-varying acceleration cases. Here the parameters compared are battery current, ultra-capacitor current, charging voltage, DC load current, and battery SOC. All the parameters have been analysed based on hybrid design in control systems enhancing the energy efficiency of electronic converters for power electronics.

Table 6

Comparative analysis is based on the constant acceleration case and the time varying acceleration case.

The above Figures 9 and 10 show comparative analysis of constant acceleration and time-varying acceleration case. Here for both cases, the proposed technique obtained optimal results in developing hybrid designs in control system while enhancing the energy efficiency of electronic converters for power electronics. The proposed technique in the constant acceleration case obtained a battery current of 92 Amps, ultracapacitor current of 89 Amps, charging voltage of 88 V, DC load current of 85 Amps, battery

Hindawi

International Transactions on Electrical Energy Systems

90 Amps, ultra-capacitor current of 85 Amps, charging voltage of 85 V, DC load current of 68 Amps, battery SOC of 74%; HEV obtained battery current of 92 Amps, ultra-capacitor current of 89 Amps, charging voltage of 89 V, DC load current of 78 Amps, battery SOC of 79%. From the above analysis, the proposed technique obtained optimal results in enhancing the energy efficiency of electronic converters for power electronics.

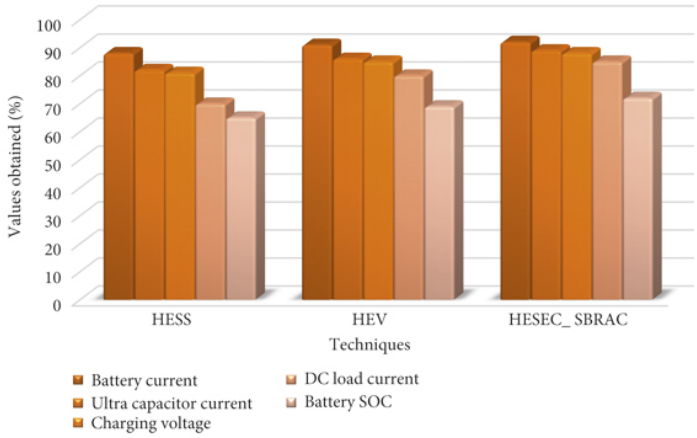

Figure 9

Comparative analysis of the constant acceleration case.

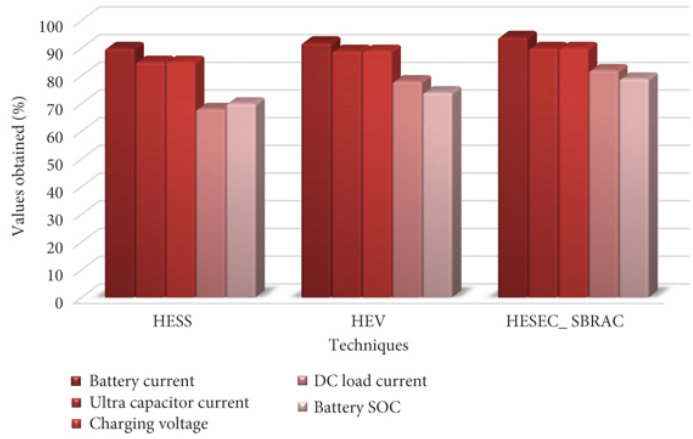

Figure 10

Comparative analysis of the constant acceleration case.

Hindawi

International Transactions on Electrical Energy Systems

synergetic battery reference adaptive controller. A PHEV's internal combustion engine with a small photovoltaic (PV) module is shown here. The effectiveness of the suggested control system's energy management is evaluated using simulations. By drawing power from batteries during peak hours and then recharging them during off-peak hours, the suggested method efficiently manages the grid's supply of electricity. This reduces the load on the converter and enables electric vehicles to charge more quickly. Regardless of changes in renewable energy supply and load, the system maintains a steady voltage. Experimental results show Constant acceleration case obtained battery current of 92 Amps, ultra-capacitor current of 89 Amps, charging voltage of 88 V, DC load current of 85 Amps, battery SOC of 72% and time-varying acceleration proposed technique obtained current of 94 Amps, ultracapacitor current of 90 Amps, charging voltage of 90 V, DC load current of 82 Amps, battery SOC of 79%.

Data Availability

The data will be avaible by corresponding author upon request.

Conflicts of Interest

The authors declare that they have no conflicts of interest.

References

1. D. Yuan, M. Sun, M. Zhao et al., "Persulfate promoted ZnIn2S4 visible light photocatalytic dye decomposition," *International Journal of Electrochemical Science*, vol. 15, pp. 8761–8770, 2020.
View at: Publisher Site | Google Scholar

2. X. Feng, Y. Zhang, L. Kang et al., "Integrated energy storage system based on triboelectric nanogenerator in electronic devices," *Frontiers of Chemical Science and Engineering*, vol. 15, no. 2, pp. 238–250, 2020.
View at: Publisher Site | Google Scholar

3. C. Y. Bu, F. J. Li, K. Yin, J. B. Pang, L. C. Wang, and K. Wang, "Research progress and prospect of triboelectric nanogenerators as self-powered human body sensors," *ACS Appl. Electron. Mater.*, vol. 2, no. 4, pp. 863–878, 2020.
View at: Publisher Site | Google Scholar

4. G. T. Xia, Y. N. Huang, F. J. Li et al., "A thermally flexible and multi-site tactile sensor for remote 3D dynamic sensing imaging," *Frontiers of Chemical Science and Engineering*, vol. 14, no. 6, pp. 1039–1051, 2020.
View at: Publisher Site | Google Scholar

5. W. L. Wang, Y. H. Li, L. W. Li, L. C. Wang, and K. Wang, "Nanoparticle structure for flexible quasi-solid-state lithium-ion batteries," *International Journal of Electrochemical Science*, vol. 15,

Hindawi

International Transactions on Electrical Energy Systems

lithium-ion batteries," *Energies*, vol. 14, no. 22, 2021.
View at: Publisher Site | Google Scholar

7. F. Mumtaz, N. Zaihar Yahaya, S. Tanzim Meraj, B. Singh, R. Kannan, and O. Ibrahim, "Review on non-isolated DC-DC converters and their control techniques for renewable energy applications," *Ain Shams Engineering Journal*, vol. 12, no. 4, pp. 3747–3763, 2021.
View at: Publisher Site | Google Scholar

8. C. Akkaldevi, S. D. Chitta, J. Jaidi, S. Panchal, M. Fowler, and R. Fraser, "Coupled electrochemical-thermal simulations and validation of minichannel cold-plate water-cooled prismatic 20 ah $LiFePO_4$ battery," *Electrochemistry (Tokyo, Japan)*, vol. 2, no. 4, pp. 643–663, 2021.
View at: Publisher Site | Google Scholar

9. K. Purohit, S. Srivastava, V. Nookala et al., "Soft sensors for state of charge, state of energy, and power loss in formula student electric vehicle," *Applied System Innovation*, vol. 4, pp. 78–85, 2021.
View at: Publisher Site | Google Scholar

10. V. G. Choudhari, A. S. Dhoble, S. Panchal, M. Fowler, and R. Fraser, "Numerical investigation on thermal behaviour of 5 × 5 cell configured battery pack using phase change material and fin structure layout," *Journal of Energy Storage*, vol. 43, Article ID 103234, 2021.
View at: Publisher Site | Google Scholar

11. K. Liu, Z. Yang, X. Tang, and W. Cao, "Automotive battery equalizers based on joint switched-capacitor and buck-boost converters," *IEEE Transactions on Vehicular Technology*, vol. 69, no. 11, pp. 12716–12724, 2020.
View at: Publisher Site | Google Scholar

12. Y. Shang, K. Liu, N. Cui, N. Wang, K. Li, and C. Zhang, "A compact resonant switched-capacitor heater for lithium-ion battery self-heating at low temperatures," *IEEE Transactions on Power Electronics*, vol. 35, no. 7, pp. 7134–7144, 2020.
View at: Publisher Site | Google Scholar

13. Y. Shang, K. Liu, N. Cui, Q. Zhang, and C. Zhang, "A sine-wave heating circuit for automotive battery self-heating at subzero temperatures," *IEEE Transactions on Industrial Informatics*, vol. 16, no. 5, pp. 3355–3365, 2020.
View at: Publisher Site | Google Scholar

14. K. Liu, X. Hu, H. Zhou, L. Tong, W. D. Widanage, and J. Marco, "Feature analyses and modeling of lithium-ion battery manufacturing based on random forest classification," *IEEE*, vol. 26, no. 6, pp. 2944–2955, 2021.
View at: Publisher Site | Google Scholar

Hindawi

International Transactions on Electrical Energy Systems

16. K. Wang, W. Wang, L. Wang, and L. Li, "An improved SOC control strategy for electric vehicle hybrid energy storage systems," *Energies*, vol. 13, no. 20, Article ID 5297, 2020.
View at: Publisher Site | Google Scholar

17. M. K. Azeem, H. Armghan, Z. e. Huma, I. Ahmad, and M. Hassan, "Multistage adaptive nonlinear control of battery-ultracapacitor based plugin hybrid electric vehicles," *Journal of Energy Storage*, vol. 32, Article ID 101813, 2020.
View at: Publisher Site | Google Scholar

18. M. S. Nazir, I. Ahmad, M. J. Khan, Y. Ayaz, and H. Armghan, "Adaptive control of fuel cell and supercapacitor based hybrid electric vehicles," *Energies*, vol. 13, no. 21, Article ID 5587, 2020.
View at: Publisher Site | Google Scholar

19. M. M. Islam, S. A. Siffat, I. Ahmad, M. Liaquat, and S. A. Khan, "Adaptive nonlinear control of unified model of fuel cell, battery, ultracapacitor and induction motor based hybrid electric vehicles," *IEEE Access*, vol. 9, pp. 57486–57509, 2021.
View at: Publisher Site | Google Scholar

20. F. Eroğlu, M. Kurtoğlu, and A. M. Vural, "Bidirectional DC–DC converter based multilevel battery storage systems for electric ˇ vehicle and large-scale grid applications a critical review considering different topologies, state-of-charge balancing and future trends," *IET Renewable Power Generation*, vol. 15, no. 5, pp. 915–938, 2021.
View at: Publisher Site | Google Scholar

21. M. Bortoluzzi, C. Correia de Souza, and M. Furlan, "Bibliometric analysis of renewable energy types using key performance indicators and multicriteria decision models," *Renewable and Sustainable Energy Reviews*, vol. 143, Article ID 110958, 2021.
View at: Publisher Site | Google Scholar

22. M. S. Miah, M. S. Hossain Lipu, S. T. Meraj et al., "Optimized energy management schemes for electric vehicle applications a bibliometric analysis towards future trends," *Sustainability*, vol. 13, no. 22, Article ID 12800, 2021.
View at: Publisher Site | Google Scholar

23. A. Katnapally, U. B. Manthati, A. Chirayarukil Raveendran, and S. Punna, "A predictive power management scheme for hybrid energy storage system in electric vehicle," *International Journal of Circuit Theory and Applications*, vol. 49, no. 11, pp. 3864–3878, 2021.
View at: Publisher Site | Google Scholar

24. J. Fang, H. Deng, N. Tashakor, F. Blaabjerg, and S. M. Goetz, "State-space modeling and control of grid-tied power converters with capacitive/battery energy storage and grid-supportive services," *IEEE Journal of Emerging and Selected Topics in Power Electronics*, vol. 19, pp. 1–17, 2021.
View at: Publisher Site | Google Scholar

Hindawi

International Transactions on Electrical Energy Systems

bidirectional DC-DC converter with intrinsic equal current sharing characteristic for electric vehicles," *IEEE Transactions on Industrial Electronics*, vol. 68, no. 2, pp. 1803–1813, 2021.
View at: Publisher Site | Google Scholar

Copyright

More related articles

No related content is available yet for this article.

Download other formats

Order printed copies

Related articles

No related content is available yet for this article.

Hindawi

International Transactions on Electrical Energy Systems

Print editions

Authors

Editors

Reviewers

Partnerships

Hindawi XML Corpus

Open Archives Initiative

Fraud prevention

ScienceDirect

Materials Today: Proceedings

Volume 46, Part 17, 2021, Pages 7618-7623

Investigations on microstructure and tensile properties of as-cast ZA-27 metal matrix composite reinforced with zircon sand

G.R. Gurunagendra [a], B.R. Raju [b], Vijayakumar Pujar [a], D.G. Amith [a], H.G. Hanumantharaju [c], Santosh Angadi [a]

Show more

https://doi.org/10.1016/j.matpr.2021.01.896

Get rights and content

Highlights

- ZA27 composites with 1.5%wt, 3.0 wt%, 4.5 wt% and 6.0 wt% zircon sand is fabricated by stir casting and the microstructure reveals the distribution of zircon sand particles.
- The ductility is low for 4.5 wt% reinforcement but improves at 6.0 wt% zircon sand of course with slightly better strength that is desirable in engineering applications.
- The dislocation density of the composites is calculated and shows an upward trend with an increase in zircon sand particles but at 6.0 wt% its value drops and correlates with the tensile strength of the 6.0 wt% ZA27 composites.

Abstract

Zinc-Aluminum alloys are employed as a bearing material in various machinery. In the present work zircon sand microparticles of size, 100 µm are dispersed in ZA-27 alloy with weight fractions of 1.5 wt%, 3.0 wt%, 4.5 wt%, and 6.0 wt% to synthesize ZA-27 metal matrix composites by stir casting. Microstructure studies using, SEM/EDAX conducted to determine the morphology of the particles and the ZA-27composites. Physical properties like density and porosity of the zircon sand microparticulate reinforced ZA-27 are evaluated and their effect on strength and ductility of the composites are evaluated using the tensile test. dispersion of zircon sand is seen in the SEM micrographs and EDAX confirms the same. The results obtained revealed an increase in tensile strength and yield strength at 3.0 wt%, 4.5 wt and 6.0 wt% at the cost of a reduction in percentage elongation when compared to ZA-27 alloy. The tensile behavior of ZA-27

composites is found to be affected by the dispersion of reinforcement in the matrix arising due to dislocation density.

Previous Next

Keywords

Density; Porosity; Dislocation density; Tensile strength; as- cast ZA-27; Micro-structure

Special issue articles Recommended articles

Cited by (1)

Optimization of Tribological Properties of Microparticulate-Reinforced ZA-27 Composites
2023, Lecture Notes in Mechanical Engineering

Scientific Research (//www.scirp.org)
An Academic Publisher

OPEN ACCESS
(/journal/openaccess.aspx)

Journal of Minerals and Materials Characterization and Engineering (journalarticles.aspx?journalid=1753) > Vol.9 No.1, January 2021 (home.aspx?issueid=14748#106925)

Microstructure, Dislocation Density and Thermal Expansion Behavior Using Thermo Elastic Models of Zircon Sand Reinforced as Cast ZA-27 Composites

G. R. Gurunagendra (articles.aspx?searchcode=G.+R.++Gurunagendra&searchfield=authors&page=1)[1*], V. Bharat (articles.aspx?searchcode=V.++Bharat&searchfield=authors&page=1)[1], B. R. Raju (articles.aspx?searchcode=B.+R.++Raju&searchfield=authors&page=1)[2], D. G. Amith (articles.aspx?searchcode=D.+G.++Amith&searchfield=authors&page=1)[1], Vijayakumar Pujar (articles.aspx?searchcode=Vijayakumar++Pujar&searchfield=authors&page=1)[1], C. Ravi Keerthi (articles.aspx?searchcode=C.+Ravi++Keerthi&searchfield=authors&page=1)[1]

[1]Global Academy of Technology, Bangalore, India (articles.aspx?searchcode=Global+Academy+of+Technology%2c+Bangalore%2c+India&searchfield=affs&page=1).

[2]The Oxford College of Engineering, Bangalore, India (articles.aspx?searchcode=The+Oxford+College+of+Engineering%2c+Bangalore%2c+India&searchfield=affs&page=1).

DOI: 10.4236/jmmce.2021.91008 (https://doi.org/10.4236/jmmce.2021.91008) **PDF (//www.scirp.org/pdf/jmmce_2021012815063580.pdf) HTML (//www.scirp.org/journal/paperinformation.aspx?paperid=106925) XML (//www.scirp.org/xml/106925.xml)** **263** Downloads **828** Views Citations (papercitationdetails.aspx?paperid=106925&JournalID=1753)

Abstract

In the present work stir casting route is used to fabricate the ZA27 Metal matrix composites containing 3 wt%, 6 wt%, 9 wt%, and 12 wt%. Zircon sand particulates of size 100 mesh. Microstructure studies using Optical Microscopy, SEM-EDAX are carried out to ascertain the distribution and morphology of particulates in the composites. Effect of zircon sand as reinforcement on bulk density, porosity, of the fabricated composites is studied. SEM studies are carried out to understand the behavior of as-cast ZA27 alloy reinforced with zircon sand. The dislocation density of the fabricated composite affects the strength of the composites and depends on the strain due to thermal mismatch and is found to increase with increase in weight% of zircon sand. However, it does not consider casting defects of voids/clustering observed in micrographs of the fabricated composite. Porosity in composites does not have influence on Coefficient of thermal expansion (CTE) of the ZA27 composites studied using thermoelastic models like Kerner and turner model and rule of mixtures of composite.

Keywords

Density (articles.aspx?searchcode=Density&searchfield=keyword&page=1&skid=0), Porosity (articles.aspx?searchcode=+Porosity&searchfield=keyword&page=1&skid=0), Dislocation Density (articles.aspx?searchcode=+Dislocation+Density&searchfield=keyword&page=1&skid=0), Thermoelastic Models (articles.aspx?searchcode=+Thermoelastic+Models&searchfield=keyword&page=1&skid=0), Rule of Mixtures (articles.aspx?searchcode=+Rule+of+Mixtures&searchfield=keyword&page=1&skid=0)

About SCIRP (http://www.scirp.org/About/Index.aspx)
SCIRP News (http://www.scirp.org/news/Index.aspx)
Submit your Manuscript (//papersubmission.scirp.org/login.jsp?sub=true&utm_campaign=submit&utm_source=www.scirp.org&utm_medium=bottom_submit_www)
Sign up (http://papersubmission.scirp.org/users/showAddUser?utm_campaign=signup&utm_source=www.scirp.org&utm_medium=bottom_signup_www)

1. Introduction

Over the years, Metal matrix composites are playing a significant role in aerospace, automotive, space engineering and other industrial applications due to their superior mechanical, tribological and thermal properties.

Matrix is made of monolithic Metal or alloy and embedded with hard particulates to augment the properties of MMC compared to the monolithic metals/alloys. Aluminum, Magnesium, titanium, copper and Zinc based alloys are widely employed as matrix materials in various applications.

Over the past few decades research on zinc-based alloys are being carried out and found to exhibit excellent tribo-mechanical properties apart from low melting point, good cast ability and machinability. Several research have proved the Zinc-Aluminum family of alloys like ZA12 and ZA27 are possessing better strength when compared to cast-iron, bronze and plastics as tribo-elements for operating at moderate temperature condition. In spite of good tribo-mechanical properties The ZA alloy exhibits dimensional instability at temperature greater than 100˚C. With heat treatment techniques of cast alloy and addition of high melting point ceramic particles to the alloy the properties of the alloy can be improved at the expense of reduction in machinability which can be reduced by addition of dry lubricants [1] [2].

Nowadays researchers are inspired to reinforce these alloys with reinforcement particles and whiskers like Al_2O_3, Sic, Garnet, glass, Tic, graphite, Agri and industrial waste etc. to achieve better mechanical, wear and thermal characteristics. There are research reports of ZA27 alloy containing more than one reinforcement to produce hybrid composites like a ceramic filler and a solid lubricant like graphite to offset the negative effects of ceramic fillers on machinability [3] [4]. Also in recent times, researchers are adding nanofillers in recent times to the as-cast ZA27 alloy and fabricating the MMC using different metallurgical processes like, stir casting, double stir casting, squeeze casting, powder metallurgy and also ultrasonic-assisted stir casting for obtaining better casting and improved properties [3] [5]. There is not much work carried out on characterization of zircon sand reinforced with ZA27 alloy especially beyond 5% weight fraction also micro-mechanical behavior of such composites [6]. Coefficient of thermal expansion (CTE) plays an important role in ZA27 materials used as tribo-elements and needs to be estimated for better performance of the elements. Thermoelastic models are used to predict the CTE of the ZA27/zircon sand composites [7]. Effects of presence of voids on dislocation density of composites and cracking/agglomeration of zircon particles in ZA27 matrix with increased weight fraction on CTE of composites and their effects on strength is addressed [8]. preparation of composites by various routes and its processing, matrix-reinforcement bonding and characterization poses significant challenge in the end use of composites, also decrease in ductility, poor matrix-reinforcement interface, particle cracking, debonding/pull out of particles and agglomeration of particulates are some of the challenges in preparation of composites. composites are subjected to age hardening to obtain better strength and improved ductility as well as tribological properties [2] [9].

Stir casting is widely adopted route in preparing these composites due to their advantages like bulk manufacturing, ease of fabrication and economy. Also, there is enough scope to investigate and understand the behavior of ZA-27 containing microparticulate zircon sand as primary reinforcement and hybrid composites with dry lubricants as secondary reinforcement.

2. Experimental Procedure (Figure 1 and Table 1)

In this work Zircon sand ($ZrsiO_4$) of particle size 100 mesh is used as a primary reinforcement in the matrix of ZA-27. Chemical composition of Zircon sand is Zircon oxide and hafnium of 65% and silica of 24% with traces of Al_2O_3, TiO_2 and Fe_2O_3 [10]. The thermal coefficients of zircon sand is low compared to other oxides of ceramics improving the interface strength, also the density of zircon sand (ρ = 4.56 g/cc) is in close proximity with the density of ZA-27 (ρ = 4.5 g/cc) alloy which reduces the problems of gravity segregation due to large density difference between matrix phase and dispersed phase (Figure 2 and Table 2).

(a)

(b)

Figure 1. (a) Zircon sand particles (b) ZA-27 ingot.

Figure 2. Particle size by sieve analysis.

Al	Mg	Cu	Fe	silicon	Zinc
25.60%	0.07%	2.10%	0.04%	0.001	Remainder

Table 1. The chemical compositions of ZA-27 alloy.

Melting point (˚C)	2500
Hardness (Mohs)	7.5
Density (g/cc)	4.5
linear coefficient of expansion (10^{-6} K)	4.5
crystal structure	Tetragonal

Table 2. Properties of zircon sand.

Preparation of ZA27 MMC by Stir Casting

Composite was fabricated by stir casting method regarded as the most economical and suitable for mass production compared to other techniques of fabrication. The setup is as shown in Figure 3. To begin with the weight of reinforcements for 3 wt%, 6 wt%, 9 wt% and 12 wt% Zircon sand to prepare 2000 g of ZA-27 alloy was calculated. Zircon sand particles were preheated to around 200˚C in an oven to remove presence of moisture in it ZA27 alloy ingots were placed in the graphite crucible and super-heated to a melting temperature and stirring was done for homogenizing temperature later the temperature was reduced to 450˚C (semi solid state) Now, the reinforcement particles are fed at a rate of 20 g/min and the mixture with continued heating is stirred at a speed of 350 rpm to create vortex for 5 minutes for better distribution of particles. 10 g of Magnesium rod was added to improve wettability and the melt is degassed using C_2Cl_6 (hex chloroethylene tablets) in order to eliminate porosity and remove air presence in the mixture. The composite was poured at 500˚C into the preheated cast iron die for better solidification [6].

3. Results and Discussion

Theoretical density and experimental density of the base alloy and composite with different weight percentage of composite is evaluated. There will be difference in the values of densities due to the voids and pores generated during casting. Due to the presence of voids mechanical properties will get reduced so it is obvious to determine the density and porosity of the composites for ascertaining the quality of composites produced. Theoretical density is calculated using the rule of mixture,

$$\rho_{theoritical} = \frac{100}{\sum_{i=1}^{n} \frac{x_i}{\rho_i}} \quad (1)$$

Figure 3. Diagram of stir casting set up.

Experimental density is determined using the Archimedes principle by measuring the known volume of water displaced by the base alloy and composite specimens. The mass of the specimen is measured using a weighing balance (make: shimadzu-Electronic balance) of readability of 0.0001 grams.

ρ = mass of the specimen/volume of water displaced

$$\%\text{Porosity} = \frac{\rho_{th} - \rho_{exp}}{\rho_{th}} \times 100 \quad (2)$$

From the values of density of base alloy and composite it is observed that density decreases with increase in reinforcement as shown in Figure 4. Porosity of the composite was found to increase with the reinforcement content (Figure 5). The increase in porosity is attributed to gas entrapment during mixing, shrinkage, and presence of air bubbles in the composite slurry.

3.1. Hardness Test (Figure 6)

Hardness is the ability of the material for indentation. Rockwell Hardness number of the bulk specimen of the base alloy and composites is measured using indentation of 1/16' ball indenter under a load of 100 Kgf for dwell time of 15 seconds. An average of values of readings obtained during the tests were taken and tabulated. The hardness was found to increase with increase in weight (%) of zircon sand particles.

Figure 4. Variation of measure density with composition of reinforcement.

Figure 5. Porosity with increase in weight percentage of zircon sand.

Figure 6. Brinell Hardness for the ZA-27 composite.

The ZA27 alloy is strengthened due to solid solution strengthening, while the ZA27 composite is dispersion strengthened due to presence of zircon sand particulates in the matrix. The hardness testing is compressive in nature and the area under the indentation is work hardened, resulting in enhanced values.

3.2. Microstructure Studies

When the Zinc alloy is solidified it results information of various phases like, $\alpha + L$, β, $\alpha + \beta$ and $\alpha + \eta$ as shown in Figure 7 The microstructure in Figure 2(a) of ZA-27 alloy reveals the Aluminum rich matrix (α FCC) and dendrite Zinc phase (η HCP), $CuZnO_4$ at 382˚C and Al_4Cu_3Zn at 275˚C [11] (Figure 7, Figure 8 and Figure 9).

The wavelength of X-rays is in the range of 0.01nm to 10nm that can penetrate through the crystal structure to reveal the properties of material while exiting out of it. XRD is are used to characterize different types of materials. Interplanar spacing (d) = Order of Reflection (n) × Wavelength (λ)/2 × sinθ using Braggs law.

Figure 7. Phase diagram, of ZA-27 alloy.

Figure 8. Optical microscope pictures of zircon sand reinforced ZA-27 (100× Magnification).

Figure 9. EDAX of ZA-27.

3.3. SEM/EDAX Studies

To study the morphology of the different composition of composites SEM (Make: TESCAN VEGA3) was used with EBSD arrangement attached with EDS detector. The micrographs reveal the presence of distribution of zircon particles and their distribution. The average size of the zircon sand particles is found to be 100 - 150 microns distributed in the matrix of ZA27 alloy and confirms the sieve analysis shown in Figure 2. The EDS detector confirms the existence of zinc, aluminum, zircon, and silicon along with the oxides due to chemical reactions at the interface.

Principle of Bragg's law is the basis for X-Ray diffraction. XRD is conducted to identify different phases present in the ZA27 composite samples using PAN-Analytical-Xpert^3 powder XRD fitted with Ni filter operated at 30 mA and 40 kV generator settings using Cu-kα radiation with a wavelength of 1.5418 Å. The diffraction angle (2θ) range is varied from 20˚ to 90˚.

XRD of the zircon sand and composites confirmed the presence of elements like zircon, silicon, and oxygen in the reinforcement as shown in Figure 10. XRD of ZA-27 composites containing 3% and 12% zircon sand reveals the presence of zirconium silicate and their compounds. The compounds are found at the interface of matrix and particles due to chemical reaction of Zinc aluminum with zircon sand (Figure 11, Figure 12 and Figure 14).

The presence of voids will bring down the strength of the composite developed. With increase in zircon sand reinforcement content there occurs agglomeration of particles because of which voids get accumulated during deformation. The agglomeration of particulates is undesirable in fabrication of metal matrix composites due to which strength of the fabricated composites certainly reduces. The strength is also obtained by good wetting of the zircon sand and ZA27 alloy, resulting in strong interface for efficient load transfer [12].

The bonding strength at the interface will affect the mechanical and physical properties like coefficient of thermal expansion, thermal conductivity, and

Figure 10. XRD of Zircon sand particles.

(a)

(b)

Figure 11. (a) SEM of Zircon sand particles (b) EDAX of Zircon sand particles.

(a)

(b)

Figure 12. (a) SEM for ZA-27 composite containing zircon sand (b) EDAX for ZA-27 composite containing zircon sand.

damping. Coefficient of thermal expansion is a major criterion for the ZA27 composites with good dimensional stability. To obtain better interface characteristics there are process variables that need to be controlled such as processing technique, pouring temperature, stirring time, stirring speed etc. as well as reinforcement content and chemical properties of matrix and reinforcement [13].

It follows from SEM pictures in Figure 13 that the multiple microcracks observed in the regions of particle agglomeration will results in reduction in ductile region of the composite The addition of the hard zircon particles as reinforcement in the ductile soft ZA-27 alloy matrix results in resistance to deformation. Subsequently, causing triaxial stress state ZA27 matrix results in the formation of voids and growth in the matrix and also debonding at the interface of the particle

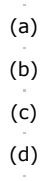

Figure 13. (a) SEM images of ZA27 composites of magnification 100×, 200×, 300×, 1000× for 3 wt%; (b) SEM images of ZA27 composites of magnification 100×, 200×, 300×, 1000× for 6 wt%; (c) SEM images of ZA27 composites of magnification 100×, 200×, 300×, 1000× for 9 wt%; (d) SEM images of ZA27 composites of magnification 100×, 200×, 300×, 1000× for 12 wt%; (e) Size of the particles distributed in ZA-27 alloy (Magnification: 100×).

and the matrix [12] Shrinkage cavities are seen in the micrographs due to porosity linking to reduction in strength of the composite. Hence, distribution of the particles is an important factor governing the behaviour of the composites. It is very essential to control particle clustering and voids to in the microstructure of the composite [6] (Figure 14).

Apart from the above challenges in processing of composites by liquid metallurgy route it is necessary to understand strong chemical bond that exists between reinforcement and matrix. It is very important to know the various advantages and limitations of fabrication techniques like liquid metallurgy, powder metallurgy, spray deposition or in-situ route of preparation of composites. Also, due consideration to be given to the disparity in the physical properties of Zircon sand as reinforcement and ZA27 matrix in order to obtain a satisfactory interface between the reinforcement and matrix [14]. Large differences in the coefficients of thermal expansion in the reinforcement and matrix lead to the formation of residual stresses in the composite during the fabrication process.

3.4. Dislocation Density of the Composite Due to Difference in CTE

Dislocation density is total length of dislocation to volume of the crystal. It is well known that microscopic movement of dislocation will be having significant effect on the macroscopic deformation of materials. Effect of ceramic particles present in ductile alloy matrix on strength and hardness has been studied earlier [15] by theories like, quench strengthening, Orowan strengthening, work hardening, grain strengthening/Hall Petch mechanism of the composites. During solidification and cooling of composite to room temperature if the particle-reinforcement interface bonding is good then tensile and compressive stresses is developed in ZA27 alloy and zircon sand particles, respectively. Because of large difference of coefficient of thermal expansion (CTE) and temperature

Figure 14. EDAX conforming the presence of reinforcement.

difference (Δ*T*) due to cooling of composites, plastic deformation of ZA27 alloy matrix is likely to occur in order to accommodate elastic residual stress that forms in matrix, CTE mismatch will be large at interface due to work hardening setting up dislocations formed during cooling of composite whose movements are arrested at particle and matrix interface and exhibits large hardness which decreases with increasing distance from interface. This is due to high density of dislocation at the interface and can be predicted using the model of [15] The dislocation density of particulate composite at the interface is given by Equation (3) where b = 0.26 nm burgers vector for zinc alloy [15] d = particle size.

$$\rho = \frac{12\Delta C \Delta T V_p}{bd\left(1 - V_p\right)} \tag{3}$$

Themal mismatch strain,

$$\Delta C = \alpha_m - \alpha_p \tag{4}$$

ΔT = Temperature difference during cooling of casting from solidus temperature.

It is understood that coefficient of thermal expansion of the composites depends on several material parameters like the composition, the microstructure of the matrix, the reinforcement volume fraction and distribution as well as residual stresses formed due to the CTE mismatch, porosity, volume fraction and the interface strength [16].

Thermo-elastic models like Kerner and Turner have been used to understand the behavior of thermal expansion of composites. It is important to note that these models can predict the CTE relying on the reinforcement content and elastic nature of the matrix [16] [17], however, they do not take into account the case of plasticity of the matrix nor the voids formed in the composites [18].

By Rule of mixture CTE (α) of composites are calculated using,

$$\alpha_c = \alpha_p V_p + \alpha_m V_m \tag{5}$$

Based on Turner model,

$$\alpha_c = \frac{\alpha_m K_m V_m + \alpha_p K_p V_p}{K_m V_m + K_p V_p} \tag{6}$$

Based on Kerner's model.

$$\alpha_c = \alpha_m V_m + \alpha_p V_p + V_m V_p \left(\alpha_p - \alpha_m\right) \times \frac{K_p - K_m}{V_m K_m + V_p K_p + \frac{3K_m K_p}{4G_m}} \tag{7}$$

where, α, E, G, K, V are CTE, Youngs modulus, Shear modulus, bulk modulus, and volume fraction, respectively. Subscripts m, p, c indicates matrix, particles, and composites.

The Bulk modulus of the material is calculated using,

$$K = \frac{E}{3\left(3 - \frac{E}{G}\right)} \tag{8}$$

It is important to understand the mechanism of the reduction in CTE values in the ZA27 composites due to presence of voids. From Table 3 it is found the CTE and elastic modulus of the reinforcement are lower and higher than those of matrix resin, respectively. When this composite is subjected to temperature rise, Thermal mismatch strain, $\Delta C = \alpha_m - \alpha_p$ is induced. This mismatch strain initiates the formation of compressive and tensile stress in the matrix and reinforcement (Table 4 and Table 5, Figure 15 and Figure 16).

Figure 15. Variation of dislocation density vs weight percent of zircon sand.

Figure 16. CTE comparison of composite using by thermoelastic models.

Material	*E* GPa	*G* Gpa	*K* Gpa	CTE/˚C
ZA27	77	31	49.7	26×10^{-6}
Zircon sand	97.1	36.5	95.27	4.5×10^{-6}

Table 3. Elastic constants and CTE of ZA27 and zircon sand.

Slmo.	Sample	Weight (%) zircon sand	Dislocation density (ρ)
1	A	0	-
2	B	3	5.69×10^{11}
3	C	6	7.89×10^{11}
4	D	9	1.19×10^{12}
5	E	12	1.57×10^{12}

Table 4. Results of dislocation density.

Sl No	Sample	Weight (%) zircon sand	CTE (Rule of mixtures)	CTE (Turners model)	CTE (Kerner's model)
1	A	0	-	-	-
2	B	3	2.10×10^{-5}	1.81×10^{-5}	1.67×10^{-5}
3	C	6	1.97×10^{-5}	1.65×10^{-5}	1.56×10^{-5}
4	D	9	1.78×10^{-5}	1.42×10^{-5}	1.60×10^{-5}
5	E	12	1.62×10^{-5}	1.28×10^{-5}	1.45×10^{-5}

Table 5. Comparison of CTE values using thermo elastic models.

If micro voids are dispersed in the matrix, they are subjected to the compressive stresses, resulting in the shrinkage of the void volume. Hence, the overall CTE of the ZA27 composite is reduced and shape of the voids results CTE reduction. The reduction of CTE values of the composite is also due to low volume fraction of the matrix and existence of voids in the composite. Hence, the ZA27 matrix, with large CTE value is reduced with increase of volume fraction of voids, affecting the overall CTE value of ZA27 composites [7] [8] [16].

If the interface between zircon sand and matrix of ZA27 is good, then a significant amount of the reduction of CTE value of the composite occurs. However, it is more likely that these high thermal stress values induce fracture at the interface. So the compressive thermal stress, which is the main driving force of the composite CTE reduction due to voids, is relaxed in this respect so that the effect of voids on CTE values are reduced [13].

4. Conclusions

The experimental density is reduced with increase in weight fraction of zircon sand and the bulk hardness of the ZA27/zircon composite prepared by stir casting route is found the increase with increase in zircon sand reinforcement. The Optical microscopy studies of the ZA27/zircon composites and microstructure obtained from SEM/EDAX and XRD studies indicate the presence and distribution of zircon sand particles and intermetallic compounds in the ZA27 matrix along with agglomeration.

The SEM pictures also show the presence of voids and particle clustering in the matrix. The role of particle-matrix interface as revealed from the microstructure of the composite is studied to understand the thermal expansion behavior of composites. Strengthening of composites due to mechanism of dislocation density is obtained analytically.

From the analytical results obtained by the rule of mixtures it is found that the value of CTE decreases with the increase in zircon sand reinforcement. The values are closely predicted by thermoelastic energy principles like Turners and Kerner's model using Equation (6) and Equation (7) in comparison to rule of mixtures Equation (5). The reason for decrease in CTE values is due to the presence of voids and agglomeration during the fabrication of the ZA27 MMC.

The dislocation density is found to increase with the increase in reinforcement content and depicts the inverse relation with CTE values. Thermoelastic models reveal that Zircon sand particles as reinforcement is affecting the augmentation of strength of the composites due to increase in dislocation density arising out of large difference in CTE values during solidification of the composites. But it does not consider casting defects like voids or poor interface between ZA27matrix and Zircon sand particulates.

Acknowledgements

All acknowledgments (if any) should be included at the very end of the paper before the references and may include supporting grants, presentations, and so forth.

Conflicts of Interest

The authors declare no conflicts of interest regarding the publication of this paper.

References

[1 Babić, M. and Ninković, R. (2004) Zn-Al Alloys as Tribomaterials. Tribology in Industry, 26, 3-7.
(../reference/referencespapers.aspx?referenceid=2916428)]

[2 (../reference/referencespapers.aspx?referenceid=2916429)] Babić, M., Ninković, R., Mitrović, S., et al. (2007) Influence of Heat Treatment on Tribological Behavior of Zn-Al Alloys. Tribology in Industry, 29, 23-31.

[3 (../reference/referencespapers.aspx?referenceid=2916430)] Shiva Kumar, N. (2018) Mechanical and Wear Behavior of ZA-27/Sic/Gr Hybrid Metal Matrix Composites. Materials Today Proceedings, 5, 19969-19975. https://doi.org/10.1016/j.matpr.2018.06.363

[4 (../reference/referencespapers.aspx?referenceid=2916431)] Hemanth Kumar, T.R., Swamy, R.P. and Chandrashekar, T.K. (2013) An Experimental Investigation on Wear Test Parameters of Metal Matrix Composites Using Taguchi Technique. Indian Journal of Engineering and Materials Sciences, 20, 329-333.

[5 (../reference/referencespapers.aspx?referenceid=2916432)] Fatile, B.O., Adewuyi, B.O. and Owoyemi, H.T. (2017) Synthesis and Characterization of ZA-27 Alloy Matrix Composites Reinforced with Zinc Oxide Nanoparticles. Engineering Science and Technology, 20, 1147-1154. https://doi.org/10.1016/j.jestch.2017.01.001

[6 Sharma, S.C., Girish, B.M., Somashekar, D.R., et al. (1999) Mechanical Properties and Fractography of Zircon-Particle-Reinforced ZA-27 (../ref Alloy Composite Materials. Composites Science and Technology, 59, 1805-1812.
erenc https://doi.org/10.1016/S0266-3538(99)00040-8
e/refe
rence
spape
rs.asp
x?
refere
nceid
=291
6433)
]
[7 Panwar, R.S. and Pandey, O.P. (2013) Study of Wear Behavior of Zircon Sand-Reinforced LM13 Alloy Composites at Elevated (../ref Temperatures. Journal of Materials Engineering and Performance, 22, 1765-1775.
erenc https://doi.org/10.1007/s11665-012-0383-0
e/refe
rence
spape
rs.asp
x?
refere
nceid
=291
6434)
]
[8 Shoba, C., Ramanaiah, N. and Rao, D.N. (2014) Ageing Behavior of Aluminum Hybrid Metal Matrix Composites. Materials Science: An (../ref Indian Journal, 3, 79-85.
erenc
e/refe
rence
spape
rs.asp
x?
refere
nceid
=291
6435)
]
[9 Prasad, D.S., Shoba, C. and Ramanaiah, N. (2014) Investigations on Mechanical Properties of Aluminum Hybrid Composites. Journal of (../ref Materials Research and Technology, 3, 79-85.
erenc https://doi.org/10.1016/j.jmrt.2013.11.002
e/refe
rence
spape
rs.asp
x?
refere
nceid
=291
6436)
]

[10 (../reference/referencespapers.aspx?referenceid=2916437)] Ramesha, V., Prasad, T.B., Nayak, V. And Neelakantha, V.L. (2018) A Study on Mechanical Properties of Al-17Si Metal Matrix Composites. IOP Conference Series: Materials Science and Engineering, 376, 012100. https://doi.org/10.1088/1757-899X/376/1/012100

[11 (../reference/referencespapers.aspx?referenceid=2916438)] Gurunagendra, G., Ravishankar, T.N., Ravikeerthi and Raju, B.R. (2019) Dry Sliding Wear Studies of Zinc Aluminium Alloy Containing Micro and Nano Solid Lubricants. International Journal of Engineering Research and Advanced Technology, 5, 7-13. https://doi.org/10.31695/IJERAT.2019.3457

[12 (../reference/referencespapers.aspx?referenceid=2916439)] Madhusudan, S., Sarcar, M.M.M. and Rao, N.B.R.M. (2016) Mechanical Properties of Aluminum-Copper(p) Composite Metallic Materials. Journal of Applied Research and Technology, 14, 293-299. https://doi.org/10.1016/j.jart.2016.05.009

[13 (../reference/referencespapers.aspx?referenceid=2916440)] Mitra, R. and Mahajan, Y.R. (1995) Interfaces in Discontinuously Reinforced Metal Matrix Composites: An Overview. Bulletin of Materials Science, 18, 405-434. https://doi.org/10.1007/BF02749771

[14 Chappell, P.J.C. (1990) Reinforcement-Matrix Interface Effects in Metal Matrix Composites. MRL Technical Note, MRL-TN-562.
(../ref
erenc
e/refe
rence
spape
rs.asp
x?
refere
nceid
=291
6441)
]
[15 Miller, W.S. and Humphreys, F.J. (1991) Strengthening Mechanisms in Particulate Metal Matrix Composites. Scripta Metallurgica et
(../ref Materialia, 25, 33-38.
erenc https://doi.org/10.1016/0956-716X(91)90349-6
e/refe
rence
spape
rs.asp
x?
refere
nceid
=291
6442)
]
[16 Hatta, H., Takei, T. and Taya, M. (2000) Effects of Dispersed Microvoids on Thermal Expansion Behavior of Composite Materials.
(../ref Materials Science and Engineering: A, 285, 99-110.
erenc https://doi.org/10.1016/S0921-5093(00)00721-8
e/refe
rence
spape
rs.asp
x?
refere
nceid
=291
6443)
]
[17 Bharat, V., Prasad, B.D. and Venkateswarlu, K. (2017) Effect of Beryllium Aluminum Cyclosilicate on Thermal Expansion Behavior of Al-
(../ref Based Composites. Journal of Minerals and Materials Characterization and Engineering, 5, 140-152.
erenc https://doi.org/10.4236/jmmce.2017.53012
e/refe
rence
spape
rs.asp
x?
refere
nceid
=291
6444)
]

[18 Nam, T.H., Requena, G. and Degischer, P. (2008) Thermal Expansion Behaviour of Aluminum Matrix Composites with Densely Packed SiC (../refPerenc Particles. Composites Part A: Applied Science and Manufacturing, 39, 856-865. https://doi.org/10.1016/j.compositesa.2008.01.011 e/refe rence spape rs.asp x? refere nceid =291 6445)]

Related Articles

- Effect of Beryllium Aluminum Cyclosilicate on Thermal Expansion Behavior of Al-Based Composites (paperinformation.aspx?paperid=76523)
- Mechanical, Thermal and Crystallization Properties of Polypropylene (PP) Reinforced Composites with High Density Polyethylene (HDPE) as Matrix (paperinformation.aspx?paperid=84748)
- Microstructure, Mechanical Properties (Strength and Hardness) and Wear Behavior of Chilled Aluminum Alloy (LM-13) Reinforced with Titanium Carbide (TiC) Metal Matrix Composites (paperinformation.aspx?paperid=93802)
- Development of Nickel Alloy Reinforced with Fused SiO2 Chilled Composites and Evaluation of Thermal Properties (Thermal Conductivity & Coefficient of Thermal Expansion) and Temperature Distribution by Finite Element Analysis (FEA) (paperinformation.aspx?paperid=79108)
- Thermo-Stamping Process of Glass and Carbon-Fibre Reinforced Polymer Composites (paperinformation.aspx?paperid=100474)

Open Special Issues (../journal/openspecialissues.aspx?journalid=1753&PubState=false)

Published Special Issues (../journal/openspecialissues.aspx?journalid=1753&PubState=true)

Special Issues Guideline (../journal/openspecialissuesguideline.aspx?journalid=1753)

E-Mail Alert (../journal/newslettersubscription.aspx?journalid=1753)

JMMCE Subscription (../journal/subscribejournal.aspx?journalid=1753)

Publication Ethics & OA Statement (../journal/publicat_ethics_statement.aspx?journalid=1753)

Frequently Asked Questions (../journal/faq.aspx?journalid=1753)

Recommend to Peers (../journal/recommendtopeers.aspx?journalid=1753)

Recommend to Library (../journal/recommendtolibrary.aspx?journalid=1753)

Contact us (../journal/contactus.aspx?journalid=1753)

Sponsors, Associates, and Links

- Materials Sciences and Applications (http://www.scirp.org/journal/msa/)
  (http://www.scirp.org/journal/msa/)
- Journal of Materials Science and Chemical Engineering (http://www.scirp.org/journal/msce/)
  (http://www.scirp.org/journal/msce/)
- Open Journal of Composite Materials (http://www.scirp.org/journal/ojcm/)
  (http://www.scirp.org/journal/ojcm/)
- New Journal of Glass and Ceramics (http://www.scirp.org/journal/njgc/)
  (http://www.scirp.org/journal/njgc/)
- Open Journal of Organic Polymer Materials (http://www.scirp.org/journal/ojopm/)
  (http://www.scirp.org/journal/ojopm/)
- Graphene (http://www.scirp.org/journal/graphene/)
  (http://www.scirp.org/journal/graphene/)

About SCIRP (http://www.scirp.org/AboutUs/Index.aspx)

SCIRP News (http://www.scirp.org/news/Index.aspx)

Submit your Manuscript (//papersubmission.scirp.org/login.jsp?sub=true&utm_campaign=submit&utm_source=www.scirp.org&utm_medium=bottom_submit_www)

Sign up (http://papersubmission.scirp.org/users/showAddUser?utm_campaign=signup&utm_source=www.scirp.org&utm_medium=bottom_signup_www)

Follow SCIRP

(https://twitter.com/Scirp_Papers) (https://www.facebook.com/Scientific-Research-Publishing-267429817016644/) (http://www.linkedin.com/company/scientific-research-publishing-inc.-usa) (http://e.weibo.com/scirp)

Contact us

customer@scirp.org (mailto:customer@scirp.org)

+86 18163351462(WhatsApp)

(http://wpa.qq.com/msgrd?v=3&uin=1655362766&site=qq&menu=yes) 1655362766 (http://wpa.qq.com/msgrd?v=3&uin=1655362766&site=qq&menu=yes)

Paper Publishing WeChat

Free SCIRP Newsletters

Add your e-mail address to receive free newsletters from SCIRP.

E-mail address

Select Journal

Subscribe

Home (//www.scirp.org/index.aspx)

Journals A-Z (../journal/indexbytitle.aspx)

Subject (../journal/index.aspx)

Books (../book/index.aspx)

Sitemap (../sitemap/index.xml)

Contact Us (../aboutus/index.aspx#ContactUs)

About SCIRP (//www.scirp.org/aboutus/index.aspx)

Publication Fees (../aboutus/publicationfees.aspx)

For Authors (../aboutus/forauthors.aspx)

Peer-Review Issues (../journal/peer-review.aspx)

Special Issues (../journal/callforspecialissueproposals.aspx)

News (../news/index.aspx)

Service (//www.scirp.org/careers/index.aspx)

Manuscript Tracking System (//papersubmission.scirp.org)

Subscription (../aboutus/subscription.aspx)

Translation & Proofreading (../careers/index.aspx)

FAQ (../aboutus/faq.aspx)

Volume & Issue (//www.scirp.org/journalvolume.html)

Policies (//www.scirp.org/aboutus/policies.aspx)

Open Access (../journal/openaccess.aspx)

Publication Ethics (../aboutus/publicationethics.aspx)

Preservation (../aboutus/preservation.aspx)

Retraction (../aboutus/retraction.aspx)

Privacy Policy (../aboutus/privacypolicy.aspx)

About SCIRP (http://www.scirp.org/AboutUs/Index.aspx)

SCIRP News (http://www.scirp.org/news/Index.aspx)

Submit your Manuscript (//papersubmission.scirp.org/login.jsp?sub=true&utm_campaign=submit&utm_source=www.scirp.org&utm_medium=bottom_submit_www)

Sign up (http://papersubmission.scirp.org/users/showAddUser?utm_campaign=signup&utm_source=www.scirp.org&utm_medium=bottom_signup_www)

ScienceDirect

Bioactive Carbohydrates and Dietary Fibre
Volume 27, May 2022, 100304

Immunomodulatory and radioprotective property of glucans isolated from lactobacillus species

Pradeepa [a], Anushri Umesh [a], Manasadeepika [a], Anushree Manjunath [a], Chithralekha Salian [a], S.M. Darshini [a], B.T. Prabhakar [b], Srinivas Mutalik [c], B.K. Manjunatha [d], S.M. Vidya [a]

Show more

Outline | Share Cite

https://doi.org/10.1016/j.bcdf.2021.100304
Get rights and content

Abstract

Bacterial exopolysaccharides (EPS) have been reported to protect the radiation induced damage during radiotherapy. Recent studies suggested that, lactic acid bacteria (LAB) and their secreted products have unique radioprotective properties. In the present study, we evaluated the ability of EPS isolated from two LAB species i.e., *Lactobacillus acidophilus* and *Lactobacillus plantarum* as a radioprotective agent against radiation induced mice small intestinal damage. EPS was isolated, identified as glucan and named as glucan A (GA) derived from *Lactobacillus acidophilus* and glucan P (GP) derived from *Lactobacillus plantarum*. GA and GP were subjected to *in vitro* immunomodulatory and *in vivo* radioprotective activity. Both GA and GP exhibited significant mitogenic activity and increased interleukin-2 (IL-2) and interleukin-10 (IL-10) secretion in a dose dependent manner. Similarly, after 9Gy whole body irradiation, glucan pre-treated mice showed improved spleen weight, reduced radiation induced hematopoietic disorder and radiation enteritis when compared to the irradiation control mice. Both glucans were also protected mice from early death and increased survival rate when compared to irradiation control. As a result, it is possible that glucan from *Lactobacillus acidophilus* and *Lactobacillus plantarum* could be served as a novel radioprotective agent to inhibit radiation-induced intestinal damage.

Previous Next

Keywords

Exopolysaccharides; Lactobacillus; Glucan; Immunomodulatory activity; Irradiation

Recommended articles

Cited by (0)

View full text

Relationship between microbial biomass and extracellular enzymes: a study of Pachamalai forested streams

PDF (https://www.nveo.org/index.php/journal/article/view/1108/1012)

K. Valarmathy, R. Stephan, B.K.Manjunath

Abstract

In forest environments, aquatic micro fungi play a critical role in organic matter breakdown. These microorganisms break down refractory substances like lignin, allowing the microbial population to effectively use organic material. In Pachamalai rainforest streams, the primary inflow of allochthonous organic materials occurs in the autumn and is enriched with luxurious microbiota.Our study aimed to determine the relationship between microbial biomass and extracellular enzymes from the streams of Pachamalai forests. The physicochemical properties of leaves and the activity of the microbial flora on the organic matter degradation were also determined.The C: N, C: P, and N: P biofilm molar ratios were calculated based on the total N, P, and C contents of two leaves species viz. Morinda tinctoria and Pongamia pinnata eaves. The hydrolytic and oxidative enzyme activity of the leaf substrata was analysed by earlier know methods.Morinda tinctoria leaves had a faster breakdown with a decrease in leaf toughness relative to P. pinnata. Extracellular enzyme assays revealed that M. tinctoria had higher hydrolytic enzyme activity when compared to P. pinnata.From our study, it is conclusive that the microbiota associated with both the leaf species have significant extracellular enzymatic activity in degrading the polysaccharides and lignin. This plays a significant role in the stream biota and influences the ecosystem.

Issue

Volume: 8 Issue: 4 (https://www.nveo.org/index.php/journal/issue/view/29)

Section

Articles

(https://www.scimagojr.com/journalsearch.php?q=21100904334&tip=sid&exact=no)

INDEXES AND PLATFORMS

ASOS indeks

SAIF Scholars Impact

CABI

CAS A DIVISION OF THE AMERICAN CHEMICAL SOCIETY

DRJI

Google Scholar

ELSEVIER Scopus

SOBIAD

OCLC WorldCat

ZDB ZEITSCHRIFTEN DATENBANK

Nat. Volatiles & Essent. Oils, 2022; 9(1): 736-744

NVEO
Natural Volatiles &
Essential Oils

Application Of RBNN Method For Identification Of Thyroid Disease Cases Using Electro Photonic Images

Indrakumar S S[1] , Prof. M S Shashidhara[2]

[2]Research Scholar Dept. of Computer Applications The Oxford College of Engineering, Bangalore-560068,India.

[2]Dept. of Computer Applications The Oxford College of Engineering, Bangalore-560068,India.

Abstract

Many diseases affect human beings, and various methods are used to understand these disease conditions. ElectroPhotonic images also help diagnose disease much earlier, like before physical symptoms appear in the body. Energy fields of Humans, Plants, and Crystals can be measured using Electro photonic imaging. A special camera is used to gather these images, referred to as an EPI camera. This paper gives insight into the detection and classification of Thyroid disease using Electro Photonic Images. Image processing is carried out using the Radial Basis Function to detect and classify Thyroid patients.

Keywords: Kirlian photography, Medical diagnosis, Energy, Aura, Chakras, Thyroid, RBNN

Introduction

According to modern science, the human organism is made of molecules, and these molecules need energy which is provided in the form of food, light, and water. The overall energy in the body creates an energy field. We are learning to measure this energy fields using the Kirlian camera.

When a human being is affected by any disease, it will appear in the form ailment in the body. Since the human body is made of cells, these cells are affected. Energy levels of the human body are captured during this process used to identify the diseases. Images collected from Non-Thyroid and Thyroid. These images are classified using the Radial Basis Function Neural Network method as Non-Thyroid and Thyroid.

1. Energy

We get energy from the universe in some form from Sun, Air, and Water. All living organisms need energy to live. All living organisms require energy from their food intake, along with these energies. The bioenergy field surrounds every human. An electrocardiogram device helps to understand the electrical activity of the Human Heart**,** and Electroencephalogram can be used to measure Brain bioenergy. Various magnetic imaging devices can measure electromagnetic fields around the human body. We have an energy system

made up of different electromagnetic fields known as bioenergy fields. There are two effects of the bioenergy field, one reflecting on the physical body and another influencing our environment. First, the human bioenergy field is affected by the external factors that emit electromagnetic waves. The effect of these waves will be negative. Cells will be affected when this negative energy affects the human body for a long time. This cellular level will show up as physical symptoms.

2. Medical Diagnosis

In standard practice, to diagnose any disease, the doctor begins to understand the patient's conditions by asking questions related to the ailments in patients, then goes thru the history and previous records treatment suggested, then does physical examinations and medical tests if required. Electrophonic images are helpful in finding out the energy levels of the body, which are then used in disease diagnosing. The Kirlian camera can capture Electro photonic images that measure human energy levels. These images also help in analyzing the changes in the subtle energy distribution.

3. Existing Systems

The two most prominent systems which are used for energy analysis are:

1. Energy Emission Analysis or EEA - Peter Mandel’s System
2. Gas Discharge Visualization Technology - Dr. Konstantin Korotkov’s System

Peter Mandel used a high-voltage analog camera in a dark room. Peter Mandel approached new holistic treatments where he believed that troubling conditions originated from the subconscious state. The EEA evaluator collects the patient's overall body-soul-spirit situation, which shows the physical, emotional, or mental state; the therapist will address the issue based on the form.

4. Electro Photonic Imaging

Scientists captured electromagnetic fields from humans and biological objects for more than two centuries. However, the complexity of the equipment used during that time slowed down the progress of the study of the effect. Finally, this phenomena was discovered by a Russian named Kirlian in 1930. They were involved in this study for several decades to study various substances, and they successfully attained more than 30 patents. Hence, the phenomenon is also known as the Kirlian Effect.

There is electrical activity in the human body. Electro photonic imaging devices can be used to measure the electrical activity of the human organism. The pattern created by the high voltage varies when the `subject's body is in a balanced condition. When there is an imbalance in the subject, it creates another pattern. There will be a difference in the patterns generated in normal and abnormal subjects. A Russian named Kirlian discovered these phenomena in 1930. There are practical applications in the area’s of Medicine, Sports, and liquid testing using Electro photonic imaging systems. The EPI system can measure physical and Emotional effects on the human energy field.

Each finger connected to one of the human body organ, like Right Thumb Finger connected to the Right eye, Left Little Finger to the Left part of the Heart, Right Thumb Finger to the Right eye, and Right Ring Finger to the Thyroid gland.

Fig: ElectroPhotonic Imaging Devices

5. Thyroid

The thyroid gland is an endocrine gland. It contains two lobes connected. Isthmus is connecting bridge between these two lobes. The thyroid gland location is at the front of the neck of the human body. The thyroid gland secretes three hormones triiodothyronine, thyroxine, and a peptide hormone, calcitonin. These hormones affect the metabolic rate, also growth, and development. Thyroid-stimulating hormone-regulated the secretion of these two hormones. Hypothalamus produces the stimulating thyroid hormone.

There are various conditions of the Thyroid depending on the functional level of this gland. Goiter is one condition that has a state of swelling, which is due to iodine deficiency. The next one is due to the cause of Grave's disease known as Hyperthyroidism. The autoimmune disease causes another condition referred to as Hypothyroidism. Even a type of cancer occurs to this gland known as Thyroid cancer which is curable by surgery or radiation. Thyroiditis is another condition caused by a viral infection. Finally, another condition named Thyroid occurs due to Hyperthyroidism with excess hormone release, which causes severe illness.

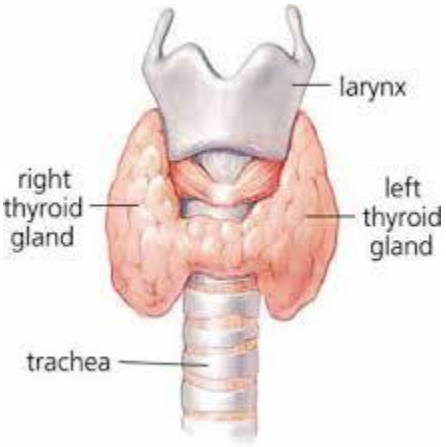

Fig: Thyroid Gland

6. Radial Basis Function Neural Networks

The radial basis function is the most broadly used and best fit for image classification. RBF is simple in architecture. The training process is faster. Also, the learning algorithm corresponds to the solution of a linear regression problem. RBF requires the determination of the number and position, which is the main drawback of this algorithm. Centers are randomly selected from the training data, and in unsupervised

methods, clustering algorithms are adopted like k-means. Center initialization in the traditional approach is more sensitive in RBF.

RBF network is an artificial neural network with input and output layers. Another layer Hidden layer carries hidden neurons and activation functions. For an input signal from the input layer corresponding input, a vector is generated by the hidden layer, and the network generates the corresponding signal.

Nodes in the hidden layer perform the radial basis transformation function.- to get final values. The output layer performs the linear combination of the outputs of the hidden layer. Classification is performed in the output layer. With respect to Training times, Multi-layer Perceptron Classification takes more time than RBNN.

Algorithm

- K- number of hidden neurons
- RBNN centers are set using a K-means clustering algorithm.
- Calculate Sigma
- Calculate actions of Radial Basis Function
- Train the output using

A Radial basis function focuses on distance from its center. Absolute values are used. Absolute values are those without their associated sign; the absolute value of -4 is 4.
A typical Gaussian function is defined as

$$f(x) = \frac{1}{\sigma\sqrt{2\pi}} e^{-\frac{(x-\mu)^2}{2\sigma^2}}$$

7. Model Building

After collecting the images using the EPI device, the next stage is to train images and build a model to predict thyroid disease. We have used Matlab for coding to train images and build the model

8. Training & Testing

Each image is read in Matlab and stored in the Matlab database. Training of both normal and Thyroid images was carried out. Once training is completed, testing is carried out for some samples.

We successfully collected 510 Normal and 520 Thyroid sample Electrophotonic images from different sources during the image collection.

80% of images were used for training, and 20% were used for testing

Inclusion Criteria

Subjects will be included for the current research based on the following criteria
Age: 25 to 50 years.
Healthy volunteers, both male and female volunteers. People who are taking Allopathy Medicine
People who are taking Ayurvedic Medicine, People who are taking Homeopathic Medicine
People who are practicing Yoga and meditation.

Exclusion Criteria

People having any acute or chronic diseases, People with missing fingers or cut in fingers
Females during menstruation or pregnancy

Normal Images	500
Thyroid Images	520
Total Images	1020

Normal Samples	50
Thyroid samples	52
Total Samples	102
Male Samples	15
Female Samples	87

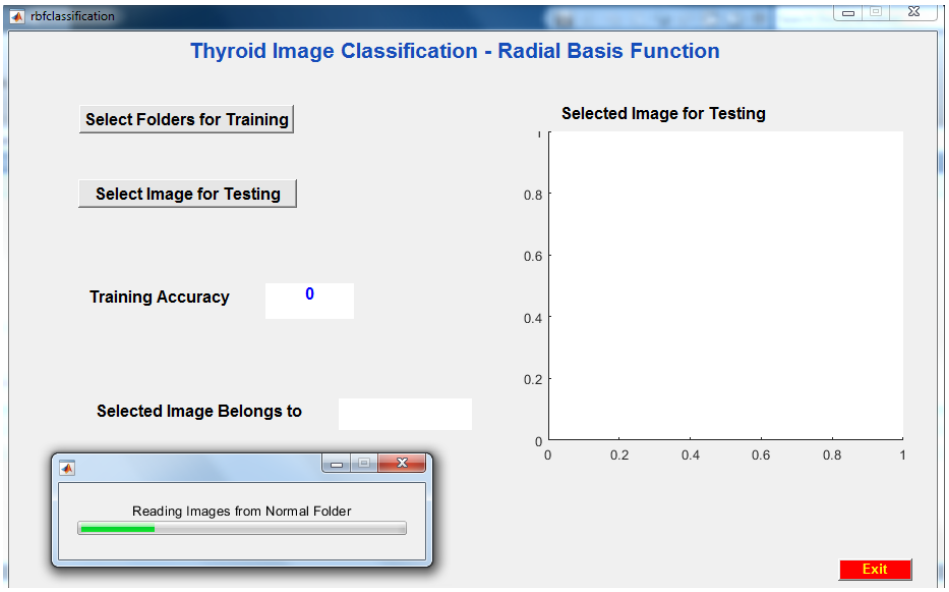

Fig: Reading images from the folder

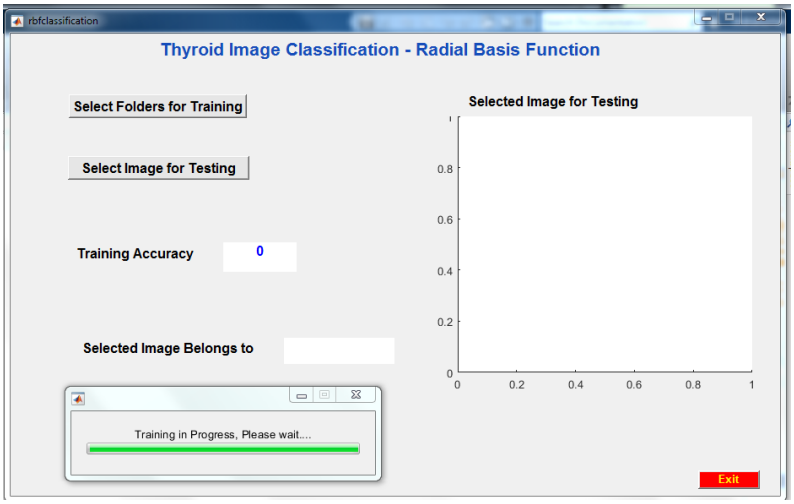

Fig: Training images

9. Results

Thyroid disease prediction is made using the Radial Basis Function algorithm with function. Five hundred sample images of Normal and Thyroid images in each category were used for training. Model is built, which is used to predict other samples. Learning rate set to .01 No of inputs as image size of 285*370 and output as single either Normal or Thyroid. The Training Accuracy rate is 95.5%.

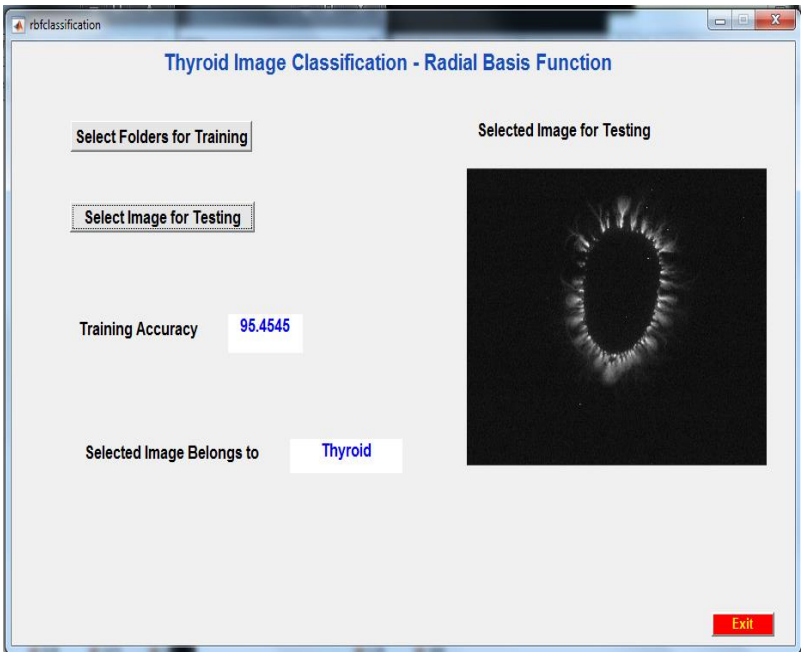

Fig: Test Result of Thyroid image

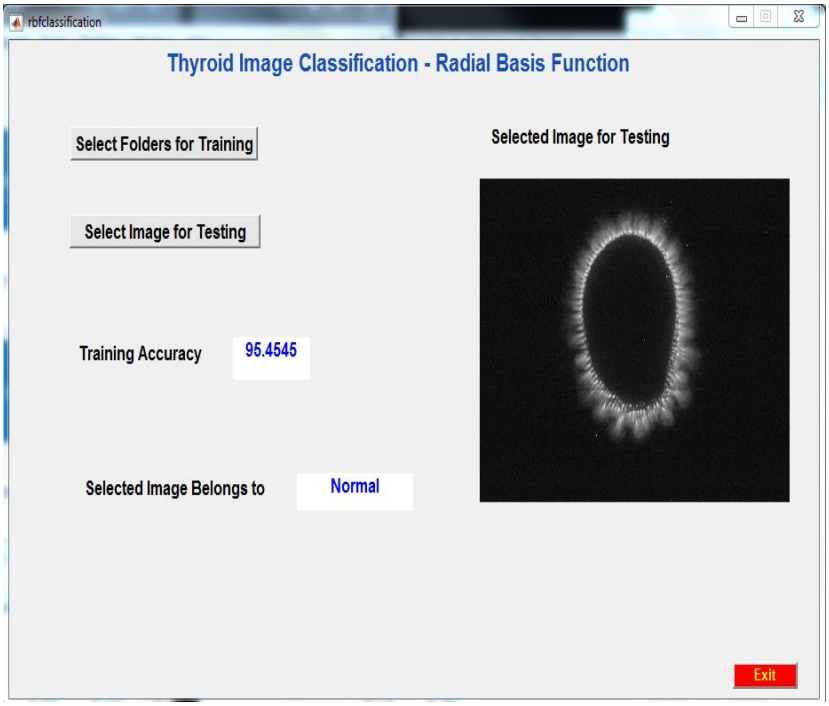

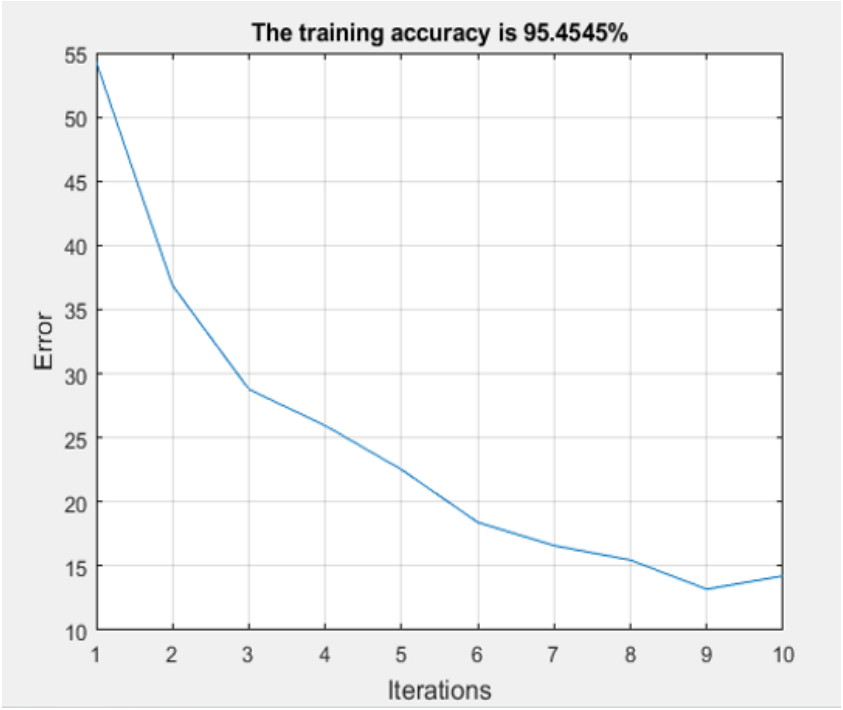

Fig: Training Accuracy

10. Conclusion

Electrophotonic images can be used to predict thyroid disease. These images also reveal the current conditions of the organs. Therefore, these images are used to diagnose thyroid disease. Collected images

can also be classified using the Radial Basis Function model. After training images, the training rate achieved 95.5%.

A confusion matrix was used to evaluate the performance of the classification model. Various measures listed below can be calculated to assess the performance of the classification model. In addition, the following parameters from the confusion matrix are helpful to compare results.

Measure	Value
Sensitivity [B / (B+C)]	0.955
Specificity SPC [E/ (D + E)]	0.955
Precision PPV [B / (B + D)]	0.955
Negative Predictive Value NPV [E / (E+ D)]	0.955
False Positive Rate FPR [D / (D + E)]	0.045
False Discovery Rate FDR [D/ (D + E)]	0.045
False Negative Rate FNR [C / (C + B)	0.045
Accuracy ACC [(B + E) / (P + N)]	0.955
F1 Score [2TP / (2B + D + C)]	0.955

Table 3: Confusion matrix measures-RBNN Method

11. References

[1] K.G.Korotkov, ''Measuring Energy Fields'', Saint Petersburg, 1999.

[2] Rosenfield, A.C. Kak, Digital Picture Processing, vol. 1 & 2, Acad. Press, NY, 1982.

[3] Rosalyn L. Bruyere, Wheels of Light (New York: Simon and Schuster, 1989),

[4] Caroline Myss, Anatomy of the Spirit (New York: Random House, Inc., 1996),

[5] Michael Tierra, Lesley Tierra, “Chinese traditional herbal medicine - Diagnosis \& treatment,” vol. 1, pp. 195, 1998.

[6] R. Rajesh, M.R. Kaimal, K. Srinivasan, “A Note on Medical Image Analysis and Visualization using Matlab,” ICGST International Journal on Graphics Vision and Image Processing, Special Issue on Medical Image Processing, pp. 352-355, 2006.

[7] Xanadu C. Halkias, Petros Maragos, “Analysis of Kirlian Images: Feature Extraction and Segmentation'', Proc. of ICSP, 2004.

[8] K.G.Korotkov, “Aura and Consciousness - Book'', 2nd Ed, Saint Petersburg, 1999.

[9] Sushrutha S, Hegde M, Nagendra H.R., et al. “Comparative study of Influence of Yajña and Yogāsana on stress level as Measured by Electron Photonic Imaging (EPI) Technique.” International Journal of Science and Research (IJSR). 2014;3(8):1402–1406.

[10] Sushrutha S, Madappa K, Nagendra H.R. “Effect of bhaishajya maha yajna on human energy field and environment.” International Journal of Innovative Research in Science & Engineering. 2015.

[11] Narajanan R. Understanding diabetes from the perspective of electro–photonic imaging (bio–well) and proposing yoga therapy for reversing Type–2 diabetes. In: Proceedings of International Scientific Congress on Bioelectrography. St Petersburg; 2017:36.

[12] Naranjan R. EPI readings of type II diabetes. In: Proceedings of International Scientific Congress on Bioelectrography. St Petersburg; 2018:16–23

[13] Kuldeep K Kushwah, et.al."Effect of Yoga based techniques on stress and health indices using electro photonic imaging technique in managers"

[14] Romesh Kumar Bhat, "Diabetes mellitus type 2 and yoga: Electro photonic imaging perspective," International Journal Yoga. 2017.

Recent Trends in Communication and Intelligent Systems pp 13–19

Implementation and Image Transformation for Ground Penetration Image Radar System

Dharamvir & M. S. Shashidhara

Conference paper | First Online: 25 May 2022

Part of the Algorithms for Intelligent Systems book series (AIS)

Abstract

Ground Penetration Radar (GPR) detects buried detonatory objects. The data collection may be view with different source of information to make use of Ground Penetration Radar System. In the normal data gives hyperbolic effects, which make the analysis and detection of targets difficult. So a focusing algorithm, Kirchoff Migration has been used for a synthetically generated GPR data pattern, The task control behavior of assigned data performs with Stepped Frequency Continuous Wave Radar (SFCW). The data is migrated, simulated in Mat Lab. Architecture has been proposed for the FPGA Implementation of the same.

Keywords

GPR **Kirchoff migration** **Interpolation**

FPGA implementation

References

1. I.A. Ruthenberg, *Curve Fitting and Migration of GPR Data for the Detection*. (Department of Computer Science and Electrical Engineering, University of Queensland, IJMRT Journal, 2018) pp. 119–126

2. R. Gupta et al., Automation and aviation radar techniques. IEEE Trans. **29**(11), 219–231 (2018)

3. A. Gunawardena, D. Longstaff, Wave equation formulation of synthetic aperture radar (SAR) algorithms in the time-space domain. IEEE Trans. GeoSci. Rem. Sens. **6** (2019)

4. D.S. Jones, *The Theory of Electromagnetism* (Pergamon Press, 2016)

5. E. Yigit, S. Demirci, C. Ozdemir, Ground penetrating radar image focusing using frequency-wave number based synthetic aperture radar technique, In *IEEE paper, Published in, International Conference on Electromagnetics in Advanced Applications, ICEAA2017*, pp. 344–347

Author information

Authors and Affiliations

Research Scholar VTU, Dept. of MCA, The Oxford College of Engineering, Bengaluru, 560068, India

Dharamvir & M. S. Shashidhara

Corresponding author

Correspondence to Dharamvir .

Editor information

Editors and Affiliations

Arya College of Engineering & IT, Jaipur, Rajasthan, India

Prof. Aditya Kumar Singh Pundir

Department of Mathematics, National Institute of Technology, Hamirpur, Himachal Pradesh, India

Dr. Neha Yadav

Department of Computer Science and Engineering, Rajasthan Technical University, Kota, Rajasthan, India

Dr. Harish Sharma

Electronics and Communication Sciences Unit, Indian Statistical Institute, Kolkata, West Bengal, India

Dr. Swagatam Das

Rights and permissions

About this paper

Cite this paper

Dharamvir, Shashidhara, M.S. (2022). Implementation and Image Transformation for Ground Penetration Image Radar System. In: Pundir, A.K.S., Yadav, N., Sharma, H., Das, S. (eds) Recent Trends in Communication and Intelligent Systems. Algorithms for Intelligent Systems. Springer, Singapore. https://doi.org/10.1007/978-981-19-1324-2_3

.RIS .ENW .BIB

DOI
https://doi.org/10.1007/978-981-19-1324-2_3

Published	Publisher Name	Print ISBN
25 May 2022	Springer, Singapore	978-981-19-1323-5

Online ISBN	eBook Packages
978-981-19-1324-2	Intelligent Technologies and Robotics Intelligent Technologies and Robotics (R0)

Technological University (3001338151)

Yantu Gongcheng Xuebao/Chinese Journal of Geotechnical Engineering

Handling Big Data Using a Data-Aware HDFS and Evolutionary Clustering Technique

Dr. M.S. Shashidhara*, Abhishek Madhusoodhanan, Monish N, Namratha T K & Subash N

Keywords: Clustering methods, Distributed Computing, Information Management, Optimization, Scalability.

Abstract

The increased use of digital empowered plans and Internet-of-Things (IoT) prompted a colossal amount of insights with divergent developments. Most noteworthy large realities answers are developed on most elevated of the Hadoop eco-framework or use its appropriated document framework (HDFS). However, trainings consume uncovered disorder in such plans when business with the present realities. Some examination overpowered these errors for accurate sorts of chart measurements, however the present realities are extra than one sort of insights. Such skill subjects head to enormous gage misfires, including predominant space required in realities places, and left-over in capitals (like control ingesting), that state of the art go lead to environmental errors (like more fossil fuel byproduct) [1], according to scholastics. We propose an information mindful part for the Hadoop eco-framework. We also propose a scattered influence technique for Hereditary Systems. Our construction lets Hadoop to accomplish the inventory of measurements and its task established on pack assessment of the insights himself. We stay skilled to hold an extensive assortment of realities types as solid as upgrade enquiry time and save practice.

PDF

Published
2022-08-10

How to Cite

Dr. M.S. Shashidhara*, Abhishek Madhusoodhanan, Monish N, Namratha T K & Subash N. (2022). Handling Big Data Using a Data-Aware HDFS and Evolutionary Clustering Technique. *Yantu Gongcheng Xuebao/Chinese Journal of Geotechnical Engineering*, *44*(8), 59–65.

Yantu Gongcheng Xuebao/Chinese Journal of Geotechnical Engineering

A Semantically Improved Marginalization Denoising Auto Encoder is Used to Detect Cyberbullying

J C Achutha*, Vishwanath S, Md Khalid Athar, Manoj Kumar M R & Vimal Joy

Keywords: Denoising, Auto-Encoder, Artificial Intelligence, CyberBullying, Word Embedding.

Abstract

Cyberbullying has become a big problem for youngsters as a result of the rise of social media.

"Teenagers" and "youthful grown-ups" are terms used to depict youths and youthful grown-ups. Because of AI procedures, modified distinguishing proof of pestering messages by means of electronic diversion is by and by possible, possibly adding to the foundation of a solid and safe virtual entertainment environment.This key area of exploration, Powerful and discriminative mathematical portrayal intake instant chat, has arrived at a defining moment. To settle this test, we offer another illustrative learning strategy in this review. Semantic-Enhanced Marginalized Denoising Auto-Encoder (smSDA) is a semantic difference in the by and large used significant learning model Stacked Denoising Auto-Encoder. The semantic extension is involved semantic dropout uproar and sparsity objectives, with the semantic dropout commotion being made using space data and the word embedding method.Our recommended framework can learn and take advantage of the idle component construction of tormenting data, bringing about a vigorous and separating message portrayal. Our proposed approaches outflank past essential literary portrayal learning techniques on two well known cyberbullying corpora (Twitter and MySpace), as indicated by broad testing.

Published
2022-08-10

How to Cite

J C Achutha*, Vishwanath S, Md Khalid Athar, Manoj Kumar M R & Vimal Joy. (2022). A Semantically Improved Marginalization Denoising Auto Encoder is Used to Detect Cyberbullying. *Yantu Gongcheng Xuebao/Chinese Journal of Geotechnical Engineering*, *44*(8), 66–73. Retrieved from http://ytgcxb.periodicales.com/index.php/CJGE/article/view/148

Issue

Vol. 44 No. 8 (2022)

Section

Articles

Keywords

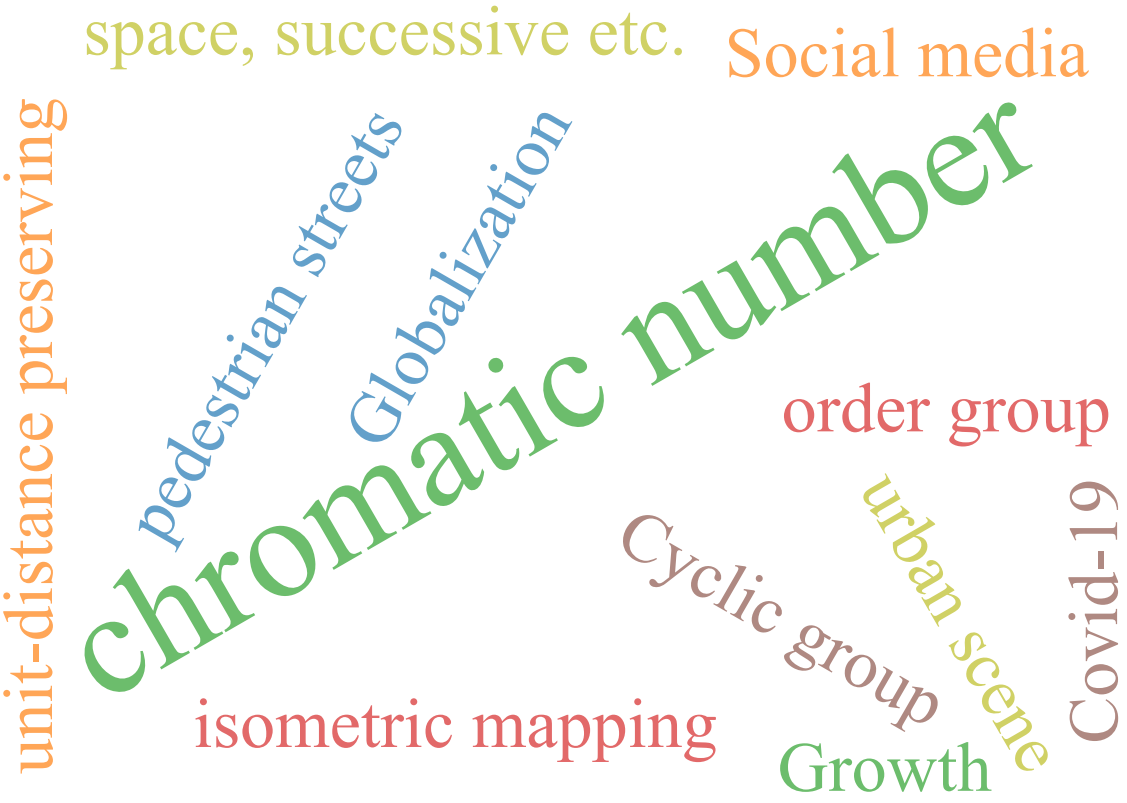

Information

For Readers

For Authors

For Librarians

Publisher

Chinese Society of Civil Engineering & Editorial Office of Chinese Journal of Geotechnical Engineering

Current Issue

ATOM 1.0

RSS 2.0

RSS 1.0

Subscription

Login to access subscriber-only resources.

Browse

Open Journal Systems

ISSN:1000-4548

Yantu Gongcheng Xuebao/Chinese Journal of Geotechnical Engineering

Operational Efficiency Improvement of Power Grid by Improving MPPT Charge Controller

Dr. Prabodh Khampariya, Savitha C & Achutha J.C

Keywords: Solar Power, Power Grid, Efficiency, photovoltaic systems.

Abstract

The growth of industry, transportation, and the media have all had a significant impact on global power use in the last several decades. There is now a lot of power being generated from non-renewable resources including coal, natural gas, oil and uranium. Because of the sluggish rate of regeneration, these resources may be depleted sooner rather than later. Photovoltaic systems that are linked to the grid are the subject of this research. Optimizing inverters as interfaces between the grid and photovoltaic systems is the primary goal of this research, which aims to send energy to the grid in accordance with the network's needs. It is not only the active power that may be controlled, but also the reactive one. This paper proposes an algorithm for creating an inverter connected to the grid that can be controlled simply and reliably. The digital control approach provides the basis for it. With this research, we're able to learn more about the limits of VSCs as inverters for delivering active and reactive electricity to the grid while also enhancing power factor and harmonic content of the injected current from solar panels

Published
2022-07-25

How to Cite

Dr. Prabodh Khampariya, Savitha C & Achutha J.C. (2022). Operational Efficiency Improvement of Power Grid by Improving MPPT Charge Controller. *Yantu Gongcheng Xuebao/Chinese Journal of Geotechnical Engineering*, *44*(7), 1–8. Retrieved from http://ytgcxb.periodicales.com/index.php/CJGE/article/view/138

More Citation Formats

Issue

Vol. 44 No. 7 (2022)

Section

Articles

Make a Submission

Keywords

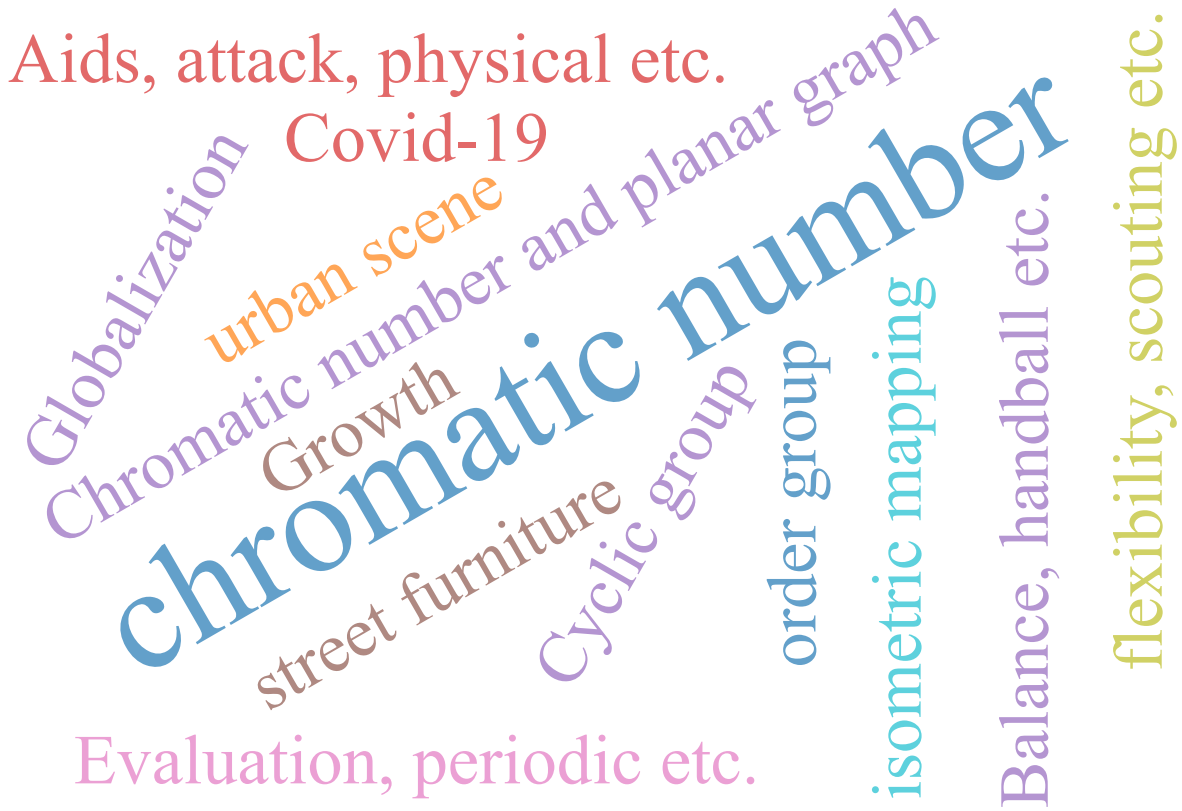

Information

For Readers

For Authors

For Librarians

Publisher

Chinese Society of Civil Engineering & Editorial Office of Chinese Journal of Geotechnical Engineering

Current Issue

ATOM 1.0

RSS 2.0

RSS 1.0

Subscription

Login to access subscriber-only resources.

Browse

Open Journal Systems

ISSN:1000-4548

NeuroQuantology
An Interdisciplinary Journal of Neuroscience and Quantum Physics
ISSN 1303 5150

DOI: 10.14704/nq.2022.20.8.NQ44532

REAL-TIME MOVIE TICKET BOOKING CHATBOT BASED ON NLP AND RASA FRAMEWORK

J C Achutha, Anmol N, Chandu A B, Dipankar Boruah, Chirag Mahadev

Abstract

A chatbot or commonly known as chatterbot can be referred as software program that can converse in an online chat discussion utilizing text or texttospeech instead of direct textual communication with a live human agent. A chatbot is program that will help customers automate conversations and connect with the customers through various instant messaging platforms. Despite the reality that many chatbots in deployment are still unable to talk fluently and cannot pass the traditional Turing tests, chatbot systems are usually created to flawlessly replicate how a person would interact as a communicator. The goal of this work is to create a chatbot that can help a user easily book cinema tickets using Natural Language Processing and backend database activity.The final model consists of all the required modules that handle reservation, allocation and retrieval of seats parallelly for more than two movies screening in the same theatre. As a result, a model which provides schedule of the movies that are being played on a particular date, information and rating about the movie the user is interested to watch, real-time seat map of available seats in the screen, temporary reservation of seats while waiting for payment confirmation, payment handling tasks through various payment gateways offering variety in payment options to the user, generation of tickets and a unique Ticket QR code for easy check-in and methods in the backend to manage data at each of the above stage, has been developed. The second objective of developing a chat bot to book tickets is to enable user to interact naturally without the burden for the user to learn new UI usages techniques, install new apps or create accounts.

Keywords

Chatbot, Movie Ticket Booking, Natural Language Processing, Ticket QR Code, Payment Gateway, RASA, RASA-X

Full Text

PDF

References

?>

Journal of Optoelectronics Laser

A comprehensive Review on power Consumption with Applied deep Analytics

Savitha C, Prabodh Khampariya, Achutha J.C

Keywords: Affordable and clean energy, micro-grid applications, micro-grid architectures, regional development, smart grid, sustainable cities, sustainable development goals.

Abstract

Generation and energy consumption are a major issue in different countries around the world. Nowadays, projects under development seek the modernization of electric power generation and distribution systems. One of the main strategies is the design of context-adaptable micro-grid architectures. The micro-grid concept focuses on a controlled, monitored and highly autonomous use of electric power supported on information technologies, for the optimization of energy transfer, minimize risks and increase the system's quality, efficiency and reliability. This article, therefore, aims to identify, classify and compare different micro-grid architectures, based on their applicability and research trends. A systematic mapping study of micro-grid architectures is conducted to examine the experimental and theoretical contributions made by the scientific community. This article categorizes and quantifies the different studies related to the subject, identifying and analysing the strengths and opportunities for improvement in the applicability of micro-grid architectures. The trends observed highlight five strategies as the most relevant, whose different characteristics contribute to an automated and intelligent organization of the distribution, control and supervision of electricity according to supply versus demand.

Published
2022-06-15

How to Cite

Savitha C, Prabodh Khampariya, Achutha J.C. (2022). A comprehensive Review on power Consumption with Applied deep Analytics. *Journal of Optoelectronics Laser*, *41*(6), 496–506. Retrieved from http://www.gdzjg.org/index.php/JOL/article/view/548

More Citation Formats

Issue

Vol. 41 No. 6 (2022)

Section

Articles

Scopus

Make a Submission

Current Issue

ATOM 1.0

RSS 2.0

RSS 1.0

Subscription

Login to access subscriber-only resources.

Publisher

Tianjin Daxue Jidian Fenxiao/Tianjin Innstitute of Technnology

Information

ISSN:1005-0086

NeuroQuantology
An Interdisciplinary Journal of Neuroscience and Quantum Physics
ISSN 1303 5150

DOI: 10.14704/nq.2022.20.8.NQ44533

Anti-fake Technology of Commodity by Using the QR Code Application

Dharamvir, Ashwini D, Apula S, Hibu Tabyo, BhimSen Singh

Abstract

QRCode are often used in the raw materials trading. One of its main idea is covering credible authentication information to avoid the customerbuying produced products. This Research Papers gives an extinct idea how the QRcode Security system interacts with a customer and it helps us to know the relation on the server and the QRCode data. It is necessary to encrypt the QRCode by using the RSA secure-ID software token and DES Algorithm. And by Comparing these procedures for the QR security Code, by using the DES and RSA algorithms, it displays the way how the expends of preceding goods are increasing, which is ultimately can be used in the antifake identification as expectation. Furthermore, this insight helps us in decrypting the QRCode and key storage of how it is introduced in the maintenance and development and with the textbook which are written and handled as a relationship of Client and Server on this research. The way and process of how the anti-fake technology detection is working, can be viewed or seen from its brands or by its specialist co-opâ€™s side or service providers side, and it is been used for detecting that when a same acquirers or identifiers coded in the QRCode are repeated many times within the specific time periods or Geographic Regions.

Keywords

QR code,Cryptography,RSA, DES.

Full Text

PDF

References

Journal Menu

Home
Editorial Board
Archives
Current Archives
Author Guidelines
Call for Submissions
Login

?>

NeuroQuantology
An Interdisciplinary Journal of Neuroscience and Quantum Physics
ISSN 1303 5150

DOI: 10.14704/nq.2022.20.8.NQ44533

Anti-fake Technology of Commodity by Using the QR Code Application

Dharamvir, Ashwini D, Apula S, Hibu Tabyo, BhimSen Singh

Abstract

QRCode are often used in the raw materials trading. One of its main idea is covering credible authentication information to avoid the customerbuying produced products. This Research Papers gives an extinct idea how the QRcode Security system interacts with a customer and it helps us to know the relation on the server and the QRCode data. It is necessary to encrypt the QRCode by using the RSA secure-ID software token and DES Algorithm. And by Comparing these procedures for the QR security Code, by using the DES and RSA algorithms, it displays the way how the expends of preceding goods are increasing, which is ultimately can be used in the antifake identification as expectation. Furthermore, this insight helps us in decrypting the QRCode and key storage of how it is introduced in the maintenance and development and with the textbook which are written and handled as a relationship of Client and Server on this research. The way and process of how the anti-fake technology detection is working, can be viewed or seen from its brands or by its specialist co-opâ€™s side or service providers side, and it is been used for detecting that when a same acquirers or identifiers coded in the QRCode are repeated many times within the specific time periods or Geographic Regions.

Keywords

QR code,Cryptography,RSA, DES.

Full Text

PDF

References

Journal Menu

Home
Editorial Board
Archives
Current Archives
Author Guidelines
Call for Submissions
Login

?>

How to Cite:
Dharamvir, D., Chandrakala, M., Patel, P., Sharma, P. P., & Kumar, P. V. (2022). Fake news detection using python. *International Journal of Health Sciences*, *6*(S3), 12513–12523. https://doi.org/10.53730/ijhs.v6nS3.9537

Fake news detection using python

Dharamvir
Asst. Professor, Department of MCA, The Oxford College of Engineering, Bengaluru, Karnataka, India – 560068
*Corresponding author email: dhiruniit@gmail.com

Chandrakala M.
MCA Final Year, Department of MCA, The Oxford College of Engineering, Bengaluru, Karnataka, India – 560068

Pooja Patel
MCA Final Year, Department of MCA, The Oxford College of Engineering, Bengaluru, Karnataka, India – 560068

Phurailatpam Paona Sharma
MCA Final Year, Department of MCA, The Oxford College of Engineering, Bengaluru, Karnataka, India – 560068

Pramodh Kumar V.
MCA Final Year, Department of MCA, The Oxford College of Engineering, Bengaluru, Karnataka, India – 560068

Abstract---This Research Paper proposed COVID-19 pandemic, a few achievement and cash related impels come to ungracefully play with identification of given data . This has presented distortion and disarray from one side of the world to the other. The issues of phony news have achieved a rising importance in the dispersing of trim reports. A broad bundle of them stop to rely on the papers, magazines, and so on and began to depend through internet based redirection completely. Online redirection changed into the focal news point of convergence for a tremendous number of individuals because of their clear access, unassuming, genuinely beguiling and quick spread. The phony substance began to spread at a gigantic speed to get inescapability over electronic redirection to divert individuals from the ceaseless major issues, in unambiguous events spreading more and quicker than the genuine data. Individuals spread counterfeit news through virtual redirection for cash related and political augmentation. Counterfeit information in all plans should be perceived quickly to keep away from a threatening outcome on society. This try makes an assessment of the appraisal related with counterfeit news divulgence, we organized and endeavored different AI

International Journal of Health Sciences ISSN 2550-6978 E-ISSN 2550-696X © 2022.
Manuscript submitted: 18 Feb 2022, Manuscript revised: 27 April 2022, Accepted for publication: 9 June 2022

calculations independently to show the productivity of the social event on the dataset. This task was executed in the Jupyter scratch cushion stage and execution was assessed.

Keywords SVM, PAC, fake news, social media, machine learning

Journal of Physics: Conference Series

Transformational Perceptive of Data Recorder for UAV Flight Automation Control System using Image Processing Techniques

Transformational Perceptive of Data Recorder for UAV Flight Automation Control System using Image Processing Techniques

Dharamvir[1], Hemanth K S [2]

[1]Research Scholar , School of CSA, REVA University , Bengaluru, India -560024

[2] Associate Professor , School of CSA, REVA University , Bengaluru, India -560024
Email : [1]dhiruniit@gmail.com , [2]hemanth.ks@reva.edu.in

***Abstract*—** Flight Data Recorders (FDRs) are readily available in the market, to be used on the Unmanned Aerial Vehicles (UAV) for onboard data recording. They have their own inbuilt sensors and characteristics and can be easily placed within the cockpit of the UAV. However, they have umpteen drawbacks. They do not have sufficient sampling rate for rapid and accurate flight automation, are either very bulky, or do not incorporate some of the necessary sensors required for post-flight analysis and are very costly. Hence, the need arises where the FDR needs to be designed to suit the requirements. We go about designing one such FDR. Our FDR incorporates a MicroStrain's 3DM- GX1 Gyro Enhanced Orientation Sensor, a Texas Instrument's GPS module and four servo motors each controlling the rudder, elevator, ailerons. The data from these devices are interpolated to increase the sampling rate and are simultaneously stored into a Secure Digital (SD) / Micro Memory Card (MMC) during the flight of the UAV. Greater sampling rates allow more rapid and accurate flight automation. SD/MMC cards allow faster and efficient data retrieval for post flight processing. Our FDR is designed to be compact, cheap and overcomes most of the drawbacks mentioned above.Therefore, we call this FDR as Smart Data Recorder(SDR).

***Keywords*—**3DM-GX1 Orientation Sensor, GPS module, servo motors and SD/MMC card, interpolation.

1. INTRODUCTION

Unmanned Aerial Vehicles (UAV) have evolved by leaps and bounds in the last quarter of the century into very intelligent, capable robotic systems. They are mainly used by military for surveillance and data acquisition purposes. UAVs vary in size, from an aircraft as small as that of our palm to one as big as that of an average car. UAVs, in general, comprise of three main features: the aircraft, Ground Control Station (GCS) and the operator.

Although the presence of a human pilot aboard the aircraft is eliminated, his presence cannot be removed completely from the mission. Right from the word 'Go' i.e. from the moment the UAV takes off till it lands safely, an operator in the GCS will have complete control of the UAV from a remote distance. The operator analyses the various sensor data, images and video obtained from the UAV and flies the aircraft in a way a normal pilot would. Hence there are chances of the mission failing due to human (operator) error. To minimize this error, the flight operation should be made as independent as possible, from human intervention. Once the co- ordinates of the destination have been uploaded to the aircraft, it should take off and maintain correct flight path and reach the destination quickly at all costs. Hence very accurate and rapid flight automation is required.

For smaller UAVs the characteristics of the FDR
used will be of utmost importance. Since flight automation depends on the feedback signals obtained from the sensors aboard, the data recorder aboard the UAV needs to be very fast, accurate and compact enough so that the overall payload factor remains virtually unaltered. In other words, the FDR needs to be

"Smart". Our SDR is designed to be fast, accurate and compact enough to be fitted onto relatively smaller UAVs.

The sampling rates in readily available FDRs are 100 samples/second or less. As this is insufficient for flight automation, we increase the sampling rate to 500 samples/s, by interpolation, in SDR. Unlike other FDRs, the SDR extracts only the necessary and sufficient parameters that are required from the sensors. Unwanted data is simply discarded and so this time is instead used for effective sampling of required data.

Also our SDR can be used for testing active flightparameters such as rudder or elevator sensitivitywhen a new flight design is to be incorporated, which otherwise cannot be determined by a wind tunnel test.

This paper discusses the Block Diagram of the SDR and hardware interconnections involved in section 2, the program flow in section 3. The resultsare explained in section 4, conclusion and future scope in sections 5 and 6 respectively.

2. SMART DATA RECORDER (SDR) BLOCKDIAGRAM

Interconnections between microcontroller and otherdevices are as shown in Fig.1. The SDR characteristics are as follows:

i. 4 analog channels to receive analog datafrom four servos.
ii. A UART port to receive data from 3DM-GX1 orientation sensor which gives -
    1. Roll, pitch and yaw
    2. X, Y, Z axis angular rates
    3. X, Y, Z axis acceleration
    4. Timer ticks
iii. A UART port to receive data from theGPS module which gives
    1. Universal Time
    2. Latitude
    3. Longitude
    4. Altitude
iv. Interpolate the above to 500 samples persecond.
v. An external removable memory (SD or MMC card) to store the interpolatedvalues.
vi. 4 PWM channels to send feedback signalsback to servos.
vii. PIC18F458 microcontroller to implementall of the above.

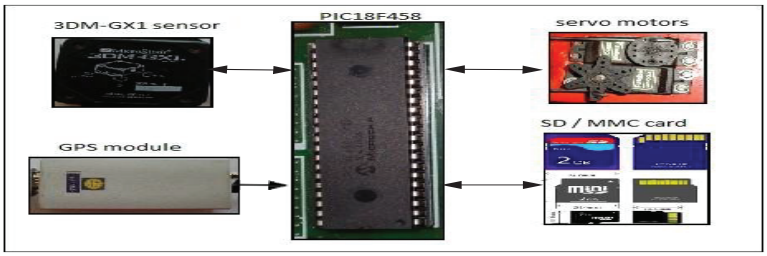

Figure 1: Block Diagram showing the connections between thesensors, GPS module, PIC

We Use the MP Lab PIC programming software and with Micro Chip C-18 tool suite to program the PIC using C language and we use the PicKit 2 programmer to download the same onto the PIC. We also use the Proteus ISIS schematic Capture toolto verify our codes via software simulation.

Both the GPS module and 3DM-GX1 have a female DB9 out pin through which data is sent out serially by UART. The PIC µc has a female DB9pin which is used for serial data transfer. Hence a male DB9 to male DB9 *Cross Connector* was designed by us for this purpose. This cross connector wire has two DB9 male pins at either end and allows successful data transfer between the PIC and the GPS or 3DM-GX1 modules.

The 3DM-GX1 sensor is capable of operating at 19200, 38400,115200 baud but we use 19200 baud. Once an ASCII '1' is sent to the 3DM-GX1, it goes into continuous data out mode and it starts to transmit 11 parameters namely time, roll, pitch, yaw, XYZ axes angular rates, XYZ axes acceleration and timer ticks [Fig.3]. The output rate is 50 samples/s and so we interpolate the data to attain 500 samples/s and store the same onto the external memory.[2]

The GPS module starts to continuously transmit data at 9600 bauds after an initial set up time of fewmin when it is switched on. From the output data, we extract the UTC, latitude, longitude and altitude from the $GPGGA set of parameters[Fig.2] and interpolate the same and save them.

The last two pins of port C of the PIC µc which are predefined by the PIC manufacturer, to be for UART transmission, is connected to a MAX 232 ICbefore connecting to the DB9 port. MAX232 is usedto convert TTL logic levels to RS232 levels.

Each analog voltage output from each the servo motors is connected to a single Port A pin of thePIC µc via (DFK RI WKH 3RUW $ SLQV serves as the input channel to the inbuilt 8 channel, 10 bit ADC embedded within the PIC. The ADC conversion clock is selected as Fosc/32 where Fosc is the crystal frequency used for the PIC. Fosc in this case is 20MHz. Also, the reference voltages to the ADC can either be given externally or the Vcc and ground pins of the PIC itself can be taken as reference. We choose the latter.

Insufficient internal memory space to store the data samples brings in the need to use an external memory. The Master Synchronous Serial Port (MSSP) module is a serial interface module on the PIC µc which we use for communicating with the SD / MMC card using Serial Peripheral Interconnect (SPI) protocol. Port C pins of the PIC are programmed to be used in SPI mode[3].

All the interpolated data is saved onto thememory card and Memory card readers can be used to read the data from the card. The Prospective task and identification transform the various inbuild signal process to makes MSPP module that is having connected Applications with different approach of application. The Logical Application of given data must have primary block of system Application Task that can be identified with different approach and applications to control the selected block data. After selecting data processing with Application used to identify maximum approach of review Applications with given prospects of signal and identical Approach. We can have control adopter to finalized available resources to control and adopt similar input channel with different set of identical control Applications. It is also performed different task of Data segments to approach and identify basic transformation in given task support system. The serial interconnect peripheral will identify the clear data to perform the applications is identified as follow in following Program Flow Application performance method and its components in system portfolio. The memory utilization and control behavior also plays vital role to connect the usability of system task with available resources . [4],[6]

b. Application of Proposed Program Flow

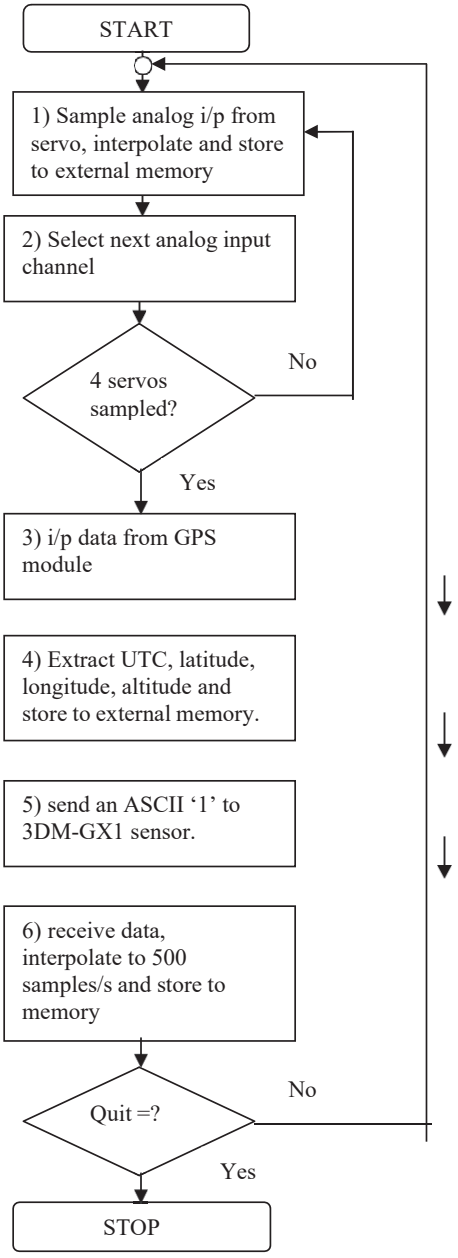

Figure 2: Application Structure flowchart for the Implementation

3. RESULTS AND ANALYSIS

A) GPS Module

The GPS module continuously outputs data with reference to the National Marine Electronics Association (NMEA) protocol, at9600 bauds, as shown in Figure.2.

Figure 3 : Analysis GPS outputted data at 9600 baud.

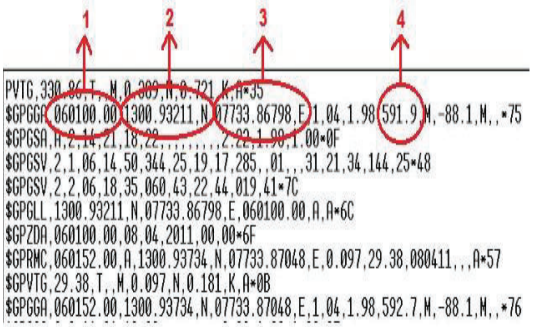

Figure 4 : Analysis of 3DM-GX1 output at 19200 Baud.

Only the following data [Fig.2] is extracted using the microcontroller and is stored onto the external memory.

1. Universal Coordinated time, in hhmmss.ssformat (000000.00 – 235959.99).
2. Latitude in ddmm.mmmm, North (N) or South (S) format.
3. Longitude in ddmm.mmmm, East (E) or West (W) format.
4. Altitude indicating mean sea level (Geoids) (-9999.9 – 17999.9)

B) 3DM-GX1 Orientation Sensor

The 3DM-GX1 outputs the data [Fig.3] in continuous mode at minimum baud rate of 19200 when an ASCII ‘1’ or ‘0x31’ is inputted to it. We use the PIC18F458 microcontroller to input the ASCII ‘1’ to the sensor using the inbuilt UART port. Data output of the sensor is at 50 samples/second and in order to achieve a higher sampling rate of 500 samples/second, we interpolatethe data before we store it on to the external memory.[7]

The following data [Fig.3] is extracted from the3DM-GX1 output:

1. Time in seconds
2. Roll
3. Pitch
4. Yaw
5. Acceleration w.r.t X-axis
6. Acceleration w.r.t Y-axis
7. Acceleration w.r.t Z-axis
8. Angular Rate w.r.t X-axis
9. Angular Rate w.r.t Y-axis
10. Angular Rate w.r.t Z-axis
11. Timer ticks indicating clock cycles of the microcontroller embedded inside the 3DM-GX1 sensor.

C) Servo Motors

All the four servo motors are connected to the PIC'sinbuilt 10 bit ADC and each motor's analog i/p to the ADC is sampled [Fig4], converted to digital by the ADC, interpolated to increase sampling rate andstored.

```
4.902 4.902 4.902 4.902 4.902 4.892 4.902 4
902 4.902 4.902 4.902 5.000 5.000 5.000 5.0
0 5.000 5.000 5.000 5.000 5.000 5.000 4.990
```

Figure 5 : Showing the ADC output.

D) SD / MMC Card

The memory capacity required to store thedata can be calculated as:-

- *3DM-GX1*

Data output = 50 samples/s.
Data output after interpolation= 500 samples/s.For 1 minute = 30000 samples/s
1 sample = 16 bit
Therefore 30000 samples = *480,000 bits/min*

- *GPS Module*

1) UTC = 72 bits/sample
Therefore for 500 samples/sec = 36000 bits.For 1 minute = *2,160,000 bits.*
2) Latitude = 88 bits/sample
Therefore for 500 samples/sec = 44000bits.For 1 minute = *2,640,000 bits.*
3) Longitude = 96 bits/sample.
Therefore for 500samples/sec = 48000bits.For 1 minute = *2,880,000 bits.*
4) Altitude = 56 bits/sample
Therefore for 500samples/sec = 28000 bits.For 1 minute = *1,680,000 bits.*

- *Servo Motors*

1 channel = 40 bits/sample.For 4 channels = 1600bits.
For 500 samples/sec = 800000bits.For 1 minute = *48,000,000 bits.*

- TOTAL

For 1 minute, total number of bits generated =

57,840,000 bits.

For a flight duration for approx 20 min, numberof bits to be stored = *1,156,800,000 bits.*

Therefore the minimum memory capacity required to store all the data is = *144,600 kiloBytes* = ***144.6 Mega Bytes***

Internal memory on board the PIC is 256 kilo Bytesand this huge capacity can be supported by using only SD / MMC cards interfaced externally to the PIC microcontroller.

4. Conclusion

Flight automation is very complex. Though SDR is just a small part of the process as a whole, it is one of the vital requisites for the automation. The method adopted by us, to increase the sampling rate by interpolating, is a simple yet very effective method to increase the overall number of data samples obtained and initiate better feedback response to the system. Also, all the parameters such as roll, pitch, yaw, acceleration, angular rates, UTC, latitude, longitude, altitude and the feedback from servo motors, which provide more than sufficient information required for a robust, accurate flight automation system, is extracted and stored by our SDR.The SDR uses only one PIC18F458 microcontroller, which comes inbuilt with most ofthe features required for efficient data extraction, and a single external SD / MMC card. Hence The SDR is compact and also cheap.Although the FDR is "Smart" in many ways, there are still areas in which the overall scope of the SDR can be improved. The PIC18F458 has a 10 bit inbuilt ADC. The resolution is only 4.88mV for a 5V analog input. Therefore by using an external ADC of higher bit conversion capability such as 16 bit we can obtain more accurate voltage of 76.25 µV for 5V analog input. But overall sampling speedwill be negatively affected and more memory will be needed to store the data.

SDR only has be ability to store the interpolated data. Feedback to the servo motors for flight automation is a highly complex and arduous task and is undergoing extensive research.

5. References

1. Muhammad Ali Mazidi, Roland McKinlay, Danny Causey, *PIC Microcontroller and Embedded Systems – Using assembly and C for PIC18.* Pearson Education. Copyright, 2018.
2. Dogan Ibrahim, *SD Card projects using PICmicrocontrollers.* Elsevier Ltd, 2019
3. Simion Dascalu, "Remote sensing using autonomous UAVs suitable for less developed countries", European Business Innovation & Research Center S.A, Romania.
4. Zak Sarris, "Survey of UAV applications in civilmarkets", Technical University of Crete,Greece. June 2020.
5. "Flight Data Recorder Systems". FederalAviation Administration. 2017-04-10. Retrieved201-04-08.
6. G. E. Blonder, "Graphical passwords," in *Lucent Technologies, Inc., Murray Hill, NJ*, U. S. Patent, Ed. United States, 2019.
7. R. Dhamija, and A. Perrig. "Déjà Vu: A User Study Using Images for Authentication". In 9th USENIX Security Symposium, 2020.
8. J. Goldberg, J. Hagman, V . Sazawal, "Doodling Our Way To Better Authentication", CHI '02 extended abstracts on Human Factors in Computer Systems, 2019.
9. W. Jansen, "Authenticating Mobile Device User through Image Selection," in *Data Security*, 2014.
10. A Sudhakar , "Authenticating Users on Handheld Devices "in *Proceedings of Canadian Information Technology Security Symposium* , 2020.
11. Jermyn, I., Mayer A., Monrose, F., Reiter, M., and Rubin., "The design and analysis of graphical passwords" in Proceedings of USENIX Security Symposium, August 2019.

Yantu Gongcheng Xuebao/Chinese Journal of Geotechnical Engineering

Carrying Out Indian Repealed Farm Regulations to a Web- Based Entrance

Prof. Mridula Shukla*, Raghu Ram S, Raghunandana Guptha D R, Radadiya Kaushik Kumar & Lavanya S

Keywords: web-based, farmers, center man, e-commerce, web-based gateway, agriculture, Bidding System, Chat Bot.

Abstract

This research is all about building a secure, user-friendly web-based gateway where farmers can sell their yields to anybody in this world and purchasers can purchase the harvests from any place, task will probably give opportunity to farmers to sell their harvests outside mandis, we want to eliminate the center man required during the exchanging cycle of the harvest by this gateway farmers won't be charged any Tax or available to be purchased of the yields our entry will likewise assist with getting more open decisions for farmers to sell their harvests, Web based business is the most broad regions for the use of data innovation and a significant part of information development. Farming is a developing piece of the web based business by developing web based gateway which helps in Advances hindrance free intra-state and between state exchange of farmer's produce, and also by implementing a contract based option in our web-based portal, The demonstrations tries to furnish farmers with a system to take part in agreement cultivating, where farmers can go into an immediate concurrence with a purchaser (prior to planting season) to offer the produce to them at pre-decided costs everything can be created utilizing our latest programming technologies.

Published
2022-08-10

Prof. Mridula Shukla*, Raghu Ram S, Raghunandana Guptha D R, Radadiya Kaushik Kumar & Lavanya S. (2022). Carrying Out Indian Repealed Farm Regulations to a Web- Based Entrance. *Yantu Gongcheng Xuebao/Chinese Journal of Geotechnical Engineering*, *44*(8), 91–96. Retrieved from http://ytgcxb.periodicales.com/index.php/CJGE/article/view/152

More Citation Formats

Issue

Vol. 44 No. 8 (2022)

Section

Articles

Make a Submission

Keywords

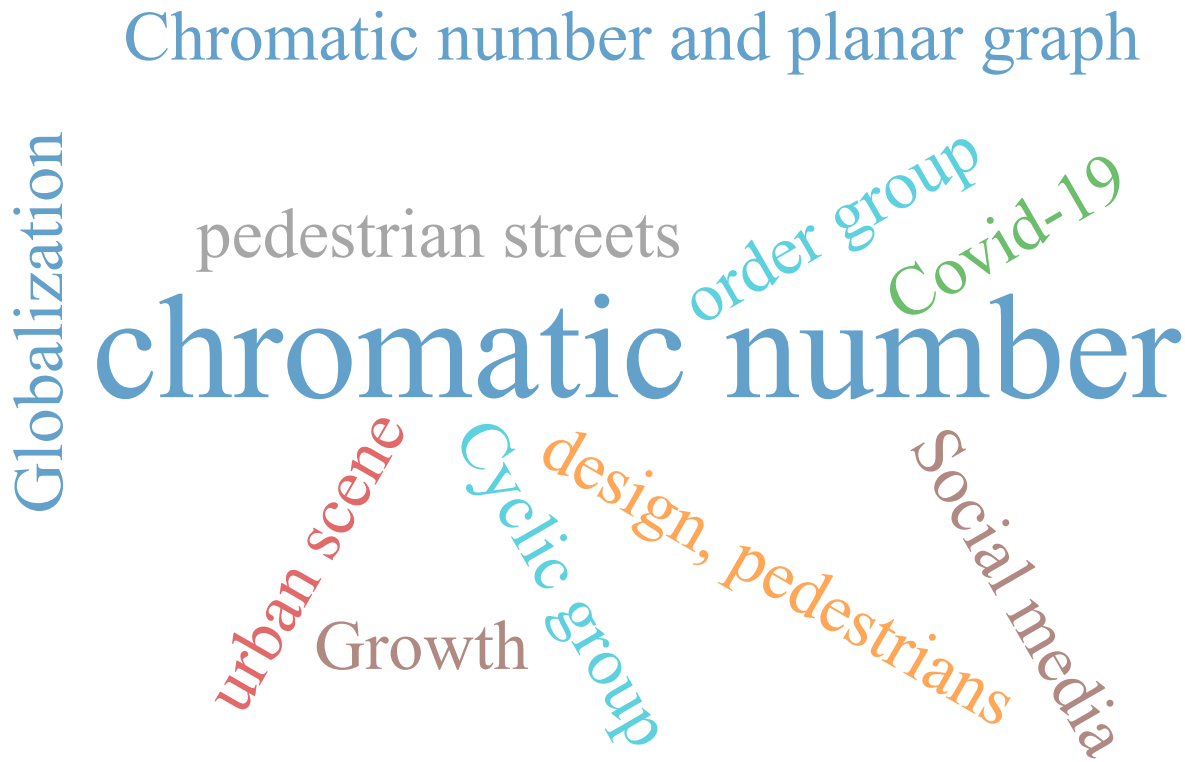

Information

For Readers

For Authors

For Librarians

Publisher

Chinese Society of Civil Engineering & Editorial Office of Chinese Journal of Geotechnical Engineering

Current Issue

ATOM 1.0

RSS 2.0

RSS 1.0

Subscription

Login to access subscriber-only resources.

Browse

Open Journal Systems

ISSN:1000-4548

Yantu Gongcheng Xuebao/Chinese Journal of Geotechnical Engineering

Farmers Trade Marketing-Agriculture Marketing Information System

Mridula Shukla*, Eswaran M, Kashti dhananjaya, Kollu BharathKumarReddy & Praveen E

Keywords: Website, Trade-Marketing, marketing Price, Billing, e-Learning, SMS benefit.

Abstract

Despite the fact that farming is a prominent occupation in India, the vast majority of those who work in it nowadays are from the lower classes and live in poverty. Advanced procedures and automated machines now rule the world, but there are no new techniques or equipment to develop in the farming industry, thus it has fallen behind. Farmers are being conned by agents in today's market, resulting in poverty in the farmer's field despite their hard work and produce. Farmers Trade Marketing will automate the entire process, making it simple to serve as the greatest solution to all of the challenges faced by farmers.

Farmers' Trade Promotion Farmers may sell their products throughout the country by using the internet and a little website knowledge. Farmers will receive updates on current crop marketing rates, as well as blogs and news on farming, marketing, and the agriculture industry from around the world. The site will also include data on overall sales and profit margins for sold commodities, as well as a consolidated perspective of many federal agriculture programs. The site sends out an SMS whenever new items or crops are added to the system.

Published
2022-08-10

How to Cite

Mridula Shukla*, Eswaran M, Kashti dhananjaya, Kollu BharathKumarReddy & Praveen E. (2022). Farmers Trade Marketing-Agriculture Marketing Information System. *Yantu Gongcheng Xuebao/Chinese Journal of Geotechnical Engineering*, *44*(8), 85–90. Retrieved from http://ytgcxb.periodicales.com/index.php/CJGE/article/view/151

More Citation Formats

Issue

Vol. 44 No. 8 (2022)

Section

Articles

Make a Submission

Keywords

Information

For Readers

For Authors

For Librarians

Publisher

Chinese Society of Civil Engineering & Editorial Office of Chinese Journal of Geotechnical Engineering

Current Issue

ATOM 1.0

RSS 2.0

RSS 1.0

Subscription

Login to access subscriber-only resources.

Browse

Open Journal Systems

ISSN:1000-4548

Yantu Gongcheng Xuebao/Chinese Journal of Geotechnical Engineering

Fake Review Detection on Yelp

Ashok B P*, Shreyas Reddy, Shrilaxmi Bannigol, Spoorti & Mahesh

Keywords: Machine Learning; Classification; Fake Reviews Detection; Online Discussion Forum

Abstract

Due to the commonness of gathering exercises in individuals' regular routine, prescribing content to a gathering of clients turns into a significant errand in numerous data frameworks. A basic issue in bunch proposal is the manner by which to total the inclinations of gathering individuals to deduce the choice of a gathering. Toward this end, we contribute an original arrangement, in particular AGREE (another way to say "Mindful Group Recommendation"), to address the inclination collection issue by gaining the conglomeration procedure from information, which depends on the new improvements of consideration organization and brain cooperative sifting (NCF). In particular, we embrace a consideration system to adjust the portrayal of a gathering, and gain the communication among gatherings and thi ngs from information under the NCF structure. In addition, since many gathering recommender frameworks likewise have bountiful associations of individual clients on things, we further coordinate the displaying of client thing collaborations into our technique. Through along these lines, we can build up the two errands of suggesting things for the two gatherings and clients. By investigating two genuine world datasets, we exhibit that our AGREE model further develops the gathering proposal execution as well as improves the suggestion for clients, particularly for cold-start clients that have no verifiable cooperation’s independently.

Published
2022-08-10

How to Cite

Ashok B P*, Shreyas Reddy, Shrilaxmi Bannigol, Spoorti & Mahesh. (2022). Fake Review Detection on Yelp. *Yantu Gongcheng Xuebao/Chinese Journal of Geotechnical Engineering*, *44*(8), 46–51. Retrieved from

http://ytgcxb.periodicales.com/index.php/CJGE/article/view/145

More Citation Formats

Issue

Vol. 44 No. 8 (2022)

Section

Articles

Make a Submission

Keywords

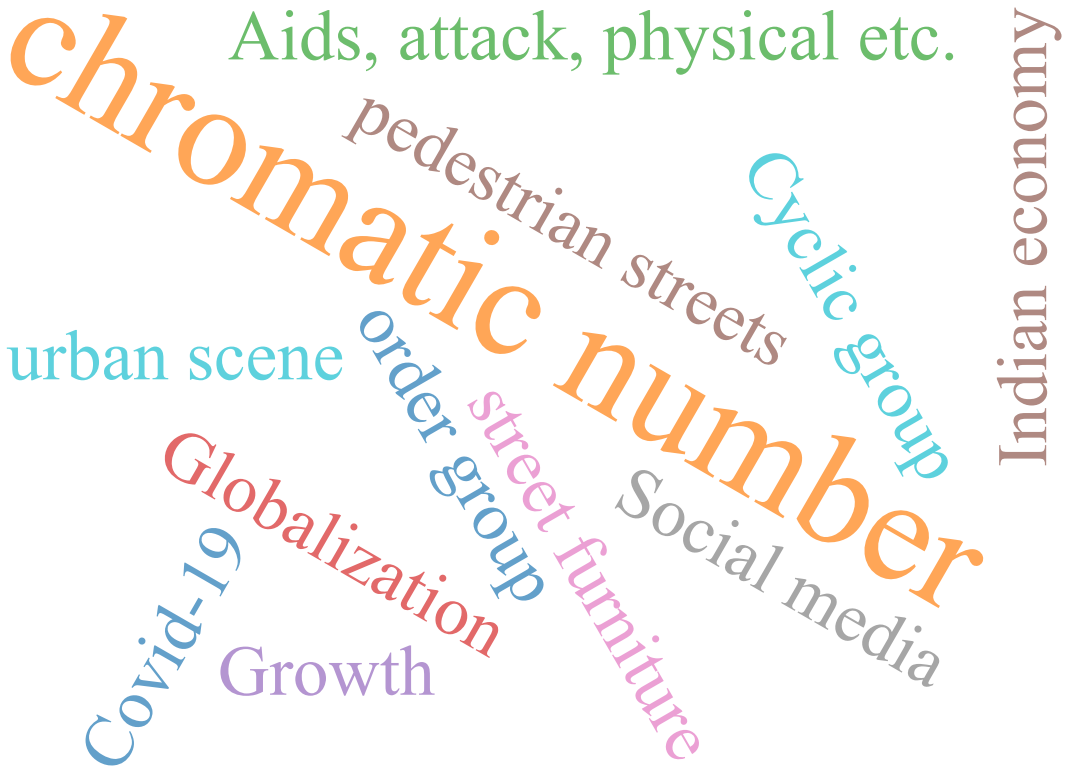

Information

For Readers

For Authors

For Librarians

Publisher

Chinese Society of Civil Engineering & Editorial Office of Chinese Journal of Geotechnical Engineering

Current Issue

ATOM 1.0

RSS 2.0

RSS 1.0

Subscription

Login to access subscriber-only resources.

Browse

Open Journal Systems

ISSN:1000-4548

Development Of an Evaluation Model for Measuring the Competencies of Business School Faculty Members

PDF (https://www.journalppw.com/index.php/jppw/article/view/437/233)

A. Sahana, Vijila. E, K. Tharaka Rami Reddy, Jaisimha D S, Priyanka Ganguly, Sharath Kumar Y

Abstract

The present study in an effort to develop a competency model for exploring the competencies of Business School faculty in the realm of knowledge, skills and abilities. The variables for the study are drawn from the Academic Performance Indicators that form the basis for the Higher Educational Institutions teachers' self-assessment framework framed by the University Grant Commission. To be a successful performer at the job, a faculty has to be competent in the fields of curriculum and pedagogy; research and consultancy; administration and governance and knowledge dissemination. There is a need to identify the competencies of management teachers in the domain of knowledge, skills and abilities. The interrelationship between knowledge, skills and abilities needs to be explored and there is a necessity to distinguish good and average performers. This study is guided by the research question: What can be the competency framework for evaluating the business faculty members? Therefore, the main objective of this study is to present a competency framework for business school faculty. Competency is a cluster of knowledge, skills and abilities that are associated to job responsibilities and can be measured to identify average and superior performers. The study was realized with faculty members working in business schools in Bengaluru, Karnataka. The population for the study comprised of faculty members working in university affiliated Business schools in urban Bengaluru and were either affiliated to Bangalore University or Visvesvaraya Technological University. Two stage simple random sampling process was used to identify a sample representative from the universe. All permanent full time faculty members working in self-financing and aided colleges formed the majority of the sample. Literature review, job description as given by AICTE and Academic Performance Indicators (API) by University Grants Commission facilitated in identifying the statements in the questionnaire. The development of the instrument was designed in three phases and is explained in detail in this paper. Exploratory Factor Analysis was used to identify and group the latent variables of the competency clusters to the domains of knowledge, skills and abilities.

Issue

Vol. 5 No. 3 (2021): Vol. 5 No. 3 (2021): Journal of Positive Psychology and Wellbeing (https://www.journalppw.com/index.php/jppw/issue/view/24)

Section

Articles

Make a Submission (https://www.journalppw.com/index.php/jppw/about/submissions)

(https://www.scimagojr.com/journalsearch.php?q=21100983356&tip=sid&exact=no)

Scopus (https://www.scopus.com/sourceid/21100983356)

Keywords

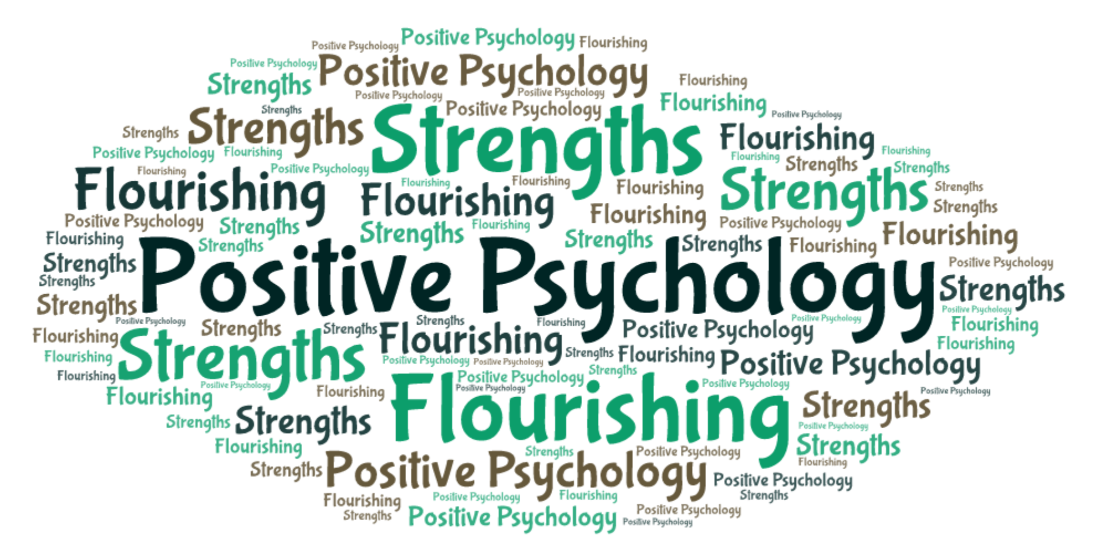
Positive Psychology
Strengths
Flourishing

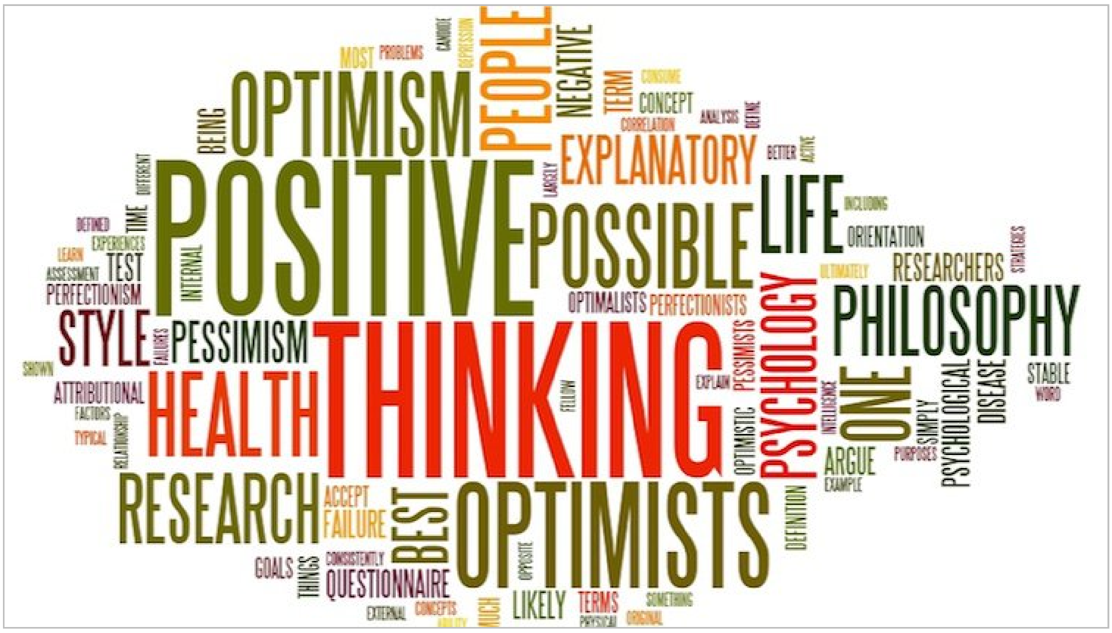
OPTIMISM
PEOPLE
NEGATIVE
EXPLANATORY
POSITIVE
POSSIBLE
LIFE
THINKING
HEALTH
PESSIMISM
STYLE
PSYCHOLOGY
PHILOSOPHY
ONE
RESEARCH
BEST
OPTIMISTS
QUESTIONNAIRE

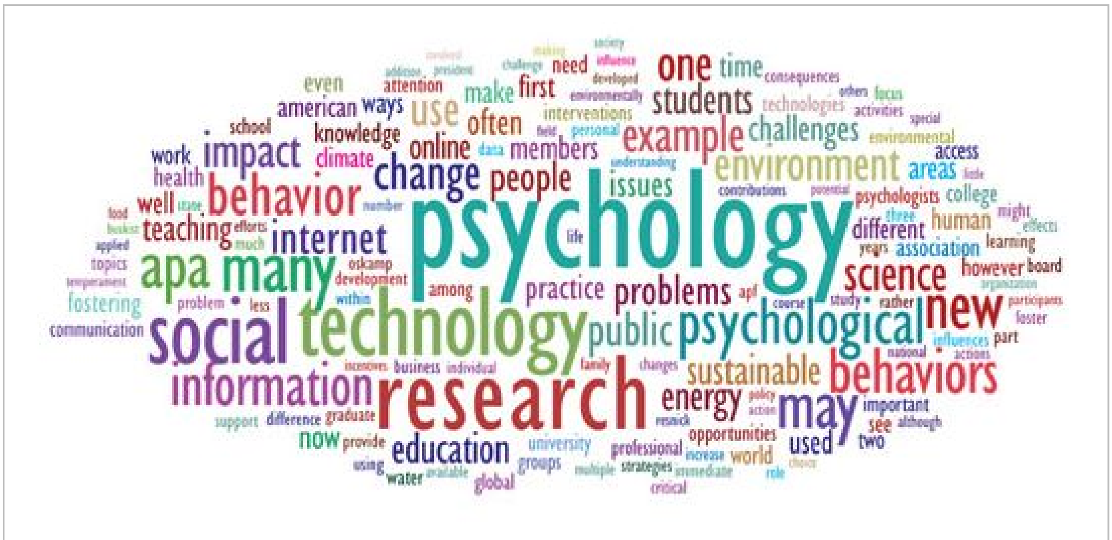
psychology
research
technology
social
behavior
information
psychological
behaviors
new
science
environment
example
change
impact
apa
many

Journal of Positive Psychology and Wellbeing (ISSN 2587-0130) is a peer-reviewed journal covering positive psychology and provides an international forum for the science of positive psychology in education and school settings. The JPPW, which is published two times a year, is an open-access that publishes research outcomes with significant contributions to the understanding and improvement of the positive psychology of education and services in school settings. The journal encompasses a full range of methodologies and orientations that include educational, cognitive, social, behavioral, preventive, cross-cultural, and developmental perspectives. The JPPW publishes research regarding the education of populations across the life span.

Artificial Intelligence in Healthcare: 21st century age of rifles - A bibliometric analysis

(https://journal.achsm.org.au/index.php/achsm/issue/view/63)

PDF (https://journal.achsm.org.au/index.php/achsm/article/view/1327/687)

Published: Dec 13, 2021

DOI: https://doi.org/10.24083/apjhm.v16i4.1327 (https://doi.org/10.24083/apjhm.v16i4.1327)

Keywords:
Artificial Intelligence, Technology, Bibliometric, Pandemic

R K Prema
Acharya Bangalore B School, Bangalore, India

M Kathiravan
The Oxford College of Engineering, Bangalore, Karnataka, India

Asmat Ara Shaikh
Bharati Vidyapeeth's Institute of Management Studies and Research, Navi Mumbai, India

Abstract

In the 21st century data, itself are information, product, and goods. The pandemic situation has given new eyes to the old invention to effectively bridge the gap between history, happenings, and technology as well as past and future. Health is requisite and every one of us would have placed our footstep one way or the another in the healthcare sector. The demand for healthcare professionals is also increasing in our country with an increasing population. To address the health need of society, this paper attempts to exhibit the studies captured on these two broad areas in the healthcare sector with a systematic literature review of bibliometric analysis. This paper will bring out the technological invention, its implications in the 21st century, relevance in the covid 19 pandemic situation, research, and facts explored in this area. Humans are the inventor and users of technology: the good we use the great will be the outcome: It all depends.

*(*The paper was presented at the 2nd Conference on Business Data Analytics: Innovation in emerging trends in management data analytics. Apeejay School of Management, Dwarka, Delhi, India. November 2021)*

How to Cite

Prema, R. K., Kathiravan, M., & Shaikh, A. A. (2021). Artificial Intelligence in Healthcare: 21st century age of rifles - A bibliometric analysis. *Asia Pacific Journal of Health Management*, *16*(4), 274-281. https://doi.org/10.24083/apjhm.v16i4.1327

More Citation Formats

Issue

Vol. 16 No. 4 (2021) (https://journal.achsm.org.au/index.php/achsm/issue/view/63)

Section

Conference Articles

0

Most read articles by the same author(s)

- Pooja Sharma, Asmat Ara Shaikh, Ameet Sao, Nitesh Rohilla, Using Technology Acceptance Model, Analyzing the Role of Telehealth Services in the Healthcare Industry During COVID-19 (https://journal.achsm.org.au/index.php/achsm/article/view/1815), Asia Pacific Journal of Health Management: Vol. 17 No. 2 (2022) (https://journal.achsm.org.au/index.php/achsm/issue/view/65)

Author Guidelines (https://journal.achsm.org.au/index.php/achsm/211)

Review Guidelines (https://journal.achsm.org.au/index.php/achsm/113)

Publication Ethics (https://journal.achsm.org.au/index.php/achsm/123)

Current Issue

ATOM 1.0
(https://journal.achsm.org.au/index.php/achsm/gateway/plugin/WebFeedGatewayPlugin/atom)

RSS 2.0
(https://journal.achsm.org.au/index.php/achsm/gateway/plugin/WebFeedGatewayPlugin/rss2)

RSS 1.0
(https://journal.achsm.org.au/index.php/achsm/gateway/plugin/WebFeedGatewayPlugin/rss)

Information

For Readers (https://journal.achsm.org.au/index.php/achsm/information/readers)

For Authors (https://journal.achsm.org.au/index.php/achsm/information/authors)

For Librarians (https://journal.achsm.org.au/index.php/achsm/information/librarians)

Make a Submission

Make a Submission (https://journal.achsm.org.au/index.php/achsm/about/submissions)

APJHM is indexed by Scopus; WOS; DOAJ (https://doaj.org/) EBSCO; Informit (https://search.informit.com.au/browseJournalTitle;res=IELHEA;issn=1833-3818); Google Scholar (https://scholar.google.co.id/scholar?as_ylo=2020&q=apjhm&hl=en&as_sdt=0,5); Crossref (https://search.crossref.org/?q=apjhm); ABDC

Subscribe to eTOC (mailto:journal@achsm.org.au)

journal@achsm.org.au (mailto:journal@achsm.org.au)

Contact us:

Platform & workflow by OJS / PKP

(https://journal.achsm.org.au/index.php/achsm/about/aboutThisPublishingSystem)

Original Research | Published: 26 May 2022

High-performance 2D photonics MOEMS pressure sensors

Yashaswini P.R., Gayathri H.N. & Srikanth P.C.

International Journal of Information Technology **14**, 2459–2468 (2022)

Abstract

A pressure sensor design is proposed based on Micro Opto-electro-mechanical systems (MOEMS) and Photonic Crystal (PhC). The objective of the proposed work is to measure pressure in the higher range. The performance of two resonator structures, ring and triangular structures made of silicon (Si) are designed and compared. The finite-difference time-domain (FDTD) tool is used for two-dimensional (2D) modeling and simulation of the resonator structures. Pressure can cause deformation resulting in a shift in wavelength. Excess pressure can affect the overall structure, reducing the sensitivity of the sensor. Hence maximum of 0 to 3 Giga Pascal (GPa) of pressure is used for sensitivity. The resonant wavelength shift for different loads is observed and tabulated. Ansys Multiphysics is the modeling tool used to extract the mechanical parameters. Through a literature

study, it is found that there are sensors developed by using PhC to measure pressure. From the simulation study, it is accomplished that the triangular resonator has provided good performance compared to the ring resonator between 0 and 2 GPa. Further, the ring resonator provided better performance between 2 and 3 GPa. This is because the propagation loss of the triangular structure is less compared to the ring structure. For the designed ring resonator structure, the Quality factor (Q-factor) obtained is 1634 and for the triangular structure, Q-Factor is 1047 for a 2 GPa pressure. The novelty of the proposed design is the ring and triangular structures and this resulted in a significant improvement of the Q-Factor compared to the published Q-Factor of 150.

References

1. Joannopoulos JD, Johnson SG, Winn JN, Meade RD (2008) Photonic crystal: molding the flow of light, 2nd edn. Princeton University Press, New Jersey

2. Yablonovitch E (1987) Inhibited spontaneous emission on solid-state physics and electronics. Phys Rev Lett 58(20):2059–2062

3. Mai TT et al (2011) Optimization and comparison of photonic crystal resonators for silicon microcantilever sensor. Sens Actuators A: Phys 165(1):16–25

4. Li B, Lee C (2010) Computational study of NEMS diaphragm sensor using triple nano-ring resonator. Procedia Eng 5:1418–1421

5. Biradar UV, Dongarge SM (2015) Refractive index of salt NaCl from aqueous solution in proc. Int J Comput Math Sci (IJCMS) 4(12):33–39

6. Chao CY, Fung W, Guo LJ (2006) Polymer microring resonators for biochemical sensing applications. IEEE J Sel Top Quantum Electron 12(1):134–142

7. Ho CP, Li B, Danner AJ, Lee C (2012) Design and modeling of 2-D photonic crystals based hexagonal triple nano-ring resonators as biosensors. Microsyst Technol 19:53–60

8. Hsiao FL, Lee C (2011) Nano-photonic biosensors using hexagonal nano-ring resonators: a computational study. J Micro/Nano-lithogr MEMS MOEMS 10:013001–013008

9. Monošík R et al (2012) Biosensors - classification, characterization and new trends. Acta ChimicaSlovaca 5(1):109–120

10. Olyaee S, Najafgholinezhad S (2013) A high-quality factor and wide measurement range biosensor based on photonic crystal nanocavity resonator. Sens Lett 11(3):483–488

11. Lai CH, Sun CK, Chang HC (2011) Terahertz antiresonant-reflecting-hollow-waveguide-based directional coupler operating at

antiresonant frequencies. Opt Lett 36:3590–3592

12. Martinez NP et al (2018) Spatially-variant photonic crystals and possible applications in proc. 2018 IEEE Res Appl Photonics In Defense Conference (RAPID). https://doi.org/10.1109/RAPID.2018.8509003

13. Pereira HNS, Rocha JN, Caballero LEP, Neto OPV (2017)Photonic crystal design tool, SBMicro 2017 - 32nd Symp.Microelectron. Technol. Devices Chip Sands, co-located Symp. 30th SBCCI - Circuits Syst. Des. 2nd INSCIT - Electron.Instrumentation, 7th WCAS - IC Des. Cases 17th SForum - Undergraduate-Student Forum, pp. 5–8, 2017, https://doi.org/10.1109/SBMicro.2017.8113020.

14. Jindal SK, Raghuwanshi SK et al (2015) Realization of MOEMS pressure sensor using mach Zehnder interferometer. J Mech Sci Technol 29:3831–3839. https://doi.org/10.1007/s12206-015-0829-z

15. Sharan P, Sandhya KV, Barya R et al (2021) Design and analysis of moems based displacement sensor for detection of muscle activity in the human body. Int j inf tecnol

13:397–402. https://doi.org/10.1007/s41870-020-00533-6

16. Ostasevicius V et al (2017) MOEMS-assisted radial pulse measurement system development. In: biomechanical microsystems. Lecture notes in computational vision and biomechanics. Springer, Cham

17. Yashaswini PR, Mamatha N, Srikanth PC (2021) Circular diaphragm-based MOEMS pressure sensor using ring resonator. Int j inf tecnol 13:213–220. https://doi.org/10.1007/s41870-020-00534-5

18. Sharan P, Deshmukh P, Roy SK (2013) Mapping of aqua constituents using photonic crystal. 2013 IEEE Reg 10 Humanit Technol Conf. https://doi.org/10.1109/R10-HTC.2013.6669063

19. Sharma P, Roy SK, Sharan P (2014) Design and simulation of photonic crystal-based biosensor for detection of different blood components. 2014 IEEE Reg 10 Symp. https://doi.org/10.1109/TENCONSpring.2014.6863019

20. Levy O et al (2005) Ultrasensitive displacement sensing using photonic crystal

waveguides. J Appl Phys Lett 98:033102

21. Romanov O, Tolstik A, Fanjul-Velez F, Ortega-Quijano N et al (2012) Modeling of light propagation in turbid media: application to biological tissues. Nonlinear Phenom Complex Syst 15:395–402

22. Nandhini VL et al (2021) Multichannel Biosensor for Skin Type Analysis. In: Patnaik S, Sethi I (eds) Advances in machine learning and computational intelligence algorithms for intelligent systems. Springer, Singapore

23. Dharchana T, Sivanantharaja A, Selvendran S (2017) Design of pressure sensor using 2D photonic crystal. Adv Nat Appl Sci 11(7):26–30

24. Upadhyaya AM, Srivastava MC, Sharan P, Roy SK (2021) Silicon nanostructure-based photonic MEMS sensor for biosensing application. J Nanophoton 15(2):026001. https://doi.org/10.1117/1.JNP.15.026001

25. Chen L et al (2019) Microcantilever aptasensor for detecting epithelial tumor marker Mucin 1 and diagnosing human breast carcinoma MCF-7 cells. Sens Actuators B 297:126759.

https://doi.org/10.1016/j.snb.2019.126759SABCEB0925-4005

26. Hardik JP et al (2015) Simultaneous MEMS-based electro-mechanical phenotyping of breast cancer. Lab Chip 15(18):3695–3706. https://doi.org/10.1039/C5LC00491HLCAHAM1473-0197

27. Shameem S et al (2018) Design, and analysis of MEMS-based capacitive pressure sensor for the detection of colon cancer. Int. J. Eng. Technol 7(1.5):77–83. https://doi.org/10.14419/ijet.v7i1.5.9126

28. Yashaswini PR et al (2021) Performance analysis of photonic crystal based biosensor for the detection of bio-molecules in urine and blood. Mater Today Proc. https://doi.org/10.1016/j.matpr.2021.06.192

29. Khongsombut E, Silapunt R, Watcharakitchakorn O (2012) A study of Photonic Crystals bending waveguide laser tip for dental treatments. 2012 IEEE Int Conf Electron Devices Solid State Circuit, EDSSC. https://doi.org/10.1109/EDSSC.2012.6482853

30. Bogaerts W et al (2005) Nanophotonic waveguides in silicon-on-insulator fabricated with CMOS technology. J Light Technol 23(1):401–412. https://doi.org/10.1109/JLT.2004.834471

31. Sharan P et al (2014) Design and modelling of photonic sensor for cancer cell detection. 2014 Int Conf IMpact E-Technology US, IMPETUS. https://doi.org/10.1109/IMPETUS.2014.6775872

32. Sharma P, Sharan P (2015) A label-free photonic crystal based optical gratings for propagation analysis of cancer cells, 2015 Int. Conf Commun Signal Process ICCSP 2015:1870–1874. https://doi.org/10.1109/ICCSP.2015.7322849

33. Olyaee S, Bahabady AM (2014) E. Leitgeb, A Diamond-shaped Bio-sensor Based on Two-dimensional Photonic Crystal Nano-ring Resonator, pp 434–437

34. Radhouene M, Najjar M, Janyani V (2020) Novel design superelliptic photonic crystal ring resonator based on channel drop filter, 2020 Int. Wirel Commun Mob Comput IWCMC 2020:1359–1363. https://doi.org/10.1109/IWCMC48107.2020.9148535

35. Ajey SS, Bhanumathi HR, Srikanth PC, Sharan P (2020) Highly sensitive photonic crystal based biosensor for Bacillus cereus. Int J Inf Technol 12(4):1393–1402. https://doi.org/10.1007/s41870-020-00507-8

36. Vijaya Shanthi K, Robinson S (2014) Two-dimensional photonic crystal based sensor for pressure sensing. Photonic Sens 4(3):248–253. https://doi.org/10.1007/s13320-014-0198-8

Author information

Authors and Affiliations

Department of ECE, Malnad College of Engineering, Hassan, Karnataka, India
Yashaswini P.R. & Srikanth P.C.

Department of Chemistry, The Oxford College of Engineering, Bangalore, Karnataka, India
Gayathri H.N.

Corresponding author

Correspondence to Yashaswini P.R..

Rights and permissions

About this article

Cite this article

P.R., Y., H.N., G. & P.C., S. High-performance 2D photonics MOEMS pressure sensors. *Int. j. inf. tecnol.* **14**, 2459–2468 (2022). https://doi.org/10.1007/s41870-022-00986-x

Received	Accepted	Published
06 March 2022	30 April 2022	26 May 2022

Issue Date

August 2022

DOI

https://doi.org/10.1007/s41870-022-00986-x

Keywords

Line defect **RSoft** **Resonant structure** **Pressure Sensor** **MOEMS**

ScienceDirect

Materials Today: Proceedings

Volume 58, Part 1, 2022, Pages 451-455

Theoretical investigation of Bragg Reflector optical sensor for the measurement of cryogenic temperature

Ranjith B. Gowda [a b], H.N. Gayathri [c], Preeta Sharan [d], K. Saara [a]

Show more

https://doi.org/10.1016/j.matpr.2022.02.482

Get rights and content

Abstract

The goal of the proposed work is to design and analyze a low temperature sensor to measure cryogenic temperature in the range of 0–120K. Proposed sensor design uses Distributed Bragg Reflector (DBR) multi-layer structure. DBR consists of high-low alternate dielectric materials arranged in one direction which acts as a one-dimensional photonic crystal (pc). Gallium Arsenide (GaAs) is used as high dielectric material and air as low dielectric material. GaAs dielectric constant is a function of the temperature and hence it can be used to detect any variation in the temperature. In this work, the number of alternate multi-layers (N) is chosen as 8 and the frequency of input electromagnetic wave is taken as 24THz. We achieved a high sensitivity of 1.525nm/K with a Q factor of 3534. The proposed sensor suits for the applications where critical low temperature measurement is needed.

Previous Next

Keywords

Photonic crystal; Cryogenic temperature; Distributed Bragg Reflector; Optical sensor; Gallium arsenide

Special issue articles Recommended articles

Cited by (3)

1-Dimensional silicon photonic crystal pressure sensor for the measurement of low pressure

2023, Results in Optics

Show abstract

Highly sensitive temperature sensor using one-dimensional Bragg Reflector for biomedical applications

2023, Biomedizinische Technik

One-dimensional optical Bragg grating sensor for the detection of urine glucose concentration

2022, Journal of Optics (India)

Enhancement of Meta Verse Capabilities by IoT Integration

Publisher: IEEE

Vivek Veeraiah ; Gangavathi P ; Shahanawaj Ahamad ; Suryansh Bhaskar Talukdar ; An… All Authors

Abstract: Due to increasing demand of Meta-verse, there is needed to enhance the performance during object detection in meta-verse environment. Several education institutions are m... **View more**

Metadata

Abstract:

Due to increasing demand of Meta-verse, there is needed to enhance the performance during object detection in meta-verse environment. Several education institutions are making use of meta-verse while many social groups are considering meta-verse for communication purpose. There are several commercial applications that are making use of meta-verse environment. It has been observed that there are lots of graphical objects present in meta-verse environment. There have been several factors that are affecting the performance of meta-verse environment. There is need to introduce image processing mechanism over meta-verse environment. The motto of research is to propose system that would allow identifying virtual objects in meta-verse efficiently without any delay. This research would integrate image processing and learning environment in order to detect object with enhanced performance.

Published in: 2022 2nd International Conference on Advance Computing and Innovative Technologies in Engineering (ICACITE)

Date of Conference: 28-29 April 2022

Date Added to IEEE *Xplore*: 18 July 2022

INSPEC Accession Number: 21884838

DOI: 10.1109/ICACITE53722.2022.9823766

ISBN Information:

Publisher: IEEE

Conference Location: Greater Noida, India

Contents

The science fiction meta-verse shown to us is a universe of endless possibilities. Avatar and Ready, Player one are good examples of how it may be visualized. According to Selina Yuan, general manager of Alibaba Cloud Intelligence's international business unit, the meta-verse is a three-dimensional digital universe in movies where players can escape physical reality, interact with each other as an avatar of their creation, and experience anything they want. The actual promise of the meta-verse rests in its capacity to make better use of the digital intelligence we currently have and visualize it in a manner that exposes fresh insights that would otherwise remained buried. Using this technology might help us address real-world issues and develop a more environmentally friendly, inclusive, and sophisticated society. No one is surprised that the Internet of Things (IoT) is leading this trend. The rise of affordable, ubiquitous sensors has hastened the development of Ambient Intelligence, which refers to the system's capacity to monitor the surroundings and react to the occupancy of people and particular events or circumstances. Mobile information technologies have fostered an increased interest in the Internet of Things (IoT) as a consequence of this.

ScienceDirect

Materials Today: Proceedings

Volume 69, Part 3, 2022, Pages 853-857

Influence of nanomaterial coated condensing surface on the productivity of evacuated tube assisted solar still

P. Gangavathi [a], G. Ramya [b], M.S. Karuna [c], K. Jeyapiriya [d], Pramod B Magade [e], D. Manirathnam [f]

Show more

https://doi.org/10.1016/j.matpr.2022.07.285

Abstract

In this current investigation, an attempt has been endeavored to examine the synergistic effect of using a nano-coated hydrophobic condensing glass as well as the integration of evacuated tubes (ETC) on the productivity of the single sloped solar still (SSS). Three numbers of SSS with the analogous configuration had been employed during the experimental trials. However, the first still was used as it is, the second still was equipped with the nano-coated condensing top glass and the third still was integrated with the ETCs in addition to the nano-coated glass. The fumed silica nanoparticles were used for preparing hydrophobic coating over the glass. The investigations were pursued in the southern part of India during the month of February in 2021. The findings evidenced that the use of both nano-coated glass and the ETCs seems to be synergistic in terms of enhancing the performance of the still and it was noted that 28.53% increment in yield was attained with such synergistic combination, comparing to the ordinary SSS. Whereas, the aforesaid increment was 15.49% more comparing to the yield of the still containing only nano-coated glass.

Previous Next

Keywords

Solar still; Nano-coating; Nano-titania; Productivity; Evacuated tubes

Special issue articles Recommended articles

ScienceDirect

Pattern Recognition Letters
Volume 152, December 2021, Pages 283-294

An improved watermarking algorithm for robustness and imperceptibility of data protection in the perception layer of internet of things

Mohammad Kamrul Hasan [a], Samar Kamil [b], Muhammad Shafiq [c], Yuvaraj S [d], E. Saravana Kumar [e], Rajiv Vincent [f], Nazmus Shaker Nafi [g]

Show more

https://doi.org/10.1016/j.patrec.2021.10.032
Get rights and content

Abstract

Emergence of Internet of Things (IoT) and modern digital applications such as digital financial services and deliveries make it easy to reproduce and re-distribute digital contents thus give room to so many copyright violations of illegal use of contents that need to be resolved. Researcher have been presenting the watermarking algorithms to prevent these illicit activities to a document before distribution. However, several issues have been identified for the digital transactions in the IoT. Thus, this research proposes a new text document image watermarking algorithm which emphasizes on two most important measures, visual quality, and robustness. To boost these measures, third least significant bit has been used for insertion. In addition, to further strengthen the technique, the Pascal Triangle is applied to determine the best position for embedding. Experimental results on the standard dataset have revealed that the proposed watermarking has achieved very encouraging results with PSNR and NCC averaged 54.95db and 0.98, respectively.

Introduction

The digital watermarking technique overcomes many challenges copyright violations, including illegal duplication or redistribution of digital content of IoT (Hasan etal. [1]). There are many research in digital contents such as text, image file, audio files and video files but for the protection of text file the area is relatively new (Kamil etal. [2]). Text file is the most common medium for today's information exchanges in 5G network architectures-based Internet of Things (IoT) platform ([3], [4], [5] Liu etal., Abiddi etal., Zhang etal.). The other digital transactions such as bitcoin is very popular that go beyond tracking ledger entries of just one specific on-chain asset (e.g., a bitcoin) to allow users to watermark a bitcoin as “token” to represent a sundry of off-chain assets purportedly. These tokens are the significant component of digital information exchanges ([4] Abidi etal.). Bitcoin tracking system using a robust secured protocol that includes asset issuance, native tracking and watermarking for the security issuance (Hasan etal. [1]). Fig.1 shows the watermarking procedure for digital transaction applications. However, securing digital context has been difficult to procure by most of the watermarking using IoT devices.

Like the general watermarking defined above, digital text watermarking is a way of hiding digital watermarks into a digital text by secretly storing some information that will help the owner tract his own text. The image-based approach secretly embeds watermark in-text images by modifying the inter line or words of the gaps between lines and words (Bhatti etal. [6]).

Using IoT, beacons, and other context-aware smart devices can help bankers improve their customer service (personalized messages). IoT-based securitysolutions is one of the top priorities for fintech providers financial operations safe and transparency. Several wearable devices offerbiometric authentication methodsfor wireless payments and money transfers can be made. The IoT solutions for fintech focused on all types of digital contest, such as data collection and processing methods. For digital data security watermarking is one of the top challenges in the IoT Fintech services. The syntactic approach embed watermark into the syntactic structure of text and its bits by applying some digital transformation like: clef ting passivation and topicalization (Hu etal. [7]). And the semantic approach incorporates some technique like: synonyms, acronyms words spelling, pre-suppositions and text meaning as text's semantics to enter the watermarking in text (Su etal. [8]).

The binary text image algorithms for text watermarking are not strong enough to withstand attacks and could be easily bypassed by re-typing. But syntactic approach mixes the algorithms with the natural language processing (NLP) and made it stronger (Wang etal. [9]). The algorithms are more protective but slow. These are inefficient syntactic analyzers and suffers the problem of syntactic and irreversible transformations (Kamil etal. [10]). The approach of semantics-based watermarking algorithms is

language dependent therefore not frequently used (Kamil etal. [11]). The synonym-based method has to be complimented with the powerful syntactic analyzer ([12], [13], [14], [15], [16], [17] Hasan etal., Lu etal., Choudhary, R. and Parmar, Zahoor etal., Vali etal., Mane and Chiddarwar). Random semantic transformation cannot be applied on some documents like: legal, poetry and quotations due to their sensitivity properties. Also, protection is needed for the semantic connotation, text's value and meaning ([17], [18], [19], [20], [21], [22]. Security is one of key issues in digital communications including Internet of Things in heterogeneous network based secure text transfer for the classified documents([23], [24], [25], [26] Amanlou etal. 2021; Memon etal. 2021; Hasan et Al., 2020; Nurelmadina etal. 2021; Hasan etal. 2019;Ghazal etal. 2020a; Ghazal etal., 2020b). Hou etal., Chauhan etal., Hasan etal., Shafiq etal.). Alginahi etal. [30] presented a repeating pattern to embed data within an image. Where the distribution of the image is done in two subsets. One process is selected and applied in a reverse way to these subsets. This is to apply the technique; if one of the subsets is augmented by a factor k, the other subset will be reduced by an equivalent quantity. the drawbackLow imperceptibility andcapacity. Dixit etal. [31] proposed a technique. They implemented textually on virtual Quran content photos, the feature of its sensitive nature in its minimal use of portraits/shades and the best textual content symbols, which impose additional constraints on the seek area for an invisible embedding. They had been powerful for giving users a higher self-belief of the authenticity content image safety and real possession of virtual media. It has been found that LSB's issue offers more distortion and is less secure due to sequential mapping. Rizzo etal. [32] have presented themultiple text images using hidden image into a single coloured image applying modified LSB substitution method. Total 6 text image had been used for hiding purpose. The method has the ability to embed/hide multiple text images in any color image. The encoded text images able to flawlessly recoverable. This coding algorithm's key benefit is that the embedded text image does not make any noticeable marks on the color image. In this study provides more security with higherimperceptibility andcapacity byproposing a new text document image watermarking algorithm which emphasises on two most important measures such as visual quality and robustness. In order to boost these measures, third least significant bit has been used for insertion. In addition, to further strengthen the technique, the Pascal Triangle is applied to determine the best position for embedding.

Therefore, some portable and robust copyright protection methods that can support all kinds of texts and provide the required protection need to be developed. The new method will address the different features of foreground, background and ensures the protection of all the text properties such as text meaning, word patterning, fluency, language rule and author writing style. The technique needs to support the embedding of large binary object (Pascal's Triangle) into an image, and allows robustness to most

common image processing tasks. The technique is more effective and produces very impressive result if relatively large text file is use compare to the size watermark. Combining the self-similarity properties of Pascal's triangles together with effective embedding method can help to produce a very reliable watermarking strategy that can provide the required robustness for JPEG compression and other geometric transformations (Wang etal. [9]).

Section snippets

Proposed method

In this research work, a new approach to improve the watermark imperceptibility and robustness was proposed. The main idea of this approach is to use black pixels of text documents for embedding watermark. In this technique, a trade-off between imperceptibility and robustness must be achieved.

To achieve the best watermark imperceptibility, the third intermediate Significant Bit (ISB) of Black pixels will be used. Pascal's Triangle will be used in the approach for embedding; this will enhance…

General research framework

As introduced above, the proposed watermarking algorithm in this research is implemented in five phases, namely: preprocessing, embedding the watermark, applying attacks, extracting the watermark and finally evaluation of the proposed algorithm (shown in Fig.2). Some of the phases are complex enough which further divide into some simpler stages as discussed in the following sub-sections.…

Experimental results and discussion

The experimental results were performed for the proposed method using 64×64 binary image and 512×512gray scale of ten different text document images was used as a cover image. The two separate approaches of white pixels between words and black pixels in-words were evaluated separately and the PSNR and NCC tests were carried out on each one and the result was compared.…

Conclusion

IoT has given the industry an exciting boost, especially regarding security and digital payment processing. Therefore, it requires security enforcement. In this context, to

ensure security, this paper presented an improved watermarking algorithm. The performance of the proposed algorithm was evaluated using an experimental approach. The attacks of Salt, Pepper, Poisson Noise and Gaussian Noise were used to test the proposed watermarking methods. The PSNR and NCC analysis were performed on the…

Declaration of Competing Interest

We would like to affirm that this manuscript is original, has not been published elsewhere and is not currently being considered for publication elsewhere and there no conflict of interest.…

Acknowledgment

This work was supported by the Universiti Kebangsaan Malaysia (UKM) under the FRGS/1/2020/ICT03/UKM/02/6.…

References (30)

S. Amanlou *et al.*

Lightweight and secure authentication scheme for IoT networks based on publish-subscribe fog computing model

Comput. Networks (2021)

M. Shafiq *et al.*

Selection of effective machine learning algorithm and Bot-IoT attacks traffic identification for internet of things in smart city

Future Generat. Comput. Syst. (2020)

M.H. Vali *et al.*

Optimized watermarking technique using self-adaptive differential evolution based on redundant discrete wavelet transform and singular value decomposition

Expert Syst. Appl. (2018)

H.T. Hu *et al.*

An improved SVD-based blind color image watermarking algorithm with mixed modulation incorporated

Inf. Sci. (Ny) (2020)

M.K. Hasan *et al.*

Lightweight Encryption Technique to Enhance Medical Image Security On Internet of Medical Things Applications
(2021)

Samar Kamil *et al.*
Challenges in multi-layer data security for video steganography
Asia-Pacific J. Inf. Technol. Multimed. (2018)

J. Liu *et al.*
A robust multi-watermarking algorithm for medical images based on DTCWT-DCT and Henon map
Appl. Sci. (2019)

M.H. Abidi *et al.*
Optimal 5G network slicing using machine learning and deep learning concepts. Computer Standards & Interfaces, 76, 103518
Int. J. Electron. Commun. (2021)

L. Zhang *et al.*
Dual DCT-DWT-SVD digital watermarking algorithm based on particle swarm optimization
Multimed. Tools Appl. (2019)

U.A. Bhatti *et al.*
Hybrid watermarking algorithm using clifford algebra with Arnold scrambling and chaotic encryption
IEEE Access (2020)

View more references

Cited by (2)

Design of Intelligent Manhole Cover Monitoring System Based on Narrow Band Internet of Things
2022, 2022 7th International Conference on Intelligent Computing and Signal Processing, ICSP 2022

The Rise of Ransomware: A Review of Attacks, Detection Techniques, and Future Challenges

2022, 2022 International Conference on Business Analytics for Technology and Security, ICBATS 2022

Recommended articles (6)

Research article

On utilizing 2D features from 3D scans to enhance the prediction of lung cancer survival rates

Pattern Recognition Letters, Volume 152, 2021, pp. 56-62

Show abstract

Research article

Deep ladder reconstruction-classification network for unsupervised domain adaptation

Pattern Recognition Letters, Volume 152, 2021, pp. 398-405

Show abstract

Research article

SnipeDet: Attention-guided pyramidal prediction kernels for generic object detection

Pattern Recognition Letters, Volume 152, 2021, pp. 302-310

Show abstract

Research article

FinPAD: State-of-the-art of fingerprint presentation attack detection mechanisms, taxonomy and future perspectives

Pattern Recognition Letters, Volume 152, 2021, pp. 225-252

Show abstract

Research article

Combined secure approach based on whale optimization to improve the data classification for data analytics

Pattern Recognition Letters, Volume 152, 2021, pp. 327-332

Show abstract

Research article

Joint object recognition and pose estimation using multiple-anchor triplet learning of canonical plane

Pattern Recognition Letters, Volume 152, 2021, pp. 372-381

Show abstract

View full text

International Journal of Communication Systems / Volume 35, Issue 11 / e5179

RESEARCH ARTICLE

An enhanced distance and residual energy-based congestion aware ant colony optimization routing for vehicular ad hoc networks

Raghu Ramamoorthy, Menakadevi Thangavelu

First published: 17 April 2022
https://doi.org/10.1002/dac.5179
Citations: 1

Summary

Due to the ad hoc nature of vehicular ad hoc networks (VANETs), routing in VANETs is challenging. Using an energy-efficient shortest path without congestion (EESPWC) increases routing efficiency by satisfying specific parameters (high throughput, high packet delivery ratio, low overhead, low end-to-end delay, low packet loss ratio, and low energy consumption). In this work, enhanced distance and residual energy-based congestion aware ant colony optimization (EDR-CAACO) for VANETs is proposed to find an EESPWC. The proposed EESPWC produces high throughput and high packet delivery ratio with low overhead and low delay. In EDR-CAACO, the roulette wheel selects the EESPWC based on the link's fitness values. The fitness value is computed based on the pheromone level of the link. The enhanced ACO (ant colony optimization) of the proposed model relies on the distance, residual, and congestion levels of the vehicles to estimate pheromone levels. For path selection, the roulette wheel relies on links that have the highest fitness value. The combination of high fitness value links provides an energy-efficient non-congested shortest route. The simulation results prove that the overall performance of EDR-CAACO is better than Improved Distance Based Ant Colony Optimization Routing (IDBACOR), Fuzzy-based Ant colony optimization (F-ANT), ant colony optimization routing algorithm (ARA), and AntNet in terms of throughput, routing overhead, packet delivery ratio, end to end delay, and packet loss rate.

DATA AVAILABILITY STATEMENT

Data sharing is not applicable to this article as no datasets were generated or analyzed during the current study.

Citing Literature

Download PDF

ScienceDirect

Engineering Failure Analysis
Volume 138, August 2022, 106376

Real time implementation of fiber Bragg grating sensor in monitoring flat wheel detection for railways

Suchandana Mishra [a], Preeta Sharan [b], K. Saara [a]

Show more

Outline | Share | Cite

https://doi.org/10.1016/j.engfailanal.2022.106376
Get rights and content

Highlights

- Rail-wheel analysis of the train.
- Real time monitoring and detection of the train wheel passage using optical sensor fiber Bragg grating sensor.
- Positions of grating sensors installed on the rail.
- Time domain and frequency spectrum analysis for the strain data induced on the rail when train passes by, to detect wheel flats.
- Reflection spectrum analysis for good wheel and bad wheel of a passenger train.

Abstract

Wheel flats are a key source of issues in railway systems, as they generate significant wear on both the infrastructure and the train carriages. Flat zones on the wheel tread are created by the wheel sliding unintentionally on the rail. They can cause serious damage to the train and accidents, so identifying worn wheels is critical for human safety and rail transit. The purpose of this study is to present the real-time implementation of fiber Bragg grating sensors on rail tracks and to investigate the train's flat wheel status. By considering passenger train running at speed 70kmph, it has been monitored for 35 *sec* in the interrogator. Real time analysis of strain induced in the rail was calculated and it has been found from the sensor reading there is peak value of strain of the order of 303.4 με which implies that wheel flatness is present whereas for normal wheel strain value is minimal up to 173.23 με. By collecting experimental strain data simulation has been done and shift in peak wavelength at 1550.804nm and reflectivity obtained was 89.3% for flat wheel. Simulation result shows that there is a remarkable wavelength shift for the flat wheel and normal wheel from the Bragg center wavelength.

Graphical abstract

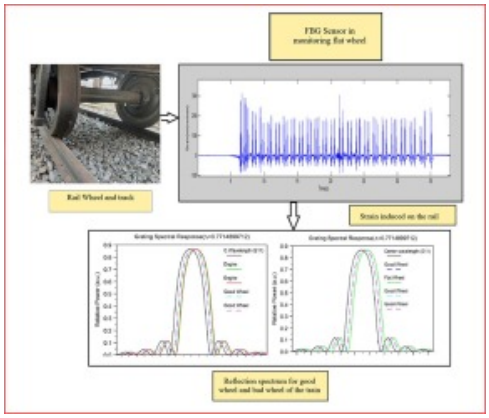

Download : Download high-res image (180KB)

Download : Download full-size image

Previous Next

Keywords

Wheel flat detection; Fiber Bragg grating; Optical sensor; Rail wheel analysis; Healthy wheel; Worn wheel; Signal processing

Recommended articles

Cited by (6)

Quasi-distributed FBG interrogation based on coherent wavelength-to-time mapping using mode-locked laser and pseudo-random barcode

2023, Optics and Laser Technology

Show abstract

Rail wheel tread defect detection using improved YOLOv3

2022, Measurement: Journal of the International Measurement Confederation

Show abstract

Optomechanical behaviour of optical sensor for measurement of Wagon weight at different speeds of the train

2023, Journal of Optics (India)

Axle Box Resonance Excitation Model Based on Wheelset Polygon and Its Resonance Characteristic Analysis in High-Speed Train

2022, Advanced Theory and Simulations

Journal of the Optical Society of America B Vol. 39, Issue 1 (/josab/issue.cfm?volume=39&issue=1), pp. 200-206 (2022)
• https://doi.org/10.1364/JOSAB.444838 (https://doi.org/10.1364/JOSAB.444838)

Sensitivity enhancement of a plasmonic biosensor for urine glucose detection by employing black phosphorous

Archana Yadav, Anil Kumar, and Preeta Sharan

Abstract

Abstract

A novel, to the best of our knowledge, optimized structure is proposed to enhance the sensitivity of a surface plasmon resonance (SPR)-based biosensor for urine glucose detection by adding a few layers of black phosphorous (BP) (two-dimensional material) over the zinc oxide (ZnO) sandwiched in between gold (Au) and silver (Ag) bimetallic layers. Results show that with an optimized thickness of 42 nm/Au, 12 nm/ZnO, .05 nm/Ag, and 2.65 nm/BP, the sensitivity of 289°/RIU can be achieved at a 633 nm operating wavelength. This is enhanced up to 1.5 times from the conventional biosensor. It is further enhanced up to 3 times with the addition of five numbers of BP sheet layers (each sheet has a thickness of 0.53 nm) over the Au/ZnO/Ag layers, as BP possesses a high absorption coefficient at the incident wavelength of 633 nm. This biosensor is rather efficient at responding to the minute change of 0.001 in the refractive index of urine samples for non-diabetic persons (0–15 mg/dL) and diabetic persons (0.625 gm/dL, 1.25 gm/dL, 2.5 gm/dL, 5 gm/dL, and 10 gm/dL) with the corresponding refractive indices of 1.335, 1.336, 1.337, 1.338, 1.341, and 1.347. It provides significant resonance shift and higher sensitivity in terms of changes in the resonance angle shift. This proposed work has the potential to detect glucose concentration levels with higher accuracy and with faster sensor responses.

Full Article (viewmedia.cfm?uri=josab-39-1-200&seq=0&html=true) | PDF Article (viewmedia.cfm?uri=josab-39-1-200&seq=0)

More Like This

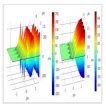

Detection of hemoglobin in blood and urine glucose level samples using a graphene-coated SPR based biosensor (/osac/abstract.cfm?uri=osac-4-8-2164)

Shahriar Mostufa, Alok Kumar Paul, and Kisalaya Chakrabarti

OSA Continuum **4**(8) 2164-2176 (2021)

Sensitivity enhancement of a graphene–barium titanate-based surface plasmon resonance biosensor with an Ag–Au bimetallic structure in the visible region (/josab/abstract.cfm?uri=josab-36-4-1108)

Lili Liu, Mei Wang, Lipeng Jiao, Ting Wu, Feng Xia, Meijie Liu, Weijin Kong, Lifeng Dong, and Maojin Yun

J. Opt. Soc. Am. B **36**(4) 1108-1116 (2019)

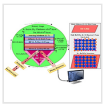

Sensitivity enhancement of the SPR biosensor for Pseudomonas bacterial detection employing a silicon-barium titanate structure (/ao/abstract.cfm?uri=ao-60-19-5588)

Yesudasu Vasimalla, Himansu Shekhar Pradhan, and Rahul Jasvantbhai Pandya

Appl. Opt. **60**(19) 5588-5598 (2021)

View More...

◁ Previous Article (abstract.cfm?uri=josab-39-1-188) Next Article ▷ (abstract.cfm?uri=josab-39-1-207)

Journal of the Optical Society of America B

Kurt Busch, Editor-in-Chief

(/josab/home.cfm)

ABOUT (/JOSAB/JOURNAL/JOSAB/ABOUT.CFM)

TUTORIALS (/JOSAB/TUTORIALS.CFM)

ISSUES IN PROGRESS (/JOSAB/UPCOMINGISSUE.CFM)

CURRENT ISSUE (/JOSAB/ISSUE.CFM)

ALL ISSUES (/JOSAB/BROWSE.CFM)

EARLY POSTING (/JOSAB/UPCOMING.CFM)

FEATURE ISSUES (/JOSAB/FEATURE.CFM)

Top

Publishing Home (/)

Journals (/about.cfm)

Conferences (/conferences.cfm)

Preprints (Optica Open) (https://opticapreprints.figshare.com/)

INFORMATION FOR

Authors (/author/author.cfm)

Reviewers (/reviewer/)

Librarians (/library/)

OPEN ACCESS INFORMATION

Open Access Statement and Policy (/submit/review/open-access-policy-statement.cfm)

Terms for Journal Article Reuse (/library/license_v2.cfm)

ScienceDirect

Engineering Failure Analysis
Volume 138, August 2022, 106376

Real time implementation of fiber Bragg grating sensor in monitoring flat wheel detection for railways

Suchandana Mishra [a], Preeta Sharan [b], K. Saara [a]

Show more

Outline | Share Cite

https://doi.org/10.1016/j.engfailanal.2022.106376
Get rights and content

Highlights

- Rail-wheel analysis of the train.
- Real time monitoring and detection of the train wheel passage using optical sensor fiber Bragg grating sensor.
- Positions of grating sensors installed on the rail.
- Time domain and frequency spectrum analysis for the strain data induced on the rail when train passes by, to detect wheel flats.
- Reflection spectrum analysis for good wheel and bad wheel of a passenger train.

Abstract

Wheel flats are a key source of issues in railway systems, as they generate significant wear on both the infrastructure and the train carriages. Flat zones on the wheel tread are created by the wheel sliding unintentionally on the rail. They can cause serious damage to the train and accidents, so identifying worn wheels is critical for human safety and rail transit. The purpose of this study is to present the real-time implementation of fiber Bragg grating sensors on rail tracks and to investigate the train's flat wheel status. By considering passenger train running at speed 70kmph, it has been monitored for 35 *sec* in the interrogator. Real time analysis of strain induced in the rail was calculated and it has been found from the sensor reading there is peak value of strain of the order of 303.4 με which implies that wheel flatness is present whereas for normal wheel strain value is minimal up to 173.23 με. By collecting experimental strain data simulation has been done and shift in peak wavelength at 1550.804nm and reflectivity obtained was 89.3% for flat wheel. Simulation result shows that there is a remarkable wavelength shift for the flat wheel and normal wheel from the Bragg center wavelength.

Graphical abstract

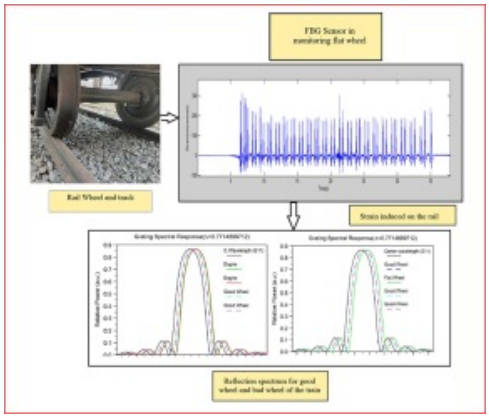

Download : Download high-res image (180KB)

Download : Download full-size image

Previous Next

Keywords

Wheel flat detection; Fiber Bragg grating; Optical sensor; Rail wheel analysis; Healthy wheel; Worn wheel; Signal processing

Recommended articles

Cited by (6)

Quasi-distributed FBG interrogation based on coherent wavelength-to-time mapping using mode-locked laser and pseudo-random barcode

2023, Optics and Laser Technology

Show abstract

Rail wheel tread defect detection using improved YOLOv3

2022, Measurement: Journal of the International Measurement Confederation

Show abstract

Optomechanical behaviour of optical sensor for measurement of Wagon weight at different speeds of the train

2023, Journal of Optics (India)

Axle Box Resonance Excitation Model Based on Wheelset Polygon and Its Resonance Characteristic Analysis in High-Speed Train

2022, Advanced Theory and Simulations

Technical Article | Published: 20 October 2021

High-Temperature Oxidation Studies of Plasma-Sprayed NiCrAlY/TiO_2 and NiCrAlY/Cr_2O_3/YSZ Cermet Composite Coatings on MDN-420 Special Steel Alloy

G. Madhu Sudana Reddy, C. Durga Prasad ✉, Gagan Shetty, M. R. Ramesh, T. Nageswara Rao & Pradeep Patil

Metallography, Microstructure, and Analysis **10**, 642–651 (2021)

Abstract

The plasma spray process was used to form 70%NiCrAlY + 30%TiO_2 and 70%NiCrAlY + 25%Cr_2O_3 + 5%YSZ cermet coatings on MDN-420 special steel alloy . Cyclic oxidation testing was conducted on coated and uncoated specimens at 700°C under a static air environment. Thermogravimetric analysis was applied to establish the oxidation kinetics. X-ray diffraction (XRD), scanning electron microscopy (SEM)/energy-dispersive x-ray spectroscopy (EDS), and electron probe microanalysis (EPMA) techniques were used to analyze the oxidized

products. The NiCrAlY + Cr_2O_3 + YSZ coating was found to be most resistive when compared with the NiCrAlY + TiO_2 coating in the aggressive oxidation environment. Net weight loss was observed for bare MDN-420 alloy due to sputtering. The oxidation resistance of the coatings was due to formation of Cr_2O_3, $NiCr_2O_4$, NiO, and Al_2O_3 phases.

Introduction

Applications such as nuclear, steam, gas turbine blades, compressor blades, and internal combustion engine parts operate in gaseous conditions, and in some cases components undergo sliding action against the hard face of a counterbody. Friction and oxidation are the major issues leading to catastrophic failure of such components [1,2,3]. These parts require elevated-temperature strength, wear, hot corrosion, and oxidation resistance to sustain such extreme working conditions [4, 5]. The structural rigidity and reliability can be provided by designing components for use in high-temperature operating conditions. However, protection of the component from oxidation cannot be provided simultaneously,

resulting in a need for surface modification to protect against material failure [6,7,8].

The thermal spray process is a superior approach for coating deposition compared with the overlay coating technique in terms of both economic and environmental aspects [9, 10]. A thicker coating can be deposited by using the thermal spray process, in the range from a few micrometers to millimeters. Chromium oxide coatings are widely used in applications involving high temperature because they enable better protection from erosion, corrosion, and oxidation environments [11,12,13]. Aluminum and chromium are included in such coatings to enable selective oxidation of Al_2O_3 and Cr_2O_3 scale that forms during the reaction of the coating with atmospheric air, thus protecting the base material from oxidation [14,15,16].

Thermal barrier coatings are actually ceramic coatings with a layered structure. This not only reduces the thermal fatigue but also protects the underlying metal from oxidation and corrosion. They can therefore help to increase the operating temperature while also improving the engine performance. The life of a part can be greatly increased by coating. Currently used coating material (yttria-stabilized zirconia) can provide considerable protection for existing engines [17,18,19]. Since TiO_2 is an excellent material for spraying with higher deposition efficiency and

cheaper coatings with tight coating, NiCrAlY + TiO_2 coatings are studied in the present work.

NiCrAlY/TiO_2 coating: This coating combination is mainly focused on improving the corrosion, erosion and oxidation resistance at elevated-temperature conditions. The titanium accelerates the formation of chromia at the metal–oxide interface, thus reducing the thermal expansion coefficient [20,21,22,23,24].

NiCrAlY/Cr_2O_3/YSZ coating: The presence of Cr_2O_3 reinforcement strengthens nickel-based coatings in terms of their tribological, hot corrosion, and oxidation resistance performance when compared with other coatings [25, 26]. Combination of these coatings with yttrium improves the adherence of alumina and chromia scales on Ni- and Co-base alloys, and changes the oxide growth from a cation to anion diffusion-controlled mode, which reduces the oxidation rate of chromia [27,28,29].

Coating materials are selected based on their performance in terms of the degradation of components in static oxidation environment, corrosion, and erosion environments. The present study considers coated and uncoated alloys in a high-temperature oxidation environment at 700°C in a static air environment. The plasma spray process was used to coat powders onto the substrate.

Experimental Procedures

Substrate and Coatings

MDN-420 special steel alloy is used to manufacture turbine blades and the components of compressors that are commonly used in power plants. The chemical composition and application of the material chosen for the present study are presented in Table 1. Substrates with dimensions of 25 mm × 25 mm × 5 mm were cut using an excimer laser micromachining system. Before applying the coating, a roughening process was carried out by impinging the substrate with Al_2O_3 powder to achieve better coating adhesion. The morphology of the coating powder is shown in Table 2. The operating parameters of the plasma spray coating process are presented in Table 3.

Table 1 Composition and application of MDN-420 special steel alloy

Table 2 Morphology of coating powders

Table 3 Plasma spray coating parameters

Cyclic Oxidation

A ceramic tubular furnace was used to study the behavior of coated and uncoated substrates in a high-temperature static oxidation environment.

The test specimens were kept in the furnace at 250°C for 2 h to dry the specimens, then weighed. This process was carried out to remove moisture present in the substrate. Cyclic oxidation experiments were conducted in a furnace at 700°C by keeping the specimen in a ceramic boat for 1 h. The heated specimens were then removed and cooled to room temperature for 20 min, then weighed. The difference in the reading and visual observations were noted. This procedure was repeated for 50 cycles. The specimens subjected to the static oxidation environment were characterized by using SEM, XRD analysis, and EDS technique.

Results and Discussion

Characterization of As-Sprayed Coatings

The morphology of the coating feedstock powders is shown in Fig. 1. The coatings were found to be denser with a laminar structure, as shown in Fig. 2. The NiCrAlY + TiO_2 and NiCrAlY + Cr_2O_3 + YSZ coatings showed a similar lamellar structure with shiny appearance of layers formed with the presence of coating elements as confirmed by EDS (Fig. 2a, b). Table 4 presents the thickness of the coatings, and the porosity and hardness of the coated specimens.

Fig. 1

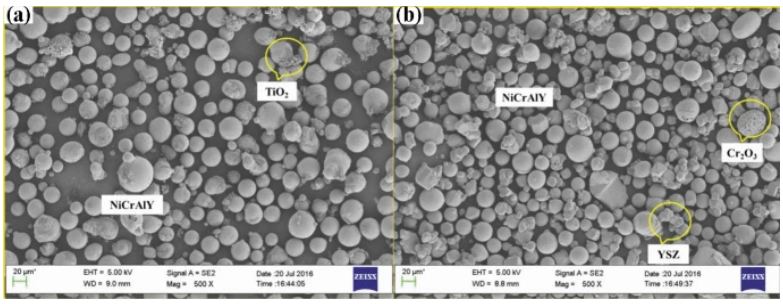

Coating powder morphology: (**a**) NiCrAlY + TiO_2 and (**b**) NiCrAlY + Cr_2O_3 + YSZ

Fig. 2

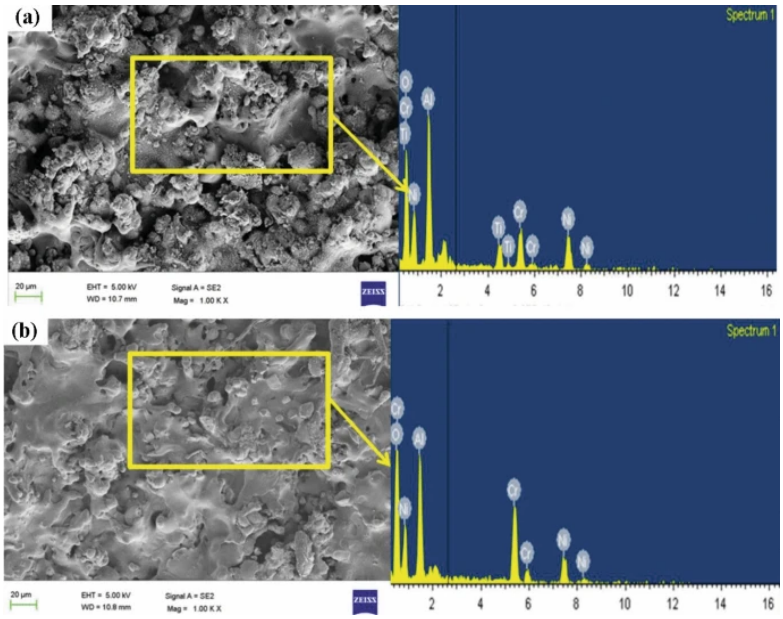

Coating morphology of (**a**) NiCrAlY + TiO_2 and (**b**) NiCrAlY + Cr_2O_3 + YSZ

Table 4 Porosity, thickness, and microhardness of coatings

Oxidation Kinetics

Macrographs of the coated specimens subjected to cyclic oxidation for 50 cycles are shown in Fig. 3.MDN420 showed a rust color after completion of

the first cycle. After the seventh cycle, a color change to brown was noticed. A color change from brown to black was observed after 25 cycles, and this trend continued until the completion of 50 cycles. In the NiCrAlY + TiO_2 coating, a light-brown color was observed after completion of three cycles on the substrate surface. A color change from brown to shiny brown appearance was noticed after the 11th cycle. Then, no further color changes were observed until the end of 50 cycles. A shiny brown color was observed for the NiCrAlY + Cr_2O_3 + YSZ coating after completion of the first cycle. A transformation of the shiny brown color to dull brown appearance was noticed after the 17th cycle. The same trend was observed with no color until the end of 50 cycles.

Fig. 3

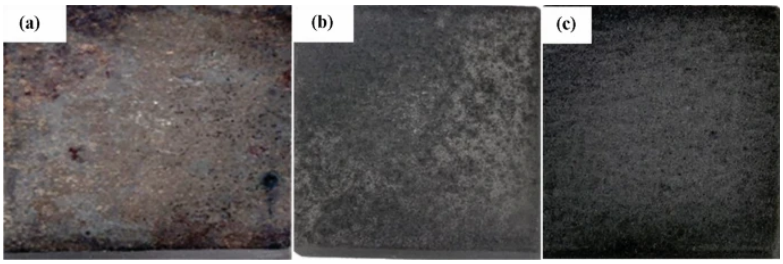

Macrographs of uncoated and coated substrates after cyclic oxidation at 700°C: (**a**) MDN-420, (**b**) NiCrAlY + TiO_2 coating, and (**c**) NiCrAlY + Cr_2O_3 + YSZ coating

Figure 4 shows a graph of the cumulative weight gain versus number of cycles, while Fig. 5 shows the weight gain squared versus the number of cycles for the coated and uncoated substrates subjected to the

cyclic oxidation environment. The weight gain for the MDN-420 alloy after completion of 50 cycles was 0.1779 mg/cm^2.The weight gain values for the NiCrAlY + TiO_2 and NiCrAlY + Cr_2O_3 + YSZ coatings after completion of 50 cycles were found to be 69.37 and 55.23 mg/cm^2, respectively. The parabolic constant (K_p) for the MDN420 alloy was 1.388×10^{-15} g^2 cm^{-4} s^{-1}. The parabolic constant (K_p) for the NiCrAlY + TiO_2 and NiCrAlY + Cr_2O_3 + YSZ coatings was 3.247×10^{-11} g^2 cm^{-4}s^{-1} and 2.361×10^{-11} g^2 cm^{-4}s^{-1}, respectively. The weight gain observed after 50 cycles and the K_p values obtained by plotting the weight gain squared (mg^2/cm^4) versus the number of cycles for the coated and uncoated specimens are presented in Table 5. A lower K_p value indicates that the coating performed better in the high-temperature static oxidation environment [7].

Fig. 4

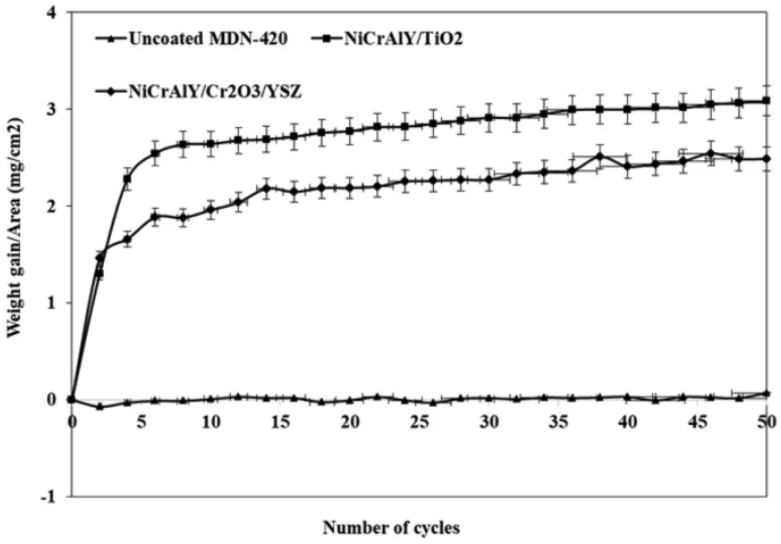

Weight gain versus number of cycles for MDN-420, NiCrAlY + TiO_2, and NiCrAlY + Cr_2O_3 + YSZ coatings

subjected to cyclic oxidation for 50 cycles in static air environment at 700°C

Fig. 5

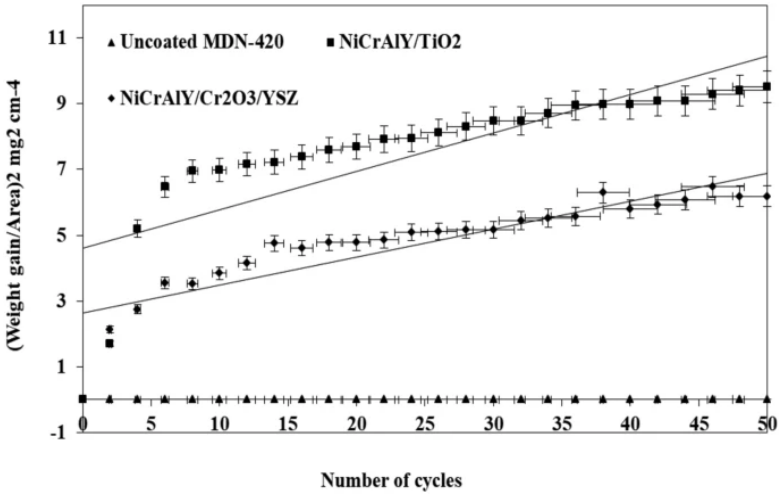

Weight gain/area^2 versus number of cycles for MDN-420, NiCrAlY + TiO_2, and NiCrAlY + Cr_2O_3 + YSZ coatings subjected to cyclic oxidation for 50 cycles in static air environment at 700°C

Table 5 K_p values of coated and uncoated MDN-420 after subjecting specimens to cyclic oxidation

XRD Analysis

Figure 6 shows the XRD analysis after specimens were exposed to the oxidation environment for 50 cycles at 700°C. The major peak of Cr_7C_3 and the minor peaks of Fe_2O_3 and FeS_2 are observed for the MDN420 alloy. For the NiCrAlY + TiO_2 coating, the major phases observed were Cr_2O_3 and $NiCr_2O_4$ with minor phases of Al_2O_3 and NiO. Major phases

of $NiCr_2O_4$, NiO, Cr_2O_3, and Al_2O_3 were observed for the NiCrAlY + Cr_2O_3 + YSZ coating. A tendency for a major phase of Al_2O_3 in NiCrAlY + Cr_2O_3 + YSZ coating was also suggested by Stroosnijder et al. [16] and Toma et al. [17].

Fig. 6

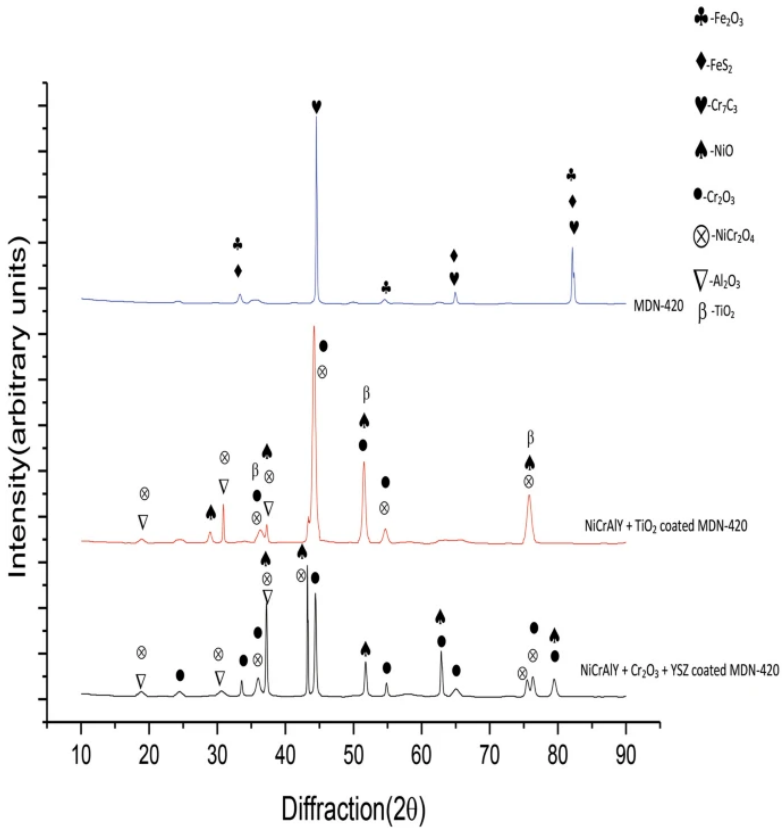

XRD patterns from coated and uncoated substrates subjected to oxidation for 50 cycles in static air environment at 700°C

SEM and EDS Analysis

SEM and EDS analysis of coated and uncoated alloys after cyclic oxidation is shown in Fig. 7. The analysis was done in selected regions. From Fig. 7, note that the uncoated substrate material exhibited a sponge-like appearance, and EDS of this area

revealed about 47.52% oxygen 21.47% iron, and 17.89% Cr with small traces of silicon and manganese. The scales that formed on the coated substrate materials were dense and free from cracks, containing O_2, Cr, Al, Ti, and Ni. Small crystal-like structures were observed across almost all the whole area of the NiCrAlY + TiO_2 coating as shown in Fig. 7. EDS analysis of this area revealed higher percentages of oxygen, chromium, and nickel (42.82% O, 11.43% Cr, and 12.62% and 23.36% Ni) with small amounts of titanium. SEM analysis of the NiCrAlY + Cr_2O_3 + YSZ coating revealed a rock crystal-like appearance on almost all areas .EDS analysis on the other hand revealed higher percentages of oxygen, nickel, and chromium (52.51% O, 12.22% Al, 13.44% Cr, and 21.83% Ni).

Fig. 7

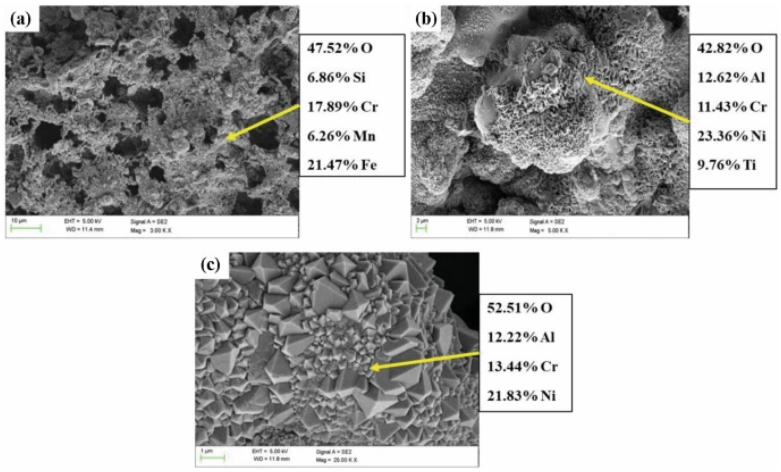

SEM and EDS analysis of uncoated and coated alloys subjected to cyclic oxidation at 700°C: (**a**) MDN-420, (**b**) NiCrAlY + TiO_2 coating, and (**c**) NiCrAlY + Cr_2O_3 + YSZ coating

EPMA

Back-scattered images of NiCrAlY + TiO_2 and NiCrAlY + Cr_2O_3 + YSZ coatings are shown in Fig. 8. Figures 9 and 10 show elemental maps of the titanium dioxide and chromium oxide coatings after cyclic oxidation for 50 h. The oxidized NiCrAlY + TiO_2 coating showed formation of scale consisting of elements such as O_2, Al, Cr, Ni, and Ti. Oxygen forms the thicker band in the uppermost part of the scale, with chromium in the subscale area, as seen in Fig. 9. Ni-rich splats were present at splat boundaries. Nickel showed a relatively higher concentration near the subsurface scale interface, indicating its diffusion from the substrate to the coating surface.

Fig. 8

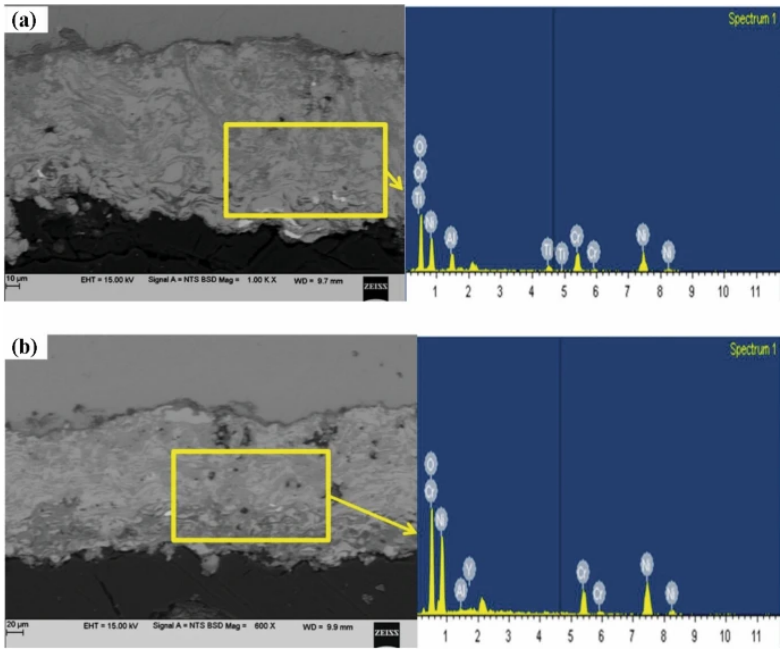

BSE images of (**a**) NiCrAlY + TiO_2 coating and (**b**) NiCrAlY + Cr_2O_3 + YSZ coating after oxidation for 50 phases at 700°C

Fig. 9

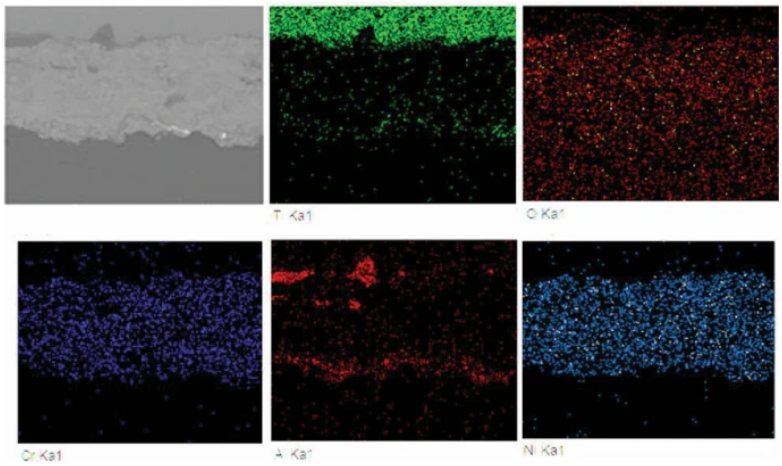

X-ray map of NiCrAlY + TiO_2 coating subjected to cyclic oxidation for 50 cycles in static air environment

Fig. 10

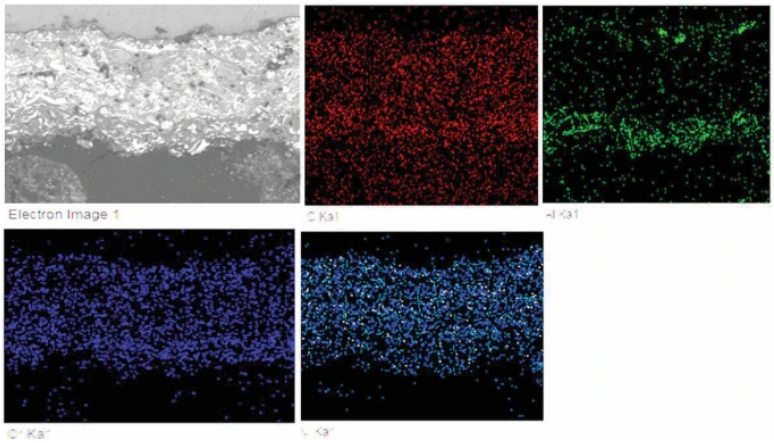

X-ray map of NiCrAlY + Cr_2O_3 + YSZ coating subjected to cyclic oxidation for 50 cycles in static air environment

The scale that formed on the surface of the NiCrAlY + Cr_2O_3 + YSZ coating mainly consisted of elements such as oxygen, aluminum, chromium, and nickel. Oxygen forms as the thicker band in the uppermost part of the scale. Just below this layer, an

intermediate band formed, enriched with chromium and nickel splats. The presence of chromium and nickel indicates that oxides of chromium were formed mostly at the splat boundaries. These elements were oxidized at the boundary areas. The other part of scale included aluminum with a lamellar splat structure.

Discussion

Coatings with the desired thickness in the range from 250–350 μm were successfully deposited on special steel alloys. Heath et al. [20] reported that thick coatings exhibit better corrosion and oxidation resistance. The measured porosity values are in good agreement with the findings of Hidalgo et al. [21], Belzunce et al. [22], Erickson et al. [23], and Chen et al. [24].

In the present investigation, the NiCrAlY + Cr_2O_3 + YSZ coating showed better oxidation resistance compared with the NiCrAlY + TiO_2 coating. A net weight loss was observed for the MDN-420 substrate alloy due to intense sputtering of the scale that formed on the substrate surface, making it difficult to measure the overall weight gain. When sputtering takes place, there is a net weight loss in the substrate alloy [22,23,24]. The formation of ternary oxide $NiCr_2O_4$ and Cr_2O_3 spinels in the scale improved the oxidation resistance of the coating in the static air environment. Similar findings were reported by Chatterje et al. [28].

The superior oxidation resistance of the NiCrAlY + Cr_2O_3 + YSZ coating was due to the formation of protective oxide scale mainly consisting of chromium oxide (Cr_2O_3), which shows minimum solubility towards atmospheric air [26, 30, 31]. Parabolic behavior and slow oxidation kinetics were observed by thermogravimetric analysis, revealing that the reaction rate is diffusion limited.

The oxidation resistance of the NiCrAlY + TiO_2 coating was due to the spinels and oxides of chromium, aluminium, and titanium that formed on the surface of the scale. The oxidation was restricted to only the external surface with a depth of a few microns, while the remainder of the coating remained in an unoxidized state.

Conclusions

- NiCrAlY/TiO_2 and NiCrAlY/Cr_2O_3/YSZ coatings were successfully deposited on MDN-420 by using the plasma spray process, achieving porosity of 2.7% and 2.9% and average microhardness of 539 and 568 Hv, respectively.
- The substrate exhibited a net weight loss and lower oxidation resistance due to intense sputtering of the scale that formed on the surface. Sputtering promoted exposure of a new layer to the oxidation environment.
- NiCrAlY + Cr_2O_3 + YSZ-coated alloys showed less weight gain when compared with NiCrAlY

+ TiO_2-coated alloys. It was evident that the formation of $NiCr_2O_4$ and Cr_2O_3 spinels in the oxide scale improved the oxidation resistance of the coating in the static air environment.

- The NiCrAlY + TiO_2 coating exhibited a slightly higher weight gain due to the spinels and oxides of chromium, aluminum, and titanium that formed on the surface of the scale. The presence of TiO_2 was noted on the surface of the oxidized coatings. Hence, the NiCrAlY + Cr_2O_3 + YSZ coating was more protective when compared with the NiCrAlY + TiO_2coating.

References

1. B.S. Sidhu, S. Prakash, Evaluation of the corrosion behaviour of plasma-sprayed Ni3Al coatings on steel in oxidation and molten salt environments at 900 °C. Surf. Coat. Technol. **166**, 89–100 (2003)

2. C.D. Prasad, S. Joladarashi, M.R. Ramesh, M.S. Srinath, B.H. Channabasappa, Comparison of high temperature wear behavior of microwave assisted HVOF Sprayed CoMoCrSi-WC-CrC-Ni/WC-12Co composite coatings. Silicon. (2020). https://doi.org/10.1007/s12633-020-00398-1

3. X.Q. Cao, R. Vassenb, D. Stoeverb, Ceramic materials for thermal barrier coatings. J. Eur.

Ceram. Soc. **24**, 1–10 (2004)

4. C.D. Prasad, S. Joladarashi, M.R. Ramesh, M.S. Srinath, B.H. Channabasappa, Microstructure and tribological resistance of flame sprayed CoMoCrSi/WC-CrC-Ni and CoMoCrSi/WC-12Co composite coatings remelted by microwave hybrid heating. J. Bio Tribo-Corrosion. **6**, 124 (2020). https://doi.org/10.1007/s40735-020-00421-3

5. J.R. Nicholls. Designing Oxidation-Resistant Coatings, Oxidation review

6. K.A. Khor, Y.W. Gu, Z.L. Dong, Plasma spraying of functionally graded Yttria stabilized Zirconia/NiCoCrAlY coating system using composite powders, *JTTEE*5, 9: 245-249

7. M. Reddy, C.D. Prasad, P. Patil, M.R. Ramesh, N. Rao, Hot corrosion behavior of plasma sprayed NiCrAlY/TiO_2 and NiCrAlY/Cr_2O_3/YSZ cermets coatings on alloy steel. Surfaces and Interfaces. **22**, 100810 (2021). https://doi.org/10.1016/j.surfin.2020.100810

8. C.D. Prasad, A. Jerri, M.R. Ramesh, Characterization and sliding wear behavior of iron based metallic coating deposited by HVOF process on low carbon steel substrate. J. Bio

Tribo-Corrosion. **6**, 69 (2020). https://doi.org/10.1007/s40735-020-00366-7

9. M. Seraffon, N.J. Simms, J. Sumner, J.R. Nicholls, The development of new bond coat compositions for thermal barrier coating systems operating under industrial gas turbine conditions. Surf. Coat. Technol. **206**, 1529–1537 (2011)

10. H. Vasudev, L. Thakur, H. Singh, A. Bansal, A study on processing and hot corrosion behaviour of HVOF sprayed Inconel718-nano Al_2O_3 coatings. Mater. Today Commun. **25**, 101626 (2020). https://doi.org/10.1016/j.mtcomm.2020.101626

11. H. Vasudev, L. Thakur, H. Singh, A. Bansal, An investigation on oxidation behaviour of high velocity oxy-fuel sprayed Inconel718-Al_2O_3 composite coatings. Surf. Coat. Technol. **393**, 125770 (2020). https://doi.org/10.1016/j.surfcoat.2020.125770

12. C.D. Prasad, S. Joladarashi, M.R. Ramesh, M.S. Srinath, B.H. Channabasappa, Effect of microwave heating on microstructure and elevated temperature adhesive wear behavior of HVOF deposited CoMoCrSi-Cr_3C_2

composite coating. Surf. Coat. Technol. **374**, 291–304 (2019). https://doi.org/10.1016/j.surfcoat.2019.05.056

13. T.W. Kerr, Hot corrosion and oxidation studies of pure nickel and Ni-Cr, Ni-Si and Ni-Cr-Si alloys at 1000_C. Report AD-A024, U.S. Department of Commerce, 1975, p. 708

14. Buta Singh Sidhu, S Prakash, High-temperature oxidation behavior of NiCrA1Y bond coats and stellite-6 plasma-sprayed coatings, *Oxidation of Metals*, 63, 314, https://doi.org/10.1007/s11085-005-3203-1.

15. C.D. Prasad, S. Joladarashi, M.R. Ramesh, M.S. Srinath, B.H. Channabasappa, Microstructure and tribological behavior of flame sprayed and microwave fused CoMoCrSi/CoMoCrSi-Cr_3C_2 coatings. Mater. Res. Express. **6**, 026512 (2019). https://doi.org/10.1088/2053-1591/aaebd9

16. M.F. Stroosnijder, R. Mevrel, M.J. Bennett, The interaction of surface engineering and high temperature corrosion protection. Mater. High Temp. **12**(1), 53–56 (1994)

17. D. Toma, W. Brandl, U. Koester, Studies on the transient stage of oxidation of VPS and HVOF

sprayed MCrAlY coatings. Surf. Coat. Technol. **120–121**, 8–15 (1999)

18. C.D. Prasad, S. Joladarashi, M.R. Ramesh, M.S. Srinath, B.H. Channabasappa, Influence of microwave hybrid heating on the sliding wear behaviour of HVOF Sprayed CoMoCrSi Coating. Mater. Res. Express. **5**, 086519 (2018). https://doi.org/10.1088/2053-1591/aad44e

19. H. Singh, S. Prakash, D. Puri, Some observations on the high temperature oxidation behavior of plasma sprayed Ni_3Al coatings Elsevier. Mater. Sci. Eng. A. **444**, 242–250 (2007)

20. G.R. Heath, P. Heimgartner, G. Irons, R. Miller, S. Gustafson, Mater. Sci. Forum. **251–254**, 809 (1997)

21. V.H. Hidalgo, F.J.B.Varela, A.C. Menendez, Proc. of the 15th Int. Thermal Spray Conf., 25–29th May, Nice, France, 1998, p. 617

22. F.J. Belzunce, V. Higuera, S. Poveda, High temperature oxidation of HFPD thermal-sprayed MCrAlY coatings. Mater. Sci. Eng. AStruct. Mater. Prop. Microstruct. Process. **297**(1–2), 162 (2001)

23. L.C. Erickson, R. Westergard, U. Wiklund, N. Axen, H.M. Hawthorne, S. Hogmark, Cohesion in plasma-sprayed coatings—a comparison between evaluation methods. Wear. **214**, 30 (1998)

24. H.C. Chen, Z.Y. Liu, Y.C. Chuang, Degradation of plasma-sprayed alumina and zirconia coatings on stainless steel during thermal cycling and hot corrosion. Thin Solid Films. **223**(1), 56 (1993)

25. Osawa, T. Itsukaichi, R. Ahmed, Influence of substrate properties on the impact resistance of WC cermet coatings, *JTTEE*, 5 14:495-501, ASM International

26. R.A. Mahesh, R. Jayaganthan, S. Prakash, Microstructural characteristics and mechanical properties of HVOF sprayed NiCrAl coating on superalloys. J. Alloy. Compd. **468**, 392–405 (2009)

27. J. Gang-Chang, L. Chang-Jiu, W. Yu-Yue, L. Wen-Ya, Microstructural characterization and abrasive wear performance of HVOF sprayed Cr_3C_2–NiCr coating. Surf. Coat. Technol. **200**, 6749–6757 (2006)

28. U.K. Chatterjee, S.K. Bose, S.K. Roy, Environmental Degradation of Metals, Marcel

Dekker, New York, 2001.S

29. C.J. Li, G.C. Ji, Y.Y. Wang, K. Sonoya, The dominant mechanism of carbon loss during HVOF spraying ofCr_3C_2-NiCr. Thin Solid Films. **419**, 137–143 (2002)

30. N.D. Prasanna, C. Siddaraju, G. Shetty, M.R. Ramesh, M. Reddy, Studies on the role of HVOF coatings to combat erosion in turbine alloys. Mater. Today Proc. **5**, 3130–3136 (2018)

31. Madhu Sudana Reddy, Pradeep P Patil, M Muniraju, K Gagan Shetty, T Nageswara Rao, Investigation & characterization of plasma sprayed cermet coatings on special steel alloy for gas turbine applications, *Materials Today: Proceedings*, 2021/2/26.

Author information

Authors and Affiliations

Department of Mechanical Engineering, The Oxford College of Engineering, Bengaluru, Karnataka, India

G. Madhu Sudana Reddy

Department of Mechanical Engineering, RV Institute of Technology and Management Bengaluru, Karnataka, 560078, India

C. Durga Prasad

Department of Mechanical Engineering, Sahyadri College of Engineering and Management, Adyar, Mangaluru, 575007, India

Gagan Shetty

Department of Mechanical Engineering, National Institute of Technology Karnataka, Surathkal, 575025, India

M. R. Ramesh

Department of Mechanical Engineering, GITAM University, Bengaluru, Karnataka, India

T. Nageswara Rao & Pradeep Patil

Corresponding author

Correspondence to C. Durga Prasad.

Ethics declarations

Conflict of Interest

The authors declare that they have no known competing financial interests or personal relationships that could have appeared to influence the work reported in this paper.

Additional information

Publisher's Note

Rights and permissions

About this article

Cite this article

Madhu Sudana Reddy, G., Durga Prasad, C., Shetty, G. *et al.* High-Temperature Oxidation Studies of Plasma-Sprayed NiCrAlY/TiO_2 and NiCrAlY/Cr_2O_3/YSZ Cermet Composite Coatings on MDN-420 Special Steel Alloy. *Metallogr. Microstruct. Anal.* **10**, 642–651 (2021). https://doi.org/10.1007/s13632-021-00784-0

Received	Revised	Accepted
16 June 2021	10 September 2021	15 September 2021

Published	Issue Date
20 October 2021	October 2021

DOI
https://doi.org/10.1007/s13632-021-00784-0

Share this article

Keywords

Thermal spray coatings **NiCrAlY/TiO_2** **NiCrAlY/Cr_2O_3/YSZ** **Oxidation** **Special steel alloys**

PAPER

Design and analysis of photonic MEMS based micro ring resonators for pressure sensing application

Prajwal P Patil[1], Sushma P Kamath[2], Anup M Upadhyaya[1] and Preeta Sharan[3,2]

Published 13 October 2021 • © 2021 IOP Publishing Ltd

Journal of Micromechanics and Microengineering, Volume 31, Number 11

Citation Prajwal P Patil *et al* 2021 *J. Micromech. Microeng.* **31** 115004

DOI 10.1088/1361-6439/ac2bb1

sharanpreeta@gmail.com

[1] Department of Mechanical Engineering, The Oxford College of Engineering, Bangalore, India

[2] Department of Electronics and Communication Engineering, The Oxford College of Engineering, Bangalore, India

[3] Author to whom any correspondence should be addressed.

Prajwal P Patil https://orcid.org/0000-0001-9421-4584

Preeta Sharan https://orcid.org/0000-0002-3549-7147

1. Received 5 June 2021
2. Accepted 30 September 2021
3. Published 13 October 2021

Abstract

The proposed work consists of a ring resonator-based pressure sensor. Double and triple ring photonic crystal resonators are configured in series and in parallel combinations. The sensing layer is designed and simulated for a varying pressure of 3–9 MPa using ansys workbench to obtain the stress and deformation experienced by the sensor. The equivalent refractive index value for every stress is computed and shift in wavelength is determined by simulation of the photonic crystal ring resonator (PCRR) structures in the optical tool. Finite-difference time-domain results show that 'three rings coupled in parallel' PCRR structure have the best sensitivity and good quality factor than other sensing configurations. A maximum sensitivity of 49.77 nm MPa^{-1} and a quality factor of 3260.25 is observed for the triple-ring parallel PCRR. The proposed type of sensor has remarkable biosensing applications.

Research Paper | Published: 11 February 2022

High-temperature oxidation behavior of plasma-sprayed NiCrAlY/TiO_2 and NiCrAlY/Cr_2O_3/YSZ coatings on titanium alloy

G. Madhu Sudana Reddy, C. Durga Prasad, Gagan Shetty, M. R. Ramesh, T. Nageswara Rao & Pradeep Patil

Welding in the World **66**, 1069–1079 (2022)

Abstract

The 70% NiCrAlY + 30% TiO_2 and 70% NiCrAlY + 25% Cr_2O_3 + 5% YSZ metallic coatings are sprayed on titanium-15 alloy of ASTM B338, Grade 2, by using the plasma spray coating technology. Cyclic oxidation studies are conducted on the uncoated and coated alloys at 700 °C under static air environment. The kinetics of oxidation is studied by using the thermo-gravimetric method. Phase, microstructural, and chemical analysis tests are performed on as-sprayed and oxidized coatings. The coated alloys are found to be more resistant when compared to the uncoated alloys. The NiCrAlY + Cr_2O_3 + YSZ coating is found to be more protective when compared to NiCrAlY + TiO_2 coating. It is concluded that the formation of Cr_2O_3,

$NiCr_2O_4$, and Al_2O_3 is attributed to the development of oxidation resistance in the coatings.

References

1. Sidhu BS, Prakash S (2003) Evaluation of the corrosion behaviour of plasma-sprayed Ni_3Al coatings on steel in oxidation and molten salt environments at 900°C. Surf Coat Technol 166:89–100

2. Cao XQ, Vassenb R, Stoeverb D (2004) Ceramic materials for thermal barrier coatings. J Eur

Ceram Soc 24:1–10

3. Durga Prasad C, Sharnappa Joladarashi, Ramesh MR, Srinath MS, Channabasappa BH (2020) Microstructure and Tribological resistance of flame sprayed CoMoCrSi/WC-CrC-Ni and CoMoCrSi/WC-12Co composite coatings remelted by microwave hybrid heating. J Bio Tribo-Corrosion 6:124. https://doi.org/10.1007/s40735-020-00421-3

4. Khor KA, Gu YW, Dong ZL (2000) Plasma spraying of functionally graded yttria-stabilized zirconia/NiCoCrAlY coating system using composite powders, Journal of Thermal Spray Technology 9(2):245–249. https://doi.org/10.1361/105996300770349999

5. Seraffon M, Simms NJ, Sumner J, Nicholls JR (2011) The development of new bond coat compositions for thermal barrier coating systems operating under industrial gas turbine conditions. Surf Coat Technol 206:1529–1537

6. Reddy MS, Prasad CD, Ramesh MR, Nageswara R (2021) Hot corrosion behaviour of plasma-sprayed NiCrAlY/TiO_2 and NiCrAlY/Cr_2O_3/YSZ cermets coatings on alloy steel, Surfaces and Interfaces Volume 22Article 100810

7. Durga Prasad C, Akhil Jerri, Ramesh MR (2020) Characterization and sliding wear behavior of iron based metallic coating deposited by HVOF process on low carbon steel substrate. J Bio Tribo-Corrosion 6: 69. https://doi.org/10.1007/s40735-020-00366-7

8. Buta Singh Sidhu, S Prakash (2005) High-temperature oxidation behavior of NiCrA1Y bond coats and stellite-6 plasma-sprayed coatings, oxidation of metals. Oxid Met 63:241–259. https://doi.org/10.1007/s11085-005-3203-1

9. Durga Prasad C, Sharnappa Joladarashi, Ramesh MR, Srinath MS, Channabasappa BH (2020) Comparison of high temperature wear behavior of microwave assisted HVOF sprayed CoMoCrSi-WC-CrC-Ni/WC-12Co composite coatings. Silicon 12:3027–3045. https://doi.org/10.1007/s12633-020-00398-1

10. Thavaraya Naik, Mahantayya Mathapathi, Durga Prasad C, Nithin HS, Ramesh MR (2022) Effect of laser post treatment on microstructural and sliding wear behavior of HVOF sprayed NiCrC and NiCrSi coatings. Surf Rev Lett 29(1):2250007 https://doi.org/10.1142/S0218625X2250007X

11. Hidalgo VH, Varela FJB, Menendez AC (1998) Proc. of the 15th Int. Thermal Spray Conf., 25–29th May, Nice, France, p. 617

12. Durga Prasad C, Sharnappa Joladarashi, Ramesh MR, Srinath MS, Channabasappa BH (2019) Effect of microwave heating on microstructure and elevated temperature adhesive wear behavior of HVOF deposited CoMoCrSi-Cr_3C_2 composite coating Surf Coatings Technol 374: 291–304. https://doi.org/10.1016/j.surfcoat.2019.05.056

13. Stroosnijder MF, Mevrel R, Bennett MJ (1994) Material high temperature. 12(1): 53–56

14. Heath GR, Heimgartner P, Irons G, Miller R, Gustafson S (1997) Mater Sci Forum 251–254:809

15. Belzunce FJ, Higuera V, Poveda S (2001) Mater Sci Eng A Struct Mater: Prop Microstruct Process 297 (1–2): 162

16. Girisha K G, K.V.Sreenivas Rao, Durga Prasad C (2018) Slurry erosion resistance of martenistic stainless steel with plasma sprayed Al_2O_3–40%TiO_2 coatings. Mater Today Proc 5: 7388–7393. https://doi.org/10.1016/j.matpr.2017.11.409

17. Madhusudana Reddy G, C Durga Prasad, Gagan Shetty, Ramesh MR, Nageswara Rao T, Pradeep Patil (2021) High temperature oxidation studies of plasma sprayed NiCrAlY/TiO_2 & NiCrAlY /Cr_2O_3/YSZ cermet composite coatings on MDN-420 special steel alloy. Metallography Microstruct Anal 10: 642–651. https://doi.org/10.1007/s13632-021-00784-0

18. Erickson LC, Westergard R, Wiklund U, Axen N, Hawthorne HM, Hogmark S (1998) Wear 214:30

19. Durga Prasad C, Sharnappa Joladarashi, Ramesh MR, Srinath MS, Channabasappa BH (2018) Influence of microwave hybrid heating on the sliding wear behaviour of HVOF sprayed CoMoCrSi coating. Mater Res Express 5: 086519. https://doi.org/10.1088/2053-1591/aad44e.

20. Chatterjee UK, Bose SK, Roy SK (2001) Environmental degradation of metals. Marcel Dekker, New York

21. Prasanna ND, Siddaraju C, Shetty G, MSRG, Ramesh MR (2018) Studies on the role of HVOF coatings to combat erosion in turbine alloys. Mater Today Proc 5 (1):3130–

3136. https://doi.org/10.1016/j.matpr.2018.01.119

22. Madhu Sudana Reddy G, Ramesh MR, Nageswara Rao, Jegadeeswaran N (2018) High Temperature oxidation behavior of plasma sprayed (WC-Co) / (Cr_3C_2-NiCr) coating On MDN-420 & titanium-15 Alloy for gas turbine application. Int J Mech Prod Eng Res Dev 8(6):227–237

23. Madhu Sudana Reddy G, Ramesh MR, Nageswara Rao, Jegadeeswaran N (2018) Characterisation & Hot corrosion studies on plasma sprayed (WC-Co) / (Cr_3C_2-NiCr) coating on titanium & special steel alloys. Int J Mech Eng Technol 8(6): 227–237

24. Durga Prasad C, Sharnappa Joladarashi, Ramesh MR, Srinath MS, Channabasappa BH (2019) Microstructure and tribological behavior of flame sprayed and microwave fused CoMoCrSi/CoMoCrSi-Cr_3C_2 coatings. Mater Res Express 6: 026512. https://doi.org/10.1088/2053-1591/aaebd9

25. Ajdelsztajn L, Picas JA, Kim GE, Bastian FL, Schoenung J, Provenzano V (2002) Oxidation behavior of HVOF sprayed nanocrystalline NiCrAlY powder. Mater Sci Eng A 338:33–43

26. Wang B, Gong J, Wang AY, Sun C, Huang RF, Wen LS (2002) Oxidation behaviour of NiCrAlY coatings on Ni-based superalloy. Surf Coat Technol 149:70–75

27. Evans HE, Taylor MP (2001) Diffusion cells and chemical failure of MCrAlY bond coats in thermal-barrier coating systems. Oxid Met 55(1–2):17–34

28. Niranatlumpong P, Ponton CB, Evans HE (2000) The failure of protective oxides on plasma-sprayed NiCrAlY overlay coatings. Oxid Met 53:241

Author information

Authors and Affiliations

Department of Mechanical Engineering, The Oxford College of Engineering, Bengaluru, Karnataka, India

G. Madhu Sudana Reddy

Department of Mechanical Engineering, RV Institute of Technology and Management Bengaluru, Karnataka, 560078, India

C. Durga Prasad

Department of Mechanical Engineering, Sahyadri College of Engineering & Management, Adyar, Mangaluru, 575007, India

Gagan Shetty

Department of Mechanical Engineering, National Institute of Technology Karnataka, Surathkal, 575025, India

M. R. Ramesh

Department of Mechanical Engineering, GITAM University, Bengaluru, Karnataka, India

T. Nageswara Rao & Pradeep Patil

Corresponding author

Correspondence to C. Durga Prasad.

Ethics declarations

Conflict of interest

The authors declare no competing interests.

Additional information

Publisher's note

Springer Nature remains neutral with regard to jurisdictional claims in published maps and institutional affiliations.

Recommended for publication by Commission I—Additive Manufacturing, Surfacing, and Thermal Cutting

Rights and permissions

About this article

Cite this article

Reddy, G.M.S., Prasad, C.D., Shetty, G. *et al.* High-temperature oxidation behavior of plasma-sprayed NiCrAlY/TiO_2 and NiCrAlY/Cr_2O_3/YSZ coatings on titanium alloy. *Weld World* **66**, 1069–1079 (2022). https://doi.org/10.1007/s40194-022-01268-7

Received	Accepted	Published
20 October 2021	01 February 2022	11 February 2022

Issue Date
June 2022

DOI
https://doi.org/10.1007/s40194-022-01268-7

Keywords

Plasma spray coatings **NiCrAlY/TiO_2** **NiCrAlY/Cr_2O_3/YSZ** **Oxidation** **Titanium alloy**

PAPER

Elevated temperature erosion performance of plasma sprayed NiCrAlY/TiO_2 coating on MDN 420 steel substrate

Madhu Sudana Reddy G[1], C Durga Prasad[2], Pradeep Patil[3], Naresh Kakur[4] and M R Ramesh[5]

Published 5 May 2022 • © 2022 IOP Publishing Ltd

Surface Topography: Metrology and Properties, Volume 10, Number 2

Citation Madhu Sudana Reddy G *et al* 2022 *Surf. Topogr.: Metrol. Prop.* **10** 025010

DOI 10.1088/2051-672X/ac6a6e

durgaprasi71@gmail.com

[1] Department of Mechanical Engineering, The Oxford College of Engineering, Bengaluru, Karnataka, India

[2] Department of Mechanical Engineering, RV Institute of Technology and Management Bengaluru, Karnataka, India

[3] Department of Mechanical Engineering, GITAM University, Bengaluru, Karnataka, India

[4] Department of Materials Science and Engineering, University of California, Irvine, United States of America

[5] Department of Mechanical Engineering, National Institute of Technology Karnataka, Surathkal, India

C Durga Prasad https://orcid.org/0000-0002-6632-0037

1. Received 25 January 2022
2. Revised 19 March 2022
3. Accepted 26 April 2022
4. Published 5 May 2022

Method: Single-anonymous
Revisions: 1
Screened for originality? Yes

Abstract

The current study deals with the erosion behaviour of a plasma-sprayed 70% NiCrAlY + 30% TiO_2 coating on MDN 420 steel substrate at extreme temperatures. The coating was characterized by using an optical microscope, Scanning Electron Microscopy and X-ray diffraction methods. The coating's porosity, microhardness, surface roughness, and adhesion strength were all examined. The solid particle erosion experiments were carried out at temperatures of 300 °C, 500 °C, and 700 °C, with impact angles of 30° and 90°. The tests were conducted by using the alumina as an erodent in the hot air jet erosion testing machine. The erosion volume loss of coated and uncoated samples was measured using an optical profilometer. It is observed that erosion resistance of the coating was found to be more when compared to the substrate for the different test temperatures chosen. As the temperature increases, the erosion resistance of the coating also found increased from 300 °C to 700 °C at both impact angles of 30° and 90°. The morphology of the eroded coating surface reveals that the generalized behaviour of the coating is ductile in nature.

PAPER

Elevated temperature erosion performance of plasma sprayed NiCrAlY/TiO_2 coating on MDN 420 steel substrate

Madhu Sudana Reddy G[1], C Durga Prasad[2], Pradeep Patil[3], Naresh Kakur[4] and M R Ramesh[5]

Published 5 May 2022 • © 2022 IOP Publishing Ltd

Surface Topography: Metrology and Properties, Volume 10, Number 2

Citation Madhu Sudana Reddy G *et al* 2022 *Surf. Topogr.: Metrol. Prop.* **10** 025010

DOI 10.1088/2051-672X/ac6a6e

durgaprasi71@gmail.com

[1] Department of Mechanical Engineering, The Oxford College of Engineering, Bengaluru, Karnataka, India

[2] Department of Mechanical Engineering, RV Institute of Technology and Management Bengaluru, Karnataka, India

[3] Department of Mechanical Engineering, GITAM University, Bengaluru, Karnataka, India

[4] Department of Materials Science and Engineering, University of California, Irvine, United States of America

[5] Department of Mechanical Engineering, National Institute of Technology Karnataka, Surathkal, India

C Durga Prasad https://orcid.org/0000-0002-6632-0037

1. Received 25 January 2022
2. Revised 19 March 2022
3. Accepted 26 April 2022
4. Published 5 May 2022

Method: Single-anonymous
Revisions: 1
Screened for originality? Yes

Abstract

The current study deals with the erosion behaviour of a plasma-sprayed 70% NiCrAlY + 30% TiO_2 coating on MDN 420 steel substrate at extreme temperatures. The coating was characterized by using an optical microscope, Scanning Electron Microscopy and X-ray diffraction methods. The coating's porosity, microhardness, surface roughness, and adhesion strength were all examined. The solid particle erosion experiments were carried out at temperatures of 300 °C, 500 °C, and 700 °C, with impact angles of 30° and 90°. The tests were conducted by using the alumina as an erodent in the hot air jet erosion testing machine. The erosion volume loss of coated and uncoated samples was measured using an optical profilometer. It is observed that erosion resistance of the coating was found to be more when compared to the substrate for the different test temperatures chosen. As the temperature increases, the erosion resistance of the coating also found increased from 300 °C to 700 °C at both impact angles of 30° and 90°. The morphology of the eroded coating surface reveals that the generalized behaviour of the coating is ductile in nature.

PAPER

Investigation of thermally sprayed NiCrAlY/TiO_2 and NiCrAlY/Cr_2O_3/YSZ cermet composite coatings on titanium alloys

G Madhu Sudana Reddy[1], C Durga Prasad[6,2], Pradeep Patil[3], Gagan Shetty[4], M R Ramesh[5] and T Nageswara Rao[3]

Published 23 June 2022 • © 2022 IOP Publishing Ltd

Engineering Research Express, Volume 4, Number 2

Citation G Madhu Sudana Reddy *et al* 2022 *Eng. Res. Express* **4** 025049

DOI 10.1088/2631-8695/ac7946

durgaprasi71@gmail.com

[1] Department of Mechanical Engineering, The Oxford College of Engineering, Bengaluru, Karnataka, India

[2] Department of Mechanical Engineering, RV Institute of Technology and Management Bengaluru, Karnataka, 560078, India

[3] Department of Mechanical Engineering, GITAM University, Bengaluru, Karnataka, India

[4] Department of Mechanical Engineering, Sahyadri College of Engineering & Management, Adyar, Mangaluru 575007, India

[5] Department of Mechanical Engineering, National Institute of Technology Karnataka, Surathkal 575025, India

[6] Author to whom any correspondence should be addressed,

C Durga Prasad https://orcid.org/0000-0002-6632-0037

1. Received 15 February 2022
2. Revised 18 May 2022
3. Accepted 15 June 2022
4. Published 23 June 2022

Method: Single-anonymous

Revisions: 2

Screened for originality? Yes

Abstract

The present work investigates the hot corrosion behavior of thermally sprayed 65 pct NiCrAlY + 35 pct TiO_2 and 65 pct NiCrAlY + 30 pct Cr_2O_3 + 5 pct YSZ coatings on titanium 15 alloys. The coatings on the titanium 15 alloy substrates exhibit a near-uniform, dense, and adherent microstructure with a porosity of 2.7 to 2.9%. Thermogravimetric studies are made to examine the hot corrosion performance of coatings in a molten salt environment of Na_2SO_4 + 60%V_2O_5 at the temperature of 700 °C for 50 cycles. One cycle is carried out by heating for a period of one hour and cooling the sample at ambient conditions. The corrosion products are analyzed based on scanning electron microscopy, energy dispersive analysis, and X-ray diffraction techniques to study the morphology, phase composition, and abundance of the high-temperature corrosion constituents. The bare titanium-15 alloy, 65 pct NiCrAlY + 35 pct TiO_2 coating and 65 pct NiCrAlY + 35 pct Cr_2O_3 + 5 pct YSZ coating produced a weight gain of 307.92 mg cm^{-2}, 42.16 mg cm^{-2} and 44.02 mg cm^{-2} respectively after the period of 50 cycles. The effective resistance of the coatings is due to the formation of $Ni_3V_2O_8$, $NiCr_2O_4$, Cr_2O_3 & AlV_2O_4 phases.

1. Introduction

Hot corrosion is a major drawback that can be seen in gas turbines, boilers, IC engines, incinerators, etc [1]. The vanadium, sulphur, and sodium are the common impurities that are present in some low-grade petroleum fuels, when coming in contact with high-temperature materials, providing a harsh environment for the hot corrosion to occur [2–4]. Hot corrosion is initiated by deposition or

condensation of corrosive species, e.g. sulphates. The condensation of sulphates on gas turbine blades takes place owing to high concentrations of alkalis in combination with high concentrations of sulphur [5–7]. Even at high concentrations of chlorine, alkali sulphates are formed, because these are the least volatile alkali species. The typical temperature range for hot corrosion in gas turbines is 600 °C–950 °C [8–10]. The upper-temperature limit is given by the dew point of the alkali sulphates. The lower temperature limit is given by the melting point of eutectics formed by the deposits and the corrosion product scale of the blade material [10–12].

Hot corrosion has been characterized as type I (high-temperature) corrosion and type II (low-temperature) corrosion. Type I hot corrosion mainly occurs at 800 °C–950 °C. It is caused by the formation of liquid alkali sulphates above their melting points, leading to the basic dissolution of the oxide scale of the blade material. Type II hot corrosion mainly occurs at 600 °C–800 °C. It is caused by the formation of a eutectic melt of $NiSO_4$ or $CoSO_4$ and alkali sulphates above the eutectic temperature. $NiSO_4$ and $CoSO_4$ are formed by the reaction of the oxide scale of the blade materials with SO_3 depending on the SO_3 partial pressure in the hot flue gas [4, 5, 13–15]. To overcome these problems of corrosion, high-strength alloys are developed to withstand high-temperature environments. But unfortunately, the alloys which are developed are not sufficient to resist corrosion at elevated temperatures; hence the thermal spray coatings are developed [16–18]. Nickel-based coatings are found to be more suitable and effective in terms of resistance to corrosion at high temperatures [19–22]. There are wide varieties of coating techniques available in the market. Plasma spraying is the most commonly and widely used thermal spraying method for coating powders on ceramics and metals [23–25]. It is been reported as one of the best technology which is successful as an economical solution and reliable to industrial problems [26–28]. The temperature produced in the plasma spray coating process makes it suitable for thermal, bio-medical & electrical applications [29, 30, 31]. The focus of the present work is to study the 65 pct NiCrAlY + 35 pct TiO_2 and 65 pct NiCrAlY + 35 pct Cr_2O_3 + 5 pct YSZ coatings behavior by using the plasma spray method on titanium-15 alloys to assess their sustainability in the harsh atmosphere of Na_2SO_4 + 60 pct V_2O_5 salt at the temperature of 700 °C. The substrate used for the present study has been procured from MDNL, Hyderabad is being used for different components in gas turbines. XRD, SEM/EDS, and X-ray elemental mapping techniques are used to characterize the uncoated and coated samples in the molten salt corrosion environment under the cyclic condition at the temperature of 700 °C.

2. Experimental details

2.1. Substrate material

The ASTM B338, Grade 2 titanium-15 alloy is chosen as a base material for the present work. The specimen dimensions of 25 mm × 25 mm × 5 mm are polished with emery sand papers to a size of 180 grit. The specimens are grit blasted by using alumina powder before plasma spray coating for better coating adhesion. The substrate chosen for the present work is used in the hot section component of gas turbine applications. Table 1 shows the chemical compounds of Titanium-15 alloy.

Table 1. Chemical composition of the substrate material.

Element	Wt %
C	0.007
O	0.1071
N	0.007
H	0.0013
Fe	0.03
Ti	Bal

2.2. Formulation of coating and its characterization

The NiCrAlY + TiO_2 and NiCrAlY + Cr_2O_3 + YSZ are used as a feedstock powders. The feedstock powders are coated on Titanium-15 alloy by using the atmospheric plasma spray method by controlling the process variables. The process variables of plasma spray coating are as shown in table 2. The surface morphology of coatings is investigated using a scanning electron microscope (SEM) (JOEL-JSM-6380LA, Japan) equipped with energy dispersive spectroscopy (EDS). In this technique, a cross-section of coating is polished with emery paper and placed under a microscope that is equipped with a CCD camera. Select a magnification that allows resolution of the voids and best fills the screen with the entire coating thickness. If some of the substrate is visible on the screen it must be masked. Once the best magnification has been determined, adjust the microscope's aperture and field diaphragms for the best resolution and contrast. XRD analysis is done by using an X-ray diffractometer (Bruker D 8 Advanced). Here Ni-filtered Cu-Ka radiation is used in an X-ray diffractometer at room temperature. The scan rate is 2° per min and the scan range from 20° to 90° is maintained.

Table 2. Process variables of plasma spray coating

Argon-gas Pressure	800000 Pa
Argon-gas Flow-rate	40000 CCM
H_2-gas (Pressure)	350000 Pa
H_2-gas (Flow rate)	5000–8000 CCM
Voltage	60–70V
Current	1350 A
Powder feed rate	100–120 gram min^{-1}
Stand-off distance	100–125 mm

In the present investigation, porosity measurement is performed by using the image analyzer according to ASTM 276B standards. A total of 20 separate fields of view in a random pattern are analyzed. After the desired number of fields has been measured, the mean value of area percentage porosity and standard deviation of the individual measurements are calculated.

According to ASTM B487 standards coating thickness is measured using an image analyzer (Biovis software). Ten readings are taken on each specimen and the average value is reported as the (mean) coating thickness.

2.3. Molten salt hot corrosion tests

The hot corrosion behavior of bare titanium-15 alloys and coatings made on titanium-15 alloys are studied under cyclic conditions in a Na_2SO_4–60 pct V_2O_5 environment at the temperature of 700 °C. The hot corrosion tests are carried out in SiC tubular furnace. 0.8g of Na_2SO_4 and 2g of V_2O_5 are thoroughly mixed with distilled water to form a salt mixture which is applied to the specimens. The specimens are cleaned with acetone and weighed using the weighing balance. Before the experiment starts, the dimension of the specimen is carefully recorded with vernier calipers to estimate the specimen surface. The specimen is roughened using emery paper to roughen the surface for the proper adhesion of the salt coat. The salt layer on the specimen is maintained within the range of 3–5 mg cm^{-2}. The salt-coated sample is kept inside the tubular furnace on a ceramic boat at a temperature of 250 °C for about 2 h to remove the moisture content. The whole process is carried out for 2 h and removed from the furnace and weighed. The 50 cycles are carried out with one hour

of heating with twenty minutes of cooling at room temperature. Test sample with the boat is weighed and recorded for each and every cycle. Changes observed with regard to oxide scale and colour change are made after each cycle.

3. Results and Discussion

3.1. Characterisation of coatings

3.1.1. SEM/EDS analysis

Figure 1 shows the morphology of two different powders which have a spherical structure with a particle size of −45 + 15 μm. Figures 2(a) and (b) shows the cross-sectional micrograph of the NiCrAlY + TiO_2 and NiCrAlY + Cr_2O_3 + YSZ coatings after being subjected to hot corrosion. It can be inferred that the coatings have dense and uniform microstructure. Oxide inclusions and voids are found to be some of the characteristics observed in coatings developed by the plasma spray method.

Figure 1. Morphology of (a) NiCrAlY + TiO_2 powder (b) NiCrAlY + Cr_2O_3 + YSZ powder.

Figure 2. BSEI image of (a) NiCrAlY + TiO_2 coating (b) NiCrAlY + Cr_2O_3 + YSZ coating after 50 cycles of hot corrosion at a temperature of 700 °C.

The EDS technique results for selected areas of NiCrAlY + TiO_2 coating shows the weight percentage of 93.76% Fe, 25.10% Cr, 36.03% Ni, 0.56% Ti are as shown in the (figure 2(a)). The NiCrAlY + Cr_2O_3 + YSZ coating shows the weight percentage of 46.23% Ni, 59.43% Cr, 94.16% Fe & 5.92% Al are as shown in the (figure 2(b)).

Figure 3(a)–(c) shows the SEM and EDS analysis for uncoated and plasma sprayed coatings at selected regions after subjecting to 50 cycles in a hot corrosion environment. Loosely bounded structure and needle-like appearance are observed in the bare titanium-15 alloy with the elemental composition of 70.67% O & 29.33% Ti which are as shown in figure 3(a).

Figure 3. SEM & EDS analysis of (a) Titanium-15 alloy (b) NiCrAlY + TiO_2 coating. (c) NiCrAlY + Cr_2O_3 + YSZ coating after 50 cycles of hot corrosion at a temperature of 700 °C.

Surface scales formed on the coated samples have a dense, massive, and crack-free consisting of O, Na, Cr, and Ni. The oxide scale formed on the NiCrAlY + TiO_2 coating (figure 3(b)) has a crystal-like appearance with a bunch of clusters noticed after the 50 cycles of hot corrosion. The EDS analysis on this area indicates the elemental composition of 48.68% O, 21.66% Na & 12.59% of Ni with the small amounts of Cr, Ti, S, Al, and V. The NiCrAlY + Cr_2O_3 + YSZ coating (figure 3(c)) have a bunch of nodules like appearance distributed uniformly throughout the substrate surface is observed. The EDS analysis of NiCrAlY + Cr_2O_3 + YSZ coating exhibits 50.45% O, 27.22% Ni & 11.01% Cr with the small quantities of Na, Al, and V.

3.1.2. Electron probe micro analyzer analysis

Figures 4 and 5 represent the X-ray elemental mapping of two different coatings after the hot corrosion of 50 cycles at a temperature of 700 °C in a Na_2SO_4–60%V_2O_5 environment. Figure 4 shows the X-Ray elemental mapping of NiCrAlY + TiO_2 coating which indicates the formation of scales consisting of O_2, Al, Cr, Fe, Ni, Ti, Na, and S. The chromium depleted layer is formed on the base of the scale followed with a thick band of chromium on the subscale area and the uppermost layer of scale is formed with a thick band of oxygen. The splat boundaries are enriched with nickel and the sub-surface interfaced with a higher concentration of Ni due to the diffusion occurring from the substrate to the coating top surface. Na and S constituents are present below the top scale, showing the penetration through the splat boundaries.

Figure 4. X-ray mapping of NiCrAlY + TiO_2 coating (cross-section).

Figure 5. X-ray mapping of NiCrAlY + Cr_2O_3 + YSZ coating (cross section).

O_2 and Na are found to be dominant on the scales formed on the top layer of NiCrAlY + Cr_2O_3 + YSZ coating which is as shown in figure 5. The intermediate layer is found to be rich in Al and Ni splats which are oxidized at their boundary and the other layer of scale has splats with lamellar structure. Oxides of chromium like V, Ni, Cr, and Fe are formed at the splat boundary.

3.1.3. Coating thickness & porosity

The coating powders are sprayed onto the substrate using the plasma spray torch by maintaining the desired thickness in the range of 250–350 μm. The porosity of the coating plays important role in terms of resistance against corrosion; a lower value of porosity indicates the coating has the better resistance in a corrosion environment. The average value of porosity is found to be 2.9% and 2.7% for NiCrAlY + TiO_2 and NiCrAlY + Cr_2O_3 + YSZ coating respectively.

3.1.4. Microhardness tests

Figure 6 represents the micro-hardness profile along the cross-section for two different coatings. The average value of micro-hardness of coatings is measured by using the Mitutoyo hardness (HM series) test equipment. Hardness values of 539 Hv & 568 Hv is found for NiCrAlY + TiO_2 & NiCrAlY + Cr_2O_3 + YSZ coating respectively. The variation of micro-hardness along the cross-section can be inferred from the oxide inclusions [12]. The increase in hardness at the boundary of coating and substrate is due to the cohesive strength and density of each splat due to the high impact velocity of the coated particles. The strain hardening effect caused during sandblasting of the substrate before coating may also be the reason for the higher hardness value of the coating [14].

Figure 6. Micro hardness profiles of NiCrAlY + TiO_2 & NiCrAlY + Cr_2O_3 + YSZ coatings.

3.1.5. Bond strength test

An adhesion strength test is carried out by using the EC-1386 Epoxy Adhesive (3M-Scotch weld) tensile machine. The macrographs of ruptured surfaces for coated samples are shown in figures 7 and 8. The adhesion strength is found to be 20.43 MPa and 21.96 MPa for NiCrAlY + TiO_2 and NiCrAlY + Cr_2O_3 + YSZ coatings respectively.

Figure 7. Adhesion test samples of NiCrAlY + TiO_2 coating.

Figure 8. Adhesion test samples of NiCrAY + Cr_2O_3 + YSZ coating.

3.1.6. X-ray diffraction Analysis

The X-Ray Diffraction analysis is carried out for the coated and the uncoated samples after 50 cycles of hot-corrosion at the temperature of 700 °C. The XRD pattern obtained is shown in figure 9. Major peaks of TiO_2 & $TiVO_4$ are observed on the Titanium-15 corroded sample [15]. The scale formation on the NiCrAlY + TiO_2 coating consists of TiO_2, $Ni_3V_2O_8$, $NiCr_2O_4$, Al_2O_3, AlV_2O_4 & Cr_2O_3 as a major phase and $Cr_2(SO_4)_3$ as a minor phase. The NiCrAlY + Cr_2O_3 + YSZ coating has AlV_2O_4, $Ni_3V_2O_8$, Al_2O_3, $NiCr_2O_4$, & Cr_2O_3 as major phases and $Cr_2(SO_4)_3$ as a minor phase. The oxides like Cr_2O_3, Al_2O_3 & $NiCr_2O_4$, present as a major phase in corroded products [5–9].

Figure 9. XRD patterns for titanium-15 alloy and plasma sprayed coatings.

3.2. Thermogravimetric analysis

The hot corroded macrographs of the bare titanium-15 alloy and the plasma sprayed coatings are as shown in figures 10(a)–(c). The formation of oxide scale on titanium-15 alloy is observed from the beginning of the first cycle and the surface is observed to be greyish brown in colour. From the 3rd cycle, the colour change is noticed to light brown. The peeling of the salt layer is observed on the substrate surface during the 4th cycle. In the 11th cycle, the light brown colour to dark brownish grey is noticed and the same trend is continued till the end of the 50th cycle. In the NiCrAlY +TiO_2 coating, the light brownish colour has observed in the 1st cycle. From the 3rd cycle, the colour change from pale brown colour to dark brown colour is observed and it is followed up to the end of the 50th cycle. In the NiCrAlY + Cr_2O_3 +YSZ coating, the glossy brown shade is observed in the 1st cycle and the same trend is continued up to the end of the 50th cycle.

Figure 10. Macrographs of hot corroded samples in Na_2SO_4–60%V_2O_5 environment. (a) Titanium-15 alloy (b) NiCrAlY + TiO_2 coating (c) NiCrAlY + Cr_2O_3 + YSZ coating.

A graphical representation of weight gain (mg/cm^2) versus time in terms of a number of cycles is plotted for the substrate and coatings are as shown in figure 11. The bare titanium-15 alloy, 65 pct NiCrAlY + 35 pct TiO_2 coating and 65 pct NiCrAlY +35 pct Cr_2O_3 + 5 pct YSZ coating produced a weight gain of 307.92 mg/ cm^2, 42.16 mg cm^{-2} and 44.02 mg cm^{-2} respectively after the period of 50 cycles. It is observed that the net weight gain is lower for the coated substrates when compared to uncoated substrates. This clearly indicates the coatings are protective against corrosion environment. A graph is plotted to analyze the parabolic relation of the weight gain with the exposure time of the sample and also (weight gain) ^{2} versus the time is plotted [8–10]. The parabolic relationship graph of alloys and coatings is shown in figure 12.

Figure 11. Weight gain/Area versus no: of cycles graph for substrate and coatings for 50 cycles of hot corrosion at a temperature of 700 °C.

Figure 12. (Weight gain/area) ^{2}/Area versus a number of cycles graph for substrate and coatings for 50 cycles of hot corrosion at a temperature of 700 °C.

From figure 11 it is observed that the bare titanium-15 alloy deviates from the parabolic rate law. As the number of cycles increases, the value of weight gain/area increases as observed in figure 11 hence indicating the oxide scale formation is un-protective in the Na_2SO_4-60%V_2O_5 molten-salt environment. The parabolic constant (Kp) value, for bare titanium-15 alloy, NiCrAlY + TiO_2 coating and NiCrAlY + Cr_2O_3 + YSZ coating is 1.568×10^{-9} g^2 $cm^{-4}s^{-1}$, $1.525 \times 10^{-11}g^2$ $cm^{-4}s^{-1}$ and $1.469 \times 10^{-11}g^2$ $cm^{-4}s^{-1}$ respectively. The K_P values are found to be in the upper limits which are calculated after 50 cycles. The lower Kp values represent the coating is more protective in sodium sulphate and vanadium pentoxide environment.

4. Discussion

The plasma spraying method is used to deposit the NiCrAlY + TiO_2 and NiCrAlY + Cr_2O_3 + YSZ powders on Titanium-15 alloys with an average coating thickness range of 250–350 μm. The two different plasma sprayed coatings show superior corrosion resistance properties compared to bare Titanium-15 alloy. The NiCrAlY + TiO_2 coating exhibits better corrosion resistance compared to NiCrAlY + Cr_2O_3 + YSZ coating. The indication of the $TiVO_4$ scales on the bare Titanium-15 alloy showed the non-protective conditions under the molten salt environment of Na_2SO_4 + 60 pct V_2O_5 at 700 °C after 50 cycles. The formation of $NiCr_2O_4$, $Ni_3V_2O_8$ & Cr_2O_3 & AlV_2O_4 spinals (figure 9) on the oxide scales inhibits the corrosion and resistance to oxidation in sodium sulphate and vanadium pentoxide environment. The salt which is induced due to the mechanism of accelerated oxidation, which will act like a catalyst and oxygen carrier, the stable binary oxides which are grown initially replaced with the ternary oxides such as $NiCr_2O_4$ during the intermediate stages of oxidation [3–5]. The Cr_2O_3 scale formation resists the differences between oxygen, and corrosive species and also protects from penetration of any particle through it. Resistance to corrosion has been improved by the formation of $NiCr_2O_4$ spinel and Cr_2O_3 (confirmed by the XRD analysis) in the scales of oxide with the environment of molten salt [6–8]. The superior hot corrosion resistance of NiCrAlY + TiO_2 coating is attributed to the protective oxide scale mainly consisting of titanium oxide (TiO_2) which has minimum solubility in highly acidic Na_2SO_4−60 pct V_2O_5 salt melt. The parabolic behavior and slow corrosion kinetics observed during thermo gravimetric study show that the reaction rate is diffusion-limited.

5. Conclusion

- The NiCrAlY / TiO_2 & NiCrAlY / Cr_2O_3 /YSZ coatings are successfully deposited using the plasma-sprayed method on bare Titanium-15 alloy with the porosity of 2.7% and 2.9% and an average micro-hardness of 539 Hv & 568 Hv respectively.

- The coated samples showed a lesser weight gain when compared to the uncoated substrate. The estimated parabolic constant values are lower for coated surfaces when compared to the uncoated surface.
- The corrosion rate is slightly higher at the initial cycles of exposure and slowly decreases and becomes stable in further cycles. This is due to the oxygen that is propagating through the coating's voids and splat boundaries, causing severe and speedy oxidation at the early stages of the cycles. Further, these oxides will lock or close down all the ways to decelerate corrosive species' diffusion in the later stages in the coating. The coating is then cramped or restricted mainly to the upper surface of the coatings.

- The NiCrAlY / TiO_2 coating shows better corrosion resistance at higher temperatures. This may be due to lower porosity and flat splat structure. The protective oxide scale mainly consists of titanium oxide (TiO_2) which has minimum solubility in highly acidic Na_2SO_4−60 pct V_2O_5 salt melt. Titanium oxide formed along the boundaries of Nickel-rich splats present in pores might have blocked the passages and have enabled coatings to develop the barriers against diffusion and penetration of corrosive species.

- Spalling and peel-off scale are observed in bare titanium-15 alloy with maximal weight gain during the hot corrosion study.

Data availability statement

All data that support the findings of this study are included within the article (and any supplementary files).

Declaration of interests

☒ The authors declare that they have no known competing financial interests or personal relationships that could have appeared to influence the work reported in this paper.

☐ The authors declare the following financial interests/personal relationships which may be considered as potential competing interests.

ScienceDirect

Journal of Molecular Structure
Volume 1237, 5 August 2021, 130380

Rational design of flavonoid based potential inhibitors targeting SARS-CoV 3CL protease for the treatment of COVID-19

Shipra Bhati [a], Vikas Kaushik [b], Joginder Singh [b]

Show more

Outline | Share Cite

https://doi.org/10.1016/j.molstruc.2021.130380
Get rights and content

Highlights

- Several flavonoid based SARS-CoV 3CLpro inhibitors were rationally designed by incorporating gamma lactam ring and various fluoro substituted heterocyclic ring systems.
- The ligands were tested for drug-likeness, oral bioavailability, toxicity, synthetic accessibility, and ADMET properties.
- Docking simulations confirmed strong binding affinity and inhibition potential of the ligands against the receptor SARS-CoV 3CL protease (3CLpro).
- Ligand L4, L8 and L14 emerged as the lead compounds.

Abstract

The current outbreak of Coronavirus Disease 2019 (COVID-19) pandemic has reported thousands of deaths worldwide due to the rapid transmission rate and the lack of antiviral drugs and vaccinations. There is an urgent need to develop potential antiviral drug candidates for the prevention of COVID-19 infection. In the present study, a series of potential inhibitors targeting SARS-CoV 3CL protease were rationally designed by incorporating gamma lactam ring, and various fluoro substituted heterocyclic ring systems to the flavonoid scaffold. The prediction of drug-likeness, oral bioavailability, toxicity, synthetic accessibility, and ADMET properties was made by computational means. Quercetin was used as standard. The binding affinity of the ligands towards the 3CL protease target was examined using docking simulations. The designed ligands possess favourable pharmacokinetic and pharmacodynamic properties. Ligand L4, L8, and L14 appeared to be the lead compounds in the series and can be considered for further *in-vivo* and *in-vitro* validation.

A Face Recognition Method In Machine Learning (ML) For Enhancing Security In Smart Home

Publisher: IEEE

Marwan Alshar'e ; Mohammad Rustom Al Nasar ; Rohit Kumar ; Manish Sharma ; Dharamvir ; Vikas Tripathi **All Authors**

Abstract: The study explores with Machine learning (ML), which is a type of neural network (AI) that empowers software programmers to start increasing prediction without being done... **View more**

Metadata

Abstract:
The study explores with Machine learning (ML), which is a type of neural network (AI) that empowers software programmers to start increasing prediction without being done with full to make this happen Exterior door security is of paramount importance and has become the cornerstone for the best and fastest security or sufficient to choose a feeling of protection to property owners, and together with technological innovations, especially in the Communication area, which tends to make emerging innovations in locking doors or windows have picked up a lot, including such locking doors and windows with faces and the others. Face - recognition technologies have also been developed and used for residential door locking mechanisms, and they are a basic and easy-to-use technology that detects the features of homeowners quite well. The advancement of facial recognition has resulted in one of the computer vision algorithms that is simple to build and has a high accuracy in recognising faces, and it has been widely utilised. When consumers review or exposure to new goods, does this have an instant influence on your suggestion system or does it take time, How do suggestions evolve as consumers interact more with the platform, many different of each sort of recommendation system in order to have a more detailed of their capabilities.

Published in: 2022 2nd International Conference on Advance Computing and Innovative Technologies in Engineering (ICACITE)

Date of Conference: 28-29 April 2022

INSPEC Accession Number: 21884745

Date Added to IEEE *Xplore*: 18 July 2022

DOI: 10.1109/ICACITE53722.2022.9823833

ISBN Information:

Publisher: IEEE

Conference Location: Greater Noida, India

Circumstantial Discussion on Security and Privacy Protection using Cloud Computing Technology

Publisher: IEEE

Melanie Lourens ; Ayesha Naureen ; Shouvik Kumar Guha ; Shahanawaj Ahamad ; Dharamvir ; Vikas Tripathi All Authors

Abstract: Cloud computing is becoming a demanding technology due to its flexibility, sensibility and remote accessibility. Apart from these applications of cloud computing, privacy... **View more**

Metadata

Abstract:
Cloud computing is becoming a demanding technology due to its flexibility, sensibility and remote accessibility. Apart from these applications of cloud computing, privacy and security are two terms that pose a circumstantial discussion. Various authors have argued on this topic that cloud computing is more secure than other data sharing and storing methods. The conventional data storing system is a computer system or smartphone storage. The argument debate also states that cloud computing is vulnerable to enormous types of attacks which make it a more concerning technology. This current study has also tried to draw the circumstantial and controversial debate on the security and privacy system of cloud computing. Primary research has been conducted with 65 cloud computing experts to understand whether a cloud computing security technique is highly secure or not. An online survey has been conducted with them where they provided their opinions based on the security and privacy system of cloud computing. Findings showed that no particular technology is available which can provide maximum security. Although the respondents agreed that blockchain is a more secure cloud computing technology; however, the blockchain also has certain threats which need to be addressed. The study has found essential encryption systems that can be integrated to strengthen security; however, continuous improvement is required.

Published in: 2022 2nd International Conference on Advance Computing and Innovative Technologies in Engineering (ICACITE)

Date of Conference: 28-29 April 2022

INSPEC Accession Number: 21884617

Date Added to IEEE *Xplore*: 18 July 2022

DOI: 10.1109/ICACITE53722.2022.9823875

ISBN Information:

Publisher: IEEE

A Comprehensive Analysis of Internet of Things (IOT) Sustained Integrity System Services with Data Management Based ON Machine Learning

Publisher: IEEE

Ch Sekhar ; Meenakshi ; Saeed Mousa ; M. K. Sharma ; V M Gobinath ; Dharamvir **All Authors**

Abstract: Internet of Things (IoT) and Machine Learning (ML) are recent trends in huge data management. Traditionally, data management was carried out by humans where big data coll... **View more**

▸ Metadata

Abstract:
Internet of Things (IoT) and Machine Learning (ML) are recent trends in huge data management. Traditionally, data management was carried out by humans where big data collection, analysis and acquisition were solely done by humans. However, IoT and ML have enabled machines rather than humans to collect big data, analyse them and develop a new business model. It has shown huge success in industry 4.0; however, during the management of big data, large-scale companies encountered certain issues. These include, lack of effective training leads to less accuracy in data management, security issues during cloud computing and security issues in blockchain as well. Therefore, this study has explained the ways to improve big data management through ML and to enhance the security of blockchain. A primary survey was carried out with 50 respondents who provided their responses to certain questions related to big data management solutions and blockchain security. Findings showed that providing training to the workers and using guidelines/policies in blockchain can increase the data management accuracy and can improve the security in cloud computing, respectively.

Published in: 2022 2nd International Conference on Advance Computing and Innovative Technologies in Engineering (ICACITE)

Date of Conference: 28-29 April 2022

Date Added to IEEE *Xplore*: 18 July 2022

▸ ISBN Information:

INSPEC Accession Number: 21884783

DOI: 10.1109/ICACITE53722.2022.9823431

Publisher: IEEE

Conference Location: Greater Noida, India

Contents

The implementation of IoT in business has opened the pathway for faster and easier transportation, manufacturing and data management. Traditionally, remote sensing and controlling devices were lacking which did not allow the management employees to monitor certain processes and carry out effective data management [1]. However, in recent days, IoT-based devices enabled the use of wireless devices to carry out effective data management. Two issues lie in the IoT system which brings some problems in business are single-point of failure and cyber-attack. Therefore, the researchers are trying to strengthen network security by implementing various techniques which will allow the business to share information without any worry [2]. The proposed technique is Blockchain security which allows the management to share data privately and record the data securely [3].